Acceptor Surrogates for Mycobacterial Glycosyltransferases

By

Mario Alejandro Martínez Farias

A dissertation submitted in partial fulfillment

of the requirements for the degree of

Doctor of Philosophy

(Chemistry)

at the

UNIVERSITY OF WISCONSIN—MADISON

2014

Date of final oral examination: June 10, 2014

The dissertation is approved by the following members of the Final Oral Committee:

Laura L. Kiessling, Professor, Departments of Chemistry and Biochemistry
Judith N. Burstyn, Professor, Department of Chemistry
Samuel H. Gellman, Professor, Department of Chemistry
Eric R. Strieter, Assistant Professor, Department of Chemistry
Tehshik P. Yoon, Associate Professor, Department of Chemistry

ACCEPTOR SURROGATES FOR MYCOBACTERIAL GLYCOSYLTRANSFERASES

Mario A. Martínez Farias

Under the supervision of Professor Laura L. Kiessling

at the University of Wisconsin-Madison

Glycans mediate a wide range of biological processes. They are a diverse and abundant class of molecules, particularly notable for their complexity. Assembly of glycan chains takes place through a template-independent process mediated by enzymes termed glycosyltransferases. The oligosaccharide portion of glycosyltransferase acceptors are frequently linked via a pyrophosphate bridge to a long lipid carrier, and all components are recognized by the enzyme. Deciphering the enzymes' function *in vitro* is complicated by the lability and amphiphilic nature of these glycan intermediates, and the challenges in accessing them synthetically. I sought to address this limitation while investigating the galactofuranosyltransferases that mediate galactan biosynthesis. Galactan is a glycan polymer consisting of 20–40 galactofuranose (Gal*f*) residues, built on a pyrophosphoryl-linked carrier lipid prior to installation onto the cell wall peptidoglycan of mycobacteria.

The galactofuranosyltransferase GlfT1 is hypothesized to prime galactan assembly by elongating a lipid-linked disaccharide pyrophosphate with 2–3 Gal*f* residues. The polymerase GlfT2 builds the full galactan chain from this oligosaccharide. Efforts to characterize GlfT1 using *O*-alkyl disaccharide acceptor analogs have failed, but it was unclear whether this resulted from instability of the enzyme *in vitro* or lack of suitable acceptors. I hypothesized that GlfT1 is restrictive for disaccharide acceptor analogs bearing a pyrophosphate, or analog thereof. I stabilized the putative GlfT1 acceptor substrate by replacing the pyrophosphate group with a phosphonophosphate.

Using synthetic acceptor substrate surrogates, I discovered that GlfT1 elongates disaccharide acceptors by 2–3 Gal*f* residues *in vitro*, generating a specific oligosaccharide pattern. In generating the +3 Gal*f* oligosaccharide, GlfT1 sets the register for the alternating β(1,5) and β(1,6) linkage pattern observed in endogenous galactan. Chain termination experiments utilizing deoxygenated UDP-Gal*f* donors and NMR spectroscopy confirmed the Gal*f*-β(1,6)-Gal*f*-β(1,5)-Gal*f* pattern on the non-reducing end of the lipid-linked phosphonophosphate. Finally, I determined that an acceptor substrate bearing the Gal*f*-β(1,5)-Rha-α(1,3)-GlcNAc trisaccharide overrides the enzyme's requirement for a pyrophosphate-containing substrate. Using this acceptor, I concluded that GlfT1 produces oligosaccharides that can be extended by the polymerase GlfT2 to generate synthetic galactan polymers of endogenous length.

_____

Laura L. Kiessling

To my parents,
whose immense courage
made this all possible.

To my wife,
my source of strength.

Acknowledgements

I have drawn strength from a number of extraordinary people in my life. I thank first and foremost my advisor, Laura Kiessling, who gave me the opportunity to pursue this magnificent goal. She guides her students on a journey of self-discovery with calm and patience. We learn how to truly become independent scientists with keen insight and ambition. The knowledge that she shares with us, and the resources that she works so hard to provide, are invaluable. She encouraged me to push forward when I wavered, and I thank her for having confidence in my potential. I leave her laboratory a much better scientist and person than I thought possible.

I have had the pleasure of working alongside extremely talented scientists. I thank my office mates, Joe Grim and Chris Brown, who made the lab a very welcoming and fun environment when I first joined. I thank Virginia Kincaid, who made a critical contribution to the GlfT1 project that opened the floodgates to so many interesting biochemical experiments. I started graduate school with no knowledge of biochemistry, and I thank three people in particular for sharing their extensive biochemistry and molecular biology expertise. Matt Levengood, Matt Kraft, and Darryl Wesener. With great patience, they taught me to how become a competent biochemist. Matt Kraft was a brilliant mentor during my middle years. I also thank all other members of the Kiessling laboratory, who have all contributed to my development as a scientist and a person.

None of the conclusions outlined in this thesis would be possible without outstanding support provided by the Chemistry and Biochemistry departments. I thank Martha Vestling for countless and lengthy discussions about mass spectrometry, as well as Charles Fry and Monica Ivancic for helping with unique NMR experiments and pulse sequences. The assistance of Kris Turkow and Kat Myhre are also acknowledged.

Professors Roman Manetsch and Georg Kleine inspired me to pursue graduate studies. Roman instilled in me his passion for chemical biology and empowered me with meaningful and important projects. Georg, as a fountain of wisdom and my trusted mentor for nearly a decade, has affected my life in so many positive ways.

I thank my parents, who sacrificed absolutely everything in their lives to secure a better future for my siblings and I. They have provided me with a source of strength that I may never match. I thank them for trusting in me, for supporting my schooling even when they could not live comfortably themselves, and for providing so much guidance and perspective. Thank you for recognizing that there was a better place, and having the courage to risk everything and take us there. It has been difficult, and we have suffered, but we might yet thrive. I hope to one day be worthy of all of the love and affection that you have selflessly given me.

Lastly, I thank my wife, Danielle, whose unwavering support replenished my energies every single day. She trusted and believed in me, and as my best friend has counseled me on countless occasions. I am an incredibly lucky man to have shared so many memories over the past five years in Madison with you. Our journey continues.

Table of Contents

Acknowledgements ..... **iv**

Table of Contents ..... **vi**

List of Figures ..... **xi**

List of Schemes ..... **xv**

List of Abbreviations ..... **xvii**

Chapter 1: Lipid-linked Acceptor Analogs for Prokaryotic Glycosyltransferases **1**

1.1 Abstract **2**

1.2 The importance of defined synthetic glycans **3**

1.3 Acceptors to interrogate cell wall glycosyltransferases **5**

1.3.1 Peptidoglycan glycosyltransferases 6

1.3.2 Cell wall transglycosylases 9

1.3.3 Wall teichoic acid glycosyltransferases 11

1.4 Acceptors for *N*-glycosylation pathways **15**

1.4.1 Bacterial N-glycan glycosyltransferases 16

1.4.2 Archaeal glycosyltransferases 19

1.5 Mycobacterial glycosyltransferases **20**

1.5.1 Peptidoglycan glycosyltransferases 20

1.5.2 Galactan glycosyltransferases 22

1.5.3 Arabinan glycosyltransferases 30

1.6 Acceptors to survey various bacterial glycosyltransferases 34

1.7 Conclusion 35

Chapter 2: Synthesis of Phosphonophosphates Acceptor Substrates for Mycobacterial Glycosyltransferases 36

2.1 Abstract 37

2.2 Introduction 38

2.3 Biosynthesis of the mycobacterial galactan 41

2.3.1 GlfT1 and GlfT2 mediate galactan assembly 42

2.3.2 Glycolipids bearing the linkage disaccharide 43

2.4 Phosphonophosphates as glycosyltransferase acceptor substrates 45

2.4.1 Synthesis of the acceptor disaccharide portion 48

2.4.2 Synthesis of (2Z,6Z)-farnesyl phosphonic acid 51

2.4.3 Moffatt-Khorana coupling to generate phosphonophosphate acceptors 52

2.4.4 Synthesis of neryl-linked phosphonophosphates 53

2.5 Conclusion 55

2.6 Experimental details 55

Chapter 3: Isoprenoid Phosphonophosphates as Acceptor Substrates for Mycobacterial Glycosyltransferases 86

3.1 Abstract 87

3.2 Introduction 88

3.3 Chemically defined conditions to investigate GlfT1 function 89

3.3.1 Reconstituting GlfT1 activity in vitro 91

3.3.2 Quantification of UDP release by GlfT1 with phosphonophosphate acceptor substrates 93

3.3.3 Kinetics analysis of GlfT1 turnover with a farnesyl-linked acceptor 94

3.4 Use of phosphonophosphate-linked oligosaccharides in galactan assembly 96

3.4.1 Isolation of phosphonophosphate-linked tetra- and pentasaccharides 97

3.4.2 NMR analysis of tetrasaccharide produced by GlfT1 99

3.4.3 GlfT2 processes phosphonophosphate-linked oligosaccharides 100

3.5 Conclusion 101

3.6 Experimental details 102

Chapter 4: A neutral acceptor processed by cell wall galactofuranosyltransferases 105

4.1 Abstract 106

4.2 Introduction 107

4.3 A lipid-linked Gal*f* acceptor bearing the disaccharide linker unit 110

4.3.1 Synthesis of a lipid-linked Galf-β(1,4)-Rha-α(1,3)-GlcNAc acceptor 111

4.3.2 Disaccharide formation with a 4'-OBz rhamnosyl donor 111

4.3.3 Disaccharide formation with a 4'-ONAP rhamnosyl donor 114

4.4 Glycosyltransferase assays with the neutral lipid-linked trisaccharide 116

4.4.1 Investigating the acceptor's utility in GlfT1 assays 116

4.4.2 Site-directed mutagenesis reveals residues important for GlfT1 catalysis 122

4.4.3 Investigating the utility of the trisaccharide acceptor in GlfT2 assays 123

4.5 Conclusion 126

4.6 Experimental details 127

Chapter 5: Structural Analysis of Galactofuranose Oligosaccharides with Chain Terminating Agents 147

5.1 Abstract 148

5.2 Introduction 149

5.3 Linkage analysis of oligosaccharides prepared by GlfT1 149

5.4 Conclusions 156

5.5 Experimental details 156

Chapter 6: Future Directions 163

6.1 Abstract 164

6.2 Introduction 165

6.3 Investigating cooperativity between cell wall galactofuranosyltransferases 165

6.3.1 An arabinogalactan biosynthetic complex 166

6.3.2 Measuring interactions between GlfT1 and GlfT2 166

6.4 Toward more complex synthetic phosphonophosphate acceptors 169

6.4.1 A synthetic lipid-linked trisaccharide phosphonophosphate acceptor 169

6.4.2 Interrogating galactofuranosyltransferase acceptor scope with an expanded carrier lipid repertoire 171

6.5 Conclusions 175

6.6 Experimental details 175

Appendix: NMR Spectra 191

Compiled References 301

List of Figures

Figure 1.1. Structures of the pentasaccharide portion of heparin, synthetic heparin analog fondaparinux sodium, antiviral glycomimetics zanamivir and oseltamivir, and antibiotic kanamycin. 4

Figure 1.2. A generic lipid-linked hexose pyrophosphate is glycosylated by a glycosyltransferase (GT) through a nucleotide-activated donor. 5

Figure 1.3. Glycosyltransferases MraY and MurG build Lipid I and Lipid II, respectively, as peptidoglycan precursors. Various modifications, particularly on Lipid I, have shed light on the activity of MurG. 7

Figure 1.4. Penicillin binding proteins (PBPs) form mature peptidoglycan from Lipid II and Lipid IV monomers through transglycosylase and transpeptidase domains. 9

Figure 1.5. Top: WTAs from *B. subtilis* 168 and *S. aureus* H. R_1 = D-Ala or α-Glc, R_2 = D-Ala or -H, R_3 = α-GlcNAc or β-GlcNAc. Middle: Wall teichoic acid biosynthesis in *B. subtilis* 168. Bottom: WTA analogs modified at the glycerol tail, the sugar residues, or the lipid carrier. 12

Figure 1.6. Oligosaccharides in the N-linked glycosylation pathway of *C. jejuni* and *M. voltae*. . 17

Figure 1.7. The glycosyltransferases GlfT1 and GlfT2 generate the galactan polymer. GlfT1 primes a decaprenyl-linked linker disaccharide with 2-3 Gal*f* residues, which is subsequently polymerized by GlfT2. 24

Figure 1.8. Acceptor substrate modifications to interrogate galactan assembly by cell wall galactofuranosyltransferases GlfT1 and GlfT2. 27

Figure 1.9. A terminal arabinan oligosaccharide motif and an acceptor substrate analog. 31

Figure 2.1. Substructure of the mycobacterial cell wall. An additional cell envelope component, lipoarabinomannan, is shown on the right. The outer membrane is omitted for clarity. 40

Figure 2.2. Galactan biosynthesis. Top: Biosynthetic pathway toward arabinogalactan. Bottom: Genes encoding the enzymes that build arabinogalactan. Galactan biosynthetic enzymes are highlighted in red. 42

Figure 2.3. GlfT1 and GlfT2 mediate galactan biosynthesis..... 43

Figure 2.4. Glycolipid acceptor substrate analogs for GlfT1. 44

Figure 2.5. Acceptor 2.04 is not a substrate for GlfT1 in the presence of donor sugar UDP-Gal*f*. 45

Figure 2.6. Replacement of the allylic phosphate (blue) and decaprenyl lipid tail in putative glycosyltransferase acceptor substrate 2.01 to a phosphonate (blue) and (2Z,6Z)-farnesyl lipid in surrogate 2.08. 46

Figure 2.7. Phosphonophosphate analogs in the chemical literature. 47

Figure 3.1. Structure of the mycobacterial mycolyl-arabinogalactan-peptidoglycan (mAGP) cell wall complex. 89

Figure 3.2. GlfT1 and GlfT2 mediate galactan biosynthesis..... 90

Figure 3.3. Acceptor substrate analogs for GlfT1. 91

Figure 3.4. Top: Representative MALDI-TOF mass spectrum obtained from a reaction mixture of compound 2.08, UDP-Gal*f*, and GlfT1. Masses corresponding to +2 and +3 Gal*f* residues were observed. Bottom: Corresponding +2 and +3 products from elongation of acceptor 2.08. The linkage pattern shown is in agreement with that of endogenous galactan. 92

Figure 3.5. Representative MALDI-TOF mass spectrum obtained from a reaction mixture of compound 2.32, UDP-Gal*f*, and GlfT1. A mass corresponding to +2 Gal*f* residues was observed. 93

Figure 3.6. Top: Glycosyltransferase activity promotes UDP release, which is monitored using a luminescence assay. Bottom: Relative output of UDP-Gal*f* turnover by GlfT1 with acceptors 2.04, 2.08, 2.32, and 2.33. 94

Figure 3.7. Relative output of UDP-Gal*f* turnover by GlfT1 with acceptors 2.08 monitored over time. 95

Figure 3.8. Analysis of a GlfT1 reaction mixture with UDP-Gal*f* and varied concentrations of acceptor 2.08. 95

Figure 3.9. Isolation of +2 Gal*f* and +3 Gal*f* products from a reaction mixture of acceptor 2.08, UDP-Gal*f*, and GlfT1. 98

Figure 3.10. MALDI-TOF MS spectrum of isolated tetrasaccharide product obtained following extension of acceptor 2.08 with GlfT1. LRMS: calcd $C_{41}H_{70}NO_{25}P_2$ $[M-H]^-$ 1038.9, observed 1038.5. 99

Figure 3.11. $^1H-^{13}C$ HSQC spectrum of isolated tetrasaccharide product obtained following extension of acceptor 2.08 with GlfT1. Labels correspond to sugar resonances in the inset structure. 100

Figure 3.12. Relative output of UDP-Gal*f* turnover by GlfT1 with +2 Gal*f* and +3 Gal*f* farnesyl-linked phosphonophosphate acceptors. 101

Figure 4.1. A lag phase, observed when GlfT2 polymerizes a disaccharide acceptor, is abolished with a tetrasaccharide acceptor. A trisaccharide acceptor may fill enough subsites to avoid a lag phase. 109

Figure 4.2. MALDI-TOF analysis of an incubation of 4.01, UDP-Gal*f* and GlfT1. 117

Figure 4.3. GlfT1 activity is abolished upon addition of 5 mM EDTA. Top: GlfT1 reaction in the presence of 10 mM $MgCl_2$ ("no EDTA"). Bottom: Reaction with no added metal and 5 mM EDTA. 119

Figure 4.4. Time course MALDI-TOF analysis of an incubation of 4.01, UDP-Gal*f* and GlfT1. .120

Figure 4.5. Isolation of +1 Gal*f* oligosaccharide produced by GlfT1. Top: MALDI-TOF MS spectrum of input reaction mixture prior to HPLC purification. Middle: Mixture of +1 and +2 Gal*f* oligosaccharides. Bottom: Purified +1 Gal*f* oligosaccharide 4.19. 121

Figure 4.6. Site-directed mutagenesis of *M. smegmatis* GlfT1 reveals the critical importance of Asp193 for GlfT1 catalysis. 122

Figure 4.7. An oligosaccharide mixture produced by GlfT1's action on 4.01 is converted to endogenous length galactan by GlfT2..... 124

Figure 4.8. GlfT2 formation of galactan polymers from acceptor 4.01 is dependent on the acceptor's concentration. 125

Figure 4.9. GlfT2 processes isolated +1 Gal*f* oligosaccharide 4.19 to long galactan polymers. .. 126

Figure 5.1. MALDI-TOF MS analysis of a GlfT1 reaction mixture with phosphonophosphate acceptor 2.08 and deoxygenated donor sugars. 152

List of Schemes

Scheme 2.1. Synthesis of rhamnolipid acceptor 2.02. 44

Scheme 2.2. Retrosynthetic analysis toward phosphonophosphate 2.08. 48

Scheme 2.3. Synthesis of donor and acceptor substrates for Rha-α(1,3)-GlcNAc glycosides. 49

Scheme 2.4. Glycosylation of silylated monosaccharides 2.15 and 2.16, followed by elaboration to phosphate 2.22. 50

Scheme 2.5. Synthesis of acetate-protected disaccharide α-phosphate 2.13. 51

Scheme 2.6. Synthesis of (2Z,6Z)-farnesyl phosphonate 2.14. 52

Scheme 2.7. Synthesis of farnesyl-linked Rha-α(1,3)-GlcNAc phosphonophosphate 2.08. 53

Scheme 2.8. Synthesis of neryl-linked Rha-α(1,3)-GlcNAc disaccharide phosphonophosphate 2.32. 54

Scheme 2.9. Synthesis of neryl-linked GlcNAc phosphonophosphate 2.33. 55

Scheme 4.1. Trisaccharide acceptor 4.01 is processed differently by GlfT1 and GlfT2. 109

Scheme 4.2. Retrosynthetic analysis of phenoxyundecenyl trisaccharide 4.01. 111

Scheme 4.3. Synthesis of differentially-protected 4-*O*-benzoyl L-rhamnosyl thioglycoside donor 4.06. 112

Scheme 4.4. Synthesis of allyl *N*-acetyl-D-glucosamine acceptor 4.07 and glycosylation with donor 4.06. 113

Scheme 4.5. Synthesis of 4-*O*-NAP L-rhamnosyl donor 4.05, glycosylation with acceptor 4.07, and elaboration to disaccharide acceptor 4.17. 114

Scheme 4.6. Preparation of alkenyl trisaccharide 4.01 via cross-metathesis. 116

Scheme 5.1. Use of deoxygenated UDP-Gal*f* donor analogs 5.01 and 5.02 as linkage determination probes. 151

Scheme 5.2. Use of 4'-deoxygenated farnesyl-linked disaccharide phosphonophosphate as GlfT1 specificity probe. 154

Scheme 5.3. Synthetic efforts toward 4'-deoxygenated phosphonophosphate acceptor 5.03. ... 155

Scheme 6.1. Trisaccharide phosphorylation toward phosphonophosphate 6.01. 170

Scheme 6.2. Synthesis of (2Z,6E)-farnesol. 172

Scheme 6.3. Synthesis of (2Z,6Z,10Z)-nerylnerol 2.ai via the *cis*-isoprenoid synthon 2.ah. 173

Scheme 6.4. Elaboration of prenyl alcohols 6.08 and 6.08 and coupling to disaccharide phosphate 2.13 may yield disaccharide phosphonophosphates. 174

List of Abbreviations

Ac	acetyl
A. baumannii	*Acinetobacter baumannii*
ABC	ATP-binding cassette
ACS-grade	American Chemical Society-grade
AG	arabinogalactan
AIBN	2,2'-azobis(2-methylpropionitrile)
Ar	aromatic
Ara*f*	D-arabinofuranose
AraT	arabinofuranosyltransferase
ATP	adenosine triphosphate
B. subtilis	*Bacillus subtilis*
Bac-2,4-diNAc	2,4-diacetamido-2,4,6-trideoxy-D-glucopyranose
BCG	*M. bovis*—bacillus Calmette-Guérin
BF_3•Et_2O	boron trifluoride diethyl etherate
BLAST	Basic Local Alignment Search Tool
Bn	benzyl
brsm	based on recovered starting material
C. difficile	*Clostridium difficile*

C. glutamicum	*Corynebacterium glutamicum*
C. jejuni	*Campylobacter jejuni*
C_{50}-P-Ara*f*	decaprenyl-monophosphoryl-arabinofuranose
CHCA	α-cyano-4-hydroxycinnamic acid
COSY	correlation spectroscopy
Cy	cyclohexane
d	doublet
DCC	*N,N*'-dicyclohexylcarbodiimide
DDQ	2,3-dichloro-5,6-dicyano-*para*-benzoquinone
DIBAL-H	diisobutylaluminum hydride
DMAP	4-(dimethylamino)pyridine
DMPU	1,3-dimethyl-3,4,5,6-tetrahydro-2(1*H*)-pyrimidone
DPA	arabinofuranosyl-β-phosphoryldecaprenol
DSP	dithiobis(succinimidylpropionate)
dTDP	thymidine 5'-diphosphate
dTDP-Rha	thymidine 5'-diphosphate rhamnose
DTT	dithiothreitol
E. coli	*Escherichia coli*
EDTA	ethylenediaminetetraacetic acid

Enz	enzyme
Et	ethyl
Et_3N	triethylamine
Et_2O	diethyl ether
EtOAc	ethyl acetate
EtOH	ethanol
FRET	Förster resonance energy transfer
Gal	D-galactose
Gal*f*	D-galactofuranose
GalNAc	*N*-acetyl-D-galactosamine
Gal*p*	D-galactopyranose
GGPP	geranylgeranyl pyrophosphate
Glc	D-glucose
Glc-2,3-diNAcA	2,3-diacetamido-2,3-dideoxy-D-glucuronic acid
GlcNAc	*N*-acetyl-D-glucosamine
GlfT1	uridine 5'-diphosphate-galactofuranosyltransferase 1
GlfT2	uridine 5'-diphosphate-galactofuranosyltransferase 2
Gro-P	poly(glycerol phosphate)
GT	glycosyltransferase

HABA	2-(4-hydroxyphenylazo)benzoic acid
HEPES	4-(2-hydroxyethyl)piperazine-1-ethanesulfonic acid
HIV	human immunodeficiency virus
His_6	hexahistidine
HPLC	high-performance liquid chromatography
HREI MS	high-resolution electron impact mass spectrometry
HRESI MS	high-resolution electrospray ionization mass spectrometry
HSQC	heteronuclear single-quantum coherence
IC_{50}	half maximal inhibitory concentration
K. pneumoniae	*Klebsiella pneumoniae*
k_{cat}	turnover number
K_d	dissociation constant
K_i	inhibition constant
K_m	Michaelis constant
LAM	lipoarabinomannan
LC-MS	liquid chromatography-mass spectrometry
LG	leaving group
LiDBB	lithium 4,4'-di-*tert*-butylbiphenylide
M. flavus	*Micrococcus flavus*

M. bovis	*Mycobacterium bovis*
M. smegmatis	*Mycobacterium smegmatis*
M. tuberculosis	*Mycobacterium tuberculosis*
M. voltae	*Methanococcus voltae*
m/z	mass-to-charge ratio
m-DAP	*meso*-diaminopimelic acid
mAG	mycolylarabinogalactan
mAGP	mycolyl-arabinogalactan-peptidoglycan
MALDI-TOF	matrix-assisted laser desorption/ionization time-of-flight
ManNAc	*N*-acetyl-D-mannosamine
ManNAcA	2-acetamido-2-deoxy-D-mannuronic acid
mCPBA	*meta*-chloroperoxybenzoic acid
MDR-TB	multidrug-resistant tuberculosis
Me	methyl
MeOH	methanol
MGT	monofunctionalglycosyltransferase
MHz	megahertz
mol/mol	mole per mole
MOPS	4-morpholinepropanesulfonic acid

MS	molecular sieves
MurNAc	*N*-acetylmuramic acid
MurNGly	*N*-glycolylmuramic acid
N. gonorrhoeae	*Neisseria gonorrhoeae*
NADH	nicotinamide adenine dinucleotide
NAP	2-naphthylmethyl
NBD	nitrobenzoxadiazole
NEt_3	triethylamine
NIS	*N*-iodosuccinimide
NMR	nuclear magnetic resonance
P	phosphate (or monophosphate)
p-TsOH	*para*-toluenesulfonic acid
PBP	penicillin-binding protein
pdb	protein data bank
PG	peptidoglycan
Ph	phenyl
P-P	pyrophosphate (or diphosphate)
q	quartet
quint	quintet

Rbo-P	poly(ribitol phosphate)
Rha	L-rhamnose
S. aureus	*Staphylococcus aureus*
S. galilaeus	*Streptomyces galilaeus*
S. venezuelae	*Streptomyces venezuelae*
STaz	*S*-thiazolinyl
STD-NMR	saturation transfer difference nuclear magnetic resonance
s	singlet
t	triplet
TB	tuberculosis
TBS	*tert*-butyldimethylsilyl
TBAF	tetra-*n*-butylammonium fluoride
TBSOTf	*tert*-butyldimethylsilyl trifluoromethanesulfonate
TGase	transglycosylase
THF	tetrahydrofuran
TLC	thin layer chromatography
TMS-Set	(ethylthio)trimethylsilane
TPase	transpeptidase
T4SS	Type IV secretion system

UDP	uridine 5'-diphosphate
UDP-Gal*f*	uridine 5'-diphosphate galactofuranose
UDP-Gal*p*	uridine 5'-diphosphate galactopyranose
UDP-GlcNAc	uridine 5'-diphosphate *N*-acetyl-D-glucosamine
UGM	uridine 5'-diphosphate-galactopyranose mutase
UMP	uridine 5'-monophosphate
UV	ultraviolet
V_{max}	maximum velocity
vol/vol	volume per volume
WHO	World Health Organization
WTA	wall teichoic acid
X-Gal	5-bromo-4-chloro-3-indolyl-β–D-galactopyranoside
XDR-TB	extensively drug resistant tuberculosis

Chapter 1: Lipid-linked Acceptor Analogs for Prokaryotic Glycosyltransferases

1.1 Abstract

Glycan-processing enzymes are ubiquitous, yet interrogating their function is challenging largely due to the complex and often labile nature of their substrates. Chemical glycobiology addresses these challenges by providing synthetic access to glycan substrates utilized to probe glycosyltransferase function. In this review, we provide an overview of prokaryotic glycosyltransferases that process lipid-linked acceptor substrates and the synthetic acceptor analogs used to probe their function. We focus on glycosyltransferases that mediate cell wall biosynthesis and bacterial N-linked glycosylation. These enzymes are involved in processes critical for microbial growth; intercepting their biosynthetic pathways can lead to the development of novel therapeutics to challenge the rise of antibiotic resistance.

1.2 The importance of defined synthetic glycans

Polysaccharides are the most abundant organic substances on the planet. This complex and diverse class of biopolymers mediates a variety of important biological processes. These can range from surface glycoconjugates critical to cell-cell recognition during fertilization and immune cell function, to high molecular-weight polymers that provide structural rigidity and serve as matrices for other conjugates.[1] Glycosylation is also emerging as a post-translational modification, where glycosylation can affect gene expression and protein function.[2,3]

Interest in elucidating the role of glycans in biology spawned the flourishing field of chemical glycobiology.[4,5] The importance of glycobiology became especially apparent when heparin, contaminated with oversulfated chondroitin sulfate, resulted in the death of a number of patients receiving anticoagulation therapy in the clinic.[6] This tragedy underlined not only the risk of sourcing clinical-grade heparin from animal byproducts, but also the broader difficulty in ensuring the purity of a heterogeneous mixture of large, highly charged polysaccharides. The discovery that a short pentasaccharide fragment derived from heparin is sufficient for anticoagulant activity led to the development of the fully synthetic heparin analog fondaparinux, marketed as Arixtra (Figure 1.1).[7,8] In addition to fondaparinux, small molecule glycan mimics such as Zanamivir (Relenza) and oseltamivir (Tamiflu) are important therapeutics in fighting influenza, and the aminoglycoside kanamycin is a potent antibiotic.[9,10] A recent herculean effort resulted in the total synthesis of a consensus glycoform of erythropoietin, an essential glycoprotein hormone involved in red blood cell production. These examples highlight the contributions that synthetic chemistry can make to the field of glycobiology.[11] The utility of these glycans and their derivatives has led to a renewed effort to understand the activity of the enzymes responsible for assembling essential glycans.

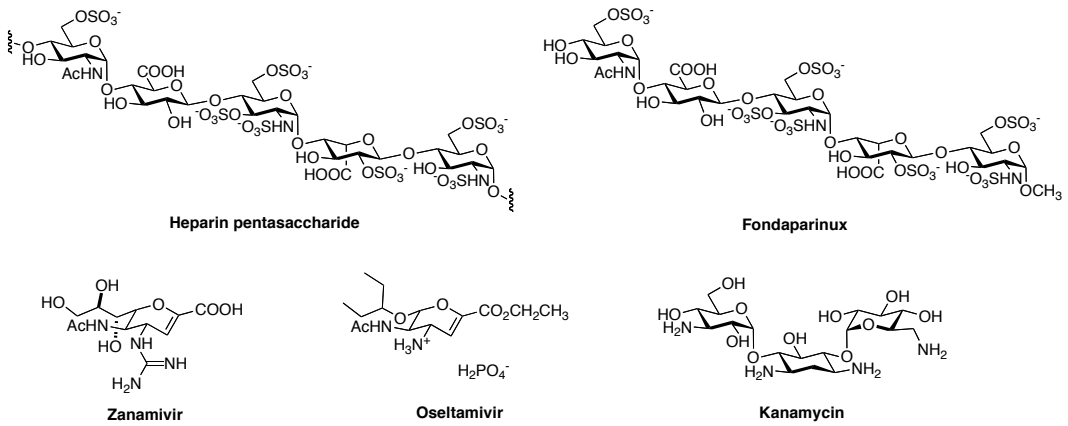

Figure 1.1. Structures of the pentasaccharide portion of heparin, synthetic heparin analog fondaparinux sodium, antiviral glycomimetics zanamivir and oseltamivir, and antibiotic kanamycin.

Glycosyltransferases are a large class of enzymes that comprise nearly 1% of the genome of eukaryotes and prokaryotes.[12] These enzymes mediate glycan assembly. Glycan assembly occurs in a template-independent fashion, wherein control of polysaccharide or polysaccharide polymer length and branching modifications is inherent to the polysaccharide biosynthetic enzymes. Building complex polysaccharides can occur either from successive addition of individual monosaccharide units or *en bloc* transfer and polymerization of large polysaccharide fragments. Glycosyltransferases (GTs) mediate the addition of a sugar from an activated donor to an acceptor substrate. The donor is typically a nucleoside-activated diphosphate but alternatively can be lipid-linked (Figure 1.2). An acceptor may be a lipid-linked mono- or pyrophosphate glycan, an amino acid residue on a protein, a nucleic acid, or a hydrophobic scaffold. An excellent review by Withers and colleagues summarizes glycosyltransferase features.[13]

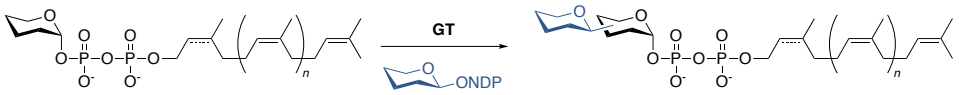

Figure 1.2. A generic lipid-linked hexose pyrophosphate is glycosylated by a glycosyltransferase (GT) through a nucleotide-activated donor.

The study of glycosyltransferases seeks to understand their basic biological function, define their scope, and develop assays to inhibit their activity. Modulation of glycosyltransferase activity has illuminated the biological targets of clinically relevant small molecules. In particular, inhibitors of prokaryotic glycosyltransferases can thwart bacterial growth. The antibiotic tunicamycin is a donor substrate analog that blocks the transfer of *N*-acetyl-D-glucosamine (GlcNAc) 1-phosphate from UDP-GlcNAc to a lipid dolichyl phosphate, consequently barring protein N-glycosylation and ultimately leading to cell death.[14] Similarly, the antibiotic moenomycin interferes with peptidoglycan biosynthesis through inhibition of cell wall transglycosylases.[15] Its mechanism of action was discovered only recently through the use of synthetic substrate analogs. This is discussed at length in the sections that follow.

In this review, we focus on the use of synthetic acceptor substrate analogs to interrogate the function and scope of prokaryotic glycosyltransferases. Particular emphasis will be placed on the glycosyltransferases of the mycobacterial cell wall. In addition, lipid-linked glycans can function as donor analogs to probe the function of oligosaccharyltransferases.[16] These excellent investigations, in addition to others highlighted below, reveal the promise of chemical synthesis in deciphering the myriad roles of carbohydrates in biology.

1.3 Acceptors to interrogate cell wall glycosyltransferases

The majority of bacteria possess a cell wall. The bacterial cell wall is a rigid, protective layer located outside of the plasma membrane. It is embedded with a complex array of proteins and accessory motifs, and provides a protective barrier critical for bacterial survival. A series of glycosyltransferases build each component of the cell wall. Acceptor substrate analogs have been essential in advancing the understanding of cell wall biosynthesis.

1.3.1 Peptidoglycan glycosyltransferases

The peptidoglycan (PG) component of cell walls is a rigid polymer that endows bacteria with their shape and the ability to withstand the osmotic pressure produced by the cytosol.[17] PG is composed of β(1,4)-linked *N*-acetyl-D-glucosamine (GlcNAc) and *N*-acetylmuramic acid (MurNAc) residues. The MurNAc residues are modified with a pentapeptide, typically L-Ala-γ-D-Glu-L-Lys-D-Ala-D-Ala. The third residue in some bacteria (such as gram-negative bacteria and mycobacteria) is *meso*-diaminopimelic acid (*m*-DAP). Other minor modifications to the pentapeptide are also observed. Cross-linking between peptide chains provides PG with its characteristic rigidity, with most cross-links occurring between residues 3 and 4 (e.g. L-Lys and D-Ala or *m*-DAP and D-Ala) or between residues 4 and 4 (e.g. D-Ala and D-Ala). Extent of cross-linking varies between species, with about 50% cross-linking in *Escherichia coli* and 70-80% in mycobacteria.[18,19]

Peptidoglycan is assembled in the cytoplasm on a C_{50} to C_{55} polyprenyl carrier lipid. Two glycosyltransferases synthesize the monomers required for peptidoglycan assembly. In *E. coli*, MraY adds a MurNAc pentapeptide residue to undecaprenyl phosphate via the nucleotide-activated donor termed Park's nucleotide, generating MurNAc(pentapeptide)-α-P-P-undecaprenol (Lipid I) (Figure 1.3).[20] Glycosyltransferase MurG adds a β-linked GlcNAc residue to the 4-hydroxyl group of MurNAc to yield Lipid II, GlcNAc-β(1,4)-MurNAc(pentapeptide)-α-

P-P-undecaprenol.[21] This lipid-linked disaccharide pyrophosphate serves as the acceptor for downstream enzymes that polymerize the monomer into peptidoglycan.

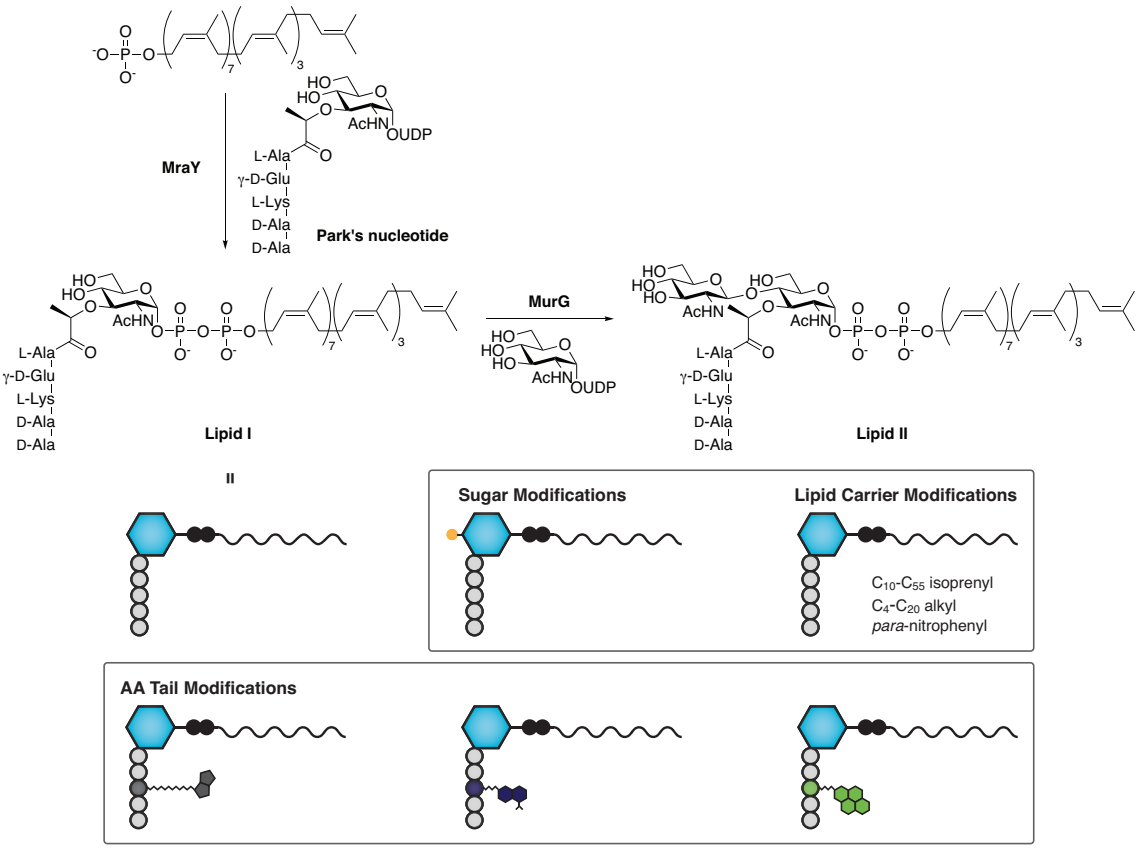

Figure 1.3. Glycosyltransferases MraY and MurG build Lipid I and Lipid II, respectively, as peptidoglycan precursors. Various modifications, particularly on Lipid I, have shed light on the activity of MurG.

Understanding the enzymes that synthesize peptidoglycan or its precursors could yield a new class of antibacterial substances. A series of probes have been developed to study the glycosyltransferases of peptidoglycan biosynthesis. Dansylated UDP-MurNAc pentapeptide substrates were useful for the development of fluorescent assays of unpurified MraY in membrane fractions.[22,23] Blanot and co-workers synthesized a fluorescent Lipid I analog to study MurG, replacing the endogenous undecaprenyl lipid carrier with the shorter dihydroheptaprenyl lipid.[24] Using a simple saturated lipid sidesteps the synthetic challenges of a highly labile allylic

pyrophosphate substrate. Incorporation of the fluorescent compound into peptidoglycan was observed in membrane fractions. The same compound was later useful for the development of an HPLC-based assay.[25] Walker and co-workers improved upon this assay by shortening the lipid carrier to a C_{10} citronellol, and relying on capture of a biotinylated L-Lys side chain instead of fluorescence.[26] This simple substrate afforded development of a purification protocol yielding active *E. coli* MurG, allowing interrogation of pure MurG for the first time.[27] The authors were able to determine kinetic parameters for MurG with the Lipid I analog and noted that MurG processed an analog bearing a truncated amino acid tail much less efficiently.

A number of subsequent studies have investigated the effect of the lipid carrier on MraY and MurG activity. The lipid is proximal to the enzyme active site, yet a number of modifications are permitted. Walker and co-workers synthesized a panel of Lipid I derivatives with no pentapeptide modifications.[28] Changes to lipid carrier length (C_{10}-C_{55}), saturation (citronellyl vs. neryl, C_{20} alkyl vs. C_{20} nerylneryl) and geometry (1 *cis* vs. 3 *cis* C_{20}) yielded the conclusion that an acceptor with a four isoprene unit carrier lipid is best for MurG activity, with a pronounced effect of lipid geometry and length. The authors found that MurNAc(pentapeptide)-α-P-P-nerylnerol is an improved substrate over endogenous Lipid I using a fluorescence assay (relative rate of 1 to 0.015). Later, Wong and co-workers synthesized a similar series of substrates with a broader set of alkyl lipid carriers and concluded that hydrophobicity of the acceptor matters.[29] The tetraprenyl carrier described by Walker and co-workers was once more determined to be the best substrate in the series (k_{cat}/K_m of 15.8 $\mu M^{-1}min^{-1}$ compared to 0.55 $\mu M^{-1}min^{-1}$ for the endogenous acceptor and 1.54 $\mu M^{-1}min^{-1}$ for a C_{20} alkyl carrier). In membrane preparations, such as *Micrococcus flavus* vesicles expressing MraY and MurG, carrier lipids of 7 prenyl units or longer were best.[30] Shorter lipid carriers (e.g. farnesyl) were tolerated, but alkyl lipids were not processed.

1.3.2 Cell wall transglycosylases

Peptidoglycan transglycosylases (TGases) and transpeptidases (TPases) are responsible for polymerizing the monomers and cross-linking the pentapeptide side chains, respectively. High-molecular-weight penicillin-binding proteins (PBPs) contain both TGase and TPase domains, and can thus process Lipid II into mature peptidoglycan. TGase domains polymerize Lipid II monomers into higher oligomers (Lipid IV, Lipid VIII, etc.), which are then cross-linked by TPase domains to form the rigid polymer (Figure 1.4). Beta-lactam antibiotics target the transpeptidase domain of penicillin-binding proteins, as do natural products such as moenomycin and vancomycin.[31-33] Just as Lipid I analogs were essential to developing purification protocols for active MurG, Lipid II analogs were sought for the development of transglycosylase assays to yield screens for novel antibacterial compounds.

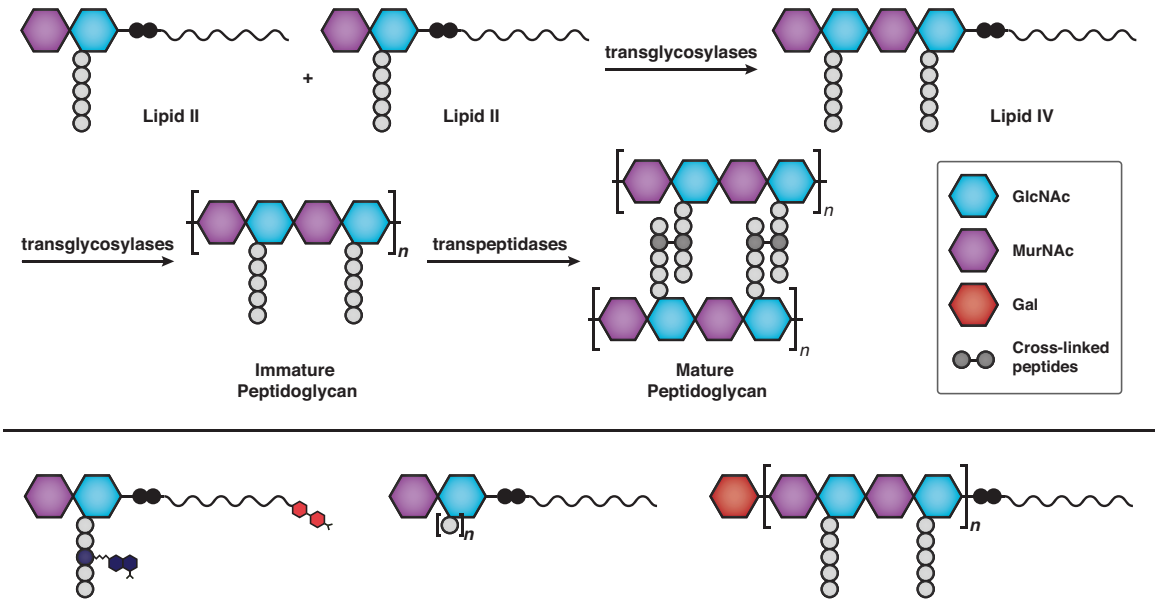

Figure 1.4. Penicillin binding proteins (PBPs) form mature peptidoglycan from Lipid II and Lipid IV monomers through transglycosylase and transpeptidase domains.

Analogs of Lipid II and Lipid IV were essential for probing the mechanism of transglycosylation. While a citronellyl-linked Lipid I analog is tolerated by MurG, Walker and

co-workers discovered that TGases are much more restrictive. Citronellyl-linked Lipid II is not processed by TGases in *E. coli* membranes, nor is a farnesyl- (C_{15}), geranylneryl-linked (C_{20}), or all-*trans* solanesyl (C_{40}) acceptor.[34] The optimal lipid carrier is all-*cis* C_{35} heptaprenyl, which outperforms the endogenous lipid carrier undecaprenol. This analog was used to study the inhibition of *E. coli* and *S. aureus* PBPs by vancomycin and other glycopeptide inhibitors.[33,35] Similarly, a Lipid IV analog bearing the heptaprenyl lipid carrier helped determine that moenomycin inhibits PBPs by binding at the elongating PG chain donor site.[36]

Kahne, Walker, and co-workers synthesized heptaprenyl-linked Lipid IV, GlcNAc-β(1,4)-MurNAc(pentapeptide)-β(1,4)-GlcNAc-β(1,4)-MurNAc(pentapeptide)-α-P-P-heptaprenol, ^{14}C-acetyl-labeled at the side chain lysine, and studied its polymerization by *E. coli* PBP1a and PBP1b.[37] PBP1b adds Lipid IV units to heptaprenyl-Lipid II sequentially, as expected. Experiments with Lipid IV bearing a nitrobenzoxadiazole (NBD) fluorophore on the lysine side chain yielded the same conclusion.[38] On the other hand, PBP1a does not require Lipid II for polymerization. The latter enzyme can catalyze synthesis of peptidoglycan directly from Lipid IV units, though not from higher oligomers. Blocking of heptaprenyl-Lipid VIII with a terminal β-(1,4)-linked galactose residue showed that these substrates can only act as glycan donors, not acceptors.[39]

The glycosyltransferase activity of TGase from various species has been studied in detail, and a proposed mechanism of PG polymerization by PBPs is established. However, the aforementioned acceptors are largely inadequate for transpeptidation. Walker, Kahne, and co-workers synthesized a heptaprenyl analog of gram-negative Lipid II to observe the transpeptidase activity of PBPs *in vitro*.[40] Gram-negative Lipid II features *m*-DAP instead of L-Lys at the 3rd position of the pentapeptide, and only peptidoglycan chains bearing this residue are polymerized by *E. coli* PBP1a and PBP1b. Thus, while TGases can form peptidoglycan chains containing L-Lys, the TPase activity is diminished.

A number of additional Lipid II derivatives with amino acid tail modifications have been developed. Schwartz and co-workers synthesized a dansylated Lipid II analog to determine the kinetic profile of *E. coli* transglycosylase PBP1b.[41] Wong and Ma solved crystal structures of *E. coli* monofunctional glycosyltransferase (MGT) with a Lipid II NBD-labeled at the lysine side chain, and a biotinylated GlcNAc-β(1,4)MurNAc(pentapeptide)-α-P-P-undecaprenol analog.[42] An elegant model for MGT transglycosylation was proposed, incorporating a detailed structural analysis supported by *in vitro* experiments. Results indicate that truncations to the pentapeptide are somewhat tolerated. The lactyl side chain in MurNAc and the first L-Ala residue are essential for TGase binding activity, but the terminal D-Ala-D-Ala dipeptide motif can be removed without much loss of activity.[43] This knowledge could be useful in the development of a new generation of antibiotics targeting TGase function.

1.3.3 Wall teichoic acid glycosyltransferases

Wall teichoic acid (WTA) is a highly anionic polymer found in the vast majority of gram-positive bacteria.[44] It represents a diverse class of cell membrane polymers within bacterial teichoic acids, consisting of alditol phosphate repeats. WTAs are bound to the peptidoglycan at the C-6 position of MurNAc residues through a phosphodiester bridge. The linkage unit is a poly(glycerol phosphate)-*N*-acetyl-D-mannosamine (ManNAc)-β(1,4)GlcNAc linkage unit, where the poly(glycerol phosphate) (Gro-P) is 2 to 3 units (Figure 1.5). This unit is followed by repeats of poly(alditol phosphate), typically modified poly(glycerol phosphate) or poly(ribitol phosphate) (Rbo-P). In *B. subtilis* 168, the major WTA polymer consists of Gro-P, and is modified at R_1 by D-alanine (D-Ala) or α-linked glucose. This WTA is typically 45–60 Gro-P units in length.[45,46] In *S. aureus* H, the polymer is Rbo-P modified at R_2 by D-Ala or –H and at R_3 by α- or β-linked GlcNAc.[47] The diversity of WTAs belies their biological importance.

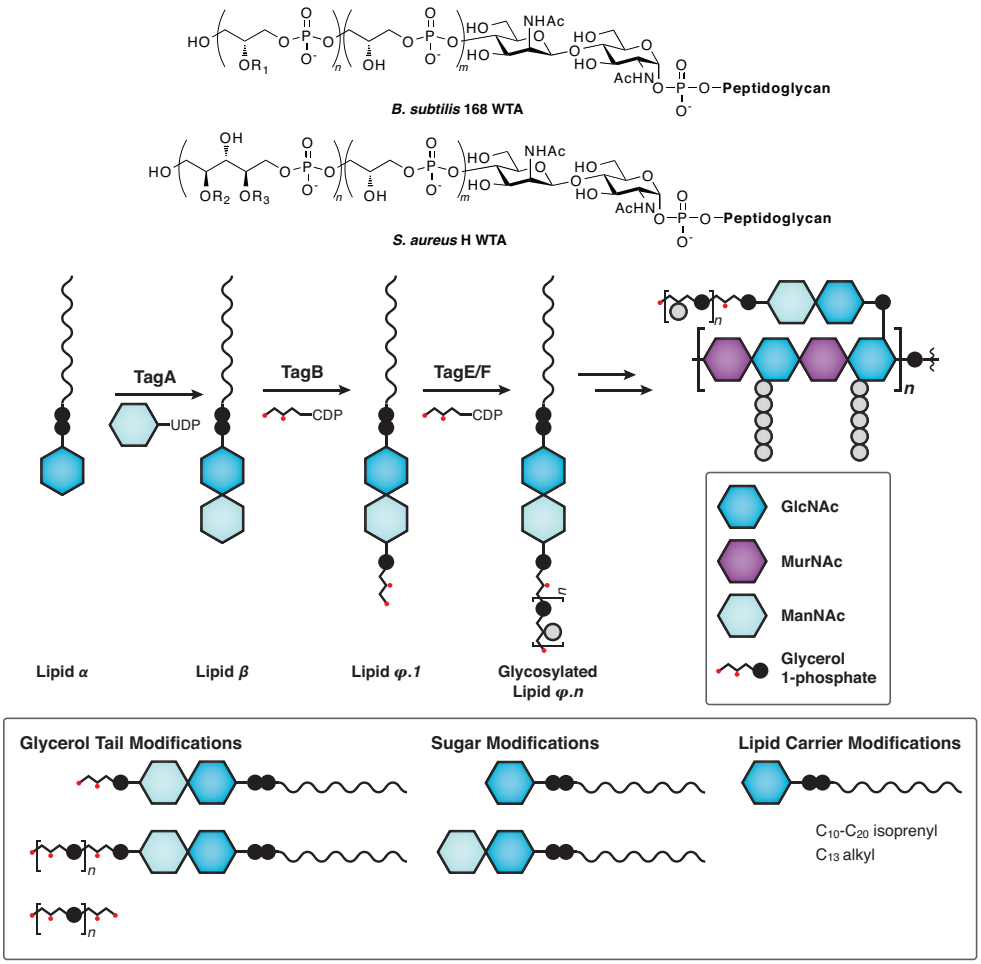

Figure 1.5. Top: WTAs from *B. subtilis* 168 and *S. aureus* H. R_1 = D-Ala or α-Glc, R_2 = D-Ala or -H, R_3 = α-GlcNAc or β-GlcNAc. Middle: Wall teichoic acid biosynthesis in *B. subtilis* 168. Bottom: WTA analogs modified at the glycerol tail, the sugar residues, or the lipid carrier.

WTAs are implicated in processes important for bacterial growth and virulence. Strains of *B. subtilis* 168 deficient in WTA develop disrupted morphologies and aberrant septation.[48,49] Colonization of nasal cells by strains of *S. aureus* lacking WTA is attenuated, supporting the assertion that WTAs are important for *S. aureus* virulence.[50,51] The highly anionic nature of WTA provides additional cellular functions, such as mediating cation homeostasis on the cell membrane.[52,53] Moreover, the volume of the polymer is modulated by the extent of D-alanyl esterification neutralizing the overall negative polyphosphate backbone.[46]

Biosynthesis of wall teichoic acid takes place in the cytoplasm and varies according to the polymer being generated.[54] In *B. subtilis* 168, *tag* (teichoic acid glycerol) genes encode the proteins mediating this process. The glycosyltransferase TagO modifies membrane-bound undecaprenyl phosphate by addition of an α-linked GlcNAc 1-phosphate from UDP-GlcNAc to form Lipid *α*, which is the substrate for TagA. TagA adds a β(1,4)-ManNAc from UDP-ManNAc, preparing Lipid *β*, the linkage unit ManNAc-β(1,4)-GlcNAc disaccharide. TagB modifies the C-4 hydroxyl of ManNAc with the first glycerol 3-phosphate unit to form Lipid *φ*.1, where donor CDP-glycerol is prepared by TagD from glycerol 3-phosphate and CTP. The enzyme TagF binds this primed linkage unit and polymerizes 30–50 glycerol 3-phosphate units onto the lipid-linked acceptor to synthesize the Gro-P WTA. Decoration of the Gro-P polymer with D-Ala and α-Glc is thought to occur prior to shuttling into the extracellular space and attachment to peptidoglycan.

Characterization of WTA biosynthetic enzymes *in vitro* is limited by the availability of the lipid-linked substrates. Walker and co-workers began a research program to characterize TagA by preparing an accessible acceptor substrate analog.[55] The endogenous undecaprenyl lipid carrier was shortened and simplified to the *n*-alkyl tridecane lipid, affording the desired TagA acceptor substrate, Lipid *α* analog GlcNAc-α-1-pyrophosphoryltridecane. Incubation with TagA and donor sugar UDP-ManNAc confirmed the enzyme's role in converting the alkyl pyrophosphate to the expected Lipid *β* ManNAc-β(1,4)-GlcNAc disaccharide. To further probe the selectivity of TagA, Walker and co-workers synthesized a series of isoprenyl α-GlcNAc pyrophosphates and measured their relative activity.[56] TagA is sensitive to the length of the isoprenyl chain (C_{10} to C_{20}), but its activity is otherwise unaffected by the geometry or saturation of the lipid. Geranylgeraniol-linked GlcNAc pyrophosphate is the best TagA substrate in the 5-member panel, and the authors' results suggest that hydrophobicity is the prevailing factor in TagA activity. Conversion of a (2Z,6Z)-farnesyl acceptor analog is inhibited by either the

disaccharide product or UDP, which was useful in determining that TagA functions via an ordered Bi-Bi mechanism.

The primase TagB is expected to mediate addition of the crucial first glycerol 3-phosphate residue to the Lipid β ManNAc-β(1,4)-GlcNAc disaccharide. Brown and co-workers confirmed this activity in membranes by incorporation of radiolabeled CDP-glycerol.[57] To investigate the activity of purified TagB *in vitro*, Walker and co-workers required access to a ManNAc-β(1,4)-GlcNAc lipid pyrophosphate. A *cis*-glycosidic linkage in the mannose series is rather challenging,[58] however, so the authors chose to prepare the TagB acceptor using a chemoenzymatic strategy via TagA.[55] Monitoring production of the phosphodiester Lipid φ.1 analog by liquid chromatography-mass spectrometry (LC–MS) confirmed TagB's activity as a glycerophosphotransferase.

The *tagE* gene has been assigned as the glycosyltransferase that mediates decoration of the poly(glycerol phosphate) backbone with α-linked glucose residues.[59] The function of this modification is not known. Brown and co-workers deleted *tagE* in *B. subtilis* 168 and demonstrated that WTAs in the Δ*tagE* strain are devoid of glycosylated Gro-P residues.[60] To confirm that TagE mediates glycosylation, they challenged purified TagE with a series of lipid $\varphi.n$ analogs, corresponding to (Gro-P)$_n$-ManNAc-β(1,4)-GlcNAc-α-P-P-tridecane. In this series of analogs, the carrier lipid has been shorted to a saturated C_{13} lipid and the Gro-P polymer length is varied from 1–80 units. Analogs of substrates for TagA (lipid α), TagB (lipid β), and TagF (lipid φ.1) were not processed as monitored by a UDP release assay. TagE has a kinetic preference for acceptors bearing longer polymers, with φ.80 analog as the best substrate, though the specificity is constant when adjusted to the concentration of Gro-P available to TagE. This enzyme may also exert control over the length of poly(glycerol phosphate), as glycosylation of a Gro-P polymer by TagE inhibits further polymerization by the polymerase TagF.

Wall teichoic acids confer *S. aureus* with resistance to peptidoglycan hydrolysis by lysozyme, which functions as a bacteriolytic component of the human immune system.[61] They also contribute to biofilm formation in this clinically important bacterium.[62] The *S. aureus* H WTA consists of a poly(ribitol phosphate) attached to a $(Gro\text{-}P)_3$-linker.[47] Using the *B. subtilis* pathway as a reference, Jiang and co-workers identified WTA biosynthetic genes in *S. aureus* through a genomic analysis of methicillin–resistant strains.[63] These genes were annotated as *tar* (teichoic acid ribitol) and assigned putative functions. Walker and co-workers utilized Lipid α analog GlcNAc-α-P-P-(2Z,6Z)-farnesol to examine the enzymes involved in this pathway.[64] This acceptor confirmed the role of TarA and TarB, homologous to *B. subtilis* TagA and TagB, respectively, in synthesizing Lipid β and Lipid φ.1. The primase TarF was found to add only one Gro-P residue to Lipid φ.1 to prepare Lipid φ.2 analog $(Gro\text{-}P)_2$-ManNAc-β(1,4)-GlcNAc-α-P-P-(2Z,6Z)-farnesol. The activity of putative Rbo-P primase TarK on this substrate could not be reproduced. In fact, the polymerase TarL adds poly(ribitol phosphate) directly onto the $(Gro\text{-}P)_2$ substrate, forming the full poly(ribitol phosphate) polymer. Production of the *S. aureus* WTA *in vitro* was accomplished chemoenzymatically through the action of purified TarA, TarB, TarF, and TarL onto the farnesyl Lipid α analog, though the synthetic wall teichoic acid is shorter than extracted, wild-type polymer.

The utility of acceptor substrate analogs is particularly relevant in wall teichoic acid glycosylation. They have served to characterize the enzymes in *B. subtilis* 168 and helped define their substrate scope. Their use *in vitro* with purified enzymes led to a revised WTA biosynthetic pathway in *S. aureus* H, which does not require a putative poly(ribitol phosphate) primase.

1.4 Acceptors for *N*-glycosylation pathways

Protein *N*-glycosylation is a conserved process in eukaryotes, bacteria, and archaea.[65,66] Prokaryotic *N*-glycosylation was first discovered in the bacterium *Campylobacter jejuni*.[67,68] The locus responsible for protein glycosylation was termed *pgl* (protein glycosylation), and it was determined that glycosylation takes place on the asparagine residue of an Asn-X-Ser/Thr, motif, where X is any amino acid except proline. Proteins are modified with an *N*-acetyl-D-galactosamine (GalNAc)-α(1,4)-GalNAc-α(1,4)-[Glc-β(1,3)]-GalNAc-α(1,4)-GalNAc-α(1,4)-GalNAc-α(1,3)-Bac-2,4-diNAc-β(1,*N*) heptasaccharide, incorporating the rare sugar bacillosamine (2,4,6-trideoxyglucopyranose, Bac).[69] The heptasaccharide is assembled on an undecaprenyl carrier lipid by a series of glycosyltransferases before being transferred *en bloc* onto the protein.

1.4.1 Bacterial N-glycan glycosyltransferases

In bacteria, assembly of the heptasaccharide takes place in the periplasm. PglC modifies undecaprenyl phosphate with Bac-2,4-diNAc-α-P, which is subsequently galactosylated by PglA. The glycosyltransferase PglJ adds a GalNAc residue to GalNAc-α(1,3)-Bac-2,4-diNAc-α-P-P-undecaprenol (Figure 1.6). The $GalNAc_2$-Bac-2,4-diNAc trisaccharide is the substrate for the downstream glycosyltransferases PglH and PglI prior to transport into the cytosol by PglK. Asparagine glycosylation is mediated by oligosaccharyltransferase PglB to form the glycoprotein.

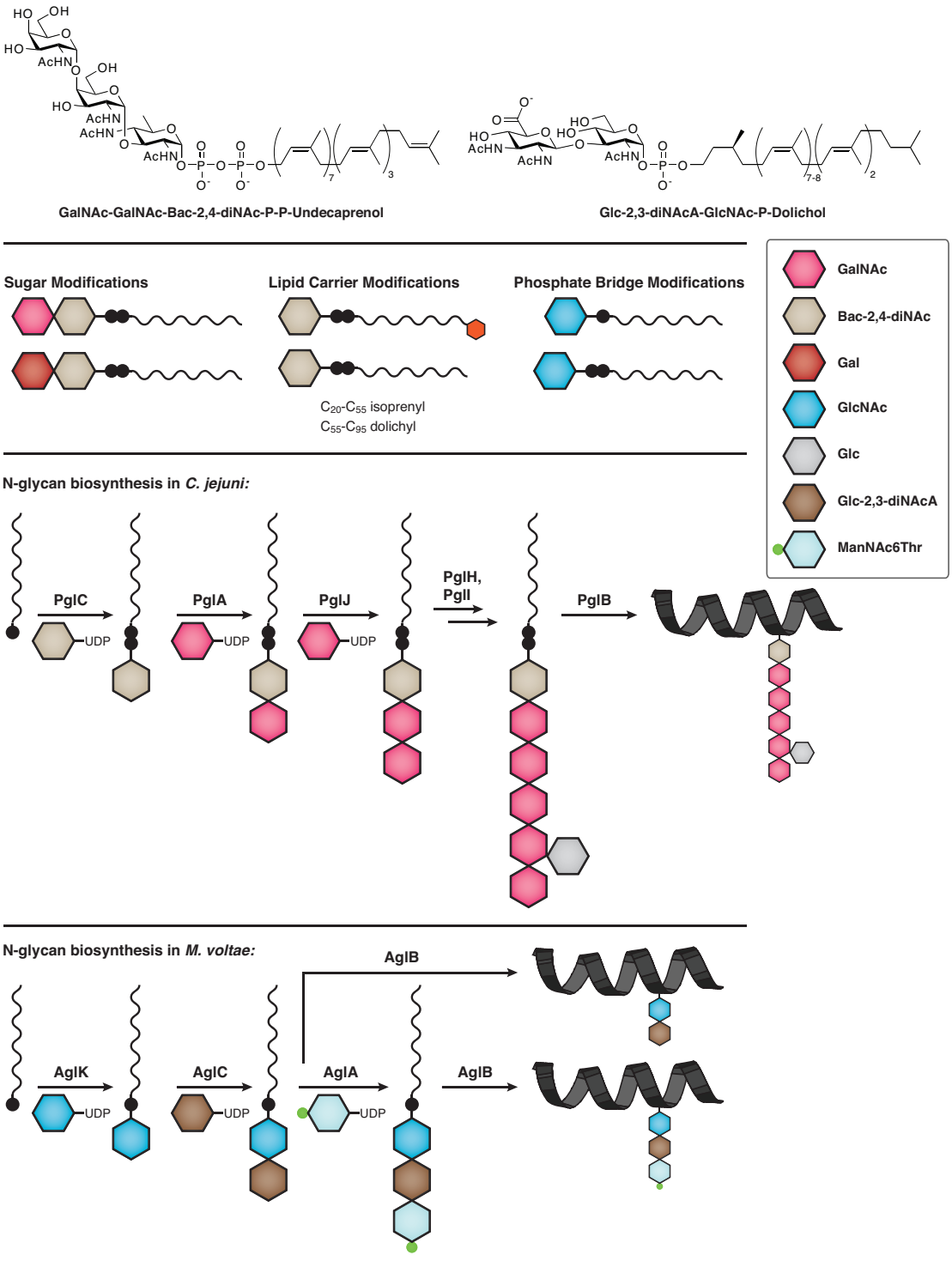

Figure 1.6. Oligosaccharides in the N-linked glycosylation pathway of *C. jejuni* and *M. voltae*.

The lipid specificity of glycosyltransferases early in the *C. jejuni* pathway, particularly PglC and PglJ, was investigated by Imperiali and co-workers.[70] To study PglJ, polyprenyl-linked [6-^{3}H]GalNAc-α(1,3)-Bac-2,4-diNAc acceptor substrates were prepared chemoenzymatically using *C. jejuni* PglC and PglA. Reaction progress by purified PglJ was assessed by incorporation of radiolabeled [6-^{3}H]GalNAc. Truncation of the endogenous lipid carrier by two isoprene units is well-tolerated, with equivalent activity for a prenol-9-linked acceptor. All other acceptors were also processed, though saturation of the α-isoprene unit led to three-fold loss of initial rate. An acceptor with an all-*trans* prenol-9 lipid carrier was equivalent to the saturated lipid analog. Along with the initial glycosyltransferase PglC, PglJ strongly favors *cis*-isoprene lipids that are unsaturated at the α-position. An acceptor substrate bearing a distal *para*-nitrophenyl lipid carrier is tolerated by *C. jejuni* PglC and PglA, as well as the homolog of PglC in *Bacteroides fragilis*, WcfS.[71,72]

There are similarities between the *C. jejuni N*-glycosylation locus and the *O*-glycosylation locus in *Neisseria gonorrhoeae*, which glycosylates serine residues.[73] PglB, analogous with *C. jejuni* PglC, modifies undecaprenyl phosphate with Bac-2,4-diNAc-α-P. PglA and PglE add two galactose residues (in analogy to *C. jejuni* PglA and PglJ) to form Gal-α(1,4)-Gal-α(1,3)-Bac-2,4-diNAc-α-P-P-undecaprenol. Transport by PglF and *O*-glycosylation by PglO yields the glycoprotein. Imperiali and co-workers characterized the glycosyltransferases in this pathway by exposing the enzymes to a panel of donor and acceptor sugars.[74] The assigned activities of purified *N. gonorrhoeae* PglA and a cell envelope fraction overexpressing PglE were confirmed. PglA catalyzed the addition of [^{3}H]Gal to Bac-2,4-diNAc-α-P-P-undecaprenol. PglE catalyzed the addition of [^{3}H]Gal to Gal-α(1,3)-Bac-2,4-diNAc-α-P-P-undecaprenol, though it can also recognize the undecapreny-linked GalNAc-α(1,3)-Bac-2,4-diNAc acceptor endogenous to *C. jejuni*. With the latter acceptor, PglE generates Gal-α(1,4)-GalNAc-α(1,3)-Bac-2,4-diNAc-α-P-P-undecaprenol with efficiency closely matching that of its endogenous *N. gonorrhoeae* substrate.

PglE did not process an acceptor bearing the Glc-α(1,3)-Bac-2,4-diNAc disaccharide, suggesting that it requires an axial 4-OH on the terminal sugar for catalysis.

1.4.2 Archaeal glycosyltransferases

Glycan intermediates in the archaeal *N*-glycosylation pathway are bound to a unique polyprenyl carrier lipid, a dolichol saturated at both the α- (proximal) and ω- (distal) units. Agl (archaeal glycosylation) enzymes in *Methanococcus voltae* generate the ManNAc(6Thr)A-β(1,4)-Glc-2,3-diNAcA-β(1,3)-GlcNAc trisaccharide, where Glc-2,3-diNAcA is 2,3-diacetamido-2,3-dideoxyglucuronic acid and ManNAc(6Thr)A is mannuronic acid modified at the 6-OH with threonine.[75] Preliminary characterization of the genes in the *agl* pathway suggested that the intermediates were bound to dolichol via a pyrophosphate linkage.[76,77] When studying the enzymes *in vitro*, Imperiali and co-workers reassigned the activity of the three glycosyltransferases and discovered that *N*-glycosylation in *M. voltae* occurs through a phosphate monoester.[78]

Activity previously assigned to AglH was reassigned to AglK, which synthesizes GlcNAc-α-P-dolichol, instead of the corresponding pyrophosphate, from UDP-GlcNAc and dolichyl phosphate. This glycosyltransferase is very selective for α-saturated C_{55}-C_{60} dolichol (similar to endogenous α,ω-saturated dolichol) over the longer C_{85}-C_{105} dolichol found in eukaryotes. The monoester product of AglK is converted to Glc-2,3-diNAcA-β(1,3)-GlcNAc-α-P-dolichol by AglC. No conversion is observed with GlcNAc-α-P-P-dolichol, implying that the enzymes in this locus are specific for phosphomonoester acceptors. The disaccharide, despite lacking the amidated mannuronic acid residue, was a substrate for the predicted oligosaccharyltransferase AglB, modifying an asparagine-containing peptide.

The functional reassignment of archaeal glycosyltransferases highlights the importance of acceptor substrate analogs in enzymology. Imperiali and co-workers discovered an *N*-glycosylation pathway not yet observed in archaea. Pathways involving membrane-associated enzymes and substrates are quite difficult to characterize, and synthetic access to substrate analogs aids the process of discovery.

1.5 Mycobacterial glycosyltransferases

Tuberculosis is the leading cause of death worldwide by a single agent. Moreover, multidrug-resistant (MDR) (resistant to 2 first-line antibiotics) and extensively drug-resistant (XDR) (resistant to 4 of the 6 first-line antibiotics) strains of tuberculosis are increasingly being encountered in the clinic.[79] Despite promising new vaccine strategies, novel small molecule therapeutics are needed to fight the scourge of tuberculosis.[80,81] The cell wall of mycobacteria possesses a unique heteropolysaccharide, so the glycosyltransferases responsible for synthesizing the mycobacterial cell wall are intriguing targets for new antitubercular agents. Given the clinical importance of these cell wall polysaccharides, as well as the context of the authors' research, a detailed analysis of substrate analogs to interrogate mycobacterial glycosyltransferases follows.

1.5.1 Peptidoglycan glycosyltransferases

Mycobacterial peptidoglycan is more rigid than other bacterial PGs, as it is about 70-80% cross-linked.[18] Most of the cross-links are between the *meso*-diaminopimelic acid (*m*-DAP) (residue 3) and D-Ala (residue 4), though a small percentage of cross-links are D-Ala to D-Ala. Importantly, the majority of muramyl residues in mycobacterial PG are *N*-glycolylated (MurNGly).[82] The Lipid II monomer in mycobacterial PG biosynthesis is therefore a GlcNAc-

β(1,4)-MurNGly pentapeptide. *N*-glycolylation is a modification special to mycobacteria and related genera in the class Actinomycetales.[83] It confers lysozyme resistance, and may otherwise stabilize PG from bactericidal degradation.[84]

In *Mycobacterium tuberculosis*, two high-molecular-weight PBPs, PonA1 and PonA2, are known to assemble peptidoglycan.[85,86] A third enzyme, PonA3, is found in other mycobacterial species.[87] Cheng and co-workers synthesized a close analog of mycobacterial Lipid II, GlcNAc-β(1,4)-MurNGly(pentapeptide)-α-P-P-undecaprenol, bearing an NBD fluorophore on the lysine side chain and the slightly longer C_{55} carrier lipid instead of endogenous C_{50} decaprenol.[88] The analog was an excellent substrate for purified *M. tuberculosis* PonA1, as assayed by HPLC. Conversion could be inhibited by moenomycin. Subsequently, Cheng and co-workers utilized a chemoenzymatic approach to access *N*-glycolyl and *N*-glycinyl Lipid I and II analogs via corresponding Park's nucleotide derivatives.[89] The nucleotides were NBD-labeled as before, and converted into Lipid II using crude *M. flavus* or *M. smegmatis* membrane fractions. *N*-glycinyl Lipid II with either L-Ala-D-Glu-L-Lys(NBD)-D-Ala-D-Ala (pentapeptide) or L-Ala-D-Glu-L-Lys(NBD) (tripeptide) are substrates for *M. tuberculosis* PonA1 (>80% conversion). These analogs bind similarly to *N*-glycolyl NBD-labeled Lipid II. A significant drop in activity is observed in substrates bearing the *N*-acetyl substituent found in typical bacterial peptidoglycan.

Modification of the lipid carrier with fluorophores has yielded assays to monitor transglycosylase activity. A Lipid II analog that incorporates a dansyl fluorophore at the distal end of a C_{20} lipid carrier is consumed by TGases from *Clostridium difficile* and *E. coli*.[90] Cheng, Cheng, Wong, and co-workers then synthesized a series of Lipid II analogs for continuous monitoring of TGase activity via Förster resonance energy transfer (FRET).[91] Optimal FRET distance was determined by altering the distance between a 7-hydroxy-4-methylcoumarin quencher on the amino acid side chain and a dabsyl group donor on the distal end of the lipid

carrier. The polyisoprene lipid length determined this distance, with pentaprenyl lipid carriers outperforming farnesyl carriers. Since the coumarin derivative self-quenches, the assay required muramidase to cleave the peptidoglycan into monomers as it was formed. Nonetheless, real-time peptidoglycan polymerization by *Acinetobacter baumannii* and *C. difficile* TGases could be observed. Consequently, the authors compared the catalytic efficiency of PBP1b homologs from *A. baumannii*, *C. difficile*, *E. coli*, and *Klebsiella pneumoniae* as well as *M. tuberculosis* PonA1. The homolog from *C. difficile* was determined to be the most active of all TGases examined. These FRET probes permitted development of a high-throughput screening assay of 120,000 compounds against *E. coli* PBP1b, leading to a naphthyl derivative with micromolar K_i values. This recent example represents a promising avenue toward the discovery of novel inhibitors of mycobacterial peptidoglycan polymerization.

1.5.2 Galactan glycosyltransferases

The mycobacterial galactan is a structural glycopolymer that anchors upper layers of the cell wall to the peptidoglycan. The cell wall in mycobacteria is largely composed of the mycolyl-arabinogalactan-peptidoglycan complex (mAGP), a heterogeneous polysaccharide covalently linked to long lipids termed mycolic acids.[92] Galactan is composed of 20-40 residues of alternating β(1,5)- and β(1,6)-linked galactofuranose (Gal*f*) residues, covalently bound to the 6-OH of MurNAc residues in the peptidoglycan backbone through a Rha-α(1,3)-GlcNAc disaccharide.[93] Gal*f* is the energetically disfavored 5-membered ring form of galactose. Galactofuranose is not present in mammals, but it is found in lower eukaryotes such as nematodes, and prokaryotes.[94,95] In addition to mycobacteria, it occurs in the lipophosphoglycan of parasitic protozoans in the genus *Leishmania*, which cause leishmaniasis, a disease of various etiologies.[96] Gal*f* is also found in cell surface glycoconjugates of *Trypanosoma cruzi*, the causative agent of Chagas disease.[97,98] The absence of Gal*f* in higher eukaryotes suggests the

enzymes responsible for its biosynthesis and incorporation as potential drug targets to combat these infections.

Biosynthesis of the mycobacterial arabinogalactan takes place on a membrane-anchored decaprenyl phosphate lipid on the cytosol leaflet of the membrane.[99] A series of glycosyltransferases act upon this lipid through a series of single glycosylation events to build the arabinogalactan complex. The glycosyltransferase WecA initiates this assembly by adding an *N*-acetyl-D-glucosamine phosphate to synthesize GlcNAc-α-P-P-decaprenol, which is the acceptor substrate for the rhamnosyltransferase WbbL.[100,101] Two galactofuranosyltransferases, GlfT1 and GlfT2, assemble the galactan polymer onto the resulting lipid-linked Rha-α(1,3)-GlcNAc disaccharide (Figure 1.7). Both of these enzymes, as well as the mutase that generates UDP-Gal*f* from UDP-Gal*p*, are essential for mycobacterial viability.[102] The lipid-linked galactan is transported to the extracytosplasmic space, modified with arabinose residues and mycolic acids, and ultimately attached to the peptidoglycan. The Rha-α(1,3)-GlcNAc disaccharide anchors the arabinogalactan heteropolysaccharide to the cell wall.[103]

GlfT1 is hypothesized to add one to three Gal*f* residues to the linker disaccharide, acting as a primase to begin the process of galactan polymerization. However, its precise function has yet to be defined unequivocally. The activity of GlfT1 produces Gal*f*-β(1,5)-Galf-β(1,4)-Rha-α(1,3)-GlcNAc-α-P-P-decaprenol, the putative substrate of the second galactofuranosyltransferase GlfT2. The polymerase GlfT2 then adds 20-40 Gal*f* residues to this lipid-linked acceptor tetrasaccharide to form galactan polymers of endogenous length. Characterizing these two enzymes is difficult, though it has been facilitated by the chemical synthesis of donor sugar UDP-Gal*f*.[104-106] The relative promiscuity of GlfT2 in binding and processing both acceptor and donor analogs has facilitated more straightforward characterization of its activity. An initial demonstration of GlfT1 and GlfT2 activity was carried

out in cell envelope preparations.[107,108] Synthetic chemistry facilitated unmasking their activity through access to susbtrate analogs that probe their acceptor selectivity.

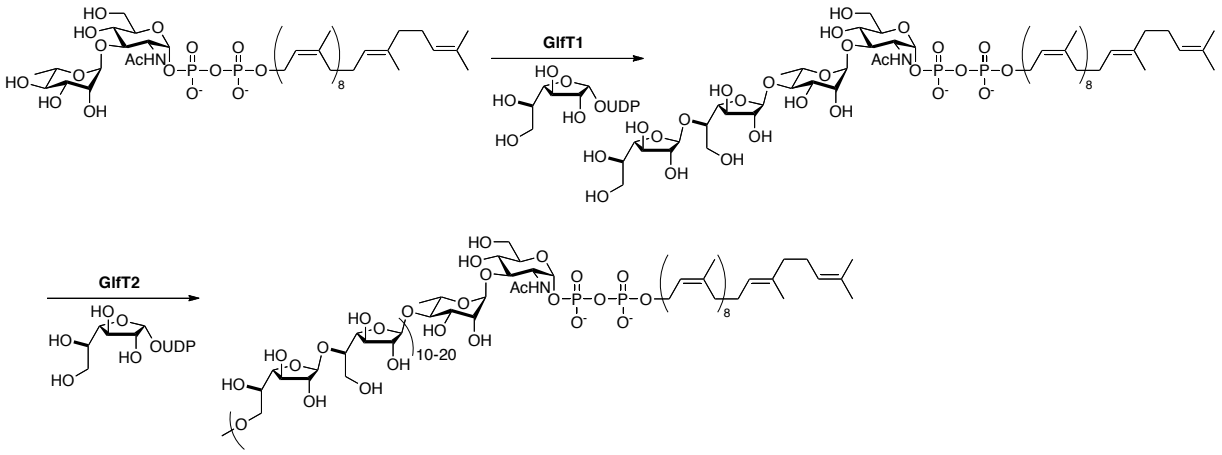

Figure 1.7. The glycosyltransferases GlfT1 and GlfT2 generate the galactan polymer. GlfT1 primes a decaprenyl-linked linker disaccharide with 2-3 Gal*f* residues, which is subsequently polymerized by GlfT2.

The galactofuranosyltransferase activity of GlfT1 has proven quite difficult to observe *in vitro*. A chemical synthesis of the endogenous mycobacterial substrate has not been reported, and the enzyme, until recently, was inactive when stripped of membrane components. As a consequence, initial experiments to demonstrate GlfT1 activity relied on acceptor substrate analogs that could be detected in a highly complex and heterogeneous environment (Figure 1.8). Besra and co-workers utilized an octyl Gal*f*-β(1,4)-Rha acceptor in a mixed enzyme assay to begin reconstituting the activity of purified *M. tuberculosis* GlfT1.[109] Incorporation of Gal*f* was monitored by thin layer chromatography, where the mutase uridine 5'diphosphate - galactopyranose mutase (UGM) included in the assay converts UDP-[^{14}C]-Gal*p* to UDP-[^{14}C]-Gal*f in situ*. A slight shift in retention is suggestive of GlfT1 activity. Subsequently, Mikušová and co-workers investigated processing of octyl Rha-α(1,3)-GlcNAc in microsomal preparations of *M. smegmatis* GlfT1 overexpressed in *E. coli*.[110] Surprisingly, GlfT1 adds one Gal*f* residue to both

octyl Rha-α(1,3)-GlcNAc and octyl Gal*f*-β(1,4)-Rha-α(1,3)-GlcNAc, as judged by incorporation of ^{14}C-labeled Gal*f*, though it presumably is capable of adding two Gal*f* residues to the disaccharide acceptor since it can process the Gal*f*-containing trisaccharide. Daniellou and Mikušová employed the same disaccharide acceptor and microsomal preparation to observe incorporation of deoxygenated donor sugars by liquid chromatography-mass spectrometry (LC-MS).[111] Both deoxygenated donor sugars appear to terminate at the +1 Gal*f* product, suggesting chain termination.

Defined conditions to unambiguously assign GlfT1 activity were lacking, primarily since suitable substrates for the enzyme were not available. Experiments with the endogenous substrate were untenable, given the instability of the allylic pyrophosphoryl-linked disaccharide. Kiessling and co-workers targeted synthetic GlfT1 acceptor substrate analogs while developing a stabilizing modification for the pyrophosphoryl group.[112] Phosphonophosphate acceptors bearing the Rha-α(1,3)-GlcNAc disaccharide were synthesized, and incubated with purified *M. smegmatis* GlfT1 expressed in *M. smegmatis*. GlfT1 was shown to process the phosphonophosphate analogs to +2 or +3 Gal*f* products. This represents the first time that GlfT1 activity has been observed in a defined system. The results implicate GlfT1 in the synthesis of the putative GlfT2 acceptor substrate, Gal*f*-β(1,5)-Galf-β(1,4)-Rha-α(1,3)-GlcNAc-α-P-P-decaprenol. Moreover, production of the +3 Gal*f* product implies that GlfT1 is a trifunctional enzyme, capable of forming the three glycosidic linkages observed in endogenous galactan. To probe the role of the lipid carrier in GlfT1 catalysis, derivatives with two lipid carriers were prepared and incubated with GlfT1. A luminescence-based assay coupling production of UDP to the luciferase/luciferin reaction was used to quantify the relative activity of the acceptor analogs. A (2Z,6Z)-farnesyl-linked acceptor is processed more efficiently than a neryl-linked acceptor, suggesting an important role for the lipid carrier in binding to GlfT1. While phosphonophosphates have been used as pyrophosphate analogs in other systems, this was the

first demonstration of their use as active glycosyltransferase acceptor substrates. Thus, the stabilization strategy may be generally applicable to studying other glycosyltransferases that process lipid-linked pyrophosphoryl glycans.

While GlfT1 appears to require complex acceptors in defined *in vitro* assays, GlfT2 is more permissive to substrate analogs. The first series of acceptor analogs described for GlfT2 were alkyl or alkenyl Gal*f*-containing disaccharides, intended to mimic the non-reducing end of the glycan. Besra and co-workers synthesized decenyl and octyl Gal*f*-β(1,5)-Gal*f* and Gal*f*-β(1,6)-Gal*f* acceptors that, when monitored by thin layer chromatography, yielded incorporation of one or two additional Gal*f* residues by membrane preparations expressing GlfT2.[113,114] Acceptors blocked at the 2-OH and 3-OH by methyl ethers appeared to serve as substrates, albeit not as efficiently.[114] Similar results were observed with GlfT2 purified from *E. coli* expressing protein folding chaperones.[109] A more comprehensive *in vitro* study was carried out by Palcic, Lowary, and co-workers.[115] Octyl Gal*f*-β(1,5)-Gal*f*-β(1,6)-Gal*f* and Gal*f*-β(1,6)-Gal*f*-β(1,5)-Gal*f* trisaccharides, in addition to arabinose-containing disaccharides and a rhamnolipid, were compared to the octyl disaccharides described above. Surprisingly, an octyl Ara*f*-β(1,6)-Gal*f* acceptor served as a substrate despite lacking the CH_2OH side chain. The related Ara*f*-β(1,5)-Gal*f* was not a substrate, since the alternating nature of GlfT2 Gal*f* addition precludes reaction at the 5-OH. Trisaccharides were the best substrates in the series, with octyl Gal*f*-β(1,5)-Gal*f*-β(1,6)-Gal*f* yielding the largest k_{cat} value. Analysis of the trisaccharide reaction mixtures by MALDI-TOF mass spectrometry showed that GlfT2 could form heptasaccharide products. However, the majority of the reaction mixture still consisted of starting material or +1/+2 Gal*f* product. While the aforementioned studies were important in deriving important acceptor features for GlfT2 catalysis, the acceptors did not yield Gal*f* polymers of endogenous length.

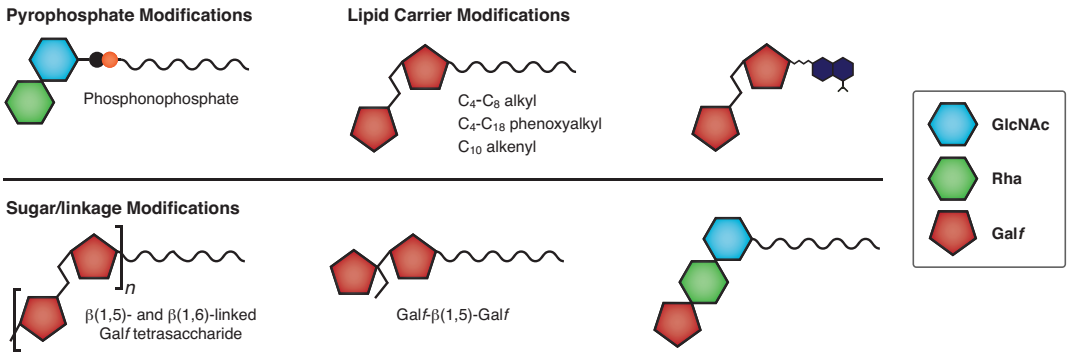

Figure 1.8. Acceptor substrate modifications to interrogate galactan assembly by cell wall galactofuranosyltransferases GlfT1 and GlfT2.

Galactan polymerization occurs through a template-independent mechanism. However, it was not known how polymer length is controlled. To study the mechanism of GlfT2 polymerization, Kiessling and co-workers synthesized a series of phenoxyalkenyl β(1,6)-linked Gal*f* disaccharides.[116] They discovered that GlfT2 builds galactan through a processive mechanism, in which an acceptor substrate remains bound to the enzyme throughout the process of polymer formation. As acceptor length grows, the polymers dissociate and yield a distribution of galactan polymers. In addition, the authors observed that acceptors with a longer lipid carrier yielded much longer Gal*f* polymers. For example, a 12-phenoxydodec-2-enyl disaccharide is processed to a polymer containing up to 27 additional Gal*f* residues, whereas a 19-phenoxy-nondec-2-enyl disaccharide is processed to a 48-mer. They hypothesize that the lipid carrier serves to tether the acceptor at a distal site, leading to additional binding interactions that discourage dissociation and termination of polymer synthesis at short galactan lengths. Kiessling and co-workers synthesized 'light' and 'heavy' acceptors to monitor processivity by single-point Gal*f* incorporation into mass-resolved acceptors.[117] 'Heavy' acceptors were perdeuterated at the phenoxy group in 12-phenoxydodec-2-enyl Gal*f*-β(1,6)-Gal*f*.[118] Incorporation of Gal*f* into heavy acceptors was reduced when enzyme was first incubated with light acceptors, indicative of a processive polymerization process.

GlfT2 exhibits a kinetic lag phase when polymerizing Gal*f* disaccharides. While there is a difference in the steady-state rate of polymerization with disaccharides bearing either β(1,5) or β(1,6) linkages, polymer distribution with either acceptor does not change dramatically. As the endogenous substrate for GlfT2 is a tetrasaccharide, Kiessling and co-workers synthesized a 12-phenoxy-dodec-2-enyl Gal*f* tetrasaccharide bearing the endogenous alternating β(1,5) or β(1,6) linkages. [117] The kinetic lag phase is abolished with this acceptor, indicating that GlfT2 catalytic efficiency improves with longer oligosaccharides, which perhaps bind to enzymatic subsites. However, despite increased initial catalytic efficiency with a tetrasaccharide acceptor, both acceptors are processed to the same polymer length. Thus, GlfT2 control over galactan length is intrinsic to the enzyme. To investigate which residues mediate catalysis, and determine the number of active sites responsible for polymerization, Kiessling and co-workers mutated DXD (or DDX) motifs conserved in glycosyltransferases.[119] Mutations in key DDD and DDA residues, predicted to form the active site via homology modeling, lead to reduced catalytic activity and disrupted polymer formation. These results suggest that GlfT2 mediates bifunctional, regioselective catalysis to generate the galactan polymer using a single active site. These mutagenesis experiments were corroborated when Lowary, Ng, and co-workers solved a crystal structure of GlfT2 bound to UDP.[120] The structure suggests that the galactan chain is synthesized in a cavity created by GlfT2 tetramers, but it's unclear whether the crystal structure represents the active form of the enzyme.

Saturation transfer difference nuclear magnetic resonance (STD-NMR) spectroscopy can provide information about substrate–protein interactions. This technique has been used to determine that mutated GlfT2 variants bind a dec-2-enyl Gal*f*-β(1,6)-Gal*f* acceptor similar to wild-type GlfT2, as well as confirm that the lipid carrier in octyl Gal*f*-β(1,5)-Gal*f*-β(1,6)-Gal*f* contributes significantly to the binding of acceptors to the enzyme.[119,121] The enzyme exhibits

flexibility in binding the acceptor carbohydrate region, as it must be catalytically competent with both extended β(1,6)-terminated and more compact β(1,5)-terminated acceptors.

The regioselective activity of galactan glycosyltransferases has been challenged with a number of donor analogs. While these experiments fall outside of the scope of the current review, synthetic acceptors for GlfT1 and GlfT2 permitted the interrogation of their donor selectivity. For example, octyl Gal*f*-β(1,5)-Gal*f*-β(1,6)-Gal*f* serves as the GlfT2 substrate in assays employed by Lowary and co-workers to incorporate donor analogs.[122,123] Kiessling and co-workers utilized 5- and 6-fluoro-UDP-Gal*f* donors as chain terminators of GlfT2 polymerization of a 12-phenoxy-dodec-2-enyl Gal*f* hexasaaccharide bearing the endogenous alternating β(1,5) or β(1,6) linkages.[124] Polymer formation was truncated when GlfT2 encountered a fluorine substituent at the position where the following linkage is to be formed. These experiments underscore the faithful regioselectivity of GlfT2 catalysis.

Inhibition of galactan formation has potential as an antimycobacterial treatment, given the role of galactan glycosyltransferases in building an essential glycopolymer. This goal has unfortunately proved elusive to date.[125,126] The inherent flexibility in the active sites of GlfT1 and GlfT2 has made it difficult to develop potent inhibitors of their activity. Nonetheless, the previous lack of substrates has been addressed, and recently developed assays to observe the activity of these enzymes may facilitate the search for inhibitors. Successful strategies targeting the mutase UGM rely on non-carbohydrate ligands to block the enzyme's active site.[127-129] This active area of research may yield potent antimycobacterial agents whose mode of action is inhibition of UDP-Gal*f* biosynthesis, which results in incomplete cell wall assembly.

1.5.3 Arabinan glycosyltransferases

The arabinan serves as an anchor for the outer membrane mycolic acids. It is a branched glycopolymer composed of α(1,5), α(1,4), and β(1,2) linked arabinofuranose (Ara*f*) residues. Three polymers of 31 Ara*f* residues make up the arabinan, each bound to the 5-hydroxyl group of the 8th, 10th, and 12th residue of galactan.[92,130] Each arabinan polymer is built exclusively from the donor sugar Ara*f*-β-P-decaprenol (DPA) by a series of membrane-associated arabinofuranosyltransferases (AraTs).[131] Many enzymes involved in arabinan synthesis have been identified, but not fully characterized. AftA adds the first three Ara*f* residues to galactan, priming arabinan biosynthesis.[132] Next, a linear series of 13 α(1,5)-linked Ara*f* may be added by EmbA/EmbB, subsequently modified by AftC or AftD to generate the first α(1,3) branch point.[133,134] A short series of 3 α(1,5)-linked Ara*f* residues is attached, followed by the final α(1,3) branch point. EmbA/EmbB work in concert with AftB, a terminal β(1,2) AraT, to generate the terminal Ara_6 motif (Figure 1.9).[135-137] Ultimately, this motif serves as the site of attachment for the mycolic acids, targeted by first-line antibiotics isoniazid and ethionamide.[138-143]

AraTs are the target of first-line antibiotic ethambutol as well as the novel benzothiazinone class of inhibitors.[144-146] A number of research programs are in place to interrogate arabinan biosynthesis. Studying AraTs is challenging given that they are not active outside of their native membrane environment and their endogenous substrate is, at a minimum, a lipid pyrophosphate-linked galactan (for AftA) or oligomers of Ara*f* linked to that core. Consequently, a series of truncated synthetic acceptors have been instrumental in assigning AraT activity to the enzymes involved in this pathway.

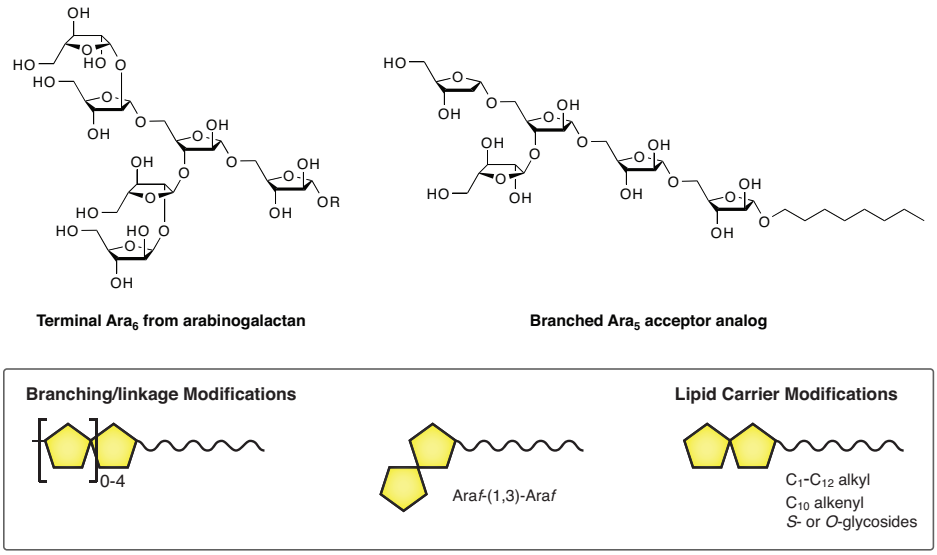

Figure 1.9. A terminal arabinan oligosaccharide motif and an acceptor substrate analog.

To observe arabinofuranosyltransferase activity, Besra and co-workers developed an assay monitoring transfer of radioactivity from [1-^{14}C]Ara*f*-β-P-decaprenol (DPA) to synthetic arabinose acceptors in *M. smegmatis* mc^{2}155 membrane extracts.[147] A series of α- and β-linked all (1,5) mono-, di-, and trisaccharide glycosides bearing O- or S-linked alkyl lipid carriers were investigated. No transfer was observed to Ara*f* monosaccharides, but there were otherwise three clear conclusions: tri-Ara*f* acceptors were markedly better than the corresponding disaccharides, α-linkages at the lipid carrier were preferred to β-linkages, and the optimal lipid carrier length was C_6 to C_8. A C_{10}-linked alkenyl acceptor had slightly reduced activity, whereas a C_{12}-linked alkyl acceptor showed a dramatic decrease in ^{14}C-Ara*f* transfer due to micelle formation. Both β(1,2)- and α(1,5)-Ara*f* arabinofuranosyltransferase activity was observed, though it is important to note that transfer of only one Ara*f* residue occurred. The complexity and length of natural arabinan would suggest that these simplified acceptors were not idea substrates for the arabinofuranosyltransferases in the membrane preparation. Nonetheless, these acceptors have been useful in defining the arabinan biosynthetic pathway in *M. smegmatis*. Later, the alkenyl

C_{10}-linked Ara*f*-α(1,5)Ara*f* acceptor was useful in determining that the *emb* gene product in *Corynebacterium glutamicum* catalyzes transfer of Ara*f* from DPA.[132] Lastly, the C_8-linked Ara*f*-α(1,5)Ara*f* acceptor was processed by *C. glutamicum* membranes overexpressing *M. tuberculosis* AftB, and linkage analysis of the +1 Ara*f* product confirmed that AftB is a terminal β(1,2)-arabinofuranosyltransferase.[137] These simple substrate analogs have clearly been helpful in establishing AraT assays.

More complex arabinofuranoside substrates yield different results with membrane extracts. Besra and co-workers synthesized larger methyl arabinofuranoside acceptors to further study AraT activity in *M. smegmatis* membranes.[148] Surprisingly, an all-α(1,5)-linked methyl Ara*f* trisaccharide outperformed the branched methyl Ara*f*-α(1,3)-[Ara*f*-α(1,5)]-Ara*f*-α(1,5)-Ara*f* tetrasaccharide. An α(1,3)-linked disaccharide is processed better than an α(1,5)-linked disaccharide, yet radioactivity incorporation on the best acceptor is only about 21%. An octyl Ara*f*-α(1,5)-Gal*f* acceptor, analogous to the disaccharide motif found in the arabinan–galactan linkage region, incorporates a single Ara*f* residue by autoradiography.[149] Thus, additional Ara*f* residues, a Gal*f* linkage, or branching complexity do not necessarily create a better acceptor. AraTs may bind preferably to di-Ara*f* or tri-Ara*f* motifs at the non-reducing end of the acceptor, suggesting a mechanism for arabinoside recognition.

The activity of EmbA and EmbB has proved difficult to decouple. Chatterjee and co-workers synthesized a linear Ara_5 acceptor, octyl Ara*f*-β(1,2)-Ara*f*-α(1,5)-Ara*f*-α(1,5)-Ara*f*-α(1,5)-Ara*f*, and investigated its processing by *M. smegmatis* mc^2155 membranes deficient in either *embA* or *embB*.[150] The assay relied on incorporation of ^{14}C-Ara*f* through DPA synthesized *in situ* from 5-phospho-^{14}C-ribose pyrophosphate (pRpp). The pentasaccharide was processed to a +2 Ara*f* product in the presence of wild-type *M. smegmatis* membranes, but membranes deficient in either *embA* or *embB* did not catalyze Ara*f* transfer. Mixing of single enzyme

membrane preparations (i.e. mixing EmbA and EmbB) restored activity. While it is difficult to arrive at a definitive conclusion, these results suggest that EmbA and EmbB cooperate to synthesize the arabinan and are functionally inactive when exposed to an Ara*f* acceptor in isolation.

Besra and co-workers employed an aminooctyl Ara*f*-α(1,5)-Ara*f*-α(1,5)-Ara*f*-α(1,5)-Ara*f*-α(1,5)-Ara*f* acceptor to determine the α(1,3)-arabinofuranosyltransferase activity of *M. smegmatis* membranes overexpressing *M. tuberculosis* Rv2673, annotated as AftC.[133] A branched Ara*f* pentasaccharide acceptor, octyl Ara*f*-α(1,5)-[Ara*f*-α(1,3)]-Ara*f*-α(1,5)-Ara*f*-α(1,5)-Ara*f* (Figure 1.9) produced an α(1,5)-linked +1 Ara*f* product in Rv2673 membrane extracts.[151] Addition of the Ara*f* residue took place at either terminus from the branch point. Interestingly, a series of additional arabinan fragments was produced, ranging from Ara_7 to Ara_{10}, as minor products. This branched acceptor, along with all α(1,5)-linked pentenyl Ara_3 and Ara_4, and an all α(1,5)-linked linear Ara_5 helped Jackson and co-workers determine that *M. smegmatis* membranes overexpressing *M. tuberculosis* Rv0236c catalyze α(1,3)-arabinofuranosyltransferase activity.[134] The enzyme has some preference for the linear Ara_5 acceptor, with lower incorporation of radioactivity in the Ara_3 and Ara_4 oligosaccharides. The gene, annotated as AftD, is essential and likely mediates the biosynthesis of important α(1,3) branches in the synthesis of both arabinogalactan and lipoarabinomannan in *M. tuberculosis*.

Synthetic lipid-linked acceptors have been essential in deciphering the arabinan biosynthetic pathway. The transmembrane nature of these enzymes has resulted in the use of complex membrane preparations for all assays determining their activity. Analysis has thus relied on incorporation of radioactivity, mass spectrometry and derivatization of the synthetic acceptors. Their solubility in organic solvents has permitted the isolation and characterization of

modified acceptor analogs, procedures that are quite challenging with natural acceptor substrates.

1.6 Acceptors to survey various bacterial glycosyltransferases

A number of active research programs study bacterial enzymes that glycosylate lipid-linked glycans. In lieu of an exhaustive overview of the field outside of the scope of this review, a few notable examples follow. A glycosyltransferase in *Mycoplasma pneumonia* extracts can add up to three galactopyranose residues to glucosylated or galactosylated diacylglycerol or ceramide.[152] The acceptor specificity of glycosyltransferases involved in *E. coli O*-antigen biosynthesis has been interrogated with phenoxyalkyl- and alkyl-linked GlcNAc-α-P-P analogs.[153-157] In addition, there is a wealth of data on additional glycosyltransferases that modify lipids or their phosphates.[158] Many of these experiments are summarized in a publication by Rush and co-workers.[159]

Similarly, a number of fundamental discoveries in the glycosylation of hydrophobic aglycones have been published in the past several years. Hung-wen Liu and workers, as well as contributions by Eguchi, Kakinuma, and Thorson yielded information about general macrolide glycosyltransferases with permissive substrate requirements.[160-164] Walsh led the study of polyketide and antibiotic glycosyltransferases, particularly those incorporating rare sugars such as novobiose and deoxyfucose.[165-167] Finally, Thorson has spearheaded the development of glycorandomization, the use of reversible glycosyltransferases to prepare a diverse library of glycosylated compounds.[168,169] The latter strategy holds promise for the development of novel glycosylated pharmaceuticals.

1.7 Conclusion

Synthetic chemistry has facilitated profound, fundamental discoveries about glycosyltransferases involved in bacterial glycan biosynthesis. From *in vitro* confirmation of proposed *in vivo* activity, to complete reassignment of biosynthetic pathways, the use of lipid-linked glycan analogs as substrates, probes, and inhibitors of these enzymes highlights the advances to our understanding of essential processes provided by chemical glycobiology. Efforts to exploit chemistry for the interrogation, and interception, of bacterial glycan biosynthesis will continue to advance our knowledge about bacterial cell wall assembly and the role of cell surface glycoconjugates in evading and co-opting the eukaryotic immune system.

Chapter 2: Synthesis of Phosphonophosphates Acceptor Substrates for Mycobacterial Glycosyltransferases

Portions of this work have been published in:

Martinez Farias, M. A.; Kincaid, V. A.; Annamalai, V. R.; Kiessling, L. L. Isoprenoid Phosphonophosphates as Glycosyltransferase Acceptor Substrates. *J. Am. Chem. Soc.* DOI: 10.1021/ja500622v.

Contributions:

Cloning and expression of GlfT1 performed by V.A. Kincaid.

Synthesis of compound **2.04** performed by V.R. Annamalai.

2.1 Abstract

Glycosyltransferases that act on polyprenol pyrophosphate substrates are challenging to study because their lipid-linked substrates are difficult to isolate from natural sources and arduous to synthesize. In the course of studying galactan glycosyltransferases, we required access to a lipid-linked pyrophosphate. The substrate is modified with 20–40 galactofuranose residues to form the mycobacterial galactan glycopolymer. Simplified glycolipids that serve as acceptors for the downstream polymerase GlfT2 are not adequate for the upstream glycosyltransferase GlfT1, which primes galactan assembly. To facilitate access to an appropriate glycosyl acceptor, we assembled phosphonophosphate analogs to serve as pyrophosphate surrogates in glycosyltransferase reactions.

2.2 Introduction

Over a million people die every year from tuberculosis (TB).[170] This infectious disease ravages the developing world, infecting over eight million people every year. TB is caused by the bacterium *Mycobacterium tuberculosis*, which spreads through aerosolization of intact bacteria in the sputum of infected individuals. The bacteria settle in the human lung, which can lead to severe and chronic pulmonary infections. In fact, only 1–3 bacteria in aerosol are needed to infect a human.[171-173] Such a low number avoids triggering a massive immune response to combat the invasion. Active infection occurs in 5–10% of infected hosts, leading to facile transmission since the majority of those infected are asymptomatic. Genetics studies have suggested that mycobacterial DNA has been present in humans for 70,000 years.[174] Tuberculosis migrated out of Africa with humans in the Neolithic period, reflecting an organism that has evolved with humans since the earliest form of our species as we know it today.

The *M. bovis*—bacillus Calmette-Guérin (BCG) vaccine, which has been administered to 3.5 billion people around the globe, has stemmed the spread of TB. BCG does not prevent pulmonary infection in adults, however, and immunization in developing countries is a major epidemiological challenge.[175] Moreover, current treatment regimes, such as the six first-line antibiotics used in the clinic, are fading in effectiveness.[176] Multidrug-resistant (MDR) and extensively drug-resistant (XDR) strains of tuberculosis are on the rise.[79] The burden of TB infection is especially damaging in immunocompromised individuals that are infected with human immunodeficiency virus (HIV) or have diabetes.[177]

Tuberculosis bacilli use a number of mechanisms to subvert the human immune system. Five different Type IV secretion systems (T4SS) are involved in transporting virulence factors across the impermeable envelope.[175] While sophisticated mechanisms in the envelope export factors important for survival and pathogenesis, this envelope also helps to protect mycobacteria from the host. Difficulties in treating *M. tuberculosis* infection include the existence of a latent

stage, in which the bacteria can evade the host immune system, the formation of dense granulomas consisting of bacilli surrounded by host immune cells, as well as the impermeability of the mycobacterial cell wall.[80,178]

The cell wall is a complex, highly heterogeneous layer that provides stiffness and remarkable protection to mycobacteria. Sections in Chapter 1 provided a detailed description of each major component of the cell wall, which will be briefly summarized here (Figure 2.1). The layer most proximal to the cell membrane is the peptidoglycan (PG), a highly cross-linked (70–80%) matrix that allows the bacteria to withstand osmotic pressure and provides the characteristic shape and rigidity.[18] PG is composed of β(1,4)-linked *N*-acetyl-D-glucosamine (GlcNAc) and *N*-glycolylmuramic acid (MurNGly) residues.[82] The MurNGly residues are modified with the pentapeptide L-Ala-γ-D-Glu-*m*-DAP-D-Ala-D-Ala, where *m*-DAP is *meso*-diaminopimelic acid. Most cross-links occur between residues 3 and 4 (*m*-DAP and D-Ala). The galactan, a polymer composed of 20–40 residues of alternating β(1,5)- and β(1,6)-linked galactofuranose (Gal*f*) residues, is covalently bound to the 6-hydroxyl group of MurNAc residues in the peptidoglycan backbone through a Rha-α(1,3)-GlcNAc linker disaccharide.[93] Three arabinan motifs, consisting of 31 branched arabinofuranose residues, are in turn bound to the 5-hydroxyl group of the 8th, 10th, and 12th residue of galactan.[92,130] Terminal arabinan residues are decorated with long fatty acids termed mycolic acids.[138] Termed the mycolyl-arabinogalactan-peptidoglycan (mAGP) complex, this lipid-linked heteropolysaccharide acts as the major protective barrier in mycobacteria.

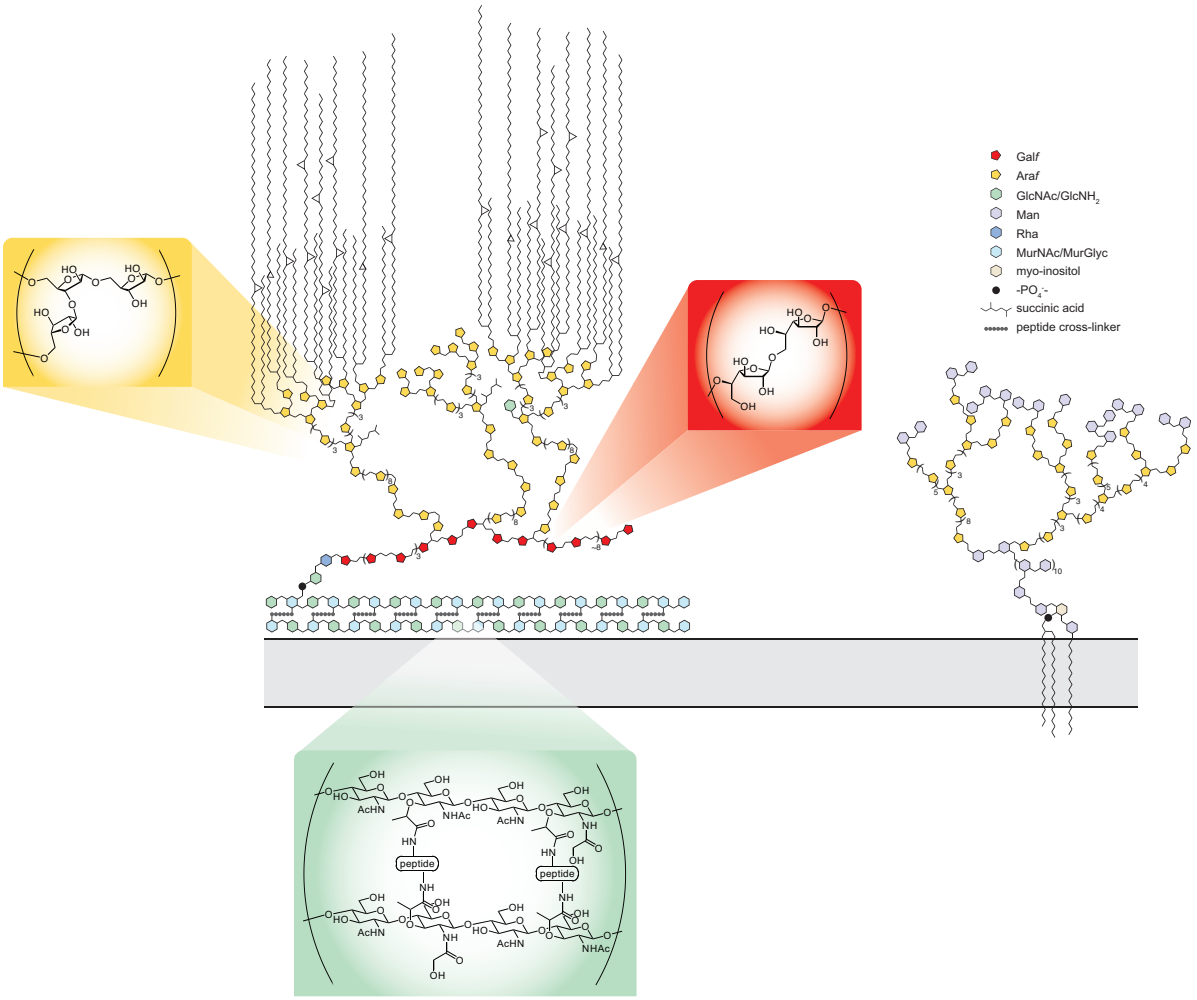

Figure 2.1. Substructure of the mycobacterial cell wall. An additional cell envelope component, lipoarabinomannan, is shown on the right. The outer membrane is omitted for clarity.

Porins, such as the T4SS described above, as well as other lipids, lipid-linked glycans, and accessory proteins are embedded in the cell wall. It is difficult to ascertain the precise presentation of the cell wall, but it is known that the outer cell wall components partition into a bilayer-like structure that essentially provides an additional cell membrane.[179] Approximations of inner cell wall structure have been aided by the solved 3-dimensional structure of soluble peptidoglycan fragments. Peptidoglycan is arranged into a helical structure with periodicity of 6 residues, extending perpendicularly from the membrane.[180] The helical structure forms cavities

that are permissive to embedded accessory motifs throughout the vertical length of the peptidoglycan.

The cell wall is a validated drug target for antitubercular therapy. Two of the four first-line drugs used to combat tuberculosis impinge upon cell wall biosynthesis. Ethambutol targets the arabinofuranosyltransferases responsible for building the arabinan domain.[144,145] Isoniazid inhibits mycolic acid biosynthesis by targeting an enoyl-acyl carrier protein reductase in the fatty acid pathway.[139,140,143] The second-line drug ethionamide also targets this reductase.[141,142] However, at least 4% of new TB infections and 20% of previously treated infections are resistant to isoniazid.[170] New targets in the cell wall are needed to thwart the rising tide of drug-resistant strains of TB.

2.3 Biosynthesis of the mycobacterial galactan

The galactan, a critical component of the mycobacterial cell wall, is composed of galactofuranose (Gal*f*), the energetically disfavored 5-membered ring isomer of galactose.[103,181] Gal*f* has not been identified in any mammalian glycans, rendering the enzymes that mediate Gal*f* incorporation potential antimycobacterial targets.[116,128] However, the mechanism by which these enzymes function, and indeed many aspects about arabinogalactan biosynthesis, are not known (Figure 2.2). The Kiessling laboratory has established a research program to interrogate cell wall biosynthesis through chemical biology. Our laboratory has established a novel mechanism for the enzyme uridine 5'-diphosphate (UDP) galactopyranose mutase (UGM), which provides the donor sugar uridine 5'-diphosphogalactofuranose (UDP-Gal*f*) required for galactan biosynthesis.[182-185] We have also developed UGM probes and inhibitors with low micromolar activity.[127,128,186,187] To further understand galactofuranose incorporation in mycobacteria, we have studied the two galactofuranosyltransferases in the biosynthetic pathway.

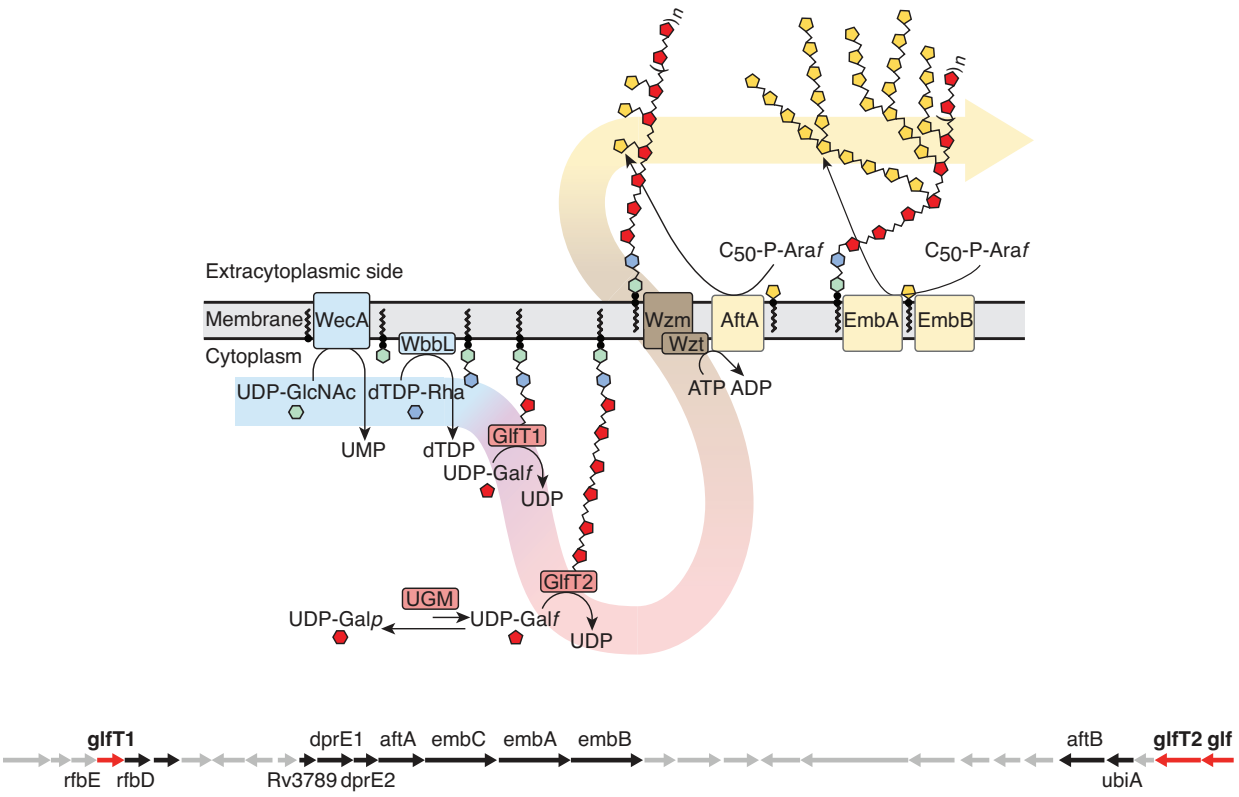

Figure 2.2. Galactan biosynthesis. Top: Biosynthetic pathway toward arabinogalactan. Bottom: Genes encoding the enzymes that build arabinogalactan. Galactan biosynthetic enzymes are highlighted in red.

2.3.1 GlfT1 and GlfT2 mediate galactan assembly

Genes encoding both cell wall galactofuranosyltransferases are essential for mycobacterial viability.[102] The *Mycobacterium tuberculosis* gene Rv3782 encodes a protein termed GlfT1. GlfT1 appears to be a galactofuranosyltransferase that primes galactan assembly. Its assigned role is to promote the elongation of decaprenyl-linked L-Rha-α-(1,3)-D-GlcNAc pyrophosphate **2.01** by one to three Gal*f* residues (Figure 2.3).[108] The resulting lipid-linked oligosaccharide is a substrate for the related galactofuranosyltransferase GlfT2, encoded by the gene Rv3808c.[116] GlfT2 assembles the bulk of the galactan, adding 20–40 Gal*f* residues to form the full-length polymer. Surprisingly, GlfT2 can process synthetic substrates bearing even a single galactofuranose residue, despite the tetrasaccharide structure of its endogenous

acceptor.[118] In principle, therefore, GlfT1 needs only to catalyze the addition of one Gal*f* residue to its substrate **2.01** (Figure 2.3). Still, experiments with membrane extracts or cell lysates suggested that GlfT1 could catalyze the addition of multiple Gal*f* residues.[108,110,111] We sought to assess the enzyme under chemically defined conditions, which required obtaining active GlfT1 and a suitable acceptor.

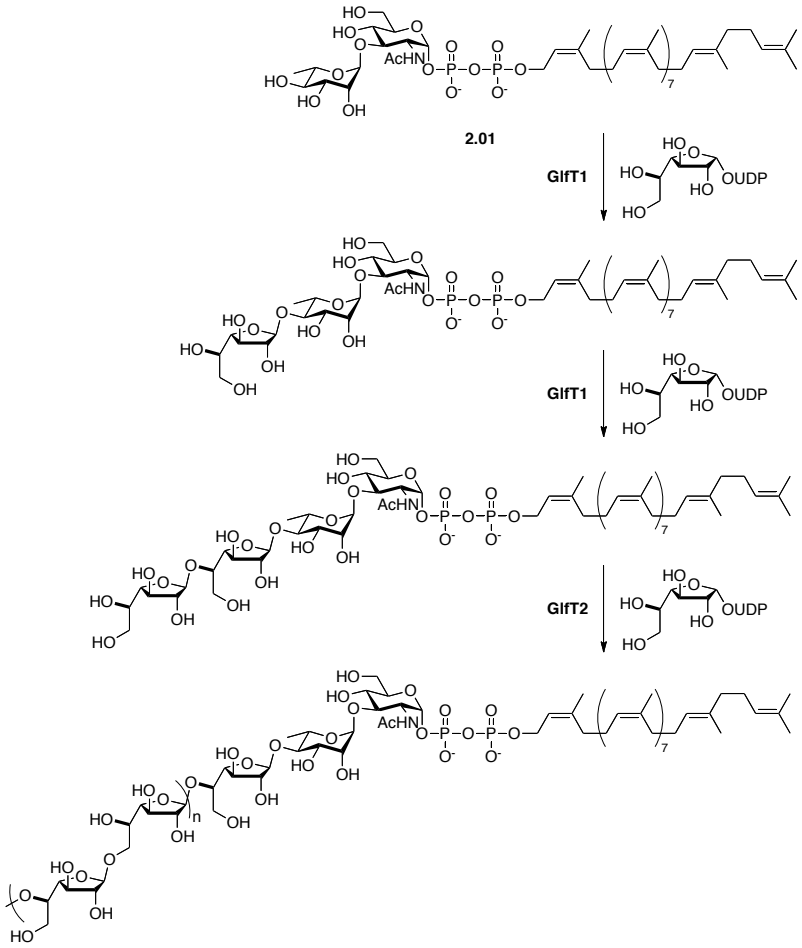

Figure 2.3. GlfT1 and GlfT2 mediate galactan biosynthesis.

2.3.2 Glycolipids bearing the linkage disaccharide

The predicted GlfT1 acceptor **2.01** is a demanding synthetic target; therefore, we considered which of its features would be required for function. As described in Chapter 1,

glycolipid acceptor substrate analogs are well tolerated by GlfT2. In analogy to these substrates, we designed a series of glycolipids that would mimic the non-reducing end of the endogenous GlfT1 acceptor (Figure 2.4). Rhamnolipids **2.02** and **2.03** as well as 12-phenoxydodec-2-enyl L-Rha-α-(1,3)-D-GlcNAc **2.04** were prepared.

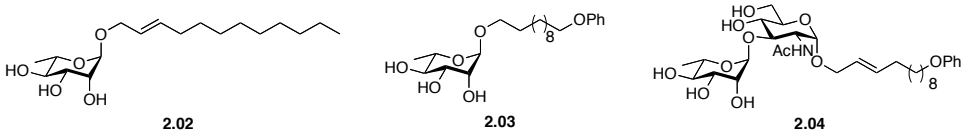

Figure 2.4. Glycolipid acceptor substrate analogs for GlfT1.

The synthetic approach toward rhamnolipid **2.02** was straightforward (Scheme 2.1). Protection of L-rhamnose with acetates afforded **2.05**, which was glycosylated with allyl alcohol using boron trifluoride-diethyl etherate to afford allyl glycoside **2.06**.[188,189] The presence of a participating group at the 2-position strongly favored formation of the α-glycoside. Cross-metathesis with 1-nonene using Grubbs I (bis[tricyclohexylphosphine]benzylidine ruthenium(IV) dichloride) catalyst yielded acetate-protected rhamnolipid **2.07**. Finally, deprotection under Zemplén conditions afforded the rhamnolipid **2.02**. We next tested the ability of the glycolipids to serve as GlfT1 substrates.

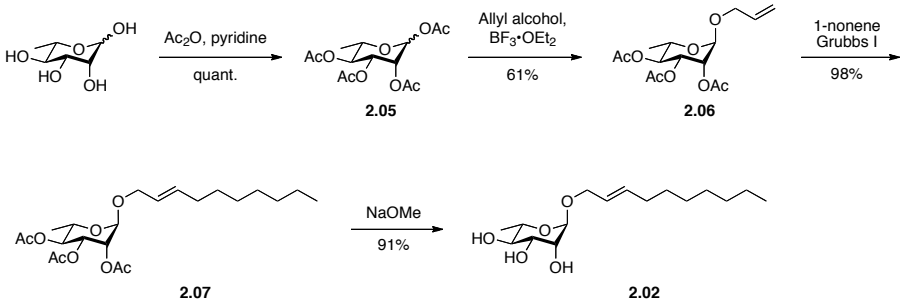

Scheme 2.1. Synthesis of rhamnolipid acceptor **2.02**.

Preparation of active, purified GlfT1 was challenging, as its activity is typically depleted when removed from its endogenous milieu. Ultimately, production of recombinant His_6-tagged *M. smegmatis* GlfT1 in *M. smegmatis* mc^2155 was successful, and the enzyme was isolated by affinity chromatography. Unfortunately, we did not observe the production of oligosaccharide products upon exposure of glycolipids **2.02**, **2.03**, and **2.04** to GlfT1 in the presence of donor sugar UDP-Gal*f* (Figure 2.5). We hypothesized that the absence of a pyrophosphate linkage yielded compounds that were poor GlfT1 substrates. Indeed, Brockhausen and co-workers have suggested that this functionality is required in substrates of enzymes that build short oligosaccharides on lipid-linked pyrophosphates.[157] Downstream polymerases, such as GlfT2, are more permissive at sites distal to their catalysis but require specific residues at the non-reducing end for catalysis. Thus, we shifted our strategy to target substrates that more closely match the endogenous acceptor.

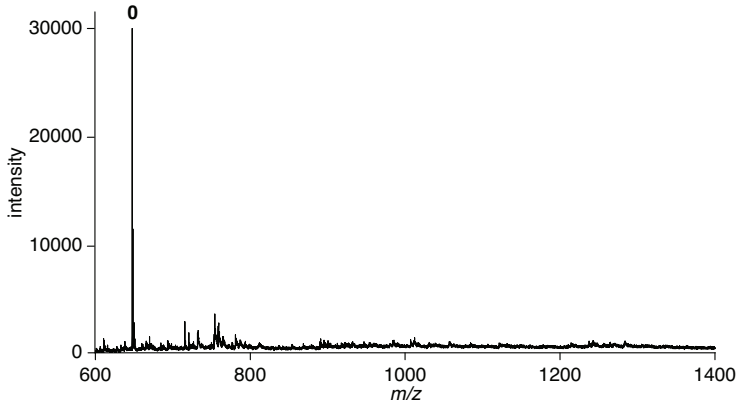

Figure 2.5. Acceptor **2.04** is not a substrate for GlfT1 in the presence of donor sugar UDP-Gal*f*.

2.4 Phosphonophosphates as glycosyltransferase acceptor substrates

Progress in understanding glycosyltransferases that modify lipid-linked oligosaccharide pyrophosphates is hindered by difficulty of isolating these biosynthetic acceptors from natural sources and the challenge of their chemical synthesis.[13,190,191] Although some acceptors have been

generated through astutely orchestrated synthetic steps,[28,37,88,192,193] the lability of the allylic pyrophosphoryl group narrows the range of transformations that can be applied to their synthesis. Our prior results with the glycolipid substrates and an analysis of literature suggested that the pyrophosphate group would be important.[26,155,157] Attempts to synthesize pyrophosphate-containing substrates analogous to **2.01** were complicated by the lability of the allylic pyrophosphate. We envisioned addressing these barriers by synthesizing an acceptor **2.08** in which the pyrophosphoryl group was replaced with a phosphonophosphate group (Figure 2.6). This stabilizing modification should mimic key features of the acceptor, while increasing the stability of intermediates en route to the target glycosyl acceptors.

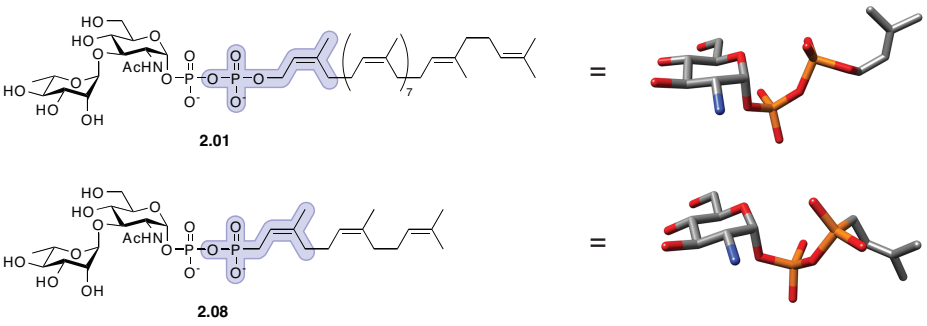

Figure 2.6. Replacement of the allylic phosphate (blue) and decaprenyl lipid tail in putative glycosyltransferase acceptor substrate **2.01** to a phosphonate (blue) and (2Z,6Z)-farnesyl lipid in surrogate **2.08**.

Phosphonophosphates are often used as pyrophosphate analogs, and their increased stability suggested that they could be more readily synthesized.[194] Some examples are highlighted in Figure 2.7. Rammler and co-workers synthesized a series of uridine phosphonophosphates such as **2.09** to mimic UDP.[195-197] Corey and Volante discovered that the phosphonophosphate functionality in geranyl derivative **2.10** could inhibit the activity of prenyltransferases.[198] Distefano and co-workers harnessed the stability of this functional group to generate photoactive farnesyl phosphonophosphate **2.11** to cross-link these enzymes.[199] In the

latter case, the parent pyrophosphate was far too labile for photoaffinity labeling. Finally, Vincent, Sinaÿ, and co-workers produced a phosphono analog of UDP-Gal*f*, **2.12**, to inhibit UGM.[200] While this analog is a modest inhibitor of UGM, the pyranose analog is slightly better.[201] However, contrary to the established literature, we sought to prepare an active glycosyltransferase substrate, as opposed to an inhibitor. We targeted surrogate **2.08** with the goal of ascertaining whether this compound could function as a GlfT1 acceptor.

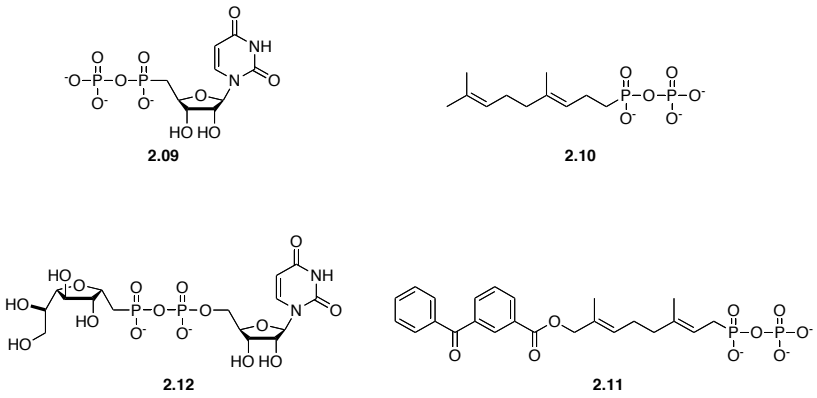

Figure 2.7. Phosphonophosphate analogs in the chemical literature.

In selecting compound **2.08**, we recognized the potential risk of generating a phosphonophosphate that is not isosteric with the pyrophosphate. Nevertheless, this risk seemed acceptable because of the increased synthetic accessibility of compound **2.08** and because enzymes, such as farnesyltransferases, bind lipid-substituted pyrophosphate and truncated phosphonophosphate derivatives similarly.[199] Because the related glycosyltransferase GlfT2 is influenced by the acceptor lipid substituent,[116] our synthetic route was designed to access acceptors with diverse lipid groups (Scheme 2.2). Thus, late-stage coupling of protected disaccharide **2.13** and lipid **2.14** would afford phosphonophosphate **2.08**. The decaprenol substituent was replaced with a (2Z,6Z)-farnesol group in **2.14**, as this shorter lipid substituent can simplify substrate handling.[202] Glycosyltransferases can be sensitive to the polyprenol lipid

alkene and its geometry,[28,70,193] so we preserved the isoprenyl alkene geometry closest to the oligosaccharide. We reasoned that if compound **2.08** was inactive, we could modify our route to identify a suitable substrate.

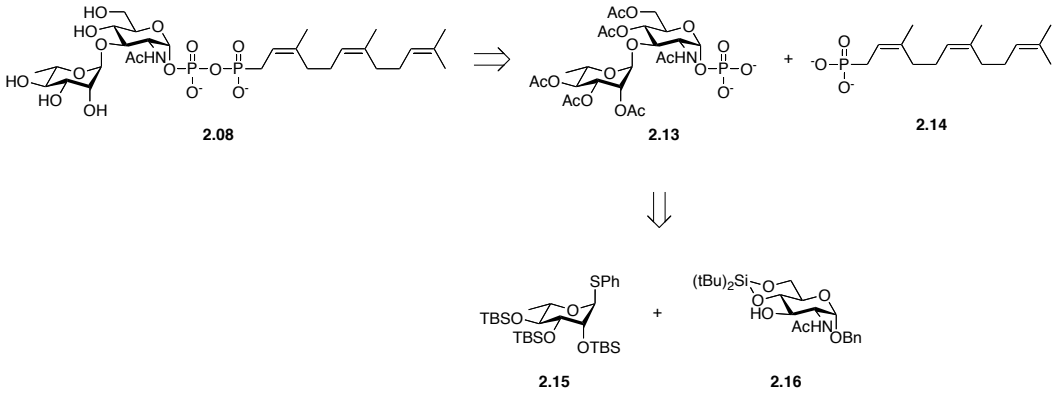

Scheme 2.2. Retrosynthetic analysis toward phosphonophosphate **2.08**.

Glycosylation of monosaccharides **2.15** and **2.16** should yield disaccharide **2.13**. We chose a thioglycoside as the activating group, since conditions for anomeric activation of this group are straightforward and it is stable under a wide range of reaction conditions.[203] Our choice of silyl protecting groups was guided by the discovery by Bols and co-workers of a conformationally arming effect on glycosylation donors.[204] Specifically, *tert*-butyldimethylsilyl (TBS)-protected thiorhamnoside **2.15** reacts to form glycosides with high selectivity for the desired α-anomer. The silylene protecting group on glycosyl acceptor **2.16** allowed for two-step isolation of the 3-hydroxyl group from *N*-acetyl-D-glucosamine.

2.4.1 Synthesis of the acceptor disaccharide portion

A four-step procedure from acetate-protected **2.05** led to donor **2.15** (Scheme 2.3). Acetate-protected **2.05** was converted to phenyl thioglycoside **2.17** using zinc(II) iodide and (phenylthio)trimethylsilane,[205] followed by deprotection under Zemplén conditions. TBS

protection of thioglycoside **2.18** under standard conditions afforded phenyl 1-thio-2,3,4-tri-*O*-*tert*-butyldimethylsilyl-L-rhamnopyranoside **2.15**.[206] To generate the acceptor, Fischer glycosylation of *N*-acetyl-D-glucosamine with benzyl alcohol in concentrated hydrochloric acid provided benzyl glucoside **2.19**.[207] We chose an anomeric benzyl group since it provided a stable, faintly UV-active linkage that could be readily removed by reductive hydrogenation. Reaction with di-*tert*-butylsilyl bis(trifluoromethanesulfonate),[208] followed by a pyridine quench, yielded the silylene-protected GlcNAc derivative **2.16**.

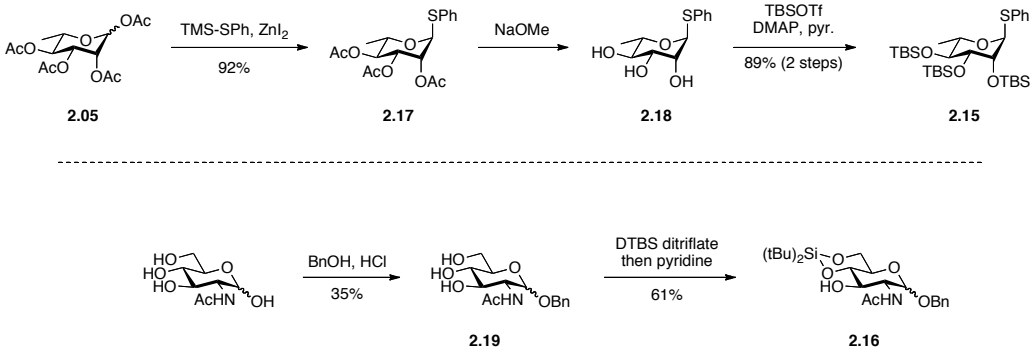

Scheme 2.3. Synthesis of donor and acceptor substrates for Rha-α(1,3)-GlcNAc glycosides.

The route to acceptor surrogate **2.08** continued with the glycosylation of compounds **2.15** and **2.16** (Scheme 2.4). Activation of the "super armed" donor **2.15** with *N*-iodosuccinimide and silver trifluoromethanesulfonate provided the desired α-glycoside **2.20**. The stereochemical outcome of the glycosylation was controlled by the silylated L-rhamnosyl donor, as formation of the β-anomer was not observed. The α-phosphoryl group was installed using a phosphitylation–oxidation sequence.[209] Hydrogenolysis afforded the anomeric lactol, which was exposed to dibenzyl N,N-diisopropylphosphoramidite in the presence of 1*H*-tetrazole.[210] The intermediate glycosyl phosphite was oxidized *in situ* to yield phosphotriester **2.21**. The benzyl protecting groups were removed by reductive hydrogenation in the presence of an amine base to afford phosphomonoester **2.22** in good yield.

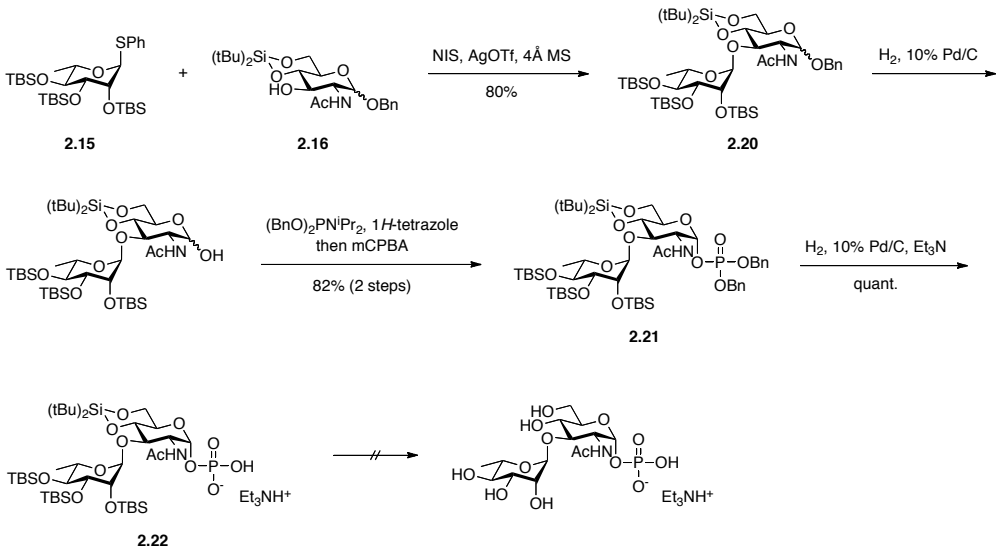

Scheme 2.4. Glycosylation of silylated monosaccharides **2.15** and **2.16**, followed by elaboration to phosphate **2.22**.

We examined whether the silyl groups could be removed at this stage. The protecting groups were inert to a variety of fluoride sources, and led to either partial cleavage or complete decomposition under more forcing conditions. A similar problem has been encountered with silyl-protected fucosides.[211] Thus, since unmasking the silyl groups late in the route was problematic, we intercepted an earlier synthetic intermediate and exchanged the silyl groups for acetate groups (Scheme 2.5). This protecting group change was beneficial, as the acylated intermediates were easier to purify and characterize.

Installation of the α-phosphoryl group from **2.23** followed the same sequence as described above (Scheme 2.5). Hydrogenolysis, followed by a phosphitylation–oxidation sequence, yielded phosphotriester **2.24**. Reductive hydrogenation in the presence of an amine base removed the benzyl protecting groups to afford phosphomonoester **2.13** in good yield, with 9:1 α:β selectivity favoring the desired anomer. Having prepared the desired phosphoglycan, our attention then turned to the lipid component.

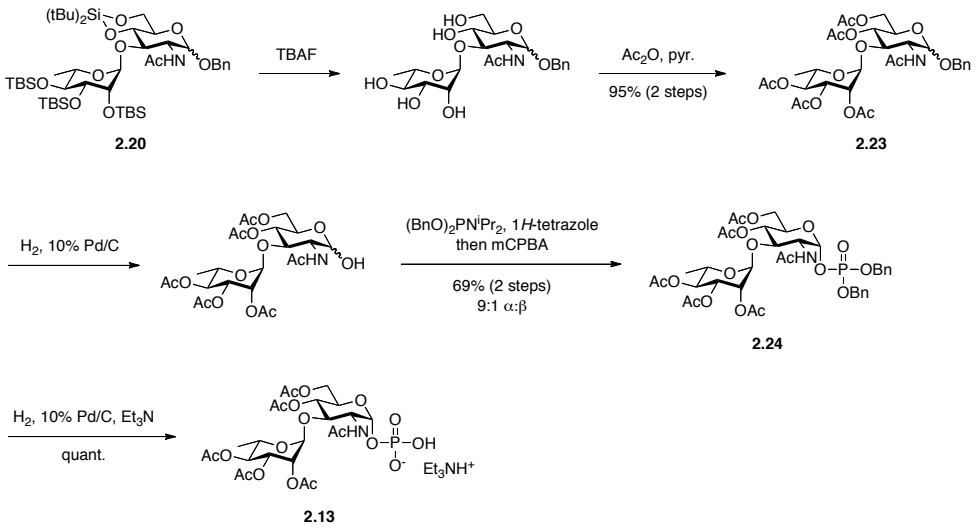

Scheme 2.5. Synthesis of acetate-protected disaccharide α-phosphate **2.13**.

2.4.2 Synthesis of (2Z,6Z)-farnesyl phosphonic acid

To prepare the C_{15} isoprenyl phosphonate **2.14**, we required acess to (2Z,6Z)-farnesol. This lipid can be generated in five steps from nerol. Specifically, nerol is converted to neryl chloride using Corey-Kim conditions, followed by addition of the dianion of ethyl acetoacetate to afford neryl β-ketoester **2.25** as a 6.6:1 mixture of Z:E isomers (Scheme 2.6).[212] The enol form of this β-ketoester was trapped with diethyl chlorophosphate in 1,3-dimethyl-3,4,5,6-tetrahydro-2(1*H*)-pyrimidone (DMPU) to yield (*E*)-enol phosphate **2.26**.[213-215] Methylation of the enol phosphate with lithium dimethyl cuprate by the method of Weiler and co-workers[216,217] afforded α,β-unsaturated ester **2.27** as a 5:1 mixture of Z:E isomers. Reduction of the ester using diisobutylaluminum hydride (DIBAL-H)[218] yielded (2Z,6Z)-farnesol **2.28** in good yield (48% over 5 steps). Conversion to diethyl phosphonate **2.29** via the Michaelis-Arbuzov reaction, followed by deprotection with bromotrimethylsilane, afforded ammonium (2Z,6Z)-farnesyl phosphonate **2.14** in good yield.

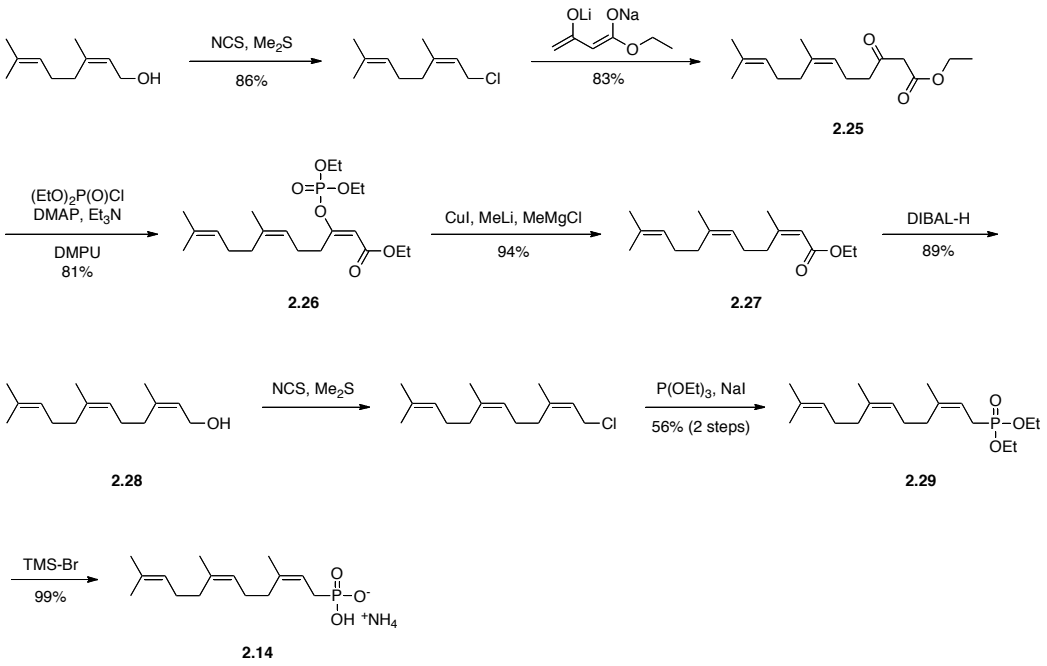

Scheme 2.6. Synthesis of (2Z,6Z)-farnesyl phosphonate **2.14**.

2.4.3 Moffatt-Khorana coupling to generate phosphonophosphate acceptors

A critical transformation was joining disaccharide **2.13** with lipid **2.14** to form the phosphonophosphate. Activation of the phosphoryl group of either coupling partner through formation of the phosphoryl chloride or phosphoryl imidazolide could result in self-coupling side products or product instability under the reaction conditions. Ultimately, Moffatt-Khorana conditions[219] were effective (Scheme 2.7). The electrophilic component, C_{15} isoprenyl phosphonomorpholidate **2.30**, was prepared by slowly dripping a solution of *N,N'*-dicyclohexylcarbodiimide (DCC) in *tert*-butanol to a refluxing solution of **2.14** and morpholine in *tert*-butanol:water. Treatment of disaccharide **2.13** and morpholidate **2.30** with 1*H*-tetrazole in pyridine yielded protected farnesyl-linked phosphonophosphate **2.31**. Finally, saponification with lithium hydroxide afforded phosphonophosphate **2.08**. Though the yield was modest, the transformation was highly reproducible.

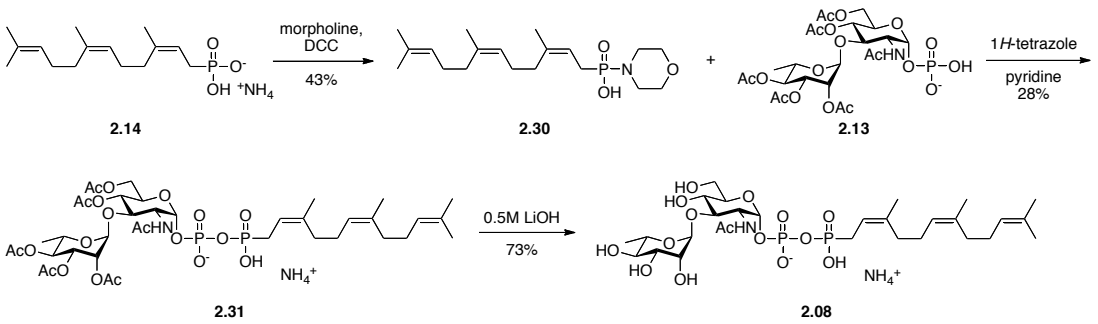

Scheme 2.7. Synthesis of farnesyl-linked Rha-α(1,3)-GlcNAc phosphonophosphate **2.08**.

2.4.4 Synthesis of neryl-linked phosphonophosphates

We exploited this convergent synthetic route to produce additional acceptors that probe structural features required for enzymatic activity. Surrogate **2.32** bearing a C_{10} isoprenyl (neryl) lipid carrier as well as surrogate **2.33** bearing only a monosaccharide were generated. To produce **2.32**, nerol was converted to phosphonomorpholidate **2.34** via the Corey-Kim and Michaelis-Arbuzov sequence described for (2Z,6Z)-farnesol above (Scheme 2.8). Diethyl phosphonate **2.35** was deprotected with bromotrimethylsilane to yield ammonium phosphonate **2.36**, and converted to morpholidate **2.34** by reaction with DCC and morpholine. Coupling with disaccharide α-phosphate **2.13** using 1*H*-tetrazole in pyridine led to acetate-protected phosphonophosphate **2.37** in 32% yield. Saponification with lithium hydroxide afforded neryl-linked Rha-α-(1,3)-GlcNAc phosphonophosphate **2.32**. This compound will be useful for probing the effect of the lipid carrier on GlfT1 activity.

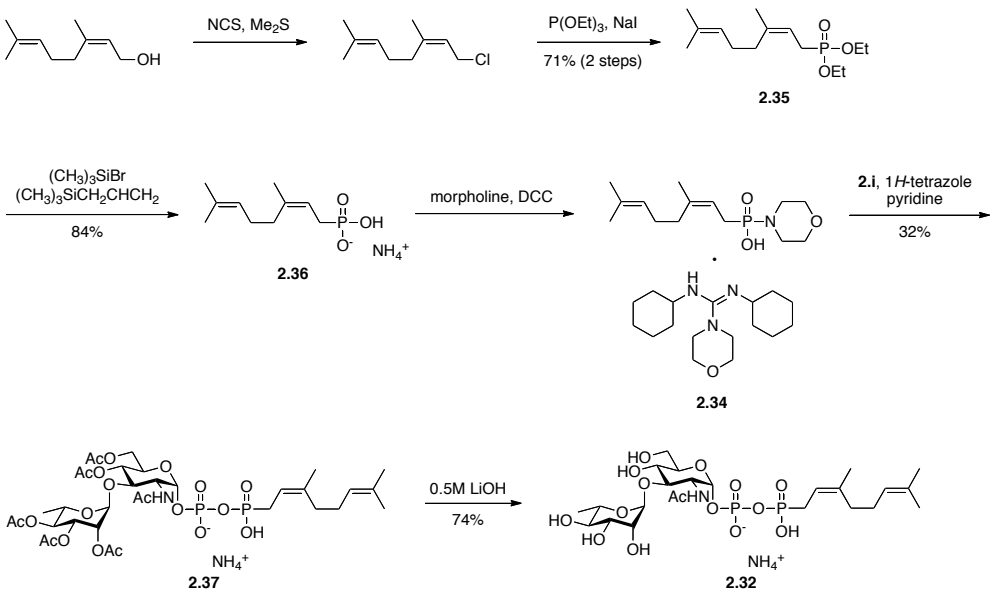

Scheme 2.8. Synthesis of neryl-linked Rha-α(1,3)-GlcNAc disaccharide phosphonophosphate **2.32**.

We sought to synthesize a phosphonophosphate that was unlikely to serve as an acceptor, and reasoned that a monosaccharide lacking the L-rhamnosyl moiety would not be processed by GlfT1. Our approach toward monosaccharide phosphonophosphate **2.33** required known GlcNAc α-phosphate **2.38** (Scheme 2.9).[209] Benzyl 2-acetamido-2-deoxy-D-glucopyranoside **2.19** was acetate-protected,[220] and the anomeric lactol of **2.39** liberated by reductive hydrogenation. One-pot phosphitylation–oxidation of lactol **2.40** afforded protected α-phosphate **2.41**. Reductive hydrogenation in the presence of an amine base yielded the desired GlcNAc α-phosphate **2.38**, which was coupled to neryl phosphonomorpholidate **2.34** as above. Saponification of acetate-protected product **2.42** afforded neryl-linked GlcNAc phosphonophosphate **2.33**. Though GlfT1 should not process this compound, we note that it could function as an acceptor surrogate for the upstream rhamnosyltransferase WbbL as well as other bacterial glycosyltransferases, such as *B. subtilis* TagA described in Chapter 1, that build glycans on lipid-linked *N*-acetyl-D-glucosamine pyrophosphates.

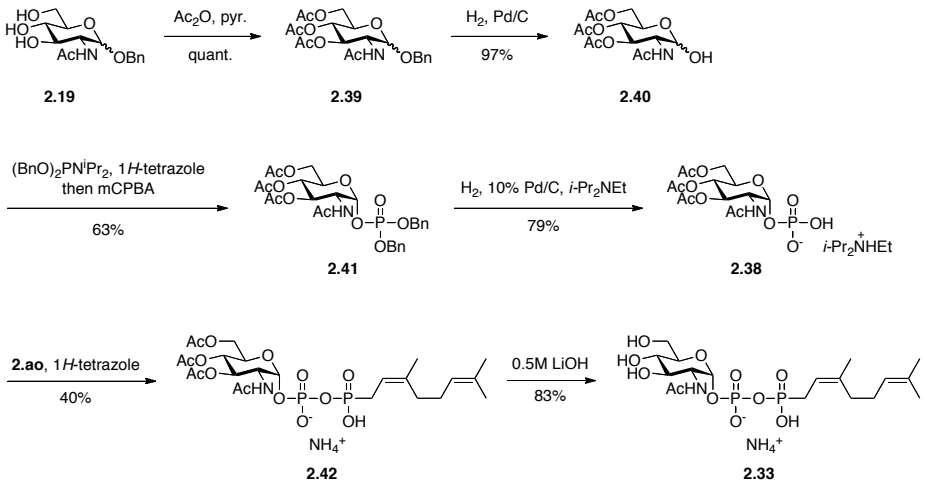

Scheme 2.9. Synthesis of neryl-linked GlcNAc phosphonophosphate **2.33**.

2.5 Conclusion

We have described the synthesis of a series of phosphonophosphate-containing glycosyltransferase acceptor substrates. These compounds were pursued as stabilized analogs of lipid-linked pyrophosphates, which will permit a wider range of synthetic manipulations on intermediate compounds. We designed a route to allow for facile diversification via late-stage coupling of a sugar phosphate with an isoprenyl phosphonomorpholidate. The stability of the allylic phosphonophosphate derivatives facilitated their synthesis and subsequent analysis. These compounds should serve as adequate acceptor substrate surrogates for galactan glycosyltransferases.

2.6 Experimental details

All compounds were purchased from Sigma Aldrich (Milwaukee, WI) or Fisher Scientific (Pittsburgh, PA). Tetrahydrofuran (THF) was distilled from sodium/benzophenone ketyl, methanol (MeOH) was distilled from magnesium, and dichloromethane (CH_2Cl_2) and

triethylamine (Et_3N) were distilled from calcium hydride. Other solvents were purified according to the guidelines in *Purification of Laboratory Chemicals*.[221] All reactions were run under argon atmosphere in oven-dried glassware unless otherwise stated. Molecular sieves were activated by heating to 600 °C in a furnace for 12 h, then cooled in a dessicator. Analytical thin layer chromatography (TLC) was carried out on E. Merck (Darmstadt) TLC plates pre-coated with silica gel 60 F254 (250 μm layer thickness). Analyte visualization was accomplished using a UV lamp and by charring with a solution of *p*-anisaldehyde (3.5 mL), acetic acid (15 mL), H_2SO_4 (50 mL), and ethanol (350 mL). Flash column chromatography was performed with Silicycle Flash Silica Gel (40-63 μm, 60 Å pore size) using reagent grade hexanes and ACS grade ethyl acetate (EtOAc), or methanol (MeOH) and CH_2Cl_2. High-performance liquid chromatography was performed on a Beckman-Coulter instrument with a Vydac Protein and Peptide C18 (22 mm x 250 mm) column, using a gradient of acetonitrile in 25 mM ammonium bicarbonate. ^1H, ^{13}C, and ^{31}P nuclear magnetic resonance (NMR) spectra were recorded on a 300 MHz spectrometer (acquired at 300 MHz for ^1H NMR, 75 MHz for ^{13}C NMR, and 121 MHz for ^{31}P NMR) a 400 MHz spectrometer (acquired at 400 MHz for ^1H NMR, 101 MHz for ^{13}C NMR, and 162 MHz for ^{31}P NMR), a 500 MHz spectrometer (acquired at 500 MHz for ^1H NMR and 126 MHz for ^{13}C NMR), or a 600 MHz spectrometer (acquired at 600 MHz for ^1H NMR and 243 MHz for ^{31}P NMR). Chemical shifts are reported relative to tetramethylsilane or residual solvent peaks in parts per million ($CHCl_3$: ^1H: 7.26, ^{13}C: 77.16; MeOH: ^1H: 3.31, ^{13}C: 49.00). Peak multiplicity is reported as singlet (s), doublet (d), doublet of doublets (dd), doublets of doublets of doublets (ddd), triplet (t), doublet of triplets (dt), etc. High resolution electrospray ionization-time of flight mass spectra (HRESI-TOF MS) were obtained on a Micromass LCT.

Penta-*O*-acetyl-L-rhamnopyranoside (2.05)

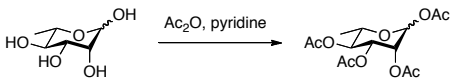

2.05

Pyridine (6.2 mL) was added to a round-bottom flask containing L-rhamnose (1.0 g, 6.1 mmol) under Ar atmosphere. The pale clear solution was cooled to 0 °C for 15 min, then acetic anhydride (2.9 mL, 30.5 mmol, 5.0 eq) was added dropwise over 30 min. After 23 h, toluene was added and the solution was concentrated under reduced pressure, followed by co-evaporation with toluene (3 x 75 mL). The pale yellow syrup was dissolved in a 1:1 (vol/vol) solution of hexanes:ethyl acetate and purified by flash column chromatography [1:1 (vol/vol) hexanes:ethyl acetate] to afford **2.05** (1.82 g, quantitative) as a clear, viscous syrup. Characterization of this compound matched a published report.[188]

Allyl 2,3,4-tri-*O*-acetyl-α-L-rhamnopyranoside (2.06)

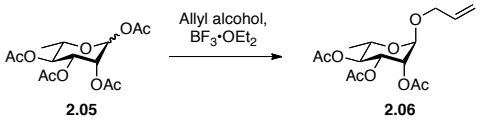

2.05 **2.06**

A solution of **2.05** (0.45 g, 1.4 mmol) in freshly distilled CH_2Cl_2 (5 mL) under Ar atmosphere was cooled to 0 °C. Allyl alcohol (0.11 mL, 2.7 mmol) and boron trifluoride diethyl etherate (0.42 mL, 3.4 mmol) were added dropwise over 15 min. The reaction stirred at 0 °C for 3 h, then warmed to ambient temperature for 2 h. The reaction was neutralized with triethylamine (0.5 mL), diluted with CH_2Cl_2, and poured into a separatory funnel. The solution was washed with a saturated solution of sodium bicarbonate, brine, dried over magnesium sulfate and concentrated under reduced pressure. Purification by flash chromatography [1:4 (vol/vol) EtOAc/hexanes] afforded **2.06** (0.27 g, 61%) as a clear oil. Characterization of this compound matched a published report.[189]

2-(*E*)-dodec-2-en-1-yl 2,3,4-tri-*O*-acetyl-α-L-rhamnopyranoside (2.07)

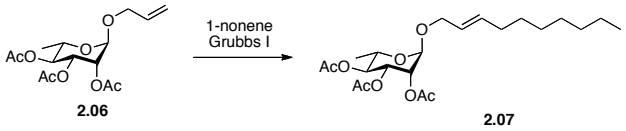

1-nonene (0.16 mL, 0.92 mmol) was added to a solution of **2.06** (50 mg, 0.15 mmol) in freshly distilled CH_2Cl_2 (2.6 mL) under Ar atmosphere, followed by bis(tricyclohexylphosphine)benzylidine ruthenium(IV) dichloride (Grubbs I catalyst, 25 mg, 0.03 mmol). The dark purple solution was heated to reflux for 3 h. An additional 18 mg of catalyst were added, followed by reflux for an additional 2 h. The reaction was cooled to ambient temperature and concentrated under reduced pressure. Purification by flash chromatography [hexanes to 1:7 (vol/vol) EtOAc:hexanes] afforded **2.07** (64 mg, 98%) as a light brown oil.

^{1}H NMR (300 MHz, $CDCl_3$) δ 5.77 – 5.62 (m, 1H, C*H*=CHCH$_2$O), 5.56 – 5.41 (m, 1H, CH=C*H*CH$_2$O), 5.30 (dd, *J* = 10.1, 3.5 Hz, 1H, H-3), 5.21 (dd, *J* = 3.5, 1.7 Hz, 1H, H-2), 5.04 (t, *J* = 9.9 Hz, 1H, H-4), 4.74 (d, *J* = 1.7 Hz, 1H, H-1), 4.14 – 4.03 (m, 1H, H-5), 4.00 – 3.81 (m, 2H, C*H*$_2$CH=), 2.12 (s, 3H, OAc), 2.02 (s, 3H, OAc), 1.96 (s, 3H, OAc), 1.44 – 1.23 (m, 8H, 4 x -C*H*$_2$-), 1.20 (d, *J* = 6.3 Hz, 3H, Me), 0.91 – 0.81 (m, 3H, CH$_2$C*H*$_3$). ^{13}C NMR (75 MHz, $CDCl_3$): δ 170.2, 170.1, 170.0, 136.3, 124.8, 96.3, 71.4, 70.1, 69.3, 68.4, 66.4, 32.4, 31.9, 29.3, 29.2, 29.1, 22.8, 21.0, 20.9, 20.8, 17.5, 14.2.

2-(*E*)-dodec-2-en-1-yl α-L-rhamnopyranoside (2.02)

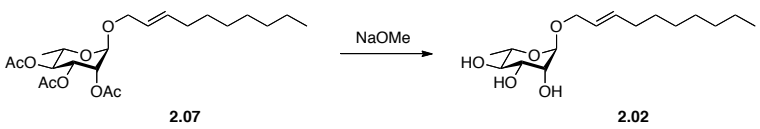

A solution of sodium methoxide in methanol (0.5 M, .75 mL, 0.38 mmol) was added to a solution of **2.07** (64 mg, 0.15 mmol) in freshly distilled MeOH (7.0 mL) under Ar atmosphere at ambient temperature. After 1 h, the reaction was neutralized with Amberlite IR-120 (H^+ form) resin, filtered, and concentrated under reduced pressure. Purification by flash chromatography [3:17 (vol/vol) EtOAc:hexanes to 3:1 (vol/vol) EtOAc:hexanes] afforded **2.02** (41 mg, 91%) as a clear film.

^{1}H NMR (500 MHz, 1:1 $CDCl_3$:CD_3OD) δ 5.68 – 5.59 (m, 1H, C*H*=CHCH$_2$O), 5.48 – 5.40 (m, 1H, CH=C*H*CH$_2$O), 4.65 (s, 1H, H-1), 4.01 (dd, *J* = 12.1, 5.7 Hz, 1H, OC*H*$_2$CH=), 3.83 (dd, *J* = 12.0, 6.9 Hz, 1H, OC*H*$_2$CH=), 3.77 – 3.72 (m, 1H, H-2), 3.60 (dd, *J* = 9.4, 3.4 Hz, 1H, H-3), 3.53 (dq, *J* = 9.2, 6.2 Hz, 1H, H-5), 3.29 (t, *J* = 9.5 Hz, 1H, H-4), 1.96 (q, *J* = 7.1 Hz, 2H, C*H*$_2$CH=), 1.32 – 1.25 (m, 2H, C*H*$_2$CH$_2$CH=), 1.25 – 1.14 (m, 11H, 4 x -C*H*$_2$-, Me), 0.80 (t, *J* = 6.8 Hz, 3H, CH$_2$C*H*$_3$). ^{13}C NMR (126 MHz, 1:1 $CDCl_3$:CD_3OD) δ 134.83, 124.88, 98.61, 72.41, 70.84, 70.45, 67.89, 67.27, 31.79, 31.33, 28.65, 28.58, 22.13, 16.70, 13.24. HRMS (ESI-TOF$^+$) for $C_{16}H_{30}NaO_5$ (M+Na$^+$) calcd 325.1986, found 325.1989.

Phenyl 2,3,4-tri-*O*-acetyl-1-thio-α-L-rhamnopyranoside (2.17)

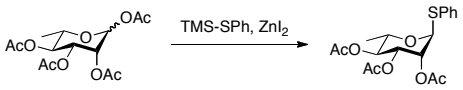

2.05 **2.17**

(Phenylthio)trimethylsilane (9.33 mL, 49.3 mmol) was added to a solution of **2.05** (8.20 g, 24.6 mmol) and zinc(II) iodide (15.4 g, 48.1 mmol) in freshly distilled CH_2Cl_2 (49.3 mL) under Ar atmosphere at ambient temperature. After 21.5 h stirring at ambient temperature, the reaction was transferred to a separatory funnel. Water (100 mL) was added, and the mixture was shaken. The layers were separated, and the aqueous layer was extracted with CH_2Cl_2 (3x).

The combined organic layers were washed with water, saturated sodium bicarbonate, brine, dried over magnesium sulfate, filtered, and concentrated under reduced pressure to a crystalline white solid. Purification by flash chromatography [hexanes to 1:3 (vol/vol) EtOAc:hexanes] afforded **2.17** (9.05 g, 96%) as a crystalline white solid. Characterization of this compound matched a published report.[205]

Phenyl 1-thio-α-L-rhamnopyranoside (2.18)

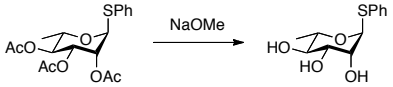

2.17 **2.18**

Freshly distilled MeOH (70.3 mL) was added to a round-bottom flask containing **2.17** (4.03 g, 10.5 mmol) under Ar atmosphere. A solution of NaOMe in MeOH (0.5M, 5.48 mL, 2.74 mmol) was added dropwise at ambient temperature. After 16 h, the reaction was neutralized by addition of Amberlite IR-120 resin (H^+ form) to pH 7. The suspension was filtered, the resin was washed with MeOH, and the filtrate was concentrated under reduced pressure to afford **2.18** (2.69 g, quantitative) as a white foam. Characterization of this compound matched a published report.[205]

Phenyl 2,3,4-tri-*O*-*tert*-butyldimethylsilyl-1-thio-L-rhamnopyranose (2.15)

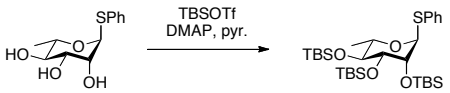

2.18 **2.15**

tert-Butyldimethylsilyl trifluoromethanesulfonate (3.58 mL, 15.6 mmol) was added dropwise to a solution of **2.18** (0.800 g, 3.12 mmol) and 4-(dimethylamino)pyridine (38.1 mg,

0.312 mmol) in anhydrous pyridine (4.0 mL) under Ar atmosphere at ambient temperature. The reaction was warmed to 50 °C and stirred for 18 h. It was cooled to 0 °C and quenched with MeOH, then poured into a separatory funnel and diluted with EtOAc. Water was added, and the layers were separated. The organic layer was washed with 1M HCl, a saturated solution of sodium bicarbonate, brine, dried over magnesium sulfate, filtered, and concentrated under reduced pressure. Purification by flash chromatography [hexanes to 2:3 (vol/vol) CH_2Cl_2:hexanes] afforded **2.15** (1.73 g, 93%) as a clear oil. Characterization of this compound matched a published report.[206]

Benzyl 2-acetamido-2-deoxy-α-D-glucopyranoside (2.19)

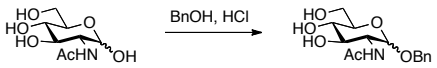

2.19

Benzyl alcohol (44.4 mL, 0.430 mol) was added to a flask containing *N*-acetyl-D-glucosamine (10.0 g, 45.2 mmol) under Ar atmosphere at ambient temperature. Concentrated hydrochloric acid (37% w/w, 1.81 mL, 22.6 mmol) was added and the mixture was warmed to 85 °C. After 6 h, the solution was cooled to ambient temperature, poured into ethyl ether (180 mL) and stored at –20 °C for 18 h. The solid was filtered and washed thoroughly with ethyl ether, affording **2.19** (12.5 g, 89%) as an off-white solid. Characterization of this compound matched a published report.[207]

Benzyl 2-acetamido-2-deoxy-4,6-*O*-di-*tert*-butylsilylene-α-D-glucopyranoside (2.16)

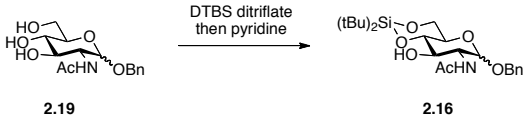

A solution of **2.19** (0.77 g, 2.5 mmol) in *N,N*-dimethylformamide (24 mL) under Ar atmosphere was cooled to –40 °C. Di-*tert*-butylsilyl bis(trifluoromethanesulfonate) (0.78 mL, 2.4 mmol) was added dropwise to the solution, and the reaction stirred for 1 h at –40 °C. The reaction was quenched by slow addition of anhydrous pyridine (0.58 mL, 7.1 mmol), then allowed to warm to ambient temperature. The reaction was partitioned between ethyl ether (70 mL) and a saturated solution of sodium bicarbonate (60 mL). The layers were separated, and the organic layer was washed with water (2 x 60 mL) and brine (60 mL). The aqueous layers were back-extracted with ethyl ether (80 mL). The combined organic layers were dried over magnesium sulfate, filtered, and concentrated under reduced pressure. The residue was coevaporated with toluene (2x). Purification by flash chromatography [hexanes to 1:1 (vol/vol) acetone:hexanes] afforded **2.16** (0.69 g, 61%) as a crystalline, white solid. Characterization of this compound matched a published report.[208]

Benzyl 2-acetamido-2-deoxy-3-*O*-(2,3,4-tri-*O*-*tert*-butyldimethylsilyl-α-L-rhamnopyranosyl)-4,6-*O*-di-tert-butylsilylene-α-D-glucopyranoside (2.20)

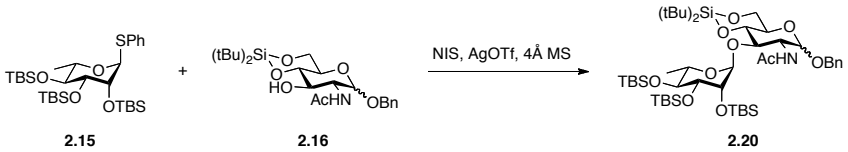

Compounds **2.15** (108 mg, 0.18 mmol, 1.5 eq) and **2.16** (54 mg, 0.12 mmol) were combined and coevaporated with toluene (3x). A stir bar and activated powdered 4 Å molecular sieves were added under Ar atmosphere, followed by CH_2Cl_2 (4.8 mL). The suspension was stirred at ambient temperature for 45 min, then cooled to –25 °C for 15 min. *N*-iodosuccinimide

(49 mg, 0.22 mmol, 1.8 eq) and silver trifluoromethanesulfonate (6 mg, 0.02 mmol, 0.2 eq) were added and the suspension stirred at –25 °C for 2 h. The reaction was warmed to –5 °C over 20 min, then filtered through Celite. The filtrate was washed with 10% v/v sodium thiosulfate, saturated sodium bicarbonate, water, and brine. The organic layer was dried over $MgSO_4$, filtered, and concentrated under reduced pressure. Purification by flash chromatography (4:1 hexanes:ethyl acetate) afforded **2.20** (91 mg, 80%) as a white, crystalline solid.

^{1}H NMR (300 MHz, $CDCl_3$): δ 7.38 – 7.24 (m, 5H, Ar), 5.72 (d, *J* = 10.0 Hz, 1H, NH), 4.90 (d, *J* = 1.9 Hz, 1H, H-1'), 4.69 (d, *J* = 3.7 Hz, 1H, H-1), 4.66 (d, *J* = 11.9 Hz, 1H, OC*H*Ar), 4.46 (d, *J* = 11.9 Hz, 1H, OC*H*Ar), 4.27 (td, *J* = 10.0, 3.7 Hz, 1H), 4.15 – 3.69 (m, 12H), 1.87 (s, 3H, NHAc), 1.19 (d, *J* = 6.2 Hz, 3H, Me), 1.06 (s, 9H, (C*H*$_3$)$_3$CSi), 0.97 (s, 9H, (C*H*$_3$)$_3$CSi), 0.93 (s, 9H, (C*H*$_3$)$_3$CSi), 0.89 (s, 9H, (C*H*$_3$)$_3$CSi), 0.85 (s, 9H, (C*H*$_3$)$_3$CSi), 0.10 (s, 3H, C*H*$_3$Si), 0.09 (s, 3H, C*H*$_3$Si), 0.08 (s, 3H, C*H*$_3$Si), 0.04 (s, 3H, C*H*$_3$Si), 0.03 (s, 3H, C*H*$_3$Si).^{13}C NMR (75 MHz, $CDCl_3$): δ 169.5, 137.1, 128.7, 128.3, 128.3, 99.4, 97.5, 76.5, 74.5, 73.3, 73.0, 72.7, 70.8, 70.1, 67.1, 66.9, 53.7, 27.8, 27.2, 26.9, 26.3, 25.8, 23.6, 22.8, 20.0, 19.3, 18.9, 18.2, 18.1, 0.1, –2.3, –3.3, –4.0, –4.0, –4.1, –4.1, –4.2. HRMS (ESI-TOF$^+$) for $C_{47}H_{89}NNaO_{10}Si_4$ (M+Na$^+$) calcd 962.5456, found 962.5453.

Dibenzyl 2-acetamido-2-deoxy-3-*O*-(2,3,4-tri-*O*-*tert*-butyldimethylsilyl-α-L-rhamnopyranosyl)-4,6-*O*-di-tert-butylsilylene-α-D-glucopyranosyl phosphate (2.21)

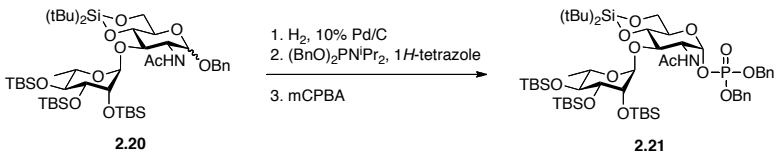

2.20 **2.21**

1. Compound **2.20** (114 mg, 121 μmol) was dissolved in ethyl acetate (12.1 mL) containing triethylamine (2.43 mL, 20% (vol/vol) w.r.t. ethyl acetate) under Ar atmosphere. Palladium on carbon (10%, 38 mg, 30% (wt/wt) w.r.t. sugar) was added, then the reaction was placed under H_2 atmosphere by evacuating the flask and backfilling with H_2 via balloon (4x). The suspension stirred vigorously at ambient temperature for 16 h. The reaction was filtered through a cotton plug and a 0.22 μm filter to afford the lactol as a clear oil that was carried onto the next step without further purification.

2. The lactol (0.10 g, 0.12 mmol) was coevaporated with toluene (3x), then dissolved in CH_2Cl_2 (6.0 mL). This solution was added via cannula to a solution of 1*H*-tetrazole (40 mg, 0.57 mmol) and dibenzyl *N*,*N*-diisopropylphosphoramidite (0.12 mL, 0.36 mmol) in CH_2Cl_2 (6.0 mL) at ambient temperature. The reaction stirred at ambient temperature for 2 h, then it was cooled to –40 °C for 15 min. *meta*-Chloroperoxybenzoic acid (77% max, 0.14 g, 0.61 mmol) was added in one portion, and the cloudy solution stirred at –40 °C for 5 min. The reaction was then allowed to warm to ambient temperature. After stirring for 2 h at ambient temperature, the reaction was diluted with CH_2Cl_2 (40 mL), washed with 10% v/v sodium thiosulfate (2 x 40 mL), saturated sodium bicarbonate (2 x 40 mL), and water (2 x 40 mL). The organic layer was dried over $MgSO_4$, filtered, and concentrated under reduced pressure. Purification by flash chromatography (hexanes to 1:4 (vol/vol) acetone:hexanes) afforded phosphotriester **2.21** (0.11 g, 82%) as a clear glass.

1H NMR (300 MHz, $CDCl_3$) δ 7.43 – 7.32 (m, 10H), 5.51 – 5.40 (m, 2H), 5.15 – 4.98 (m, 5H), 4.78 (d, *J* = 1.8 Hz, 1H), 4.37 – 4.24 (m, 1H), 4.12 – 3.71 (m, 7H), 1.71 (s, 3H, NHAc), 1.23 (d, *J* = 6.8 Hz, 3H, Me), 1.06 (s, 9H, $(CH_3)_3CSi$), 0.97 (s, 9H, $(CH_3)_3CSi$), 0.92 (s, 9H, $(CH_3)_3CSi$), 0.91 (s, 9H, $(CH_3)_3CSi$), 0.86 (s, 9H, $(CH_3)_3CSi$), 0.10 (s, 3H, CH_3Si), 0.09 – 0.07 (m, 9H, 3 x CH_3Si), 0.05 (s, 3H, CH_3Si), 0.02 (s, 3H, CH_3Si). ^{31}P NMR (121 MHz, $CDCl_3$): δ -0.91.

2-Acetamido-2-deoxy-3-*O*-(2,3,4-tri-*O*-*tert*-butyldimethylsilyl-α-L-rhamnopyranosyl)-4,6-*O*-di-tert-butylsilylene-α-D-glucopyranosyl phosphate (2.22)

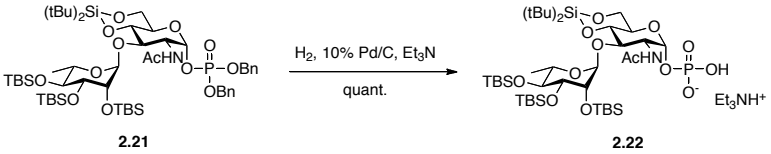

Triethylamine (0.80 mL, 20% v/v w.r.t. ethanol) was added to a solution of phosphotriester **2.21** (0.11 g, 99 μmol) in ethanol (4.0 mL) under Ar atmosphere. Palladium on carbon (10%, 11 mg, 10% (wt/wt) w.r.t. sugar) was added, then the reaction was placed under H_2 atmosphere by evacuating the flask and backfilling with H_2 via balloon (4x). The suspension stirred vigorously at ambient temperature for 17 h. The reaction was filtered through a cotton plug and a 0.22 μm filter to afford **2.22** as a waxy white solid.

HRMS (ESI-TOF$^-$) for $C_{40}H_{83}NO_{13}PSi_4$ ($M-H^-$) calcd 928.4684, found 928.4709.

Benzyl 2-acetamido-2-deoxy-3-*O*-(2,3,4-tri-*O*-acetyl-α-L-rhamnopyranosyl)-4,6-di-*O*-acetyl-α-D-glucopyranoside (2.23)

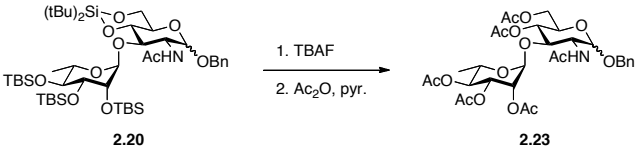

Compound **2.20** (0.78 g, 0.82 mmol) was treated with TBAF (1.0 M in THF, 8.2 mL, 8.2 mmol, 15.0 eq) under Ar atmosphere at ambient temperature for 18 h, and then concentrated under reduced pressure. The residue was taken up in pyridine (3.5 mL) under Ar atmosphere, then cooled to 0 °C. Acetic anhydride (8.0 mL) was added dropwise, then the solution was

allowed to warm to ambient temperature. After 18 h, the reaction was diluted with MeOH and concentrated under reduced pressure. Partial purification by flash chromatography [hexanes to 2:1 (vol/vol) hexanes:acetone] afforded a syrup. The syrup was diluted in EtOAc, washed with 1M HCl (2x), saturated sodium bicarbonate, brine, dried over magnesium sulfate, filtered, and concentrated under reduced pressure to afford **2.23** (0.52 g, 95% over 2 steps) as a foam.

^{1}H NMR (300 MHz, $CDCl_3$): δ 7.43 – 7.27 (m, 5H, Ar), 5.75 (d, *J* = 9.6 Hz, 1H, NH), 5.17 – 5.05 (m, 2H), 5.00 (t, *J* = 10.3 Hz, 1H), 4.91 (d, *J* = 3.4 Hz, 2H), 4.80 (s, 1H), 4.69 (d, *J* = 11.8 Hz, 1H), 4.50 (d, *J* = 11.8 Hz, 1H), 4.42 (dt, *J* = 10.0, 5.2 Hz, 1H), 4.17 (dd, *J* = 12.3, 4.3 Hz, 1H), 4.01 (d, *J* = 12.3 Hz, 1H), 3.94 – 3.76 (m, 4H), 2.12 (s, 3H, OAc), 2.10 (s, 3H, OAc), 2.07 (s, 3H, OAc), 2.04 (s, 3H, OAc), (s, 3H, OAc), 1.94 (s, 3H, NHAc), 1.13 (d, *J* = 6.1 Hz, 3H, Me). ^{13}C NMR (75 MHz, $CDCl_3$): δ 170.8, 170.6, 170.5, 170.1, 169.6, 169.5, 136.6, 128.8, 128.5, 128.4, 99.7, 97.0, 80.3, 70.7, 70.2, 70.2, 70.1, 69.0, 68.4, 67.5, 62.1, 60.5, 53.9, 51.9, 51.6, 31.8, 29.8, 29.4, 25.7, 23.3, 21.2, 21.0, 20.9, 20.7, 20.4, 17.3, 14.3, 13.8. HRMS (ESI-TOF$^+$) for $C_{31}H_{42}NO_{15}$ ($M+H^+$) calcd 668.2549, found 668.2855.

Dibenzyl 2-acetamido-2-deoxy-3-*O*-(2,3,4-tri-*O*-acetyl-α-L-rhamnopyranosyl)-4,6-di-*O*-acetyl-α-D-glucopyranosyl phosphate (2.24)

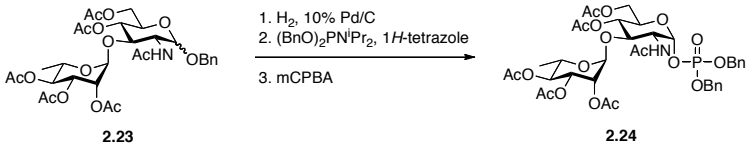

1. Compound **2.23** (30 mg, 45 μmol) was dissolved in ethanol (4.5 mL) under Ar atmosphere. Palladium on carbon (15 mg, 10%) was added, then the reaction was placed under H_2 atmosphere by evacuating the flask and backfilling with H_2 via balloon (4x). The suspension stirred vigorously at ambient temperature for 45 h. The reaction was filtered through a cotton

plug and a 0.22 μm filter to afford the lactol as a clear oil that was carried onto the next step without further purification.

2. The lactol (26 mg, 45 μmol) was coevaporated with toluene (3x), then dissolved in CH_2Cl_2 (2.3 mL). This solution was added via cannula to a solution of 1*H*-tetrazole (15 mg, 0.21 mmol) and dibenzyl *N*,*N*-diisopropylphosphoramidite (46 μL, 0.14 mmol) in CH_2Cl_2 (2.3 mL) at ambient temperature. The reaction stirred at ambient temperature for 2 h, then it was cooled to −40 °C for 15 min. *meta*-Chloroperoxybenzoic acid (77% max, 43 mg, 0.25 mmol) was added in one portion, and the cloudy solution stirred at −40 °C for 10 min. The reaction was then allowed to warm to ambient temperature. After stirring for 1.5 h at ambient temperature, the reaction was diluted with CH_2Cl_2 (15 mL), washed with 10% v/v sodium thiosulfate (2 x 20 mL), saturated sodium bicarbonate (2 x 20 mL), and water (2 x 20 mL). The organic layer was dried over $MgSO_4$, filtered, and concentrated under reduced pressure. Purification by flash chromatography (3:2 acetone:hexanes) afforded phosphotriester **2.24** (26 mg, 69%) as a light yellow oil.

^{1}H NMR (300 MHz, $CDCl_3$): δ 7.41 – 7.30 (m, 10H, Ar), 5.61 (dd, *J* = 5.7, 3.3 Hz, 1H, H-1), 5.54 (d, *J* = 9.6 Hz, 1H), 5.19 – 4.93 (m, 8H), 4.75 (d, *J* = 1.7 Hz, 1H, H-1'), 4.52 – 4.33 (m, 1H), 4.07 (dd, *J* = 13.0, 4.5 Hz, 1H), 3.98 – 3.75 (m, 3H), 3.71 – 3.59 (m, 1H), 2.16 (s, 3H, OAc), 2.08 (s, 3H, OAc), (s, 2 x 3 H, 2 x OAc), 1.95 (s, 3H, OAc), 1.89 (s, 3H, NHAc), 1.14 (d, *J* = 6.2 Hz, 3H, Me). ^{31}P NMR (121 MHz, $CDCl_3$): δ -2.34. HRMS (ESI-TOF$^+$) for $C_{38}H_{48}NNaO_{18}P$ ($M+Na^+$) calcd 860.2502, found 860.2528.

2-Acetamido-2-deoxy-3-*O*-(2,3,4-tri-*O*-acetyl-α-L-rhamnopyranosyl)-4,6-di-*O*-acetyl-α-D-glucopyranosyl phosphate (2.13)

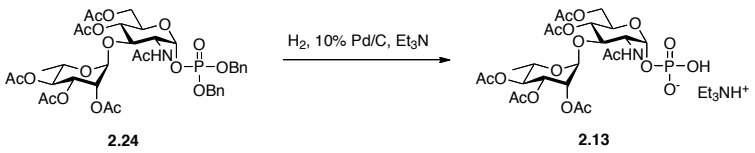

2.24 **2.13**

Triethylamine (0.60 mL, 20% v/v w.r.t. ethanol) was added to a solution of phosphotriester **2.24** (26 mg, 30 μmol) in ethanol (3.0 mL) under Ar atmosphere. Palladium on carbon (3.0 mg, 10%) was added, then the reaction was placed under H_2 atmosphere by evacuating the flask and backfilling with H_2 via balloon (4x). The suspension stirred vigorously at ambient temperature for 17 h. The reaction was filtered through a cotton plug and a 0.22 μm filter to afford **2.13** (28 mg, quant.) as a white solid.

^{1}H NMR (300 MHz, $CDCl_3$): δ 5.43 (dd, *J* = 6.9, 3.2 Hz, 1H, H-1), 5.17 (dd, *J* = 3.3, 2.0 Hz, 1H), 5.14 – 5.06 (m, 2H), 5.01 – 4.92 (m, 3H), 4.26 – 4.16 (m, 3H), 4.13 – 4.00 (m, 2H), 3.92 – 3.80 (m, 1H), 3.16 (q, *J* = 7.3 Hz, 15H, CH_3CH_2N), 2.12 (s, 3H, OAc), 2.08 (s, 3H, OAc), 2.06 (s, 3H, OAc), 2.04 (s, 3H, OAc), 2.03 (s, 3H, OAc), 1.93 (s, 3H, NHAc), 1.30 (t, *J* = 7.3 Hz, 22H, CH_3CH_2N), 1.14 (d, *J* = 6.2 Hz, 3H, Me). ^{13}C NMR (126 MHz, CD_3OD): δ 178.3, 172.6, 171.2, 170.3, 170.1, 170.1, 169.7, 99.3, 93.8 (d), 78.5, 70.7, 69.9, 69.7, 69.0, 68.5, 67.0, 61.8, 53.2 (d), 46.1, 22.4, 21.6, 20.0, 19.4, 19.3, 19.2, 16.4, 7.8. ^{31}P NMR (162 MHz, CD_3OD): δ -0.65. HRMS (ESI-TOF$^-$) for $C_{24}H_{35}NO_{18}P$ (M^-) calcd 656.1597, found 656.1610.

(*Z*)-Ethyl 7,11-dimethyl-3-oxododeca-6,10-dienoate (2.25)

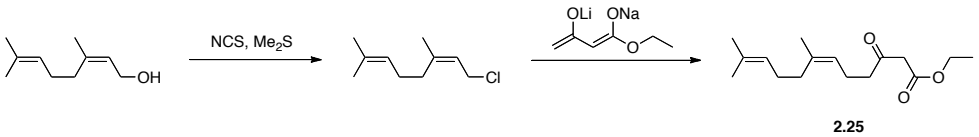

2.25

1. A solution of N-chlorosuccinimide (1.78 g, 13.3 mmol) in freshly distilled CH_2Cl_2 (24 mL) under Ar atmosphere was cooled to –30 °C. After 20 min, dimethyl sulfide (1.04 mL, 14.2

mmol) was added dropwise to the white suspension, and the reaction was warmed to 0 °C. After 20 min at 0 °C, the suspension was cooled to –30 °C for 10 min. Nerol (2.11 mL, 12.0 mmol) was added dropwise, and the suspension was stirred at 0 °C for 3 h. The reaction was then allowed to warm to ambient temperature. After 45 min, the reaction was diluted with hexanes, filtered, washed with brine, dried over magnesium sulfate, filtered, and concentrated under reduced pressure to afford crude neryl chloride (1.78 g, 86%) as a yellow oil.

2. Oil-free sodium hydride was prepared by washing a 60% dispersion of NaH in mineral oil with anhydrous pentane under N_2 in a fritted funnel. This preparation of oil-free NaH (792 mg, 19.8 mmol) was suspended in freshly distilled tetrahydrofuran (27.3 mL) and cooled to 0 °C. Ethyl acetoacetate (2.28 mL, 18.0 mmol) was added dropwise. After 10 min, *n*-butyllithium (2.63M in hexanes, 7.19 mL, 18.9 mmol) was added slowly over 5 minutes. After 10 min, a solution of neryl chloride (1.78 g) in freshly distilled tetrahydrofuran (5 mL) was added to the suspension at 0 °C. After 35 min, the reaction was quenched by addition of 3M HCl (20 mL). The biphasic mixture was partitioned between ethyl ether (75 mL) and water (75 mL). The aqueous layer was extracted with ethyl ether (3 x 75 mL). The combined organic layers were washed with water (3 x 50 mL), brine (50 mL), dried over magnesium sulfate, filtered, and concentrated under reduced pressure. Purification by flash chromatography [7:13 (vol/vol) CH_2Cl_2:hexanes to 3:2 (vol/vol) CH_2Cl_2:hexanes] afforded **2.25** (2.27 g, 83% brsm, 6.6:1 *Z*:*E*) as a light yellow oil. Characterization of this compound matched a published report.[212]

(2*E*,6*Z*)-Ethyl 3-((diethoxyphosphoryl)oxy)-7,11-dimethyldodeca-2,6,10-trienoate (2.26)

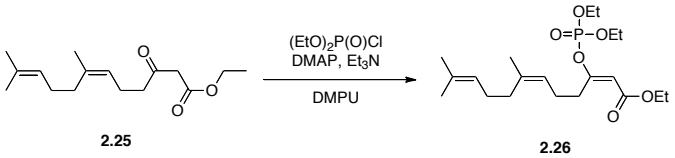

2.25 **2.26**

A solution of 4-(dimethylamino)pyridine (70 mg, 0.58 mmol) and triethylamine (0.80 mL, 5.8 mmol) in 1,3-dimethyl-3,4,5,6-tetrahydro-2(1*H*)-pyrimidone (DMPU, 11 mL) containing activated 4Å powdered molecular sieves under Ar atmosphere was cooled to 0 °C. An ice-cooled solution of **2.25** (1.4 g, 5.1 mmol) in DMPU (6.0 mL) was added via cannula using positive nitrogen pressure. The bright yellow solution stirred at 0 °C for 1 h, then it was cooled to –20 °C. Diethyl chlorophosphate (0.83 mL, 5.8 mmol) was added dropwise, and the cooling bath was removed. The reaction stirred at ambient temperature for 16 h. It was diluted with ethyl ether and acidified to pH ~2 with 1M HCl to afford a biphasic mixture. The layers were separated, and the aqueous layer was extracted with ethyl ether (3x). The combined organic layers were washed with a saturated solution of copper(II) sulfate (2x), brine (2x), dried over magnesium sulfate, filtered, concentrated under reduced pressure. Purification by flash chromatography [1:9 (vol/vol) EtOAc:hexanes to 1:3 (vol/vol) EtOAc:hexanes] afforded **2.26** (1.7 g, 81%) as a light yellow oil. Characterization of this compound matched a published report.[212]

(2*Z*,6*Z*)-Ethyl 3,7,11-trimethyldodeca-2,6,10-trienoate (2.27)

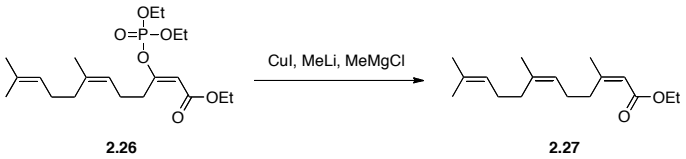

2.26 **2.27**

A suspension of copper(I) iodide (76 mg, 0.40 mmol) in freshly distilled tetrahydrofuran (3.3 mL) under Ar atmosphere was cooled to 0 °C. Methyllithium (1.6M in Et_2O, 0.25 mL, 0.40 mmol) was added dropwise and the reaction stirred at 0 °C for 10 min. The reaction was cooled

to –30 °C for 10 min, followed by dropwise addition of methylmagnesium chloride (3.0M in THF, 0.18 mL, 0.53 mmol). After 20 min, a solution of **2.26** (53 mg, 0.13 mmol) in freshly distilled tetrahydrofuran (3.3 mL) was added dropwise via cannula using positive nitrogen pressure. The greenish brown suspension stirred at –30 °C for 3.5 h. It was poured into an ice-cold solution of saturated ammonium chloride in a separatory funnel and diluted with ethyl ether. The organic layer was rinsed with a saturated solution of ammonium chloride until the aqueous layer was no longer blue. The organic layer was washed with brine, dried over magnesium sulfate, filtered, and concentrated under reduced pressure. Purification by flash chromatography [1:4 (vol/vol) CH_2Cl_2:hexanes] afforded **2.27** (33 mg, 94%, 5:1 *Z*:*E*) as a clear oil. Characterization of this compound matched a published report.[212]

(2*Z*,6*Z*)-Farnesol (2.28)

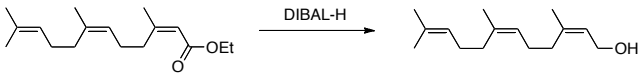

2.27 **2.28**

A solution of **2.27** (1.28 g, 4.83 mmol) in freshly distilled toluene (60.4 mL) under Ar atmosphere was cooled to –78 °C. Diisobutylaluminum hydride (DIBAL-H, 1.0M in toluene, 16.9 mL, 16.9 mmol) was added dropwise. After 1.5 h, the reaction was quenched by addition of a saturated solution of sodium potassium tartrate (120 mL). The clear biphasic mixture was transferred to a separatory funnel and diluted with EtOAc. The layers were separated, and the aqueous layer was extracted with EtOAc (3x). The combined organic layers were washed with brine, dried over magnesium sulfate, filtered, and concentrated under reduced pressure. Purification by flash chromatography [hexanes to 1:9 (vol/vol) EtOAc:hexanes] afforded **2.28** (0.928 g, 86%, 14:1 *Z*:*E*) as a clear film. Characterization of this compound matched a published report.[218]

Diethyl ((2*Z*,6*Z*)-3,7,11-trimethyldodeca-2,6,10-trien-1-yl)phosphonate (2.29)

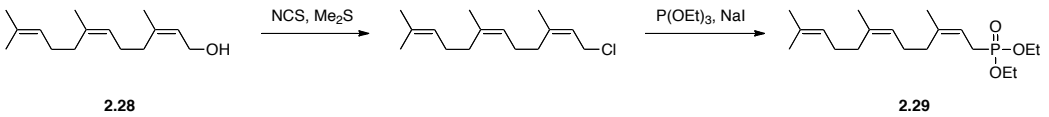

2.28 **2.29**

A solution of *N*-chlorosuccinimide (155 mg, 1.16 mmol, 1.11 eq) in CH_2Cl_2 (2.10 mL) under Ar atmosphere was cooled to –30 °C for 15 min. Methyl sulfide (91.0 μL, 1.23 mmol, 1.18 eq) was added and the solution was warmed to 0 °C for 20 min. The solution was cooled to –30 °C for 10 min, then a solution of **2.28** (233 mg, 1.05 mmol) in CH_2Cl_2 (2.1 mL) was added dropwise via cannula. The solution was warmed to 0 °C and stirred for 1.5 h before warming to ambient temperature. After stirring at ambient temperature for 1 h, the reaction was diluted with hexanes, filtered, and washed with brine (2x). The organic layer was dried over $MgSO_4$, filtered, and concentrated under reduced pressure to afford crude (2*Z*,6*Z*)-farnesyl chloride (203 mg). Sodium iodide (25 mg, 0.17 mmol) and triethyl phosphite (320 μL, 1.86 mmol) were added under Ar atmosphere, and the suspension stirred vigorously at 110 °C for 19 h. The reaction was cooled to ambient temperature, diluted with Et_2O, and washed with saturated sodium thiosulfate (2x) and brine. The organic layer dried over $MgSO_4$, filtered, and concentrated under reduced pressure. Purification by flash chromatography (3:2 ethyl acetate:hexanes) afforded **2.29** (203 mg, 70%) as a clear oil.

^{1}H NMR (400 MHz, $CDCl_3$): δ 5.20 (q, *J* = 7.1 Hz, 1H, vinyl CH), 5.12 (m, 2H, 2 x vinyl CH), 4.16 – 4.01 (m, 4H, OC*H*$_2$CH$_3$), 2.56 (dd, *J* = 21.8, 7.3 Hz, 2H, =CHC*H*$_2$P), 2.05 (d, *J* = 9.5 Hz, 8H, -C*H*$_2$-), 1.75 (d, *J* = 5.0 Hz, 3H, Me), 1.69 (s, 2 x 3H, 2 x Me), 1.61 (s, 3H, Me), 1.31 (t, *J* = 7.1 Hz, 6H, OCH$_2$C*H*$_3$). ^{13}C NMR (101 MHz, $CDCl_3$): δ 140.1 (d), 135.5, 131.4, 124.5, 124.2, 113.1 (d), 61.7, 61.6, 32.2, 32.2, 31.87, 26.6, 26.2 (d), 26.0 (d), 25.6, 23.5, 23.4, 23.3, 17.6, 16.4, 16.4.

^{31}P NMR (162 MHz, $CDCl_3$): δ 28.7. HRMS (ESI-TOF$^+$) for $C_{19}H_{36}O_3P$ (M+H$^+$) calcd 343.2397, found 343.2409.

((2*Z*,6*Z*)-3,7,11-Trimethyldodeca-2,6,10-trien-1-yl)phosphonate (2.14)

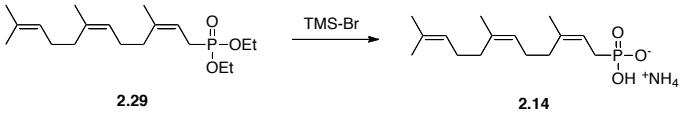

2.29 **2.14**

Compound **2.29** (34 mg, 0.10 mmol) was coevaporated with toluene (3 x 1.5 mL), then dissolved in CH_2Cl_2 (1.4 mL) under Ar atmosphere. Allyltrimethylsilane (23 μL, 0.15 mmol, 1.5 eq) and bromotrimethylsilane (42 μL, 0.32 mmol, 3.2 eq) were added dropwise at ambient temperature and the reaction stirred for 24 h. Additional bromotrimethylsilane (0.13 mL, 9.6 eq) was added to ensure complete deprotection. The reaction stirred for an additional 4 h. The reaction was concentrated under reduced pressure, then diluted with 0.9 mL of 1.0 M ammonium bicarbonate, flash-frozen and lyophilized to afford **2.14** (31 mg, 97%) as an off-white fluffy solid.

^{1}H NMR (400 MHz, CD_3OD): δ 5.34 (q, *J* = 7.0 Hz, 1H, vinyl CH), 5.21 – 5.10 (m, 2H, 2 x vinyl CH), 2.37 (dd, *J* = 20.8, 7.5 Hz, 2H, =CHC*H*$_2$P), 2.12 – 2.03 (m, 8H, -C*H*$_2$-), 1.72 (m, 3H, Me), 1.68 (s, 2 x 3H, 2 x Me), 1.62 (s, 3H, Me). ^{13}C NMR (126 MHz, CD_3OD): δ 137.5 (d), 136.0, 132.3, 126.3, 125.4, 119.4 (d), 33.2 (d), 32.9, 30.3 (d), 27.7, 27.3 (d), 25.9, 23.9 (d), 23.7, 17.7. ^{31}P NMR (162 MHz, CD_3OD): δ 21.4. HRMS (ESI-TOF$^-$) for $C_{15}H_{27}O_3P$ (M-H$^-$) calcd 285.1625, found 285.1636.

Morpholino((2*Z*,6*Z*)-3,7,11-trimethyldodeca-2,6,10-trien-1-yl)phosphinic acid, *N*,*N*′-dicyclohexyl-4-morpholinecarboxamidine salt (2.30)

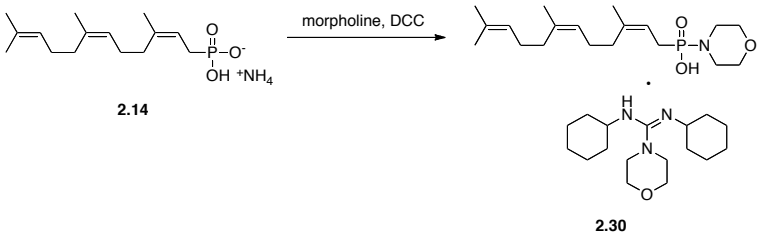

Morpholine (73 μL, 0.84 mmol, 8 eq) was added to a solution of **2.14** (31 mg, 0.11 mmol) in 1:1 *tert*-butanol:water (10.5 mL) under Ar atmosphere at ambient temperature. The solution stirred at ambient temperature for 10 min, then it was heated to 100 °C. After refluxing for 15 min, a solution of dicyclohexylcarbodiimide (433 mg, 2.1 mmol, 20 eq) in *tert*-butanol (3.5 mL) was added over 2.5 h. The reaction was refluxed for an additional 3 h before being concentrated under reduced pressure. The residue was taken up in water (40 mL) and washed with diisopropyl ether (3x). The aqueous layer was flash-frozen and lyophilized. The residue was taken up in methanol (1.5 mL) and loaded onto two Waters Oasis Plus MAX cartridges connected in series. Product eluted with 50 mM ammonium bicarbonate, pH 8.25. Further purification by flash chromatography (80:20:1 $CHCl_3$:MeOH:Et_3N) afforded **2.30** (27.6 mg, 43%) as a white solid.

^{1}H NMR (400 MHz, CD_3OD): δ 8.52 (s, 1H, NH), 5.29 (q, *J* = 7.3 Hz, 1H, vinyl CH), 5.17 – 5.04 (m, 2H, 2 x vinyl CH), 3.72 – 3.68 (m, 10H), 3.63 – 3.57 (m, 1H), 3.53 (t, *J* = 4.6 Hz, 4H), 3.38 (t, *J* = 4.8 Hz, 9H), 3.30 – 3.24 (m, 5H), 3.13 (s, 1H), 3.01 (q, *J* = 4.5 Hz, 4H), 2.30 (dd, *J* = 19.2, 7.7 Hz, 2H, =CHC*H*$_2$P), 2.12 – 1.99 (m, 7H), 1.95 – 1.83 (m, 12H), 1.83 – 1.75 (m, 9H), 1.75 – 1.60 (m, 16H), 1.58 (s, 1H), 1.56 – 1.49 (m, 1H), 1.46 – 1.24 (m, 25H), 1.24 – 1.08 (m, 7H). ^{13}C NMR (126 MHz, CD_3OD): δ 157.9, 134.9, 134.7, 130.9, 124.9, 124.8 (d), 124.0, 118.1 (d), 117.3, 67.5 (d), 65.9, 63.7, 54.6, 48.4, 45.1, 43.0, 33.1, 31.9, 31.5, 31.5 (d), 29.4, 27.8, 26.3, 25.9, 24.9, 24.7, 24.6 (d), 22.5, 22.4, 22.3, 16.4. ^{31}P NMR (162 MHz, CD_3OD): δ 21.4. HRMS (ESI-TOF$^-$) for $C_{19}H_{33}NO_3P$ (M-H$^-$) calcd 354.2203, found 354.2210.

(2-Acetamido-2-deoxy-3-*O*-(2,3,4-tri-*O*-acetyl-α-L-rhamnopyranosyl)-4,6-di-*O*-acetyl-α-D-glucopyranosyl phosphoryl) ((2*Z*,6*Z*)-3,7,11-trimethyldodeca-2,6,10-trien-1-yl)phosphonate (2.31)

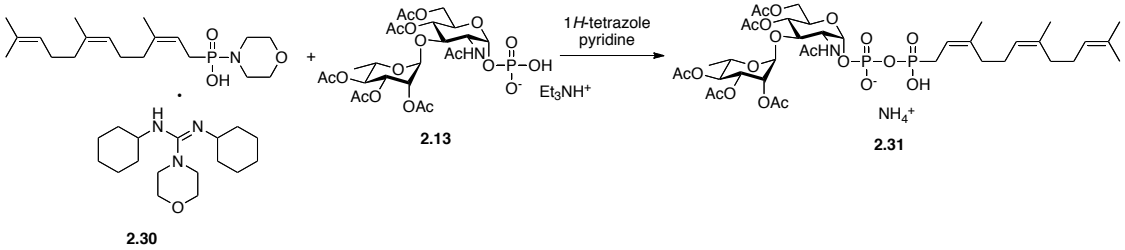

Compounds **2.13** (11 mg, 12 μmol) and **2.30** (16 mg, 25 μmol, 2.0 eq) were coevaporated with toluene (2 x 1.5 mL) and pyridine (2 x 1.5 mL) then placed on high vacuum overnight. A stir bar and 1*H*-tetrazole (2.8 mg, 40 μmol, 3.2 eq) were added under Ar atmosphere, followed by pyridine (0.25 mL). The reaction stirred at ambient temperature for 5 d. It was diluted with methanol and concentrated to dryness. The crude was purified by semi-preparative HPLC on a C18 column (25% B for 5 min, 25% B to 70% B over 45 min, A = 50 mM ammonium bicarbonate and B = acetonitrile). Fractions containing compound **2.31** were pooled and concentrated to a white solid.

^{31}P NMR (162 MHz, CD_3OD): δ 15.41 (d, *J* = 27.4 Hz), -12.90 (d, *J* = 27.6 Hz). HRMS (ESI-TOF$^+$) for $C_{39}H_{64}N_2O_{20}P_2$ ($M+NH_4^+$) calcd 943.3601, found 943.3612.

(2-Acetamido-2-deoxy-3-*O*-(α-L-rhamnopyranosyl)-α-D-glucopyranosyl phosphoryl) ((2*Z*,6*Z*)-3,7,11-trimethyldodeca-2,6,10-trien-1-yl)phosphonate (2.08)

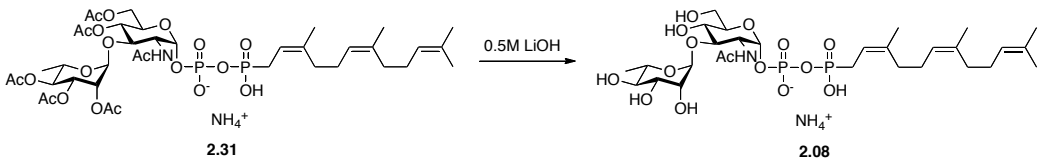

Fractions containing compound **2.31** were treated with 0.5 M lithium hydroxide (1.0 mL) at ambient temperature for 4 h. The reaction mixture was neutralized, and purified immediately by semi-preparative HPLC on a C18 column (25% B for 5 min, 25% B to 70% B over 45 min, A = 50 mM ammonium bicarbonate and B = acetonitrile). Compound **2.08** eluted at 29 min (1.8 mg, 20% over 2 steps) as a white solid.

^{1}H NMR (500 MHz, D_2O): δ 5.45 (dd, *J* = 7.3, 3.1 Hz, 1H, vinyl CH), 5.29 – 5.17 (m, 3H, 2 x vinyl CH, H-1), 4.85 (s, 1H, H-1'), 4.08 (dt, *J* = 10.3, 3.0 Hz, 1H), 3.99 (dq, *J* = 10.1, 6.3 Hz, 1H, H-5'), 3.94 (ddd, *J* = 10.6, 4.8, 2.2 Hz, 1H), 3.90-3.68 (m, 5H), 3.57 (t, *J* = 9.6 Hz, 1H), 3.41 (t, *J* = 9.7 Hz, 1H, H-4'), 2.56 (dd, *J* = 21.5, 7.6 Hz, 2H, =CHC*H*$_2$P), 2.14 – 2.04 (m, 12H, -C*H*$_2$-, NHAc), 1.73 (d, *J* = 4.8 Hz, 3H, Me), 1.68 (s, 2 x 3H, 2 x Me), 1.62 (s, 3H, Me), 1.22 (t, *J* = 6.2 Hz, 3H, Me). ^{13}C NMR (126 MHz, D_2O): δ 163.8, 139.5 (d), 137.1, 133.7, 125.3, 124.4, 115.5 (d), 101.5, 94.5 (d), 79.5, 73.3, 71.9, 70.8, 70.2, 68.9, 68.2, 60.4, 53.3, 31.5 (d), 31.2, 28.5 (d), 25.9, 25.6 (d), 25.0, 22.8 (d), 22.5, 22.2, 17.0, 16.5. ^{31}P NMR (162 MHz, D_2O): δ 16.63 (d, *J* = 28.4 Hz), -13.09 (d, *J* = 28.4 Hz). HRMS (ESI-TOF$^+$) for $C_{29}H_{55}N_2O_{15}P_2$ (M+NH_4^+) calcd 733.3073, found 733.3052.

(*Z*)-diethyl (3,7-dimethylocta-2,6-dien-1-yl)phosphonate (2.35)

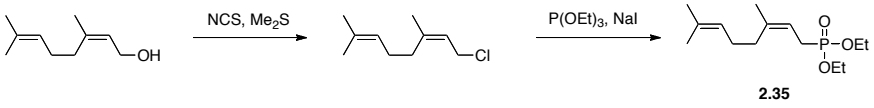

2.35

1. A solution of N-chlorosuccinimide (1.78 g, 13.3 mmol) in freshly distilled CH_2Cl_2 (24 mL) under Ar atmosphere was cooled to –30 °C. After 20 min, dimethyl sulfide (1.04 mL, 14.2 mmol) was added dropwise to the white suspension, and the reaction was warmed to 0 °C. After 20 min at 0 °C, the suspension was cooled to –30 °C for 10 min. Nerol (2.11 mL, 12.0 mmol) was added dropwise, and the suspension was stirred at 0 °C for 3 h. The reaction was then allowed to

warm to ambient temperature. After 45 min, the reaction was diluted with hexanes, filtered, washed with brine, dried over magnesium sulfate, filtered, and concentrated under reduced pressure to afford crude neryl chloride as a yellow oil.

2. Sodium iodide (0.360 g, 2.40 mmol) and triethyl phosphite (4.53 mL, 26.4 mmol) were added to neryl chloride (~12 mmol) under Ar atmosphere and heated to 110 °C. After 13 h, the reaction was cooled to ambient temperature and diluted with ethyl ether. The solution was washed with a saturated solution of sodium thiosulfate (2x), brine, dried over magnesium sulfate, filtered, and concentrated under reduced pressure. Purification by flash chromatography [hexanes to 2:3 (vol/vol) EtOAc:hexanes] afforded **2.35** (2.35 g, 71% over 2 steps) as a light yellow oil.

^{1}H NMR (300 MHz, $CDCl_3$): δ 5.25 – 5.15 (m, 1H, vinyl CH), 5.14 – 5.07 (m, 1H, vinyl CH), 4.16 – 4.03 (m, 4H, OC*H*$_2$$CH_3$), 2.57 (dd, *J* = 21.8, 7.7 Hz, 2H, =CHC*H*$_2$P), 2.10 – 2.05 (m, 4H, -C*H*$_2$-), 1.78 – 1.72 (m, 3H, Me), 1.69 (s, 3H, Me), 1.61 (s, 3H, Me), 1.31 (t, *J* = 7.1 Hz, 6H, OCH_2CH_3). ^{31}P NMR (121 MHz, $CDCl_3$): δ 28.7. HRMS (ESI-TOF$^+$) for $C_{14}H_{28}O_3P$ ($M+H^+$) calcd 275.1771, found 275.1761.

(*Z*)-(3,7-dimethylocta-2,6-dien-1-yl)phosphonate (2.36)

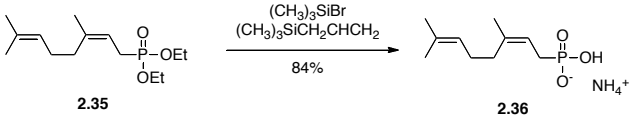

2.35 2.36

Compound **2.35** (0.32 g, 1.18 mmol) was coevaporated with freshly distilled toluene (3x) and kept under high-vacuum overnight. It was dissolved in freshly distilled CH_2Cl_2 (16.8 mL) under Ar atmosphere. Allyltrimethylsilane (0.281 mL, 1.77 mmol) and bromotrimethylsilane (0.498 mL, 3.77 mmol) were added dropwise at ambient temperature. After 5 h stirring at

ambient temperature, the reaction was concentrated under reduced pressure. The residue was taken up in a 1M aqueous solution of ammonium bicarbonate (4 mL), then flash-frozen and lyophilized. The residue was taken up in water, flash-frozen, and lyophilized twice to remove excess salt, affording **2.36** (0.28 g, quant.) as a fluffy white solid.

^{1}H NMR (300 MHz, 25 mM $NaHCO_3$ in D_2O): δ 5.35 – 5.24 (m, 2H, 2 x vinyl CH), 2.42 (dd, *J* = 20.5, 7.8 Hz, 2H, =CHC*H*$_2$P), 2.15 (s, 4H, -C*H*$_2$-), 1.80 – 1.76 (m, 3H, Me), 1.73 (s, 3H, Me), 1.68 (s, 3H, Me). ^{31}P NMR (121 MHz, 25 mM $NaHCO_3$ in D_2O): δ 22.8. ESI-MS ($M-H^-$) for $C_{10}H_{18}O_3P$ calcd 217.1 found 217.0.

(*Z*)-(3,7-dimethylocta-2,6-dien-1-yl)(morpholino)phosphinic acid (2.34)

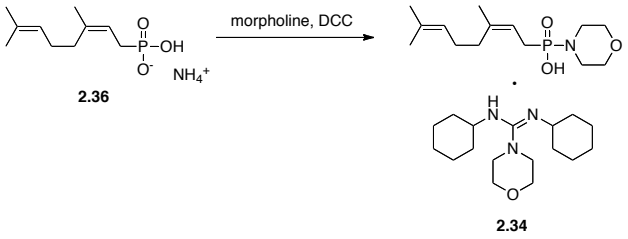

Morpholine (0.7 mL, 8.0 mmol) was added to a solution of **2.36** (0.24 g, 1.0 mmol) in 1:1 v/v *tert*-butanol:water (100 mL) under N_2 atmosphere at ambient temperature. The solution was warmed to 100 °C. After 30 min at 100 °C, a solution of dicyclohexylcarbodiimide (4.13 g, 20.0 mmol) in *tert*-butanol (33 mL) was added slowly via syringe pump over 2.5 h. The solution stirred an additional 3 h at 100 °C, cooled to ambient temperature, and concentrated under reduced pressure. The residue was taken up in water and washed with ethyl ether (3x). The aqueous layer was concentrated under reduced pressure to afford **2.34** (0.60 g) as a white solid.

^{1}H NMR (500 MHz, CD_3OD): δ 8.52 (br s, 1H), 5.32 (q, *J* = 7.1 Hz, 1H), 5.17-5.11 (m, 1H), 3.76-3.72 (m, 6H), 3.59-3.54 (m, 4H), 3.44-3.39 (m, 6H), 3.37-3.32 (m, 2H), 3.05 (q, *J* = 4.2 Hz,

4H), 2.35 (dd, *J* = 19.3, 7.5 Hz, 2H), 2.11-2.07 (m, 4H), 1.99 - 1.87 (m, 6H), 1.87-1.75 (m, 6H), 1.74-1.64 (m, 9H), 1.62 (s, 3H), 1.48-1.32 (m, 9H). ^{13}C NMR (126 MHz, CD_3OD): δ 159.3, 137.0 (d), 132.4, 125.4, 119.6 (d), 68.9, 68.9, 67.3, 56.0, 49.8, 46.4, 34.4, 33.2, 30.0, 29.0, 27.5, 27.5, 26.3, 26.2, 26.0, 23.8 (d), 17.8. ^{31}P NMR (162 MHz, CD_3OD): δ 21.0. HRMS (ESI-TOF$^-$) for $C_{14}H_{25}NO_3P$ (M^-) calcd 286.157, found 286.1593.

(2-Acetamido-2-deoxy-3-*O*-(2,3,4-tri-*O*-acetyl-α-L-rhamnopyranosyl)-4,6-di-*O*-acetyl-α-D-glucopyranosyl phosphoryl) ((*Z*)-(3,7-dimethylocta-2,6-dien-1-yl)phosphonate (2.37)

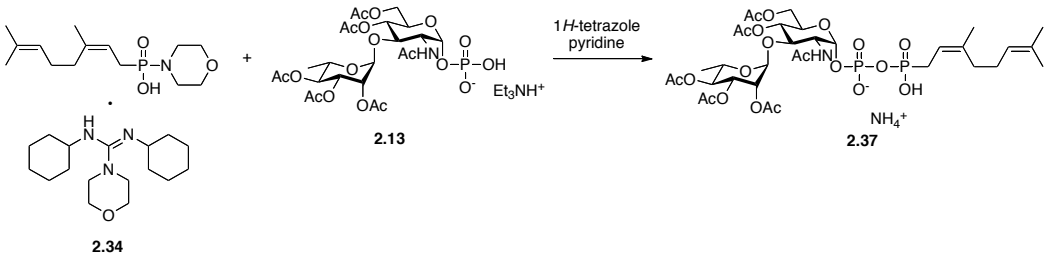

Compounds **2.13** (triethylammonium salt, 39 mg, 45 μmol) and **2.34** (66 mg, 0.11 mmol) were combined, coevaporated with anhydrous pyridine (3 x 1.5 mL) and kept under high vacuum overnight. 1*H*-tetrazole (13 mg, 0.18 mmol) and anhydrous pyridine (0.26 mL) were added, and the solution stirred at ambient temperature for 5 d. It was concentrated under reduced pressure and coevaporated with toluene (3x). The residue was taken up in MeOH and loaded onto a Bio-Gel P-2 column (2.5 cm x 30 cm). Fractions containing product eluted with 0.25 M ammonium bicarbonate, and concentrated under reduced pressure. The residue was taken up in water and further purified by loading onto two Waters Sep-Pak Plus C18 cartridges connected in series. Gradient elution [0.05 M ammonium bicarbonate to MeOH] afforded fractions containing product. The residue was purified by semi-preparative HPLC on a C18

column (20% B for 5 min, 20% B to 60% B over 45 min, A = 20 mM ammonium bicarbonate and B = acetonitrile). Compound **2.37** eluted at 40 min (13 mg, 32%) as a white solid.

^{1}H NMR (400 MHz, D_2O): δ 5.50 (dd, *J* = 7.0, 3.0 Hz, 1H, H-1), 5.31 – 5.19 (m, 3H), 5.19 – 5.11 (m, 3H), 5.04 (s, 1H, H-1'), 4.97 (t, *J* = 9.7 Hz, 1H), 4.40 (dd, *J* = 12.7, 2.2 Hz, 1H), 4.32 – 4.26 (m, 2H), 4.20 – 4.10 (m, 2H), 3.99 – 3.91 (m, 1H), 2.64 – 2.50 (m, 2H, =CHC*H*$_2$P), 2.18 (s, 3H, OAc), 2.16 – 2.09 (m, 10H, 2 x OAc, -C*H*$_2$-), 2.10 (s, 3H, OAc), 2.07 (s, 3H, OAc), 2.00 (s, 3H, NHAc), 1.75 (d, *J* = 4.3 Hz, 3H, Me), 1.69 (s, 3H, Me), 1.63 (s, 3H, Me), 1.20 (d, *J* = 6.2 Hz, 3H, Me). ^{31}P NMR (162 MHz, D_2O): δ 16.78 (d, *J* = 27.6 Hz), -13.35 (d, *J* = 28.6 Hz). HRMS (ESI-TOF$^-$) for $C_{34}H_{52}NO_{20}P_2$ (M-H) calcd 856.2563, found 856.2584.

(2-Acetamido-2-deoxy-3-*O*-(α-L-rhamnopyranosyl)-α-D-glucopyranosyl phosphoryl) ((*Z*)-(3,7-dimethylocta-2,6-dien-1-yl)phosphonate (2.32)

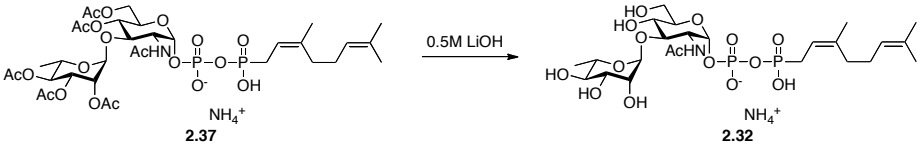

Compound **2.37** (13 mg, 14 μmol) was treated with 0.5 M lithium hydroxide (1.0 mL) at ambient temperature for 4.5 h. The reaction mixture was neutralized, and purified immediately by semi-preparative HPLC on a C18 column (20% B for 5 min, 20% B to 60% B over 45 min, A = 20 mM ammonium bicarbonate and B = acetonitrile). Compound **2.32** eluted at 13 min (7.2 mg, 74%) as a white solid.

^{1}H NMR (500 MHz, D_2O): δ 5.44 (dd, *J* = 7.1, 3.1 Hz, 1H, H-1), 5.28 – 5.17 (m, 2H, 2 x vinyl CH), 4.84 (s, 1H, H-1'), 4.08 (dt, *J* = 10.3, 2.9 Hz, 1H), 4.02 – 3.95 (m, 1H, H-5'), 3.94 – 3.90 (m, 1H), 3.89 – 3.66 (m, 5H), 3.57 (t, *J* = 9.6 Hz, 1H), 3.40 (t, *J* = 9.6 Hz, 1H, H-4'), 2.55 (dd, *J* = 21.5, 7.6 Hz, 2H, =CHC*H*$_2$P), 2.15 – 2.08 (m, 4H, -C*H*$_2$-), 2.07 (s, 3H, NHAc), 1.72 (d, *J*

= 4.7 Hz, 3H, Me), 1.67 (s, 3H, Me), 1.61 (s, 3H, Me), 1.21 (d, *J* = 6.3 Hz, 3H, Me). ^{13}C NMR (126 MHz, D_2O): δ 166.4, 139.6 (d), 133.7, 124.3, 115.4 (d), 101.4, 94.5 (d), 79.5, 73.3, 71.9, 70.7, 70.2, 68.9, 68.2, 60.4, 53.3 (d), 31.2, 28.5 (d), 25.8, 24.9, 22.7 (d), 22.2, 17.0, 16.5. ^{31}P NMR (162 MHz, D_2O): δ 17.13 (d, *J* = 28.1 Hz), -13.01 (d, *J* = 28.1 Hz). HRMS (ESI-TOF$^+$) for $C_{24}H_{47}N_2O_{15}P_2$ ($M+NH_4^+$) calcd 665.2447, found 665.2438.

Benzyl 2-acetamido-2-deoxy-3,4,6-tri-*O*-acetyl-D-glucopyranoside (2.39)

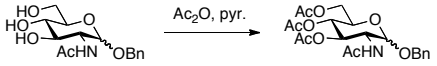

2.19 **2.39**

A solution of **2.19** (0.92 g, 3.0 mmol) and 4-(dimethylamino)pyridine (3.6 mg, 30 μmol) in anhydrous pyridine (3 mL) was cooled to 0 °C under Ar atmosphere. Acetic anhydride (1.4 mL, 14.8 mmol) was added dropwise, then the solution was allowed to warm to ambient temperature. After 24 h, the reaction was concentrated under reduced pressure and coevaporated with toluene (3x). Purification by flash chromatography [CH_2Cl_2 to 5:95 (vol/vol) MeOH:CH_2Cl_2] afforded **2.39** (1.3 g, quantitative) as an oil. Characterization of this compound matched a published report.[220]

2-Acetamido-2-deoxy-3,4,6-tri-*O*-acetyl-D-glucopyranose (2.40)

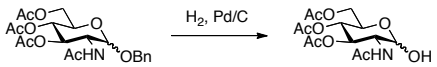

2.39 **2.40**

Palladium on carbon (10%, 0.44 g) was added to a solution of **2.39** (0.87 g, 2.0 mmol) in freshly distilled MeOH (20 mL), and the flask was evacuated/backfilled with H_2 via balloon (4x). The reaction stirred vigorously at ambient temperature for 16 h, then it was filtered through

Celite (rinsed with MeOH) and a 0.22 μm filter, and concentrated under reduced pressure to afford **2.40** (0.68 g, 97%) as a white foam. Characterization of this compound matched a published report.[209]

Dibenzyl 2-acetamido-2-deoxy-3,4,6-tri-*O*-acetyl-D-glucopyranosyl phosphate (2.41)

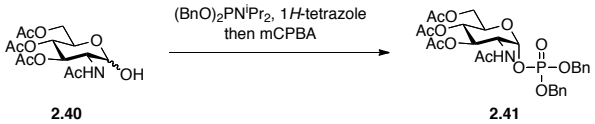

Lactol **2.40** (0.66 g, 1.9 mmol) was coevaporated with freshly distilled toluene, then dissolved in freshly distilled CH_2Cl_2 (13.6 mL) under Ar atmosphere. In a separate flask, 1*H*-tetrazole (0.63 g, 8.9 mmol) was dissolved in freshly distilled CH_2Cl_2 (13.6 mL) under Ar atmosphere. Dibenzyl *N,N*-diisopropyl phosphoramidite (Toronto Research Chemicals, 1.9 mL, 5.7 mmol) was added to the tetrazole suspension slowly. The lactol solution was rapidly transferred into the amidite/tetrazole solution via cannula at ambient temperature using positive nitrogen pressure. After 3 h, *meta*-chloroperoxybenzoic acid (77% max, 2.3 g, 10.5 mmol) was added in one portion. After 2 h, the reaction was diluted with CH_2Cl_2, washed with a 10% (w/w) solution of sodium thiosulfate (2x), a saturated solution of sodium bicarbonate (2x), water (2x), dried over magnesium sulfate, filtered, and concentrated under reduced pressure. Purification by flash chromatography [hexanes to 3:2 (vol/vol) acetone:hexanes] afforded **2.41** (0.93 g, 63%) as a white solid. Characterization of this compound matched a published report.[209]

2-Acetamido-2-deoxy-3,4,6-tri-*O*-acetyl-D-glucopyranosyl phosphate (2.38)

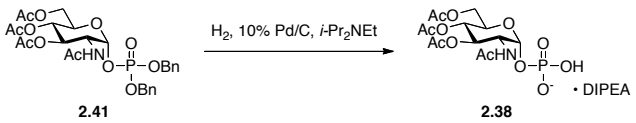

Diisopropylethylamine (0.76 mL) was added to a solution of **2.41** (0.32 g, 0.53 mmol) in MeOH (7.6 mL). Palladium on carbon (10%, 0.16 g, 50% w/w w.r.t. sugar) was added, and the flask was evacuated/backfilled with H_2 via balloon (4x). The reaction stirred vigorously at ambient temperature for 4 h, then it was filtered through Celite (rinsed with MeOH) and a 0.22 μm filter, and concentrated under reduced pressure to afford **2.38** (0.31 g, 79%) as a white solid. Characterization of this compound matched a published report.[209]

(2-Acetamido-2-deoxy-3,4,6-tri-*O*-acetyl-α-D-glucopyranosyl phosphoryl) ((*Z*)-(3,7-dimethylocta-2,6-dien-1-yl)phosphonate (2.42)

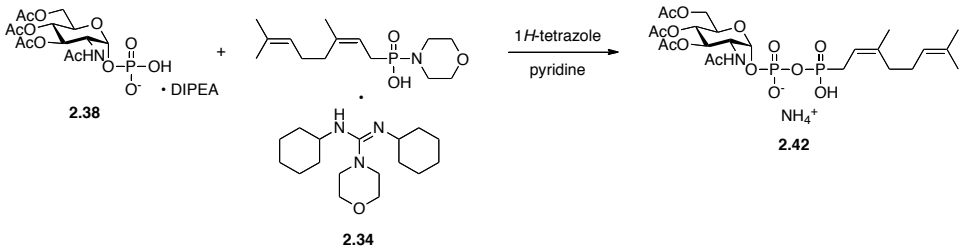

Compounds **2.38** (diisopropylethylammonium salt, 40 mg, 54 μmol) and **2.34** (63 mg, 0.11 mmol) were combined, coevaporated with anhydrous pyridine (3 x 1.0 mL), and placed under high vacuum overnight. 1*H*-tetrazole (12 mg, 0.17 mmol) and anhydrous pyridine (0.3 mL) were added under Ar atmosphere, and the solution stirred at ambient temperature for 3 d. The solution was concentrated under reduced pressure and coevaporated with toluene (2x). Partial purification was achieved by chromatography through a Biogel P-2 column (2.5 mm x 30 mm), eluting with 0.25 M ammonium bicarbonate. Fractions containing product were concentrated under reduced pressure. The residue was taken up in water and loaded onto two

Waters Sep-Pak Plus C18 cartridges connected in series. Elution with 1:2 (vol/vol) MeOH:50 mM ammonium bicarbonate (pH 8.25) afforded **2.42** (14 mg, 40%) as a white solid.

^{1}H NMR (400 MHz, D_2O): δ 5.56 (dd, *J* = 6.9, 3.2 Hz, 1H, H-1), 5.32 (t, *J* = 10.0 Hz, 1H, H-3), 5.28 – 5.19 (m, 2H, 2 x vinyl CH), 5.14 (t, *J* = 9.8 Hz, 1H, H-4), 4.45 (dd, *J* = 12.7, 2.4 Hz, 1H, H-2), 4.41 – 4.30 (m, 2H, H-6, H-6'), 4.18 (d, *J* = 12.5 Hz, 1H, H-5), 2.68 – 2.54 (m, 2H, CH_2P), 2.16 - 2.10 (m, 6H, 2 x Me), 2.08 (s, 3H, Me), 2.03 (s, 3H, Me), 2.00 (s, 3H, Me), 1.75 (d, *J* = 4.3 Hz, 4H, 2 x -CH_2-), 1.68 (s, 3H, Me), 1.63 (s, 3H, Me). ^{31}P NMR (162 MHz, D_2O): δ 17.57 (d, *J* = 27.3 Hz), -13.45 (d, *J* = 25.3 Hz). HRMS (ESI-TOF$^+$) for $C_{24}H_{39}NNaO_{14}P_2$ (M+Na$^+$) calcd 650.1739, found 650.1731.

(2-Acetamido-2-deoxy-α-D-glucopyranosyl phosphoryl) ((*Z*)-(3,7-dimethylocta-2,6-dien-1-yl)phosphonate (2.33)

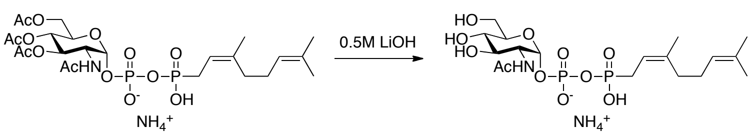

2.42 2.33

Compound **2.42** (14 mg, 22 μmol) was treated with 0.5 M lithium hydroxide (2.0 mL) at ambient temperature for 4.5 h. The reaction mixture was neutralized, and purified immediately by semi-preparative HPLC on a C18 column (0% B for 5 min, 0% B to 50% B over 50 min, A = 20 mM ammonium bicarbonate and B = acetonitrile). Compound **2.33** eluted at 38 min (9.6 mg, 83%) as a white solid.

^{1}H NMR (600 MHz, D_2O): δ 5.49 (dd, *J* = 7.2, 3.3 Hz, 1H), 5.32 – 5.23 (m, 2H), 4.00 (dt, *J* = 10.2, 3.0 Hz, 1H), 3.96 (ddd, *J* = 10.2, 4.5, 2.3 Hz, 1H), 3.90 (dd, *J* = 12.4, 2.3 Hz, 1H), 3.87 – 3.79 (m, 2H), 3.60 – 3.53 (m, 1H), 2.59 (dd, *J* = 21.5, 7.7 Hz, 2H), 2.20 – 2.12 (m, 4H), 2.09 (s,

3H), 1.76 (d, *J* = 4.8 Hz, 3H), 1.71 (s, 3H), 1.66 (s, 3H). ^{13}C NMR (126 MHz, D_2O): δ 174.8, 139.6 (d), 133.7, 124.4, 115.5 (d), 94.4 (d), 73.0, 71.1, 69.6, 60.4, 53.7, 31.2, 28.5 (d), 25.8 (d), 24.9, 22.7 (d), 22.2, 17.0. ^{31}P NMR (243 MHz, D_2O): δ 16.77 (d, *J* = 28.1 Hz), -12.98 (d, *J* = 28.1 Hz). HRMS (ESI-TOF$^-$) for $C_{18}H_{32}NO_{11}P_2$ (M^-) calcd 500.1456, found 500.1461.

Chapter 3: Isoprenoid Phosphonophosphates as Acceptor Substrates for Mycobacterial Glycosyltransferases

Portions of this work have been published in:

Martinez Farias, M. A.; Kincaid, V. A.; Annamalai, V. R.; Kiessling, L. L. Isoprenoid Phosphonophosphates as Glycosyltransferase Acceptor Substrates. *J. Am. Chem. Soc.* DOI: 10.1021/ja500622v.

Contributions:

Cloning and expression of GlfT1 performed by V.A. Kincaid.

3.1 Abstract

Glycosyltransferases that act on polyprenol pyrophosphate substrates are challenging to study because their lipid-linked substrates are difficult to isolate from natural sources and arduous to synthesize. To facilitate access to an appropriate glycosyl acceptor, we assembled phosphonophosphate analogs and showed these are effective substrate surrogates for GlfT1, the essential product of mycobacterial gene *Rv3782*. Using chemically defined conditions, we found that the galactofuranosyltransferase GlfT1 catalyzes the formation of a tetrasaccharide sequence en route to assembly of the mycobacterial galactan.

3.2 Introduction

Mycobacterial resistance to antibiotic treatment is thought to stem from the impermeability of the cell wall and active efflux of antibiotics. In the latter case, efflux pumps actively pump antibiotics that pass through the cell wall into the inner membrane out of the cell.[222,223] Active efflux of first-line antibiotic isoniazid by the transporter MmpL7, an example of many antibiotics pumped out of cells by various transporters, presents a difficult challenge in treatment of mycobacterial infections.[224] Understanding the assembly of the primary mycobacterial barrier, the cell wall, could provide new avenues to disrupt mycobacterial growth.

The structure of the mycolyl-arabinogalactan-peptidoglycan (mAGP) complex that makes up the cell wall is known (Figure 3.1). As discussed in Chapter 1, the use of acceptor substrate analogs has clarified a variety of mechanistic process in cell wall biosynthesis. Peptidoglycan assembly, from glycan chain formation to transpeptidation, is now fairly well understood. While factors that control galactan polymerization by the polymerase GlfT2 are becoming clearer, precisely how this galactofuranose polysaccharide is synthesized as mycobacteria grow and divide is not understood. With acceptor substrate surrogates from Chapter 2, we sought to illuminate the process of galactan biosynthesis.

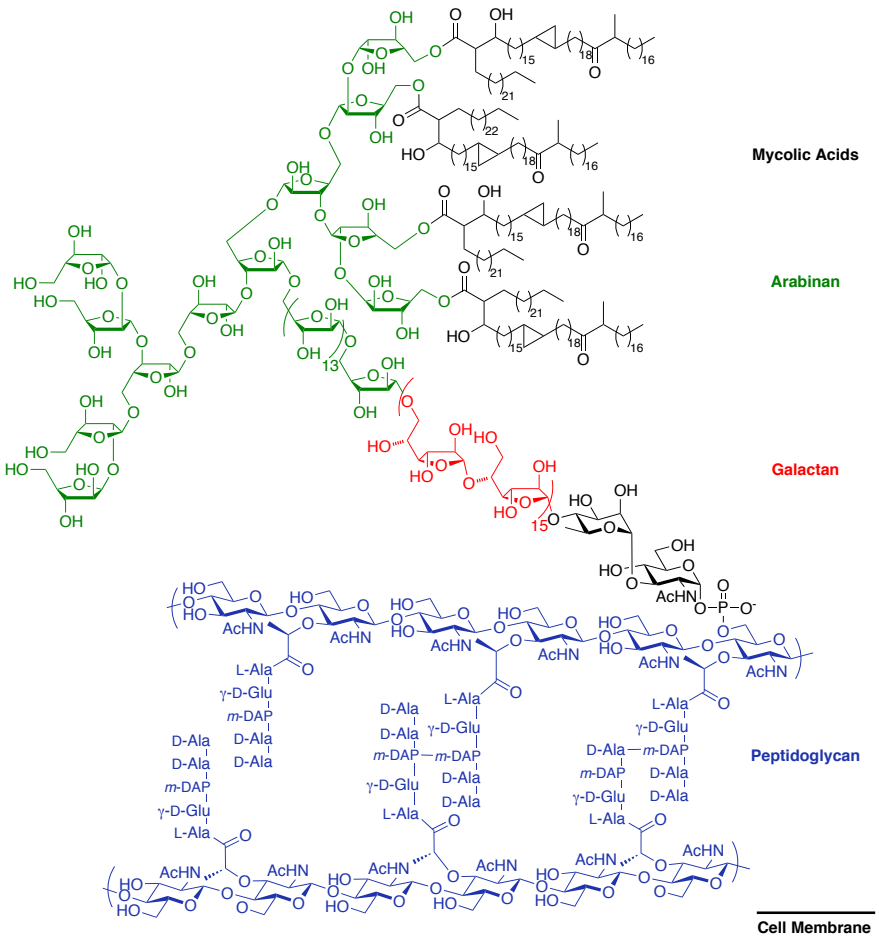

Figure 3.1. Structure of the mycobacterial mycolyl-arabinogalactan-peptidoglycan (mAGP) cell wall complex.

3.3 Chemically defined conditions to investigate GlfT1 function

Despite the wealth of knowledge about cell wall structure and function, the early steps of galactan biosynthesis are poorly understood. A hypothetical stepwise mechanism for assembly is depicted in Figure 2.3. Specifically, GlfT1 is thought to catalyze the addition of one to three Gal*f* residues to decaprenyl-linked Rha-α(1,3)-GlcNAc pyrophosphate **2.01**. However, it has proved elusive to define its activity because previous reports noted loss of activity upon stripping the enzyme from the cell envelope.[108] *E. coli* lysates overexpressing *M. smegmatis* GlfT1 may add one Gal*f* residue to octyl Rha-α(1,3)-GlcNAc, but these studies monitored activity by migration

of radiolabeled products by thin-layer chromatography and the reaction was carried out in a complex mixture of enzymes, lipids, and other biosynthetic intermediates (62.5% *E. coli* lysate by volume). The purported products are not consistent with our results. We were unable to detect any activity in a defined system (e.g., recombinant GlfT1 and substrates) using 12-phenoxydoc-2-enyl Rha-α(1,3)-GlcNAc, which is similar to octyl Rha-α(1,3)-GlcNAc used in prior experiments.[110] In light of the provocative questions regarding GlfT1 function, we interrogated its activity under chemically defined conditions.

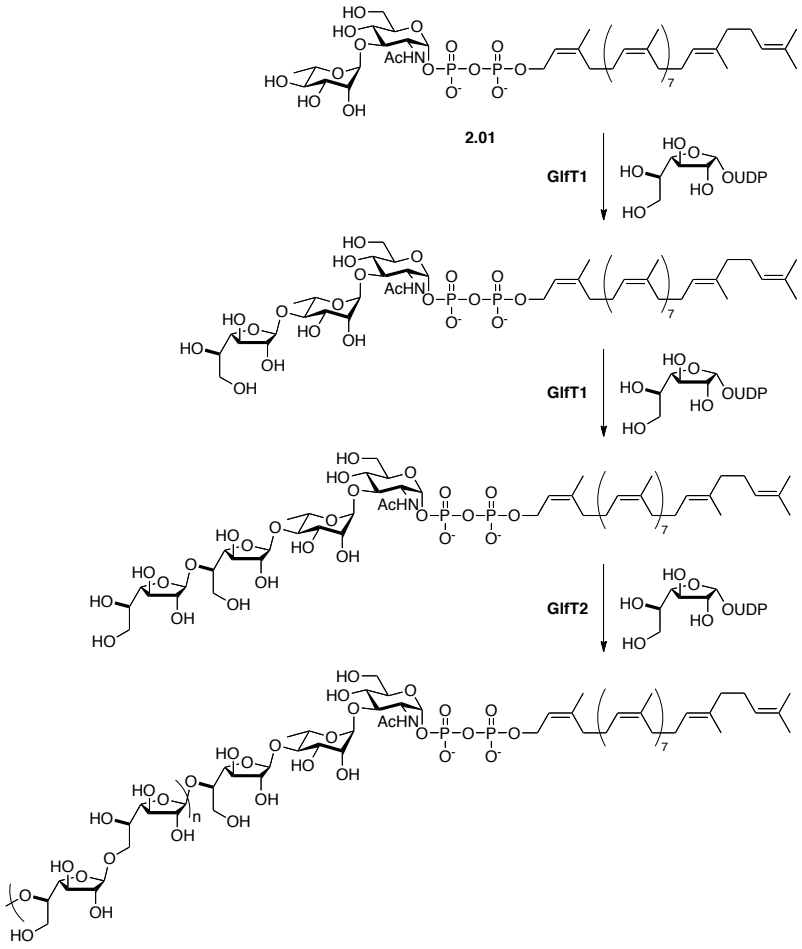

Figure 3.2. GlfT1 and GlfT2 mediate galactan biosynthesis.

3.3.1 Reconstituting GlfT1 activity in vitro

To date, GlfT1 activity has not been assessed in a defined system. Thus, we had no mechanism to validate enzymatic activity when we observed no processing of the simpler glycolipid acceptors **2.02** and **2.04** described in Chapter 2 (Figure 3.3). Lack of galactofuranosyltransferase activity could result from the inadequacy of the acceptors or from an inert enzyme. Phosphonophosphate acceptors such as **2.08** and **2.32** could resolve this dilemma, since we could provide GlfT1 substrates that we were confident would serve as good mimics of the endogenous acceptor.

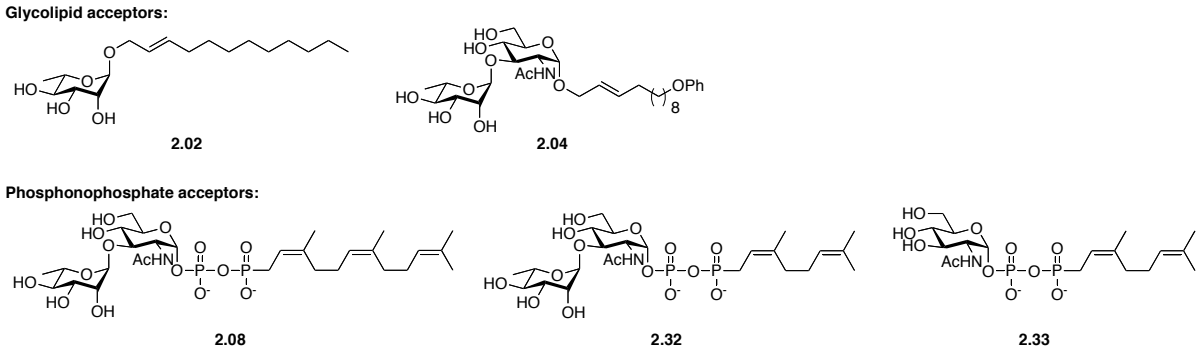

Figure 3.3. Acceptor substrate analogs for GlfT1.

With phosphonophosphate-linked acceptor surrogates in hand, we tested their ability to serve as substrates using purified GlfT1. Recombinant His_6-tagged *M. smegmatis* GlfT1 was produced in *M. smegmatis* mc^2155 and isolated by affinity chromatography. Exposure of disaccharide **2.08** to GlfT1 in the presence of donor sugar UDP-Gal*f*[106] resulted in the production of oligosaccharide products (Figure 3.4), indicating that compound **2.08** is an effective substrate. Analysis by matrix-assisted laser desorption/ionization time-of-flight (MALDI-TOF) mass spectrometry indicated that the major product of GlfT1 catalysis is an acceptor extended by +2 Gal*f* units. A product extended by +3 Gal*f* units is also observed. GlfT1 consumes nearly all of the acceptor to produce these oligosaccharides.

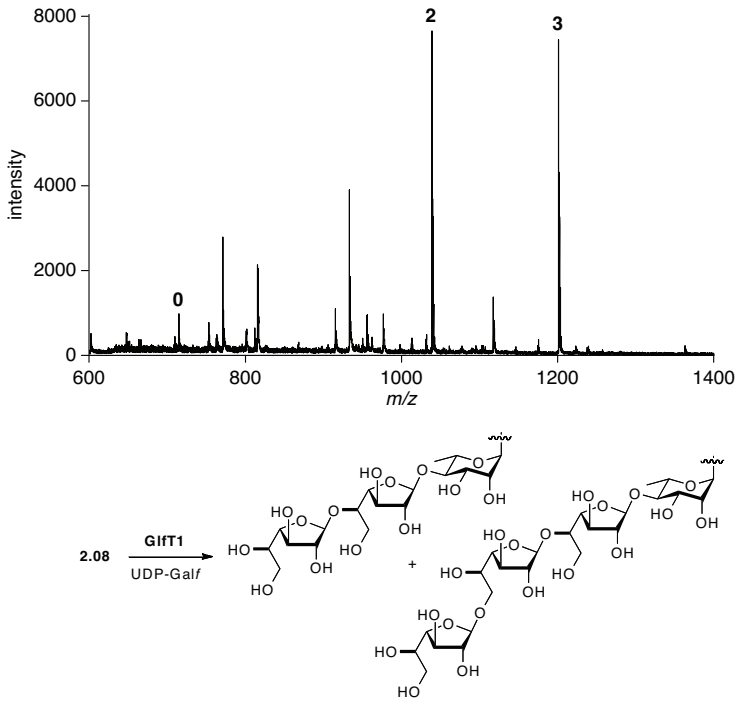

Figure 3.4. Top: Representative MALDI-TOF mass spectrum obtained from a reaction mixture of compound **2.08**, UDP-Gal*f*, and GlfT1. Masses corresponding to +2 and +3 Gal*f* residues were observed. Bottom: Corresponding +2 and +3 products from elongation of acceptor **2.08**. The linkage pattern shown is in agreement with that of endogenous galactan.

The +1 product was not detected, a relevant finding given that the polymerase GlfT2 can elongate an acceptor with a single Gal*f* residue.[118] We postulate that the ability of GlfT2 to generate a polymer with faithfully alternating β-(1,5) and β-(1,6) linkages depends on the ability of GlfT1 to catalyze the formation of the +2 Gal*f* disaccharide. In this way, GlfT1 sets the register for polymerization by GlfT2.[116,117,119] The +2 disaccharide product may also lead to more efficient polymerization by GlfT2. We previously showed that GlfT2 exhibits a kinetic lag phase when polymerizing a lipid-linked Gal*f* disaccharide.[116] The lag phase was abrogated with a substrate bearing a Gal*f* tetrasaccharide, as this oligosaccharide presumably fills the monomer subsites during polymerization.[117] Thus, the tetrasaccharide product generated by the action of GlfT1 should be processed rapidly by GlfT2.

Neryl-linked acceptor surrogate **2.32** also served as an acceptor for the enzyme (Figure 3.5). As with **2.08**, no +1 Gal*f* product is observed. With both of the active phosphonophosphate substrates, the +1 Gal*f* intermediate is completely consumed by GlfT1 and converted to the +2 Gal*f* product. This result is particularly striking with acceptor **2.32**, given that some acceptor remains as observed by MALDI-TOF MS. We conclude that an isoprenyl-linked phosphonophosphate trisaccharide bearing a terminal Gal*f* residue is an excellent acceptor substrate for GlfT1. To compare the relative efficiency of these acceptors, however, we required a quantitative means of assessing catalysis.

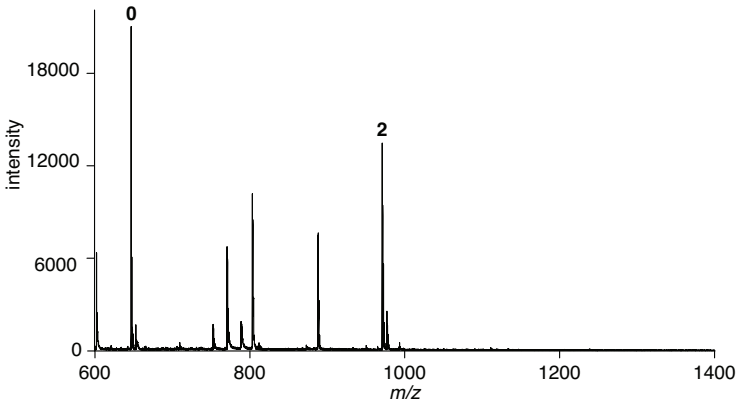

Figure 3.5. Representative MALDI-TOF mass spectrum obtained from a reaction mixture of compound **2.32**, UDP-Gal*f*, and GlfT1. A mass corresponding to +2 Gal*f* residues was observed.

3.3.2 Quantification of UDP release by GlfT1 with phosphonophosphate acceptor substrates

The identity of the lipid carrier can affect a substrate's ability to serve as a glycosyl acceptor. We therefore analyzed the efficiency of elongation of substrates bearing different lipids by quantifying the amount of UDP released upon GlfT1 addition. Specifically, the assay employed couples UDP production to the luciferase/luciferin reaction, wherein UDP production by GlfT1 is related linearly to increases in luminescence (Figure 3.6, top).[225] The luminescence readout is fitted to a standard curve made from a dilution series of known UDP concentrations.

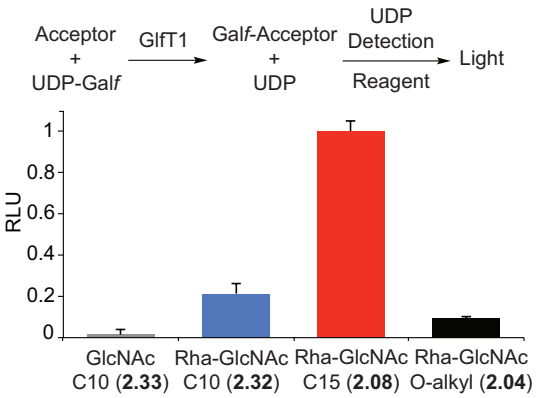

Figure 3.6. Top: Glycosyltransferase activity promotes UDP release, which is monitored using a luminescence assay. Bottom: Relative output of UDP-Gal*f* turnover by GlfT1 with acceptors **2.04**, **2.08**, **2.32**, and **2.33**.

As expected, no GlfT1 activity was observed with monosaccharide **2.33**, highlighting that GlfT1 requires a substrate bearing the disaccharide Rha-α(1,3)-GlcNAc (Figure 3.6, bottom). Minor production of UDP was observed with the catalytically inactive alkyl disaccharide **2.04**. The difference between C_{10}-linked **2.32** and C_{15}-linked **2.08** was pronounced. GlfT1 treatment produces almost five times as much UDP in the presence of acceptor **2.08** than with **2.32**. These data indicate the longer (2Z,6Z)-farnesyl lipid of acceptor **2.08** renders it a markedly better substrate for the enzyme. We previously found that the lipid substituent is important in the binding of acceptor substrates to GlfT2,[116] and our results suggest a similar role for GlfT1 acceptors.

3.3.3 Kinetics analysis of GlfT1 turnover with a farnesyl-linked acceptor

We utilized the luminescence assay to observe the kinetics of elongation by GlfT1. Reaction conditions were tuned to observe UDP production under saturating conditions of donor sugar UDP-Gal*f*. Production of UDP over time was measured and an early time point was chosen for further analysis (Figure 3.7).

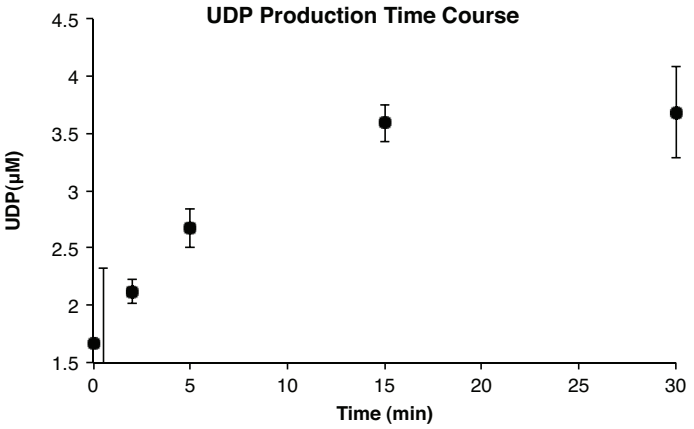

Figure 3.7. Relative output of UDP-Gal*f* turnover by GlfT1 with acceptors **2.08** monitored over time.

GlfT1 was challenged with varied concentrations of acceptor, from 0.2–200 μM of **2.08**. By fitting the rates of UDP production at each of these concentrations to the Michaelis-Menten equation, we determined an apparent K_m of 86 ± 25 μM for acceptor **2.08** and an apparent V_{max} of 1.53 ± 0.16 μM/min (Figure 3.8). These values are in the range of what is expected for the endogenous substrate.

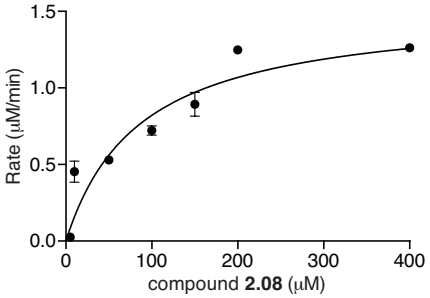

Figure 3.8. Analysis of a GlfT1 reaction mixture with UDP-Gal*f* and varied concentrations of acceptor **2.08**.

The ability of the phosphonophosphate analogs to serve as effective substrates reveals fundamental features of the galactofuranosyltransferase GlfT1. These acceptors, the closest mimics of the natural substrate available, are processed to lipid-linked oligosaccharides by GlfT1. Moreover, our studies indicate that the activity of GlfT1 outside of the endogenous mycobacterial milieu is robust—it does not require the presence of membranes or cell envelope. Though similar GT-A domains and significant amino acid sequence identity (24% by ClustalO alignment) suggest an evolutionary link between GlfT1 and GlfT2, our results highlight their distinct roles in galactan assembly. Specifically, GlfT1 does not process O-alkyl disaccharides. It requires a lipid-linked pyrophosphate group or analog thereof substituted with the disaccharide L-Rha-α(1,3)-D-GlcNAc, which it elongates by two to three Gal*f* residues. In contrast to the polymerase GlfT2, GlfT1 does not form longer polymers and its substrate preference appears to be more narrowly defined. Indeed, GlfT2 is a relatively promiscuous carbohydrate polymerase that can act on varied truncated lipid-linked acceptors.[115,118] The high specificity of GlfT1 and its ability to append at least two Gal*f* residues should increase the kinetics of polymerization by GlfT2 and its ability to generate a polysaccharide of defined sequence. Thus, GlfT1 has a critical role in controlling galactan biosynthesis.

3.4 Use of phosphonophosphate-linked oligosaccharides in galactan assembly

Two prevailing factors could govern the oligosaccharide product distribution obtained in the mixtures described above: intrinsic length control by GlfT1 via dissociation of products from the enzyme active site, or limited enzymatic stability leading to poor turnover of acceptor intermediates. If the product distribution is intrinsic to GlfT1, longer oligosaccharides should not be observed upon re-exposure of the mixture to the enzyme.

We sought to take advantage of the defined conditions of the *in vitro* assays by isolating preparative quantities of the oligosaccharide products. This material permits the dissection of factors governing the observed product distribution, in addition to providing material analogous to the endogenous acceptor substrate for the polymerase GlfT2.

3.4.1 Isolation of phosphonophosphate-linked tetra- and pentasaccharides

Several GlfT1 reaction mixtures with acceptor **2.08** were combined, and the oligosaccharides were separated from reaction components by semi-preparative reverse-phase high-performance liquid chromatography (HPLC). The desired fractions were pooled and analyzed by MALDI-TOF MS. A mixture of +2 Gal*f* and +3 Gal*f* oligosaccharides was isolated, corresponding to chemoenzymatically-prepared endogenous acceptor substrate surrogates for GlfT2 (Figure 3.9, top).

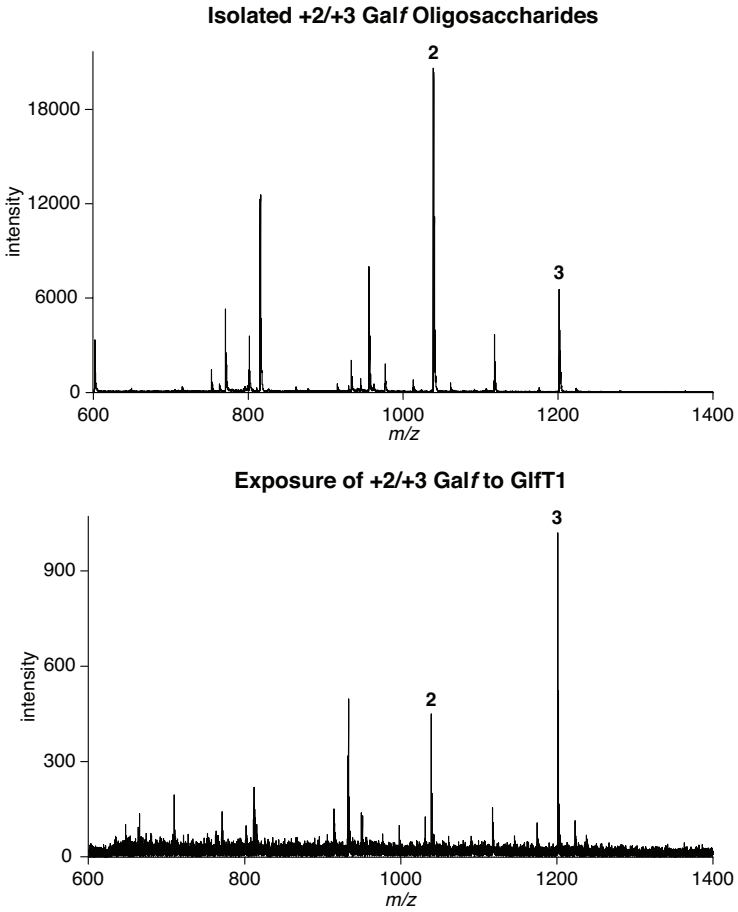

Figure 3.9. Isolation of +2 Gal*f* and +3 Gal*f* products from a reaction mixture of acceptor **2.08**, UDP-Gal*f*, and GlfT1.

Intrinsic control of oligosaccharide distribution by GlfT1 can be demonstrated by re-exposure of the isolated +2 Gal*f* and +3 Gal*f* mixture to the enzyme. The terminal products should not be processed into larger oligosaccharides upon re-exposure. Indeed, incubation of the isolated +2/+3 Gal*f* mixture with UDP-Gal*f* and GlfT1 resulted in a similar +2/+3 Gal*f* population, albeit enriched in +3 Gal*f* (Figure 3.9, bottom). The product distribution is otherwise unchanged, suggesting that the observed glycans represent the terminal products generated by GlfT1, independent of the starting mixture.

3.4.2 NMR analysis of tetrasaccharide produced by GlfT1

Separation of the +2 and +3 products by HPLC proved difficult. However, a single species was desired to structurally characterize the GlfT1 product via nuclear magnetic resonance (NMR) spectroscopy. Thus, conditions to favor formation of solely the +2 Gal*f* tetrasaccharide product by GlfT1 were desired. Ultimately, a higher concentration of acceptor in a mixture containing less enzyme was found to yield solely the +2 Gal*f* product as analyzed by MALDI-TOF MS. A series of reactions were purified by semi-preparative HPLC. Fractions containing the +2 Gal*f* material were isolated and analyzed by MALDI-TOF MS (Figure 3.10).

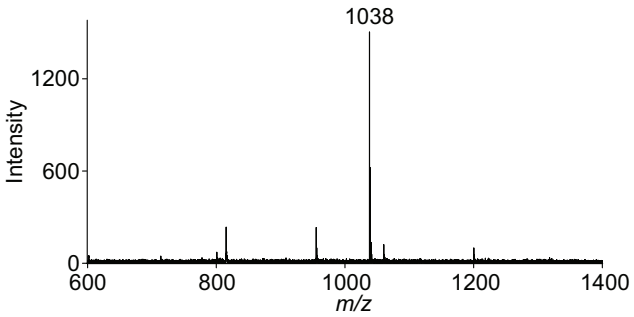

Figure 3.10. MALDI-TOF MS spectrum of isolated tetrasaccharide product obtained following extension of acceptor **2.08** with GlfT1. LRMS: calcd $C_{41}H_{70}NO_{25}P_2$ $[M-H]^-$ 1038.9, observed 1038.5.

NMR spectroscopy was utilized to analyze the isolated product. Two-dimensional experiments, specifically a $^1H-^{13}C$ heteronuclear single-quantum coherence (HSQC) experiment to provide one-bond correlations and a $^1H-^1H$ correlation spectroscopy (COSY) experiment, permitted the assignment of the anomeric protons (Figure 3.11). The chemical shifts of the anomeric protons in the product correspond to those obtained for the Gal*f* residues obtained for synthetic octyl Gal*f*-β(1,5)-Gal*f*-β(1,4)-Rha-α(1,3)-GlcNAc.[226]

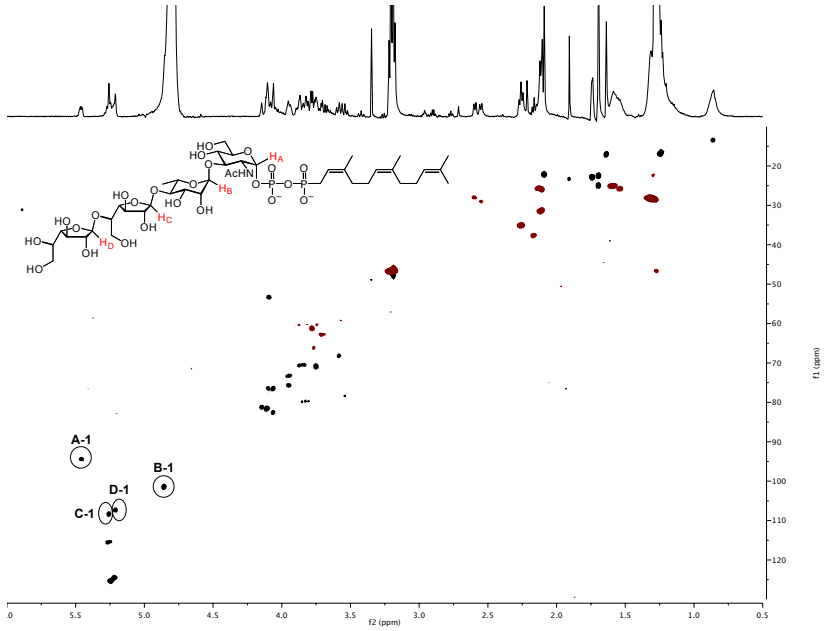

Figure 3.11. $^{1}H-^{13}C$ HSQC spectrum of isolated tetrasaccharide product obtained following extension of acceptor **2.08** with GlfT1. Labels correspond to sugar resonances in the inset structure.

Our NMR data are consistent with the tetrasaccharide structure of the synthetic alkyl glycoside, leading to the conclusion that GlfT1 constructs the tetrasaccharide with the expected β(1,4) and β(1,5) linkages. Along with the chain termination experiments in Chapter 5 (*vide infra*), we have determined that GlfT1 produces a Gal*f*-β(1,6)-Gal*f*-β(1,5)-Gal*f*-β(1,4)-Rha-α(1,3)-GlcNAc pentasaccharide. This unit sets the alternating pattern propagated by the polymerase GlfT2, and produces the precise structure of the galactan.

3.4.3 GlfT2 processes phosphonophosphate-linked oligosaccharides

The preparative isolation of phosphonophosphate-linked tetrasaccharides and pentasaccharides provided a unique opportunity to probe GlfT2 function. The polymerase has been interrogated *in vitro* solely with alkyl or alkenyl lipid-linked acceptor substrates. Thus, we

sought to study GlfT2 polymerization with surrogates that more closely resemble its endogenous tetrasaccharide substrate. We compared the efficiency of elongation of substrates presenting different oligosaccharides by quantifying the amount of UDP released upon GlfT2 addition (Figure 3.12).

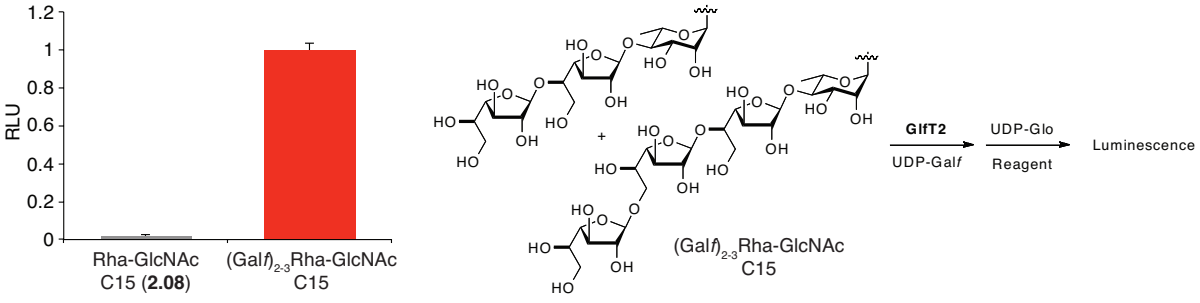

Figure 3.12. Relative output of UDP-Gal*f* turnover by GlfT1 with +2 Gal*f* and +3 Gal*f* farnesyl-linked phosphonophosphate acceptors.

No UDP production corresponding to GlfT2 activity is observed with disaccharide acceptor **2.08**, as GlfT2 requires an acceptor presenting a Gal*f* residue on the non-reducing end. On the other hand, robust activity is observed with the tetra- and pentasaccharides mixture. This result corroborates our expectations of GlfT2 activity. We expect that the isoprenyl lipid carrier and phosphonophosphate bridge render these compounds as markedly better substrates for the enzyme over alkenyl acceptors. Analysis of these reaction mixtures by mass spectrometry has proved challenging, however. Observing polysaccharides by MALDI-TOF MS in the negative mode is difficult.[227,228] Ion suppression by sodium ions in the reaction buffer further dampens the signal output. Efforts to strip buffer components from Gal*f* polymers are ongoing.

3.5 Conclusion

Our studies of GlfT1 highlight the utility of the phosphonophosphate-containing glycosyltransferase acceptor substrates. The ability of phosphonophosphates to substitute for pyrophosphates in glycosyl acceptors can facilitate the synthesis of complex glycosyltransferase acceptors. Glycosyltransferases in prokaryotes, eukaryotes and archaea that act on pyrophosphate-linked acceptors are ubiquitous, including enzymes that mediate peptidoglycan assembly[37,40] and that generate O-[74,229] and N-linked[192] glycans. We anticipate that the use of related compounds will facilitate characterization of the activity of the large family of glycosyltransferases that use pyrophosphate-containing acceptors.

3.6 Experimental details

Routine assays with GlfT1 were carried out in 35 μL final volume containing 2 μM GlfT1-His_6, 100 μM acceptor substrate and 300 μM UDP-Gal*f* in 50 mM 4-morpholinepropanesulfonic acid (MOPS), pH 7.9, 10 mM $MgCl_2$ and 5 mM β-mercaptoethanol. Reactions were incubated at 37 °C for 2 h, quenched with 35 μL of a 1:1 v/v mixture of chloroform:methanol, and evaporated to dryness on a SpeedVac SC100 (Varian). The dried mixtures were re-suspended in 35 μL of water, desalted with a ZipTip C18 pipette tip (Millipore), eluting with a 1:1 (vol/vol) solution of 20 mM ammonium bicarbonate:acetonitrile. The eluent solution was spotted onto a stainless steel plate for MALDI-TOF MS analysis as a 1:2 (vol/vol) mixture with 2-(4-hydroxyphenylazo)benzoic acid matrix containing diammonium citrate matrix. The matrix solution was prepared by saturating a 1:1 (vol/vol) water:acetonitrile solution with 2-(4-hydroxyphenylazo)benzoic acid, and adding aqueous diammonium citrate (0.2 M) to a final concentration of 25 mM. MALDI spectra were recorded in negative reflectron mode on a Bruker Ultraflex III instrument. In UDP measurement experiments, three replicates of a GlfT1 reaction mixture were incubated at 37 °C for 2 h, then aliquoted in triplicate into white microwell plates and mixed 1:1 with a reagent coupling UDP production to the luciferase/luciferin reaction.

Luminescence was measured on a Tecan Infinite M1000 after incubating for 1 h at ambient temperature. The luminescence readout was fitted to a standard curve made from a dilution series of known UDP concentrations measured in the same microwell plate. In kinetics experiments, three replicates of reaction mixtures containing 0.2 μM GlfT1-His_6, 0.2–200 μM acceptor substrate and 150 μM UDP-Gal*f* in 50 mM 4-morpholinepropanesulfonic acid (MOPS), pH 7.9, 10 mM $MgCl_2$ and 5 mM β-mercaptoethanol were quenched after 5 min by treatment with the reagent coupling UDP production to the luciferase/luciferin reaction and analyzed as described above. The results were fitted to the Michaelis-Menten equation using GraphPad (La Jolla, California) Prism 6.

For isolation of GlfT1 products, multiple reactions were carried out in 100 μL final volume containing 2 μM GlfT1-His_6, 1 mM acceptor substrate and 1 mM UDP-Gal*f* in 50 mM 4-morpholinepropanesulfonic acid (MOPS), pH 7.9, 10 mM $MgCl_2$ and 5 mM β-mercaptoethanol. Reactions were incubated at 37 °C for 2 h, quenched with 100 μL of a 1:1 v/v mixture of chloroform:methanol, and evaporated to dryness on a SpeedVac SC100. The dried mixtures were re-suspended in 100 μL of water, combined, and purified by semi-preparative high-performance liquid chromatography on a Beckman-Coulter instrument with a Vydac Protein and Peptide C18 (22 mm x 250 mm) column, using a gradient of acetonitrile in 25 mM ammonium bicarbonate. Fractions containing product were analyzed by MALDI-TOF MS as described above.

For isolation of solely +2 Gal*f* product for NMR spectroscopy analysis, several reactions with a total volume of 100 μL, containing 0.5 μM GlfT1-His_6, 2 mM acceptor substrate and 1.6 mM UDP-Gal*f* in 50 mM 4-morpholinepropanesulfonic acid (MOPS), pH 7.9, 10 mM $MgCl_2$ and 5 mM β-mercaptoethanol, were incubated at 37 °C. Following 2 h, the reactions were filtered through a 10,000 molecular weight cutoff centrifugal filter and separated by HPLC. The identity of the product-containing fraction was analyzed by MALDI-TOF mass spectrometry and NMR

spectroscopy. ^{1}H and ^{13}C nuclear magnetic resonance (NMR) spectra were recorded on a 500 MHz spectrometer (acquired at 500 MHz for ^{1}H NMR and 126 MHz for ^{13}C NMR). Chemical shifts are reported relative to residual solvent peaks in parts per million (HDO: ^{1}H: 4.79, ^{13}C referenced to ^{1}H).

Assays with GlfT2 were carried out in 30 μL final volume with 0.2 μM His_6-GlfT2, 200 μM acceptor substrate and 1.25 mM UDP-Gal*f* in 50 mM HEPES, pH 7.0, 25 mM $MgCl_2$ and 100 mM NaCl. Reactions were incubated at ambient temperature for 20 h, quenched with 30 μL of a 1:1 v/v mixture of chloroform:methanol, and evaporated to dryness on a SpeedVac SC100. The dried mixtures were re-suspended in 30 μL of water, and processed as above.

Chapter 4: A neutral acceptor processed by cell wall galactofuranosyltransferases

Contributions:

Cloning and expression of GlfT1, mutagenesis and experiments with GlfT1 mutants performed by V.A. Kincaid.

4.1 Abstract

The galactofuranosyltransferase GlfT1 is highly specific for complex acceptor substrates that are structurally related to its endogenous substrate. We reasoned that a substrate bearing its +1 Gal*f* product, a Gal*f*-β(1,4)-Rha-α(1,3)-GlcNAc trisaccharide, would flout the enzyme's stringent acceptor requirements. Thus, I targeted the synthesis of a neutral acceptor substrate for GlfT1 linked to a 12-phenoxydodec-2-enyl lipid carrier at the reducing end. Such a substrate could serve as a GlfT2 substrate as well, since GlfT2 has relaxed acceptor specificity and the acceptor bears a Gal*f* residue at the non-reducing end. The neutral trisaccharide is an excellent substrate for GlfT1, as it is entirely consumed and processed to Gal*f* oligosaccharides. Quantitative analysis by monitoring release of UDP revealed that this acceptor is comparable to a farnesyl-linked phosphonophosphate disaccharide as a GlfT1 substrate. Our results imply that the intermediate +1 Gal*f* trisaccharide motif is processed rapidly. Moreover, this trisaccharide can also serve as an acceptor substrate for the polymerase GlfT2, though it is a poor substrate. The trisaccharide permits the tandem use of both glycosyltransferases to synthesize galactan chains of endogenous lengths.

4.2 Introduction

The galactofuranosyltransferases GlfT1 and GlfT2 cooperate to assemble the mycobacterial galactan on a decaprenyl-linked Rha-α-(1,3)-GlcNAc pyrophosphate. As observed in Chapter 3, GlfT1 can rapidly assemble Gal*f* oligosaccharides of 1–3 units on the acceptor substrate, but does not otherwise polymerize Gal*f* to form full-length galactan. GlfT2 is a polymerizing glycosyltransferase, and consequently produces the majority of the galactan chain by stepwise addition of 20–40 Gal*f* residues to the growing acceptor polymer. We were interested in defining the acceptor limits of these enzymes' activity, specifically related to processing intermediate Gal*f* oligosaccharides.

The Kiessling laboratory has demonstrated[116] that *O*-alkenyl Gal*f* oligosaccharides are acceptor substrates for GlfT2. These acceptors are processed efficiently despite the lack of a Rha-α(1,3)-GlcNAc linker disaccharide as well as the pyrophosphate bridge. Remarkably, GlfT2 can even process an acceptor substrate bearing only a Gal*f* monosaccharide,[118] provided that the lipid carrier is of sufficient length. A phenoxydodecenyl-linked monosaccharide is processed efficiently, for example, whereas phenoxyoctenyl-linked monosaccharide is inactive. Despite polymerizing monosaccharide and disaccharide acceptors, GlfT2 processes shorter acceptors slowly. The enzyme exhibits a kinetic lag phase with lipid-linked disaccharide acceptors.[116] The rate of polymerization is slow at first, but hastens when the acceptor has been lengthened. The lag phase is abolished when the enzyme is exposed to a tetrasaccharide acceptor.[117] These results suggest that GlfT2 requires a minimum threshold of subsites to be filled by the growing acceptor chain. Once enough subsites are filled, GlfT2 binds the acceptor tightly and processes it readily.

Despite their difference in activity, GlfT1 and GlfT2 are structurally related. Analysis of the amino acid sequence of GlfT1 and GlfT2 suggests the enzymes are paralogs, with 24% identity by ClustalO[230] alignment. Similarly, a structural homology model of GlfT1 using the SWISS-MODEL program[231-233] is assembled from matching to a GlfT2 crystal structure. The

sequence of GlfT2 (637 a.a.) is nearly twice as large as that of GlfT1 (304 a.a.), yet their active site topology may be similar, leading them to process structurally related acceptor substrates.

The galactofuranosyltransferase activity of GlfT1 and GlfT2 could overlap in the processing of a +1 Gal*f* acceptor substrate, bearing the Galf-β-(1,4)-Rha-α-(1,3)-GlcNAc motif. Mikušová and co-workers[110,111] have suggested that GlfT1 adds a single galactofuranose residue to a decaprenyl-linked Rha-α-(1,3)-GlcNAc pyrophosphate. In this scenario, GlfT1 maintains the regulatory role presented in Chapter 3 (*vide supra*), though it fails to address how galactan can be formed regioselectively without a template or register. The implication, as a consequence, is that GlfT2 must recognize the +1 Gal*f* trisaccharide and process it efficiently to form full-length galactan.

However, GlfT2 appears to be inefficient in catalyzing addition of the first Gal*f*-β-(1,5)-Gal*f* linkage, given the lag phase it exhibits when processing a Gal*f* disaccharide. As GlfT1 catalyzes the addition of the first Gal*f* residue readily, the ability of GlfT2 to carry out this activity may be irrelevant physiologically. To examine this hypothesis, we sought to determine the relative activity of both enzymes for a trisaccharide acceptor substrate *in vitro*. In particular, we were interested in a trisaccharide that bears the Rha-α(1,3)-GlcNAc linker disaccharide. To this end, I designed an acceptor substrate **4.01** that could be processed differentially by GlfT1 and GlfT2 (Scheme 4.1). We hypothesized that GlfT1 will process a trisaccharide acceptor quickly, catalyzing the addition of 1 to 2 additional Gal*f* residues. The response by GlfT2 could be more nuanced, as the acceptor bears only one Gal*f* residue. Galactan formation should occur rapidly and efficiently if rhamnose and GlcNAc can fill subsites in the GlfT2 active site. Interrogation of the enzyme with acceptor **4.01** could also illuminate how many subsites need to

be filled to abolish a kinetic lag phase (Figure 4.1).

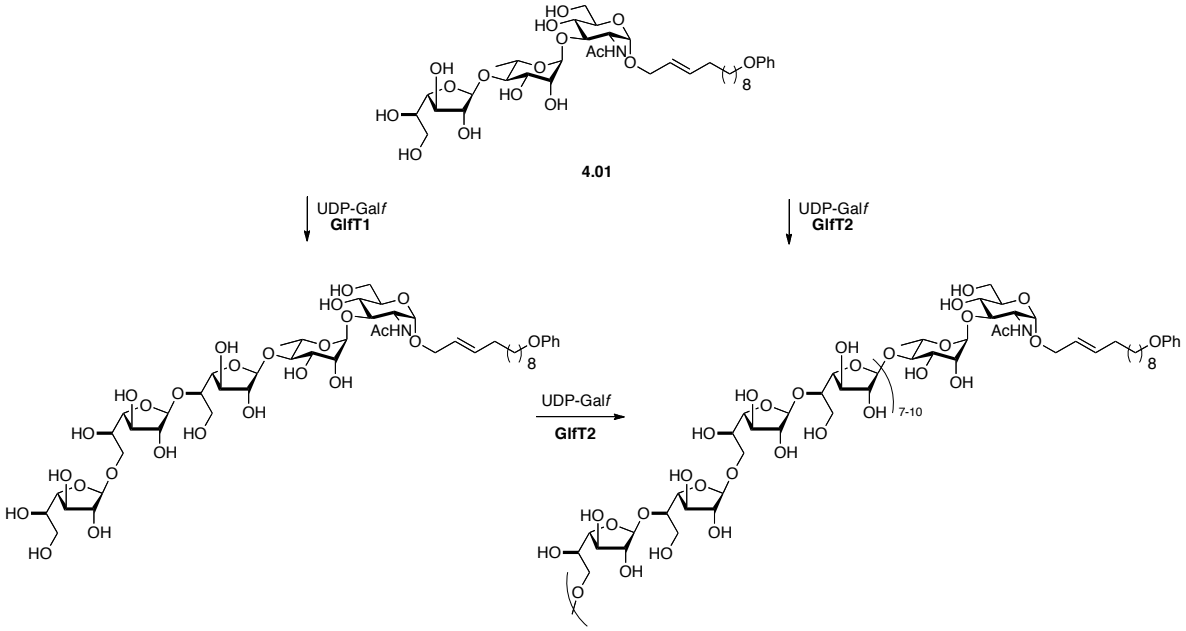

Scheme 4.1. Trisaccharide acceptor **4.01** is processed differently by GlfT1 and GlfT2.

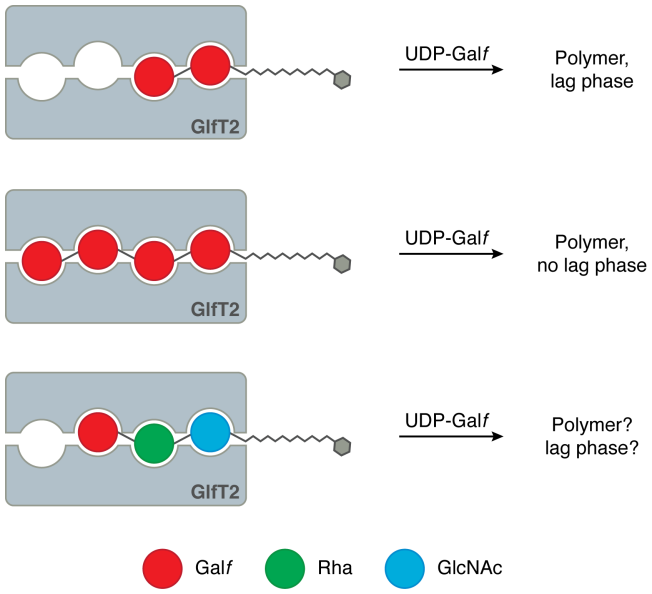

Figure 4.1. A lag phase, observed when GlfT2 polymerizes a disaccharide acceptor, is abolished with a tetrasaccharide acceptor. A trisaccharide acceptor may fill enough subsites to avoid a lag phase.

4.3 A lipid-linked Gal*f* acceptor bearing the disaccharide linker unit

Preparing a simplified acceptor substrate that would be suitable for GlfT1 was the primary concern when undertaking these experiments. As noted in Chapter 2, simplified acceptors that do not bear a pyrophosphate, or phosphonophosphate, are inactive substrates. Our rationale was that trisaccharide acceptor **4.01** would gain sufficient binding affinity from the additional Gal*f* monosaccharide. This compound should then be a suitable acceptor for processing by GlfT1. There are several advantages to pursuing a neutral acceptor, particularly simpler purification of synthetic intermediates and straightforward analysis by MALDI-TOF MS. Both of these advantages are buttressed by expertise in the Kiessling laboratory in the handling, analysis, and biochemical experiments involving related molecules.

4.3.1 Synthesis of a lipid-linked Galf-β(1,4)-Rha-α(1,3)-GlcNAc acceptor

Our approach toward trisaccharide acceptor **4.01** revolved about the cross-metathesis coupling of allyl-functionalized trisaccharide **4.02** and 11-phenoxy-1-undecene **4.03**[116] (Scheme 4.2). This strategy has proved highly effective in the preparation of various lipid-linked oligosaccharides.[118] Trisaccharide **4.02** in turn is prepared from thioglycosides **4.04** and **4.05** or **4.06**, and 2-acetamido-1-*O*-allyl-2-deoxy-D-glucopyranose **4.07**.

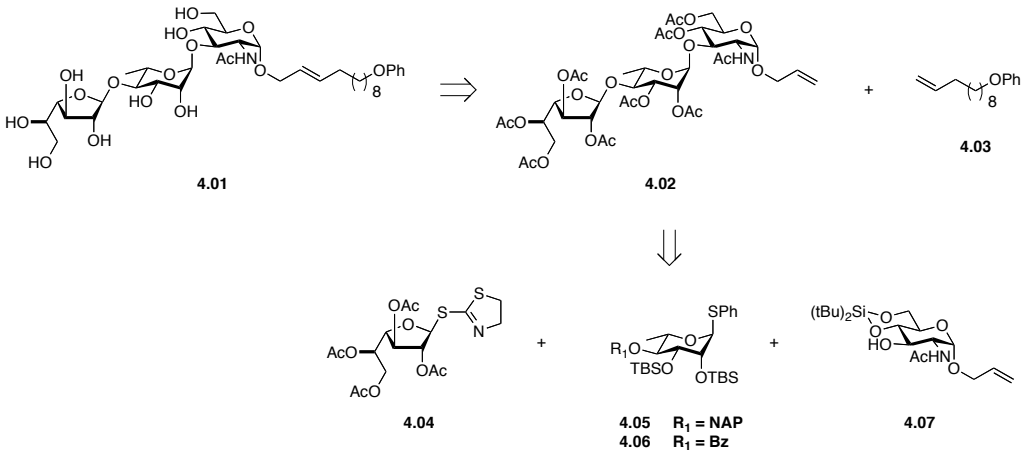

Scheme 4.2. Retrosynthetic analysis of phenoxyundecenyl trisaccharide **4.01**.

4.3.2 Disaccharide formation with a 4'-OBz rhamnosyl donor

Preparation of phenyl thioglycosides **4.05** or **4.06** requires differential protection of the hydroxyl group at the 4-position of L-rhamnose. Our initial efforts focused on 4-*O*-benzoyl thioglycoside **4.06**, since the benzoyl protecting group is commonly employed in carbohydrate chemistry (Scheme 4.3). Acetate-protected phenyl thioglycoside **4.08**,[205] obtained as described in Chapter 2, was deprotected under Zemplén conditions to provide thioglycoside **4.09**. Differential protection was achieved by simultaneous protection of the 2- and 3-position hydroxyl groups as the acetonide. To this end, crude thioglycoside **4.09** was reacted with 2,2-dimethoxypropane using 10-camphorsulfonic acid as acid catalyst to provide 2,3-*O*-isopropylidene derivative **4.10** in 93% yield over two steps. Protection of the 4-hydroxyl as the

benzoyl ester was achieved with benzoyl chloride in pyridine, yielding **4.11** in quantitative yield. A protecting group swap at this point was required to reach conformationally-armed donor **4.06**. Deprotection of the isopropylidene group from **4.11** in aqueous acetic acid afforded **4.12**. The crude material was reacted with *tert*-butyldimethylsilyl trifluoromethanesulfonate (TBSOTf) and 4-(dimethylamino)pyridine (DMAP) in pyridine to provide 4-*O*-benzoyl donor thioglycoside **4.06** in 98% yield over two steps.

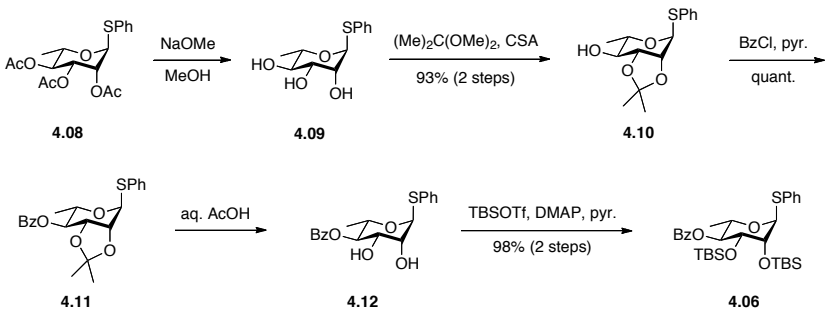

Scheme 4.3. Synthesis of differentially-protected 4-*O*-benzoyl L-rhamnosyl thioglycoside donor **4.06**.

The acceptor monosaccharide was readily prepared from *N*-acetyl-D-glucosamine (GlcNAc) in two steps (Scheme 4.4). Allylation[234] of GlcNAc was achieved with allyl alcohol and acetyl chloride, affording **4.13** in 77% yield. The 4- and 6-hydroxyl positions were selectively protected with the di-*tert*-butylsilylene group, using di-*tert*-butylsilyl bis(trifluoromethanesulfonate) in *N*,*N*-dimethylformamide.[208] This protecting strategy provided glucosamine acceptor **4.07** bearing a free 3-OH group in two steps. Glycosylation of donor **4.06** and acceptor **4.07** was effected with *N*-iodosuccinimide (NIS) and silver trifluoromethanesulfonate in the presence of 4 Å molecular sieves at –78 °C. Disaccharide **4.14** was isolated in 26% yield, with a significant amount of recovered, unreacted donor sugar.

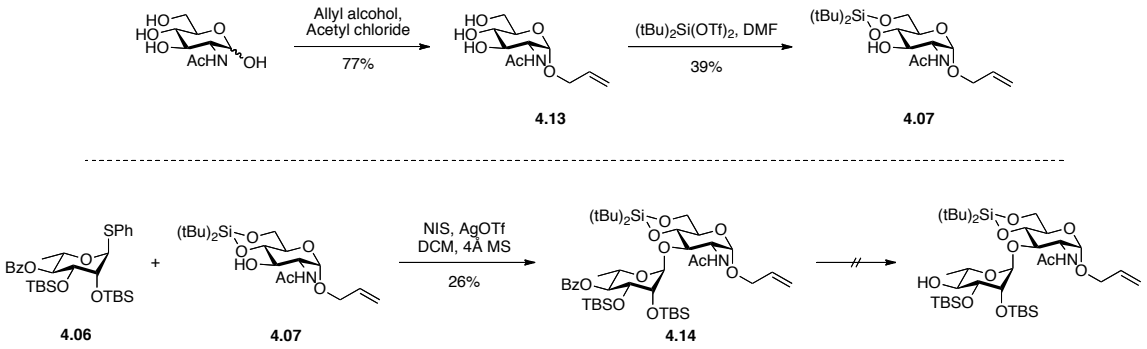

Scheme 4.4. Synthesis of allyl *N*-acetyl-D-glucosamine acceptor **4.07** and glycosylation with donor **4.06**.

Surprisingly, the 4-*O*-benzoyl substituent has a dramatic effect on the reactivity of donor **4.06**. As noted in Chapter 2, a 2,3,4-tri-*O*-*tert*-butyldimethylsilyl L-rhamnosyl phenylthioglycoside is conformationally "super-armed" for glycosylation, reacting quickly at -78 °C. The fully silylated donor provides a quantitative yield of disaccharide using a GlcNAc acceptor. We had hoped that differential protection of the 4-OH as the benzoate ester would not adversely affect the reactivity of the donor sugar. The ester substituent is electronically disarming, overriding the steric bulk provided by the aromatic substituent. Despite the low yield, disaccharide **4.14** was accessible, and a series of attempts were made to remove the 4-*O*-benzoyl group for further manipulations. Regrettably, this compound was inert to Zemplén conditions, so alternative deprotection conditions were necessary. More forcing conditions leading to benzoyl deprotection with diisobutylaluminum hydride (DIBAL-H) are well precedented.[235-237] The primary concern was concomitant deprotection of the *tert*-butyldimethylsilyl groups, which can occur quantitatively at ambient temperature.[238] Since silyl groups are inert under the reaction conditions at –78 °C,[237] we proceeded with the hope that a cooled DIBAL-H solution would only remove the protecting group at the 4-position. Unfortunately, complete decomposition was observed by thin layer chromatography when disaccharide **4.14** was exposed to DIBAL-H at –78 °C. Given the low yield in the glycosylation to form **4.14** and the difficulty in

removing the 4-*O*-benzoyl group, an alternative protecting group was required.

4.3.3 Disaccharide formation with a 4'-ONAP rhamnosyl donor

The 2-naphthylmethyl (NAP) protecting group[239] is quickly gaining popularity in carbohydrate chemistry.[240-243] As a benzyl-type protecting group, it donates electron density and electronically arms a monosaccharide as a donor for glycosylations. Moreover, we reasoned that the steric bulk of the naphthyl substituent may contribute to the conformational arming of 2,3-di-*O*-*tert*-butyldimethylsilyl L-rhamnosyl donor **4.05** (Scheme 4.5). To prepare this donor, acetonide **4.10** was reacted with 2-(bromomethyl)naphthalene and sodium hydride to afford a 4-*O*-NAP derivative. This intermediate was converted to 2,3-di-*O*-*tert*-butyldimethylsilyl derivative **4.05** using similar reaction conditions to those that provided donor **4.06**.

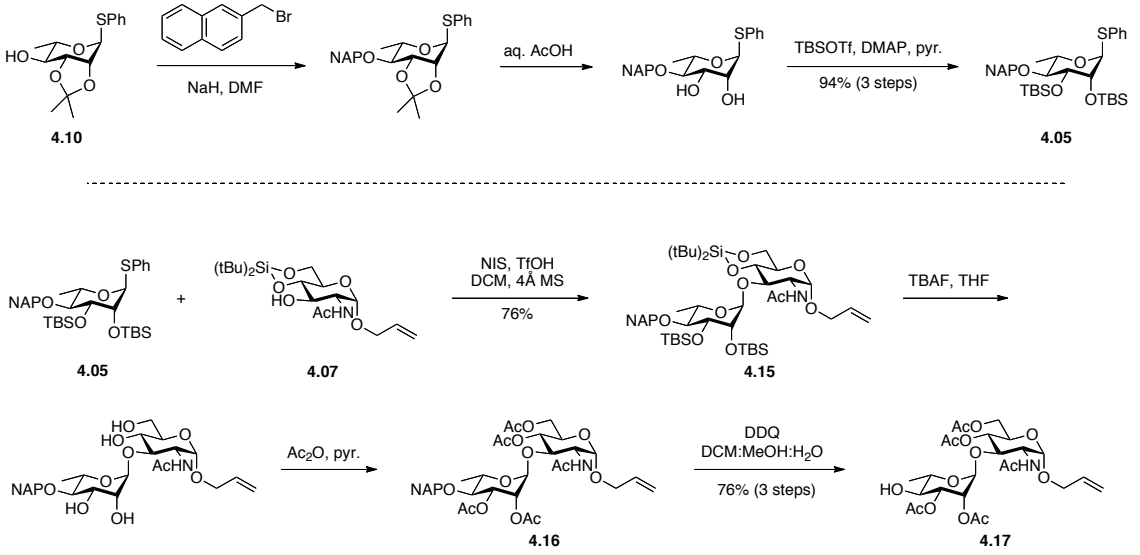

Scheme 4.5. Synthesis of 4-*O*-NAP L-rhamnosyl donor **4.05**, glycosylation with acceptor **4.07**, and elaboration to disaccharide acceptor **4.17**.

Glycosylation of **4.05** and **4.07** was effected by the addition of NIS and trifluoromethanesulfonic acid. As expected, the conformationally-armed donor provided α-

linked disaccharide **4.15** in 76% yield. To avoid complications in later synthetic steps, such as unsuccessful late-stage removal of the silyl protecting groups, these groups were globally cleaved with tetra-*n*-butylammonium fluoride (TBAF) in tetrahydrofuran. The disaccharide was re-protected with acetate esters using acetic anhydride in pyridine, affording disaccharide **4.16**. Oxidative cleavage of the 4'-*O*-NAP ether was accomplished using 2,3-dichloro-5,6-dicyano-1,4-benzoquinone (DDQ)[240] in a dichloromethane:methanol:water mixture. Disaccharide **4.17** bearing a free 4'-OH was isolated in 76% yield over 2 steps. Acetate protecting groups are prone to migration to neighboring hydroxyl groups upon prolonged storage. To prevent erosion of this material, it was carried on to the next synthetic step shortly after purification to avoid migration from the 2'- and 3'-*O*-acetyl protecting groups.

The crucial next step was glycosylation of acceptor **4.17** with a suitable Gal*f* donor. In the course of preparing a series of Gal*f* oligosaccharides, the Kiessling group explored Gal*f* donors that can be activated orthogonally to other donors in a mixture.[244] These donors were inspired by the investigations of Demchenko and co-workers[245,246] on the utility of glycosyl thioimidates with the general formula $SCR_1=NR_2$ as glycosyl donors. A Gal*f* donor bearing an anomeric *S*-thiazolinyl (STaz) group (**4.04**) is particularly useful. This donor is stable under a variety of typical reaction conditions, yet activates readily using only silver trifluoromethanesulfonate to provide glycosides in high yield. Thus, STaz donor **4.04** was chosen as the glycosyl donor in the glycosylation with **4.17** (Scheme 4.6). Glycosylation with silver trifluoromethanesulfonate proceeded smoothly to provide trisaccharide **4.02** in good yield. The next step involved addition of a lipid carrier via cross-metathesis.

The lipid carrier has a substantial impact on the efficiency of polymerization by the glycosyltransferase GlfT2.[116] Phenoxyundecenyl lipid carrier **4.03**[116] is an ideal lipid for GlfT2 polymerization, in that it yields polymers of endogenous length and the acceptor is entirely consumed. This lipid length may be optimal for a GlfT1 acceptor as well. Additionally, the lipid-

conjugated glycoside does not form micelles under the concentrations used in the *in vitro* assay. Moreover, the majority of oligosaccharides used to interrogate GlfT2 are conjugated to lipid **4.03**, making it the wisest choice for comparing the relative efficiency of **4.01** with other GlfT2 acceptors. The lipid was attached *via* ruthenium-catalyzed cross metathesis of **4.02** and **4.03**, employing Grubbs I catalyst (bis(tricyclohexylphosphine)benzylidine ruthenium(IV) dichloride). Removal of the acetate protecting groups under Zemplén conditions provided lipid-linked trisaccharide **4.01**. The prevailing question at this point was whether **4.01** would be a suitable acceptor for both GlfT1 and GlfT2.

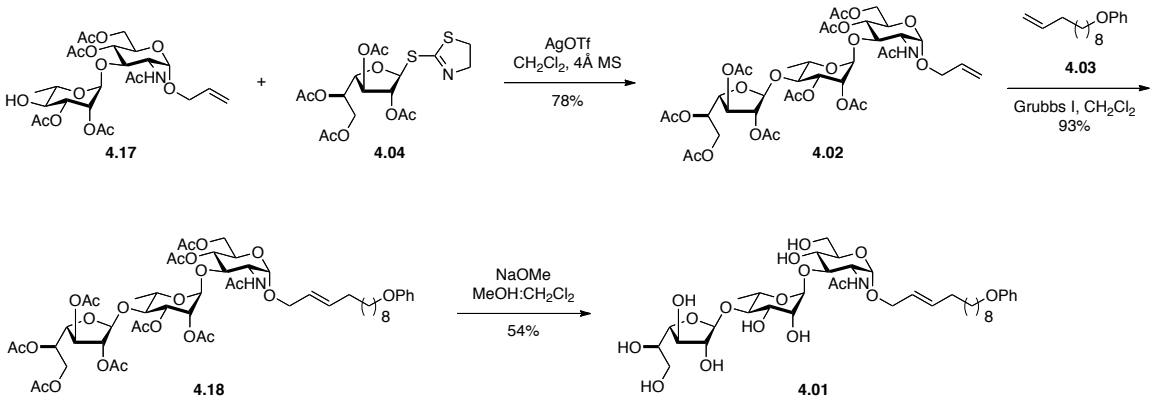

Scheme 4.6. Preparation of alkenyl trisaccharide **4.01** via cross-metathesis.

4.4 Glycosyltransferase assays with the neutral lipid-linked trisaccharide

4.4.1 Investigating the acceptor's utility in GlfT1 assays

The ability of trisaccharide **4.01** to act as a glycosyltransferase acceptor was first tested with GlfT1. This glycosyltransferase is restrictive for specific acceptor substrates. In our hands, only phosphonophosphate-linked acceptors (see Chapters 2 and 3) are processed by the enzyme.[112] However, we were confident that the additional Gal*f* residue on acceptor **4.01** would yield elongated oligosaccharides when incubated with GlfT1. Its ability to serve as an acceptor

was interrogated under the assay conditions developed for GlfT1,[112] and analyzed by MALDI-TOF mass spectrometry.

GlfT1 processes acceptor **4.01** quite efficiently. The acceptor is completely consumed to provide a mixture of Gal*f* oligosaccharides. The predominant products are +1 to +3 Gal*f* oligosaccharides (tetrasaccharides to hexasaccharides), with some evidence of a +4 (heptasaccharide) product (Figure 4.2). While we expected to observe robust processing of the acceptor, the observation of longer oligosaccharide products was surprising.

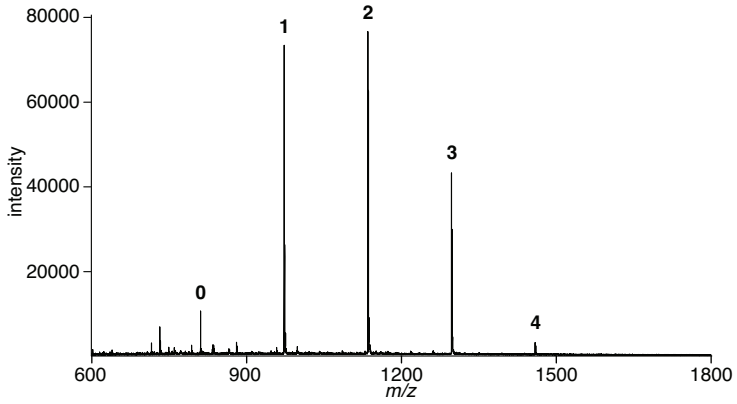

Figure 4.2. MALDI-TOF analysis of an incubation of **4.01**, UDP-Gal*f* and GlfT1.

The unexpected lengths of oligosaccharides produced by GlfT1 upon processing **4.01** may provide rather meaningful insight into how GlfT1 controls the length of its products. We posit that pyrophosphate- and phosphonophosphate-containing acceptors are likely coordinated tightly to a positive charge in the active, either a magnesium ion bound to a DDX motif or a positively-charged amino acid. This coordination holds the acceptor in place while processing is taking place, and oligosaccharide length is controlled. In the case of the lipid-linked trisaccharide, the lack of an ion-coordinating functional group may lead to the acceptor 'sliding' in the active site. This added flexibility then permits processing of additional Gal*f* residues. After addition of more than three Gal*f* residues, the acceptor is likely too large for the active site cavity

and dissociates. It has been suggested that cavity volume may have a similar effect in galactan length control by GlfT2.[120] In this model, the pyrophosphate is coordinated by a magnesium ion bound to an active site DDD motif. The volume of a cavity formed between monomers in a tetramer observed in a crystal structure may limit the maximum length of each galactan chain.

As noted above, the activity of GlfT1 should depend on coordination of Mg^{2+} by aspartate residues in the active site. The metal is presumed to coordinate to the pyrophosphate group in UDP-Gal*f*. Assays with the enzyme are usually carried out in the presence of added metal in the form of 10 mM magnesium chloride. In the absence of added divalent metal such as magnesium or manganese, no enzymatic turnover should occur. To test this hypothesis, 5 mM ethylenediaminetetraacetic acid (EDTA) was added in place of added metal to a GlfT1 reaction mixture. EDTA should chelate any adventitious metal, sequestering it from solution and shutting down GlfT1 activity. Indeed, addition of EDTA completely abolishes the glycosyltransferase activity of GlfT1 (Figure 4.3). A minor peak corresponding to the +1 product is evident, but the predominant component of the reaction mixture is unreacted starting material. Thus, a divalent metal is necessary for GlfT1 activity.

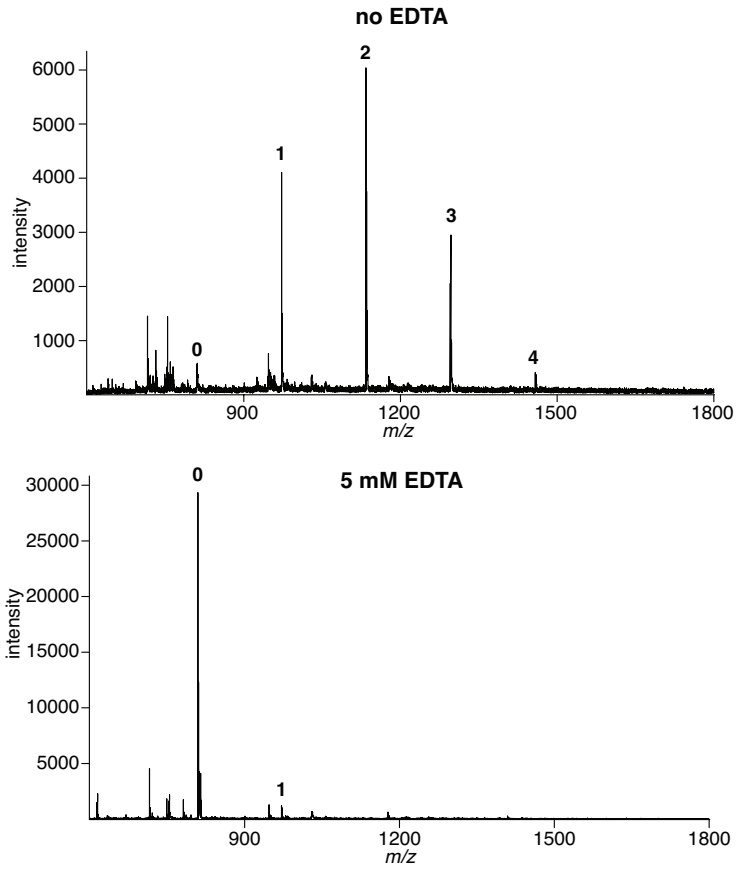

Figure 4.3. GlfT1 activity is abolished upon addition of 5 mM EDTA. Top: GlfT1 reaction in the presence of 10 mM $MgCl_2$ ("no EDTA"). Bottom: Reaction with no added metal and 5 mM EDTA.

As discussed in Chapter 3, analysis of phosphonophosphates by negative-mode MALDI-TOF is a labor-intensive protocol. Analysis of neutral sugars such as **4.01**, on the other hand, is relatively straightforward by positive-mode MALDI-TOF mass spectrometry. The Kiessling laboratory has an established protocol for analyzing neutral oligosaccharides in positive-mode MALDI mass spectrometry.[116] Sample clean-up prior to spotting on a target is not necessary when spotted in a 1:3 ratio to a α-cyano-4-hydroxycinnamic acid (CHCA) matrix. We sought to take advantage of the neutral oligosaccharides by probing various features of GlfT1 catalysis. In particular, we were interested in learning how quickly the GlfT1 reaction reached equilibrium.

The product distribution over time was analyzed by MALDI-TOF MS. Aliquots of a GlfT1 reaction mixture with UDP-Gal*f* and **4.01** were quenched at 0, 0.5, 1, 2, 4, 8, 16, 32, 64, and 128-minute time points. The intensity of molecular ions corresponding to **4.01** and the resulting oligosaccharides were used to determine their composition in the mixture (Figure 4.4). An estimated 65% of **4.01** is converted to a +1 product within one minute of exposure to GlfT1 and UDP-Gal*f*. The mixture reaches equilibrium after 32 minutes of exposure, where a 5:52:40:3 distribution of +0:+1:+2:+3 occurs. Typical GlfT1 reaction mixtures are quenched after 2 hours of incubation at 37 °C. These results confirm that the mixture at that time point is representative of the reaction equilibrium.

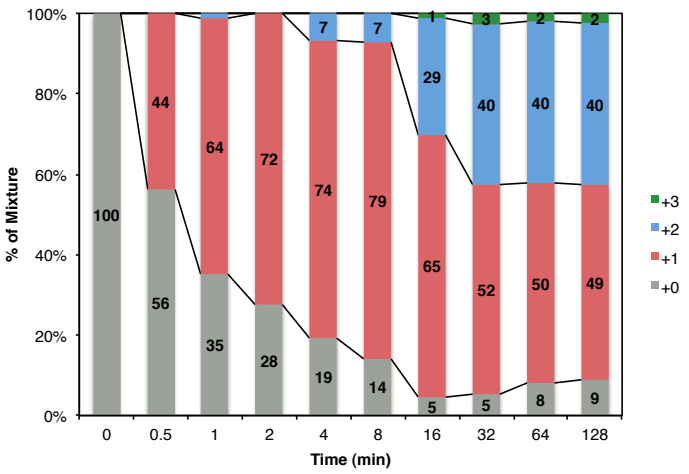

Figure 4.4. Time course MALDI-TOF analysis of an incubation of **4.01**, UDP-Gal*f* and GlfT1.

An isolated +1 oligosaccharide could be useful to further probe how GlfT1 controls its product distribution. A series of enzyme to donor and acceptor ratios were screened to optimize production of +1 Gal*f*, then scaled up in volume. A GlfT1 concentration of 0.2 μM, and equivalent concentrations of donor and acceptor at 1 mM (5000-fold excess over enzyme) provided largely a +1 Gal*f* product (Figure 4.5, top). The reaction mixture was purified on an analytical C18 HPLC column. Each collected fraction was analyzed by MALDI-TOF MS. An

aliquot enriched in +1 Gal*f* with a small percentage of +2 Gal*f* was obtained (Figure 5, middle) as well as an aliquot containing solely +1 Gal*f* **4.19** (Figure 4.5, bottom).

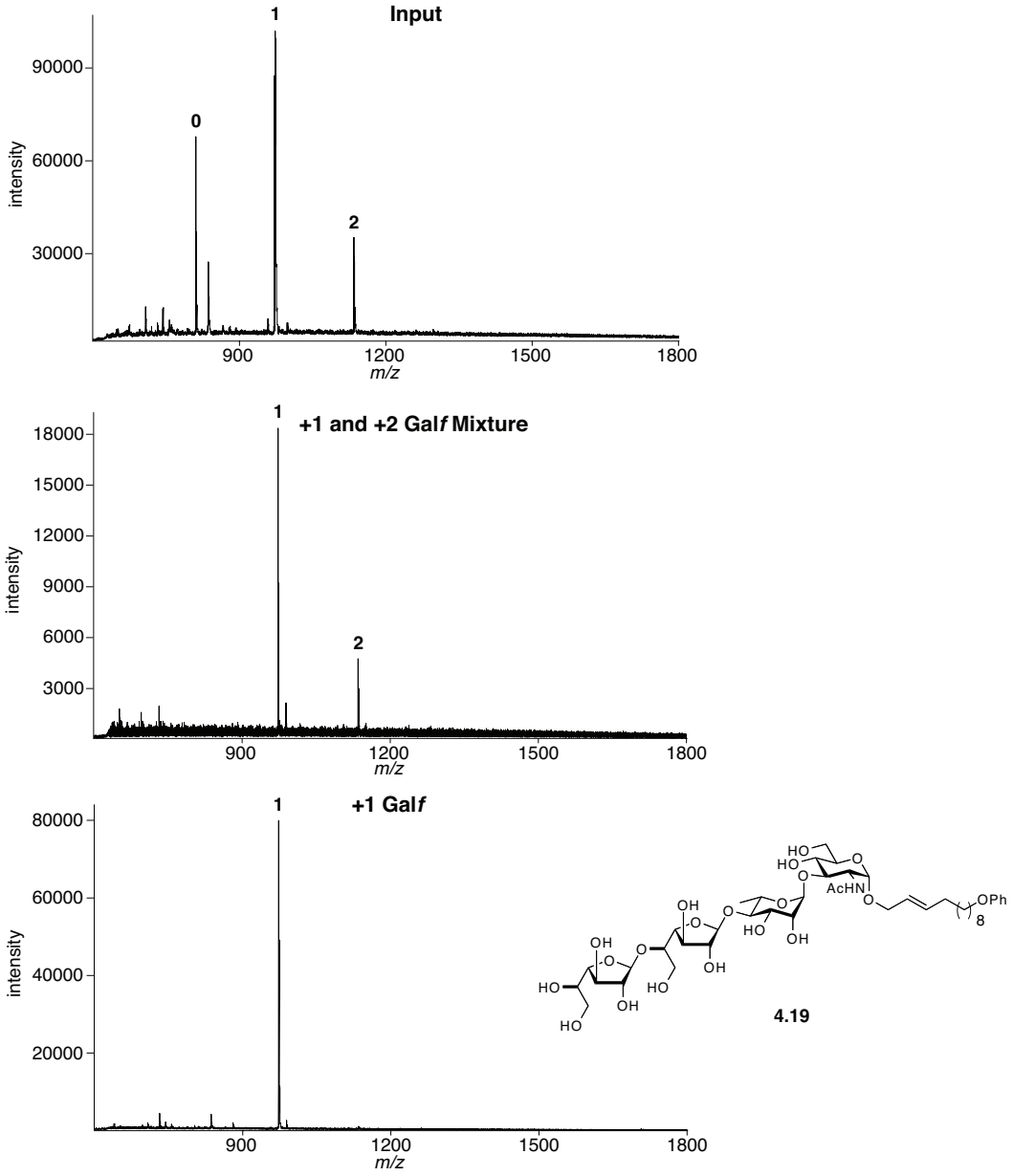

Figure 4.5. Isolation of +1 Gal*f* oligosaccharide produced by GlfT1. Top: MALDI-TOF MS spectrum of input reaction mixture prior to HPLC purification. Middle: Mixture of +1 and +2 Gal*f* oligosaccharides. Bottom: Purified +1 Gal*f* oligosaccharide **4.19**.

4.4.2 Site-directed mutagenesis reveals residues important for GlfT1 catalysis

Site-directed mutagenesis has revealed which residues in GlfT2 are critical for mediating catalysis.[119] The primary sequence of GlfT1 contains DXD (or DDX) motifs conserved in glycosyltransferases. Analysis by BLAST (Basic Local Alignment Search Tool) revealed two DDX motifs are conserved across the 50 closest homologs to *M. tuberculosis* GlfT1. We predicted that residues DDD (Asp93-Asp95) and residues DEV (Asp193-Val195) are required for glycosyltransferase activity. Based on a homology model of GlfT1 based on *M. tuberculosis* GlfT2, residues ^{193}DEV^{195} may be important for binding the acceptor substrate. Mutations to this site are not tolerated. Galactofuranosyltransferase activity is completely abolished in a GlfT1 variant bearing the D193A mutation (Figure 4.6). Greatly attenuated activity is observed in a D193E mutant.

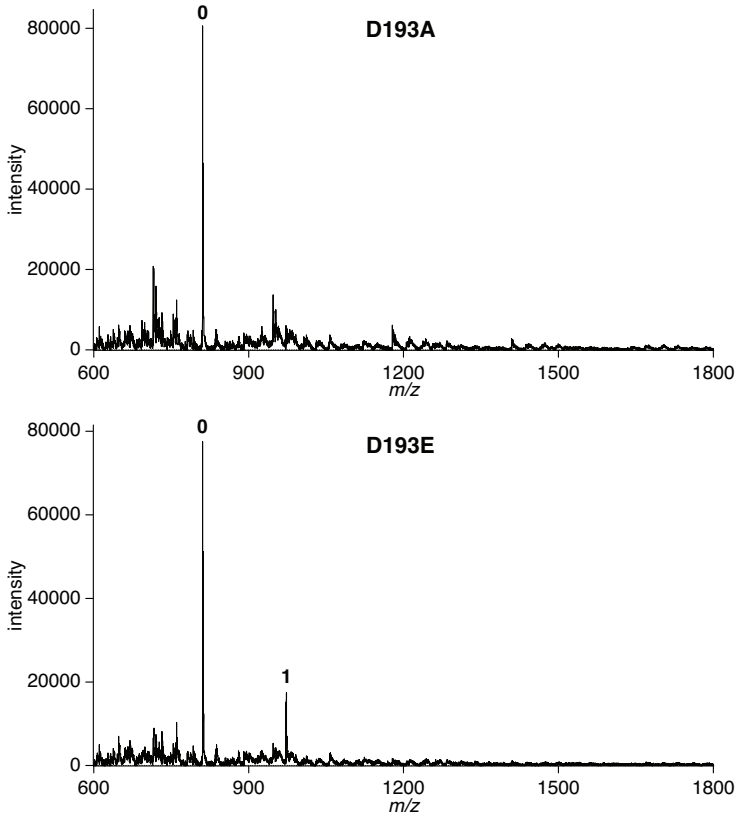

Figure 4.6. Site-directed mutagenesis of *M. smegmatis* GlfT1 reveals the critical importance of Asp193 for GlfT1 catalysis.

Analogy with the GT-2 domain in GlfT2 and other glycosyltransferases allowed the rapid determination of residues that are required for GlfT1 to process an acceptor substrate. Further characterization of mutated GlfT1 variants is ongoing, including mutation of residues predicted to be important for donor binding.

4.4.3 Investigating the utility of the trisaccharide acceptor in GlfT2 assays

The activity of GlfT2 has not been examined with acceptors bearing the linker disaccharide. Since GlfT1 processes acceptor **4.01** efficiently into short oligosaccharides, we reasoned that GlfT2 would process the products of GlfT1 catalysis into full-length galactan polymers. Thus, we used a typical GlfT1 reaction with acceptor **4.01** as the 'acceptor substrate' in a routine GlfT2 polymerization assay. GlfT2 polymerizes the short oligosaccharides prepared by GlfT1 (+1 to +3 Gal*f*) very effectively (Figure 4.7). In fact, the length of Gal*f* polymers corresponds to galactan of endogenous length.

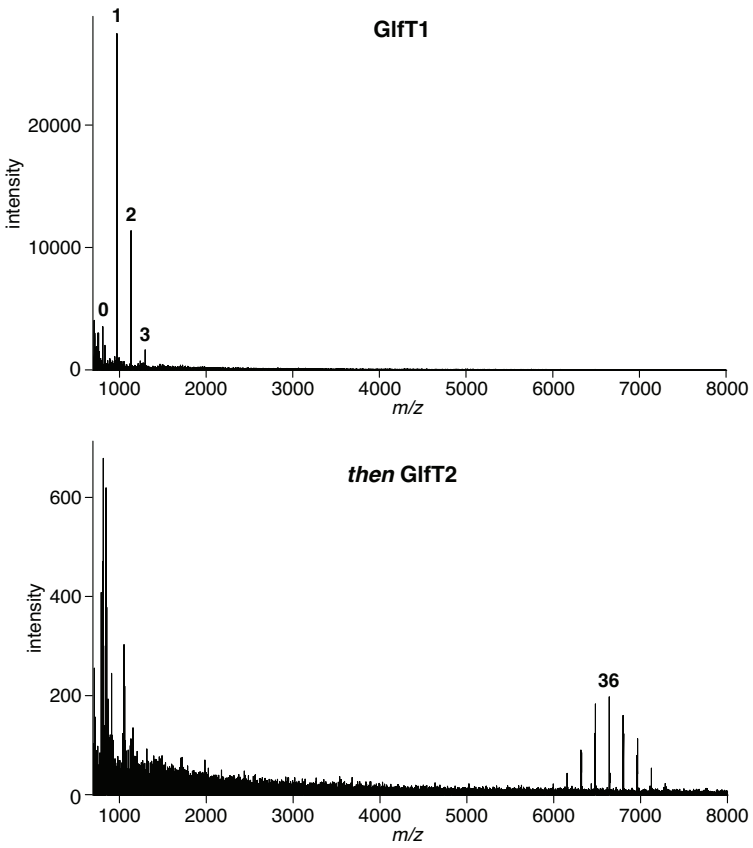

Figure 4.7. An oligosaccharide mixture produced by GlfT1's action on **4.01** is converted to endogenous length galactan by GlfT2.

We expected efficient assembly of galactan on Gal*f* oligosaccharides built from **4.01**. GlfT2 can polymerize from a single Gal*f* tethered to the phenoxydodec-2-enyl lipid carrier.[118] Consequently, we studied whether **4.01** would be processed directly by GlfT2. Indeed, GlfT2 polymerizes this acceptor to form galactan of endogenous length when incubated at concentrations of 0.2 μM GlfT2 and 40 μM acceptor (Figure 4.8). In analogy with prior experiments with GlfT2, the concentration of acceptor greatly influences the polymer length.[116] With 40 μM acceptor, the polymer length is about +35 Gal*f* units; at 200 μM, the distribution has changed to +28 Gal*f*; at 2 mM acceptor, the distribution of polymer has shifted to +13 Gal*f*. Therefore, GlfT2 exhibits a similar mechanism of polymerization when processing acceptor **4.01** in comparison to oligosaccharide acceptors that contain only galactofuranose residues.

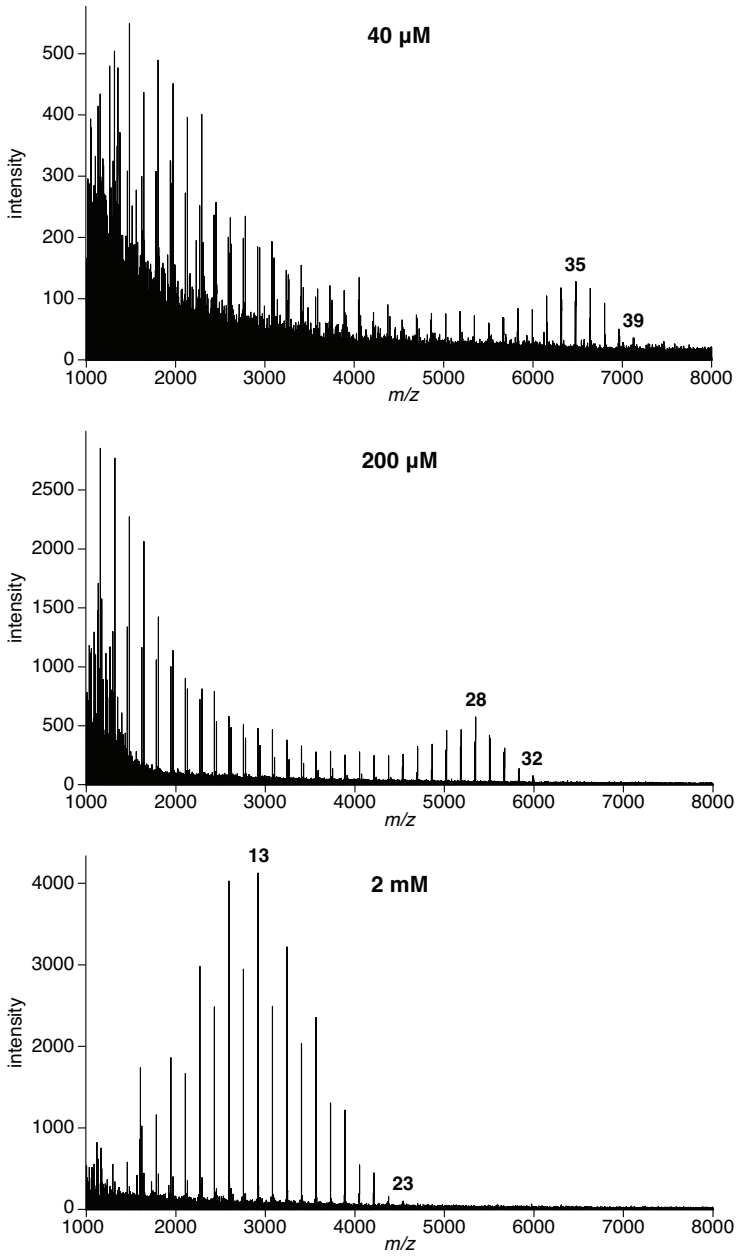

Figure 4.8. GlfT2 formation of galactan polymers from acceptor **4.01** is dependent on the acceptor's concentration.

Finally, the +1 Gal*f* product (**4.19**) obtained from GlfT1 processing of **4.01** afforded a unique opportunity. This product corresponds to 12-phenoxydoc-2-enyl Galf-β(1,5)-Galf-β(1,4)-

Rha-α(1,3)-GlcNAc, if it is produced by GlfT1 in agreement with the linkages observed in mycobacterial galactan. The oligosaccharide portion is the tetrasaccharide motif in the endogenous GlfT2 acceptor substrate. Incubation of Glft2 with acceptor **4.19** in the presence of UDP-Gal*f* provided long Gal*f* polymers (Figure 4.9). Polymers of this length are typically observed with Gal*f* oligosaccharides bearing much longer lipid carriers (19-phenoxynondec-2-ene). Thus, our results imply that the linker disaccharide may play an important and influential role in the binding of acceptor substrates to GlfT2 for efficient polymerization.

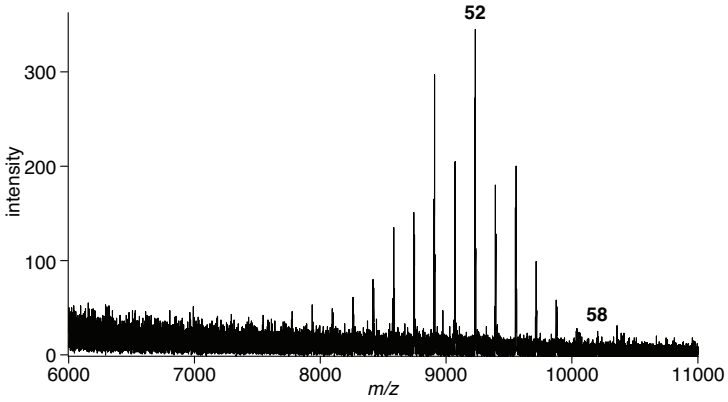

Figure 4.9. GlfT2 processes isolated +1 Gal*f* oligosaccharide **4.19** to long galactan polymers.

4.5 Conclusion

Neutral oligosaccharides bearing the linker disaccharide and a single Gal*f* residue can be processed by both galactofuranosyltransferases involved in mycobacterial cell wall assembly. These experiments were accessible through the multistep chemical synthesis of complex Gal*f*-containing trisaccharides. GlfT1 is sensitive to EDTA treatment, and a time course analysis determined that Gal*f* oligomer formation occurs rapidly upon addition of GlfT1 to a mixture of acceptor and UDP-Gal*f* in buffer. Importantly, GlfT1 and GlfT2 process this acceptor differently, as only short Gal*f* oligomers are formed by the action of GlfT1 while GlfT2 forms full-length galactan polymers. We have effected the relay synthesis of galactan polymers by the action of

both GlfT1 and GlfT2. Moreover, the linker disaccharide appears to have a significant effect on the length of Gal*f* polymers generated by the polymerase GlfT2.

4.6 Experimental details

All compounds were purchased from Sigma Aldrich (Milwaukee, WI) or Fisher Scientific (Pittsburgh, PA). Tetrahydrofuran (THF) was distilled from sodium/benzophenone ketyl, methanol (MeOH) was distilled from magnesium, and dichloromethane (CH_2Cl_2) and triethylamine (Et_3N) were distilled from calcium hydride. Other solvents were purified according to the guidelines in *Purification of Laboratory Chemicals*.[221] All reactions were run under argon atmosphere in oven-dried glassware unless otherwise stated. Molecular sieves were activated by heating to 600 °C in a furnace for 12 h, then cooled in a dessicator. Analytical thin layer chromatography (TLC) was carried out on E. Merck (Darmstadt) TLC plates pre-coated with silica gel 60 F254 (250 μm layer thickness). Analyte visualization was accomplished using a UV lamp and by charring with a solution of *p*-anisaldehyde [(4.5 mL), acetic acid (15 mL), H_2SO_4 (50 mL), and ethanol (350 mL)]. Flash column chromatography was performed with Silicycle Flash Silica Gel (40–63 μm, 60 Å pore size) using reagent grade hexanes and ACS grade ethyl acetate (EtOAc), or methanol (MeOH) and CH_2Cl_2. High-performance liquid chromatography was performed on a Beckman-Coulter instrument with a Thermo Scientific Hypersil Gold C18 (5 μm, 4.6 mm x 250 mm) column, using a gradient of acetonitrile in water. ^1H and ^{13}C nuclear magnetic resonance (NMR) spectra were recorded on a 300 MHz spectrometer (acquired at 300 MHz for ^1H NMR and 75 MHz for ^{13}C NMR) a 400 MHz spectrometer (acquired at 400 MHz for ^1H NMR and 101 MHz for ^{13}C NMR), or a 500 MHz spectrometer (acquired at 500 MHz for ^1H NMR and 126 MHz for ^{13}C NMR). Chemical shifts are reported relative to tetramethylsilane or residual solvent peaks in parts per million ($CHCl_3$: ^1H: 7.26, ^{13}C: 77.16; MeOH: ^1H: 4.31, ^{13}C: 49.00; HDO: ^1H: 4.79). Peak multiplicity is reported as

singlet (s), doublet (d), doublet of doublets (dd), doublets of doublets of doublets (ddd), triplet (t), doublet of triplets (dt), etc. High resolution electrospray ionization-time of flight mass spectra (HRESI-TOF MS) were obtained on a Micromass LCT.

Routine assays with GlfT1 were carried out in 35 μL final volume containing 2 μM GlfT1-His_6, 100 μM acceptor substrate and 300 μM UDP-Gal*f* in 50 mM 4-morpholinepropanesulfonic acid (MOPS), pH 7.9, 10 mM $MgCl_2$ and 5 mM β-mercaptoethanol. Reactions were incubated at 37 °C for 2 h, quenched with 35 μL of a 1:1 v/v mixture of chloroform:methanol, and evaporated to dryness on a SpeedVac SC100 (Varian). The dried mixtures were re-suspended in 35 μL of a 1:1 v/v mixture of water:acetonitrile and spotted onto a stainless steel plate for MALDI-TOF MS analysis as a 1:3 v/v mixture with α-cyano-4-hydroxycinnamic acid matrix. MALDI spectra were recorded in positive reflectron mode on a Bruker Ultraflex III instrument. In UDP measurement experiments, three replicates of a GlfT1 reaction mixture were incubated at 37 °C for 2 h, then aliquoted in triplicate into white microwell plates and mixed 1:1 with a reagent coupling UDP production to the luciferase/luciferin reaction. Luminescence was measured on a Tecan Infinite M1000 after incubating for 1 h at ambient temperature. The luminescence readout was fitted to a standard curve made from a dilution series of known UDP concentrations measured in the same microwell plate.

Routine assays with GlfT2 were carried out in 30 μL final volume with 0.2 μM His_6-GlfT2, 200 μM acceptor substrate and 1.25 mM UDP-Gal*f* in 50 mM HEPES, pH 7.0, 25 mM $MgCl_2$ and 100 mM NaCl. Reactions were incubated at ambient temperature for 20 h, quenched with 30 μL of a 1:1 v/v mixture of chloroform:methanol, and evaporated to dryness on a SpeedVac SC100. The dried mixtures were re-suspended in 30 μL of a 1:1 v/v mixture of water:acetonitrile and processed as above.

Isolation of +1 Oligosaccharide. The GlfT1 assays were carried out in 5 x 100 μL final volume, containing 0.2 μM GlfT1-His_6, 1 mM acceptor **4.01** and 1 mM UDP-Gal*f* in 50 mM

4-morpholinepropanesulfonic acid (MOPS), pH 7.9, 10 mM $MgCl_2$ and 5 mM β-mercaptoethanol. Reactions were incubated at 37 °C for 2 h, then injected directly onto the HPLC column for purification. Gradient elution from 40% (v/v) acetonitrile (0.1% acetic acid) in water (0.1% acetic acid) to 90% acetonitrile in water (0.1% acetic acid) over 25 minutes eluted three major peaks, which were collected separately. The content of each peak was determined by MALDI-TOF MS, and each respective fraction was evaporated and resuspended in a 1:1 v/v mixture of water:methanol. The acceptor concentration was determined by measuring the absorbance of the solutions at 250 nm (ε = 912 M^{-1} cm^{-1}).

EDTA Assay. This assay was carried out in 10 μL final volume containing 2 μM GlfT1-His_6, 100 μM acceptor substrate and 300 μM UDP-Gal*f* in 50 mM 4-morpholinepropanesulfonic acid (MOPS), pH 7.9, 5 mM EDTA and 5 mM β-mercaptoethanol. Reactions were incubated at 37 °C for 2 h, quenched with 10 μL of a 1:1 v/v mixture of chloroform:methanol, and evaporated to dryness on a SpeedVac SC100 (Varian). The dried mixtures were re-suspended in 10 μL of a 1:1 mixture of water:acetonitrile and analyzed by positive-mode MALDI-TOF MS as described above.

Phenyl 2,3,4-tri-*O*-acetyl-1-thio-α-L-rhamnopyranoside (4.08)

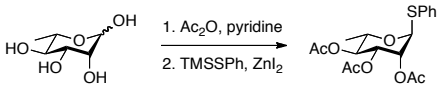

4.08

1. Pyridine (6.2 mL) was added to a round-bottom flask containing L-rhamnose (1.0 g, 6.1 mmol) under Ar atmosphere. The pale clear solution was cooled to 0 °C for 15 min, then acetic anhydride (2.9 mL, 30.5 mmol, 5.0 eq) was added dropwise over 30 min. After 23 h, toluene was added and the solution was evaporated under reduced pressure, followed by co-evaporation with toluene (3 x 75 mL). The pale yellow syrup was dissolved in a 1:1 (vol/vol)

solution of hexanes:ethyl acetate and purified by flash column chromatography [1:1 (vol/vol) hexanes:ethyl acetate]. Per-*O*-acetylated L-rhamnopyranoside was isolated as a clear, viscous syrup. Characterization of this compound matched a published report.[188]

2. (Phenylthio)trimethylsilane (4.71 mL, 24.9 mmol) was added to a solution of 1,2,3,4-tetra-*O*-acetyl-L-rhamnopyranoside (4.13 g, 12.5 mmol) and zinc(II) iodide (7.75 g, 24.3 mmol) in freshly distilled CH_2Cl_2 (24.9 mL) under Ar atmosphere at ambient temperature. After 16 h stirring at ambient temperature, the reaction was transferred to a separatory funnel. Water (50 mL) was added, and the mixture was shaken. The layers were separated, and the aqueous layer was extracted with CH_2Cl_2 (3x). The combined organic layers were washed with water, a saturated solution of sodium bicarbonate, brine, dried over magnesium sulfate, filtered, and concentrated under reduced pressure to a crystalline white solid. Purification by flash chromatography [hexanes to 1:3 (vol/vol) EtOAc:hexanes] afforded **4.08** (4.37 g, 92%) as a crystalline white solid. Characterization of this compound matched a published report.[205]

Phenyl 1-thio-α-L-rhamnopyranoside (4.09)

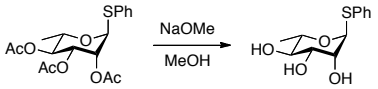

4.08 **4.09**

Freshly distilled MeOH (8.7 mL) was added to a round-bottom flask containing **4.08** (0.5 g, 1.3 mmol) under Ar atmosphere. A solution of NaOMe in MeOH (0.5 M) was added dropwise at ambient temperature. After 22 h, the reaction was neutralized by addition of Amberlite IR-120 resin (H^+ form) to pH 7. The suspension was filtered, the resin was washed with MeOH, and the filtrate was concentrated under reduced pressure to afford **4.09** as a white foam. Characterization of this compound matched a published report.[205]

Phenyl 2,3-*O*-isopropylidene-1-thio-α-L-rhamnopyranoside (4.10)

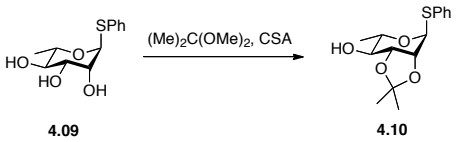

4.09 **4.10**

±-10-Camphorsulfonic acid (0.035 g, 0.15 mmol) was added to a flask containing **4.09** (0.77 g, 4.0 mmol) under Ar atmosphere. 2,2-Dimethoxypropane (1.7 mL, 22 mmol) was added, and the solution stirred at ambient temperature for 30 min. The solution was neutralized to pH 7 with triethylamine and concentrated under reduced pressure to a viscous orange oil. Purification by flash chromatography [hexanes to 7:13 (vol/vol) EtOAc:hexanes] afforded **4.10** (0.82 g, 93%) as a white crystalline solid. Characterization of this compound matched a published report.[247]

Phenyl 4-*O*-benzoyl-2,3-*O*-isopropylidene-1-thio-α-L-rhamnopyranoside (4.11)

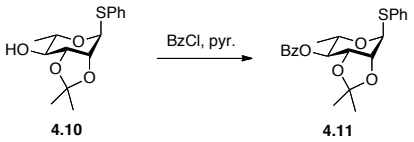

4.10 **4.11**

A solution of **4.10** (0.51 g, 1.7 mmol) in pyridine (1.3 mL) was cooled to 0 °C for 15 min. Benzoyl chloride (0.44 mL, 4.8 mmol) was added dropwise. The cooling bath was removed after 30 min at 0 °C. After 2.5 h, a saturated solution of sodium bicarbonate (15 mL) was added. Chloroform (25 mL) was added, and the layers were separated. The organic layer was washed with a saturated solution of sodium bicarbonate, brine, then dried over magnesium sulfate, filtered, and concentrated under reduced pressure. The residue was co-evaporated with toluene (2 x 25 mL). Purification by column chromatography [hexanes to 3:17 (vol/vol) EtOAc:hexanes]

afforded **4.10** (0.69 g, quant.) as a clear oil. Characterization of this compound matched a published report.[247]

Phenyl 4-*O*-benzoyl-1-thio-α-L-rhamnopyranoside (4.12)

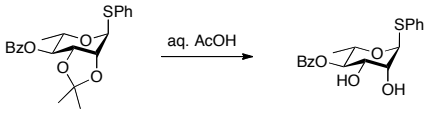

4.11 **4.12**

A suspension of **4.10** (0.69 g, 1.7 mmol) in a 4:1 (vol/vol) acetic acid:water solution (5 mL, 0.4 M) was heated to 80 °C under N_2 atmosphere. Solids dissolved after 5 min. After 2 h, the solution was cooled to ambient temperature and concentrated under reduced pressure to a clear oil. The oil was diluted in a minimal volume of a 1:1 (vol:vol) EtOAc:MeOH solution and purified by flash column chromatography. Elution from 1:3 (vol:vol) EtOAc:hexanes to 1:1 (vol/vol) EtOAc:hexanes afforded **4.12** (0.62 g, quant.) as a white solid. Characterization of this compound matched a published report.[247]

Phenyl 4-*O*-benzoyl-2,3-di-*O*-*tert*-butyldimethylsilyl-1-thio-α-L-rhamnopyranoside (4.06)

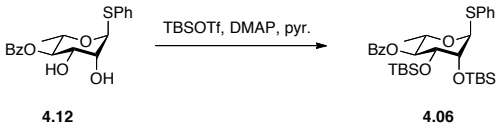

4.12 **4.06**

Compound **4.12** (0.72 g, 2.0 mmol) and 4-(dimethylamino)pyridine (0.025 g, 0.20 mmol) were dissolved in anhydrous pyridine (2.51 mL) under Ar atmosphere. *tert*-Butyldimethylsilyl trifluoromethanesulfonate (2.3 mL, 10.1 mmol) was added dropwise. The flask was fitted with a water-cooled condenser and heated to 50 °C. After 24 h, the cloudy solution was cooled first to ambient temperature, then to 0 °C in an ice bath. The reaction was

quenched by dropwise addition of methanol (4 mL). The solution was transferred to a separatory funnel, diluted with ethyl acetate and water, shaken, and the layers were separated. The organic layer was washed with hydrochloric acid (1 M), a saturated solution of sodium bicarbonate, brine, then dried over magnesium sulfate, filtered, and concentrated under reduced pressure to a light yellow oil. The oil was co-evaporated with toluene (2 x 10 mL) and chloroform (2 x 10 mL). Purification by flash column chromatography [hexanes to 1:9 (vol/vol) EtOAc:hexanes] afforded **4.06** (1.2 g, 98%) as a crystalline white solid.

^{1}H NMR (300 MHz, $CDCl_3$) δ 8.10 – 8.04 (m, 2H, Ar), 7.61 – 7.53 (m, 1H, Ar), 7.52 – 7.42 (m, 4H, Ar), 7.37 – 7.24 (m, 3H, Ar), 5.47 (t, *J* = 9.5 Hz, 1H, H-4), 5.34 (d, *J* = 1.5 Hz, 1H, H-1), 4.39 – 4.24 (m, 1H, H-5), 4.18 – 4.13 (m, 1H, H-2), 4.08 (dd, *J* = 9.5, 2.5 Hz, 1H, H-3), 1.23 (d, *J* = 6.2 Hz, 3H, Me), 0.94 (s, 9H, $(CH_3)_3CSi$), 0.75 (s, 9H, $(CH_3)_3CSi$), 0.14 (s, 3H CH_3Si), 0.08 (s, 3H, CH_3Si), 0.06 (s, 3H, CH_3Si), –0.04 (s, 3H, CH_3Si). HRMS (ESI-TOF$^+$) for $C_{31}H_{48}NaO_5SSi_2$ ($M+Na^+$) calcd 611.2654, found 611.2644.

Allyl 2-acetamido-2-deoxy-α-D-glucopyranoside (4.13)

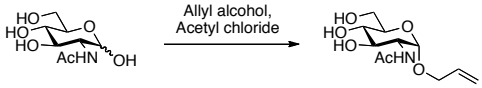

4.13

A round-bottom flask containing allyl alcohol (16.6 mL, 244 mmol, 27.1 eq) under N_2 atmosphere was cooled to 0 °C. Acetyl chloride (2.19 mL, 30.7 mmol, 4.4 eq) was added dropwise. After 5 min, *N*-acetyl-D-glucosamine (2.00 g, 9.0 mmol, 1.0 eq) was added in one portion. The suspension was fitted with a reflux condenser and warmed to 70 °C. After 3 h, the reaction was cooled to ambient temperature and neutralized with solid sodium bicarbonate. The suspension was filtered through Celite (rinsed with methanol). The amber-colored filtrate was concentrated under reduced pressure. The residue was dissolved in minimum ethanol, and **4.13**

was precipitated by addition of ethyl ether (350 mL). The suspension was filtered, affording compound **4.13** (1.81 g, 77%) as an off-white solid. Characterization of this compound has been reported.[234]

Allyl 2-acetamido-2-deoxy-4,6-*O*-di-*tert*-butylsilylene-α-D-glucopyranoside (4.07)

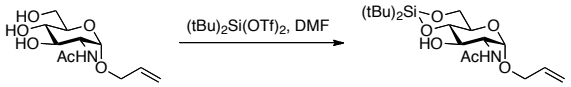

4.13 **4.07**

Anhydrous *N,N*-dimethylformamide (34.9 mL) was added to a flame-dried round-bottom flask containing **4.13** (1.77 g, 6.79 mmol) under Ar atmosphere. The solution was cooled to –40 °C for 20 min. Di-*tert*-butylsilyl di(trifluoromethanesulfonate) (2.10 mL, 6.45 mmol) was added dropwise. The cloudy solution stirred at –40 °C for 1.5 h. Anhydrous pyridine (1.65 mL, 20.4 mmol) was added, and the cooling bath was removed. After 20 min, the reaction was poured into a separatory funnel containing ethyl ether (150 mL). A saturated solution of sodium bicarbonate (150 mL) was added, the mixture was shaken, and the layers were separated. The organic layer was washed with water (2 x 125 mL) and brine (100 mL). The combined aqueous layers were extracted with ethyl ether (150 mL), and the combined organic layers were dried over magnesium sulfate, filtered, and concentrated under reduced pressure. Purification by column chromatography afforded **4.07** (1.06 g, 39%).

^{1}H NMR (400 MHz, $CDCl_3$) δ 5.96 – 5.80 (m, 1H, C*H*=CH_2), 5.34 – 5.15 (m, 2H, CH=C*H*$_2$), 4.84 (d, *J* = 4.6 Hz, 1H, H-1), 4.21 – 4.12 (m, 2H), 4.12 – 4.06 (m, 1H), 4.03 – 4.93 (m, 1H), 4.93 – 4.83 (m, 1H), 4.78 – 4.67 (m, 3H), 2.94 (br s, 1H, 4-OH), 2.04 (s, 3H, NHAc), 1.06 (s, 9H, (C*H*$_3$)$_3$CSi), 0.99 (s, 9H, (C*H*$_3$)$_3$CSi). ^{13}C NMR (101 MHz, $CDCl_3$) δ 170.9, 134.6, 117.9, 96.8, 78.1, 72. 9, 68.5, 66.6, 54.3, 27.6, 27.1, 24.5, 22.8, 20.0. HRMS (ESI-TOF$^+$) for $C_{19}H_{36}NO_6Si$ ($M+H^+$) calcd 402.2307, found 402.2304.

Allyl 2-acetamido-2-deoxy-3-O-(4-*O*-benzoyl-2,3-di-*O*-*tert*-butyldimethylsilyl-*α*-L-rhamnopyranosyl)-4,6-*O*-di-*tert*-butylsilylene-*α*-D-glucopyranoside (4.14)

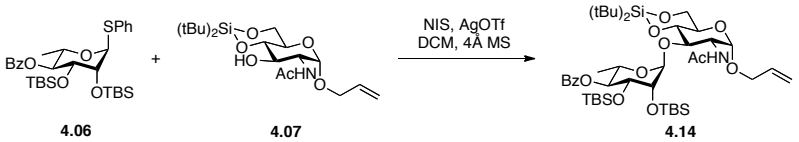

Monosaccharides **4.07** (97 mg, 0.24 mmol) and **4.06** (0.17 g, 0.30 mmol) were combined in a round-bottom flask, coevaporated with anhydrous toluene (3 x 10 mL), and kept under high-vacuum overnight. Activated 4 Å molecular sieve beads and freshly distilled CH_2Cl_2 (9.6 mL) were added under Ar atmosphere. The clear solution stirred at ambient temperature for 50 min, then it was cooled to –78 °C for 20 minutes. *N*-iodosuccinimide (95 mg, 0.42 mmol) and silver trifluoromethanesulfonate (12 mg, 0.048 mmol) were added under subdued light and the clear solution stirred at –78 °C for 2 h. The solution was warmed to –30 °C over 1 h. The cooling bath was removed, and after 1 h the dark red solution was filtered. The filtrate was transferred to a separatory funnel, washed with a 10% (w/w) solution of sodium thiosulfate, a saturated solution of sodium bicarbonate, water, brine, dried over magnesium sulfate, filtered, and concentrated under reeducated pressure to a yellow oil. Purification by flash chromatography [hexanes to 3:17 (vol/vol) acetone:hexanes] afforded **4.14** (56 mg, 26%) as a clear oil.

^{1}H NMR (300 MHz, $CDCl_3$) δ 8.02 – 7.96 (m, 2H, Ar), 7.59 – 7.50 (m, 1H, Ar), 7.45 – 7.36 (m, 2H, Ar), 5.95 – 5.80 (m, 1H, C*H*=CH_2), 5.77 (d, *J* = 10.1 Hz, 1H, NH), 5.51 – 5.38 (m, 1H, H-4'), 5.35 – 5.19 (m, 2H, CH=C*H*$_2$), 5.02 (d, *J* = 1.9 Hz, 1H, H-1'), 4.67 (d, *J* = 4.7 Hz, 1H, H-1), 4.46 – 4.31 (m, 2H), 4.22 – 4.08 (m, 4H), 4.05 – 4.76 (m, 6H), 2.01 (s, 3H, NHAc), 1.17 (m, 12H, (C*H*$_3$)$_3$CSi, Me), 0.98 (s, 9H, (C*H*$_3$)$_3$CSi), 0.94 (s, 9H, (C*H*$_3$)$_3$CSi), 0.71 (s, 9H, (C*H*$_3$)$_3$CSi), 0.16 (s,

3H, CH_3Si), 0.07 (s, 3H, CH_3Si), 0.04 (s, 3H, CH_3Si), –0.08 (s, 3H, CH_3Si). HRMS (ESI-TOF$^+$) for $C_{44}H_{78}NO_{11}Si_3$ (M+H$^+$) calcd 880.4878, found 880.4868.

Phenyl 4-*O*-(2-naphthyl)methyl-2,3-di-*O*-*tert*-butyldimethylsilyl-1-thio-α-L-rhamnopyranoside (4.05)

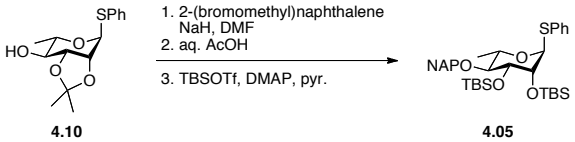

4.10 **4.05**

1. Anhydrous *N,N*-dimethylformamide (1.7 mL) was added to **4.10** (0.34 g, 1.1 mmol) in a round-bottom flask under Ar atmosphere. The solution was cooled to 0 °C. Oil-free NaH (33 mg, 1.4 mmol) was prepared by rinsing 55 mg of a 60% suspension of NaH in mineral oil in a flame-dried fritted filter under N_2 atmosphere with anhydrous pentane (6 mL). This NaH preparation was added to the solution of 4.10 in one portion. After 30 min at 0 °C, 2-(bromomethyl)naphthalene (0.30 g, 1.4 mmol) was added in one portion and the cooling bath was removed. After 2 h, the reaction was quenched with methanol and concentrated under reduced pressure. The residue was taken up in CH_2Cl_2 (20 mL) and transferred to a separatory funnel. The solution was shaken with brine (15 mL), the layers were separated, and the aqueous layer was extracted with CH_2Cl_2 (5 mL). The combined organic layers were dried over magnesium sulfate, filtered, and concentrated under reduced pressure. Purification by flash chromatography [hexanes to 3:17 (vol:vol) EtOAc:hexanes] afforded phenyl 2,3-*O*-isopropylidene-4-*O*-(2-naphthyl)methyl-1-thio-α-L-rhamnopyranoside as a crystalline solid (0.42 g, 85%, 98% based on recovered starting material).

^{1}H NMR (300 MHz, $CDCl_3$) δ 7.88 – 7.77 (m, 4H, Ar), 7.55 – 7.42 (m, 5H, Ar), 7.36 – 7.20 (m, 3H, Ar), 5.74 (s, 1H, H-1), 5.07 (d, *J* = 11.7 Hz, 1H, 1 x OC*H*Ar), 4.80 (d, *J* = 11.7 Hz, 1H, 1 x OC*H*Ar), 4.40 – 4.33 (m, 2H, H-2, H-3), 4.25 – 4.06 (m, 1H, H-5), 4.40 – 4.29 (m, 1H, H-4),

1.51 (s, 3H, (C*H*$_3$)C), 1.39 (s, 3H, (C*H*$_3$)C), 1.25 (d, *J* = 6.2 Hz, 3H, Me). HRMS (ESI-TOF$^+$) for $C_{26}H_{32}NO_4S$ (M+NH_4^+) calcd 454.2047, found 454.2046.

2. A suspension of 2,3-*O*-isopropylidene-4-*O*-(2-naphthyl)methyl-1-thio-α-L-rhamnopyranoside (0.20 g, 0.46 mmol) in a 4:1 (vol/vol) acetic acid:water solution (1.2 mL, 0.4 M) was heated to 80 °C under N_2 atmosphere. Solids dissolved after 5 min. After 2 h, the solution was cooled to ambient temperature and concentrated under reduced pressure to a clear oil. The oil was diluted in a minimal volume of a 1:1 (vol:vol) EtOAc:MeOH solution and purified by flash column chromatography. Elution from 1:3 (vol:vol) EtOAc:hexanes to 4:6 (vol/vol) EtOAc:hexanes afforded 4-*O*-(2-naphthyl)methyl-1-thio-α-L-rhamnopyranoside (0.17 g, 94%) as a white solid.

^{1}H NMR (300 MHz, 1:1 $CDCl_3$:CD_3OD) δ 7.88 – 7.77 (m, 4H, Ar), 7.56 – 7.40 (m, 5H, Ar), 7.33 – 7.17 (m, 3H, Ar), 5.44 (d, *J* = 1.6 Hz, 1H, H-1), 5.10 (d, *J* = 11.3 Hz, 1H, 1 x OC*H*Ar), 4.83 (d, *J* = 11.3 Hz, 1H, 1 x OC*H*Ar), 4.27 – 4.13 (m, 2H, H-2, H-5), 4.96 (dd, *J* = 9.3, 4.4 Hz, 1H, H-3), 4.55 (t, *J* = 9.3 Hz, 1H, H-4), 1.31 (d, *J* = 6.2 Hz, 3H, Me). ^{13}C NMR (75 MHz, 1:1 $CDCl_3$:CD_3OD) δ 135.5, 134.0, 132.9, 132.6, 130.9, 128.4, 127.5, 127.3, 127.1, 126.7, 126.2, 125.6, 125.5, 125.3, 88.0, 81.0, 74.6, 72.4, 71.6, 68.2, 17.0. HRMS (ESI-TOF$^+$) for $C_{23}H_{24}NaO_4S$ (M+Na^+) calcd 419.1288, found 419.1284.

3. 4-*O*-(2-Naphthyl)methyl-1-thio-α-L-rhamnopyranoside (0.17 g, 0.43 mmol) and 4-(dimethylamino)pyridine (5.2 mg, 43 μmol) were dissolved in anhydrous pyridine (2.8 mL) under Ar atmosphere. *tert*-Butyldimethylsilyl trifluoromethanesulfonate (0.49 mL, 2.1 mmol) was added dropwise. The flask was fitted with a water-cooled condenser and heated to 50 °C. After 18 h, the cloudy solution was cooled first to ambient temperature, then to 0 °C in an ice bath. The reaction was quenched by dropwise addition of methanol (3 mL). The solution was transferred to a separatory funnel, diluted with ethyl acetate and water, shaken, and the layers were separated. The organic layer was washed with hydrochloric acid (1 M), a saturated solution

of sodium bicarbonate, brine, then dried over magnesium sulfate, filtered, and concentrated under reduced pressure to a light yellow oil. The oil was co-evaporated with toluene (2 x 10 mL) and chloroform (2 x 10 mL). Purification by flash column chromatography [hexanes to 1:9 (vol/vol) EtOAc:hexanes] afforded **4.05** (0.27 g, quantitative) as a crystalline white solid.

^{1}H NMR (300 MHz, $CDCl_3$) δ 7.82 – 7.74 (m, 4H, Ar), 7.46 – 7.36 (m, 5H, Ar), 7.27 – 7.11 (m, 3H, Ar), 5.26 (d, *J* = 1.6 Hz, 1H, H-1), 5.01 (d, *J* = 11.8 Hz, 1H, 1 x OC*H*Ar), 4.73 (d, *J* = 11.8 Hz, 1H, 1 x OC*H*Ar), 4.18 – 4.95 (m, 3H, H-2, H-3, H-5), 4.59 (t, *J* = 9.2 Hz, 1H, H-4), 1.21 (d, *J* = 6.2 Hz, 3H, Me), 0.95 (s, 9H, $(CH_3)_3C$), 0.93 (s, 9H, $(CH_3)_3C$), 0.14 (br s, 3 x 3H, 3 x $SiCH_3$), 0.05 (s, 3H, $SiCH_3$). HRMS (ESI-TOF$^+$) for $C_{35}H_{56}NO_4SSi_2$ ($M+NH_4^+$) calcd 642.3464, found 642.3486.

Allyl 2-acetamido-2-deoxy-3-*O*-(4-*O*-(2-naphthyl)methyl-2,3-di-*O*-*tert*-butyldimethylsilyl-α-L-rhamnopyranosyl)-4,6-*O*-di-*tert*-butylsilylene-α-D-glucopyranoside (4.15)

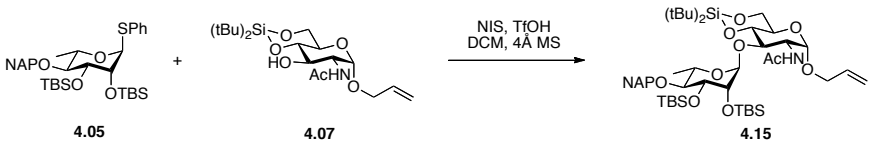

Monosaccharides **4.07** (0.11 g, 0.28 mmol) and **4.05** (0.21 g, 0.34 mmol) were combined in a round-bottom flask, co-evaporated with anhydrous toluene (3 x 10 mL), and kept under high-vacuum overnight. Activated 4 Å molecular sieve powder and freshly distilled CH_2Cl_2 (11.2 mL) were added under Ar atmosphere. The clear solution stirred at ambient temperature for 1 h, then it was cooled to –65 °C for 20 minutes. *N*-iodosuccinimide (0.13 g, 0.56 mmol) was added in one portion. After 5 min, trifluoromethanesulfonic acid (25 μL, 0.28 mmol) was added, and the solution quickly (<5 min) became orange and the color deepened over time to coral. The suspension was allowed to warm to –45 °C over 2.25 h. Freshly distilled triethylamine was then

added, causing a color change from coral to canary yellow. The suspension stirred at −45 °C for 5 min, then it was filtered through Celite and diluted with CH_2Cl_2. The solution was washed with 10% (wt/wt) sodium thiosulfate, a saturated solution of sodium bicarbonate, brine, dried over magnesium sulfate, filtered, and concentrated under reduced pressure to an orange film. Purification by flash chromatography [hexanes to 5:15 (vol/vol) EtOAc:hexanes] afforded **4.15** (0.19 g, 76%) as a foam.

^{1}H NMR (400 MHz, $CDCl_3$) δ 7.92 – 7.79 (m, 4H, Ar), 7.58 – 7.49 (m, 2H, Ar), 7.45 – 7.41 (m, 1H, Ar), 5.94 (ddt, *J* = 16.2, 10.8, 5.7 Hz, 1H, C*H*=CH_2), 5.82 (d, *J* = 10.0 Hz, 1H, NH), 5.41–5.23 (m, 2H, CH=C*H*$_2$), 5.14 – 5.01 (m, 2H, H-1', 1 x OC*H*Ar), 4.82 – 4.71 (m, 2H, H-1, 1 x OC*H*Ar), 4.45 – 4.33 (m, 2H), 4.28 – 4.13 (m, 3H), 4.10 – 4.82 (m, 5H), 4.54 (t, *J* = 9.4 Hz, 1H, H-4'), 2.06 (s, 3H, NHAc), 1.30 (d, *J* = 6.1 Hz, 3H, Me), 1.20 (s, 9H, (C*H*$_3$)$_3$Si), 1.10 (s, 9H, (C*H*$_3$)$_3$Si), 1.02 (s, 9H, (C*H*$_3$)$_3$C), 0.97 (s, 9H, (C*H*$_3$)$_3$C), 0.25 (s, 3H, SiC*H*$_3$), 0.17 – 0.12 (2 s, 2 x 3 H, 2 x SiC*H*$_3$), 0.09 (s, 3H, SiC*H*$_3$). ^{13}C NMR (101 MHz, $CDCl_3$) δ 169.7, 137.0, 134.5, 134.4, 132.7, 127.8, 127.8, 127.6, 126.0, 125.5, 125.3, 125.1, 118.1, 99.6, 97.1, 81.4, 76.4, 74.8, 74.9, 74.1, 72.6, 68.7, 68.4, 67.1, 66.9, 54.7, 27.8, 27.2, 26.4, 25.9, 24.9, 22.9, 20.0, 18.8, 18.3, 18.3, −4.0, −4.2, −4.3, −4.4. HRMS (ESI-TOF$^+$) for $C_{48}H_{82}NO_{10}Si_3$ (M+H$^+$) calcd 916.5242, found 916.5251.

Allyl 2-acetamido-2-deoxy-3-*O*-(4-*O*-(2-naphthyl)methyl-2,3-di-*O*-acetyl-α-L-rhamnopyranosyl)-4,6-di-*O*-acetyl-α-D-glucopyranoside (4.16)

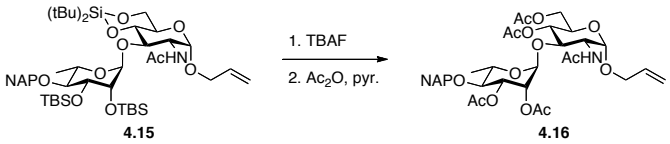

4.15 4.16

1. Freshly distilled tetrahydrofuran (2.4 mL) was added to a round-bottom flask containing **4.15** (0.18 g, 0.20 mmol) under Ar atmosphere. A solution of tetra-*n*-butylammonium fluoride (TBAF) in tetrahydrofuran (1.0 M, 2.41 mL, 2.41 mmol) was added,

and the clear solution stirred at ambient temperature. After 14 h, the reaction was concentrated under reduced pressure to afford crude allyl 2-acetamido-2-deoxy-3-*O*-(4-*O*-(2-naphthyl)methyl-α-L-rhamnopyranosyl)-α-D-glucopyranoside as a brown oil that was taken on to the next step immediately.

2. The crude allyl 2-acetamido-2-deoxy-3-*O*-(4-*O*-(2-naphthyl)methyl-α-L-rhamnopyranosyl)-α-D-glucopyranoside (~0.20 mmol) was dissolved in anhydrous pyridine (2.0 mL) under Ar atmosphere. The solution was cooled to 0 °C for 15 min prior to dropwise addition of acetic anhydride (4.0 mL). The solution was allowed to slowly warm to ambient temperature while stirring overnight. After 5 h, the reaction was diluted with methanol and concentrated under reduced pressure to a brown oil that was co-evaporated with toluene (2 x 5 mL). The oil was taken up in EtOAc (30 mL) and washed with a 1M solution of hydrochloric acid (2x), a saturated sodium of sodium bicarbonate, brine, dried over magnesium sulfate, filtered, and concentrated under reduced pressure to a faint brown film. Purification by flash chromatography [hexanes to 4:1 (vol/vol) EtOAc:hexanes] afforded **4.16** (144 mg, 99% over 2 steps) as a clear oil.

^{1}H NMR (400 MHz, $CDCl_3$) δ 7.88 – 7.70 (m, 4H, Ar), 7.52 – 7.34 (m, 3H, Ar), 5.94 – 5.82 (m, 1H, C*H*=CH), 5.74 – 5.64 (m, 1H, CH=C*H*), 5.35 – 5.06 (m, 4H), 4.91 – 4.70 (m, 4H), 4.49 – 4.30 (m, 2H), 4.21 – 4.03 (m, 4H), 4.03 – 4.95 (m, 1H), 4.94 – 4.72 (m, 2H), 4.68 – 4.44 (m, 2H), 2.13 (s, 3H, OAc), 2.11 – 2.09 (2 s, 2 x 3H, 2 x OAc), 2.04 (s, 3H, OAc), 1.91 (s, 3H, NHAc), 1.30 – 1.23 (m, 3H, Me). HRMS (ESI-TOF$^+$) for $C_{36}H_{49}N_2O_{14}$ ($M+NH_4^+$) calcd 734.3179, found 734.3182.

Allyl 2-acetamido-2-deoxy-3-*O*-(2,3-di-*O*-acetyl-α-L-rhamnopyranosyl)-4,6-di-*O*-acetyl-α-D-glucopyranoside (4.17)

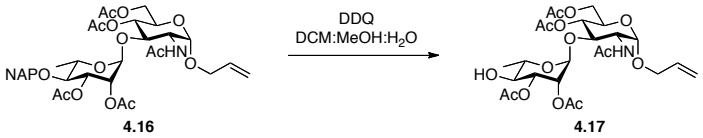

A round-bottom flask containing **4.16** (42 mg, 59 μmol) was placed under Ar atmosphere. Freshly distilled MeOH (0.6 mL), freshly distilled CH_2Cl_2 (2.3 mL), and two drops of water were added, followed by 2,3-dichloro-5,6-dicyano-*para*-benzoquinone (20 mg, 88 μmol) in one portion. The dark brown solution stirred at ambient temperature for 15 h. The reaction was concentrated under reduced pressure to a brown solid that was taken up in dichloromethane and transferred to a separatory funnel. The solution was washed with a solution of saturated sodium bicarbonate until the organic layer was clear, then washed with water, dried over magnesium sulfate, filtered, and concentrated under reduced pressure to a brown film. Purification by flash chromatography [CH_2Cl_2 to 4:96 (vol/vol) MeOH:CH_2Cl_2] afforded **4.17** (26 mg, 77%) as a white solid.

^{1}H NMR (400 MHz, $CDCl_3$) δ 5.89 (ddt, *J* = 16.1, 10.5, 5.9 Hz, 1H, C*H*=CH_2), 5.72 (d, *J* = 9.7 Hz, 1H, NH), 5.36 – 5.22 (m, 2H), 5.14 – 5.02 (m, 2H), 4.98 (dd, *J* = 10.0, 4.4 Hz, 1H), 4.89 – 4.79 (m, 2H), 4.46 – 4.30 (m, 2H), 4.21 – 4.04 (m, 4H), 4.03 – 4.96 (m, 1H), 4.93 – 4.71 (m, 3H), 4.68 – 4.50 (m, 2H), 2.12 (s, 3H, OAc), 2.10 (s, 3H, OAc), 2.09 – 2.07 (2 s, 2 x 3H, 2 x OAc), 2.05 (s, 3H, NHAc), 1.28 (d, *J* = 5.9 Hz, 3H, Me).

Thiazolyl 2,3,4,5-tetra-*O*-acetyl-D-galactofuranoside (4.04)

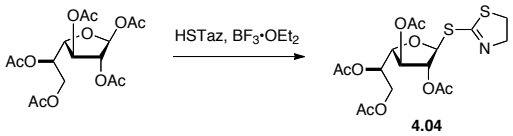

Penta-*O*-acetyl-D-galactofuranoside[248] (1.2 g, 4.0 mmol) was added to a round-bottom flask, co-evaporated with freshly distilled toluene (3 x 10 mL), and kept under high-vacuum overnight. Activated 4 Å molecular sieve sticks and 2-thiazoline-2-thiol (0.72 g, 6.0 mmol) were added under Ar atmosphere, followed by freshly distilled CH_2Cl_2 (23 mL). The reaction was cooled to 0 °C for 10 minutes. Boron trifluoride diethyl etherate (0.74 mL, 6.0 mmol) was added dropwise, and the reaction stirred at 0 °C for 15 minutes. The cooling bath was then removed. After 8 h, the reaction was quenched with triethylamine (0.8 mL), diluted with CH_2Cl_2, filtered and transferred to a separatory funnel. The solution was washed with a saturated solution of sodium bicarbonate, brine, dried over magnesium sulfate, filtered, and concentrated under reduced pressure to a light yellow oil. Purification by flash column chromatography [CH_2Cl_2 to 4:96 (vol/vol)CH_2Cl_2:MeOH] afforded **4.04** as a clear oil. Characterization of this compound matched a previous report.[244]

Allyl 2-acetamido-2-deoxy-3-*O*-(2,3-di-*O*-acetyl-4-*O*-(2,3,4,5-tetra-*O*-acetyl-β-D-galactofuranosyl)-α-L-rhamnopyranosyl)-4,6-di-*O*-acetyl-α-D-glucopyranoside (4.02)

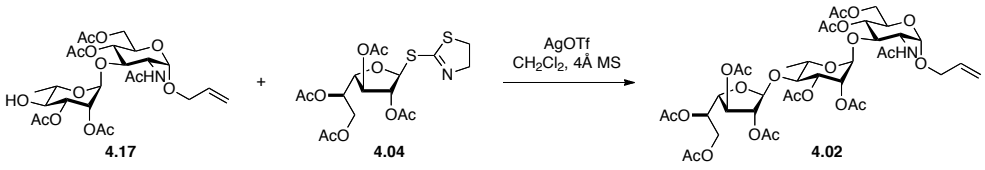

Compounds **4.17** (25 mg, 43 μmol) and **4.04** (39 mg, 87 μmol) were combined in a round-bottom flask, co-evaporated with anhydrous toluene (3 x 3 mL), and kept under high-vacuum overnight. Activated 4 Å molecular sieve powder and freshly distilled CH_2Cl_2 (1.5 mL) were added under Ar atmosphere. The clear solution stirred at ambient temperature for 1 h, then it was cooled to 0 °C for 20 min. Silver trifluoromethanesulfonate (34 mg, 0.13 mmol) was added, and the reaction stirred at 0 °C for 30 min, then it was warmed to ambient temperature.

After 4.5 h at ambient temperature, the reaction was filtered through Celite (rinsed with CH_2Cl_2), washed with a saturated solution of sodium bicarbonate, water, brine, dried over magnesium sulfate, filtered, and concentrated under reduced pressure to a clear film. Purification by flash column chromatography [CH_2Cl_2 to 3:97 MeOH:CH_2Cl_2] afforded **4.02** (31 mg, 78%) as a clear film.

^{1}H NMR (400 MHz, $CDCl_3$) δ 5.89 (ddt, *J* = 16.8, 10.4, 6.1 Hz, 1H, C*H*=CH_2), 5.68 (d, *J* = 9.7 Hz, 1H, NH), 5.43 – 5.35 (m, 1H, H-5”), 5.33 – 5.23 (m, 3H, CH=C*H*$_2$, H-1”), 5.22 – 5.05 (m, 2H, H-2’, H-3’), 5.02 – 4.99 (m, 1H, H-3”), 4.92 (t, *J* = 1.5 Hz, 1H, H-2”), 4.87 (d, *J* = 4.6 Hz, 1H, H-1), 4.76 (d, *J* = 1.6 Hz, 1H, H-1’), 4.46 – 4.39 (m, 1H, H-2), 4.32 – 4.25 (m, 3H, H-3, H-4”), 4.25 – 4.09 (m, 4H, 2 x H-6, 2 x H-6”), 4.09 – 4.97 (m, 2H, OC*H*$_2$CH=CH_2), 4.89 – 4.77 (m, 3H, H-4, H-5, H-5’), 4.63 (t, *J* = 9.8 Hz, 1H, H-4’), 2.13 (s, 3H, OAc), 2.12 – 2.11 (m, 3 x 3H, 3 x OAc), 2.10 (s, 3H, OAc), 2.07 (s, 3H, OAc), 2.06 (s, 2 x 3H, 2 x OAc), 1.99 (s, 3H, NHAc), 1.22 (d, *J* = 6.2 Hz, 3H, Me). ^{13}C NMR (101 MHz, $CDCl_3$) δ 170.9, 170.7, 170.6, 170.5, 170.3, 170.1, 169.6, 169.6, 169.2, 134.2, 118.7, 106.6, 99.8, 96.9, 81.2, 80.9, 80.1, 76.4, 75.6, 71.7, 70.4, 69.4, 68.8, 68.3, 68.1, 62.5, 62.2, 51.8, 24.4, 21.3, 21.2, 21.1, 20.9, 20.9, 20.9, 20.8, 20.8, 17.6. HRMS (ESI-TOF$^+$) for $C_{39}H_{59}N_2O_{23}$ ($M+NH_4^+$) calcd 924.3504, found 924.3535.

11-Phenoxy-1-undecene (4.03)

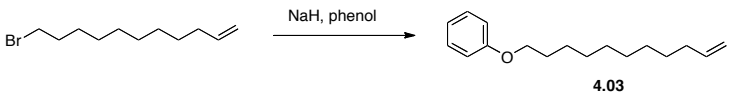

4.03

Phenol (0.94 g, 10.0 mmol, 20 eq) was dissolved in tetrahydrofuran (4.0 mL), followed by addition of NaH (0.40 g, 10.0 mmol, 2.0 eq). A solution of 11-bromo-1-undecene (1.1 mL, 5.0 mmol) in tetrahydrofuran (2.0 mL) was added. The reaction was heated and refluxed for 45 h. The reaction was cooled to ambient temperature and quenched with a saturated solution of

ammonium chloride (8.0 mL). The mixture was diluted with ethyl acetate (20 mL) and shaken. The organic layer was washed with a saturated solution of ammonium chloride (20 mL), water (20 mL), and brine (20 mL). The organic layer was dried over magnesium sulfate, filtered, and concentrated under reduced pressure to yield a crude brown liquid. Purification by flash column chromatography (hexanes) afforded **4.03** as a clear oil. Characterization of this compound matched a published report.[116]

12-Phenoxy-dodec-2-enyl 2-acetamido-2-deoxy-3-*O*-(2,3-di-*O*-acetyl-4-*O*-(2,3,4,5-tetra-*O*-acetyl-β-D-galactofuranosyl)-α-L-rhamnopyranosyl)-4,6-di-*O*-acetyl-α-D-glucopyranoside (4.18)

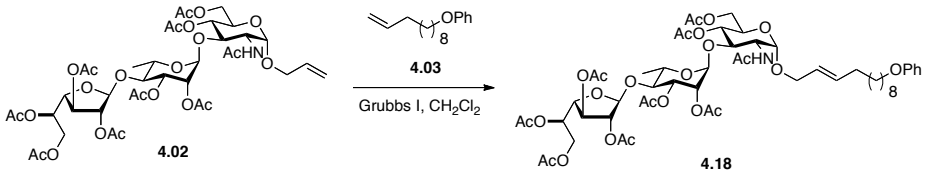

Compound **4.03** (11 mg, 46 μmol) and bis(tricyclohexylphosphine)benzylidine ruthenium(IV) dichloride (1.3 mg, 1.5 μmol) were added to a round-bottom flask containing **4.02** (7.0 mg, 7.7 μmol) under Ar atmosphere. Freshly distilled CH_2Cl_2 (0.4 mL) was added, and the solution was warmed to 45 °C for 4 h. The reaction was cooled to ambient temperature and concentrated under reduced pressure to a reddish brown solid. Purification by flash chromatography [CH_2Cl_2 to 3:97 MeOH:CH_2Cl_2] afforded **4.18** (9.1 mg, 93%) as a solid.

^{1}H NMR (400 MHz, $CDCl_3$) δ 7.31 – 7.24 (m, 2H, Ar), 6.96 – 6.87 (m, 3H, Ar), 5.72 (m, 1H, C*H*=CH), 5.63 (d, *J* = 9.7 Hz, 1H, NH), 5.55 – 5.44 (m, 1H, CH=C*H*), 5.38 (dt, *J* = 8.8, 4.8 Hz, 1H, H-5”), 5.28 (s, 1H, H-1”), 5.15 – 4.98 (m, 4H, H-2’, H-3’, H-3”), 4.91 (s, 1H, H-2”), 4.84 (d, *J* = 4.4 Hz, 1H, H-1), 4.75 (s, 1H, H-1’), 4.41 (td, *J* = 10.1, 4.6 Hz, 1H, H-2), 4.30 – 4.13 (m, 5H, H-3, H-4”, 2 x H-6, 2 x H-6”), 4.12 – 4.02 (m, 2H, OC*H*$_2$CH), 4.95 (t, *J* = 6.5 Hz, 2H,

C*H*$_2$OPh), 4.87 – 4.75 (m, 3H, H-4, H-5, H-5'), 4.62 (t, *J* = 9.7 Hz, 1H, H-4'), 2.13 (s, 3H, OAc), 2.11 (s, 3 x 3H, 3 x OAc), 2.10 (s, 3H, OAc), 2.08 – 2.05 (m, 12H, 3 x OAc, OCH$_2$*CH*$_2$), 1.98 (s, 3H, NHAc), 1.78 (p, *J* = 6.7 Hz, 2H, C*H*$_2$CH$_2$OPh) 1.48 – 1.25 (m, 12H, -C*H*$_2$-), 1.22 (d, *J* = 6.2 Hz, 3H, Me). HRMS (ESI-TOF$^+$) for $C_{54}H_{81}N_2O_{24}$ (M+NH_4^+) calcd 1141.5174, found 1141.5148.

12-Phenoxy-dodec-2-enyl 2-acetamido-2-deoxy-3-*O*-(4-*O*-(β-D-galactofuranosyl)-α-L-rhamnopyranosyl)-α-D-glucopyranoside (4.01)

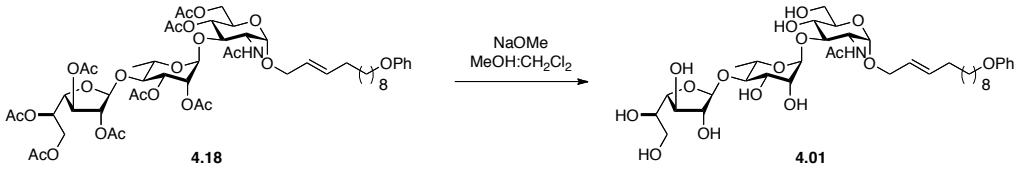

A solution of NaOMe in MeOH (0.5 M, 60 μL, 30 μmol) was added to a solution of **4.18** (6.6 mg, 5.9 μmol) in 3:1 (vol/vol) MeOH:CH_2Cl_2 under Ar atmosphere. The reaction stirred at ambient temperature for 4.5 h. The reaction was quenched with Amberlite IR-120 resin (H^+ form), filtered through a pad of cotton, and concentrated under reduced pressure. Purification by flash chromatography [95:5 (vol/vol) EtOAc:MeOH to 70:30 EtOAc:MeOH] afforded **4.01** (2.5 mg, 54%) as a clear film, as a 10:1 α:β mixture.

^{1}H NMR (500 MHz, CD_3OD) δ 7.28 – 7.21 (m, 2H, Ar), 6.92 – 6.86 (m, 3H, Ar), 5.81 – 5.71 (m, 1H, C*H*=CH), 5.63 – 5.54 (m, 1H, CH=C*H*), 5.27 (d, *J* = 1.7 Hz, 1H, H-1"), 4.84 (d, *J* = 1.4 Hz, 1H, H-1), 4.74 (d, *J* = 4.4 Hz, 1H, H-1'), 4.15 (dd, *J* = 12.4, 5.3 Hz, 1H), 4.08 – 4.93 (m, 8H), 4.85 – 4.77 (m, 2H), 4.75 – 4.67 (m, 4H), 4.65 – 4.59 (m, 3H), 4.55 (t, *J* = 9.6 Hz, 1H), 4.43 – 4.38 (m, 1H), 2.09 – 2.03 (m, 2H, OCH$_2$CH=CHC*H*$_2$), 1.99 (s, 3H, NHAc), 1.80 – 1.72 (m, 2H, C*H*$_2$CH$_2$OPh), 1.48 (p, *J* = 7.0 Hz, 2H, C*H*$_2$(CH$_2$)$_2$OPh), 1.43 – 1.31 (m, 10H, -C*H*$_2$-), 1.26 (d, *J* = 6.2 Hz, 3H, Me). ^{13}C NMR (126 MHz, CD_3OD) δ 174.4, 160.6, 136.5, 130.4, 126.8, 121.5, 115.5, 110.2, 102.8, 97.5, 84.4, 84.5, 81.2, 79.0, 78.5, 74.0, 74.0, 72.6, 72.2, 70.7, 68.9, 68.8, 64.7, 62.6,

54.6, 34.4, 30.6, 30.5, 30.5, 30.5, 30.3, 27.2, 22.6, 18.4. HRMS (ESI-TOF$^+$) for $C_{38}H_{65}N_2O_{16}$ ($M+NH_4^+$) calcd 805.4329, found 805.4330.

Chapter 5: Structural Analysis of Galactofuranose Oligosaccharides with Chain Terminating Agents

Portions of this work are described in a manuscript being prepared for publication:

Martinez Farias, M. A.; Yamatsugu, K.; Brown, C. D.; Kiessling, L. L. Structural Analysis of Galactofuranose Oligosaccharides with Chain Terminating Agents.

Contributions:

Synthesis of the deoxygenated UDP-Gal*f* analogs performed by C.D. Brown and K. Yamatsugu.

Cloning and expression of GlfT1 performed by V.A. Kincaid.

5.1 Abstract

Chain terminating agents are excellent probes of biopolymer sequence and specificity. We hypothesized that we could use chain terminating agents in a mass spectrometry-based assay to analyze the linkage structure of mycobacterial cell wall glycans. In this assay, incorporation of nucleotide-sugar donor analogs deoxygenated at key positions truncates glycan formation and provides a pattern that resolves the position of the next glycosidic linkage. We confirm that the non-reducing-end of the product generated by the mycobacterial galactofuranosyltransferase GlfT1 is a Gal*f*-β(1,6)-Gal*f*-β(1,5)-Gal*f* oligosaccharide. The use of nucleotide-sugar donor analogs as substrate probes of oligosaccharide structure complements current methods of carbohydrate structural analysis. Furthermore, synthetic efforts toward a deoxygenated acceptor substrate are described.

5.2 Introduction

Structural data of complex glycans is crucial in probing the function of the carbohydrate-processing enzymes that build them. Subtle differences in the valency or architecture can dramatically alter the presentation of a glycan.[249] Our laboratory has established a research program investigating the assembly of galactan, an essential structural glycopolymer found in the cell wall of mycobacteria.[112,116-119,124] Galactan is a polymer of galactofuranose (Gal*f*) that consists of 30–40 Gal*f* units arranged in an alternating β(1,5) and β(1,6) pattern.[115,119,124,181] Its assembly is mediated by the galactofuranosyltransferases GlfT1 and GlfT2. GlfT1 elongates decaprenyl-linked Rha-α(1,3)-GlcNAc pyrophosphate with 2–3 galactofuranose (Gal*f*) residues. This lipid-linked oligosaccharide is then processed by the polymerase GlfT2 to yield the full-length galactan polymer.

5.3 Linkage analysis of oligosaccharides prepared by GlfT1

Since the galactan anchors upper cell wall components targeted by antitubercular drugs,[176] we were interested in the origin of its alternating pattern structure. We have recently defined the function of GlfT1 in vitro and shown that it mediates the critical first steps in galactan assembly.[112] Herein, we confirm the linkage structure of Gal*f* oligomers generated upon processing of farnesyl-linked disaccharide phosphonophosphate **2.08** by GlfT1 in the presence of nucleotide-sugar donor UDP-Gal*f*. We postulate that GlfT1 is responsible for setting the register for the alternating pattern observed in endogenous galactan.

Traditional carbohydrate structural analysis methods can be extremely powerful. However, the functionality of the oligosaccharides processed by GlfT1 poses a series of challenges for these approaches,[250-254] and limited quantities of phosphonophosphate-linked oligosaccharides for analysis restricted the utility of alternative methods such as NMR

spectroscopy. We therefore pursued a mass spectrometry-based approach that would yield critical structural information while requiring minute amounts of sample. Chain termination agents are suitable reagents for this purpose.

The use of chain termination agents to sequence polymers is well established, particularly with respect to DNA sequencing by the Sanger method.[255] We have previously demonstrated that fluorinated nucleotide-sugar donors are excellent chain terminators when assaying the sequence fidelity of the polymerase GlfT2.[124] Deoxygenated nucleotide-sugar donor analogs, however, are typically designed as inhibitors of glycosyltransferase function.[111,122] We recognized that these probes could be useful for structural analysis of growing oligosaccharide chains. In analogy to Sanger sequencing, we utilize incorporated deoxysugars as probes of oligosaccharide structure. This mass spectrometry-based assay provides a clear read-out of the linkages formed by GlfT1. Truncation of the growing polysaccharide chain with the appropriate deoxysugar correlates to the regiochemistry of the following linkage. The binding affinity these analogs is expected to be similar to the endogenous donor,[111] and the specificity of the galactofuranosyltransferase avoids a 'mistaken' glycosidic linkage.

GlfT1 catalyzes the addition of 2–3 Gal*f* residues to acceptor **2.08** from donor nucleotide-sugar UDP-Gal*f*. We reasoned that in generating a +3 Gal*f* product, GlfT1 sets the register for the alternating β(1,5) and β(1,6) pattern of endogenous galactan. Thus, we expected GlfT1 to generate a Gal*f*-β(1,6)-Gal*f*-β(1,5)-Gal*f* pattern at the non-reducing end. Incorporated nucleotide-sugar donors deoxygenated at the 5- or 6-hydroxyl positions should probe the structure of this oligosaccharide. For example, if the oligosaccharide chain is truncated upon incorporation of a 5-deoxysugar, the next residue is (1,5)-linked. Alternatively, truncation upon incorporation of a 6-deoxysugar would suggest that the next residue is (1,6)-linked. Thus, we reasoned that nucleotide-sugar donor analogs **5.01** and **5.02** would be excellent structural

probes (Scheme 5.1). The donor analogs were synthesized through coupling UMP with the corresponding galactofuranosyl phosphates[111] as described previously.[106,256]

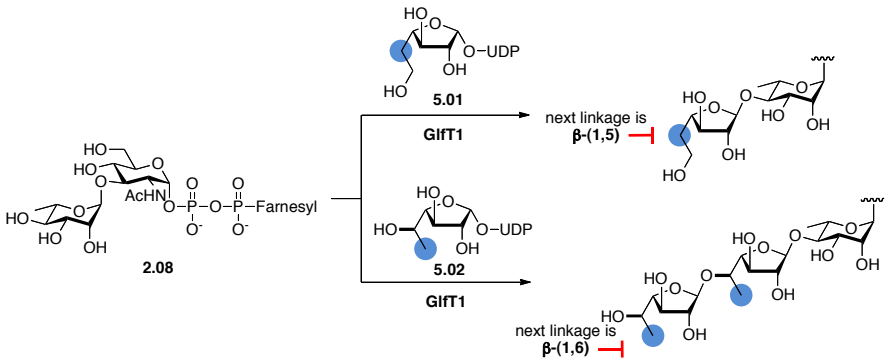

Scheme 5.1. Use of deoxygenated UDP-Gal*f* donor analogs **5.01** and **5.02** as linkage determination probes.

We exposed phosphonophosphate acceptor **2.08** to donors **5.01** and **5.02** in the presence of purified *M. smegmatis* GlfT1 and analyzed each reaction mixture by MALDI-TOF mass spectrometry. As described in Chapter 3, GlfT1 processes acceptor **2.08** to a mixture of +2 and +3 Gal*f* oligosaccharides by GlfT1 (Figure 5.1C). This galactofuranosyltransferase activity corresponds to the enzyme's expected function in mycobacterial cell wall biosynthesis. Incubation with donor **5.01** leads to the formation of a truncated +1 5H-Gal*f* oligosaccharide (Figure 5.1A). This result indicates that the addition of a second Gal*f* residue specifically at the 5-position is blocked. Alternatively, incorporation of two 6H-Gal*f* units from **5.02** is expected. Indeed, incubation of **2.08** with donor **5.02** in the presence of GlfT1 produces a mixture of +1 6H-Gal*f* and +2 6H-Gal*f* oligosaccharides (Figure 5.1B). Thus, the addition of a third Gal*f* residue at the 6-position is blocked.

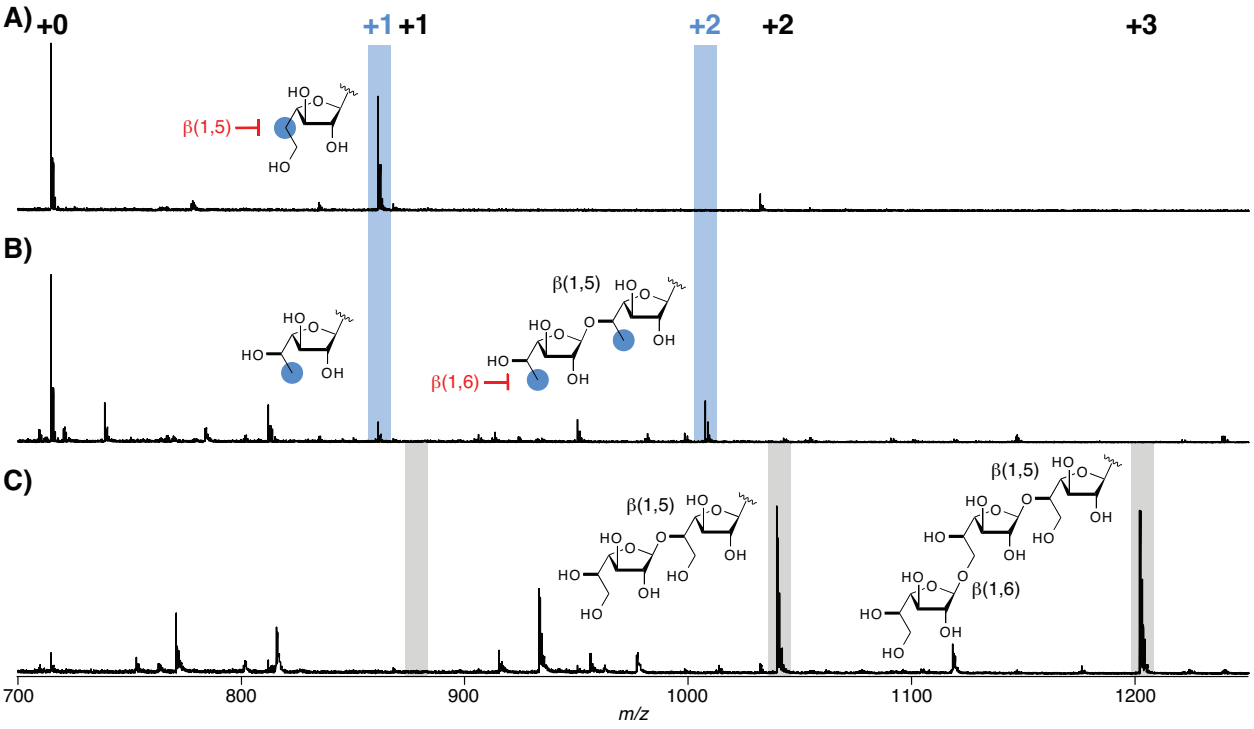

Figure 5.1. MALDI-TOF MS analysis of a GlfT1 reaction mixture with phosphonophosphate acceptor **2.08** and deoxygenated donor sugars.

Taken together, the incorporated deoxysugars reveal the linkage structure of the non-reducing end of the lipid-linked oligosaccharide. Incorporation of two 6H-Gal*f* residues indicates a terminal Gal*f*-β(1,6)-Gal*f* linkage. Incorporation of one 5H-Gal*f* indicates that the penultimate linkage is Gal*f*-β(1,5)-Gal*f*. Thus, the structure of the non-reducing end is Gal*f*-b(1,6)-Gal*f*-b(1,5)-Gal*f*. The sugars are presumed to be β-linked, given structural homology of GlfT1 with inverting glycosyltransferases. This configuration corresponds to the orientation of endogenous galactan. Importantly, these experiments confirm our hypothesis that GlfT1 sets the register for galactan pattern deposition.

Since glycan assembly occurs in a template-independent fashion, our results provide insight into how the galactan pattern emerges. We postulate that the more restrictive[112] galactofuranosyltransferase GlfT1 not only primes galactan biosynthesis, but also sets the

alternating pattern register for the polymerase. The polymerase GlfT2 builds the galactan with a faithfully alternating β(1,5) and β(1,6) pattern, and terminates a chain when it cannot propagate the pattern.[124] The remarkable fidelity of GlfT2 implies an important physiological role for the precise pattern of this polymer. Despite participating in the addition of only 2–3 residues of a ~35-residue carbohydrate polymer, GlfT1 is critically important for assembly of the galactan.

An assay for oligosaccharide structural analysis was developed, wherein the galactofuranosyltransferase GlfT1 reports the linkages it is forming as it processes an acceptor substrate by incorporating deoxygenated Gal*f* analogs. Assaying the glycosyltransferase with readily accessible reagents in an activity assay, we have determined that GlfT1 generates an oligosaccharide with a non-reducing-end Gal*f*-β(1,6)-Gal*f*-β(1,5)-Gal*f* trisaccharide. An operationally simple assay consisting of straightforward MALDI-TOF analysis of crude enzymatic reaction mixtures avoided laborious, destructive derivatization protocols, and required only picomoles of sample for analysis.

To completely characterize the three linkages formed by GlfT1 via deoxygenated sugars, however, required access to a deoxygenated acceptor substrate. GlfT1 adds the first Gal*f* linkage to the 4-hydroxyl position of rhamnose, as confirmed by NMR spectroscopy in Chapter 3. In the context of our results with deoxygenated donor sugars above, we expected that 4'-deoxygenated acceptor surrogate **5.03** would not serve as a suitable GlfT1 acceptor (Scheme 5.2). This acceptor would not only report the nature of the first linkage formed by GlfT1, but also test its ability to make a mistaken linkage.

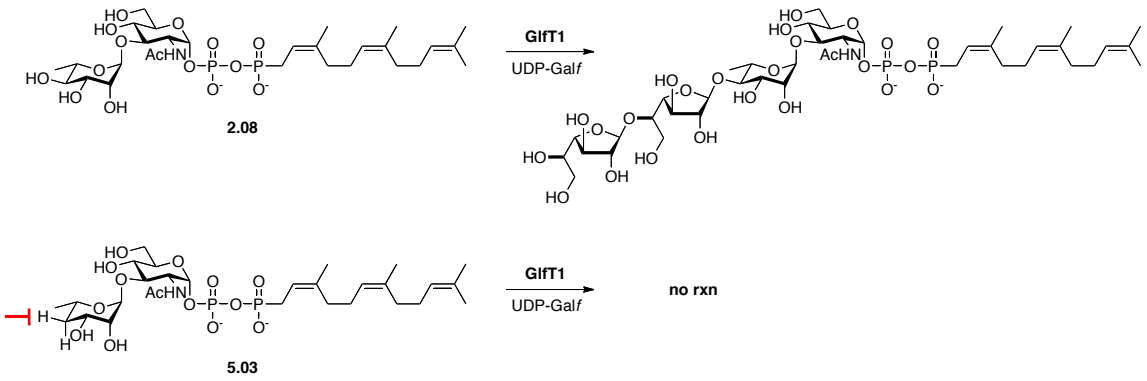

Scheme 5.2. Use of 4'-deoxygenated farnesyl-linked disaccharide phosphonophosphate as GlfT1 specificity probe.

Intermediates previously synthesized in Chapter 4 provided elaborated monosaccharides to target acceptor analog **5.03** (Scheme 5.3). Glycosylation of silyl-protected 4'-*O*-naphthyl rhamnosyl thioglycoside **4.05** and benzyl glucosamine **2.16** with *N*-iodosuccinimide and trifluoromethanesulfonic acid yielded 4'-*O*-naphthyl disaccharide **4.04** in good yield. At this junction, the silyl protecting groups were exchanged for acetate groups to provide **4.05**. The 4'-hydroxyl was exposed by oxidative removal of the naphthyl protecting group with DDQ. Isolating this position set up the possibility of deoxygenating the disaccharide.

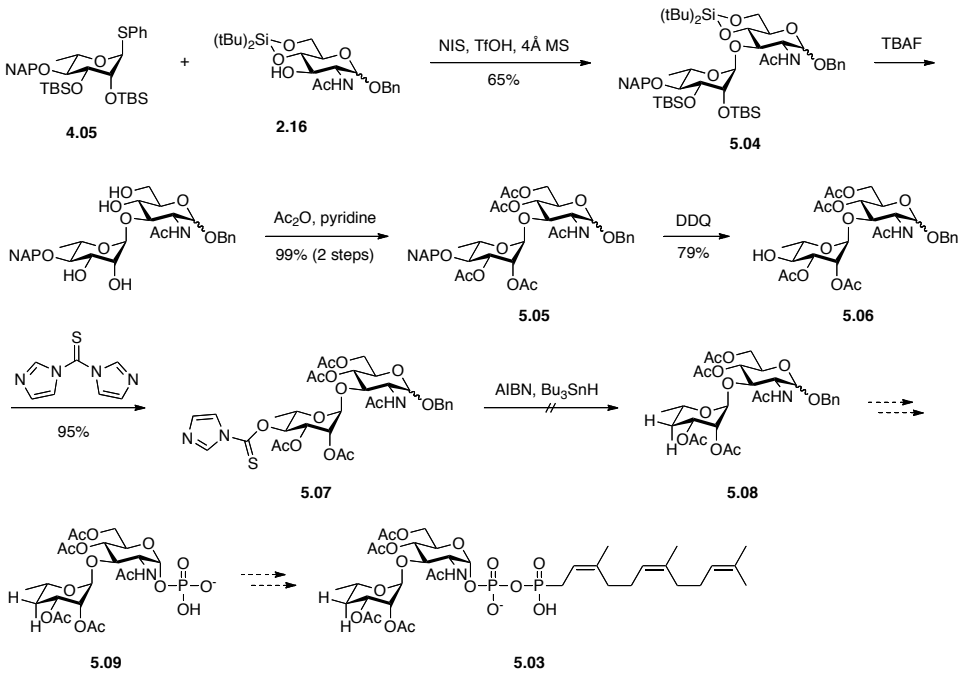

Scheme 5.3. Synthetic efforts toward 4'-deoxygenated phosphonophosphate acceptor **5.03**.

We pursued deoxygenation of the 4'-hydroxyl group using the protocol developed by Barton-McCombie.[257] This method involves radical deoxygenation of a thiocarbonyl derivative with tributyltin hydride in the presence of a radical initiator. Pozsgay and Neszmelyi, among others, have utilized Barton-McCombie deoxygenation to prepare deoxy glycosides.[258] Alcohol **5.06** was converted to thiocarbonyl derivative **5.07** by reaction with 1,1'-thiocarbonyldiimidazole in excellent yield. Unfortunately, treatment of thiocarbonyl **5.07** with 2,2'-azobis(2-methylpropionitrile) (AIBN) and tributyltin hydride resulted in decomposition. No **5.08** could be isolated from the complex mixture. It is known that substitution reactions on activated 4-hydroxyl groups on rhamnopyranosides can lead to a number of side products,[259] though these side products were not expected in a Barton-McCombie deoxygenation. Alternative methods for radical deoxygenation of acceptor **5.03**, such as the use of tris(trimethylsilyl)silane,[260] will be pursued. Elaboration of **5.08** would produce 4'-

deoxygenated phosphate **5.09**, which can be coupled to (2Z,6Z)-farnesyl phosphonomorpholidate to yield **5.03**.

5.4 Conclusions

The capability to examine linkage specificity could be useful and general for other glycosyltransferases. The extension to probing incorporation of pools of deoxygenated nucleotide-sugar donors into complex glycans is especially attractive. Species of *Shigella*[261] and *Salmonella*[262] have over 30 O-antigen biosynthetic gene clusters. Painstaking and remarkable efforts have defined the function of the majority of these genes. We posit that deoxygenated nucleotide-sugar pools can streamline the structural characterization of rare glycans assembled by organisms that contain numerous putative biosynthetic gene clusters. In addition to this method, a synthetic effort toward a 4'-deoxygenated disaccharide phosphonophosphate acceptor was described. An alternative deoxygenation method to the Barton-McCombie protocol may provide access to this acceptor.

5.5 Experimental details

All compounds were purchased from Sigma Aldrich (Milwaukee, WI) or Fisher Scientific (Pittsburgh, PA). Tetrahydrofuran (THF) was distilled from sodium/benzophenone ketyl, methanol (MeOH) was distilled from magnesium, and dichloromethane (CH_2Cl_2) was distilled from calcium hydride. Other solvents were purified according to the guidelines in *Purification of Common Laboratory Chemicals*.[221] All reactions were run under argon atmosphere in oven-dried glassware unless otherwise stated. Molecular sieves were activated by heating to 600 °C in a furnace for 12 h, then cooled in a dessicator. Analytical thin layer chromatography (TLC) was carried out on E. Merck (Darmstadt) TLC plates pre-coated with silica gel 60 F254 (250 μm

layer thickness). Analyte visualization was accomplished using a UV lamp and by charring with a solution of *p*-anisaldehyde (3.5 mL), acetic acid (15 mL), H_2SO_4 (50 mL), and ethanol (350 mL). Flash column chromatography was performed with Silicycle Flash Silica Gel (40-63 μm, 60 Å pore size) using reagent grade hexanes and ACS grade ethyl acetate (EtOAc) or ACS grade acetone, or methanol (MeOH) and CH_2Cl_2. ^1H and ^{13}C nuclear magnetic resonance (NMR) spectra were recorded on a 300 MHz spectrometer (acquired at 300 MHz for ^1H NMR and 75 MHz for ^{13}C NMR) a 400 MHz spectrometer (acquired at 400 MHz for ^1H NMR and 101 MHz for ^{13}C NMR), or a 500 MHz spectrometer (acquired at 500 MHz for ^1H NMR and 126 MHz for ^{13}C NMR). Chemical shifts are reported relative to tetramethylsilane or residual solvent peaks in parts per million ($CHCl_3$: ^1H: 7.26, ^{13}C: 77.16; MeOH: ^1H: 3.31, ^{13}C: 49.00; HDO: ^1H: 4.79). Peak multiplicity is reported as singlet (s), doublet (d), doublet of doublets (dd), doublets of doublets of doublets (ddd), triplet (t), doublet of triplets (dt), etc. High resolution electrospray ionization-time of flight mass spectra (HRESI-TOF MS) were obtained on a Micromass LCT. Matrix-assisted laser desorption/ionization-time of flight mass spectra (MALDI-TOF MS) were obtained on a Bruker Ultraflex III.

Assays with GlfT1 were carried out in 35 μL final volume containing 2 μM GlfT1-His_6, 100 μM acceptor substrate and 300 μM donor sugar (UDP-Gal*f*, 5-deoxy-UDP-Gal*f*, or 6-deoxy-UDP-Gal*f*) in 50 mM 4-morpholinepropanesulfonic acid (MOPS), pH 7.9, 10 mM $MgCl_2$ and 5 mM β-mercaptoethanol. Reactions were incubated at 37 °C for 2 h, quenched with 35 μL of a 1:1 v/v mixture of chloroform:methanol, and evaporated to dryness on a SpeedVac SC100 (Varian). The dried mixtures were re-suspended in 35 μL of water, desalted with a ZipTip C18 pipette tip (Millipore), eluting with a 1:1 (vol/vol) solution of 20 mM ammonium bicarbonate:acetonitrile. The eluent solution was spotted onto a stainless steel plate for MALDI-TOF MS analysis as a 1:2 (vol/vol) mixture with 2-(4-hydroxyphenylazo)benzoic acid matrix containing diammonium citrate. The matrix solution was prepared by saturating a 1:1 (vol/vol) water:acetonitrile solution

with 2-(4-hydroxyphenylazo)benzoic acid, and adding aqueous diammonium citrate (0.2 M) to a final concentration of 25 mM. MALDI spectra were recorded in negative reflectron mode on a Bruker Ultraflex III instrument.

Benzyl 2-acetamido-2-deoxy-3-*O*-(4-*O*-(2-naphthyl)methyl-2,3-di-*O*-*tert*-butyldimethylsilyl-α-L-rhamnopyranosyl)-4,6-*O*-di-*tert*-butylsilylene-α-D-glucopyranoside (5.04)

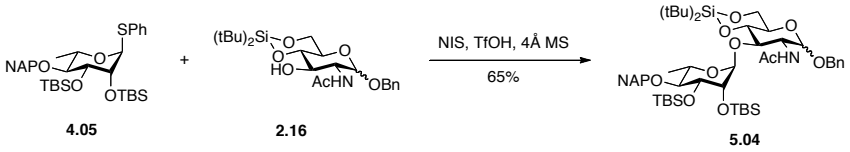

Monosaccharides **2.16** (28 mg, 62 μmol) and **4.05** (50 mg, 80 μmol) were combined in a round-bottom flask, coevaporated with anhydrous toluene (3 x 10 mL), and kept under high-vacuum overnight. Activated 4 Å molecular sieve powder and freshly distilled CH_2Cl_2 (3.0 mL) were added under Ar atmosphere. The clear solution stirred at ambient temperature for 1 h, then it was cooled to –78 °C for 20 min. N-iodosuccinimide (35 mg, 0.12 mmol) was added in one portion. After 5 min, trifluoromethanesulfonic acid (30 μL, 0.34 mmol) was added, and the solution quickly became orange and the color deepened over time to coral. The suspension stirred at –78 °C for 2 h, then was allowed to warm to –60 °C over 30 min. Freshly distilled triethylamine (~5 drops) was added after 30 min at –60 °C, causing a color change from coral to canary yellow. The suspension stirred at –55 °C for 10 min, then it was filtered and diluted with CH_2Cl_2. The solution was washed with 10% (wt/wt) sodium thiosulfate, a saturated solution of sodium bicarbonate, brine, dried over magnesium sulfate, filtered, and evaporated under reduced pressure to a brown film. Purification by flash chromatography [hexanes to 3:7 (vol/vol) EtOAc:hexanes] afforded **5.04** (39 mg, 65 %) as a cloudy glass.

^{1}H NMR (300 MHz, $CDCl_3$) δ 7.84 – 7.71 (m, 4H, Ar), 7.50 – 7.27 (m, 8H, Ar), 5.66 (d, *J* = 10.0 Hz, 1H, H-1), 4.99 (d, *J* = 12.4 Hz, 1H, OC*H*Ar), 4.92 (d, *J* = 1.9 Hz, 1H, H-1'), 4.74 – 4.64 (m, 3H, H-3, OC*H*Ar, OC*H*Ph), 4.46 (d, *J* = 11.9 Hz, 1H, OC*H*Ph), 4.35 – 4.18 (m, 2H, H-2, H-5'), 4.09 – 3.93 (m, 3H, H-3', H-4, H-5), 3.91 – 3.73 (m, 3H, H-2', 2 x H-6), 3.45 (t, *J* = 9.4 Hz, 1H, H-4'), 1.87 (s, 3H, NHAc), 1.20 (d, *J* = 6.1 Hz, 3H, Me), 1.10 (s, 9H, (CH_3)$_3$Si), 1.00 (s, 9H, (CH_3)$_3$Si), 0.92 (s, 9H, (CH_3)$_3$Si), 0.88 (s, 9H, (CH_3)$_3$Si), 0.15 (s, 3H, CH_3Si), 0.06 (s, 3H, CH_3Si), 0.04 (s, 3H, CH_3Si), -0.01 (s, 3H, CH_3Si). HRMS (ESI-TOF$^+$) for $C_{52}H_{87}N_2O_{10}Si_3$ (M+NH_4^+) calcd 983.5664, found 983.5671.

Benzyl 2-acetamido-2-deoxy-3-*O*-(4-*O*-(2-naphthyl)methyl-2,3-di-*O*-acetyl-α-L-rhamnopyranosyl)-4,6-di-*O*-acetyl-α-D-glucopyranoside (5.05)

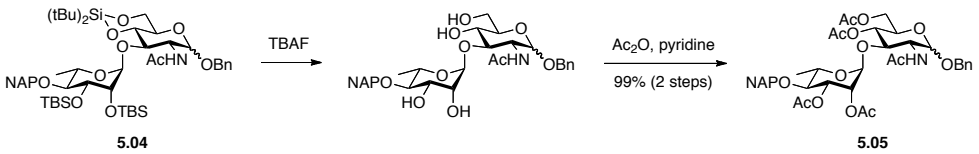

1. Freshly distilled tetrahydrofuran (0.4 mL) was added to a round-bottom flask containing **5.04** (39 mg, 40 μmol) under Ar atmosphere. A solution of tetra-*n*-butylammonium fluoride (TBAF) in tetrahydrofuran (1.0 M, 0.60 mL, 0.60 mmol) was added, and the clear solution stirred at ambient temperature. Some starting material remained as judged by thin layer chromatography after 22 h, so an additional aliquot of TBAF in THF (1.0 M, 2.5 mL, 2.5 mmol) was added. After 46 h total, the reaction was warmed to 40 °C for 5 h, when analysis by thin layer chromatography deemed the reaction complete. The reaction was cooled to ambient temperature and evaporated under reduced pressure to afford crude benzyl 2-acetamido-2-deoxy-3-*O*-(4-*O*-(2-naphthyl)methyl-α-L-rhamnopyranosyl)-α-D-glucopyranoside as a brown oil that was taken on to the next step immediately.

2. The crude benzyl 2-acetamido-2-deoxy-3-*O*-(4-*O*-(2-naphthyl)methyl-α-L-rhamnopyranosyl)-α-D-glucopyranoside (~40 μmol) was dissolved in anhydrous pyridine (1.5 mL) under Ar atmosphere. The solution was cooled to 0 °C for 15 min prior to dropwise addition of acetic anhydride (2.5 mL). The solution was allowed to slowly warm to ambient temperature while stirring overnight. After 17 h, the reaction was diluted with methanol and evaporated under reduced pressure to a brown oil that was co-evaporated with toluene (3 x 5 mL). Purification by flash chromatography [hexanes to 2:3 (vol/vol) acetone:hexanes] afforded **5.05** (30 mg, 99% over 2 steps) as a crystalline solid.

^{1}H NMR (400 MHz, $CDCl_3$) δ 7.86 – 7.66 (m, 4H, Ar), 7.50 – 7.27 (m, 8H, Ar), 6.20 (d, *J* = 6.7 Hz, NH) 5.67 (d, *J* = 9.6 Hz, 1H, H-1), 5.19 (dd, *J* = 9.9, 3.3 Hz, 1H, H-3'), 5.15 – 5.08 (m, 2H, H-2'), 4.92 (d, *J* = 3.6 Hz, 1H, H-3), 4.87 – 4.73 (m, 3H, H-1', OC*H*$_2$Ar), 4.68 (d, *J* = 11.8 Hz, 1H, OC*H*Ph), 4.49 (d, *J* = 11.7 Hz, 1H, OC*H*Ph), 4.42 (td, *J* = 10.2, 3.6 Hz, 1H, H-2), 4.16 (dd, *J* = 12.3, 4.4 Hz, 1H, H-5), 4.04 – 3.99 (m, 1H, H-4), 3.93 – 3.80 (m, 3H, H-5', 2 x H-6), 3.48 (t, *J* = 9.6 Hz, 1H, H-4'), 2.12 (s, 3H, OAc), 2.10 (s, 3H, OAc), 2.06 (s, 3H, OAc), 2.03 (s, 3H, OAc), 1.91 (s, 3H, NHAc), 1.27 (d, *J* = 6.2 Hz, 3H, Me). ^{13}C NMR (101 MHz, $CDCl_3$) δ 170.9, 170.4, 170.4, 169.4, 136.6, 135.7, 133.2, 132.9, 128.7, 128.4, 128.3, 128.1, 127.9, 127.7, 126.1, 126.0, 125.9, 125.5, 99.4, 97.0, 79.3, 78.5, 74.7, 71.4, 70.7, 70.1, 70.0, 68.8, 68.3, 62.1, 53.8, 52.0, 31.8, 29.3, 23.2, 21.2, 21.0, 20.9, 20.8, 17.8. HRMS (ESI-TOF$^+$) for $C_{40}H_{51}N_2O_{14}$ ($M+NH_4^+$) calcd 783.3335, found 783.3309.

Benzyl 2-acetamido-2-deoxy-3-*O*-(2,3-di-*O*-acetyl-α-L-rhamnopyranosyl)-4,6-di-*O*-acetyl-α-D-glucopyranoside (5.06)

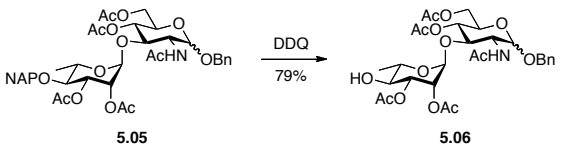

5.05 **5.06**

A round-bottom flask containing **5.05** (191 mg, 0.249 mmol) was placed under Ar atmosphere. Freshly distilled MeOH (2.6 mL), freshly distilled CH_2Cl_2 (10.4 mL), and water (60 μL) were added, followed by 2,3-dichloro-5,6-dicyano-*para*-benzoquinone (84.7 mg, 0.373 mmol) in one portion. The dark brown solution stirred at ambient temperature for 24 h. The reaction was evaporated under reduced pressure to a brown solid that was taken up in dichloromethane and transferred to a separatory funnel. The solution was washed with a solution of saturated sodium bicarbonate until the organic layer was clear, then washed with water, dried over magnesium sulfate, filtered, and evaporated under reduced pressure to a brown film. Purification by flash chromatography [CH_2Cl_2 to 4:96 (vol/vol) MeOH:CH_2Cl_2] afforded **5.06** (122 mg, 79%) as a white solid.

^{1}H NMR (400 MHz, $CDCl_3$) δ 7.42 – 7.29 (m, 5H), 5.78 (d, *J* = 9.7 Hz, 1H, NH), 5.12 – 5.05 (m, 1H, H-4), 5.03 (dd, *J* = 3.2, 2.0 Hz, 1H, H-2'), 4.96 (dd, *J* = 9.9, 3.3 Hz, 1H, H-3'), 4.89 (d, *J* = 3.6 Hz, 1H, H-1), 4.79 (d, *J* = 1.7 Hz, 1H, H-1'), 4.69 (d, *J* = 11.7 Hz, 1H, OC*H*Ar), 4.49 (d, *J* = 11.8 Hz, 1H, OC*H*Ar), 4.38 (td, *J* = 10.2, 3.7 Hz, 1H, H-2), 4.17 (dd, *J* = 12.3, 4.6 Hz, 1H, 1 x H-6), 4.01 (dd, *J* = 12.3, 2.3 Hz, 1H, 1 x H-6), 3.90 – 3.70 (m, 3H, H-3, H-5, H-5'), 3.52 (t, *J* = 9.7 Hz, 1H, H-4'), 2.87 (s, 1H, OH), 2.10 (s, 3H, OAc), 2.10 (s, 3H, OAc), 2.08 (s, 3H, OAc), 2.03 (s, 3H, OAc), 2.01 (s, 3H, NHAc), 1.27 (d, *J* = 6.1 Hz, 3H, Me). HRMS (ESI-TOF$^+$) for $C_{31}H_{49}N_2O_{14}$ ($M+NH_4^+$) calcd 643.2709, found 643.2704.

Benzyl 2-acetamido-2-deoxy-3-*O*-(2,3-di-*O*-acetyl-4-*O*-(1H-imidazole-1-carbonothioyl)-α-L-rhamnopyranosyl)-4,6-di-*O*-acetyl-α-D-glucopyranoside (5.07)

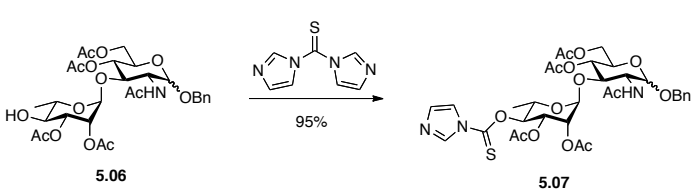

A bright yellow solution of **5.06** (22 mg, 35 μmol) and 1,1'-thiocarbonyldiimidazole (8.5 mg, 48 μmol) in freshly distilled toluene (0.42 mL) was heated to 90 °C. After 4 hours at 90 °C, the reaction was cooled to ambient temperature, diluted with CH_2Cl_2, and washed with a saturated solution of sodium bicarbonate, brine, dried over magnesium sulfate, filtered, and evaporated under reduced pressure to a bright yellow film. Purification by flash chromatography [CH_2Cl_2 to 3:97 (vol/vol) MeOH:CH_2Cl_2] afforded **5.07** (25 mg, 95%) as a crystalline white solid.

^{1}H NMR (500 MHz, $CDCl_3$) δ 8.34 (s, 1H, imid. H-2), 7.56 (s, 1H, imid. H-5), 7.43 – 7.30 (m, 5H, Ar), 7.04 (s, 1H, imid. H-4), 5.88 (t, *J* = 10.0 Hz, 1H, H-3), 5.73 (d, *J* = 9.8 Hz, 1H, NH), 5.37 (dd, *J* = 10.1, 3.3 Hz, 1H, H-4), 5.17 – 5.12 (m, 2H, H-2', H-3'), 4.92 (d, *J* = 3.7 Hz, 1H, H-1), 4.86 – 4.83 (d, *J* = 1.5 Hz, 1H, H-1'), 4.70 (d, *J* = 11.7 Hz, 1H, OC*H*Ar), 4.51 (d, *J* = 11.7 Hz, 1H, OC*H*Ar), 4.46 (td, *J* = 10.2, 3.7 Hz, 1H, H-2), 4.20 (dd, *J* = 12.4, 4.4 Hz, 1H, 1 x H-6), 4.10 (dq, *J* = 12.5, 6.3 Hz, 1H, H-5'), 4.02 (dd, *J* = 12.4, 2.1 Hz, 1H, 1 x H-6), 3.88 (ddd, *J* = 10.1, 4.0, 2.3 Hz, 1H, H-5), 3.86 – 3.81 (m, 1H, H-4'), 2.18 (s, 3H, OAc), 2.12 (s, 3H, OAc), 2.07 (s, 3H, OAc), 2.04 (s, 3H, OAc), 1.89 (s, 3H, NHAc), 1.22 (d, *J* = 6.2 Hz, 3H, Me). ^{13}C NMR (126 MHz, $CDCl_3$) δ 183.9, 170.9, 170.6, 170.5, 169.6, 169.4, 137.8, 136.6, 131.2, 128.9, 128.7, 128.5, 117.8, 100.0, 97.0, 81.3, 79.3, 70.5, 70.3, 70.0, 68.7, 68.4, 67.4, 62.0, 51.9, 23.4, 21.3, 21.1, 20.9, 20.7, 17.4. HRMS (ESI-TOF$^+$) for $C_{33}H_{42}N_3O_{14}S$ ($M+H^+$) calcd 736.2383, found 736.2393.

Chapter 6: Future Directions

6.1 Abstract

Complexes of biosynthetic enzymes mediate the production of capsular polysaccharides and O-polysaccharides in *E. coli*, and are assumed to exist in the synthesis of complex cell wall polysaccharides. Preliminary evidence has suggested the association of certain enzymes involved in mycobacterial arabinogalactan assembly. We hypothesize that the galactofuranosyltransferases GlfT1 and GlfT2 interact to assemble the galactan polymer, and seek to ascertain the existence of such an intimate interaction. Chemical cross-linking will provide evidence of physical proximity between GlfT1 and GlfT2, while two-hybrid and protein reporter constructs in *E. coli* and *M. smegmatis* will provide further support for the existence of the arabinogalactan biosynthetic complex. Additionally, the synthesis of precursors toward lipid-linked trisaccharide phosphonophosphate acceptor substrates for GlfT1 and GlfT2, such as benzyl Gal*f*-β(1,4)-Rha-α(1,3)-GlcNAc and (2Z,6Z,10Z)-nerylnerol, is described. The substrates produced from these intermediates will investigate the effect of more complex acceptor substrates on galactofuranosyltransferase catalytic efficiency.

6.2 Introduction

The research described in the preceding chapters represents foundational experiments challenging galactan biosynthetic enzymes with lipid-linked phosphonophosphate substrates and related analogs. Having established viable and modular synthetic routes, defined the activity of the glycosyltransferase GlfT1, and developed assays to monitor its catalytic efficiency, we will now transition into investigating the association of these enzymes and their participation in biosynthetic complexes. These experiments will allow us to gain insight into cell wall biosynthesis in live bacteria.

6.3 Investigating cooperativity between cell wall galactofuranosyltransferases

The existence of biosynthetic complexes involved in bacterial polysaccharide assembly is widely assumed. Preorganization near or in a membrane of enzymes processing membrane-anchored glycolipids is an elegant mechanism to prevent biosynthetic intermediates from drifting about in the membrane. Evidence of protein complexes in capsular polysaccharide biosynthesis has supported this assumption.[263,264] Complex formation is most important in the synthesis of cell wall and cell surface polysaccharides, processes which usually require translocation of lipid-linked glycan intermediates from the cytoplasm to the periplasm by specific transporters. Biosynthetic complexes of transporters and oligosaccharide biosynthetic enzymes have been discovered in *E. coli* lipopolysaccharide synthesis. Both ABC (ATP-binding cassette) transporter-dependent and Wzy polymerase-dependent processes form membrane-associated clusters, even though some proteins required for assembly are not part of the complex.[265,266] It is probable that mycobacteria possess a complex of biosynthetic enzymes responsible for arabinogalactan assembly.

6.3.1 An arabinogalactan biosynthetic complex

Some evidence of the existence of an arabinogalactan biosynthetic complex has been described. Using a bacterial two-hybrid assay, Nigou, Jackson, and co-workers discovered an association between Rv3789 and GlfT1.[267] Rv3789 is a transporter likely involved in translocation of Ara*f*-β-P-decaprenol (DPA) from the cytosol to the periplasm. As GlfT1 is a fairly sensitive enzyme, interaction with the membrane-bound Rv3789 may serve to stabilize it. Interestingly, no association was observed between Rv3789 and GlfT2. Since the complex does not have to account for every enzyme in a biosynthetic pathway, it is possible that Rv3789 and GlfT1 are part of a complex that does not require GlfT2. We seek to obtain further evidence about preorganization of arabinogalactan biosynthetic enzymes near the cytosolic leaflet of the mycobacterial cell membrane.

6.3.2 Measuring interactions between GlfT1 and GlfT2

Interaction between GlfT1 and GlfT2 may mediate galactan biosynthesis. Cooperativity between glycosyltransferases has been observed in the glycosylation of macrolide antibiotics. The glycosyltransferase DesVII from *Streptomyces venezuelae* requires the presence of DesVIII for function, just as the glycosyltransferase EryCIII requires EryCII.[268,269] Similarly, AknS from *S. galilaeus* exhibits attenuated activity in the absence of the auxiliary protein AknT. Coexpression of these proteins restores full AknS activity.[270] This last example in particular may yield insight into the cooperativity between GlfT1 and GlfT2. Specifically, while the two enzymes are clearly active in isolation, their association *in vitro* or in bacteria may lead to a more productive complex.

Certain clues appear to lend credence to a GlfT1/GlfT2 complex. In a coupled spectrophotometric assay to measure GlfT2 activity, a K_m of 380 μM was obtained for nucleotide-sugar donor UDP-Gal*f*.[271] This value is unusually large, particularly when the

equilibrium generated by UGM lies far on the side of UDP-Gal*p* (93:7 UDP-Gal*p*:UDP-Gal*f*).[272] The concentration of UDP-Gal*p* in a bacterial cell is <1.5 mM, making it difficult to conceive that such a large pool of UDP-Gal*f* would exist in the cytosol of mycobacteria.[273] We postulate that interaction between GlfT1 and GlfT2 in mycobacteria may lead to K_m values that more accurately reflect the likely physiological concentration of UDP-Gal*f*. These results may be obtained in the course of experiments investigating broader aspects of their association. Several avenues are available to study the interaction of these two enzymes.

To investigate the functional relationship between GlfT1 and GlfT2, the enzymes will be coexpressed in *E. coli*. Expression of *M. smegmatis* GlfT1 in *E. coli* has produced active enzyme, but its activity is greatly attenuated in comparison to enzyme expressed in *M. smegmatis*. Introduction of a plasmid encoding both galactofuranosyltransferases will probe whether inclusion of GlfT2 stabilizes or otherwise activates GlfT1. Alternatively, an inactive mutant of either galactofuranosyltransferase can be utilized to assess its effect on the other enzyme's activity. Specifically, a GlfT2 variant bearing a D372A mutation is catalytically inactive.[119] Comparison of the catalytic efficiency of GlfT1 in the presence of D372A GlfT2 will clarify any positive association. This experiment takes advantage of materials that are currently available to the laboratory. Alternatively, comparison of the catalytic efficiency of GlfT2 in the presence of inactive mutant D193A GlfT1 will be similarly instructive.

To monitor the physical proximity of GlfT1 and GlfT2, the coexpressed enzymes will be chemically cross-linked. The amine-reactive reagent dithiobis(succinimidylpropionate) (DSP) will be utilized, as it is suitable for membrane-associated proteins and the cross-links can be broken with dithiothreitol (DTT).[263] The enzymes will be cross-linked in a cell lysate and the cross-linked products will be enriched by affinity chromatography. The cross-links will be broken by incubation with DTT, and the protein bands separated by SDS-PAGE will be excised and analyzed by MALDI-TOF. Since false positives from artificial crowding of proteins in

solution due to overexpression can be problematic with chemical cross-linking, alternative reporter protocols will be pursued in parallel.

The bacterial two-hybrid adenylate cyclase system has been utilized to observe association of GlfT1 and the translocase Rv3789.[267] Two-hybrid systems rely on domains of a single enzyme re-associating through the interaction of two proteins tethered to each domain. Typically, reconstitution of the enzyme leads to transcriptional activation of a gene that provides a readout of the interaction. We will fuse *M. smegmatis* GlfT1 and *M. tuberculosis* GlfT2 to the appropriate adenylate cyclase subunits using commercially available plasmids.[274] Insertion of these plasmids into *E. coli* BTH101 will be followed by plating the bacteria on Luria-Bertani agar containing X-Gal (5-bromo-4-chloro-3-indolyl-β-D-galactopyranoside) essentially as described.[274] A blue-colored phenotype will be observed if the enzymes are interacting, and the interaction will be quantified by established protocols.[275]

It is possible that protein expression may be problematic in *E. coli*. There appear to be factors specific to mycobacteria that contribute to proper GlfT1 activity. Johnsson and co-workers have described a protein sensor system in *M. smegmatis* that is based on the reconstitution of an enzyme involved in tryptophan and histidine biosynthesis, HisA.[276] Cells of *M. smegmatis* □*hisA* were transformed with plasmid pairs that encoded the two HisA domains, both encoding GlfT1. Growth of the *hisA*-deficient strain in the absence of exogenous tryptophan provided evidence that GlfT1 may self-associate in mycobacteria. We seek to adapt this experiment to study GlfT1 and GlfT2 by incorporating plasmid pairs encoding these enzymes. An important caveat for these experiments is that they rely on growth of viable bacteria as a readout. In parallel with the cross-linking experiments above, however, we expect to observe conclusive evidence of galactofuranosyltransferase association.

6.4 Toward more complex synthetic phosphonophosphate acceptors

The polymerase GlfT2 can process acceptors bearing a single Galf residue. In Chapter 4, a lipid-linked acceptor bearing the Gal*f*-β(1,4)-Rha-α(1,3)-GlcNAc trisaccharide was demonstrated to serve as a suitable acceptor for GlfT1, and a poor acceptor for GlfT2. Nonetheless, lipid-linked trisaccharides can be processed by both cell wall galactofuranosyltransferases. In the former case, the galactofuranose residue dramatically improves turnover by GlfT1. An acceptor that bears a phosphonophosphate bridge should improve the efficiency of this trisaccharide. To explore the relative activity of GlfT1 and GlfT2 for trisaccharide acceptors bearing the bridging phosphonophosphate, we required access to an acceptor such as **6.01** (Scheme 6.1).

6.4.1 A synthetic lipid-linked trisaccharide phosphonophosphate acceptor

The route toward **6.01** began with the glycosylation of 4-*O*-naphthyl rhamnosyl thioglycoside **4.05** with benzyl glucoside **2.16** using *N*-iodosuccinimide and trifluoromethanesulfonic acid. The exclusively α-linked disaccharide **6.02** was obtained in nearly quantitative yield. A protecting group swap was effected by treatment with tetra-*n*-butylammonium fluoride, followed by taking up the crude material in acetic anhydride and pyridine. The 4'-*O*-naphthyl protecting group of disaccharide **6.03** was removed by oxidative cleavage with DDQ to afford 4'-OH acceptor **6.04**. Glycosylation with thiazolyl Gal*f* donor **4.04** using silver trifluoromethanesulfonate then afforded the desired trisaccharide building block **6.05**.

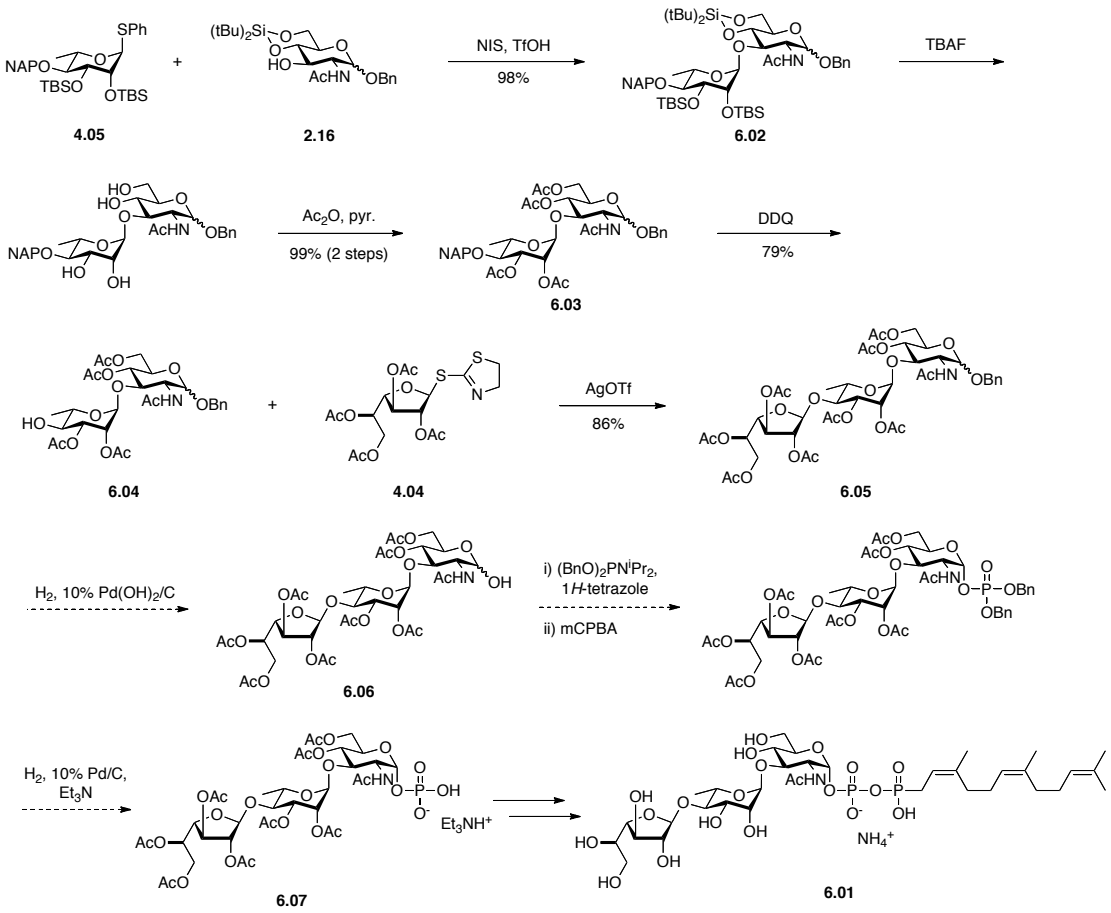

Scheme 6.1. Trisaccharide phosphorylation toward phosphonophosphate **6.01**.

From the protected trisaccharide **6.05**, a four-step hydrogenolysis, phosphitylation-oxidation, and hydrogenolysis sequence should afford the critical trisaccharide phosphate **6.07**. Coupling to a suitable lipid phosphonomorpholidate, such as the (2Z,6Z)-farnesyl phosphonomorpholidate described in Chapter 2, will provide ready access to acceptor **6.01**. Efforts to complete this sequence to date have been unsuccessful. Hydrogenolysis using 10% palladium on carbon did not yield any product **6.06**. Use of Pearlman's catalyst appeared to effect conversion to the anomeric lactol, but the subsequent phosphitylation-oxidation sequence on the crude lactol was not successful. An alternative phosphorylation strategy may be required to reach this complex trisaccharide phosphomonoester.

6.4.2 Interrogating galactofuranosyltransferase acceptor scope with an expanded carrier lipid repertoire

The identity and geometry of the carrier lipid of a glycosyltransferase acceptor substrate can have a remarkable effect on the enzyme's ability to process the acceptor. This effect in a number of glycosyltransferases was thoroughly covered in Chapter 1. In addition, however, the geometry of the carrier lipid can have a marked effect on the permeability of a membrane.[277] The polyprenol specificity of a number of dolichyl-processing glycosyltransferases has been examined in detail. Comparison of dolichyl stereochemistry,[278] length,[279,280] and extent of saturation[159,281,282] have revealed that the specificity is often enzyme- or organism-specific.

To further explore the effect of carrier lipid length and geometry on acceptor processing by cell wall galactofuranosyltransferases, we sought to expand our carrier lipid repertoire. To compare the lipid geometry in farnesyl-linked acceptors, we desired (2Z,6E)-farnesol **6.08** to complement our experiments with (2Z,6Z)-farnesol. This alcohol can be accessed in four steps from commercially available geranyl bromide (Scheme 6.2). Reaction of this allylic bromide with the dianion of ethyl acetoacetate afforded geranyl β-ketoester **6.09**.[212] The enolate was trapped with diethyl chlorophosphate in 1,3-dimethyl-3,4,5,6-tetrahydro-2(1*H*)-pyrimidone (DMPU) to yield (*E*)-enol phosphate **6.10**.[213-215] Methylation of the enol phosphate with lithium dimethyl cuprate by the method of Weiler and co-workers[216,217] afforded α,β-unsaturated ester **6.11**. Reduction of the ester using diisobutylaluminum hydride (DIBAL-H)[218] yielded (2Z,6E)-farnesol **6.08**.

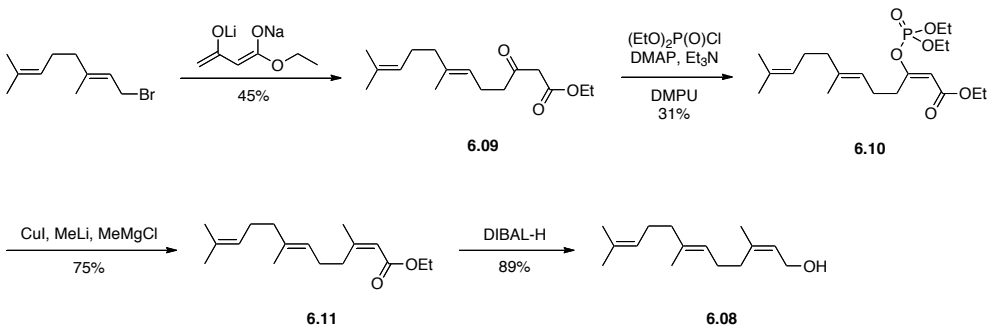

Scheme 6.2. Synthesis of (2Z,6E)-farnesol.

To prepare longer lipid carriers, we desired a method by which the lipid could be elongated strictly by (Z)-isoprene units. This can be accomplished using a 10-carbon building block **6.12** termed the *cis*-isoprenoid synthon (Scheme 6.3).[283] This synthon consists of an 'inner' allylic chloride to serve as the electrophile in chain extension, while an 'outer' protected allylic alcohol can be unmasked to serve as the terminal unit or further processed to become a nucleophile for chain extension.

Synthon **6.12** is accessed from nerol (Scheme 6.3). Protection of the alcohol as the *tert*-butyldiphenylsilyl ether **6.13** is followed by epoxidation at the distal ω-isoprene unit with *meta*-chloroperoxybenzoic acid to afford epoxide **6.14**.[284] Oxidative cleavage of the epoxide with periodic acid[285] yielded aldehyde **6.15**. The second isoprene unit was installed with high selectivity for the (Z)-isomer via a Still-Gennari olefination.[286,287] Reaction of aldehyde **6.15** with 2-[bis(2,2,2-trifluoroethoxy)phosphonyl]propionic acid ethyl ester in the presence of potassium hexamethyldisilazide and 18-crown-6 afforded the desired (Z)-α,β-unsaturated ester **6.16** with high stereoselectivity (10:1 Z:E). The ester was reduced with DIBAL-H to allylic alcohol **6.17**, and a Corey-Kim reaction on the allylic alcohol furnished allylic chloride **6.12**, the desired *cis*-isoprenoid synthon.

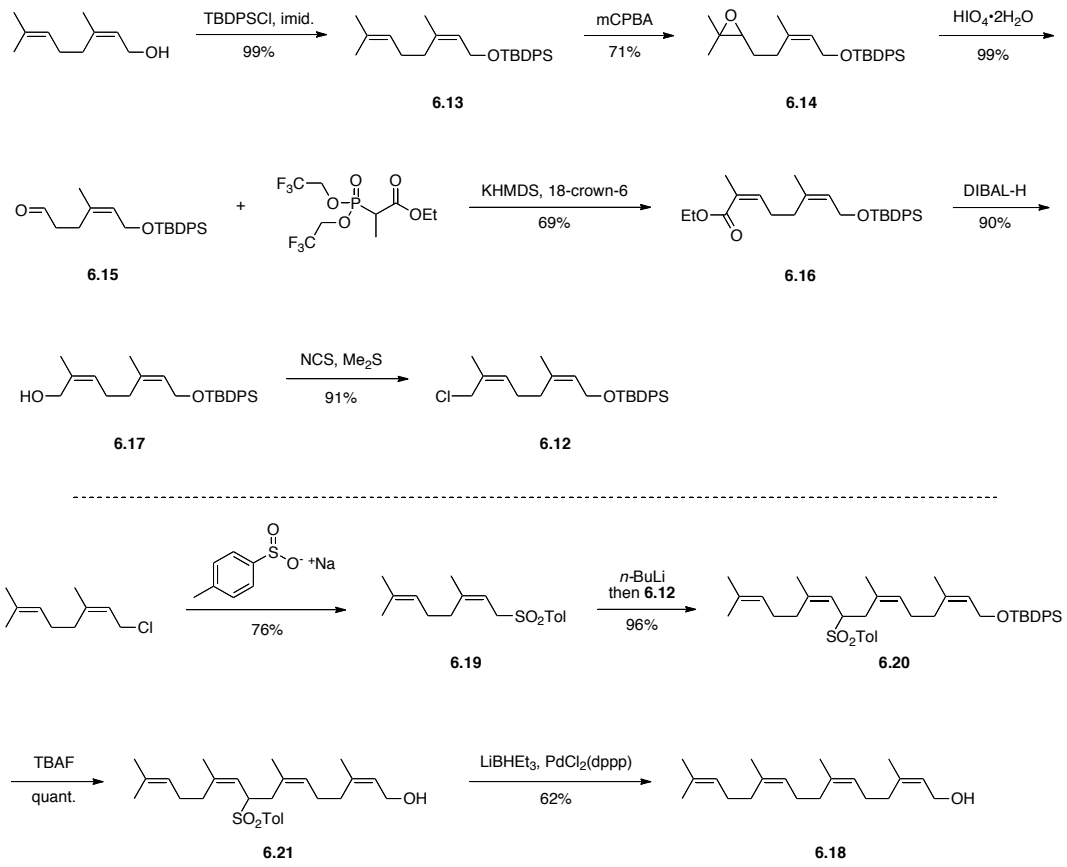

Scheme 6.3. Synthesis of (2Z,6Z,10Z)-nerylnerol **2.ai** via the *cis*-isoprenoid synthon **2.ah**.

We first targeted all-*cis* prenyl alcohol (2Z,6Z,10Z)-nerylnerol **6.18**. The *cis*-isoprenoid synthon methodology requires the use of an allylic sulfonate as the nucleophile. Thus, neryl chloride was generated from nerol as described in Chapter 2 and reacted with sodium *para*-toluenesulfinate to yield allylic sulfonate **6.19**. Deprotonation of **6.19** with *n*-butyllithium in a solution of 4:1 v/v tetrahydrofuran:1,3-dimethyl-3,4,5,6-tetrahydro-2(1*H*)-pyrimidinone (DMPU),[288] followed by addition of allylic chloride **6.12** afforded the coupling product **6.20** in excellent yield. At this point, we found that removal of the silyl groups was required prior to desulfonylation. If reductive removal of the sulfonate was attempted on the TBDPS-protected **6.20**, C-O bond cleavage occurred and yielded a hydrocarbon byproduct as the major product. The same byproduct was obtained when desulfonylation was attempted with lithium 4,4'-di-

tert-butylbiphenylide (LiDBB). Thus, silyl deprotection of sulfone **6.20** using tetra-*n*-butylammonium fluoride yielded allylic alcohol **6.21** in quantitative yield. Reductive desulfonylation[289] with lithium triethylborohydride ($LiBHEt_3$, Super-Hydride) and (1,3-bis(diphenylphosphino)propane)palladium(II) dichloride [$PdCl_2$(dppp)] afforded (2Z,6Z,10Z)-nerylnerol **6.18**.[43] This methodology can be used to generate a progressively longer series of (Z)-isoprenyl alcohols.[36]

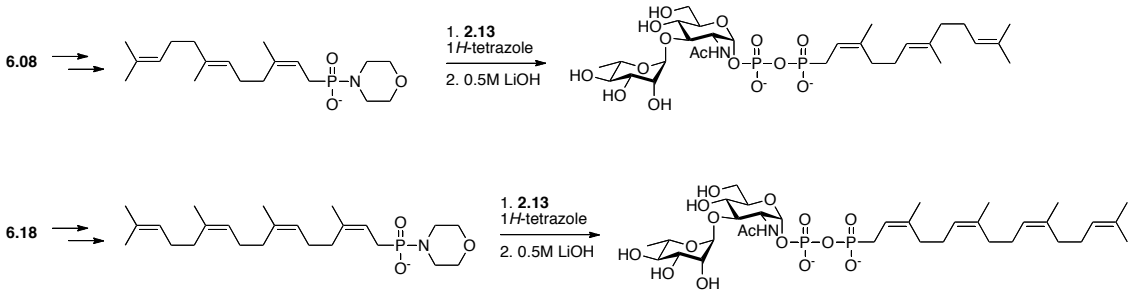

Scheme 6.4. Elaboration of prenyl alcohols **6.08** and **6.08** and coupling to disaccharide phosphate **2.13** may yield disaccharide phosphonophosphates.

The two lipids synthesized above can be elaborated to disaccharide phosphonophosphates as described in Chapter 2 (Scheme 6.4). Briefly, the allylic alcohols **6.08** and **6.18** will be converted to phosphonomorpholidates via a four-step protocol. Reaction with Rha-α(1,3)-GlcNAc-α-phosphate **2.13** in the presence of 1*H*-tetrazole in pyridine, followed by saponification of the acetate protecting groups, should produce the desired phosphonophosphates. The acceptor derived from (2Z,6E)-farnesol **6.08** would explore the effect of the penultimate isoprene unit, which is (Z) in the best GlfT1 acceptor substrate. Alternatively, the acceptor derived from (2Z,6Z,10Z)-nerylnerol **6.18** maintains the (Z) geometry about that isoprene unit. This derivative will instead investigate whether an extended lipid carrier improves the ability of an acceptor surrogate to be processed efficiently by GlfT1.

Ultimately, isolation of oligosaccharides prepared by GlfT1 from this scaffold will serve to interrogate the efficiency of GlfT2 polymerization from highly complex acceptor substrates.

6.5 Conclusions

A series of future experiments have been described that will explore the persistence of biosynthetic complexes involved in arabinogalactan assembly. Chemical cross-linking and two-hybrid/protein reporter experiments will determine whether the galactofuranosyltransferase GlfT1 and GlfT2 associate *in vitro* as well as in *E. coli* or *M. smegmatis*. In addition, a route toward a Galf-β(1,4)-Rha-α(1,3)-GlcNAc phosphomonoester and the chemical synthesis of two prenyl alcohols have been described. These two lipids will be elaborated to di- or trisaccharide phosphonophosphates to investigate the effect of the lipid carrier on cell wall galactofuranosyltransferases.

6.6 Experimental details

All compounds were purchased from Sigma Aldrich (Milwaukee, WI) or Fisher Scientific (Pittsburgh, PA). Tetrahydrofuran (THF) was distilled from sodium/benzophenone ketyl, methanol (MeOH) was distilled from magnesium, and dichloromethane (CH_2Cl_2) was distilled from calcium hydride. Other solvents were purified according to the guidelines in *Purification of Common Laboratory Chemicals*. All reactions were run under argon atmosphere in oven-dried glassware unless otherwise stated. Molecular sieves were activated by heating to 600 °C in a furnace for 12 h, then cooled in a dessicator. Analytical thin layer chromatography (TLC) was carried out on E. Merck (Darmstadt) TLC plates pre-coated with silica gel 60 F254 (250 μm layer thickness). Analyte visualization was accomplished using a UV lamp and by charring with a

solution of *p*-anisaldehyde (3.5 mL), acetic acid (15 mL), H_2SO_4 (50 mL), and ethanol (350 mL). Flash column chromatography was performed with Silicycle Flash Silica Gel (40-63 μm, 60 Å pore size) using reagent grade hexanes and ACS grade ethyl acetate (EtOAc) or ACS grade acetone, or methanol (MeOH) and CH_2Cl_2. ^1H, ^{13}C, and ^{31}P nuclear magnetic resonance (NMR) spectra were recorded on a 300 MHz spectrometer (acquired at 300 MHz for ^1H NMR, 75 MHz for ^{13}C NMR, and 121 MHz for ^{31}P NMR) a 400 MHz spectrometer (acquired at 400 MHz for ^1H NMR, 101 MHz for ^{13}C NMR, and 162 MHz for ^{31}P NMR), or a 500 MHz spectrometer (acquired at 500 MHz for ^1H NMR and 126 MHz for ^{13}C NMR). Chemical shifts are reported relative to tetramethylsilane or residual solvent peaks in parts per million ($CHCl_3$: ^1H: 7.26, ^{13}C: 77.16; MeOH: ^1H: 3.31, ^{13}C: 49.00; HDO: ^1H: 4.79). Peak multiplicity is reported as singlet (s), doublet (d), doublet of doublets (dd), doublets of doublets of doublets (ddd), triplet (t), doublet of triplets (dt), etc. High resolution electrospray ionization-time of flight mass spectra (HRESI-TOF MS) were obtained on a Micromass LCT.

Benzyl 2-acetamido-2-deoxy-3-*O*-(4-*O*-(2-naphthyl)methyl-2,3-di-*O*-*tert*-butyldimethylsilyl-α-L-rhamnopyranosyl)-4,6-di-*O*-acetyl-α-D-glucopyranoside (6.02)

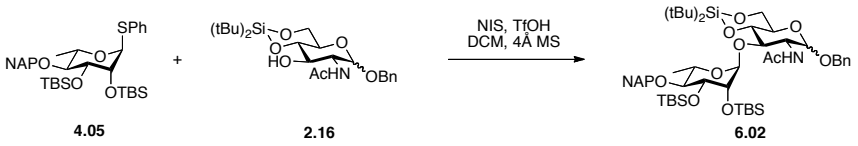

Monosaccharides **2.16** (1.35 g, 2.98 mmol) and **4.05** (2.80 g, 4.48 mmol) were combined in a round-bottom flask, coevaporated with anhydrous toluene (3 x 20 mL), and kept under high-vacuum overnight. Activated 4 Å molecular sieve powder and freshly distilled CH_2Cl_2 (120 mL) were added under Ar atmosphere. The clear solution stirred at ambient temperature for 2 h, then it was cooled to −78 °C for 20 minutes. N-iodosuccinimide (1.34 g, 5.97 mmol) was

added in one portion. After 5 min, trifluoromethanesulfonic acid (30 μL, 0.34 mmol) was added. The suspension stirred at –78 °C for 2.75 h, then additional trifluoromethanesulfonic acid (0.5 mL) was added. The reaction was warmed to –60 °C over 30 min. Freshly distilled triethylamine (2 mL) was added, causing a color change from coral to canary yellow. The suspension was filtered and diluted with CH_2Cl_2. The solution was washed with 10% (wt/wt) sodium thiosulfate, a saturated solution of sodium bicarbonate, brine, dried over magnesium sulfate, filtered, and concentrated under reduced pressure to a brown film. Purification by flash chromatography [hexanes to 2:8 (vol/vol) EtOAc:hexanes] afforded **6.02** (2.83 g, 98%) as a cloudy glass.

^{1}H NMR (300 MHz, $CDCl_3$) δ 7.84 – 7.70 (m, 4H, Ar), 7.50 – 7.26 (m, 8H, Ar), 5.66 (d, *J* = 10.0 Hz, 1H, NH), 4.99 (d, *J* = 12.4 Hz, 1H, 1 x OC*H*Ar), 4.92 (d, *J* = 1.9 Hz, 1H, H-1'), 4.72 – 4.63 (m, 3H, H-1, 2 x OC*H*Ar), 4.46 (d, *J* = 11.9 Hz, 1H, 1 x OC*H*Ar), 4.34 – 4.22 (m, 2H, H-2, H-5'), 4.10 – 3.92 (m, 3H, H-3, H-3'), 3.90 – 3.76 (m, 4H, H-2'), 3.45 (t, *J* = 9.4 Hz, 1H, H-4'), 1.87 (s, 3H, NHAc), 1.20 (d, *J* = 6.1 Hz, 3H, Me), 1.10 (s, 9H, (C*H*$_3$)$_3$CSi), 1.00 (s, 9H, (C*H*$_3$)$_3$CSi), 0.92 (s, 9H, (C*H*$_3$)$_3$CSi), 0.88 (s, 9H, (C*H*$_3$)$_3$CSi), 0.15 (s, 3H, C*H*$_3$Si), 0.06 (s, 3H, C*H*$_3$Si), 0.04 (s, 3H, C*H*$_3$Si), 0.01 (s, 3H, C*H*$_3$Si). ^{13}C NMR (101 MHz, $CDCl_3$) δ 171.2, 169.9, 137.1, 136.9, 136.3, 133.4, 133.3, 132.9, 132.7, 128.7, 128.3, 128.3, 128.0, 128.0, 127.8, 127.7, 127.5, 126.5, 126.1, 126.0, 125.9, 125.8, 125.5, 125.2, 125.1, 99.4, 97.4, 95.1, 81.3, 80.7, 77.4, 76.4, 75.0, 74.8, 74.0, 73.8, 73.0, 72.6, 70.1, 68.8, 68.7, 67.0, 66.9, 60.5, 53.7, 27.8, 27.8, 27.1, 26.4, 26.3, 25.9, 25.9, 23.6, 22.8, 21.1, 20.0, 18.8, 18.4, 18.2, 18.2, 14.3, –4.1, –4.1, –4.2, –4.3, –4.3, –4.3, –4.4, –4.4. HRMS (ESI-TOF$^+$) for $C_{52}H_{87}N_2O_{10}Si_3$ (M+NH_4^+) calcd 983.5664, found 983.5671.

Benzyl 2-acetamido-2-deoxy-3-*O*-(4-*O*-(2-naphthyl)methyl-2,3-di-*O*-acetyl-α-L-rhamnopyranosyl)-4,6-*O*-di-tert-butylsilylene-α-D-glucopyranoside (6.03)

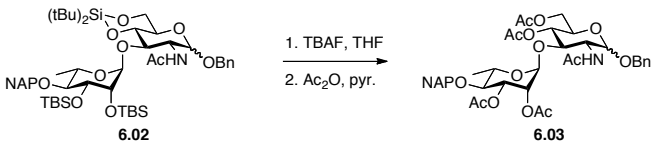

1. Freshly distilled tetrahydrofuran (0.4 mL) was added to a round-bottom flask containing **6.02** (39 mg, 40 μmol) under Ar atmosphere. A solution of tetra-*n*-butylammonium fluoride (TBAF) in tetrahydrofuran (1.0 M, 0.60 mL, 0.60 mmol) was added, and the clear solution stirred at ambient temperature. Some starting material remained as judged by thin layer chromatography after 22 h, so an additional aliquot of TBAF in THF (1.0 M, 2.5 mL, 2.5 mmol) was added. After 46 h total, the reaction was warmed to 40 °C for 5 h, when analysis by thin layer chromatography deemed the reaction complete. The reaction was cooled to ambient temperature and concentrated under reduced pressure to afford crude benzyl 2-acetamido-2-deoxy-3-*O*-(4-*O*-(2-naphthyl)methyl-α-L-rhamnopyranosyl)-α-D-glucopyranoside as a brown oil that was taken on to the next step immediately.

2. The crude benzyl 2-acetamido-2-deoxy-3-*O*-(4-*O*-(2-naphthyl)methyl-α-L-rhamnopyranosyl)-α-D-glucopyranoside (~40 μmol) was dissolved in anhydrous pyridine (1.5 mL) under Ar atmosphere. The solution was cooled to 0 °C for 15 min prior to dropwise addition of acetic anhydride (2.5 mL). The solution was allowed to slowly warm to ambient temperature while stirring overnight. After 17 h, the reaction was diluted with methanol and concentrated under reduced pressure to a brown oil that was coevaporated with toluene (3 x 5 mL). Purification by flash chromatography [hexanes to 2:3 (vol/vol) acetone:hexanes] afforded **6.03** (30 mg, 99% over 2 steps) as a crystalline solid.

^{1}H NMR (400 MHz, $CDCl_3$) δ 7.84 – 7.70 (m, 4H, Ar), 7.50 – 7.29 (m, 8H, Ar), 5.67 (d, *J* = 9.6 Hz, 1H, NH), 5.19 (dd, *J* = 9.9, 3.3 Hz, 1H, H-3'), 5.15 – 5.07 (m, 2H), 4.92 (d, *J* = 3.6 Hz, 1H, H-1'), 4.89 – 4.73 (m, 3H, 2 x OC*H*Ar), 4.68 (d, *J* = 11.8 Hz, 1H, 1 x OC*H*Ar), 4.49 (d, *J* = 11.7 Hz, 1H, 1 x OC*H*Ar), 4.42 (td, *J* = 10.2, 3.6 Hz, 1H, H-2), 4.16 (dd, *J* = 12.3, 4.4 Hz, 1H), 4.05 –

3.99 (m, 1H), 3.94 – 3.80 (m, 3H, H-5'), 3.48 (t, *J* = 9.6 Hz, 1H, H-4'), 2.12 (s, 3H, OAc), 2.10 (s, 3H, OAc), 2.06 (s, 3H, OAc), 2.03 (s, 3H, OAc), 1.91 (s, 3H, NHAc), 1.27 (d, *J* = 6.2 Hz, 3H, Me). ^{13}C NMR (101 MHz, $CDCl_3$) δ 171.0, 170.5, 170.5, 169.5, 136.7, 135.8, 133.3, 133.0, 128.8, 128.5, 128.4, 128.1, 128.0, 127.8, 126.2, 126.1, 126.0, 125.6, 99.5, 97.1, 79.4, 78.5, 74.8, 71.5, 70.7, 70.2, 70.0, 68.8, 68.4, 62.2, 53.9, 52.1, 29.4, 23.3, 21.2, 21.1, 21.0, 20.9, 17.9. HRMS (ESI-TOF$^+$) for $C_{40}H_{51}N_2O_{14}$ ($M+NH_4^+$) calcd 783.3335, found 783.3309.

Benzyl 2-acetamido-2-deoxy-3-*O*-(2,3-di-*O*-acetyl-α-L-rhamnopyranosyl)-4,6-di-*O*-acetyl-α-D-glucopyranoside (6.04)

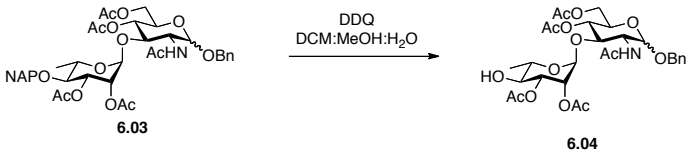

A round-bottom flask containing **6.03** (0.19 g, 0.25 mmol) was placed under Ar atmosphere. Freshly distilled MeOH (2.6 mL), freshly distilled CH_2Cl_2 (10.4 mL), and water (60 μL) were added, followed by 2,3-dichloro-5,6-dicyano-*para*-benzoquinone (85 mg, 0.37 mmol) in one portion. The dark brown solution stirred at ambient temperature for 24 h. The reaction was concentrated under reduced pressure to a brown solid that was taken up in dichloromethane and transferred to a separatory funnel. The solution was washed with a solution of saturated sodium bicarbonate until the organic layer was clear, then washed with water, dried over magnesium sulfate, filtered, and concentrated under reduced pressure to a brown film. Purification by flash chromatography [CH_2Cl_2 to 4:96 (vol/vol) MeOH:CH_2Cl_2] afforded **6.04** (0.12 gg, 79%) as a white solid.

^{1}H NMR (300 MHz, $CDCl_3$) δ 7.43 – 7.29 (m, 5H, Ar), 5.65 (d, *J* = 9.7 Hz, 1H, NH), 5.14 – 5.06 (m, 1H), 5.02 (dd, *J* = 3.3, 2.1 Hz, 1H), 4.97 (dd, *J* = 9.9, 3.3 Hz, 1H, H-3'), 4.89 (d, *J* =

3.7 Hz, 1H, H-1'), 4.80 (d, *J* = 1.8 Hz, 1H), 4.69 (d, *J* = 11.8 Hz, 1H, 1 x OC*H*Ar), 4.49 (d, *J* = 11.7 Hz, 1H, 1 x OC*H*Ar), 4.40 (td, *J* = 10.0, 3.7 Hz, 1H, H-2), 4.18 (dd, *J* = 12.4, 4.5 Hz, 1H), 4.01 (dd, *J* = 12.3, 2.3 Hz, 1H), 3.91 – 3.68 (m, 3H, H-5'), 3.59 – 3.47 (m, 1H, H-4'), 2.11 (s, 2 x 3H, OAc), 2.08 (s, 3H, OAc), 2.05 (s, 3H, OAc), 2.02 (s, 3H, NHAc), 1.28 (d, *J* = 6.1 Hz, Me). HRMS (ESI-TOF$^+$) for $C_{29}H_{43}N_2O_{14}$ ($M+NH_4^+$) calcd 643.2709, found 643.2704.

Benzyl 2-acetamido-2-deoxy-3-*O*-(2,3-di-*O*-acetyl-4-*O*-(2,3,4,5-tetra-*O*-acetyl-β-D-galactofuranosyl)-α-L-rhamnopyranosyl)-4,6-di-*O*-acetyl-α-D-glucopyranoside (6.05)

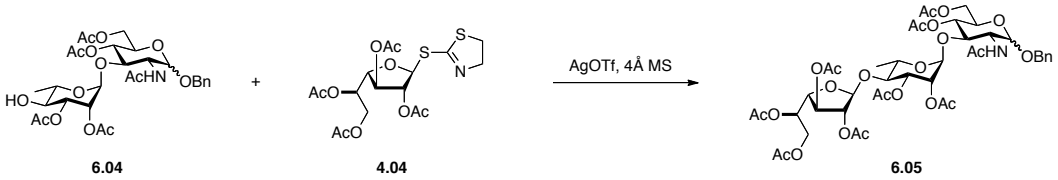

6.04 4.04 6.05

Compounds **6.04** (0.12 g, 0.20 mmol) and **4.04** (0.18 g, 0.39 mmol) were combined in a round-bottom flask, coevaporated with anhydrous toluene (3 x 4 mL), and kept under high-vacuum overnight. Activated 4 Å molecular sieve powder and freshly distilled CH_2Cl_2 (6.5 mL) were added under Ar atmosphere. The clear solution stirred at ambient temperature for 1 h, then it was cooled to 0 °C. Silver trifluoromethanesulfonate (0.15 g, 0.59 mmol) was added, and the reaction stirred at 0 °C for 5 min, then it was warmed to ambient temperature. After 4.5 h at ambient temperature, the reaction was filtered through Celite (rinsed with CH_2Cl_2), washed with a saturated solution of sodium bicarbonate, water, brine, dried over magnesium sulfate, filtered, and concentrated under reduced pressure to a clear film. Purification by flash column chromatography [CH_2Cl_2 to 3:97 MeOH:CH_2Cl_2] afforded **6.05** (0.16 g, 86%) as a clear film.

^{1}H NMR (400 MHz, $CDCl_3$): δ 7.42 – 7.29 (m, 5H, Ar), 6.16 (d, *J* = 6.8 Hz, 1H), 5.64 (d, *J* = 9.7 Hz, 1H), 5.41 – 5.35 (m, 2H), 5.30 (d, *J* = 8.2 Hz, 1H), 5.27 (s, 1H, H-1"), 5.20 – 5.15 (m,

1H), 5.14 – 5.11 (m, 1H), 5.10 (s, 1H), 5.06 (dd, *J* = 9.6, 3.5 Hz, 1H), 5.03 – 4.96 (m, 2H), 4.94 – 4.87 (m, 3H, H-1), 4.74 (d, *J* = 1.7 Hz, 1H, H-1'), 4.71 – 4.65 (m, 2H), 4.61 – 4.47 (m, 2H), 4.42 (td, *J* = 10.2, 3.7 Hz, 1H), 4.32 – 4.08 (m, 7H), 4.01 (dd, *J* = 12.3, 2.3 Hz, 1H), 3.88 – 3.77 (m, 4H), 3.71 – 3.58 (m, 2H), 2.13 (s, 3H, OAc), 2.12 – 2.09 (m, 12H, 3 x OAc), 2.09 – 2.07 (m, 6H, 2 x OAc), 2.07 – 2.04 (m, 12H, 3 x OAc), 1.98 (s, 3H, NHAc), 1.22 (d, *J* = 6.2 Hz, 3H, Me). HRMS (ESI-TOF$^+$) for $C_{43}H_{61}N_2O_{23}$ ($M+NH_4^+$) calcd 973.3660, found 973.3685.

(*E*)-Ethyl 7,11-dimethyl-3-oxododeca-6,10-dienoate (6.09)

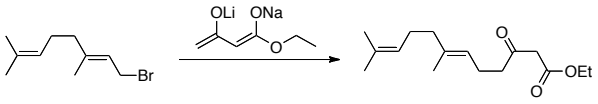

6.09

Oil-free sodium hydride was prepared by washing a 60% dispersion of NaH in mineral oil with anhydrous pentane under N_2 in a fritted funnel. This preparation of oil-free NaH (0.66 g, 17 mmol) was suspended in freshly distilled tetrahydrofuran (23 mL) and cooled to 0 °C. Ethyl acetoacetate (0.63 mL, 15 mmol) was added dropwise. After 10 min, *n*-butyllithium (2.63 M in hexanes, 6.0 mL, 16 mmol) was added slowly over 5 minutes. Geranyl bromide (1.6 mL, 8.0 mmol) was added to this suspension at 0 °C. After 20 min, the reaction was quenched by addition of 3M hydrochloric acid (8 mL). The biphasic mixture was partitioned between ethyl ether (150 mL) and water (150 mL). The aqueous layer was extracted with ethyl ether (2 x 100 mL). The combined organic layers were washed with water (3 x 100 mL), brine (100 mL), dried over magnesium sulfate, filtered, and concentrated under reduced pressure. Purification by flash chromatography [hexanes to 1:9 (vol/vol) EtOAc:hexanes] afforded **6.09** (0.96 g, 45%) as a light orange oil. Characterization of this compound matched a published report.[212]

(2*E*,6*E*)-ethyl 3-((diethoxyphosphoryl)oxy)-7,11-dimethyldodeca-2,6,10-trienoate (6.10)

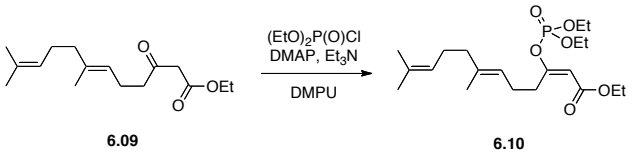

A solution of 4-(dimethylamino)pyridine (13 mg, 0.11 mmol) and triethylamine (0.15 mL, 1.1 mmol) in 1,3-dimethyl-3,4,5,6-tetrahydro-2(1*H*)-pyrimidone (DMPU, 1.8 mL) under Ar atmosphere was cooled to 0 °C. An ice-cooled solution of **6.09** (0.25 g, 0.94 mmol) in DMPU (1.2 mL) was added via cannula using positive nitrogen pressure. The bright yellow solution stirred at 0 °C for 50 min, then it was cooled to –20 °C. Diethyl chlorophosphate (0.15 mL, 1.1 mmol) was added dropwise, and the cooling bath was removed. The reaction stirred at ambient temperature for 16 h. It was diluted with ethyl ether and acidified to pH ~2 with 1M HCl to afford a biphasic mixture. The layers were separated, and the aqueous layer was extracted with ethyl ether. The combined organic layers were washed with a saturated solution of copper(II) sulfate (2x), brine, dried over magnesium sulfate, filtered, and concentrated under reduced pressure. Purification by flash chromatography [1:9 (vol/vol) EtOAc:hexanes to 3:7 (vol/vol) EtOAc:hexanes] afforded **6.10** (0.12 g, 31%) as a light yellow oil. Characterization of this compound matched a published report.[212]

(2*Z*,6*E*)-ethyl 3,7,11-trimethyldodeca-2,6,10-trienoate (6.11)

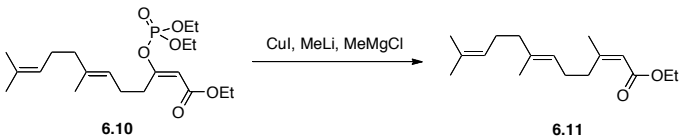

A suspension of copper(I) iodide (0.17 g, 0.88 mmol) in freshly distilled tetrahydrofuran (7.3 mL) under Ar atmosphere was cooled to 0 °C. Methyllithium (1.6M in Et_2O, 0.55 mL, 0.88 mmol) was added dropwise and the reaction stirred at 0 °C for 10 min. The reaction was cooled to –30 °C for 10 min, followed by dropwise addition of methylmagnesium chloride (3.0M in THF, 0.39 mL, 1.2 mmol). After 20 min, a solution of **6.10** (0.12 g, 0.29 mmol) in freshly distilled tetrahydrofuran (7.3 mL) was added via cannula using positive nitrogen pressure. The greenish brown suspension stirred at –30 °C for 3 h. It was poured into an ice-cold solution of saturated ammonium chloride in a separatory funnel and diluted with ethyl ether. The organic layer was rinsed with a saturated solution of ammonium chloride until the aqueous layer was no longer blue. The organic layer was washed with brine, dried over magnesium sulfate, filtered, and concentrated under reduced pressure. Purification by flash chromatography [1:4 (vol/vol) CH_2Cl_2:hexanes to 2:3 (vol/vol) CH_2Cl_2:hexanes] afforded **6.11** (58 mg, 75%) as a clear oil. Characterization of this compound matched a published report.[212]

(2*Z*,6*E*)-Farnesol (6.08)

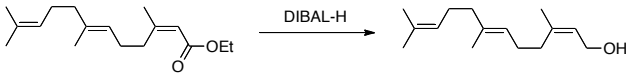

6.11 **6.08**

A solution of **6.11** (58 mg, 0.22 mmol) in freshly distilled toluene (5.0 mL) under Ar atmosphere was cooled to –78 °C. Diisobutylaluminum hydride (DIBAL-H, 1.0M in toluene, 0.77 mL, 0.77 mmol) was added dropwise. After 1.5 h, the reaction was quenched by addition of a saturated solution of sodium potassium tartrate (12 mL). The clear biphasic mixture was transferred to a separatory funnel and diluted with EtOAc. The layers were separated, and the aqueous layer was extracted with EtOAc (3 x 10 mL). The combined organic layers were washed with brine (20 mL), dried over magnesium sulfate, filtered, and concentrated under reduced

pressure. Purification by flash chromatography [hexanes to 1:9 (vol/vol) EtOAc:hexanes] afforded **6.08** (43 mg, 89%) as a clear film. Characterization of this compound matched a published report.[218]

(*Z*)-tert-butyl((3,7-dimethylocta-2,6-dien-1-yl)oxy)diphenylsilane (6.13)

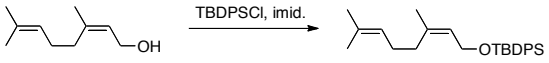

6.13

A solution of nerol (1.2 mL, 7.0 mmol) and imidazole (1.1 g, 15 mmol) in anhydrous *N,N*-dimethylformamide (6.4 mL) under Ar atmosphere was cooled to 0 °C. *tert*-Butylchlorodiphenylsilane (2.0 mL, 7.7 mmol) was added dropwise. The solution was stirred at ambient temperature for 2 h, then it was quenched with water (10 mL). The mixture was transferred to a separatory funnel and extracted with ethyl ether (3 x 15 mL). The combined organic layers were washed with a saturated solution of sodium bicarbonate, brine, dried over magnesium sulfate, filtered, and concentrated under reduced pressure to afford **6.13** (2.8 g, quantitative) as a clear oil. Characterization of this compound matched a published report.[284]

(*Z*)-tert-butyl((5-(3,3-dimethyloxiran-2-yl)-3-methylpent-2-en-1-yl)oxy)diphenylsilane (6.14)

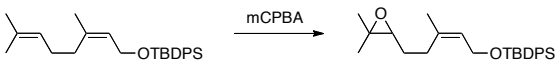

6.13 **6.14**

A solution of **6.13** (1.3 g, 3.2 mmol) in chloroform (13 mL) under Ar atmosphere was cooled to 0 °C. *meta*-Chloroperoxybenzoic acid (77% max, 0.79 g, 3.5 mmol) was added in one portion and the suspension stirred at 0 °C for 1 h. It was diluted with chloroform (40 mL) and

transferred to a separatory funnel. The suspension was washed with water, a saturated solution of sodium bicarbonate, brine, dried over magnesium sulfate, filtered, and concentrated under reduced pressure. Purification by flash chromatography [hexanes to 3:1 (vol/vol) CH_2Cl_2:hexanes] afforded **6.14** (0.93 g, 71%) as a clear oil. Characterization of this compound matched a published report.[284]

(*Z*)-6-((tert-butyldiphenylsilyl)oxy)-4-methylhex-4-enal (6.15)

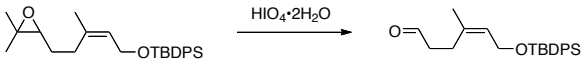

6.14 **6.15**

A solution of **6.14** (0.93 g, 2.3 mmol) in anhydrous ethyl ether (3.0 mL) under Ar atmosphere was cooled to 0 °C. It was transferred via cannula to an ice-cooled solution of periodic acid dihydrate (0.62 g, 2.7 mmol) in freshly distilled tetrahydrofuran (23 mL) using positive nitrogen pressure. The clear solution stirred at 0 °C for 2 h before being filtered, diluted with ethyl ether, washed with water, a saturated solution of sodium bicarbonate, brine, dried over magnesium sulfate, and concentrated under reduced pressure to afford **6.15** (0.83 g, 99%) as an off-white oil. This compound was carried onto the next step without further purification.

(2*Z*,6*Z*)-ethyl 8-((tert-butyldiphenylsilyl)oxy)-2,6-dimethylocta-2,6-dienoate (6.16)

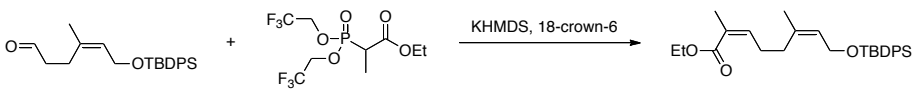

6.15 **6.16**

2-[bis(2,2,2-trifluoroethoxy)phosphonyl]propionic acid ethyl ester (0.67 mL, 2.7 mmol) was added to a solution of 18-crown-6 (1.9 g, 7.3 mmol) in freshly distilled tetrahydrofuran (17

mL) under Ar atmosphere. The solution was cooled to –78 °C prior to slow addition of potassium bis(trimethylsilyl)amide (0.5M in toluene, 5.8 mL, 2.9 mmol). After 30 min, a solution of **6.15** (0.89 g, 2.4 mmol) in freshly distilled tetrahydrofuran (7.3 mL) was added dropwise via cannula using positive nitrogen pressure and the mixture stirred at -78 °C for 1 h. A saturated solution of ammonium chloride (50 mL) and ethyl ether (30 mL) were added, and the layers were separated. The aqueous layer was extracted with ethyl ether (5 x 20 mL), and the combined organic layers were washed with brine, dried over magnesium sulfate, filtered, and concentrated under reduced pressure. Purification by flash chromatography [hexanes to 1:19 (vol/vol) EtOAc:hexanes] afforded **6.16** (0.75 g, 69%, 10:1 Z:E) as a clear oil. Characterization of this compound matched a published report.[290]

(2*Z*,6*Z*)-8-((tert-butyldiphenylsilyl)oxy)-2,6-dimethylocta-2,6-dien-1-ol (6.17)

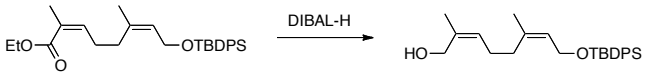

6.16 **6.17**

Diisobutylaluminum hydride (DIBAL-H, 1.0M in toluene, 4.13 mL, 4.13 mmol) was added dropwise to a solution of **6.16** (0.745 g, 1.65 mmol) in freshly distilled toluene (16.5 mL) under Ar atmosphere at –78 °C. After stirring for 1 h at –78 °C, the solution was poured into a saturated solution of sodium potassium tartrate (50 mL) at ambient temperature, diluted with ethyl acetate, and stirred vigorously for 0.5 h. The layers were separated, and the aqueous layer was extracted with EtOAc (3 x 40 mL). The combined organic layers were washed with brine, dried over magnesium sulfate, filtered, and concentrated under reduced pressure. Purification by flash chromatography [1:9 (vol/vol) EtOAc:hexanes to 1:4 (vol/vol) EtOAc:hexanes] afforded **6.17** (0.605 g, 90%) as a clear oil. Characterization of this compound matched a published report.[290]

tert-Butyl(((2_Z_,6_Z_)-8-chloro-3,7-dimethylocta-2,6-dien-1-yl)oxy)diphenylsilane (6.12)

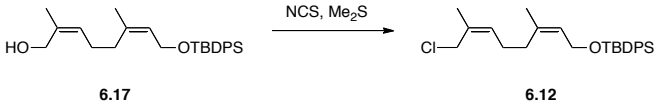

6.17 **6.12**

Methyl sulfide (64 μL, 0.87 mmol) was added to a solution of N-chlorosuccinimide (0.11 g, 0.84 mmol) in CH_2Cl_2 (1.7 mL) under Ar atmosphere at –30 °C. The suspension was warmed to 0 °C. After stirring at 0 °C for 40 min, the solution was cooled to –30 °C. Then, a solution of **6.17** (0.31 g, 0.76 mmol) in CH_2Cl_2 (1.7 mL) was added dropwise via cannula using positive Ar pressure. After 30 min at 0 °C, the reaction was warmed to ambient temperature. After 1.5 h, the reaction was diluted with hexanes, washed with brine (2x), dried over magnesium sulfate, filtered, and concentrated under reduced pressure to afford **6.12** (0.30 g, 91%) as an off-white oil. This compound was carried onto the next step without further purification.

(_Z_)-1-((3,7-dimethylocta-2,6-dien-1-yl)sulfonyl)-4-methylbenzene (6.19)

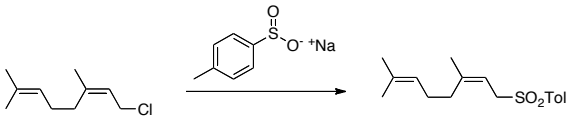

6.19

Methyl sulfide (0.693 mL, 9.44 mmol) was added to a solution of N-chlorosuccinimide (1.186 g, 8.88 mmol) in freshly distilled CH_2Cl_2 (16.0 mL) cooled to -30 °C. The suspension was warmed to 0 °C. After 20 min at 0 °C, it was cooled to -30 °C. Nerol (1.41 mL, 8.0 mmol) was added dropwise and the reaction was warmed to 0 °C. After 1.5 h, the reaction was warmed to ambient temperature. After 3 h, the reaction was diluted in hexanes, filtered, washed with brine

(2x), dried over magnesium sulfate, filtered, and concentrated under reduced pressure to afford crude neryl chloride (1.153 g, 84%) as a runny oil.

The crude neryl chloride was dissolved in anhydrous *N*,*N*-dimethylformamide (10.3 mL) under Ar atmosphere. Sodium *para*-toluenesulfinate (1.309 g, 7.34 mmol) was added, and the suspension stirred at ambient temperature for 15 h. It was diluted with water (50 mL) and extracted with diisopropyl ether (3 x 30 mL). The combined organic layers were washed with saturated sodium bicarbonate (40 mL), brine (40 mL), dried over magnesium sulfate, filtered, and concentrated under reduced pressure. Purification by flash chromatography [hexanes to 1:9 (vol/vol) EtOAc:hexanes] afforded **6.19** (1.473 g, 76%) as a white solid. Characterization of this compound matched a published report.[291]

tert-Butyldiphenyl(((2*Z*,6*Z*,10*Z*)-3,7,11,15-tetramethyl-9-tosylhexadeca-2,6,10,14-tetraen-1-yl)oxy)silane (6.20)

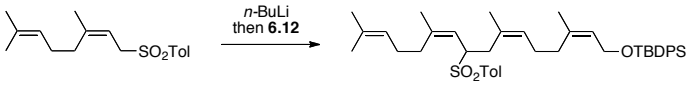

6.19 **6.20**

n-Butyllithium (2.2 M in hexanes, 0.30 mL, 0.76 mmol) was added dropwise to a solution of **6.19** (0.28 g, 0.97 mmol) in freshly distilled tetrahydrofuran (5.3 mL) and DMPU (1.3 mL) under Ar atmosphere at –78 °C. After 2 h, a solution of **6.12** (0.30 g, 0.69 mmol) in tetrahydrofuran (3.0 mL) was added dropwise via cannula using positive Ar pressure. After 2 h at –78 °C, the cooling bath was removed. After 15 min, the reaction was poured into water and ethyl ether, and the layers were separated. The aqueous layer was extracted with ethyl ether (2x), and the combined organic layers were washed with brine, dried over magnesium sulfate, filtered, and concentrated under reduced pressure. Purification by flash chromatography [hexanes to 3:47 (vol/vol) EtOAc:hexanes] afforded **6.20** (0.45 g, 96%).

^{1}H NMR (400 MHz, $CDCl_3$): δ 7.72 – 7.64 (m, 6H), 7.45 – 7.33 (m, 7H), 7.28 (d, *J* = 8.0 Hz, 2H), 5.38 (t, *J* = 6.0 Hz, 1H), 5.04 (t, *J* = 6.3 Hz, 1H), 4.92 (d, *J* = 10.6 Hz, 1H), 4.86 (d, *J* = 5.6 Hz, 1H), 4.16 (dd, *J* = 6.5, 1.4 Hz, 2H), 3.80 (td, *J* = 10.9, 2.9 Hz, 1H), 2.69 – 2.60 (m, 1H), 2.44 – 2.35 (m, 4H), 1.95 – 1.79 (m, 4H), 1.66 (q, *J* = 1.2 Hz, 4H), 1.62 (t, *J* = 1.5 Hz, 6H), 1.54 (d, *J* = 1.5 Hz, 3H), 1.52 – 1.48 (m, 4H), 1.04 (s, 9H). ^{13}C NMR (101 MHz, $CDCl_3$): δ 135.6, 129.6, 129.4, 129.2, 128.2, 127.6, 125.3, 123.6, 117.6, 63.4, 60.7, 32.1, 32.0, 30.3, 26.9, 26.4, 26.1, 25.7, 23.7, 23.4, 23.3, 21.6, 17.7. HRMS (ESI-TOF$^+$) for $C_{43}H_{58}O_3SSi$ (M+Na^+) calcd 705.3769, found 705.3774.

(2*Z*,6*Z*,10*Z*)-3,7,11,15-tetramethyl-9-tosylhexadeca-2,6,10,14-tetraen-1-ol (6.21)

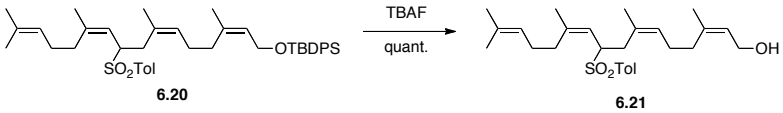

6.20 **6.21**

Tetra-*n*-butylammonium fluoride (1.0 M in tetrahydrofuran, 1.38 mL, 1.38 mmol) was added to a solution of **6.20** (0.236 g, 0.345 mmol) in freshly distilled tetrahydrofuran (3.4 mL) at ambient temperature under Ar atmosphere. The solution stirred at ambient temperature for 4 h, then it was concentrated under reduced pressure. Purification by flash chromatography [hexanes to 2:3 (vol/vol) EtOAc:hexanes] afforded **6.21** (0.153 g, quant.) as a clear oil.

^{1}H NMR (500 MHz, $CDCl_3$): δ 7.75 – 7.68 (m, 2H), 7.41 – 7.34 (m, 2H), 5.43 (t, *J* = 7.1 Hz, 1H), 5.19 (br s, 1H), 4.97 (d, *J* = 10.5 Hz, 1H), 4.88 (br s, 1H), 4.08 (d, *J* = 7.1 Hz, 2H), 3.89 – 3.81 (m, 1H), 2.76 (d, *J* = 12.9 Hz, 1H), 2.42 (s, 3H), 2.09 – 2.00 (m, 4H), 1.72 (s, 3H), 1.66 (s, 3H), 1.64 (s, 3H), 1.62 (s, 3H), 1.52 (s, 3H). ^{13}C NMR (126 MHz, $CDCl_3$): δ 145.3, 144.5, 139.5, 135.4, 134.9, 131.1, 129.7, 129.5, 129.3, 128.1, 127.8, 124.7, 123.6, 117.7, 63.6, 59.0, 32.1, 32.0, 30.2, 26.8, 26.7, 26.1, 25.7, 23.8, 23.6, 23.4, 21.7, 19.1, 17.8. HRMS (ESI-TOF$^+$) for $C_{27}H_{44}NO_3S$ (M+NH_4^+) calcd 462.3037, found 462.3049.

(2*Z*,6*Z*,10*Z*)-Nerylnerol (6.18)

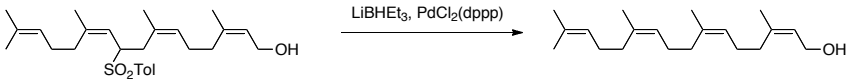

6.21 **6.18**

A solution of **6.21** (39 mg, 87 μmol) and (1,3-bis(diphenylphosphino)propane)palladium(II) dichloride [$PdCl_2$(dppp)], 2.6 mg, 4.3 μmol) in freshly distilled tetrahydrofuran (0.87 mL) under Ar atmosphere was cooled to 0 °C. Lithium triethylborohydride (1.0 M in tetrahydrofuran, 0.43 mL, 0.43 mmol) was added dropwise via syringe pump over 2 h. After stirring at 0 °C for an additional 4.5 h, the solution was warmed to ambient temperature. After stirring at ambient temperature for 15 h, the solution was diluted with ethyl ether, washed with saturated ammonium chloride, saturated sodium bicarbonate, brine, dried over magnesium sulfate, filtered, and concentrated under reduced pressure. Purification by flash chromatography [hexanes to 2:23 (vol/vol) EtOAc:hexanes] afforded **6.18** (16 mg, 62%) as a clear oil. Characterization of this compound matched a published report.[43]

Appendix: NMR Spectra

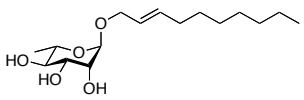

2.02

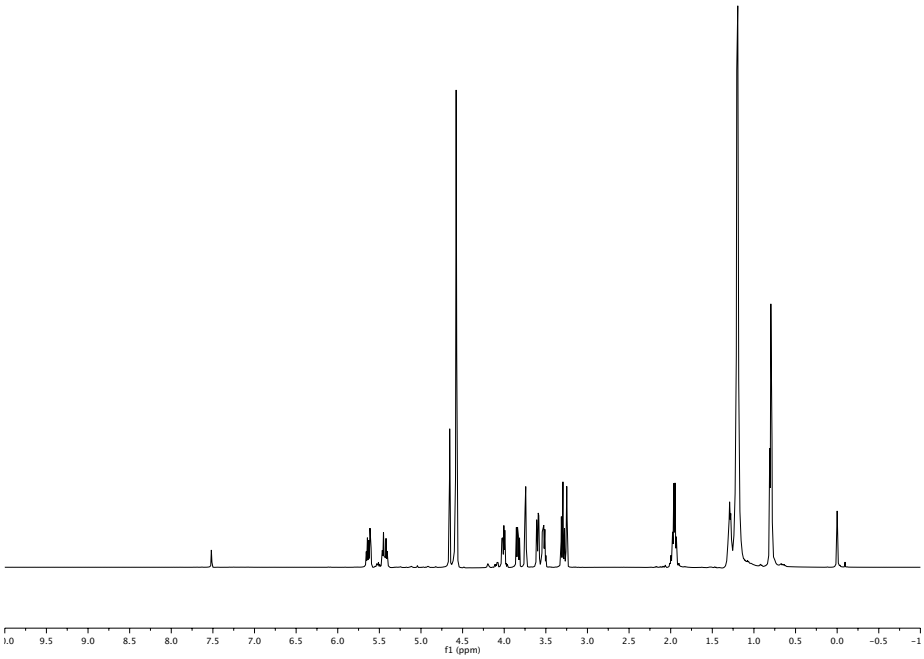

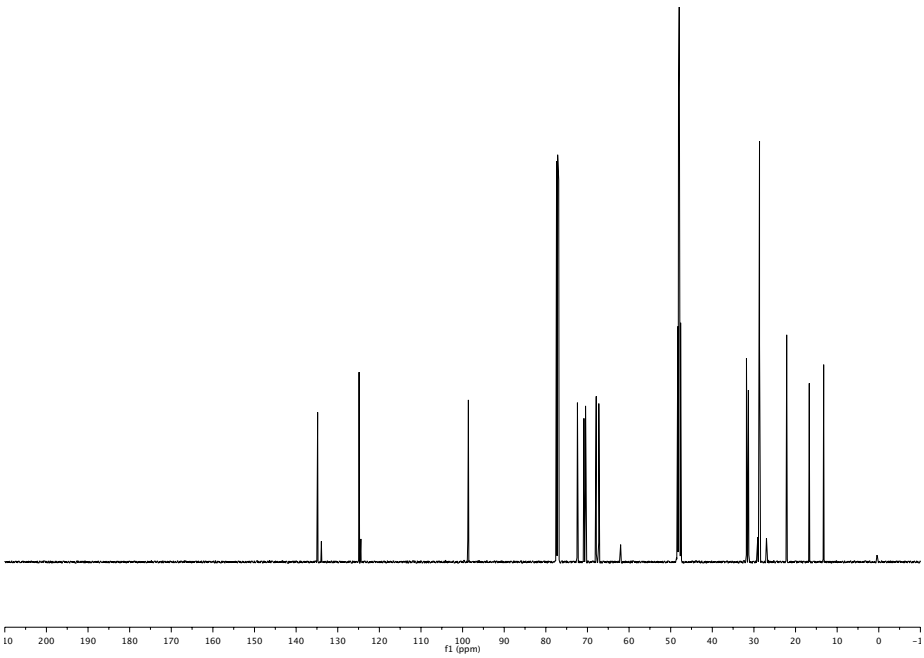

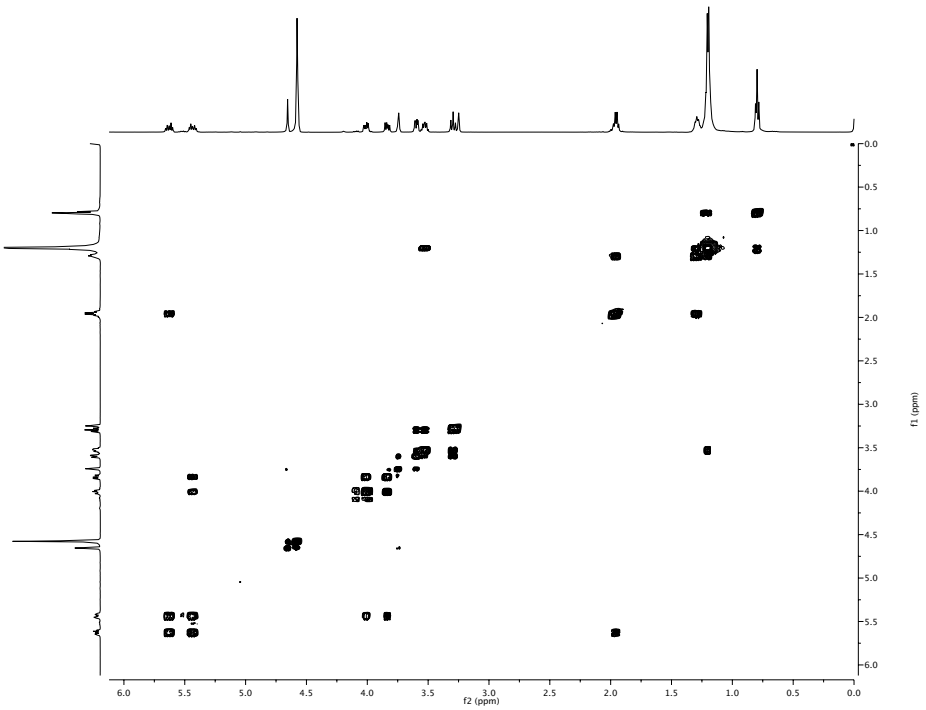
f2 (ppm)
f1 (ppm)

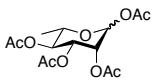
OAc
AcO
O
AcO
OAc

2.05

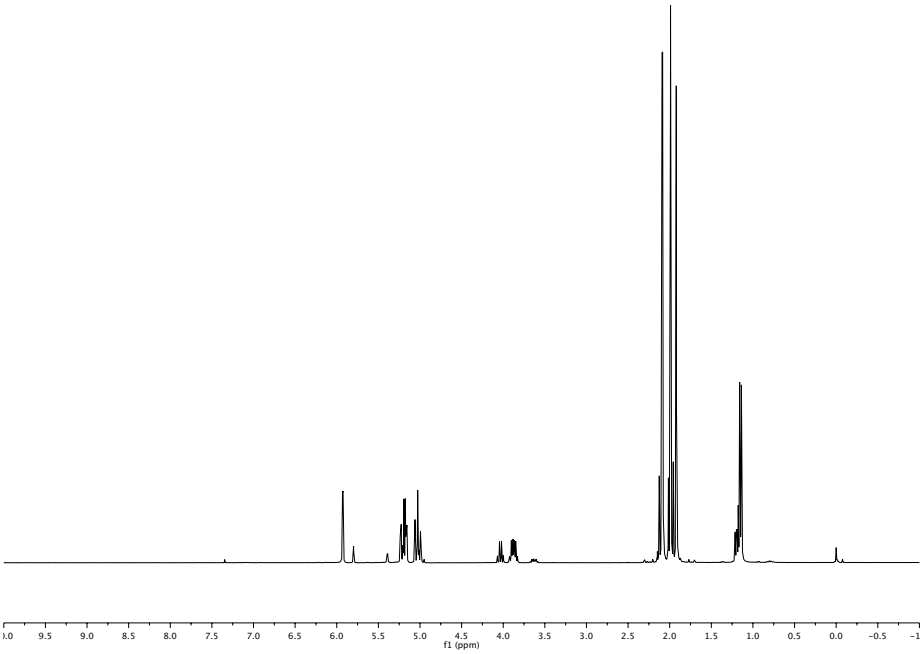
10.0
9.5
9.0
8.5
8.0
7.5
7.0
6.5
6.0
5.5
5.0
4.5
4.0
3.5
3.0
2.5
2.0
1.5
1.0
0.5
0.0
−0.5
−1
f1 (ppm)

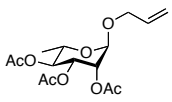
O
AcO
O
AcO
OAc

2.06

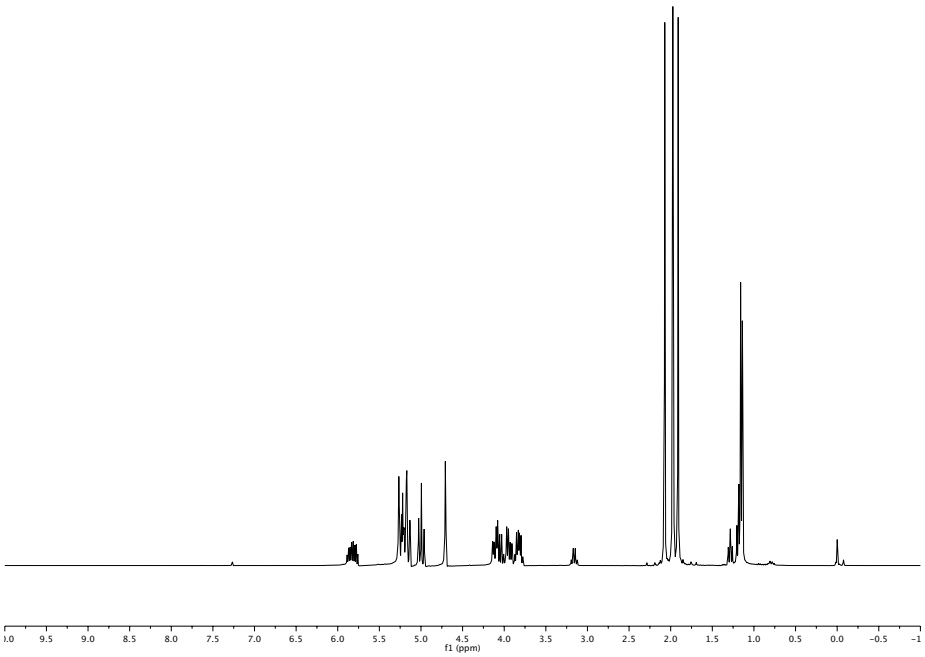
9.5
9.0
8.5
8.0
7.5
7.0
6.5
6.0
5.5
5.0
4.5
4.0
3.5
3.0
2.5
2.0
1.5
1.0
0.5
0.0
−0.5
f1 (ppm)

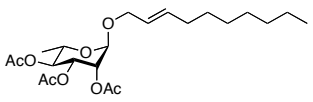
O
AcO
O
AcO
OAc

2.07

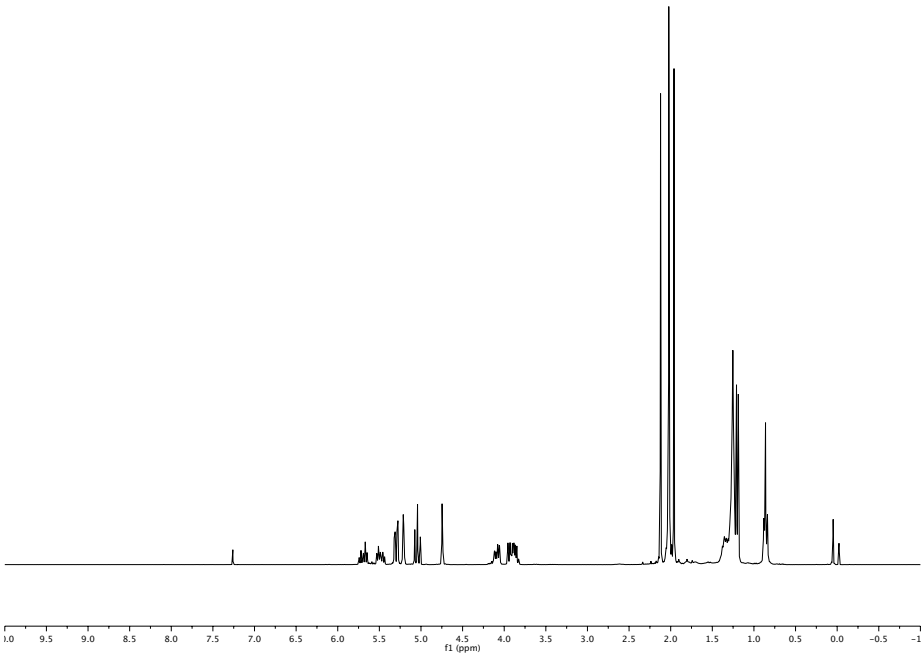
9.5 9.0 8.5 8.0 7.5 7.0 6.5 6.0 5.5 5.0 4.5 4.0 3.5 3.0 2.5 2.0 1.5 1.0 0.5 0.0 −0.5
f1 (ppm)

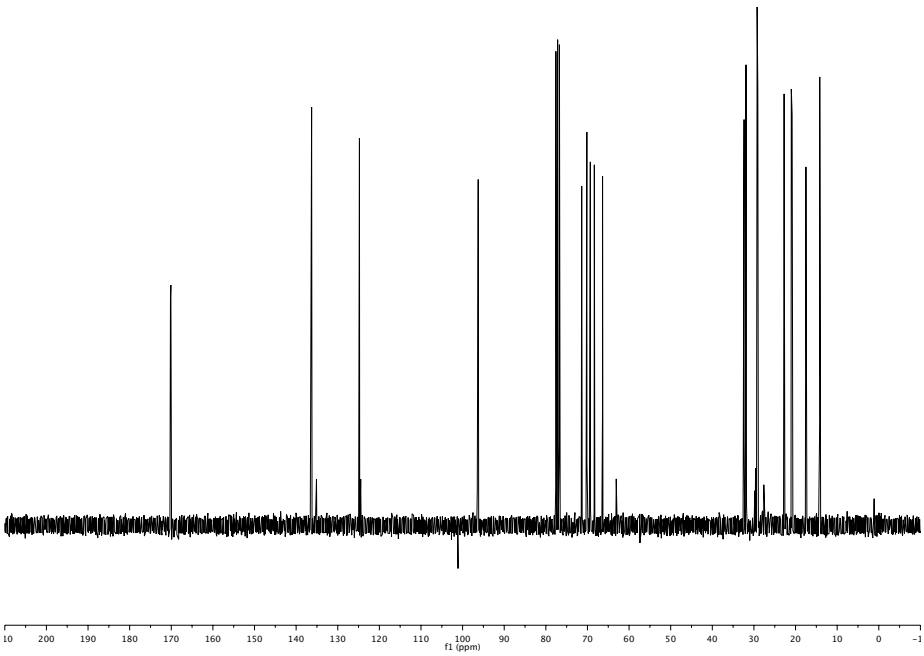
200 190 180 170 160 150 140 130 120 110 100 90 80 70 60 50 40 30 20 10 0
f1 (ppm)

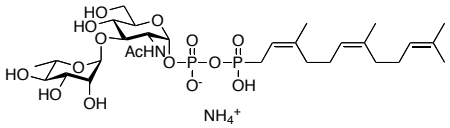
HO
HO
O
AcHN
O
O
P
O
O
P
O
OH
HO
O
HO
OH
NH4+

2.08

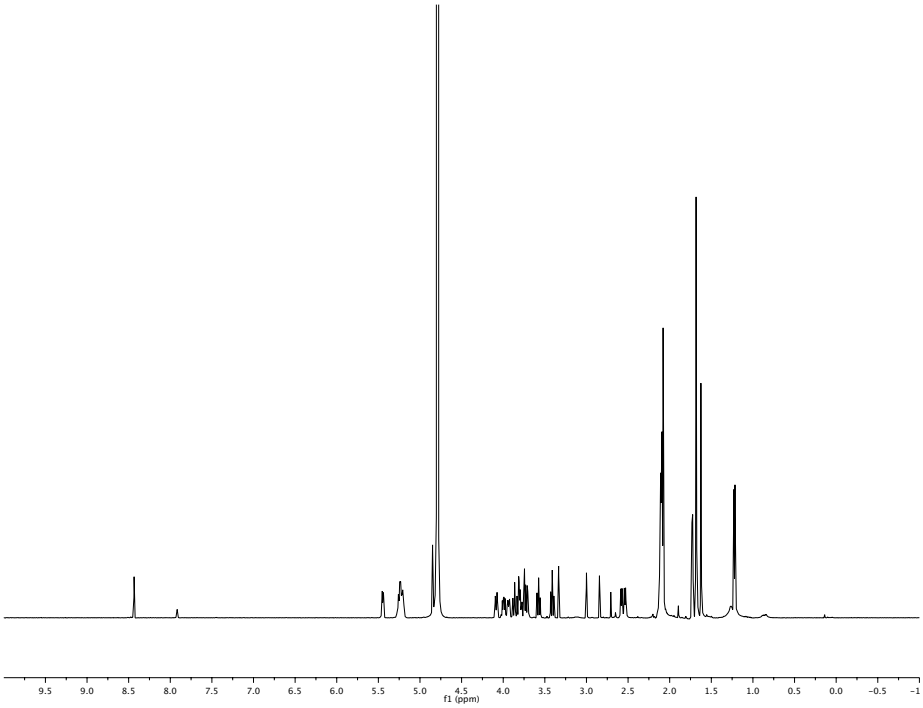
9.5 9.0 8.5 8.0 7.5 7.0 6.5 6.0 5.5 5.0 4.5 4.0 3.5 3.0 2.5 2.0 1.5 1.0 0.5 0.0 −0.5 −1
f1 (ppm)

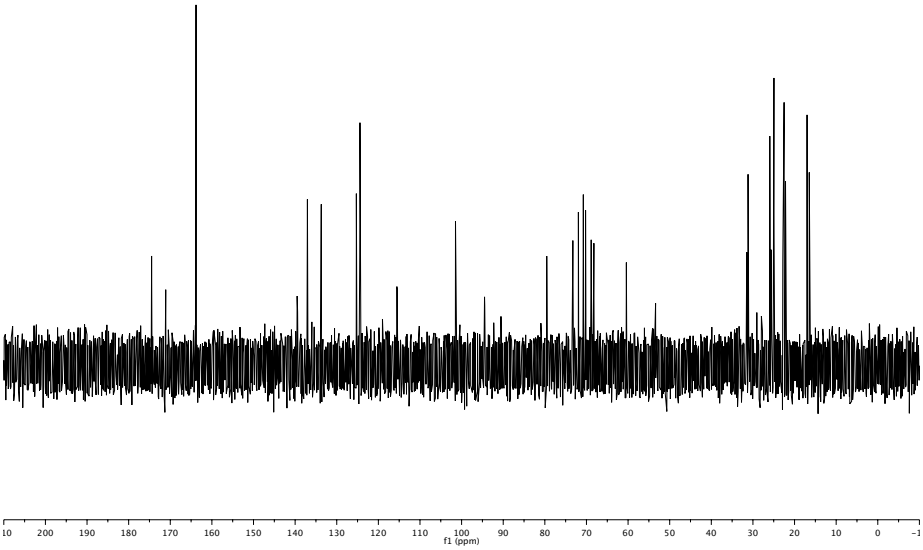
10 200 190 180 170 160 150 140 130 120 110 100 90 80 70 60 50 40 30 20 10 0 −1
f1 (ppm)

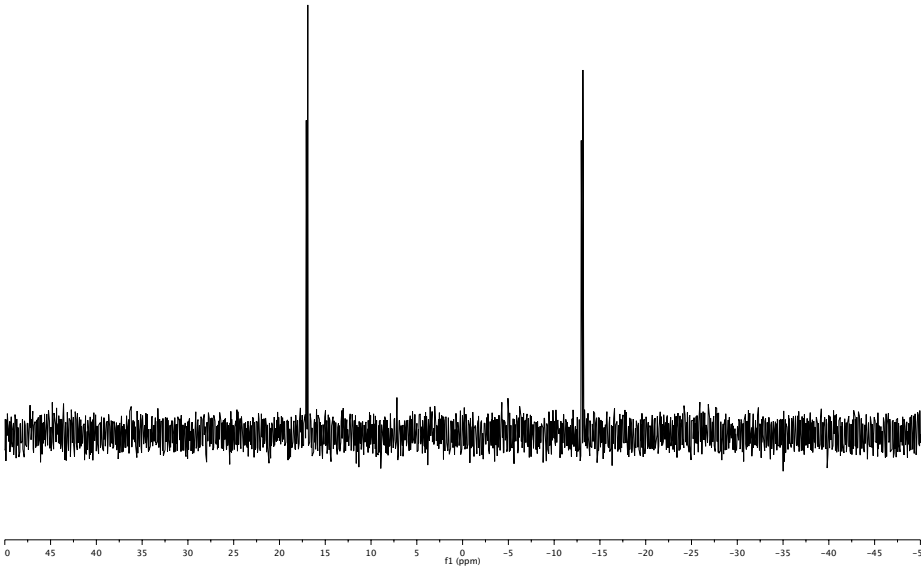
0
45
40
35
30
25
20
15
10
5
0
−5
−10
−15
−20
−25
−30
−35
−40
−45
f1 (ppm)

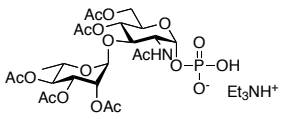

2.13

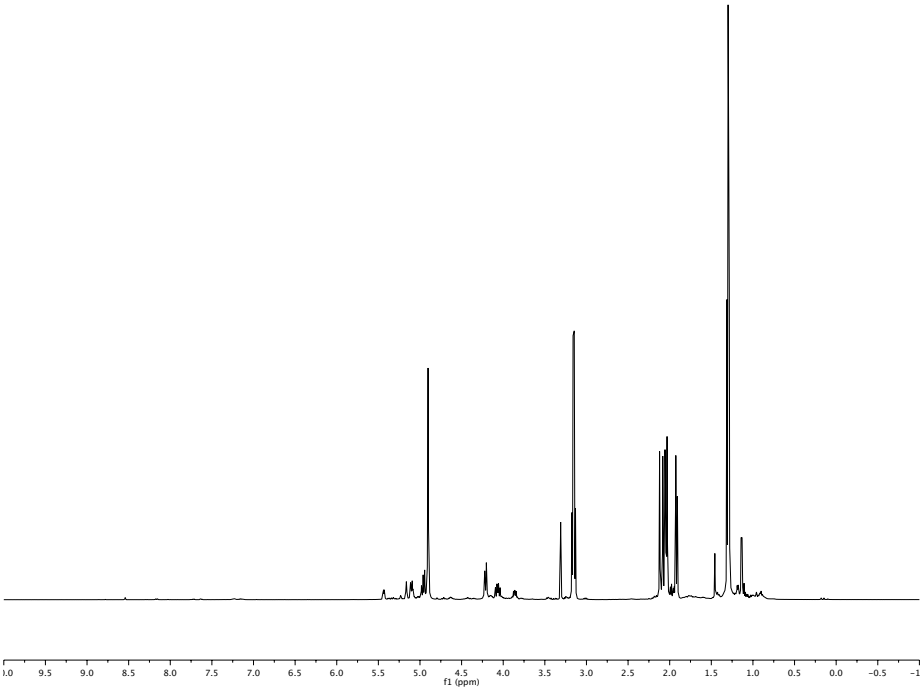

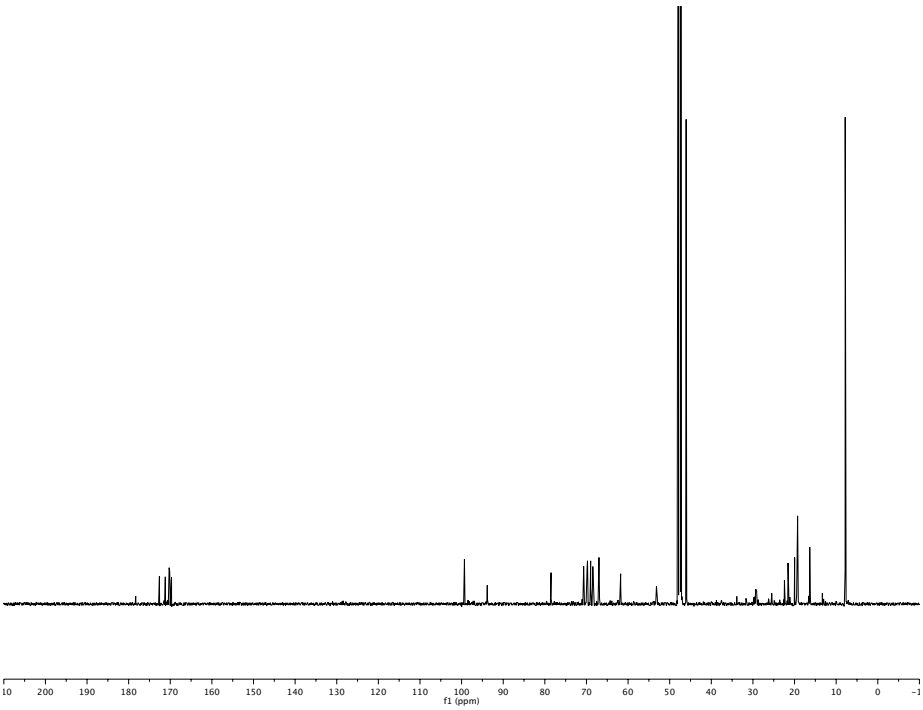

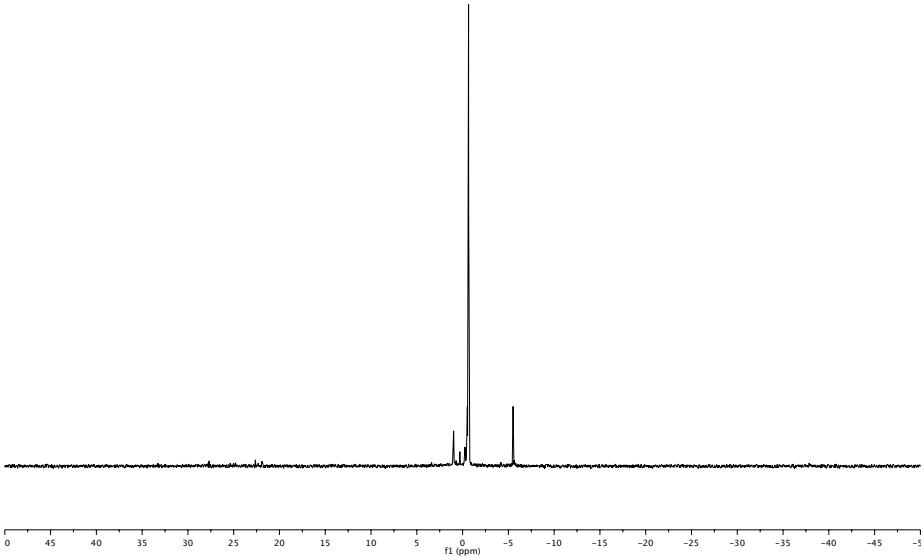
0
45
40
35
30
25
20
15
10
5
0
−5
−10
−15
−20
−25
−30
−35
−40
−45
f1 (ppm)

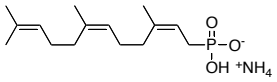
O
P–O-
OH +NH4

2.14

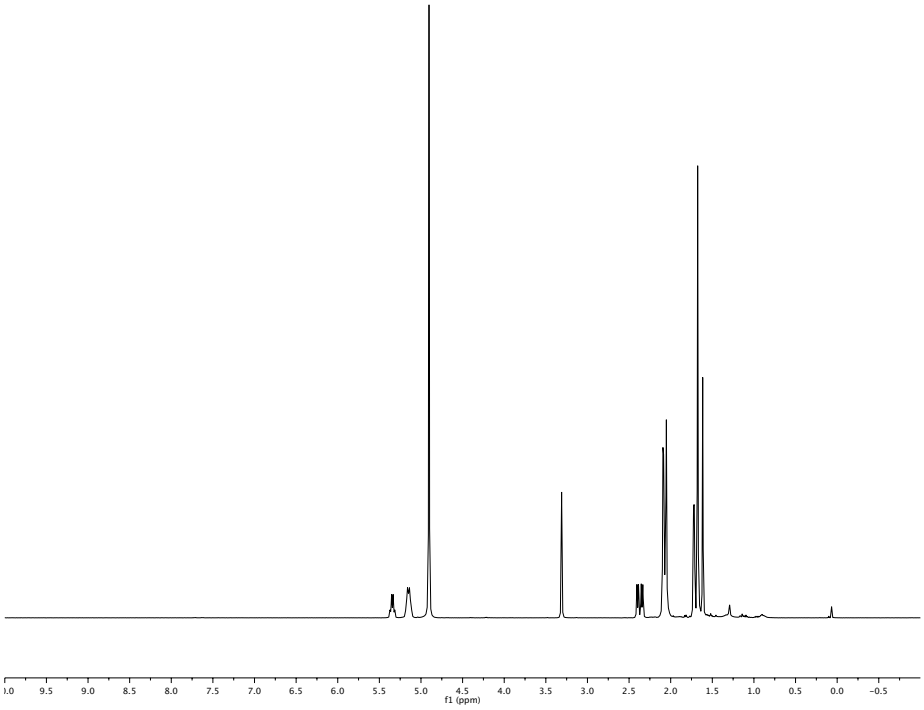
9.5
9.0
8.5
8.0
7.5
7.0
6.5
6.0
5.5
5.0
4.5
4.0
3.5
3.0
2.5
2.0
1.5
1.0
0.5
0.0
−0.5
f1 (ppm)

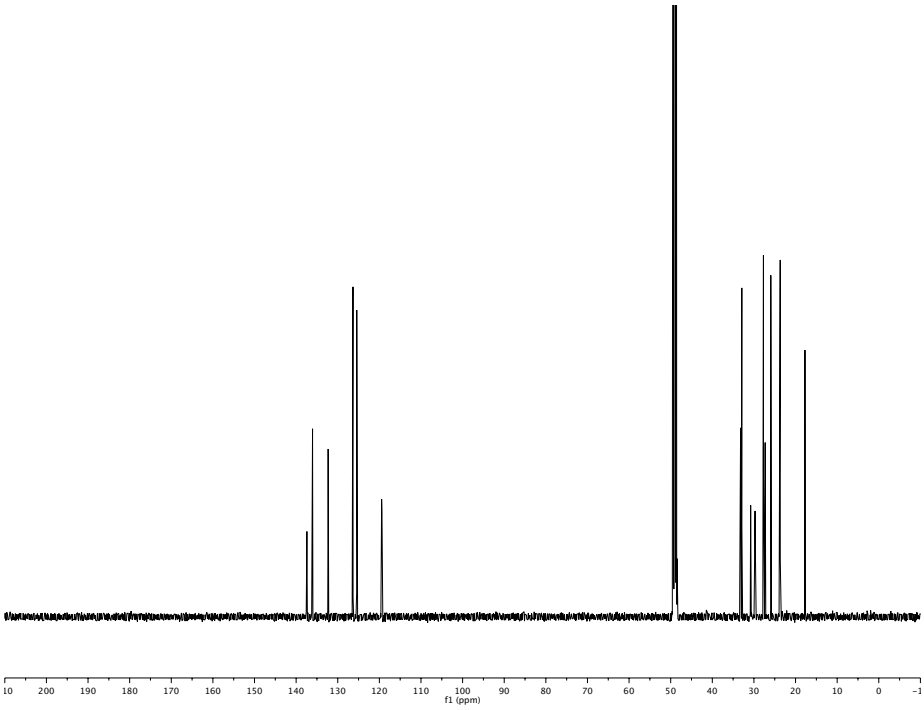
200
190
180
170
160
150
140
130
120
110
100
90
80
70
60
50
40
30
20
10
0
f1 (ppm)

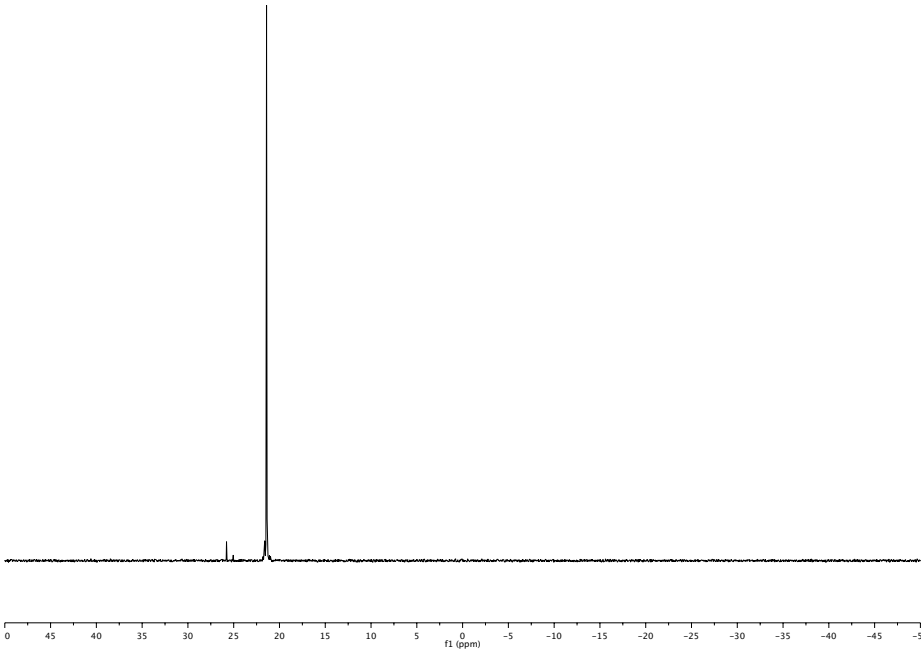
0
45
40
35
30
25
20
15
10
5
0
−5
−10
−15
−20
−25
−30
−35
−40
−45
f1 (ppm)

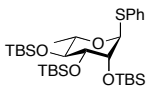

2.15

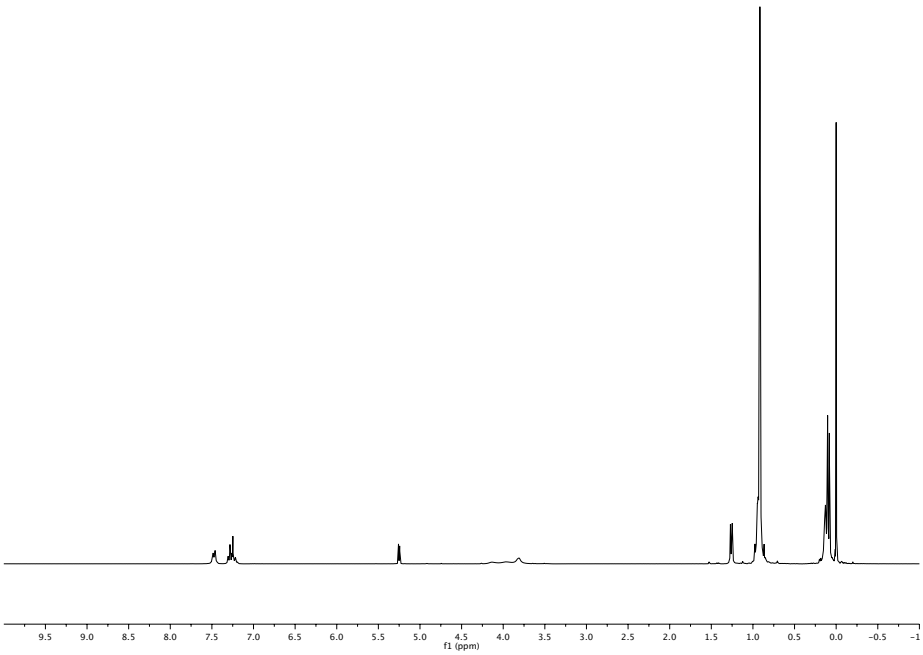

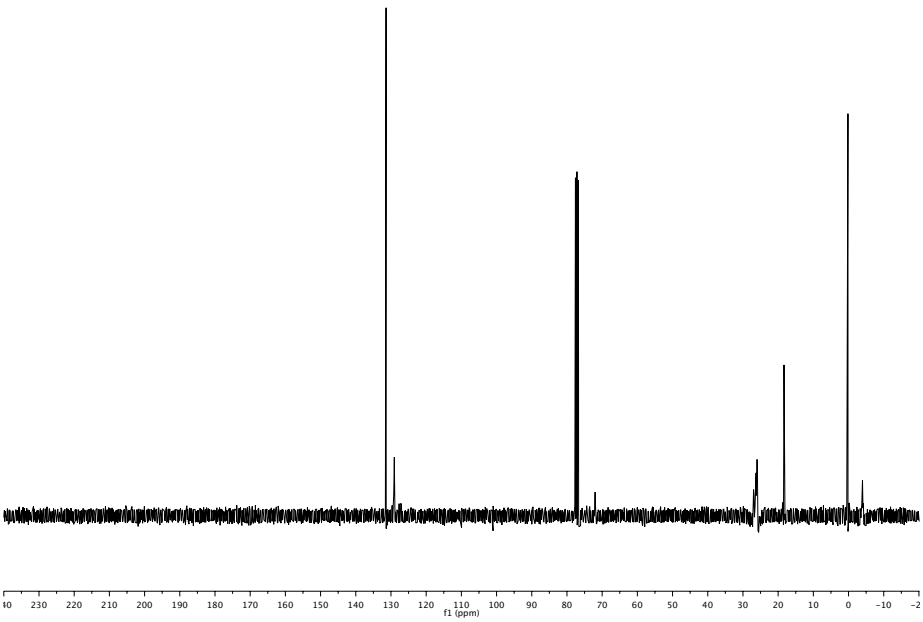

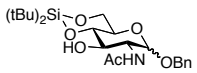

2.16

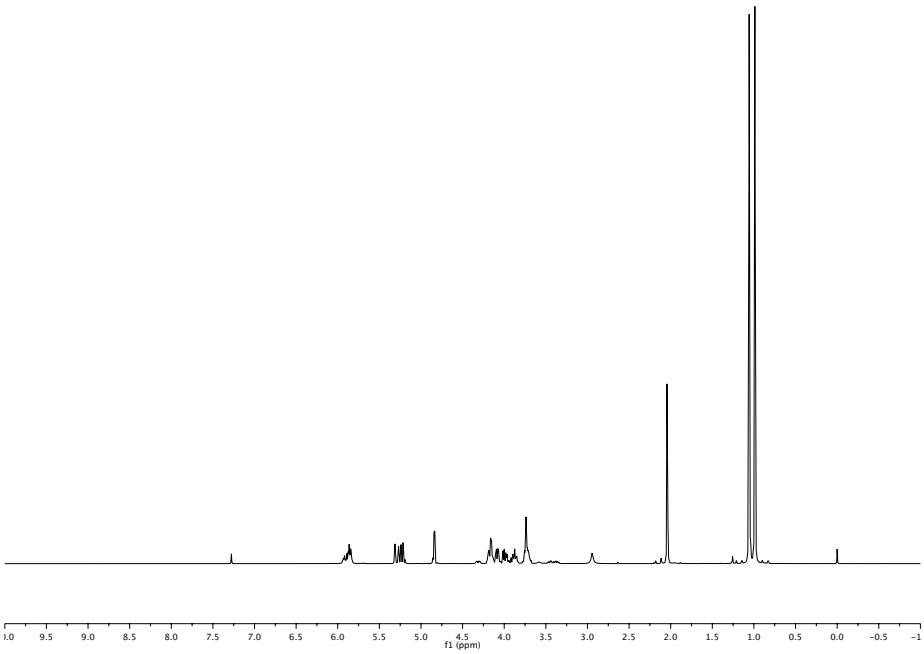

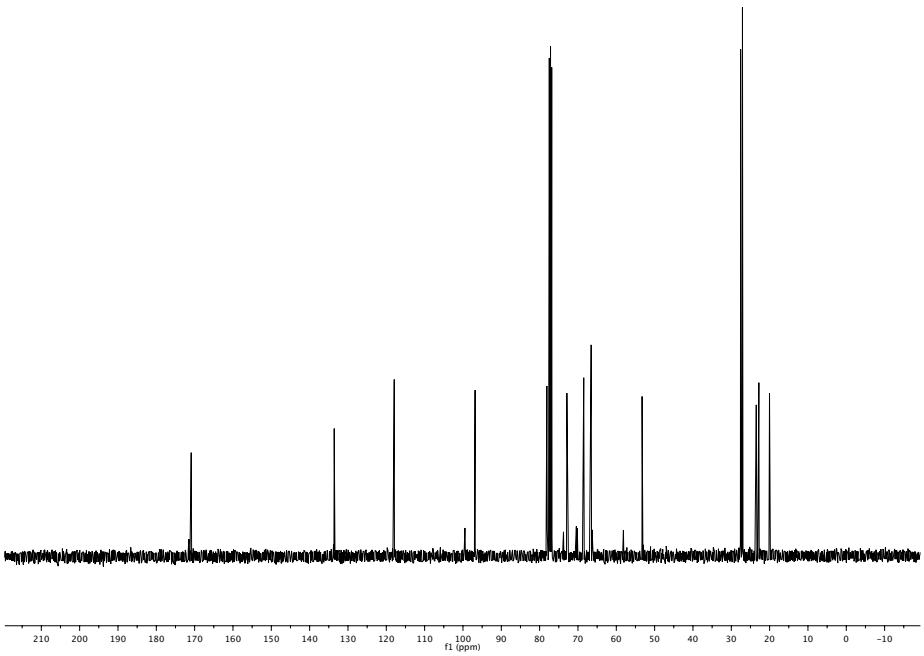

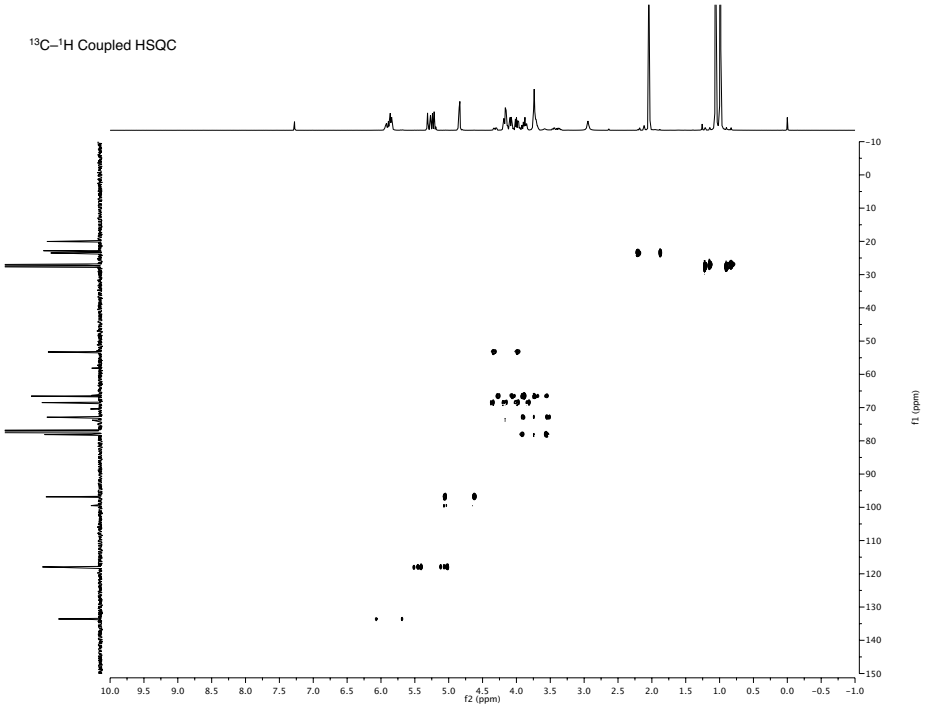
^{13}C–^{1}H Coupled HSQC
f2 (ppm)
f1 (ppm)

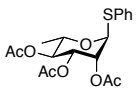
SPh
AcO
O
AcO
OAc

2.17

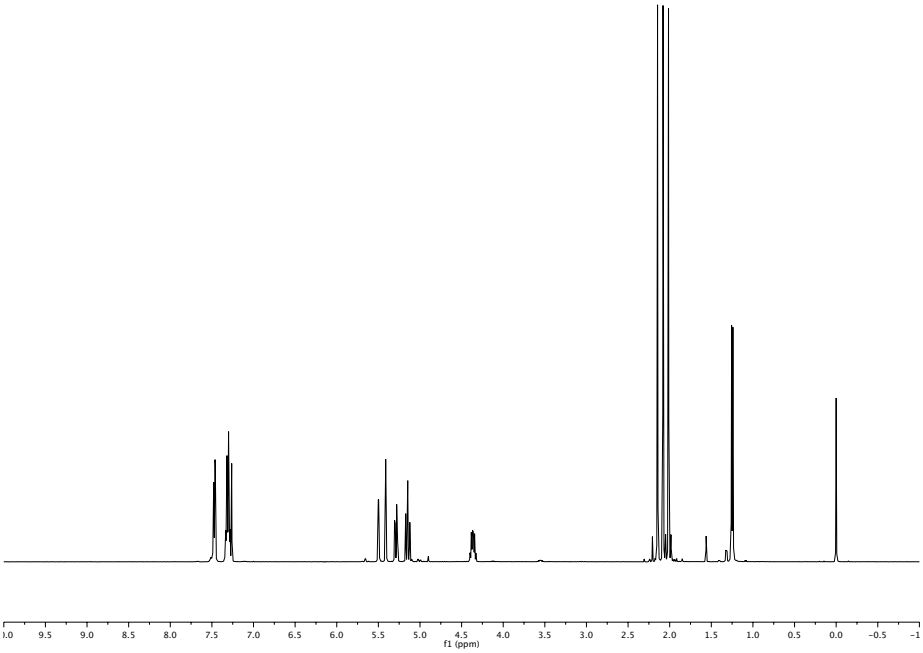
9.5
9.0
8.5
8.0
7.5
7.0
6.5
6.0
5.5
5.0
4.5
4.0
3.5
3.0
2.5
2.0
1.5
1.0
0.5
0.0
−0.5
f1 (ppm)

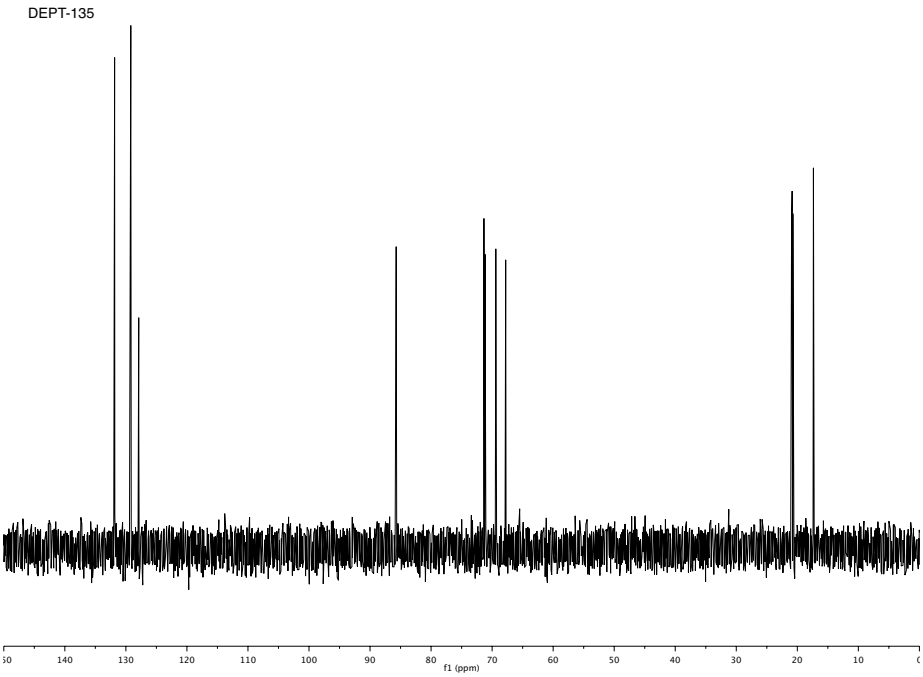
DEPT-135
140
130
120
110
100
90
80
70
60
50
40
30
20
10
f1 (ppm)

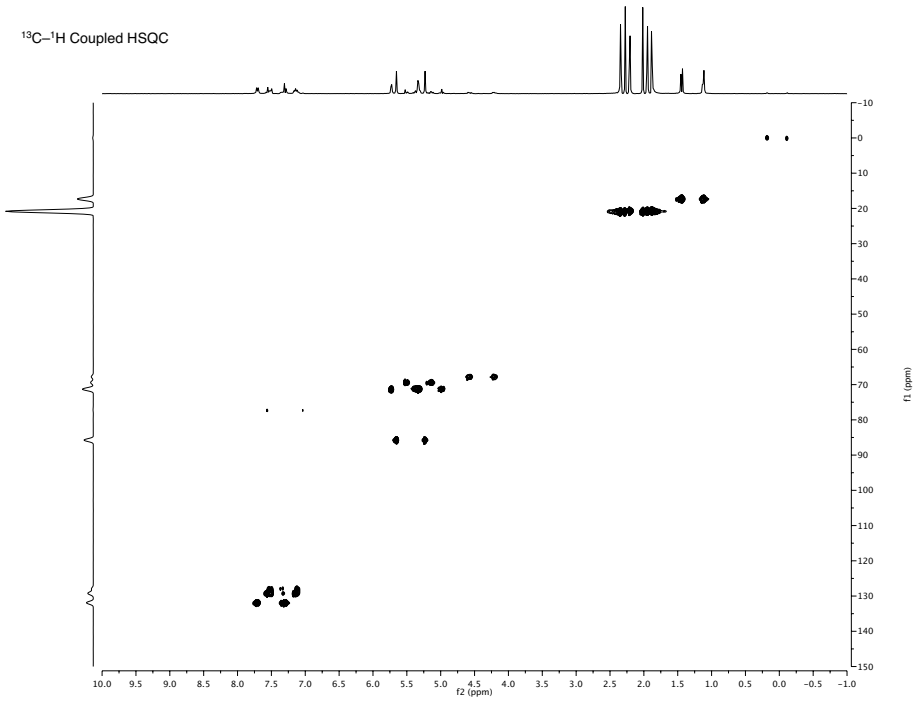
^{13}C–^{1}H Coupled HSQC
f1 (ppm)
f2 (ppm)

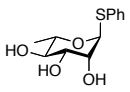
SPh
HO
O
HO
OH

2.18

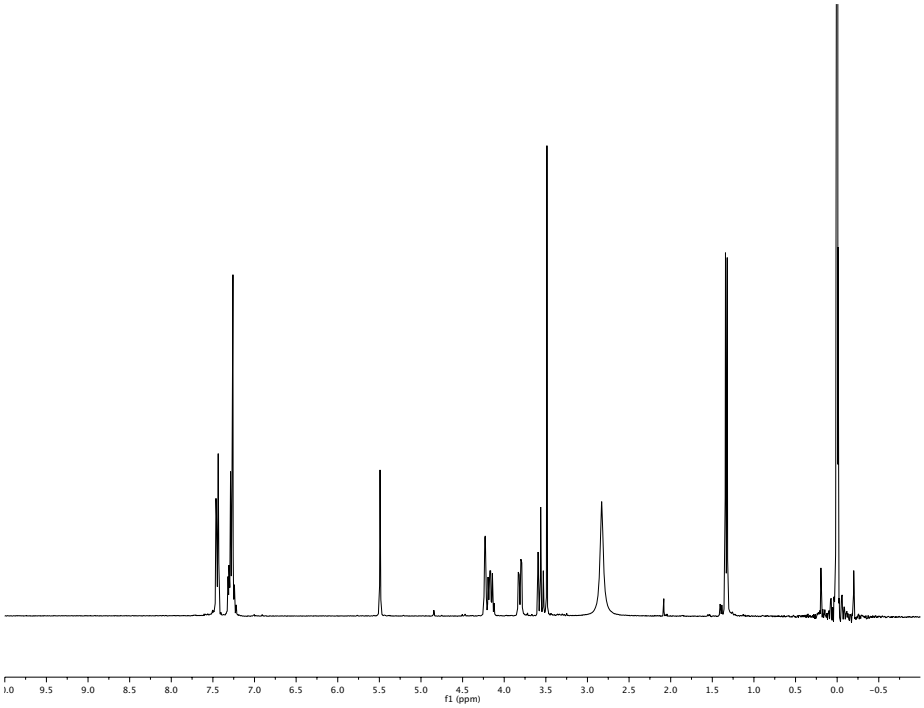
9.5
9.0
8.5
8.0
7.5
7.0
6.5
6.0
5.5
5.0
4.5
4.0
3.5
3.0
2.5
2.0
1.5
1.0
0.5
0.0
−0.5
f1 (ppm)

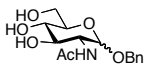
HO
HO
HO
O
AcHN
OBn

2.19

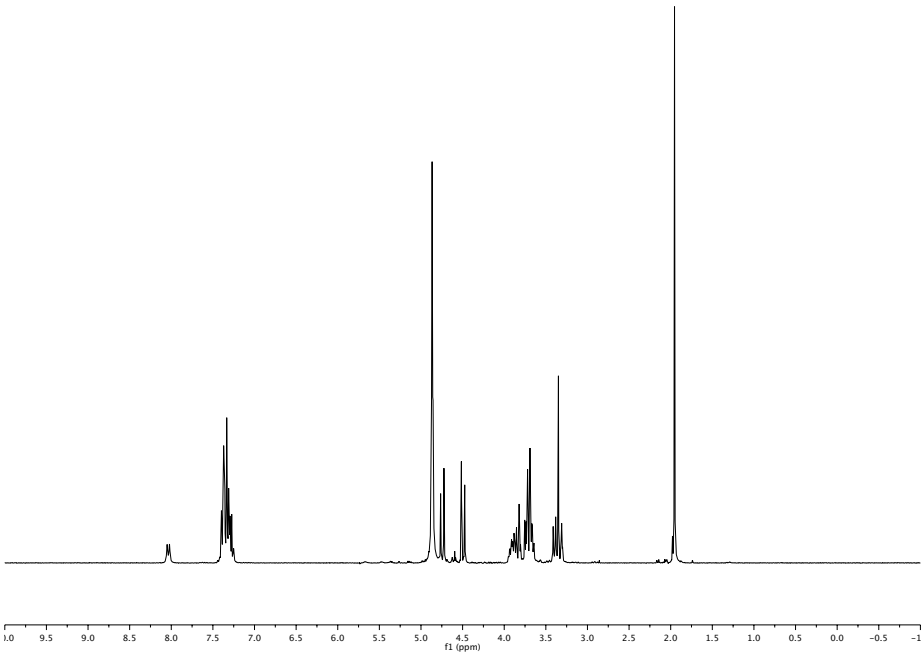
10.0
9.5
9.0
8.5
8.0
7.5
7.0
6.5
6.0
5.5
5.0
4.5
4.0
3.5
3.0
2.5
2.0
1.5
1.0
0.5
0.0
−0.5
−1
f1 (ppm)

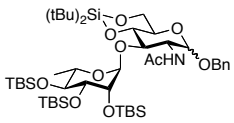
(tBu)2Si
O
O
O
O
AcHN
OBn
TBSO
O
TBSO
OTBS

2.20

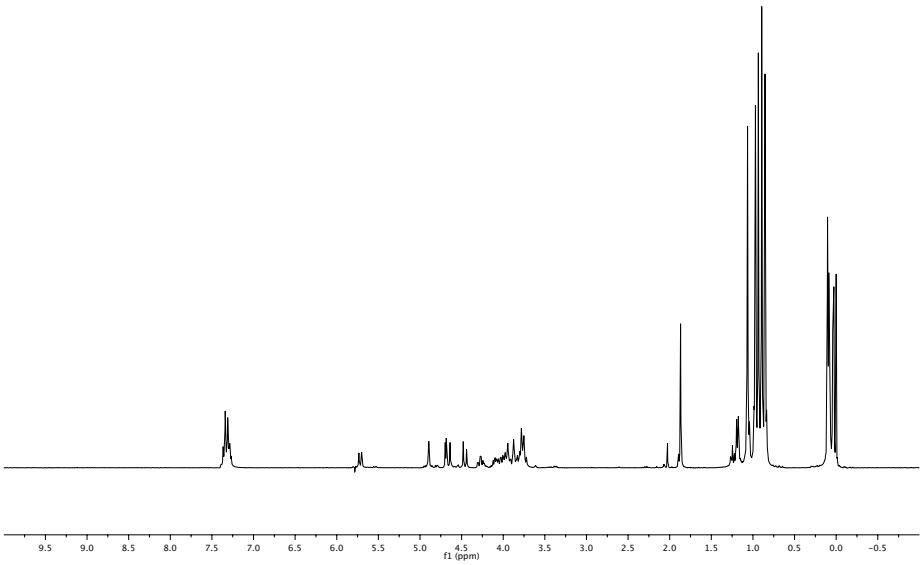
9.5 9.0 8.5 8.0 7.5 7.0 6.5 6.0 5.5 5.0 4.5 4.0 3.5 3.0 2.5 2.0 1.5 1.0 0.5 0.0 −0.5
f1 (ppm)

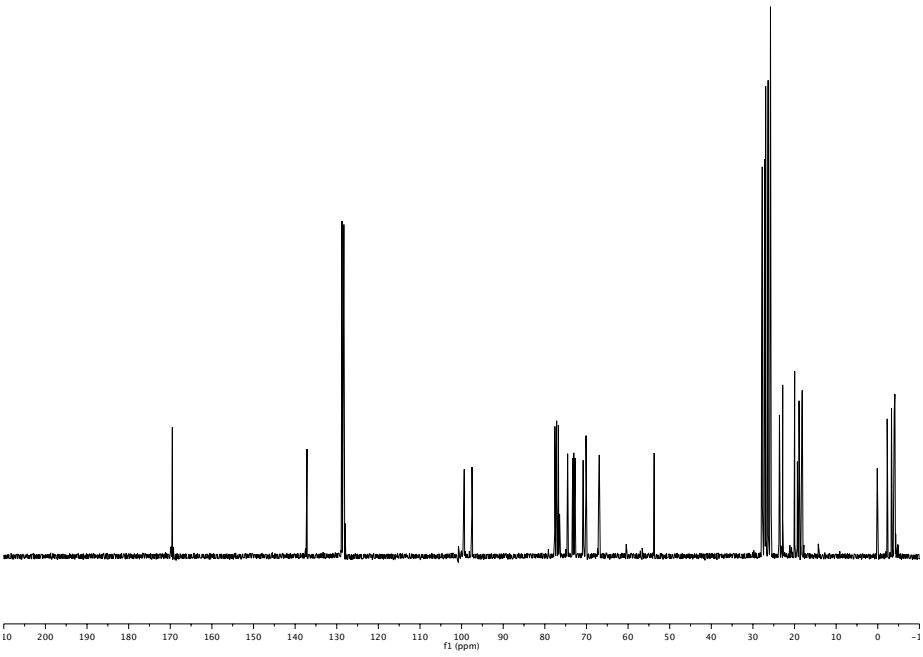
10 200 190 180 170 160 150 140 130 120 110 100 90 80 70 60 50 40 30 20 10 0 −1
f1 (ppm)

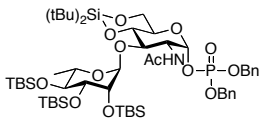

2.21

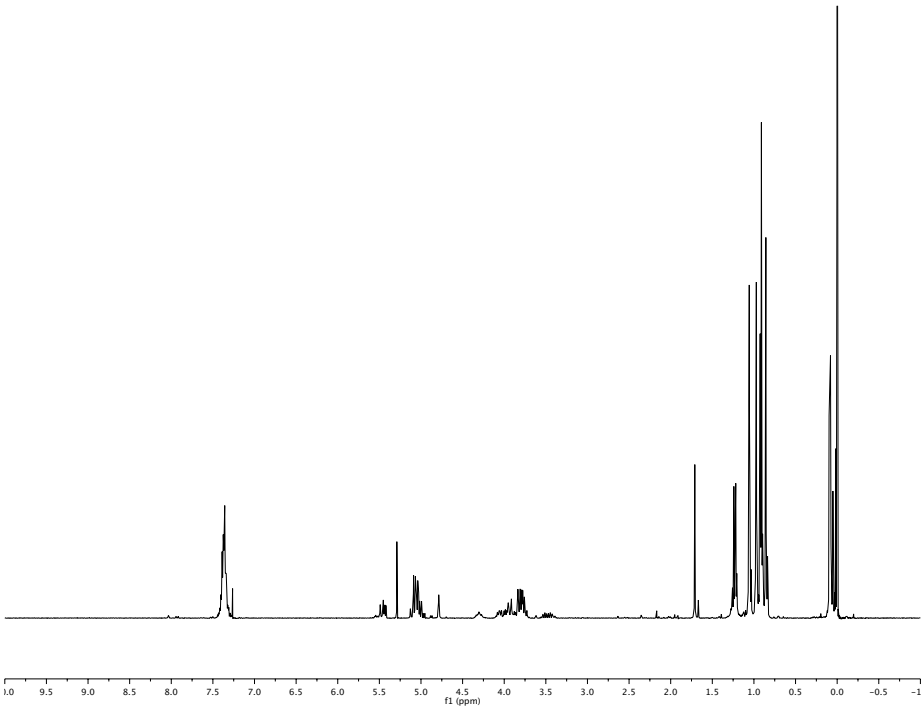

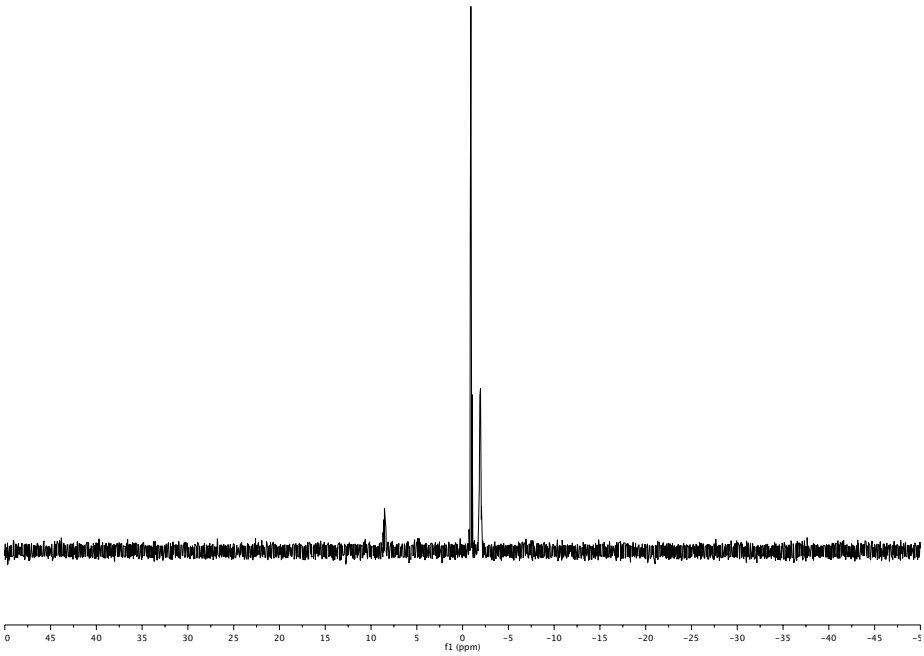

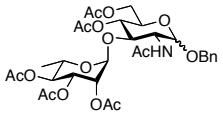
AcO
AcO
O
AcHN
OBn
AcO
O
AcO
OAc

2.23

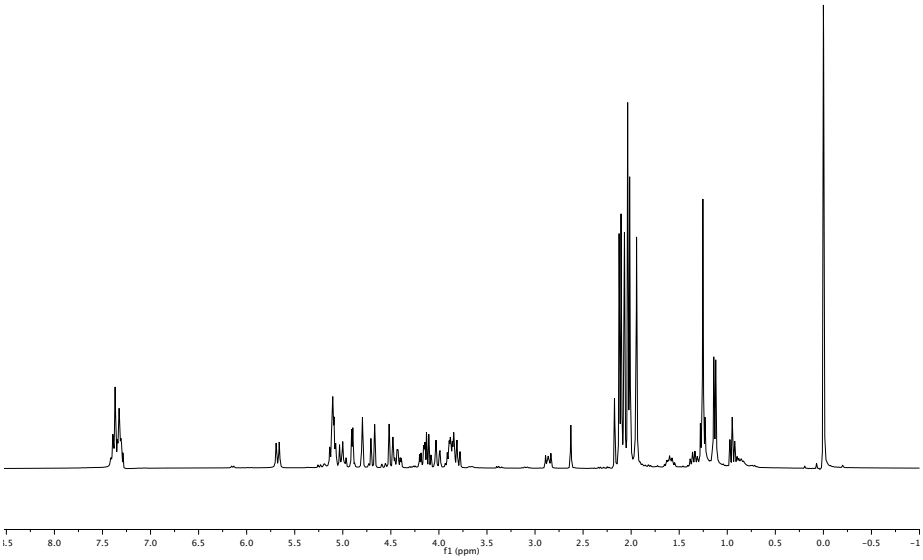
8.0
7.5
7.0
6.5
6.0
5.5
5.0
4.5
4.0
3.5
3.0
2.5
2.0
1.5
1.0
0.5
0.0
−0.5
f1 (ppm)

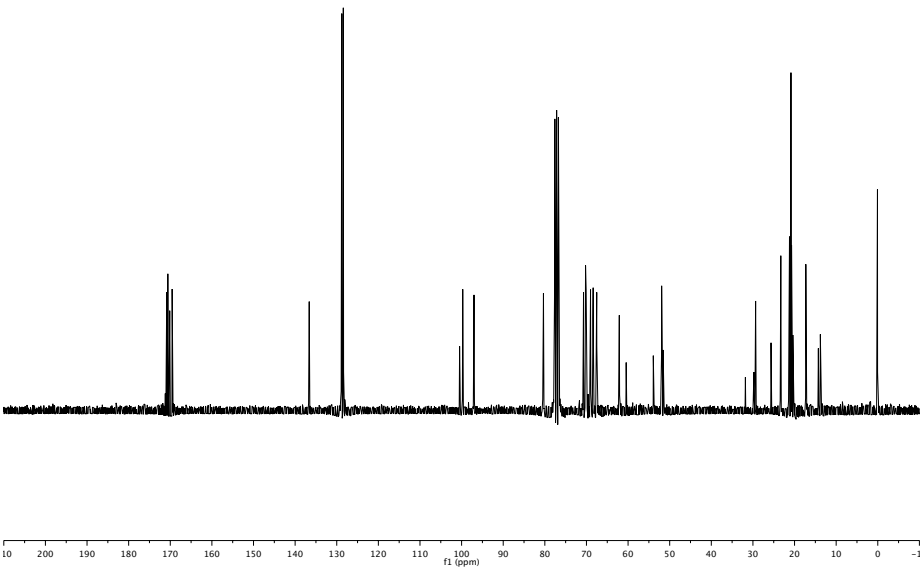
200
190
180
170
160
150
140
130
120
110
100
90
80
70
60
50
40
30
20
10
0
f1 (ppm)

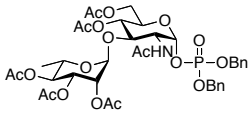

2.24

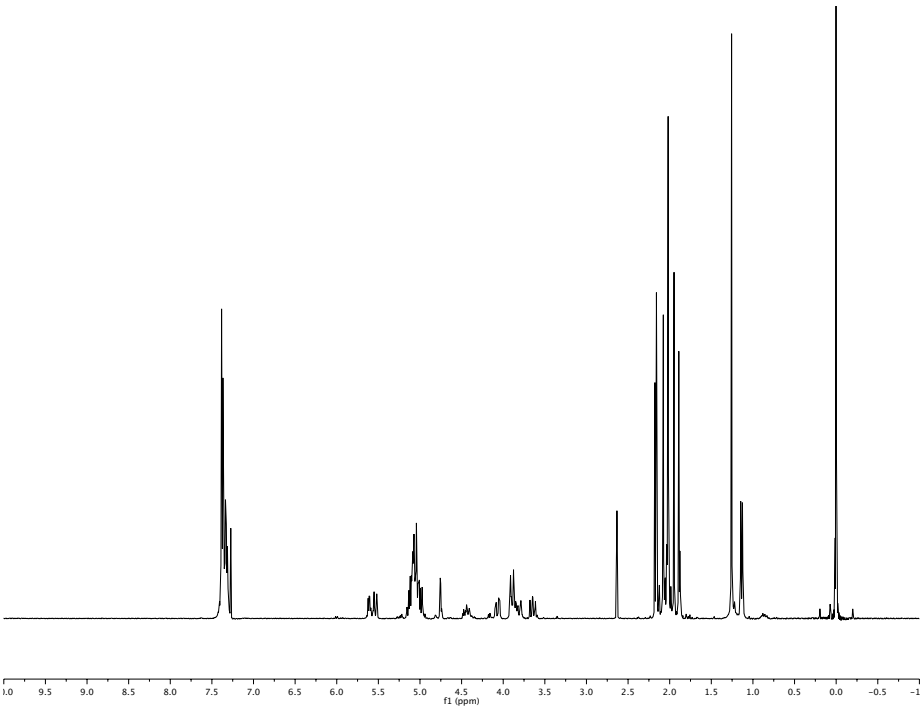

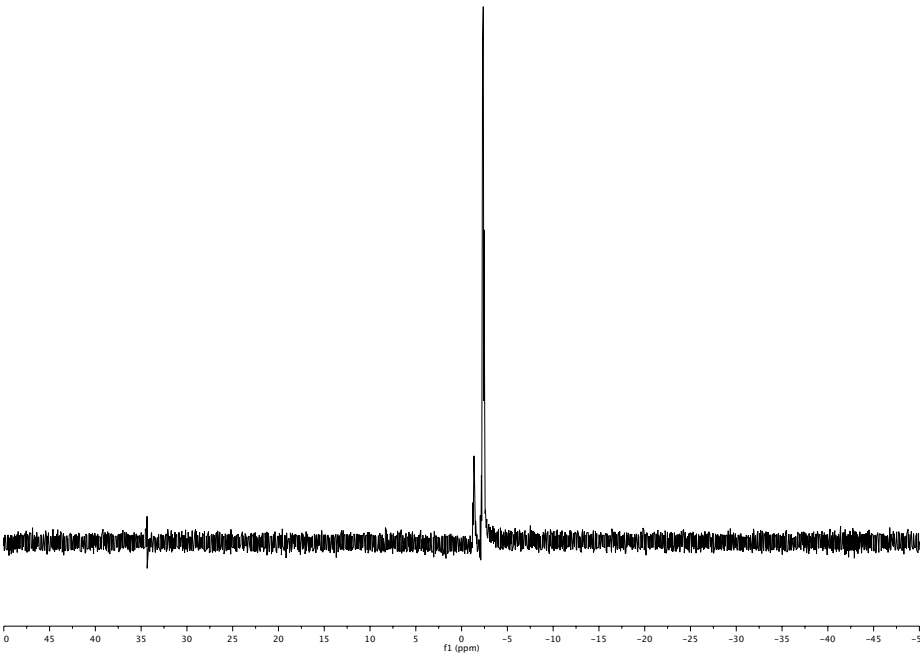

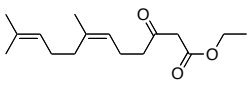

2.25

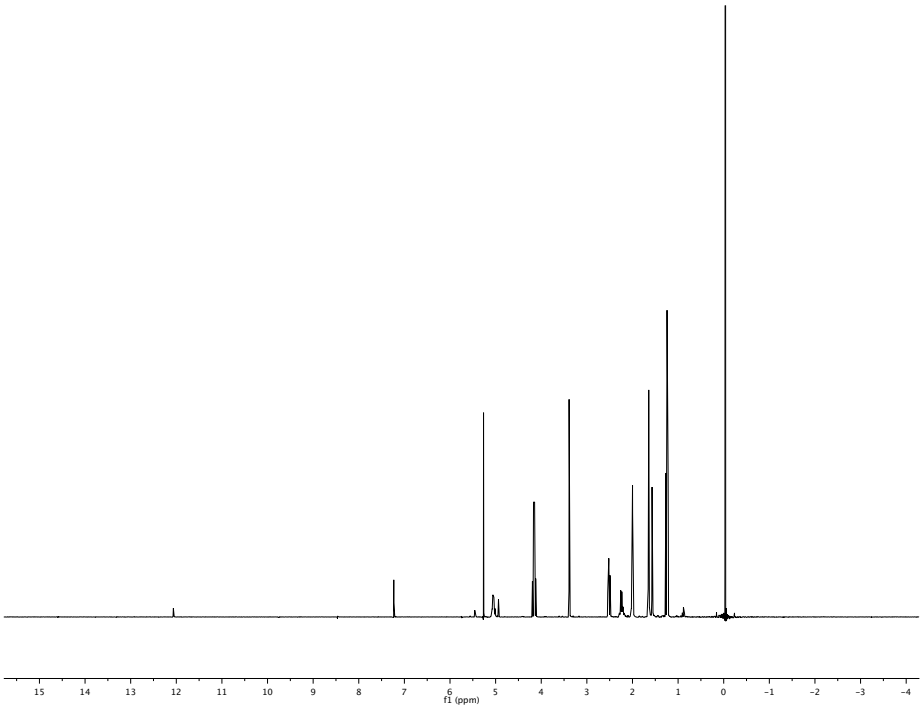

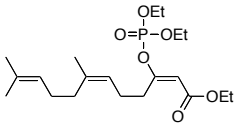
OEt
O=P–OEt
O
OEt
O

2.26

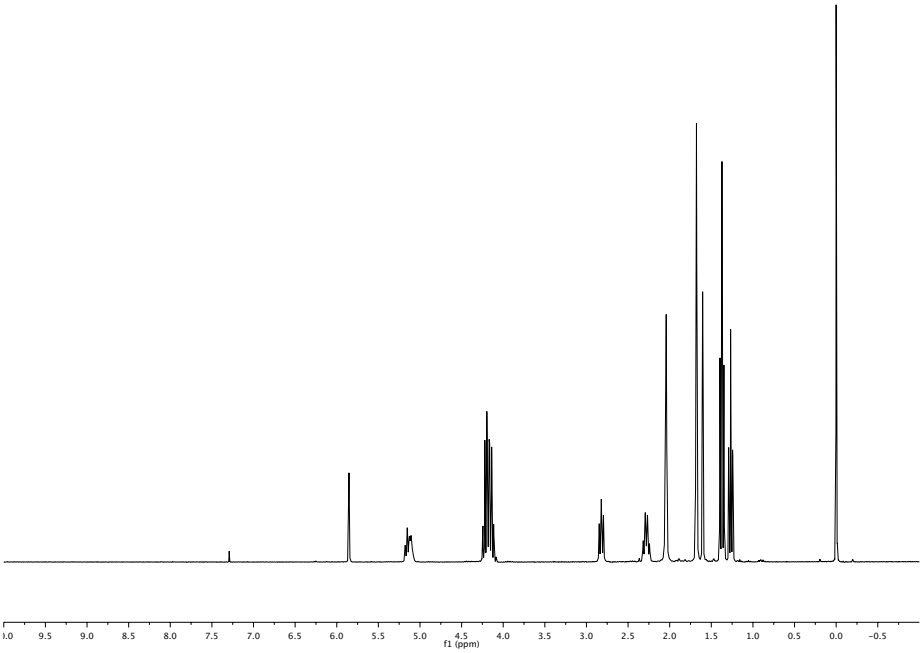
9.5 9.0 8.5 8.0 7.5 7.0 6.5 6.0 5.5 5.0 4.5 4.0 3.5 3.0 2.5 2.0 1.5 1.0 0.5 0.0 -0.5
f1 (ppm)

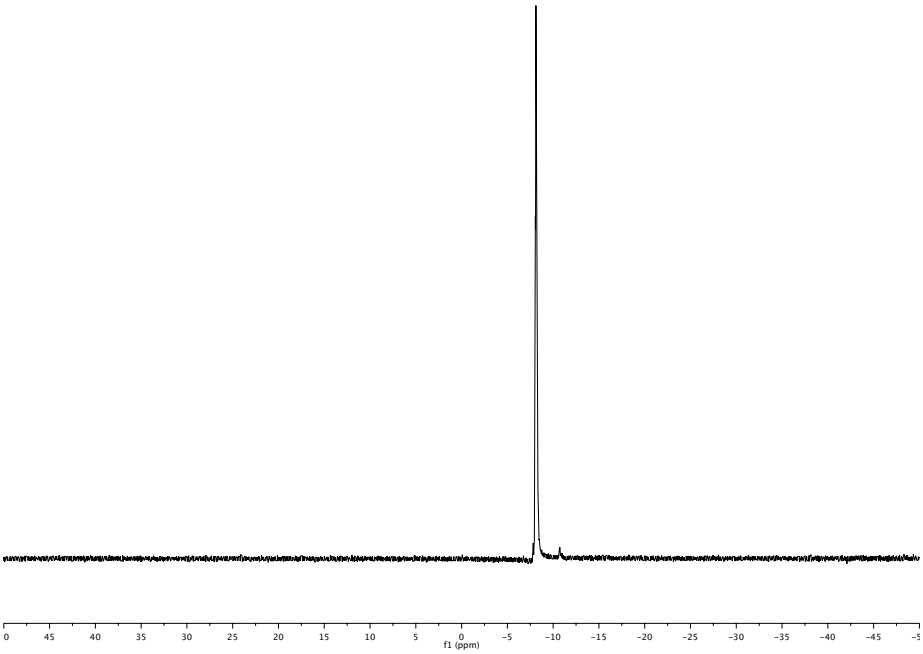
45 40 35 30 25 20 15 10 5 0 -5 -10 -15 -20 -25 -30 -35 -40 -45
f1 (ppm)

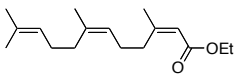
OEt
O

2.27

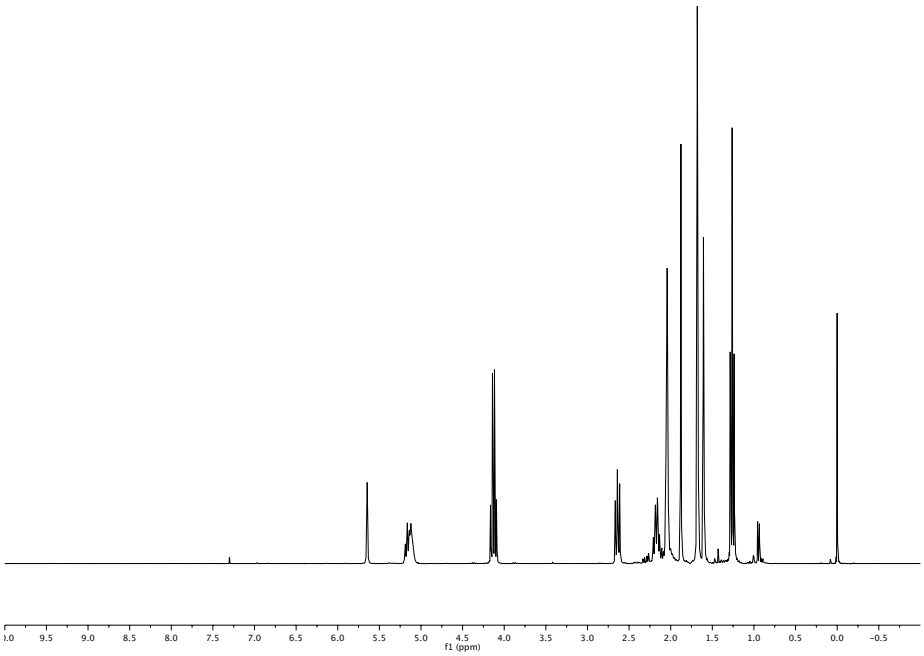
9.5
9.0
8.5
8.0
7.5
7.0
6.5
6.0
5.5
5.0
4.5
4.0
3.5
3.0
2.5
2.0
1.5
1.0
0.5
0.0
−0.5
f1 (ppm)

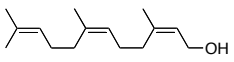

2.28

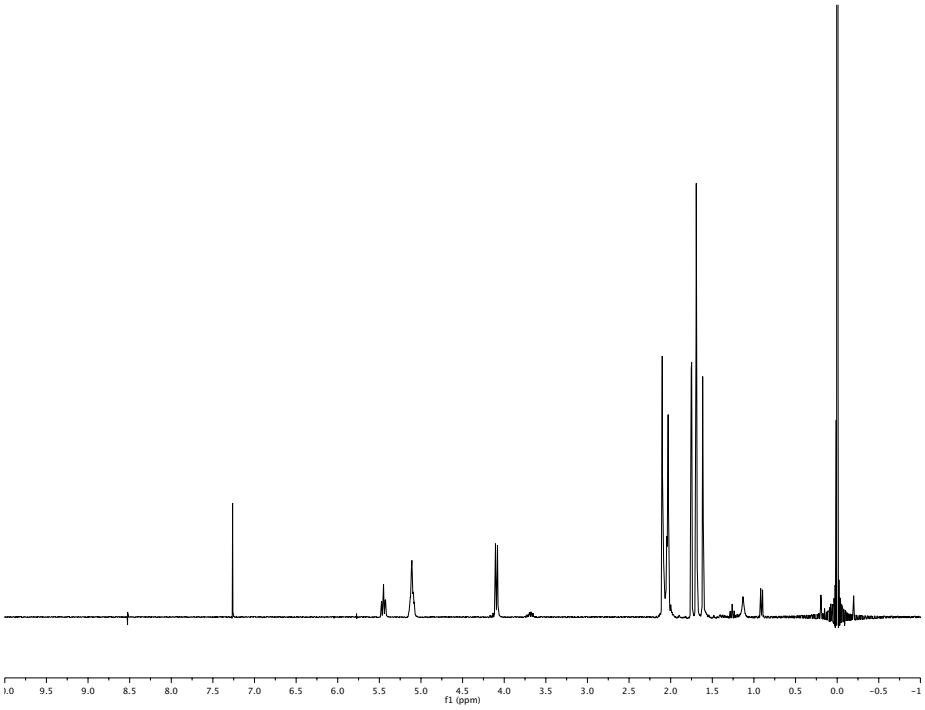

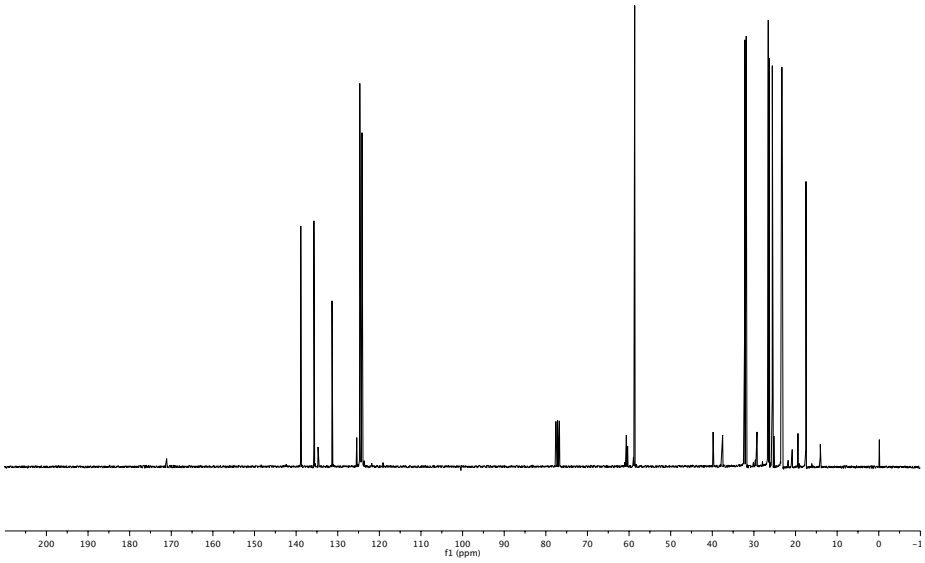

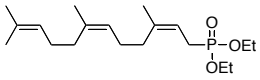

2.29

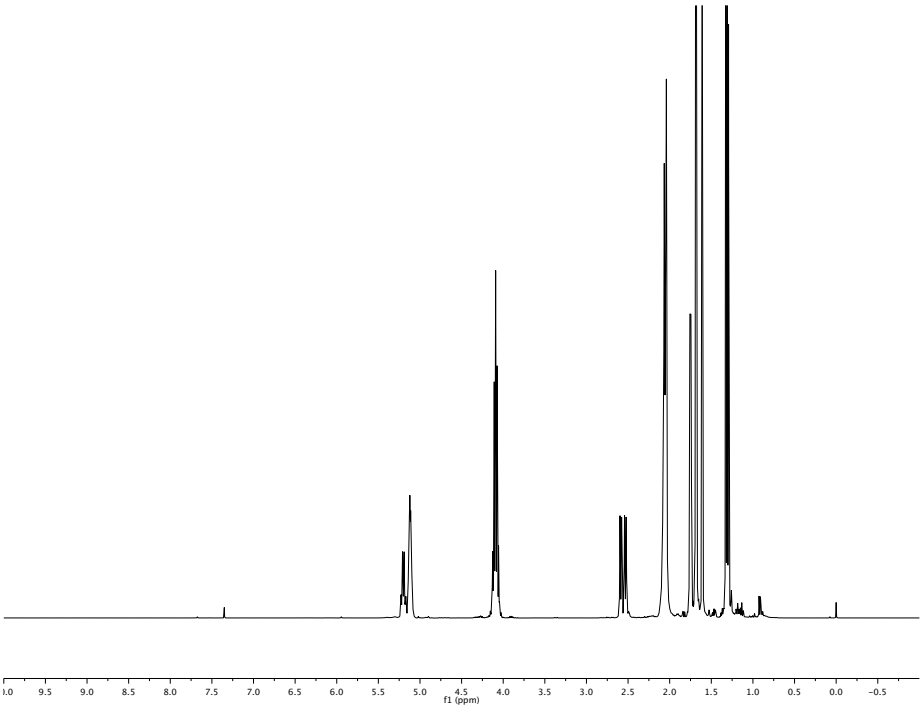

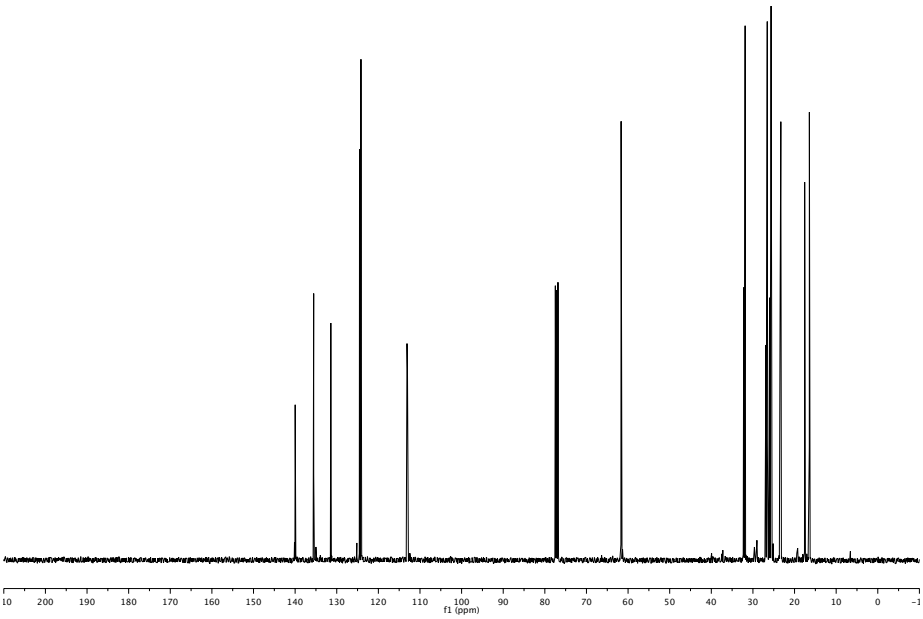

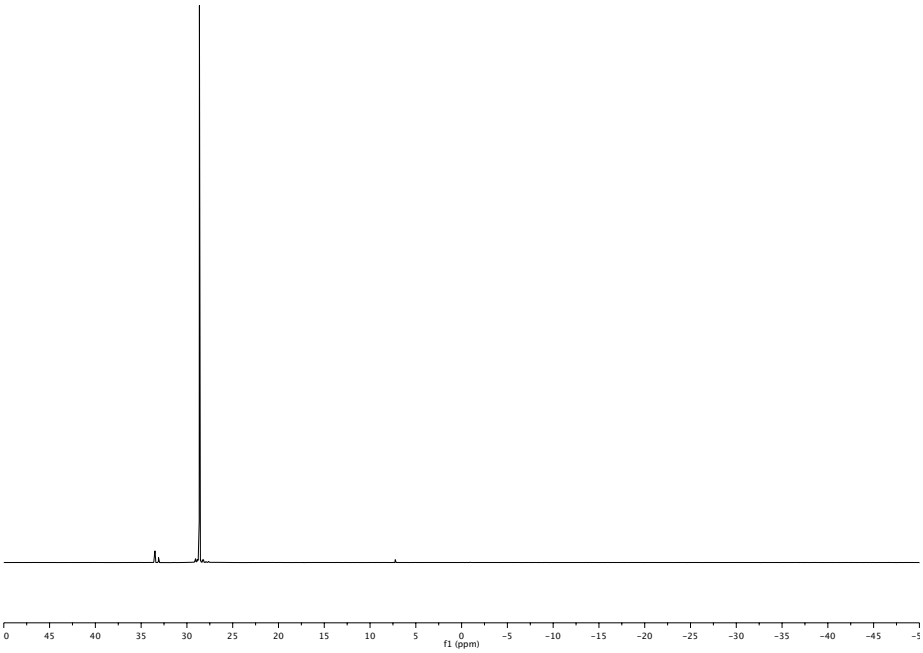
0
45
40
35
30
25
20
15
10
5
0
−5
−10
−15
−20
−25
−30
−35
−40
−45
f1 (ppm)

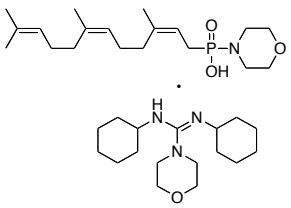

2.30

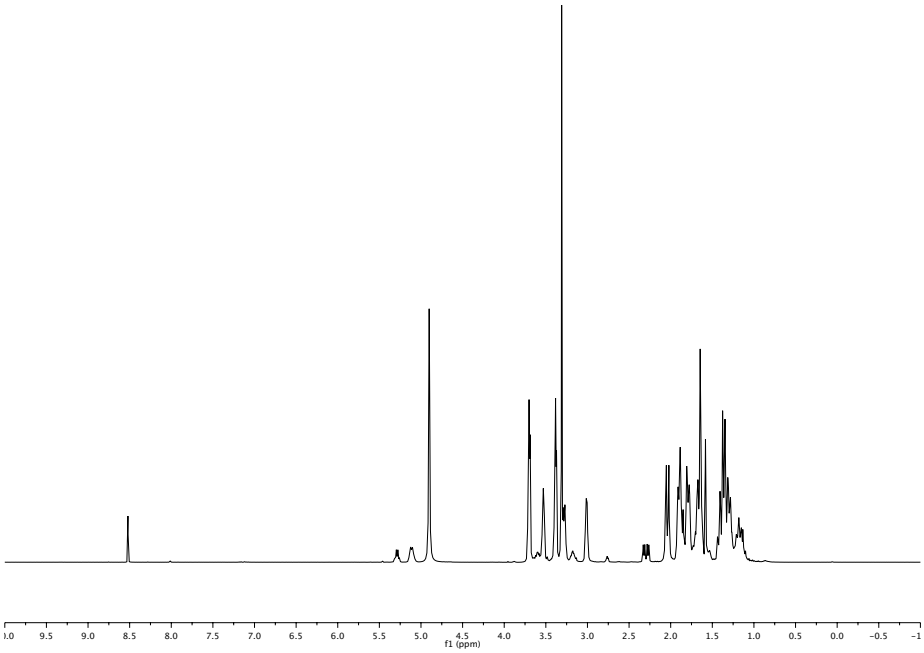

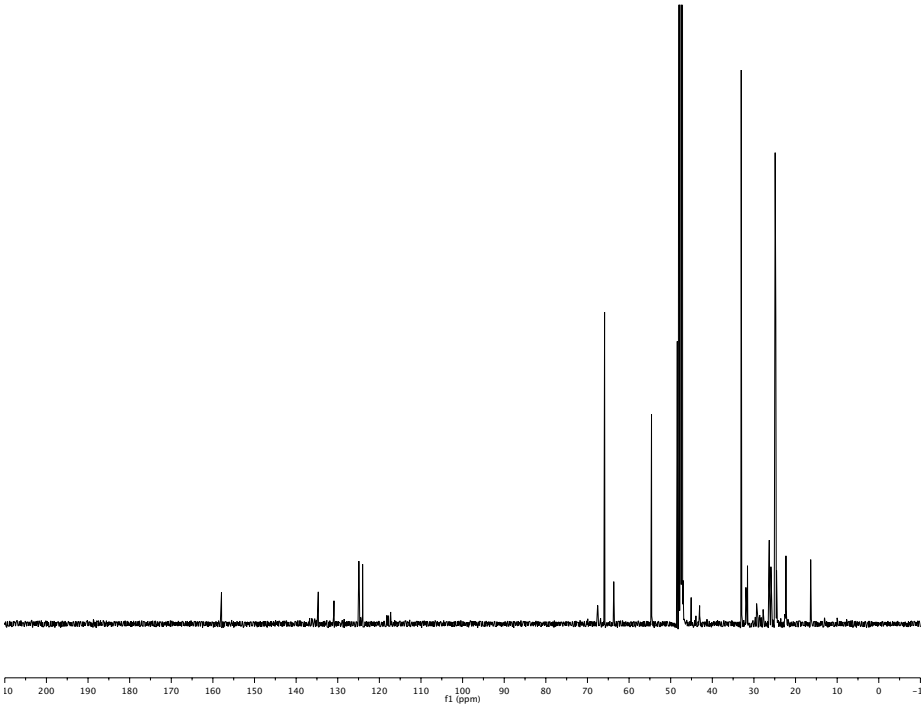
f1 (ppm)

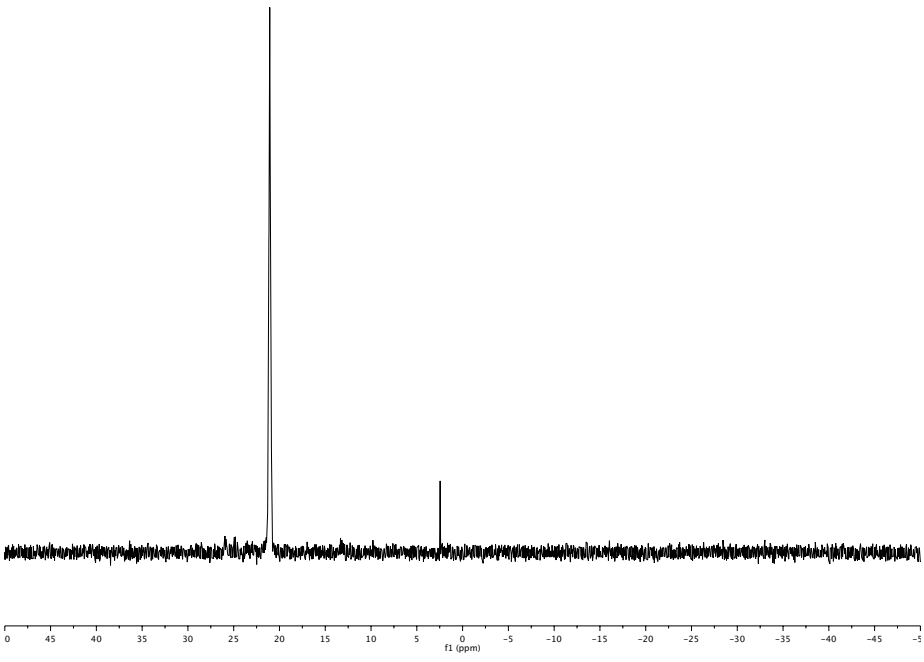
f1 (ppm)

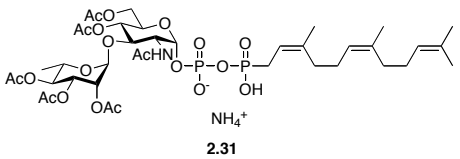

2.31

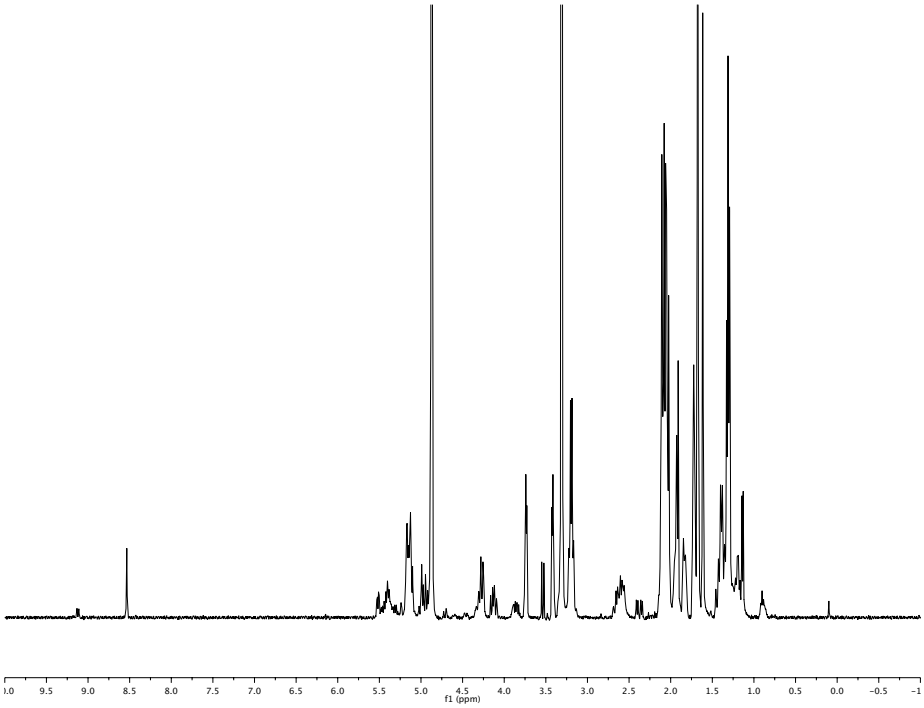

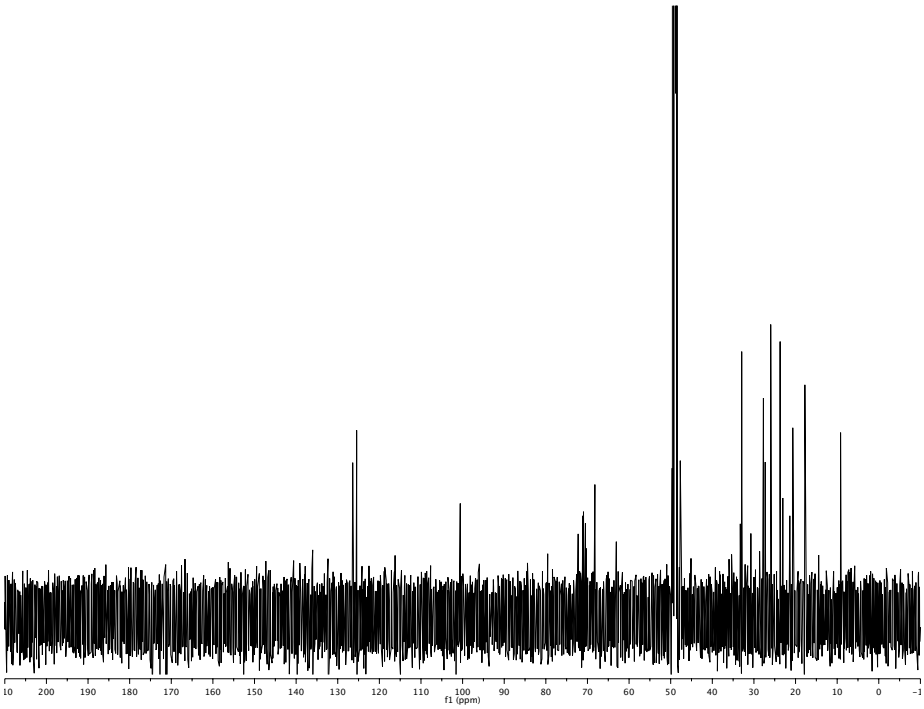

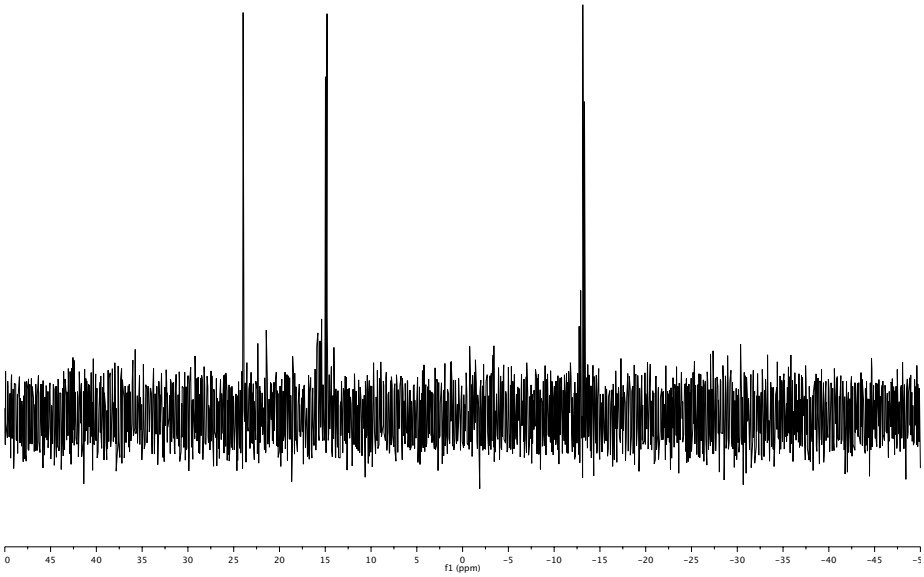
0
45
40
35
30
25
20
15
10
5
0
−5
−10
−15
−20
−25
−30
−35
−40
−45
f1 (ppm)

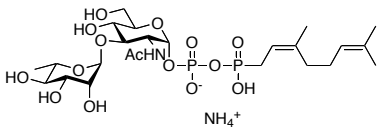
HO
HO
O
AcHN
O
O
O
P
O
O
P
O
HO
HO
O
OH
OH
NH4+

2.32

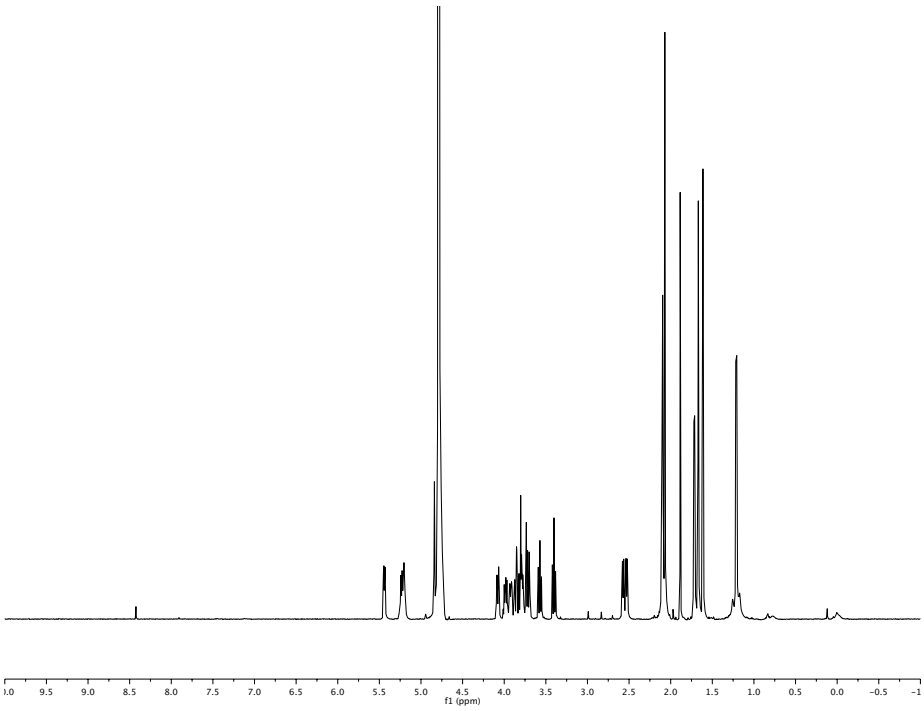
9.5
9.0
8.5
8.0
7.5
7.0
6.5
6.0
5.5
5.0
4.5
4.0
3.5
3.0
2.5
2.0
1.5
1.0
0.5
0.0
−0.5
f1 (ppm)

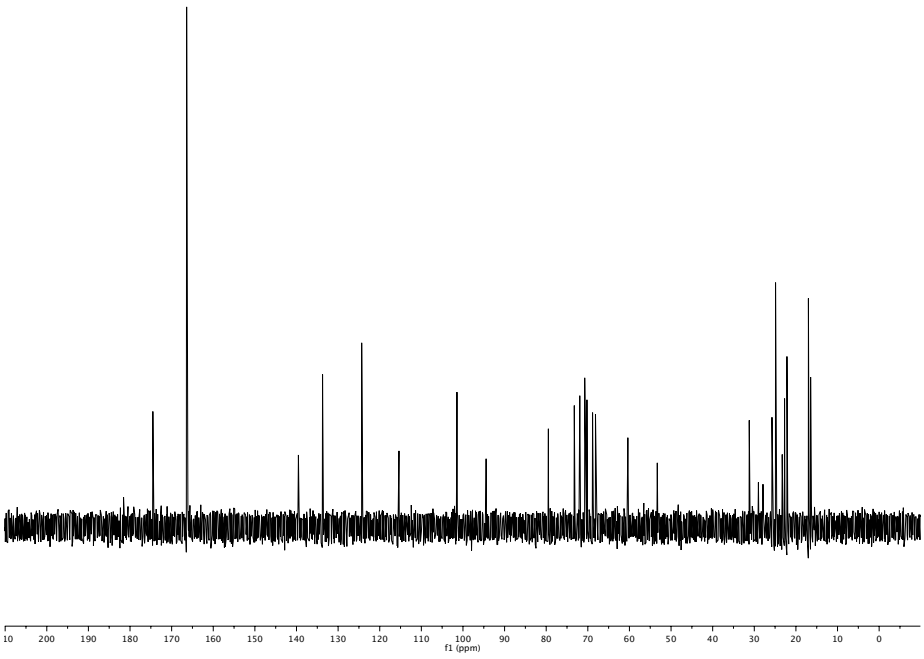
200
190
180
170
160
150
140
130
120
110
100
90
80
70
60
50
40
30
20
10
0
f1 (ppm)

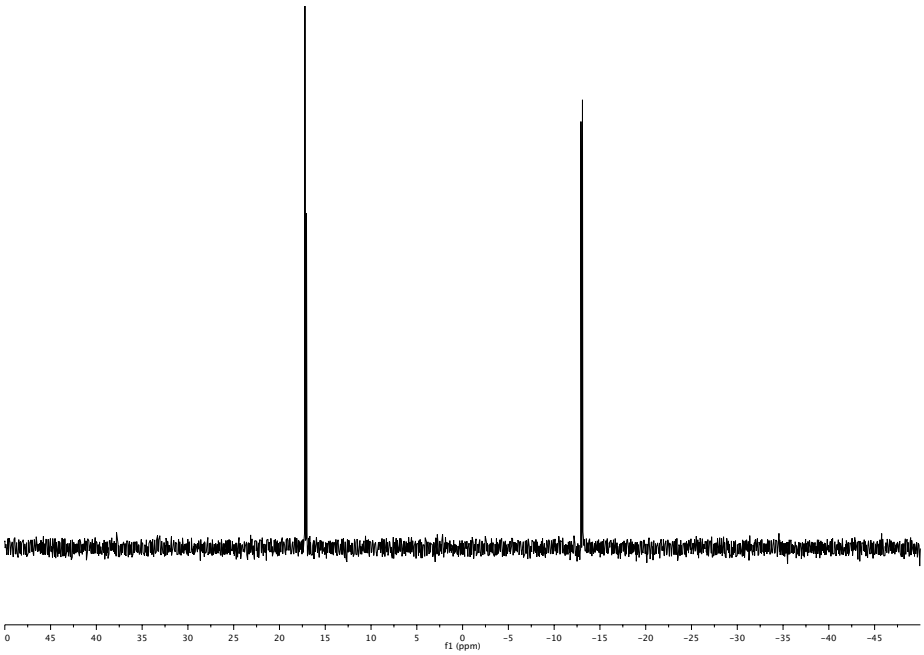
0
45
40
35
30
25
20
15
10
5
0
−5
−10
−15
−20
−25
−30
−35
−40
−45
f1 (ppm)

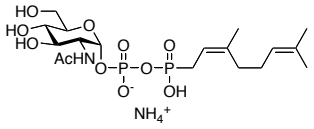

2.33

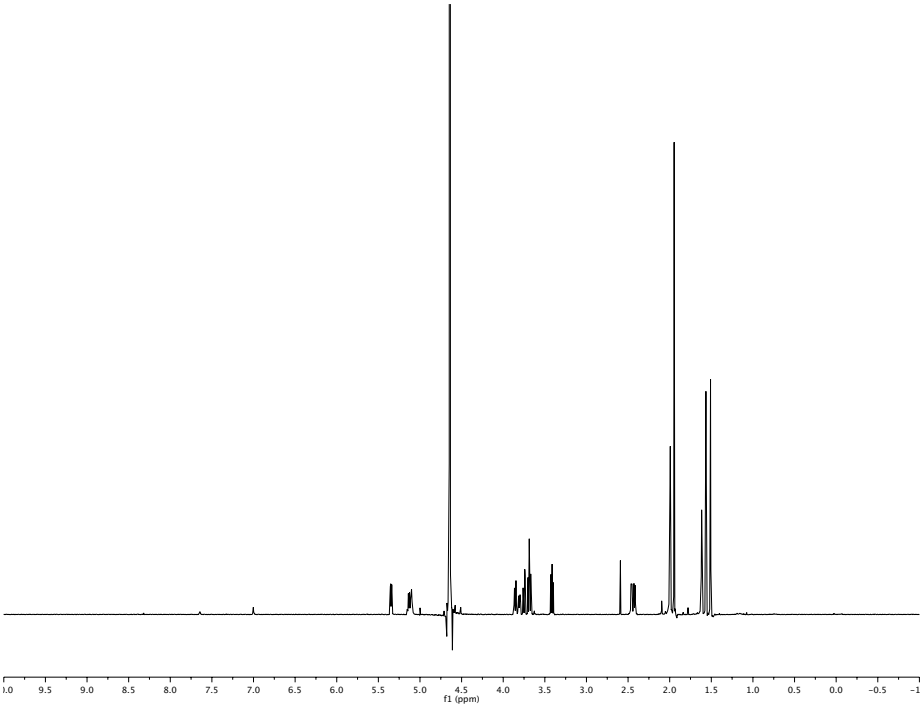

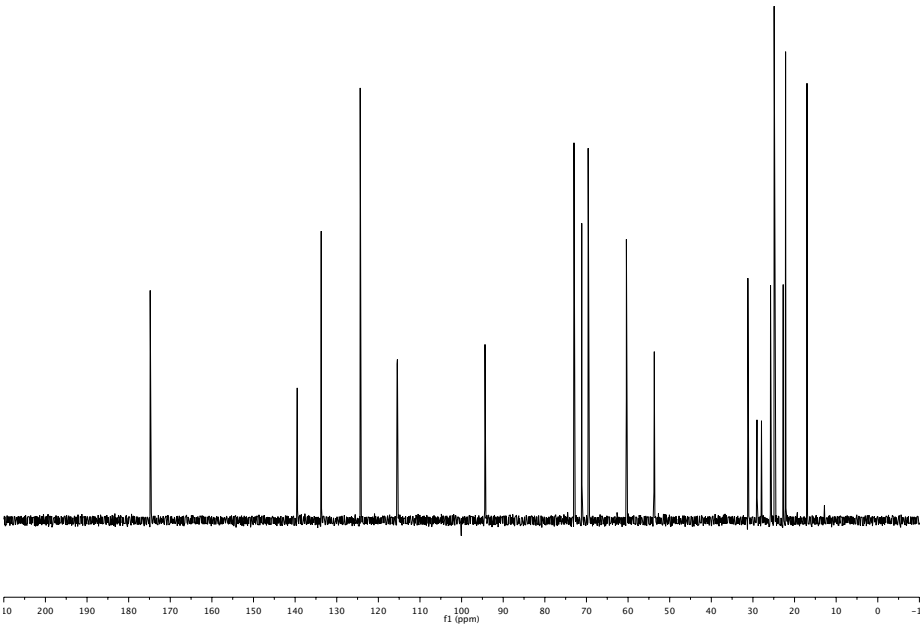

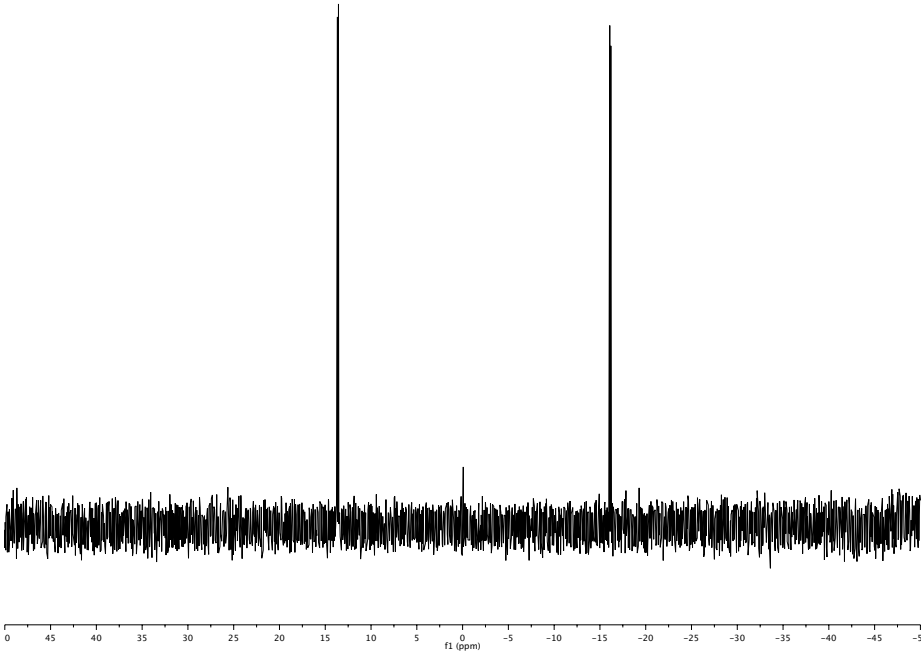
0
45
40
35
30
25
20
15
10
5
0
−5
−10
−15
−20
−25
−30
−35
−40
−45
f1 (ppm)

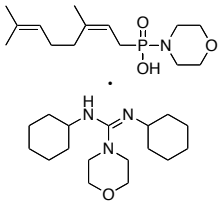

2.34

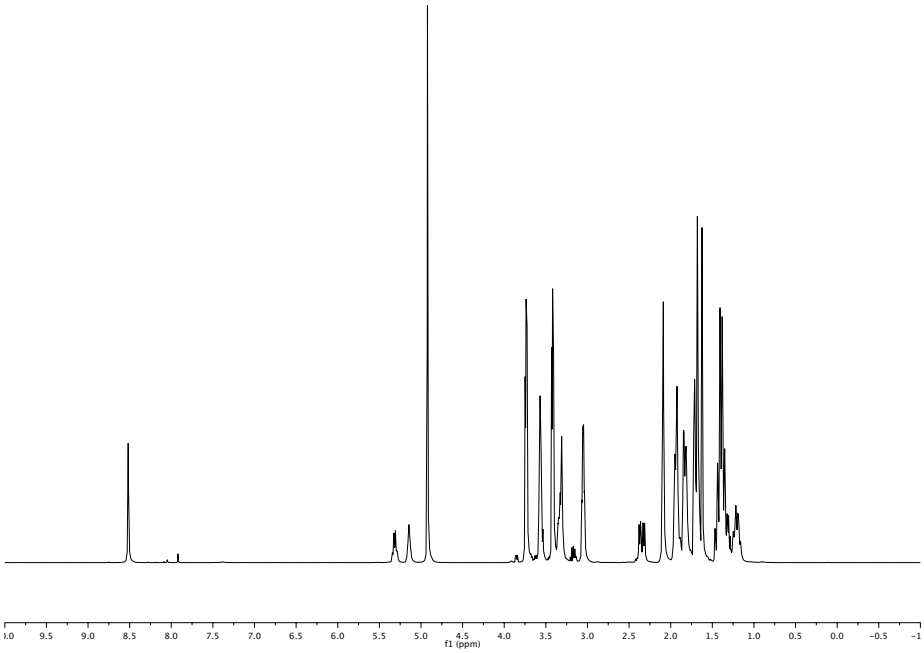

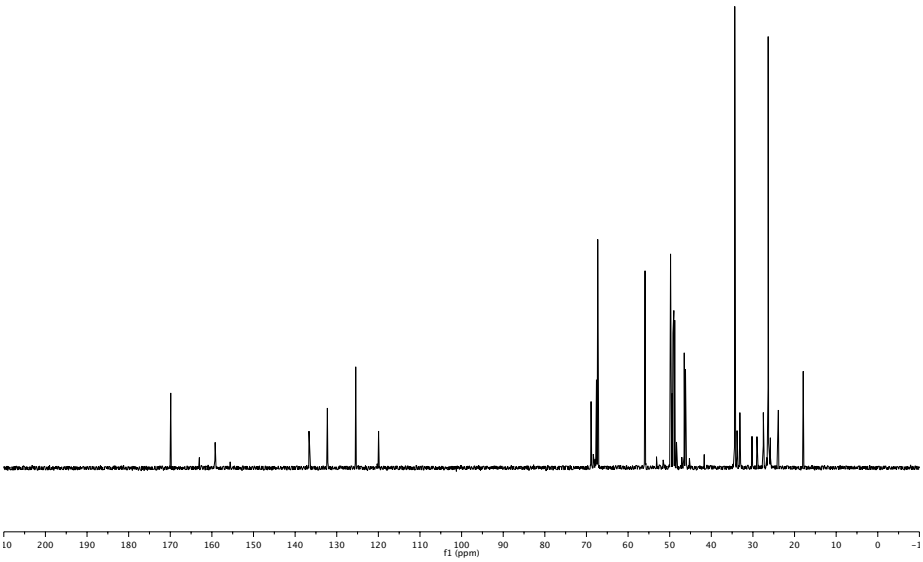
f1 (ppm)

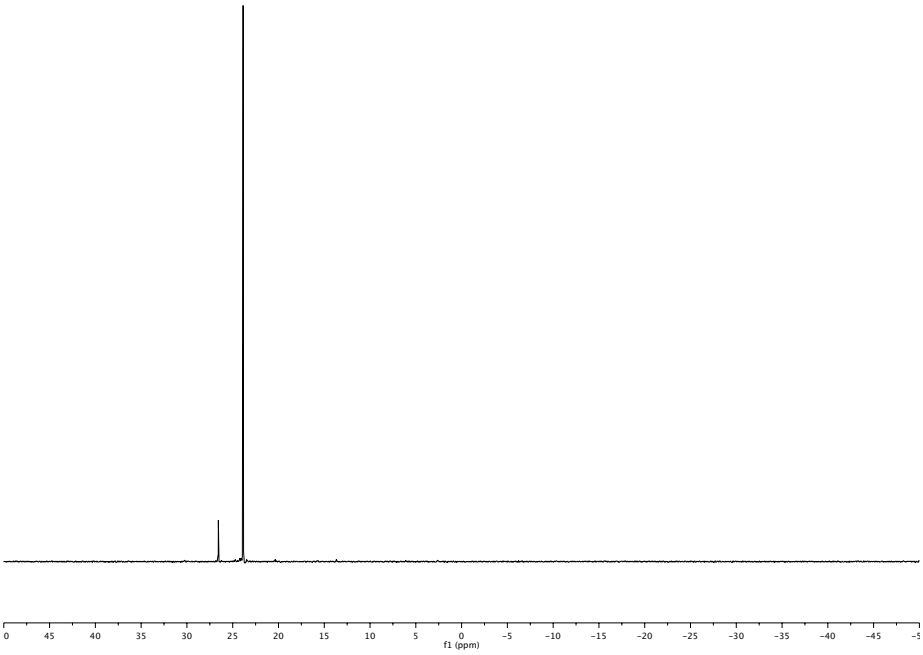
f1 (ppm)

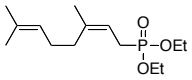

2.35

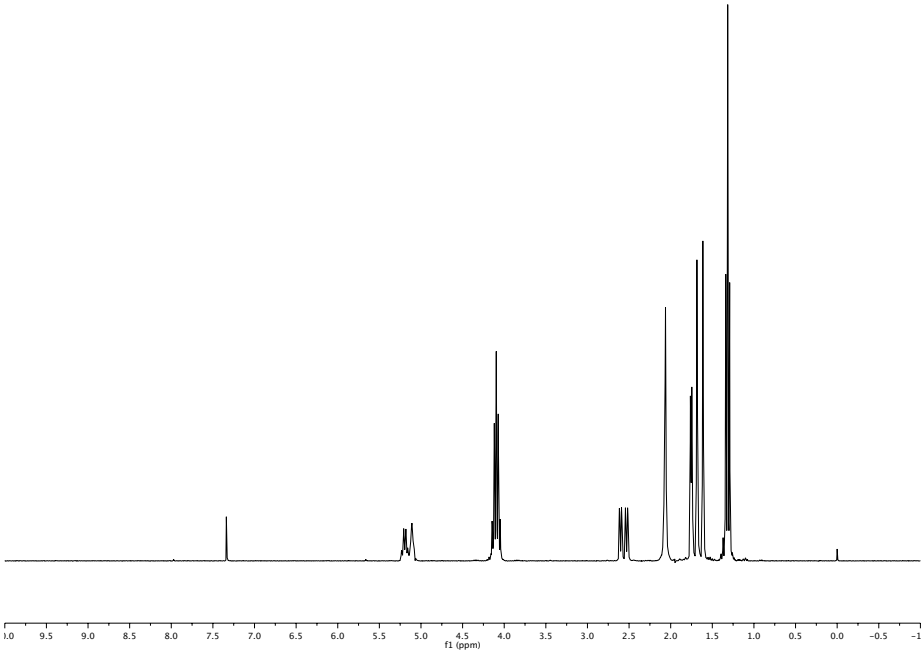

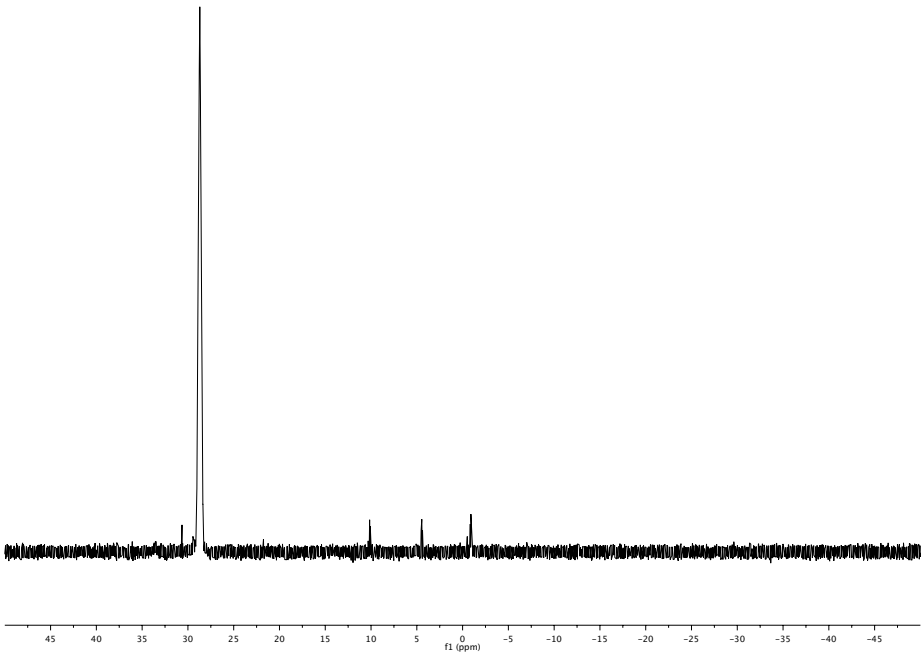

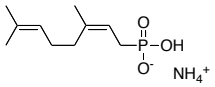

2.36

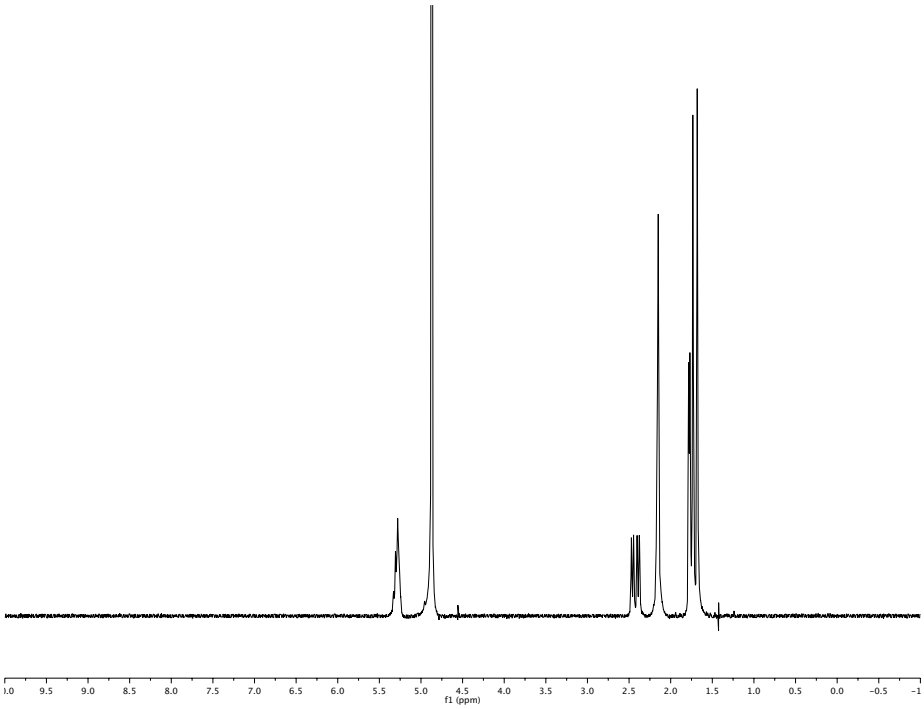

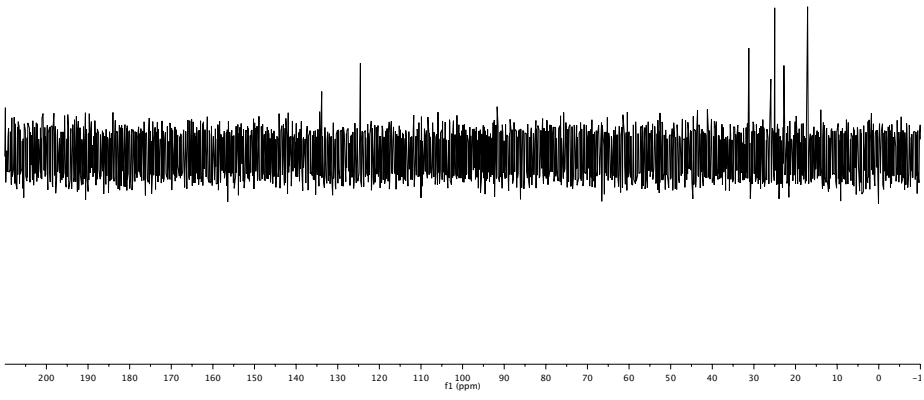

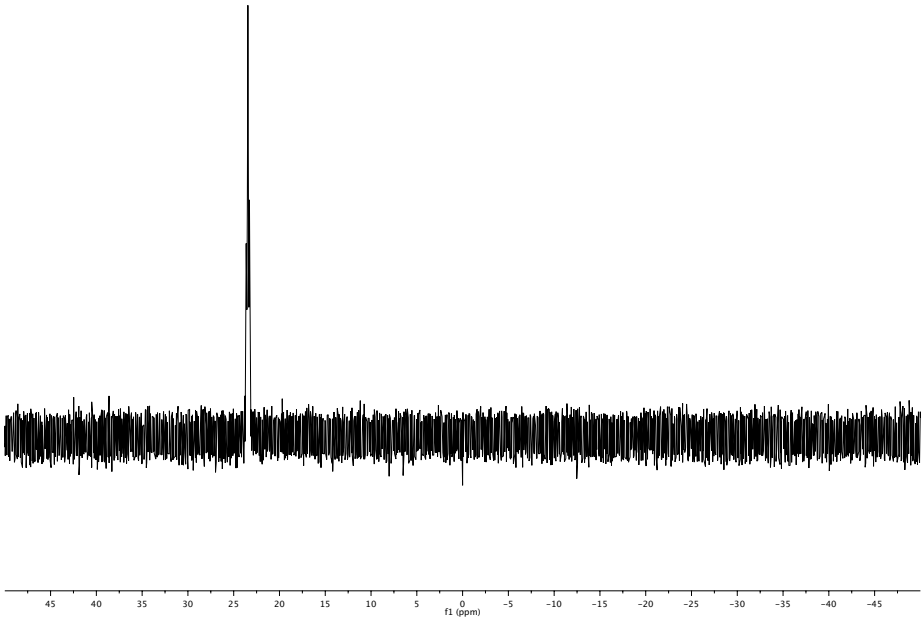
45
40
35
30
25
20
15
10
5
0
−5
−10
−15
−20
−25
−30
−35
−40
−45
f1 (ppm)

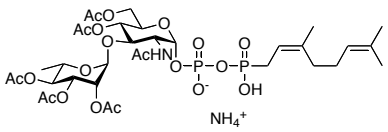
AcO
AcO
O
AcHN
O
O
P
O
O
O
P
OH
AcO
O
AcO
OAc
NH_4^+

2.37

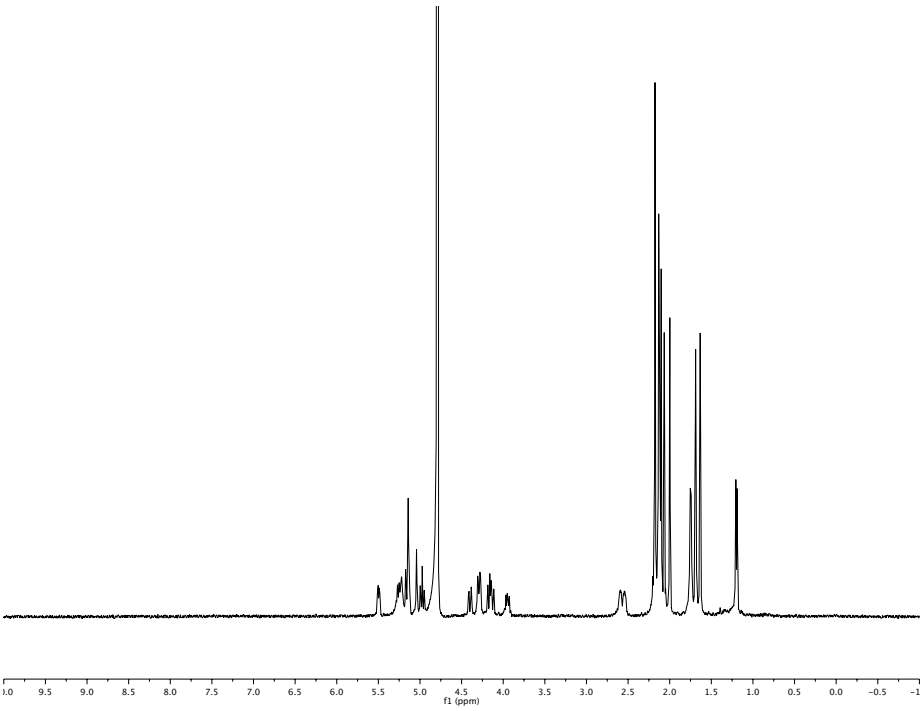
9.5 9.0 8.5 8.0 7.5 7.0 6.5 6.0 5.5 5.0 4.5 4.0 3.5 3.0 2.5 2.0 1.5 1.0 0.5 0.0 −0.5
f1 (ppm)

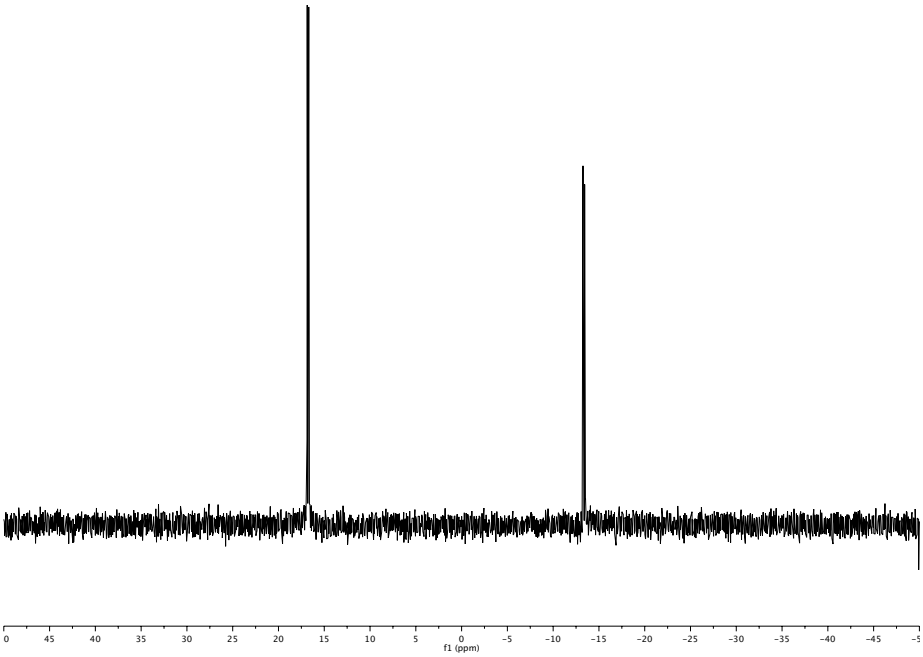
45 40 35 30 25 20 15 10 5 0 −5 −10 −15 −20 −25 −30 −35 −40 −45
f1 (ppm)

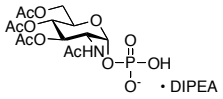
AcO
AcO
AcO
AcHN
O
O
P
OH
O⁻
• DIPEA

2.38

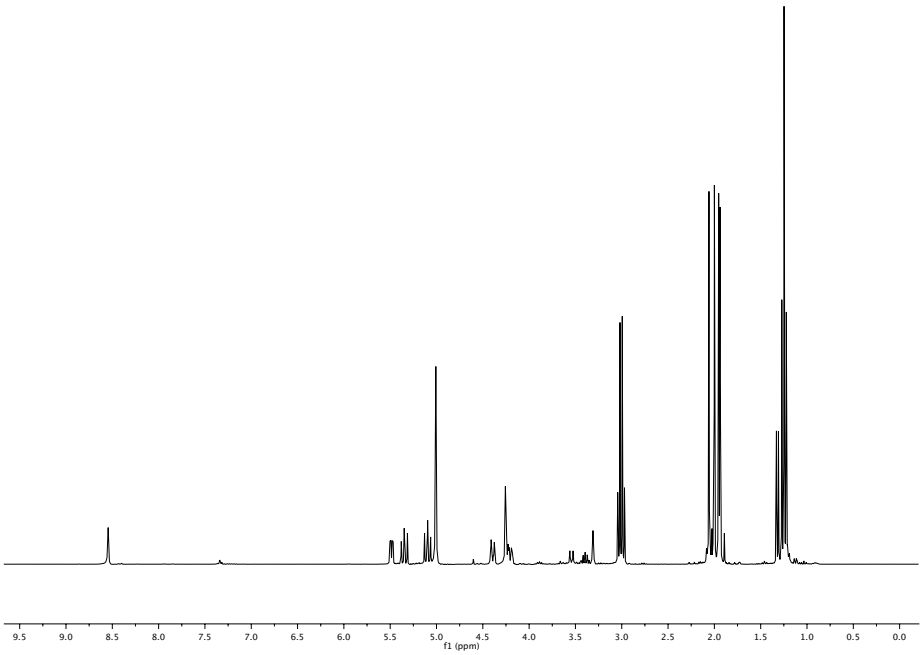
9.5 9.0 8.5 8.0 7.5 7.0 6.5 6.0 5.5 5.0 4.5 4.0 3.5 3.0 2.5 2.0 1.5 1.0 0.5 0.0
f1 (ppm)

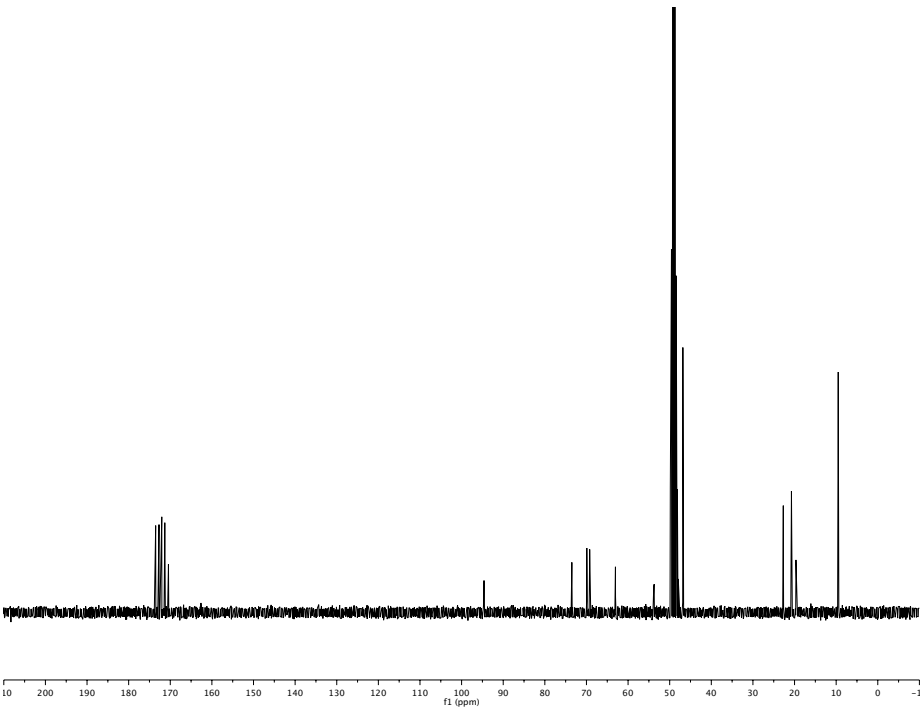
200 190 180 170 160 150 140 130 120 110 100 90 80 70 60 50 40 30 20 10 0
f1 (ppm)

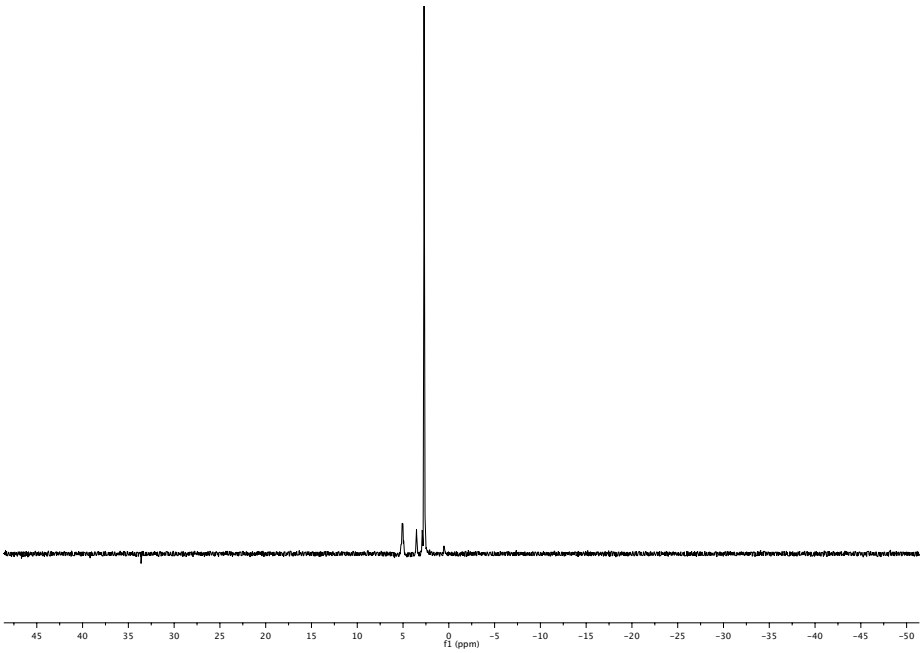
45 40 35 30 25 20 15 10 5 0 −5 −10 −15 −20 −25 −30 −35 −40 −45 −50
f1 (ppm)

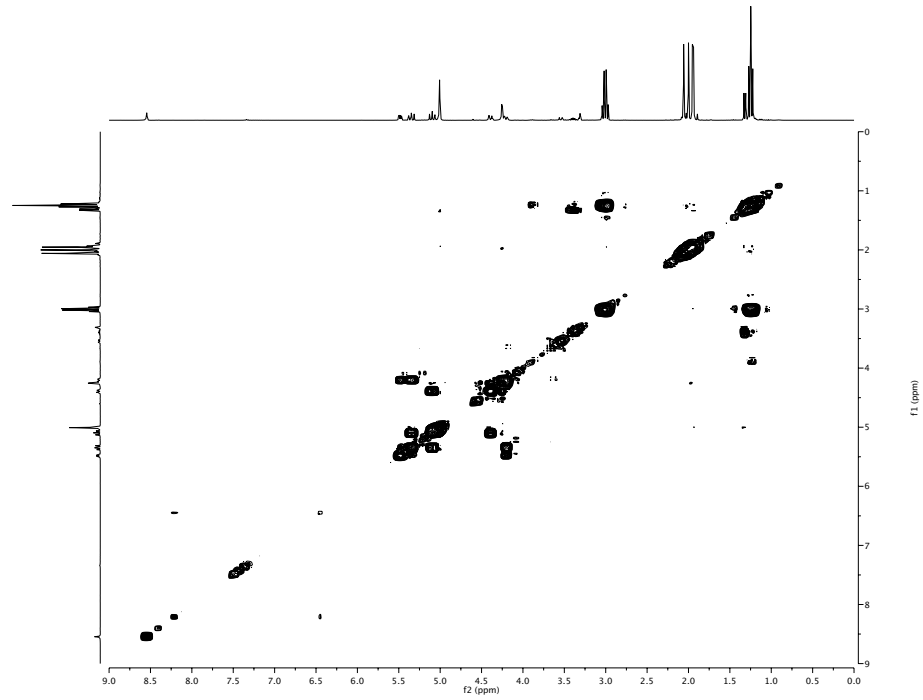
9.0 8.5 8.0 7.5 7.0 6.5 6.0 5.5 5.0 4.5 4.0 3.5 3.0 2.5 2.0 1.5 1.0 0.5 0.0
f2 (ppm)
0 1 2 3 4 5 6 7 8 9
f1 (ppm)

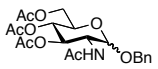

2.39

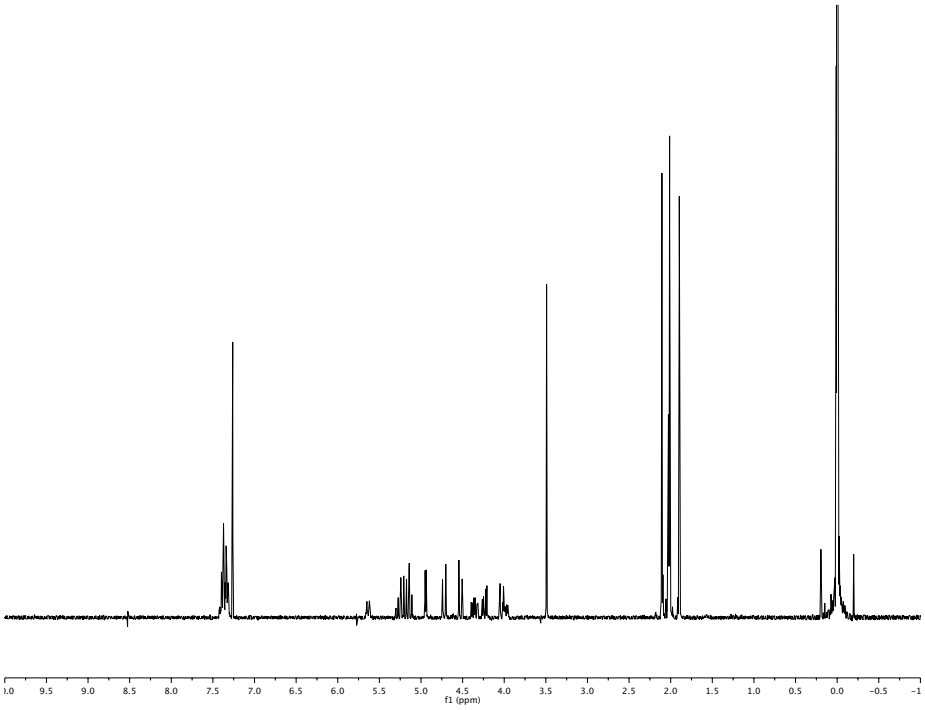

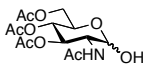

2.40

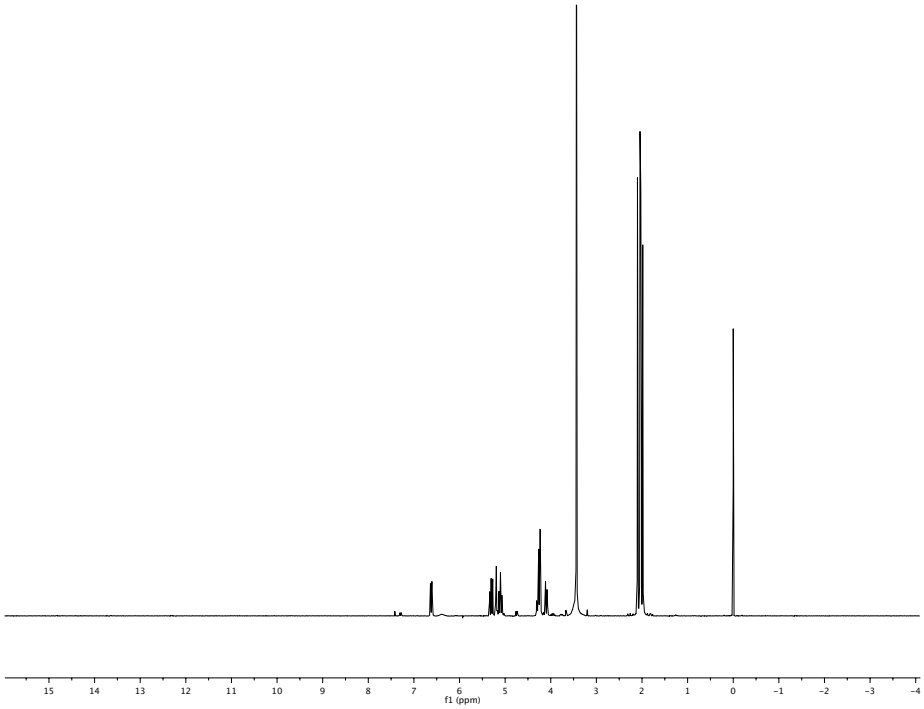

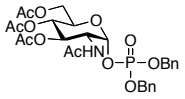
AcO
AcO
AcO
AcHN
O
O
P
OBn
OBn

2.41

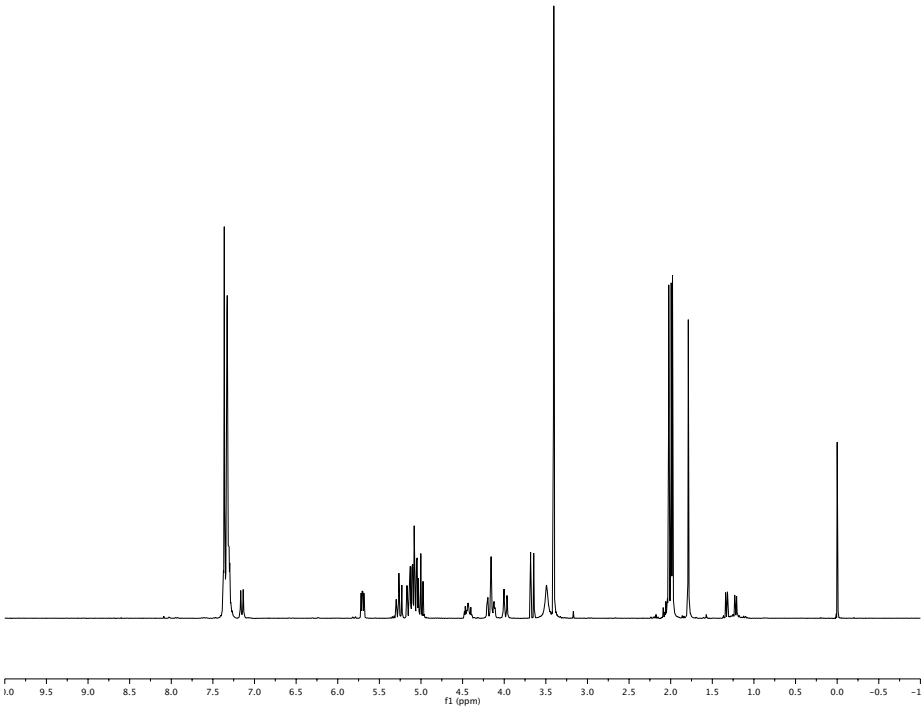
9.5 9.0 8.5 8.0 7.5 7.0 6.5 6.0 5.5 5.0 4.5 4.0 3.5 3.0 2.5 2.0 1.5 1.0 0.5 0.0 −0.5
f1 (ppm)

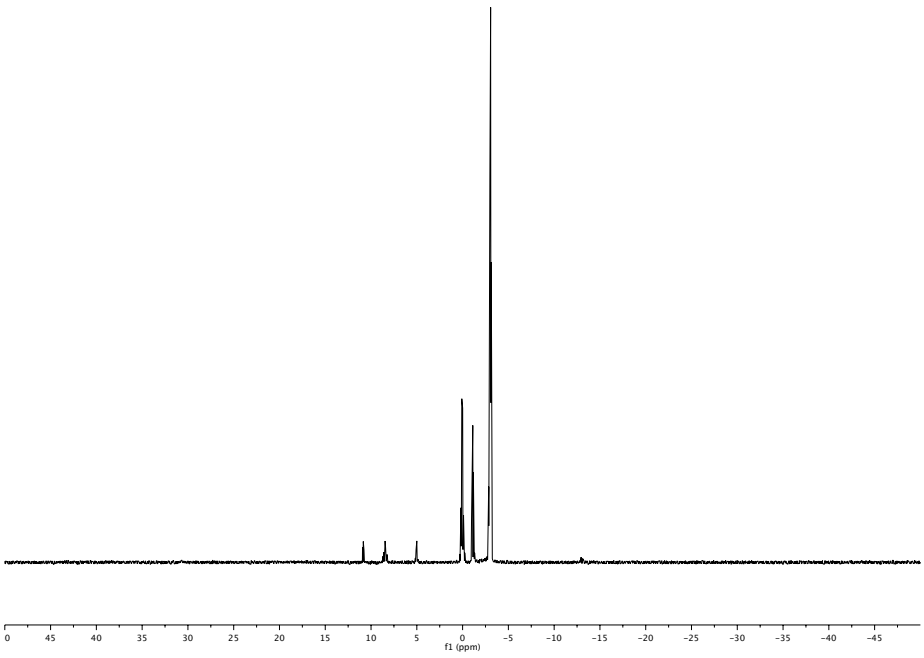
45 40 35 30 25 20 15 10 5 0 −5 −10 −15 −20 −25 −30 −35 −40 −45
f1 (ppm)

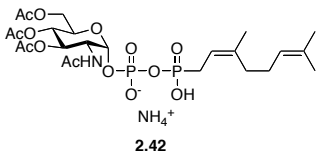

2.42

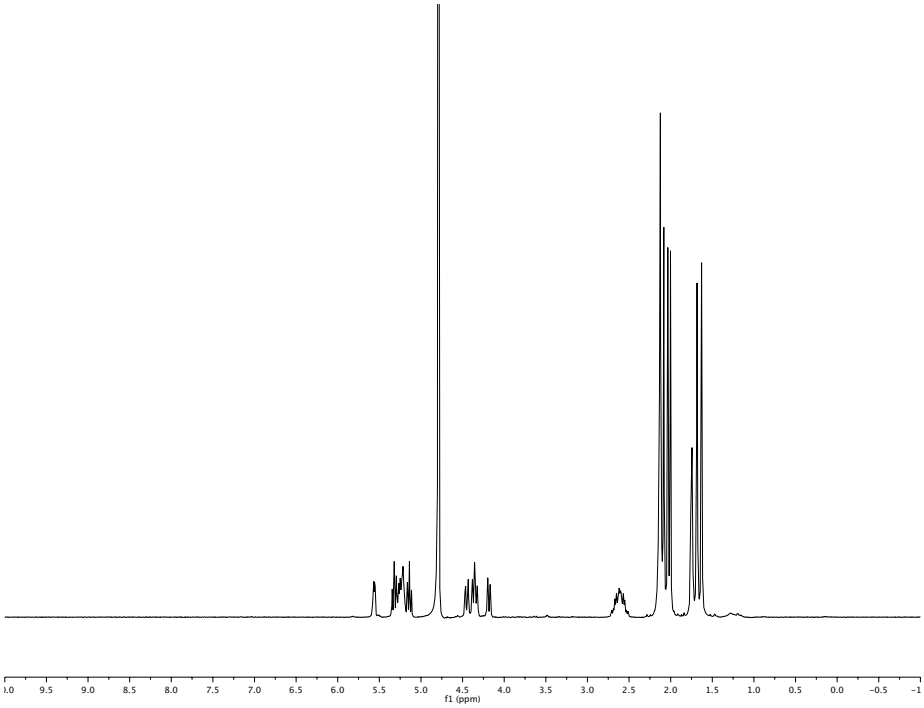

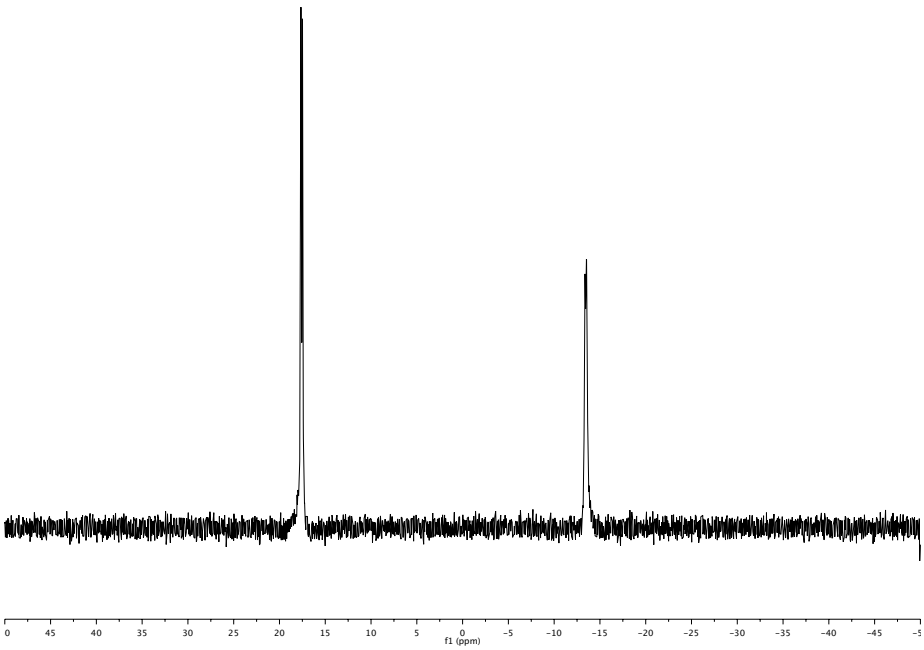

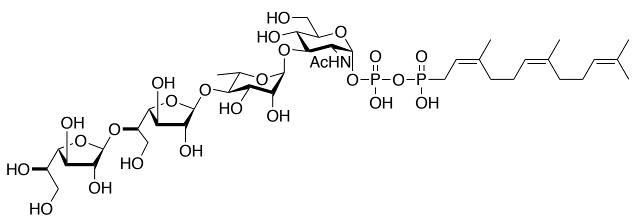
HO
HO
O
AcHN
O
O
O
P
P
OH
OH
OH
HO
OH
HO
OH
HO
OH
HO
HO
OH

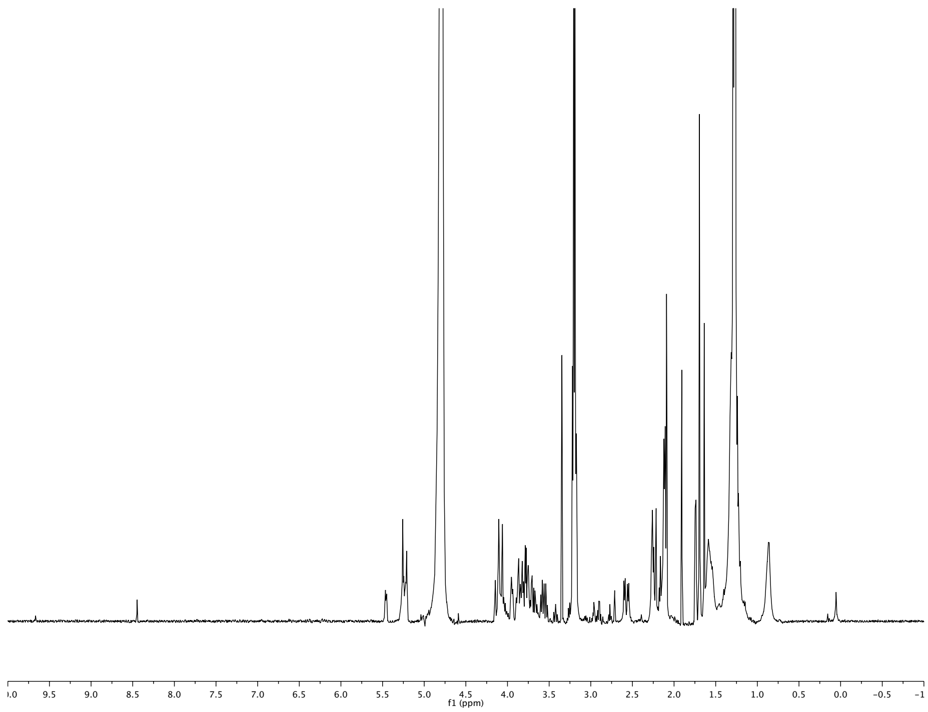
9.5
9.0
8.5
8.0
7.5
7.0
6.5
6.0
5.5
5.0
4.5
4.0
3.5
3.0
2.5
2.0
1.5
1.0
0.5
0.0
-0.5
f1 (ppm)

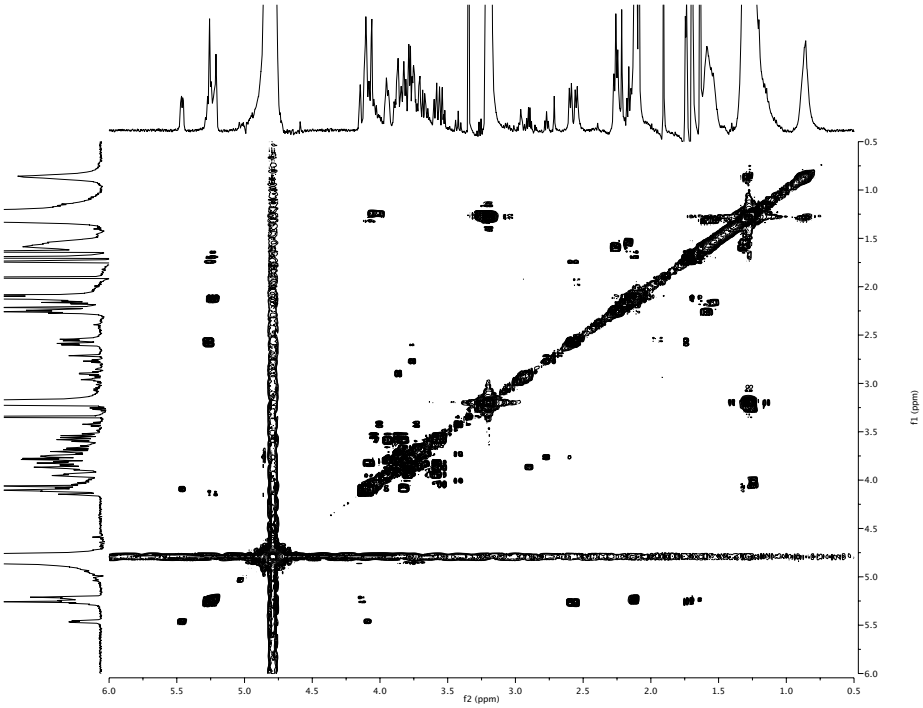
f2 (ppm)
f1 (ppm)

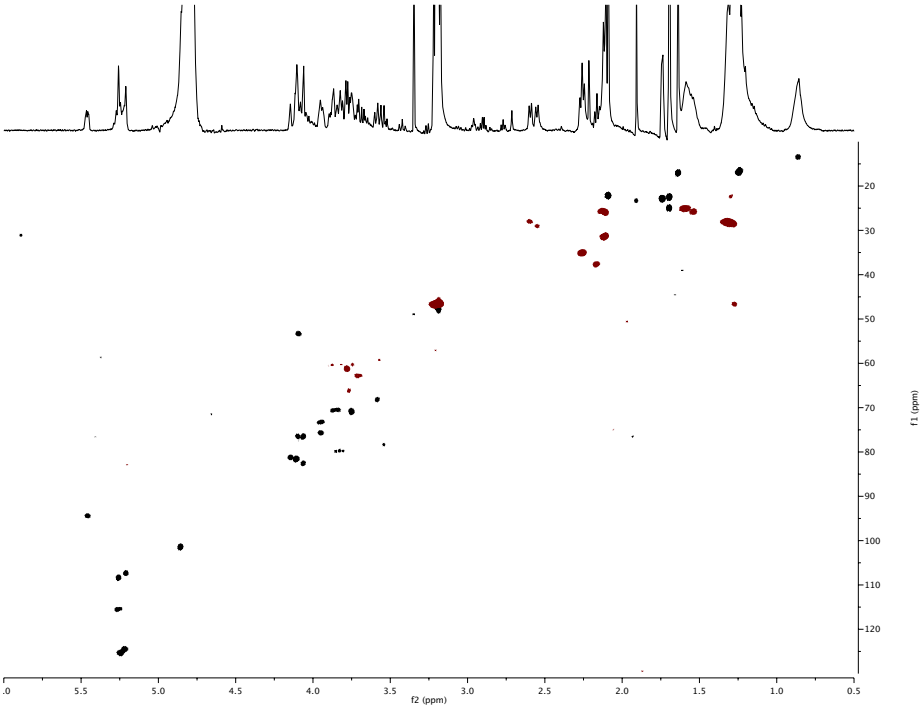
f2 (ppm)
f1 (ppm)

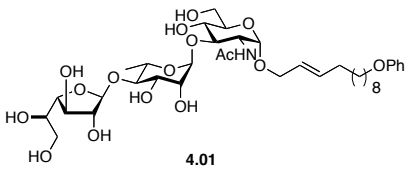
HO
HO
O
AcHN
O
OPh
8
OH
O
O
O
HO
HO
OH
OH
HO

4.01

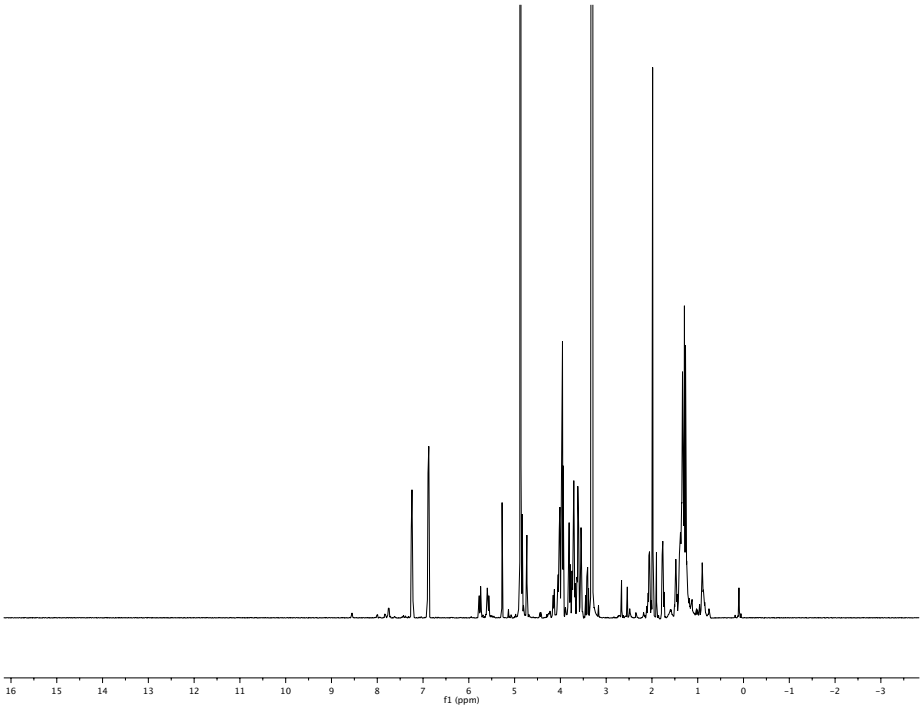
16 15 14 13 12 11 10 9 8 7 6 5 4 3 2 1 0 −1 −2 −3
f1 (ppm)

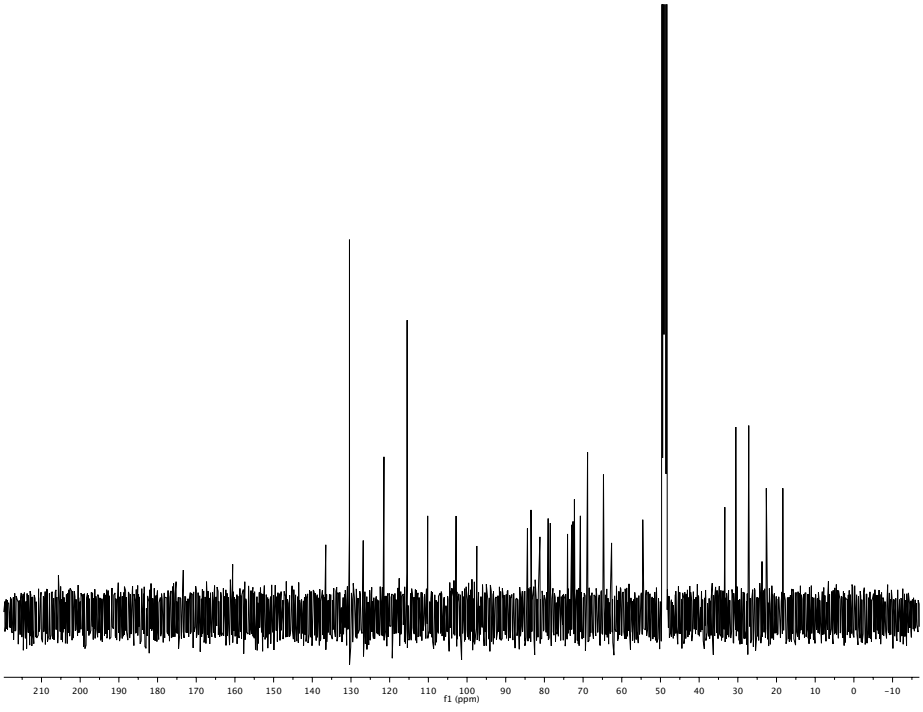
210 200 190 180 170 160 150 140 130 120 110 100 90 80 70 60 50 40 30 20 10 0 −10
f1 (ppm)

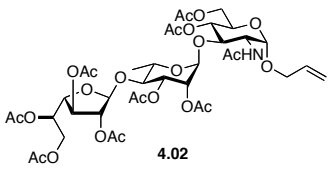

4.02

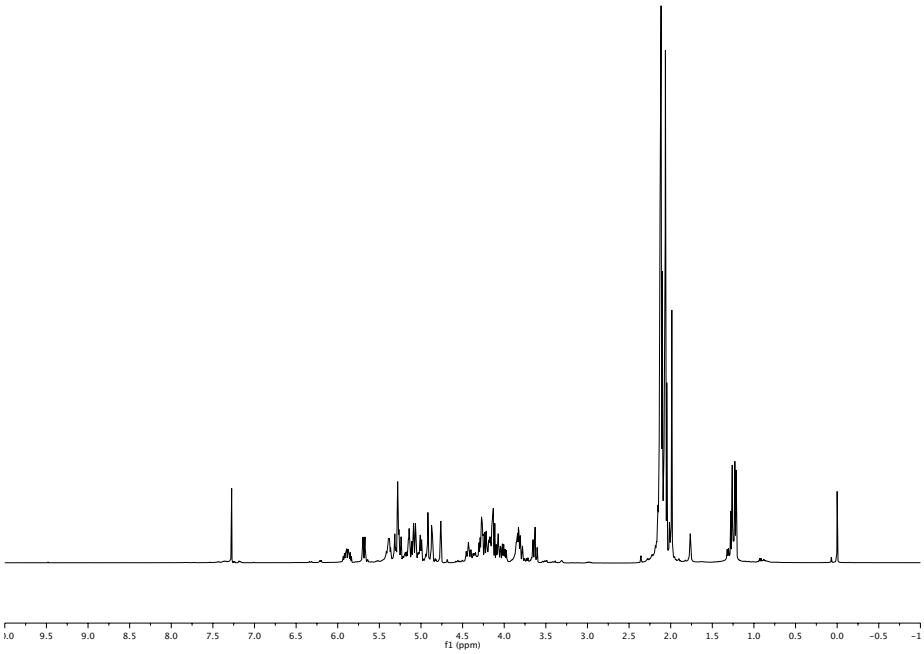

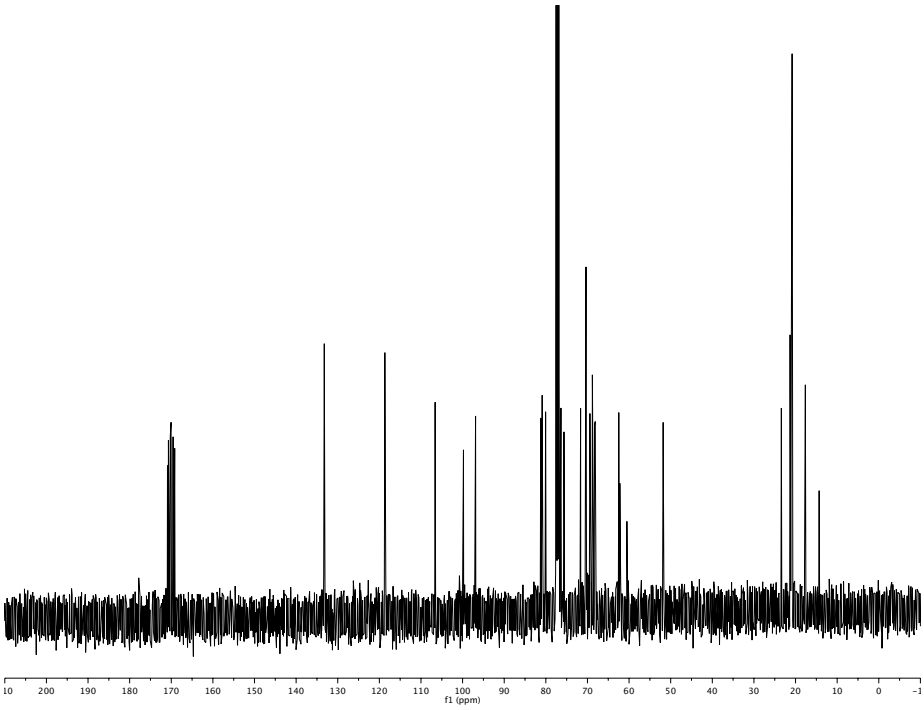

$^{1}H–^{1}H$ COSY

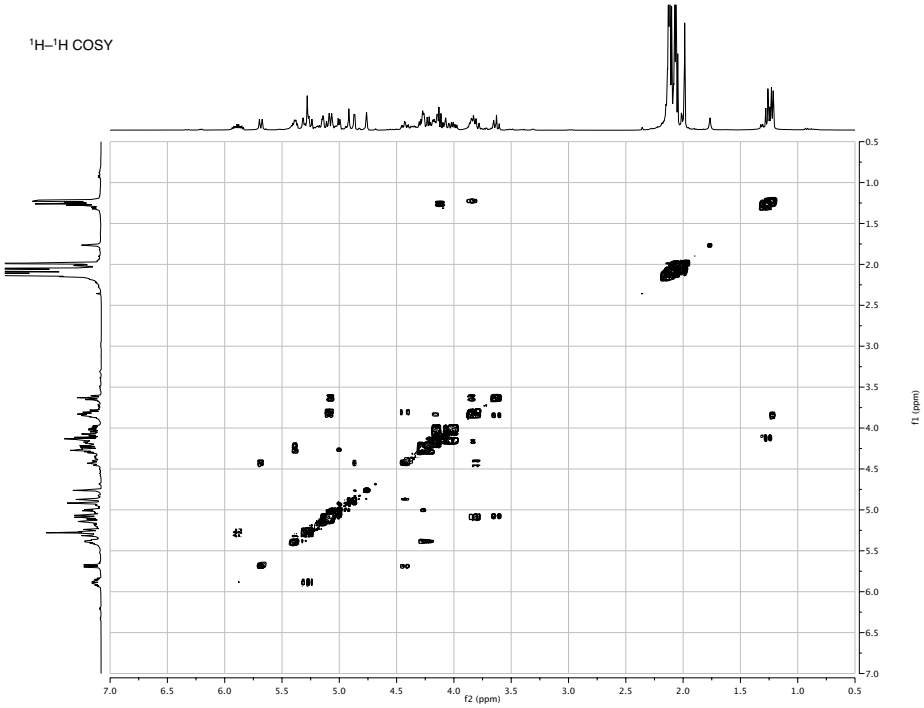

$^{13}C–^{1}H$ HSQC

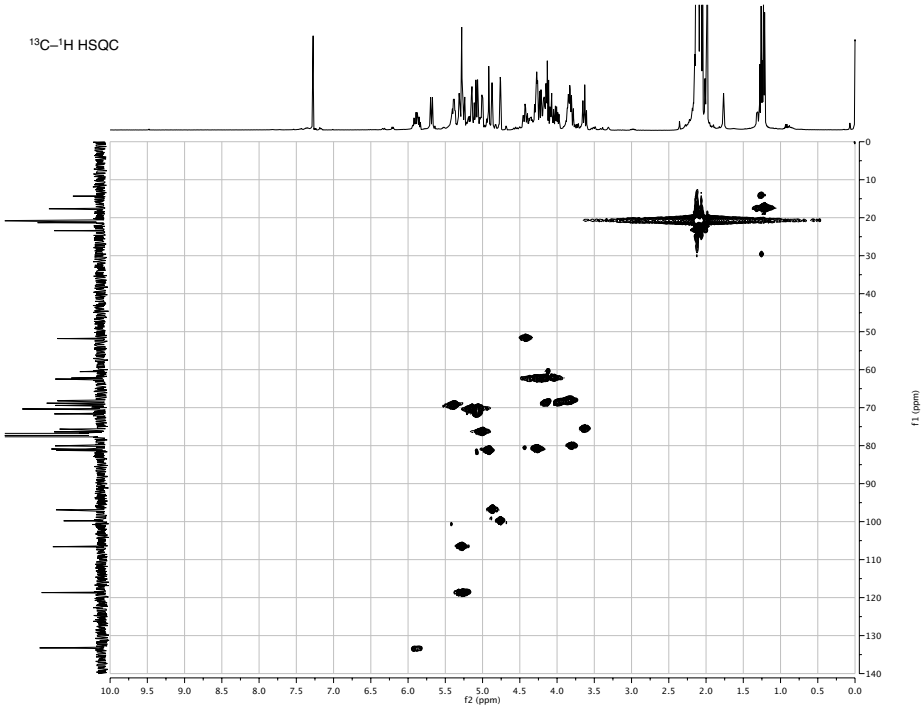

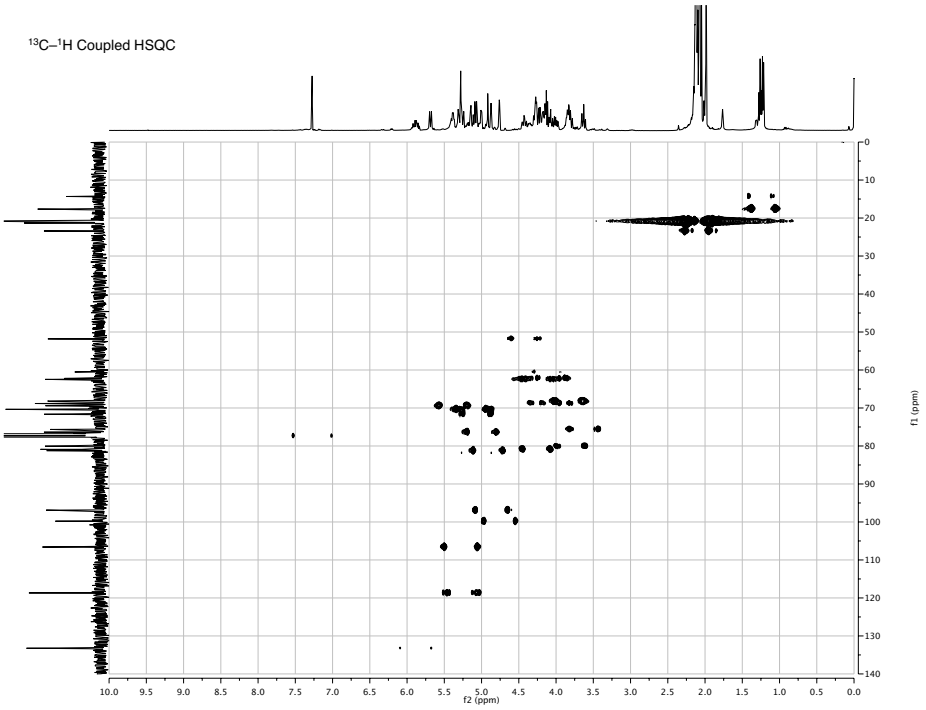
^{13}C–^{1}H Coupled HSQC
f2 (ppm)
f1 (ppm)

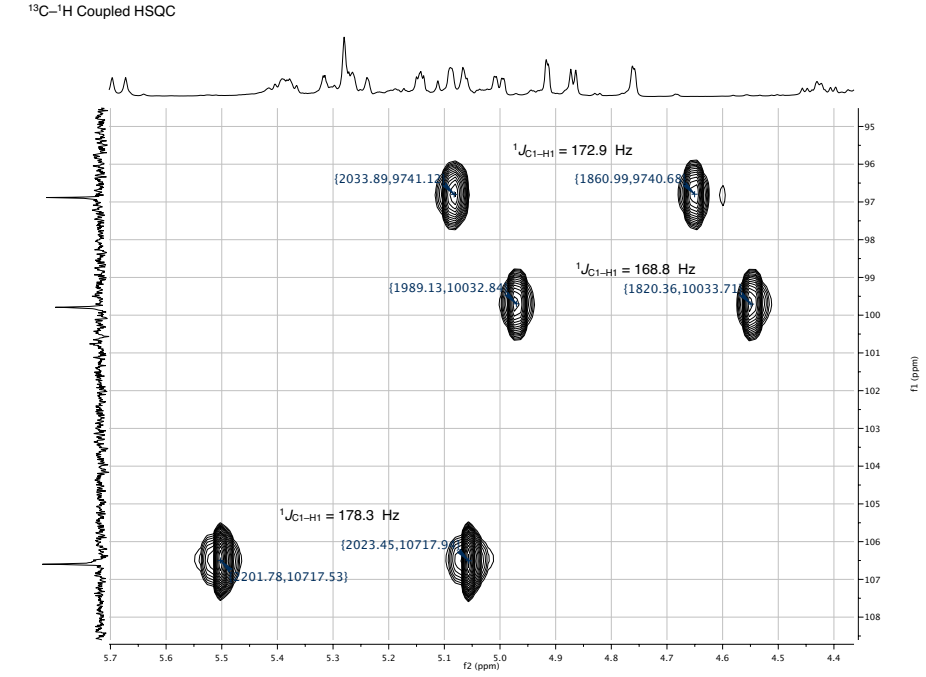
^{13}C–^{1}H Coupled HSQC
$^{1}J_{C1-H1}$ = 172.9 Hz
{2033.89,9741.12}
{1860.99,9740.68}
$^{1}J_{C1-H1}$ = 168.8 Hz
{1989.13,10032.84}
{1820.36,10033.71}
$^{1}J_{C1-H1}$ = 178.3 Hz
{2023.45,10717.96}
{2201.78,10717.53}
f2 (ppm)
f1 (ppm)

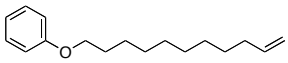

4.03

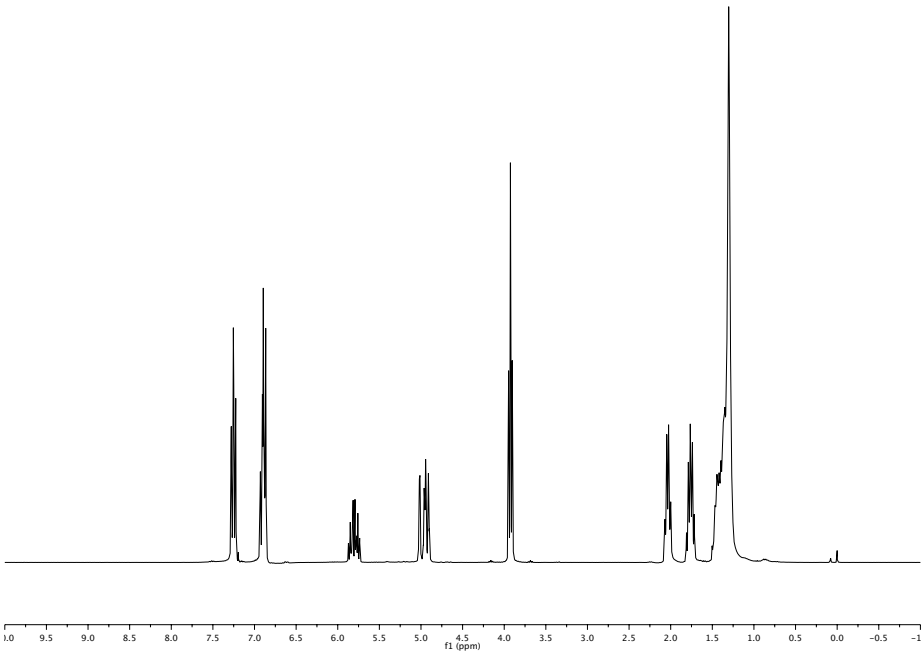

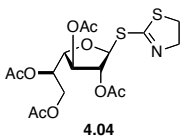
OAc
S
S
N
AcO
OAc
AcO

4.04

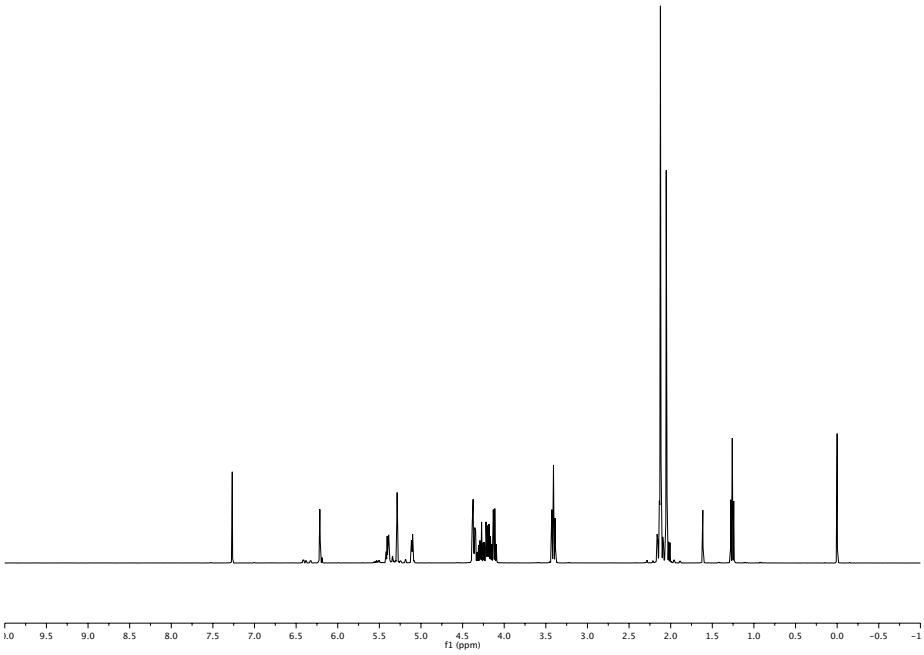
9.5
9.0
8.5
8.0
7.5
7.0
6.5
6.0
5.5
5.0
4.5
4.0
3.5
3.0
2.5
2.0
1.5
1.0
0.5
0.0
−0.5
f1 (ppm)

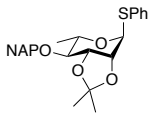
SPh
NAPO
O
O
O

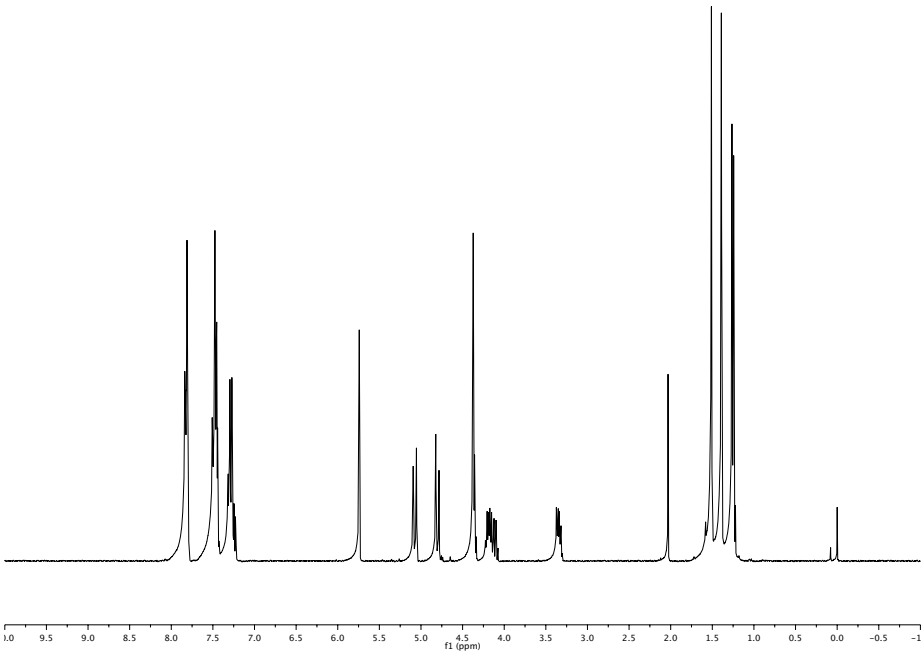
9.5
9.0
8.5
8.0
7.5
7.0
6.5
6.0
5.5
5.0
4.5
4.0
3.5
3.0
2.5
2.0
1.5
1.0
0.5
0.0
−0.5
f1 (ppm)

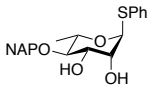
SPh
NAPO
O
HO
OH

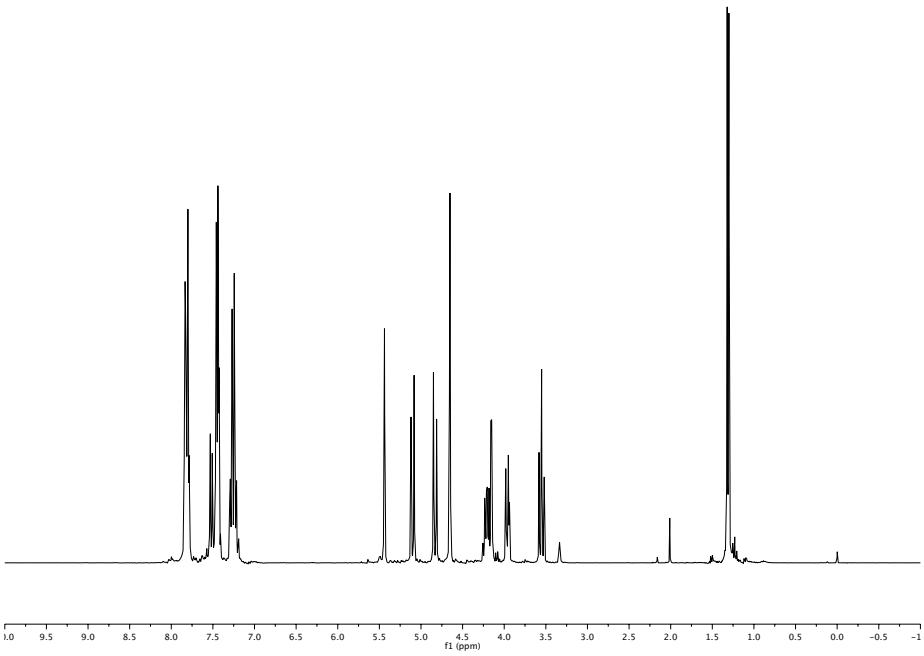
9.5 9.0 8.5 8.0 7.5 7.0 6.5 6.0 5.5 5.0 4.5 4.0 3.5 3.0 2.5 2.0 1.5 1.0 0.5 0.0 −0.5
f1 (ppm)

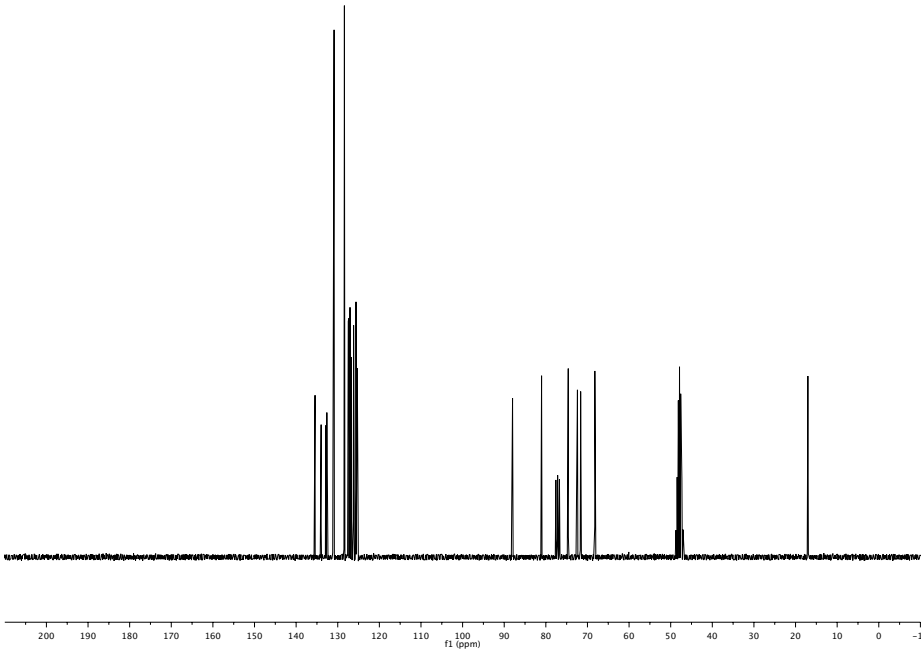
200 190 180 170 160 150 140 130 120 110 100 90 80 70 60 50 40 30 20 10 0
f1 (ppm)

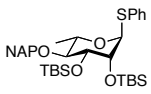

4.05

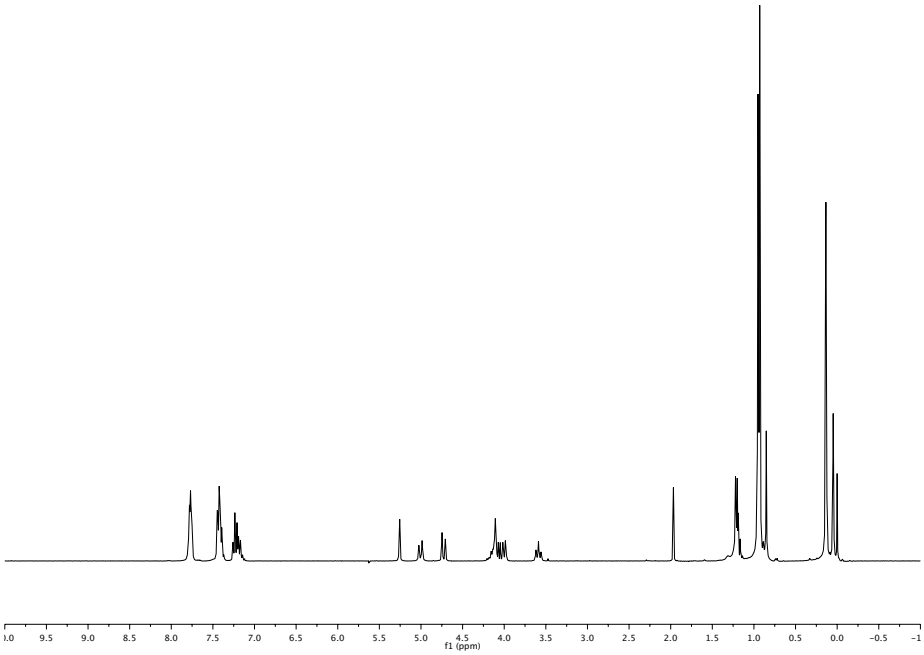

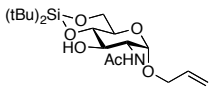
(tBu)2Si
O
O
HO
AcHN
O

4.07

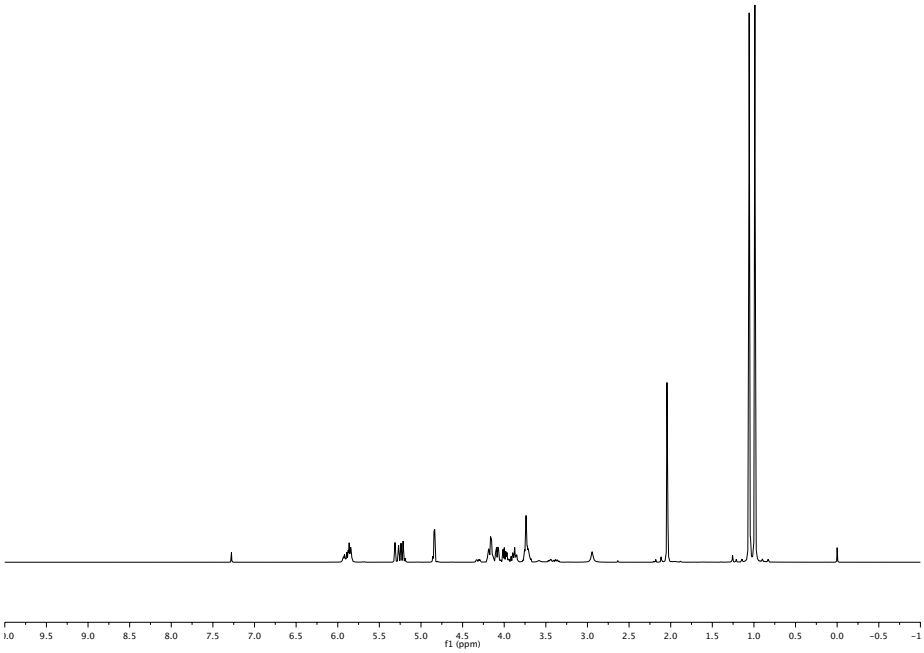
9.5
9.0
8.5
8.0
7.5
7.0
6.5
6.0
5.5
5.0
4.5
4.0
3.5
3.0
2.5
2.0
1.5
1.0
0.5
0.0
−0.5
f1 (ppm)

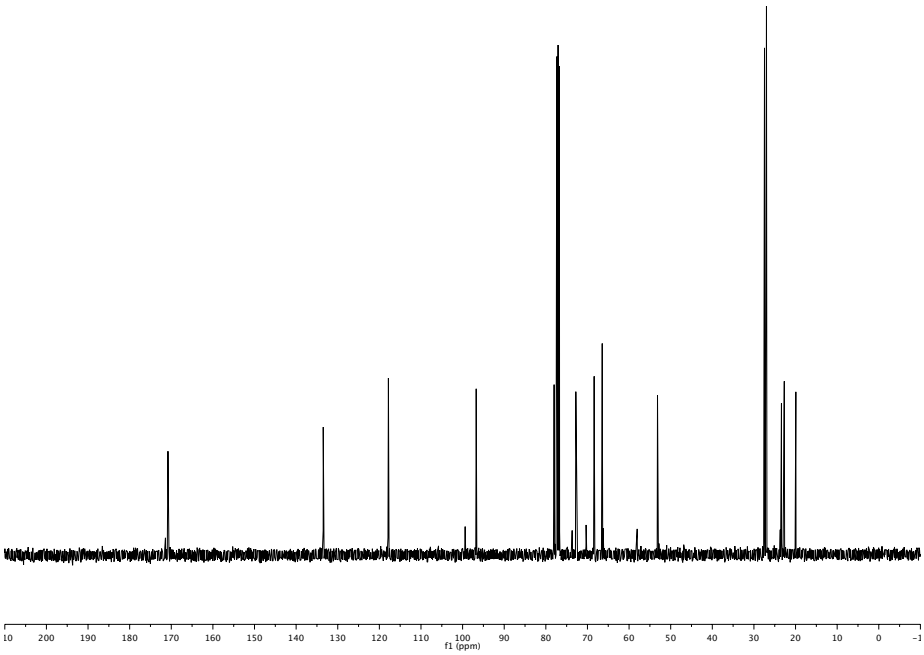
200
190
180
170
160
150
140
130
120
110
100
90
80
70
60
50
40
30
20
10
0
f1 (ppm)

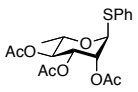

4.08

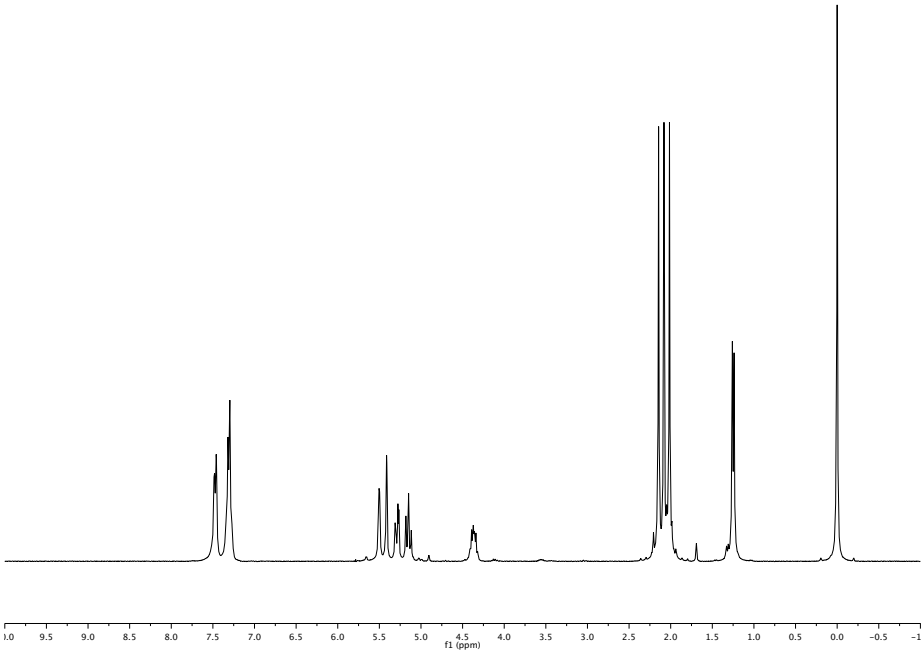

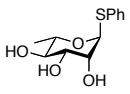

4.09

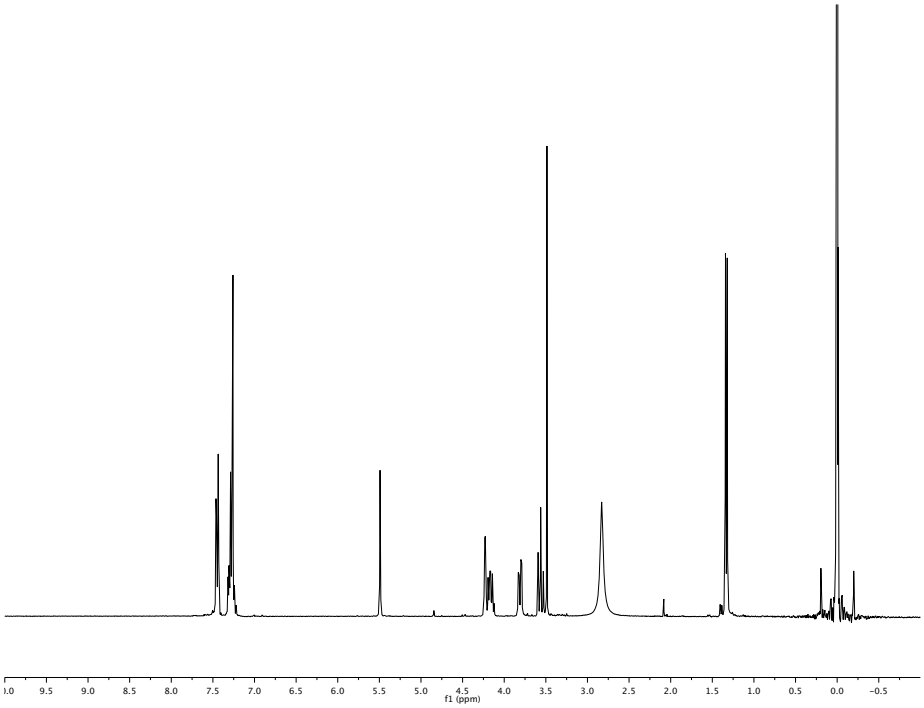

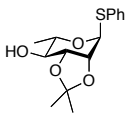
SPh
HO
O
O
O

4.10

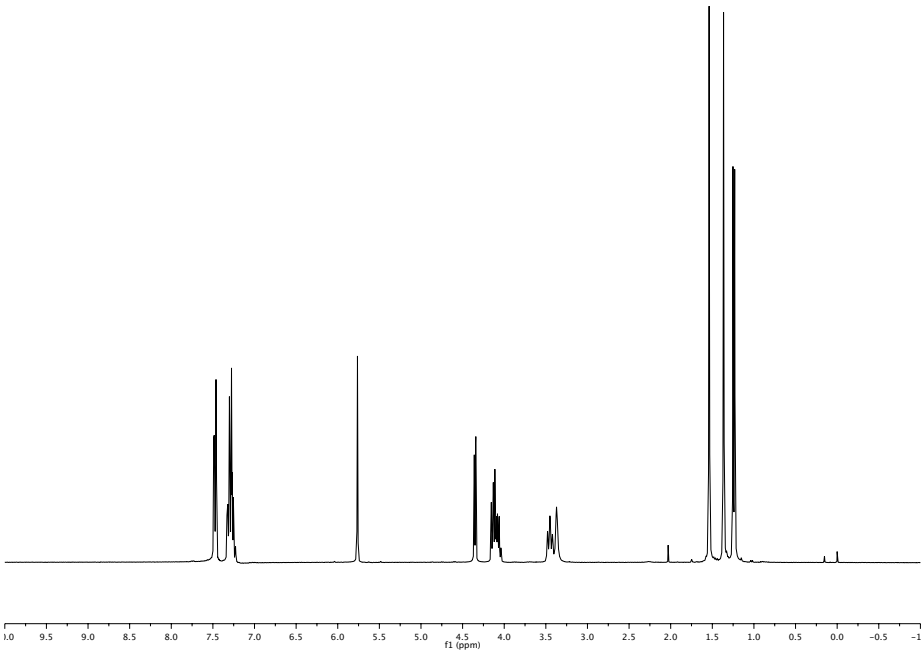
9.5
9.0
8.5
8.0
7.5
7.0
6.5
6.0
5.5
5.0
4.5
4.0
3.5
3.0
2.5
2.0
1.5
1.0
0.5
0.0
−0.5
f1 (ppm)

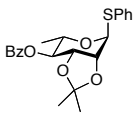
SPh
BzO
O
O
O

4.11

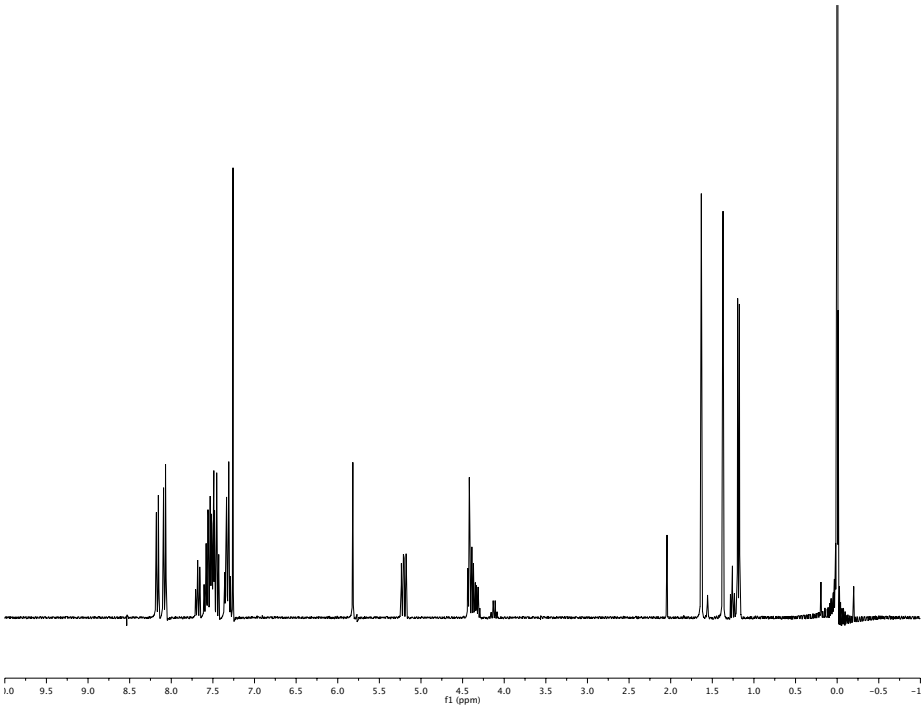
9.5
9.0
8.5
8.0
7.5
7.0
6.5
6.0
5.5
5.0
4.5
4.0
3.5
3.0
2.5
2.0
1.5
1.0
0.5
0.0
−0.5
f1 (ppm)

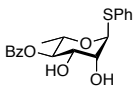
SPh
BzO
O
HO
OH

4.12

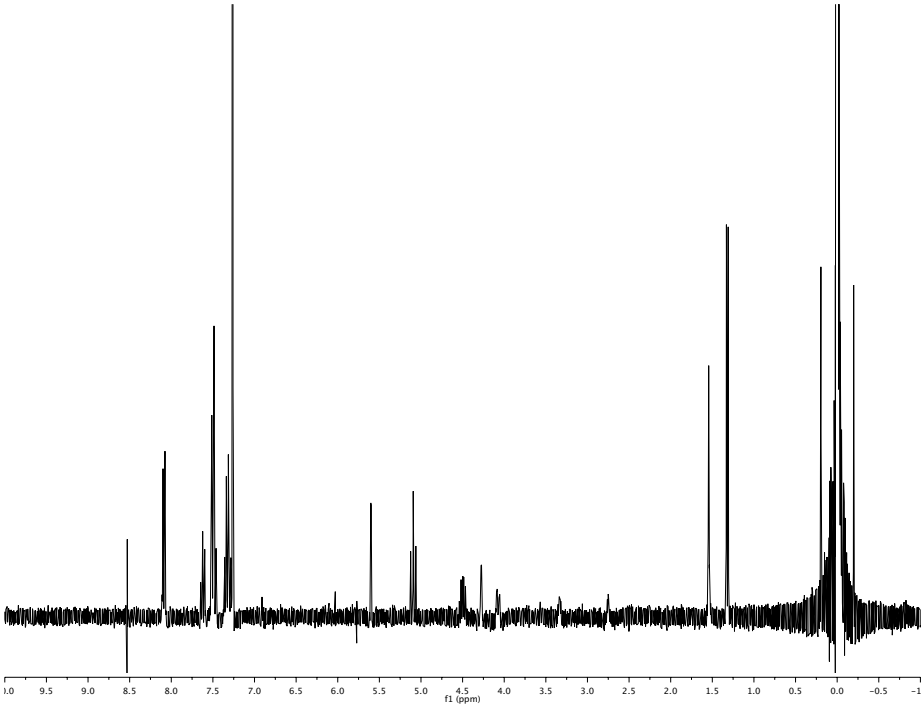
9.5
9.0
8.5
8.0
7.5
7.0
6.5
6.0
5.5
5.0
4.5
4.0
3.5
3.0
2.5
2.0
1.5
1.0
0.5
0.0
−0.5
−1
f1 (ppm)

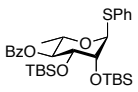
SPh
O
BzO
TBSO
OTBS

4.06

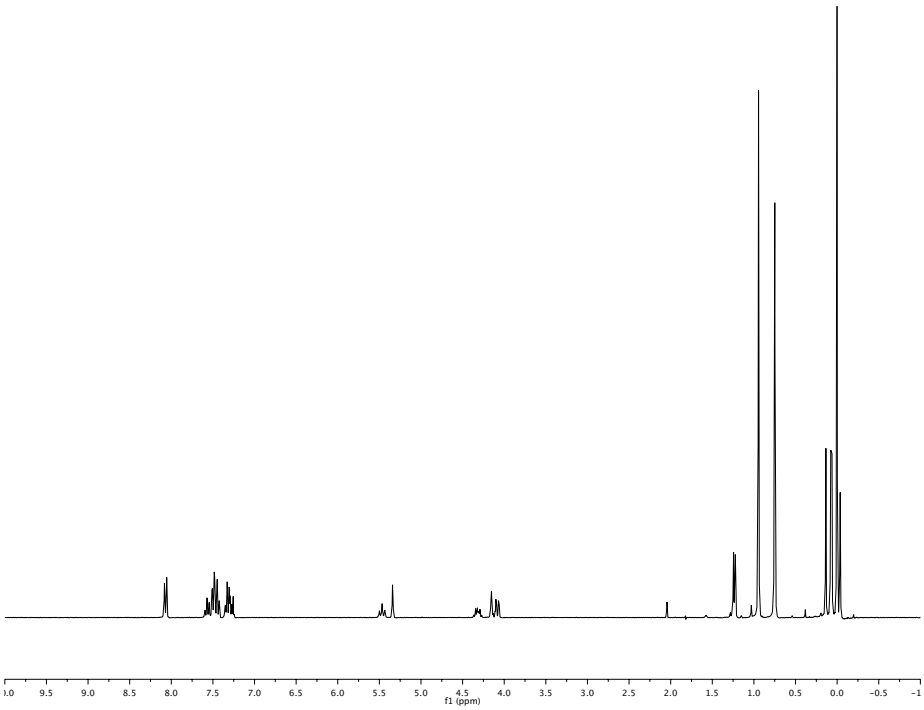
9.5
9.0
8.5
8.0
7.5
7.0
6.5
6.0
5.5
5.0
4.5
4.0
3.5
3.0
2.5
2.0
1.5
1.0
0.5
0.0
−0.5
f1 (ppm)

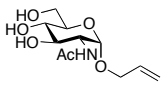
HO
HO
HO
AcHN
O
O

4.13

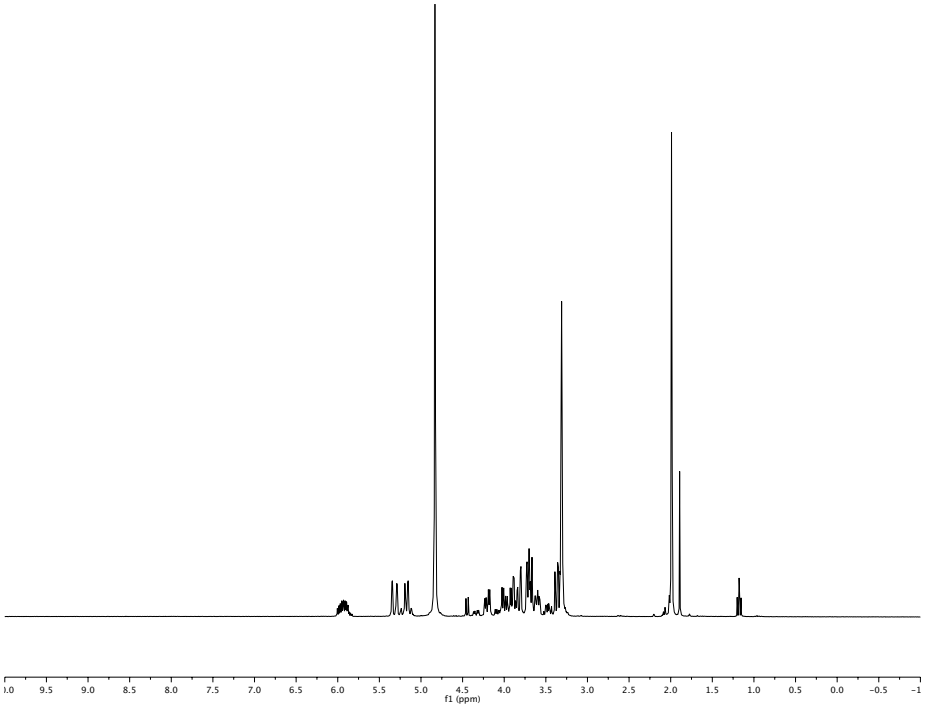
9.5
9.0
8.5
8.0
7.5
7.0
6.5
6.0
5.5
5.0
4.5
4.0
3.5
3.0
2.5
2.0
1.5
1.0
0.5
0.0
−0.5
f1 (ppm)

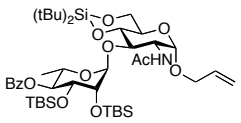
(tBu)2Si
O
O
O
O
AcHN
O
BzO
O
TBSO
OTBS

4.14

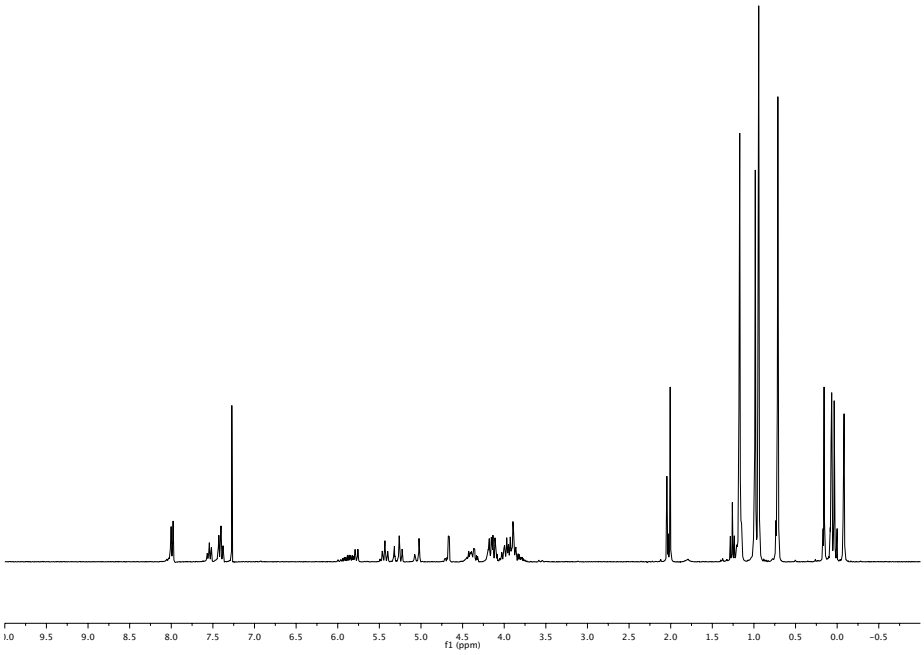
9.5
9.0
8.5
8.0
7.5
7.0
6.5
6.0
5.5
5.0
4.5
4.0
3.5
3.0
2.5
2.0
1.5
1.0
0.5
0.0
−0.5
f1 (ppm)

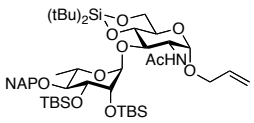
(tBu)2Si
O
O
O
O
AcHN
O
NAPO
O
TBSO
OTBS

4.15

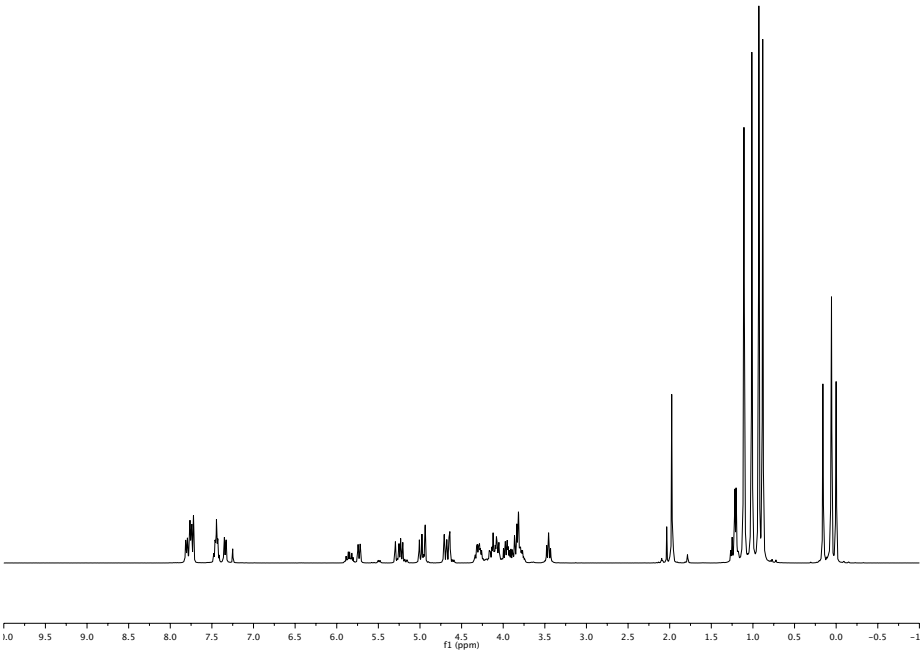
9.5
9.0
8.5
8.0
7.5
7.0
6.5
6.0
5.5
5.0
4.5
4.0
3.5
3.0
2.5
2.0
1.5
1.0
0.5
0.0
−0.5
f1 (ppm)

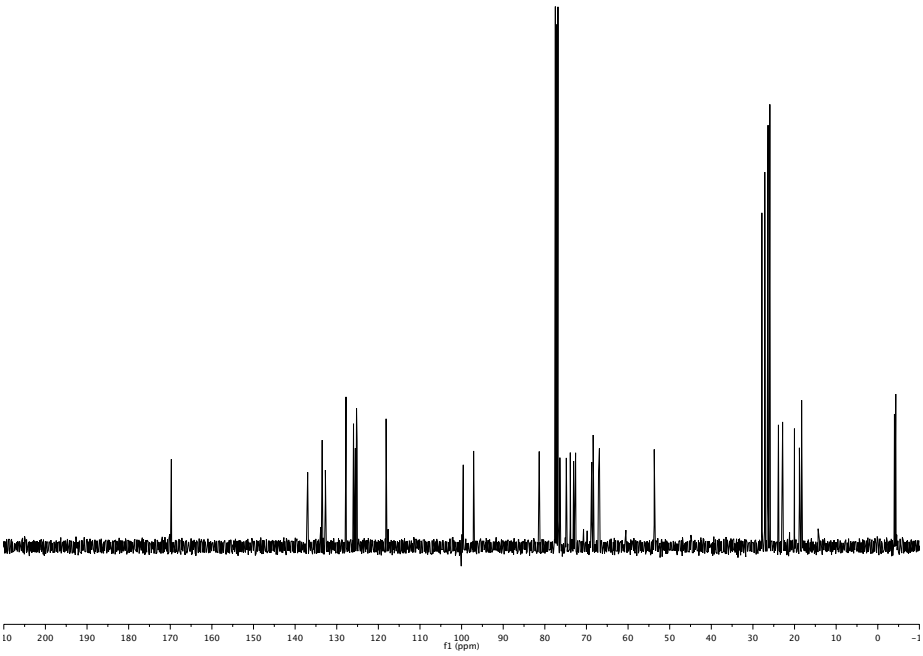
200
190
180
170
160
150
140
130
120
110
100
90
80
70
60
50
40
30
20
10
0
f1 (ppm)

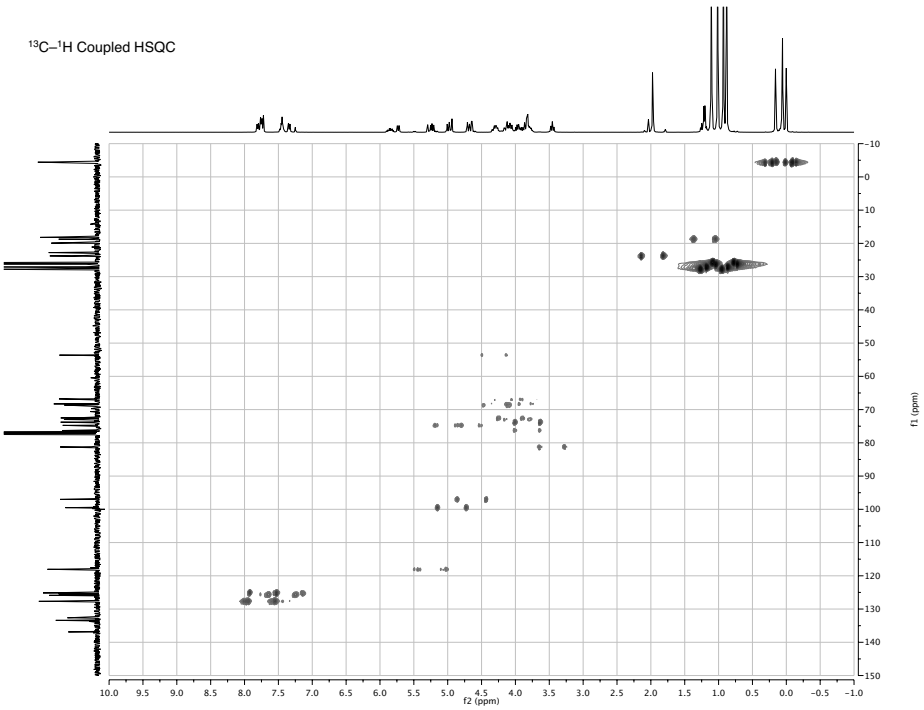
^{13}C–^{1}H Coupled HSQC
f2 (ppm)
f1 (ppm)

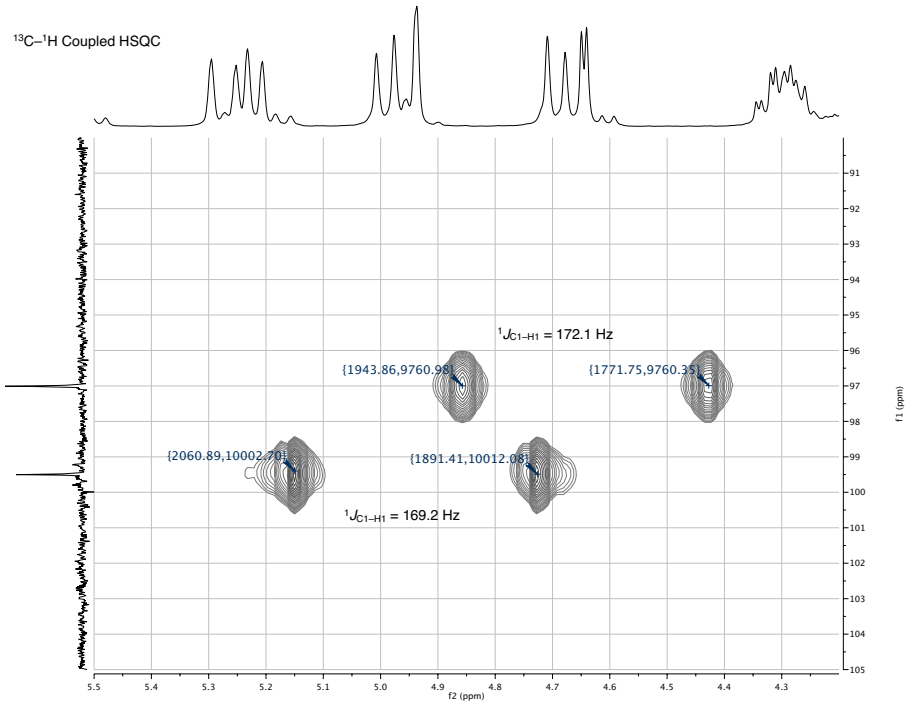
^{13}C–^{1}H Coupled HSQC
$^{1}J_{C1-H1}$ = 172.1 Hz
{1943.86,9760.98}
{1771.75,9760.35}
{2060.89,10002.70}
{1891.41,10012.08}
$^{1}J_{C1-H1}$ = 169.2 Hz
f2 (ppm)
f1 (ppm)

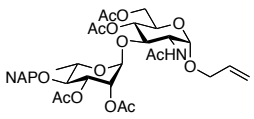
AcO
AcO
O
AcHN
O
NAPO
O
AcO
OAc

4.16

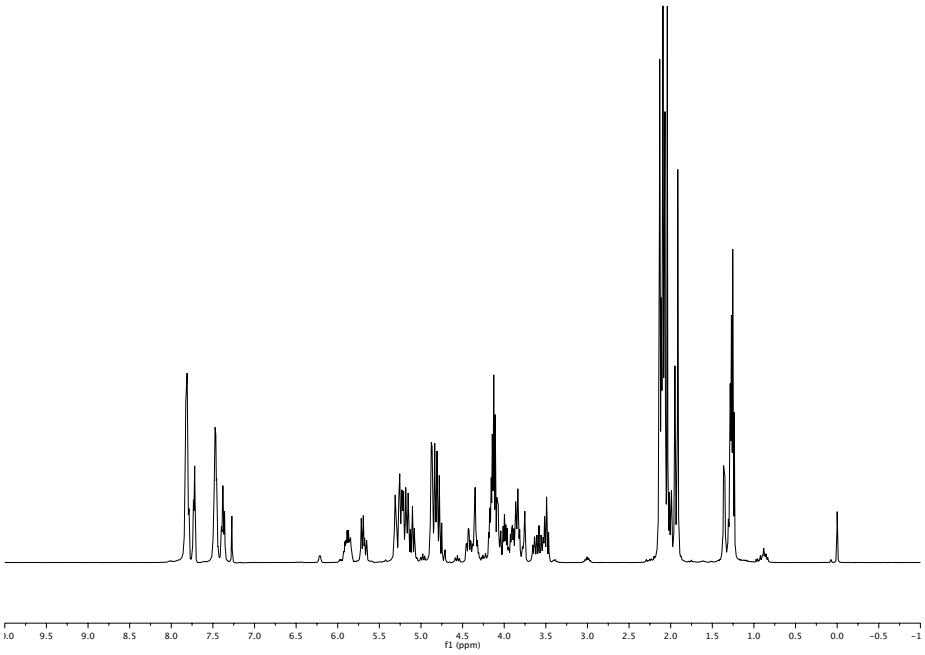
f1 (ppm)

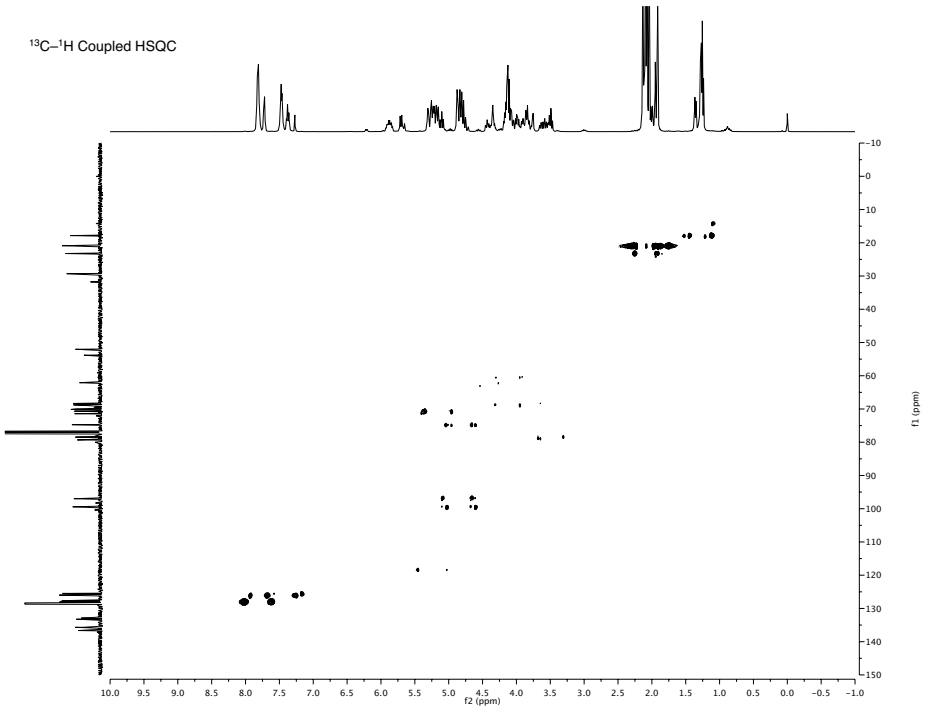
^{13}C–^{1}H Coupled HSQC
f2 (ppm)
f1 (ppm)

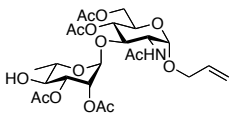
AcO
AcO
O
O
AcHN
O
HO
O
AcO
OAc

4.17

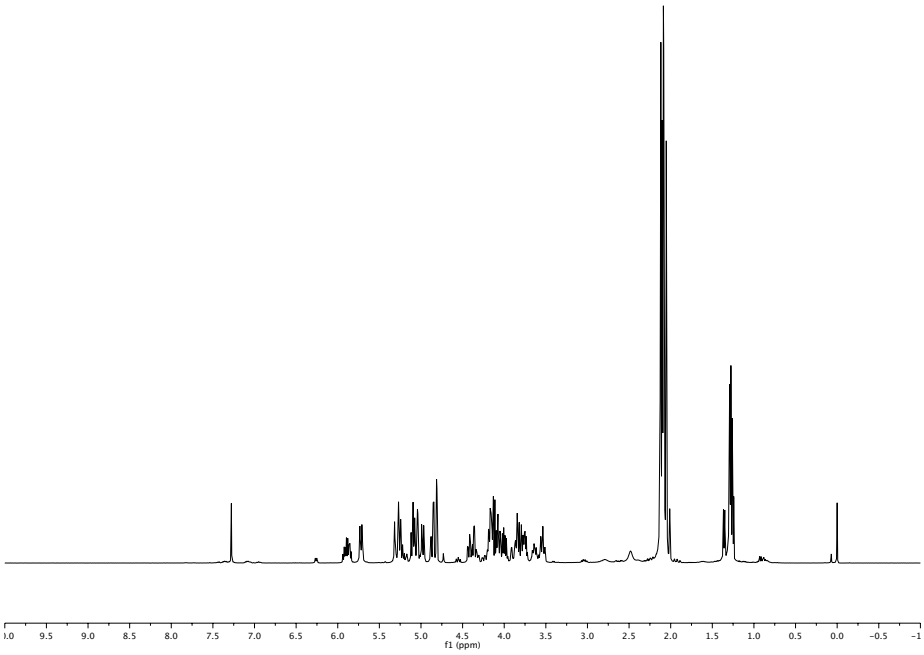
9.5
9.0
8.5
8.0
7.5
7.0
6.5
6.0
5.5
5.0
4.5
4.0
3.5
3.0
2.5
2.0
1.5
1.0
0.5
0.0
−0.5
f1 (ppm)

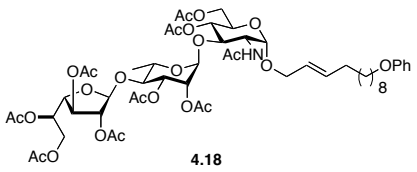

4.18

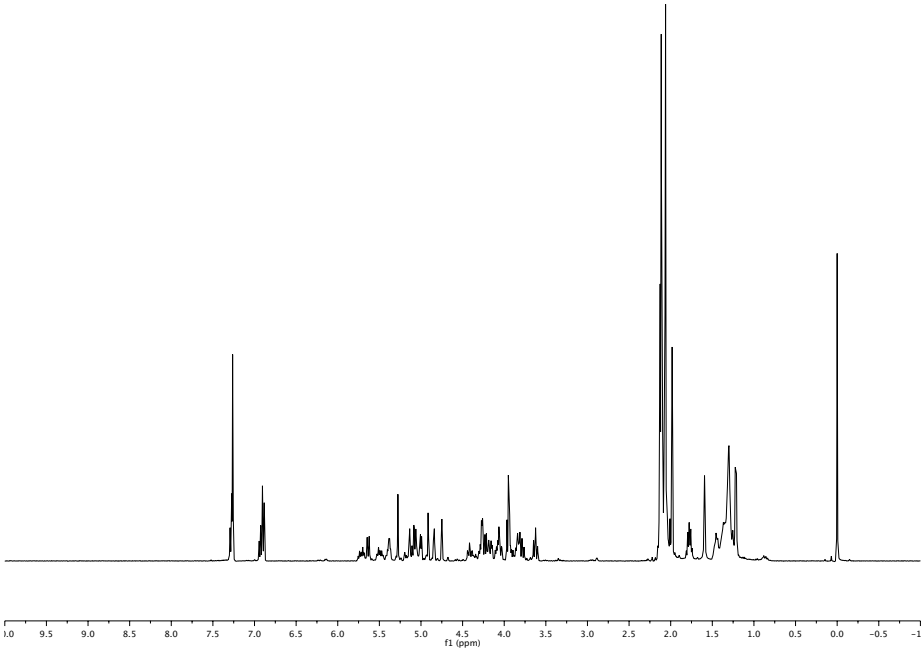

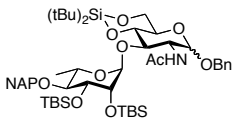
(tBu)2Si
O
O
O
O
AcHN
OBn
NAPO
O
TBSO
OTBS

5.04

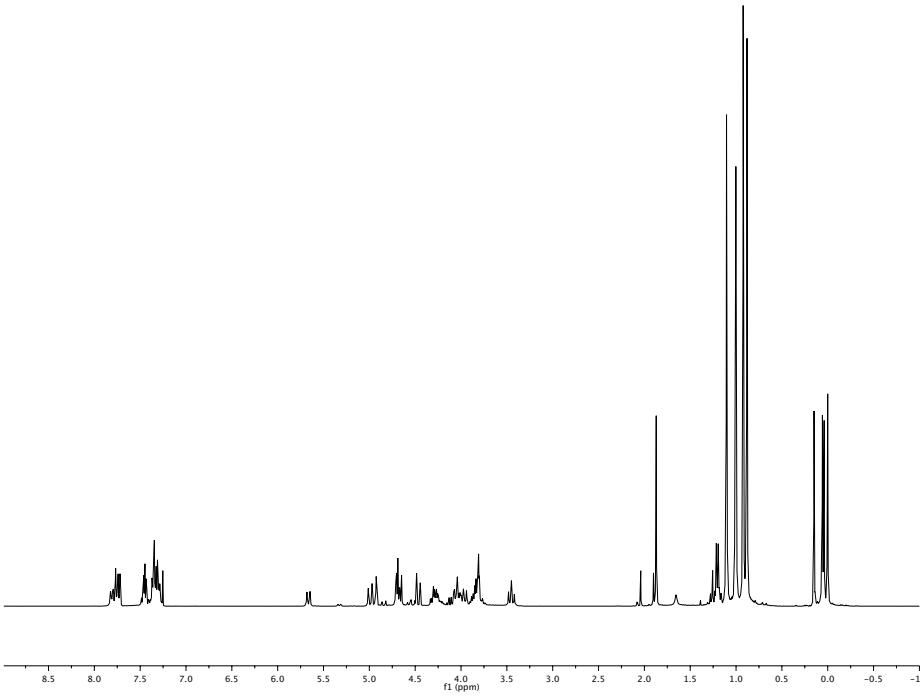
8.5 8.0 7.5 7.0 6.5 6.0 5.5 5.0 4.5 4.0 3.5 3.0 2.5 2.0 1.5 1.0 0.5 0.0 −0.5 −1
f1 (ppm)

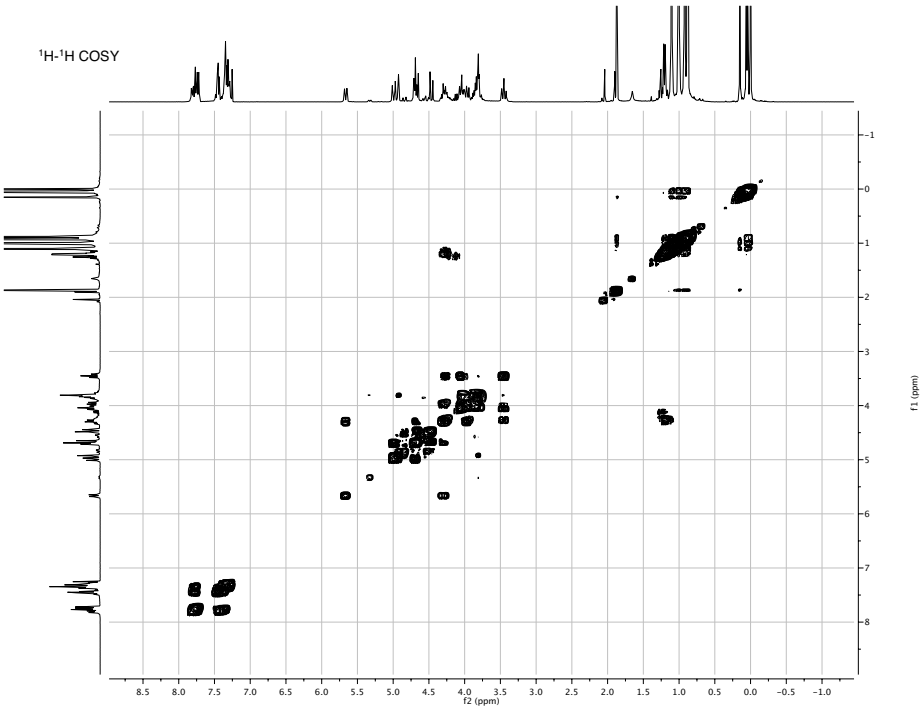
¹H-¹H COSY
8.5 8.0 7.5 7.0 6.5 6.0 5.5 5.0 4.5 4.0 3.5 3.0 2.5 2.0 1.5 1.0 0.5 0.0 −0.5 −1.0
f2 (ppm)
f1 (ppm)

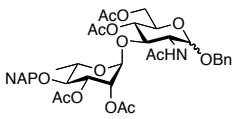

5.05

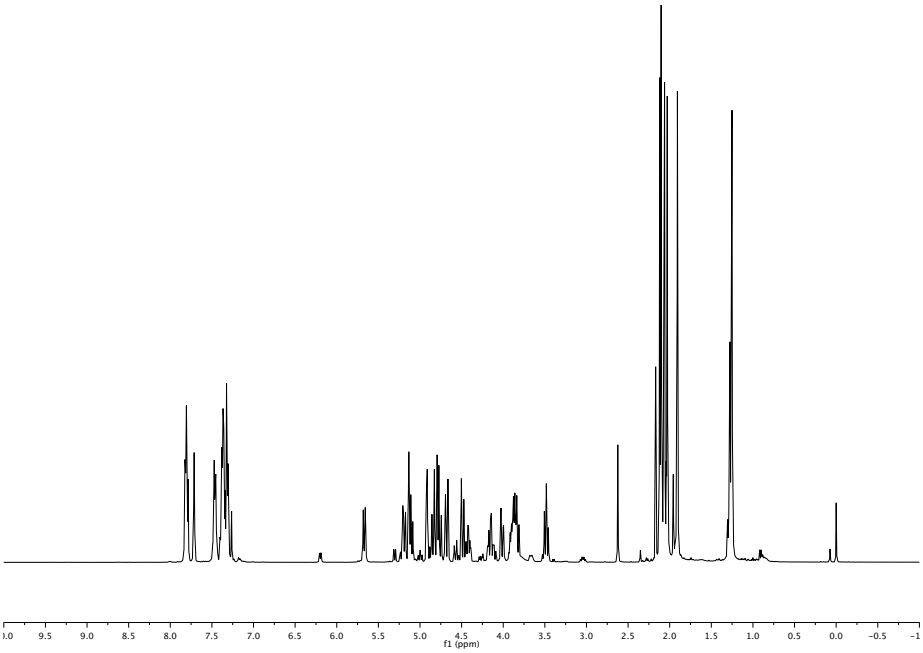

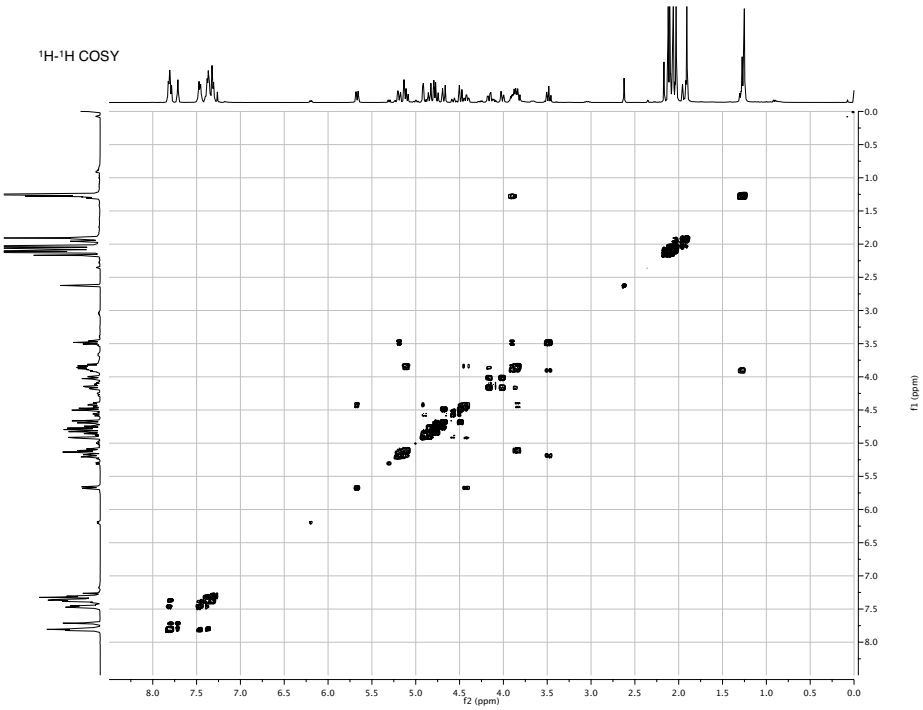

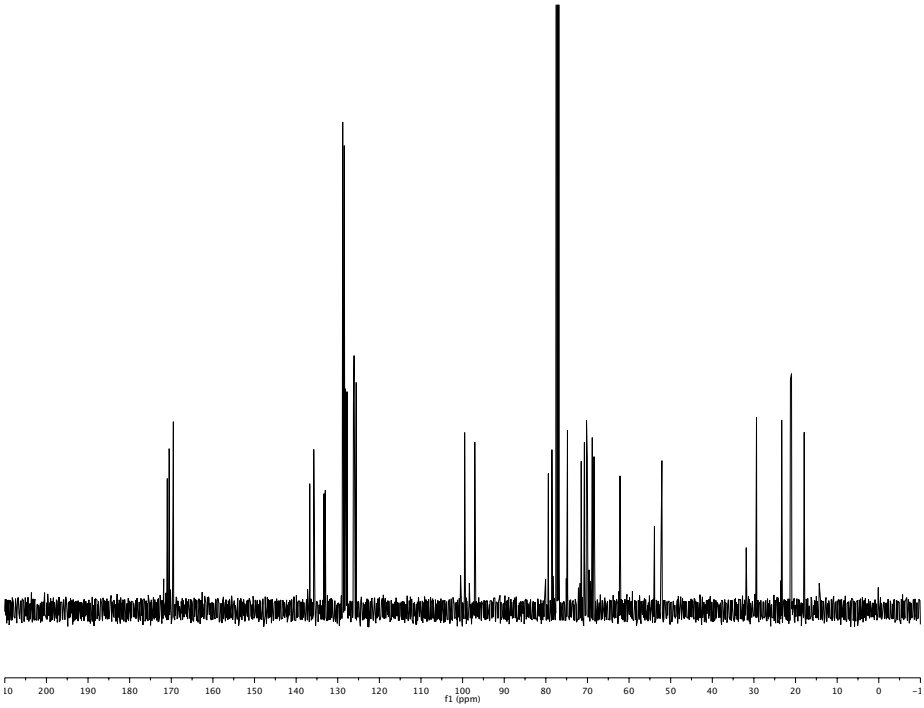
f1 (ppm)

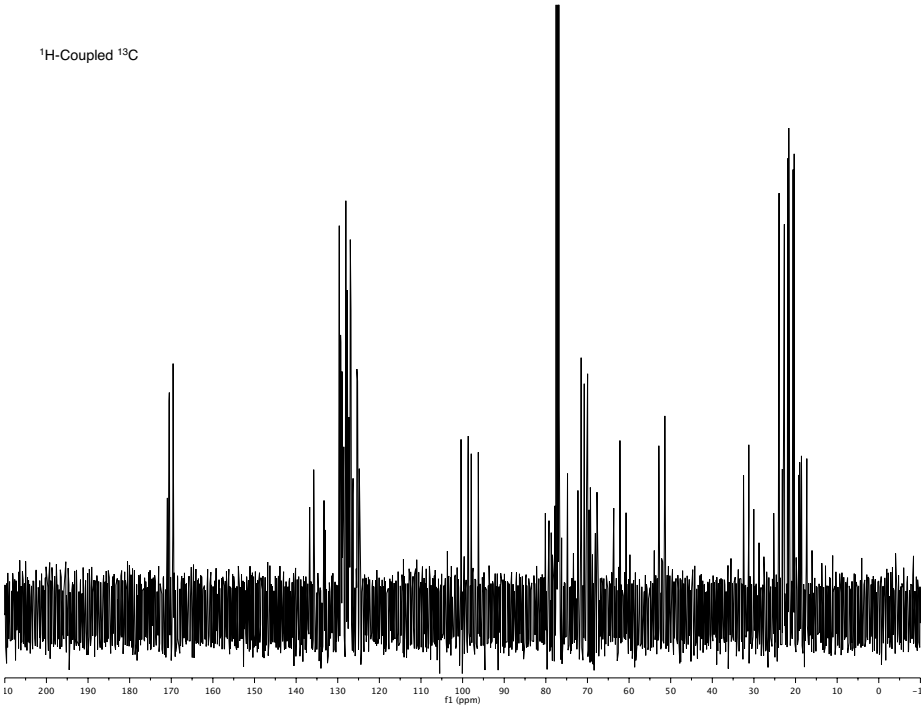
^{1}H-Coupled ^{13}C
f1 (ppm)

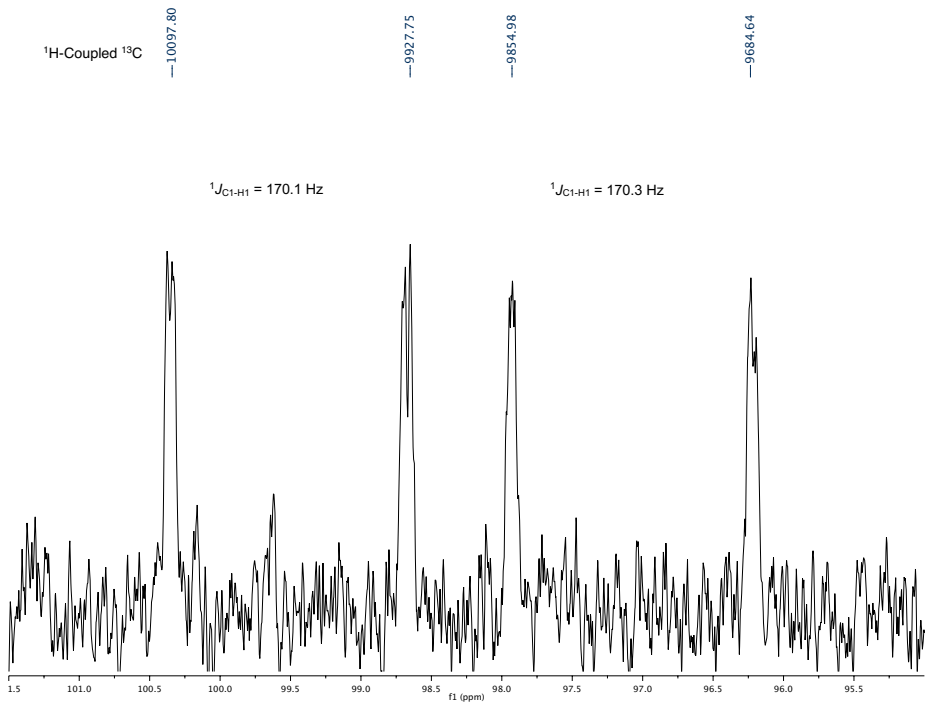
^{1}H-Coupled ^{13}C
10097.80
9927.75
9854.98
9684.64
$^{1}J_{C1-H1}$ = 170.1 Hz
$^{1}J_{C1-H1}$ = 170.3 Hz
1.5
101.0
100.5
100.0
99.5
99.0
98.5
98.0
97.5
97.0
96.5
96.0
95.5
f1 (ppm)

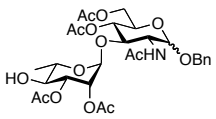

5.06

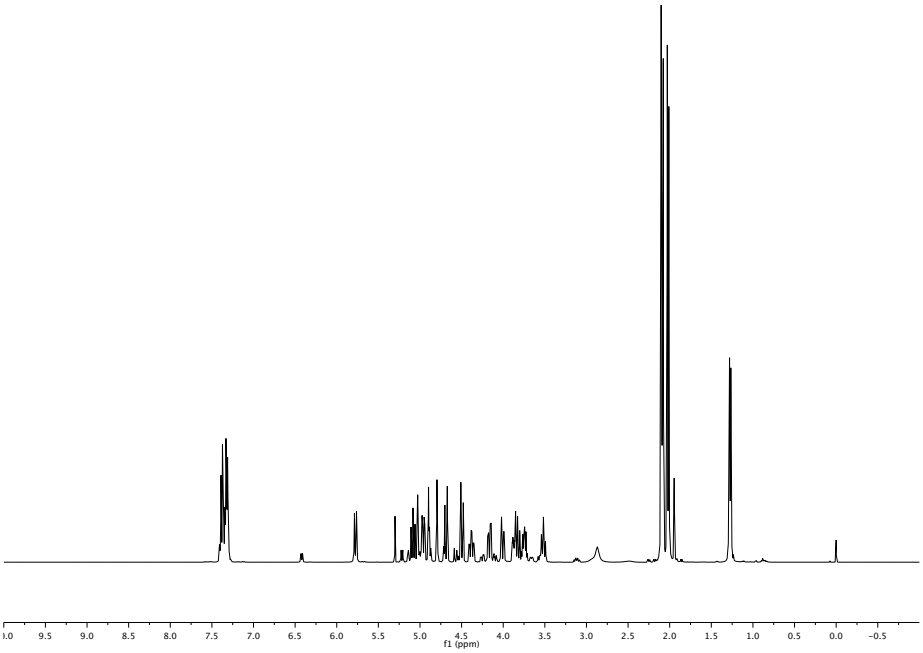

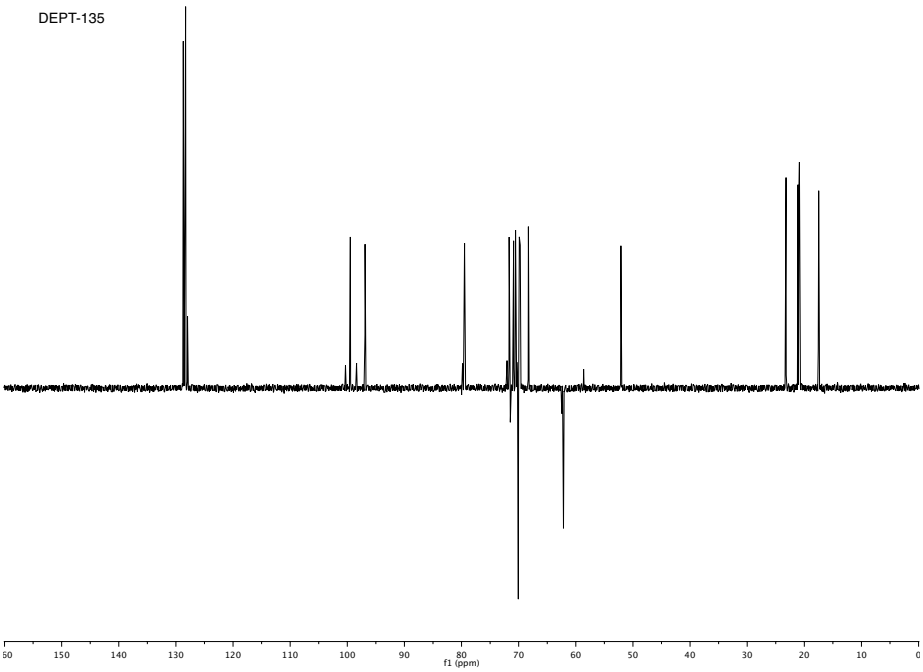

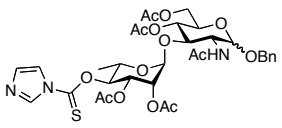

5.07

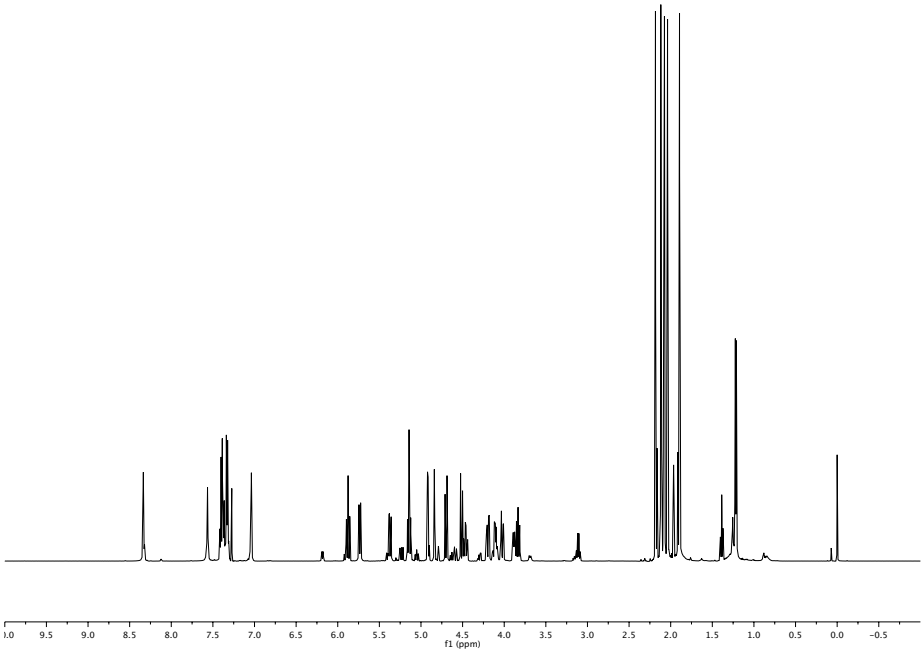

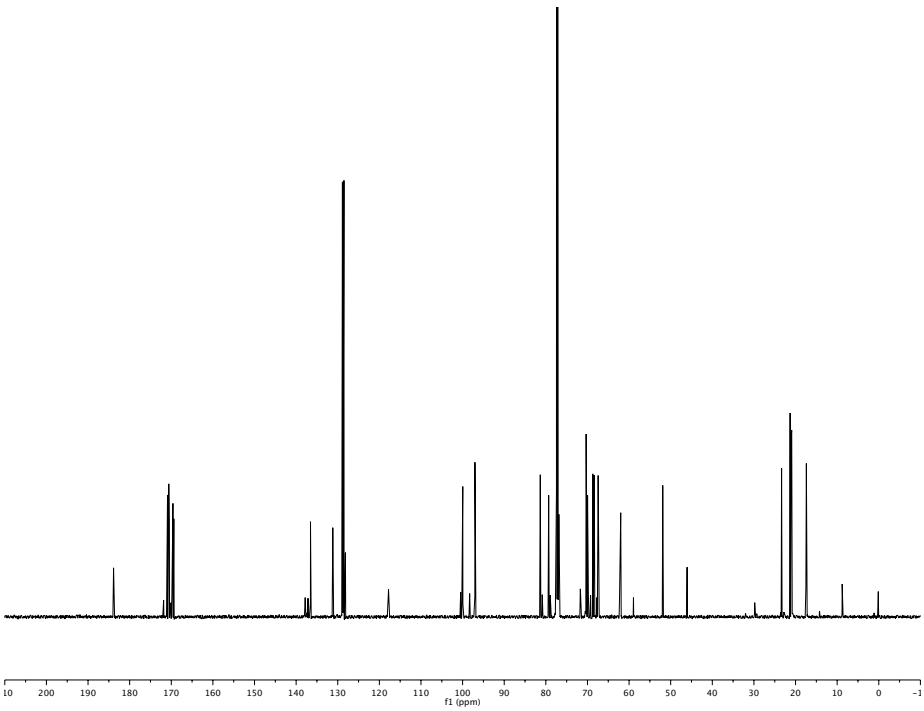

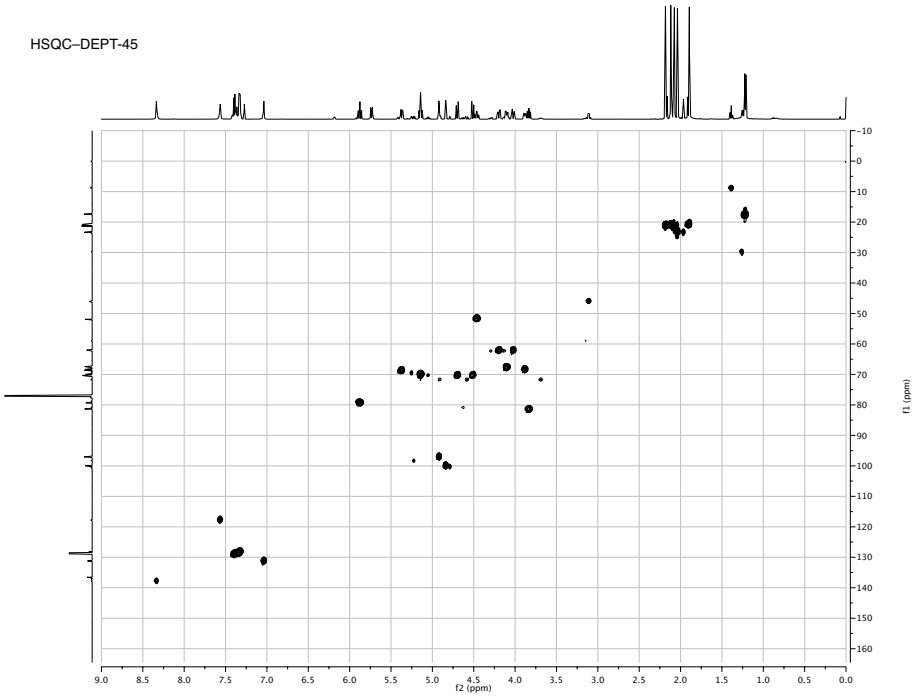
HSQC–DEPT-45
f2 (ppm)
f1 (ppm)

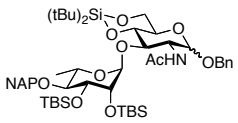
(tBu)2Si
O
O
O
O
AcHN
OBn
NAPO
O
TBSO
OTBS

6.02

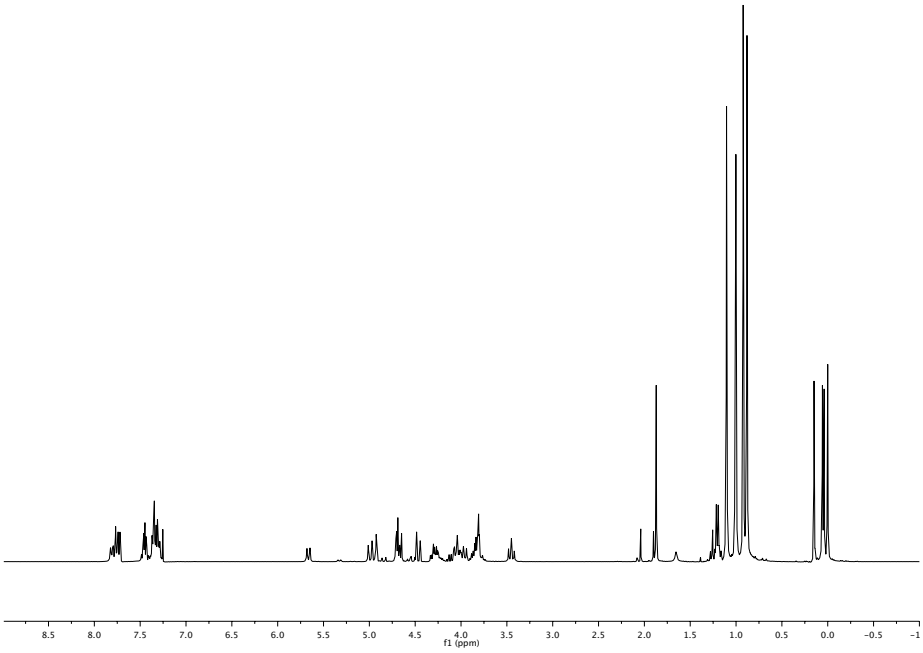
8.5
8.0
7.5
7.0
6.5
6.0
5.5
5.0
4.5
4.0
3.5
3.0
2.5
2.0
1.5
1.0
0.5
0.0
−0.5
−1
f1 (ppm)

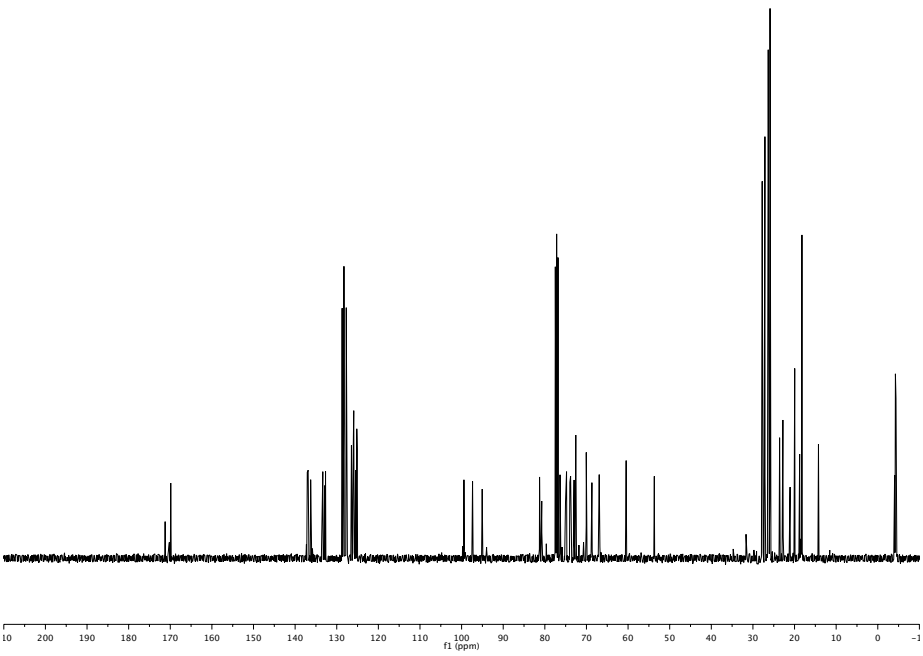
10
200
190
180
170
160
150
140
130
120
110
100
90
80
70
60
50
40
30
20
10
0
−1
f1 (ppm)

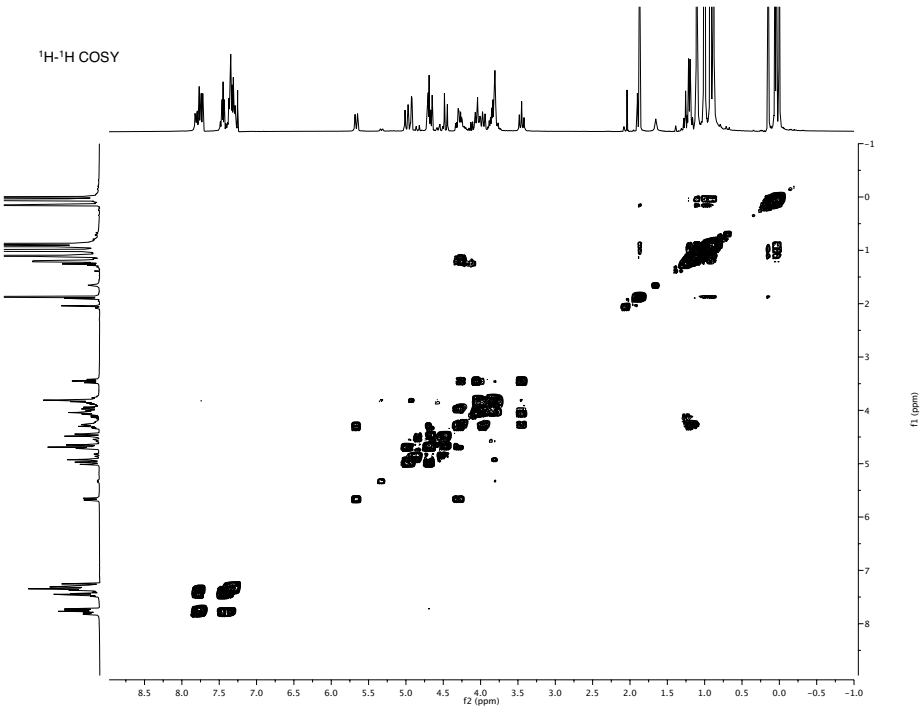
^{1}H-^{1}H COSY
f2 (ppm)
f1 (ppm)

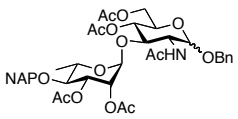

6.03

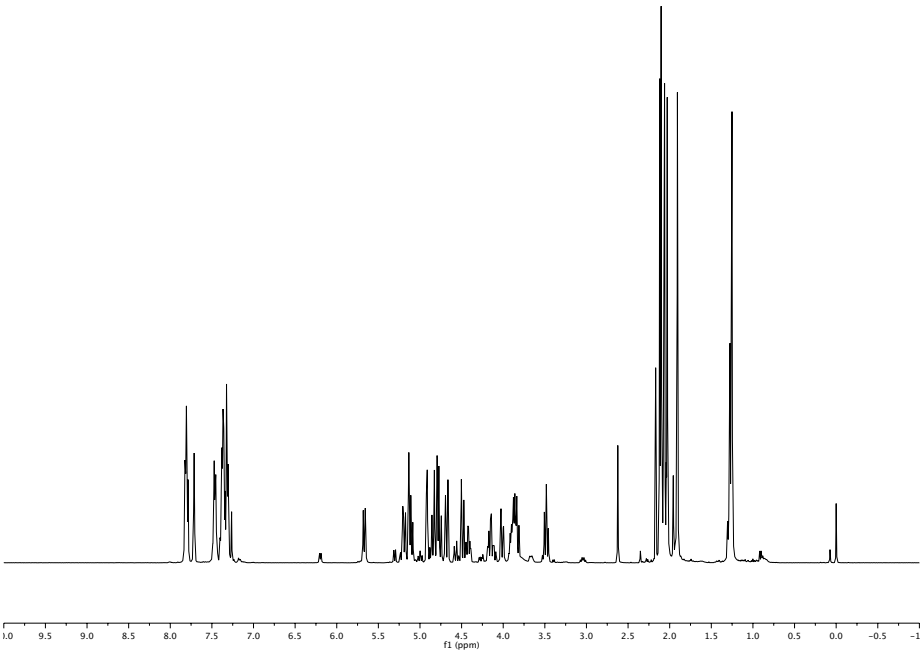

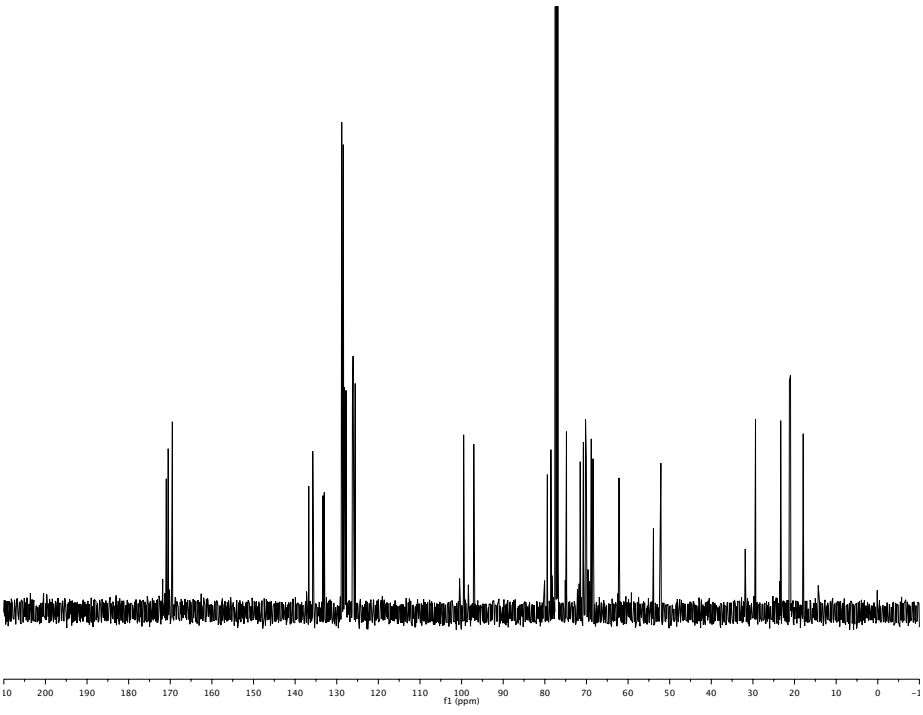

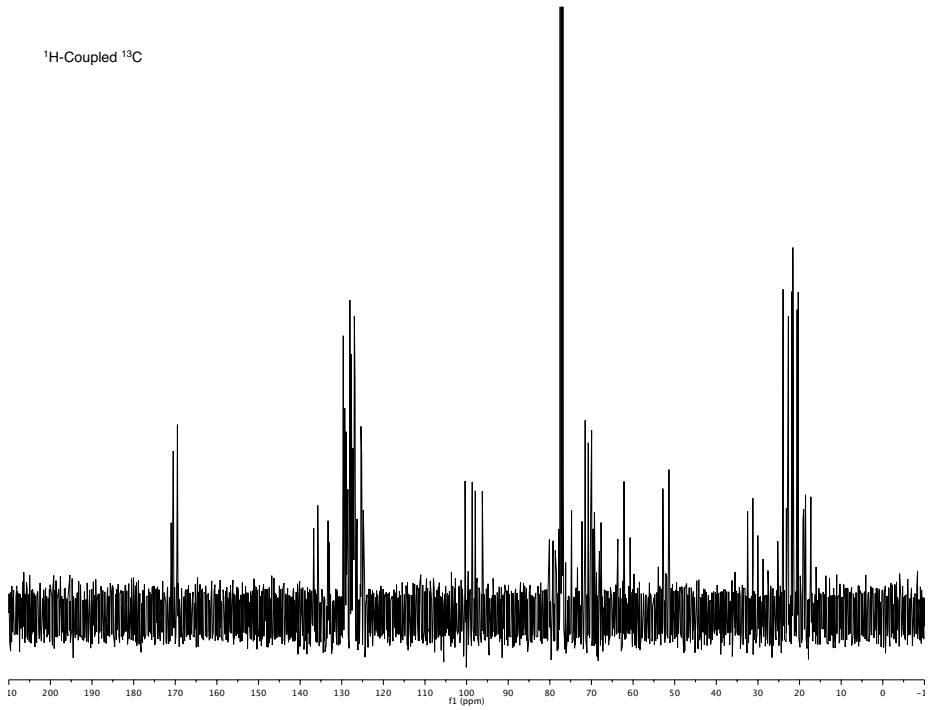
^{1}H-Coupled ^{13}C
f1 (ppm)

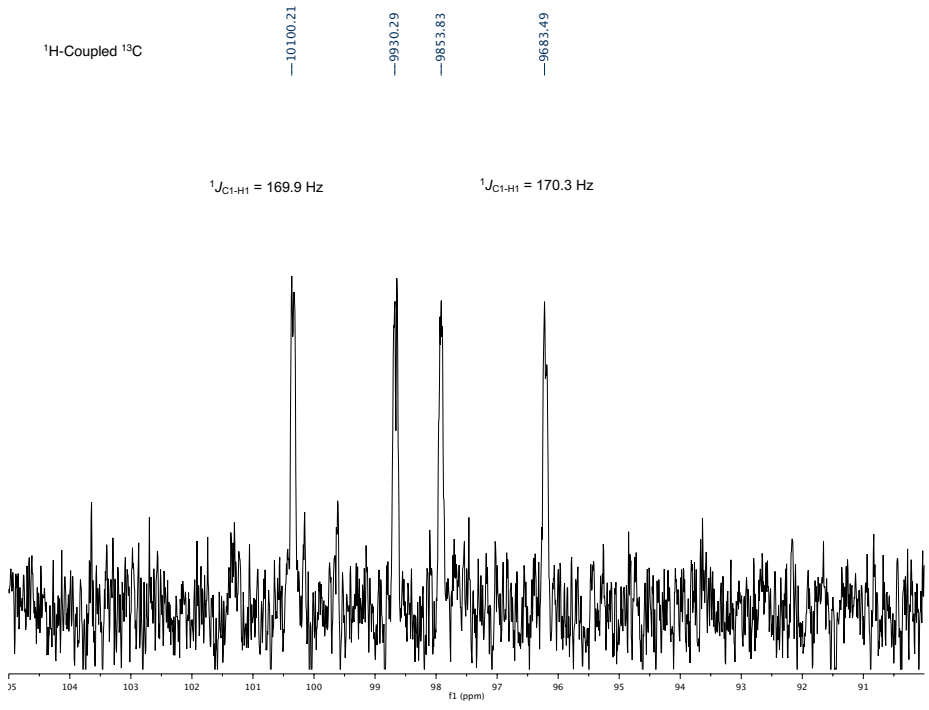
^{1}H-Coupled ^{13}C
10100.21
9930.29
9853.83
9683.49
$^{1}J_{C1-H1}$ = 169.9 Hz
$^{1}J_{C1-H1}$ = 170.3 Hz
f1 (ppm)

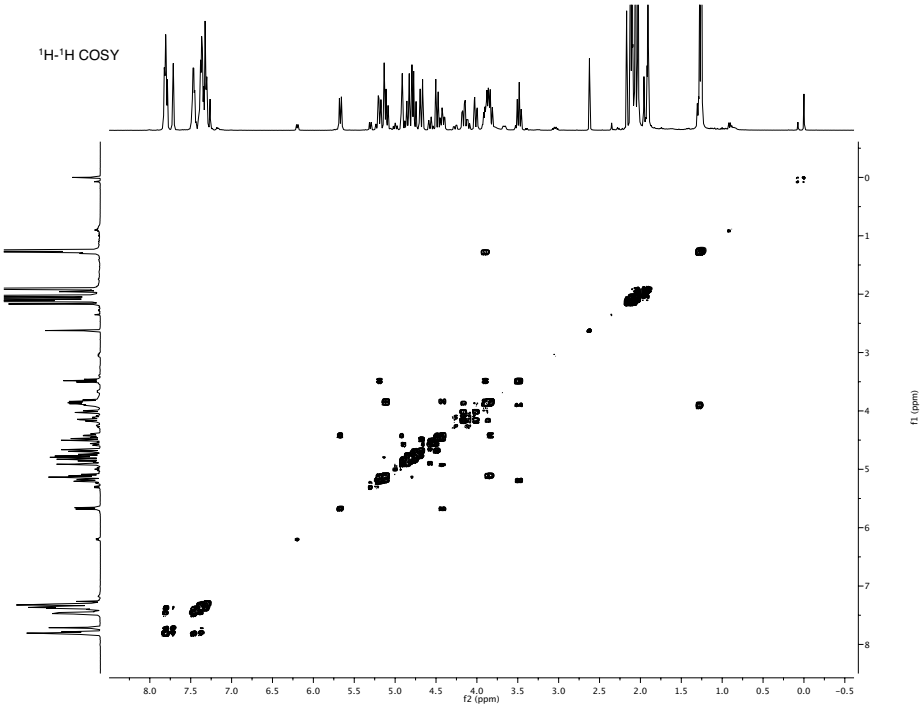
^{1}H-^{1}H COSY
f2 (ppm)
f1 (ppm)

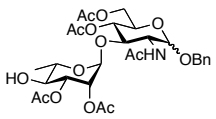
AcO
AcO
O
O
AcHN
OBn
HO
O
AcO
OAc

6.04

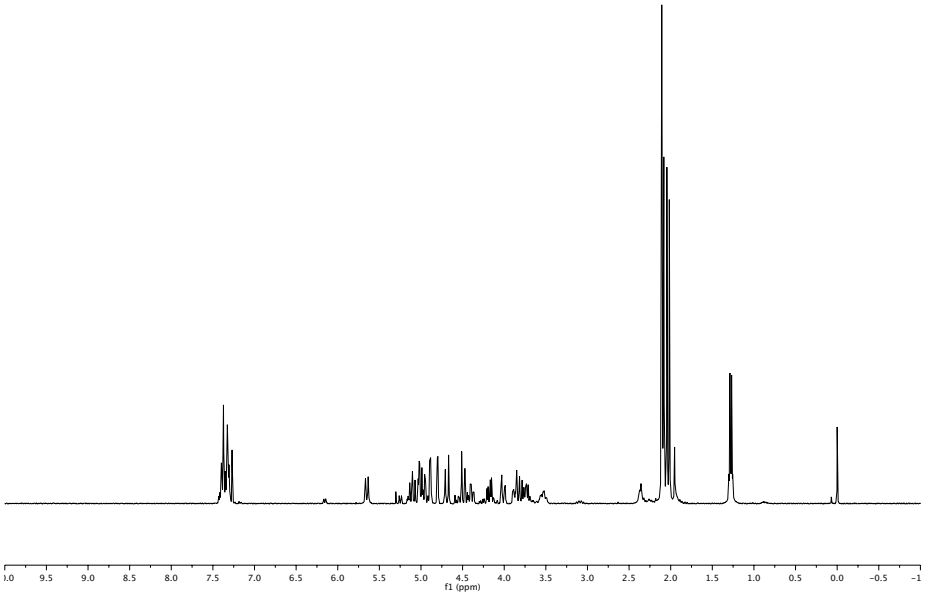
9.5
9.0
8.5
8.0
7.5
7.0
6.5
6.0
5.5
5.0
4.5
4.0
3.5
3.0
2.5
2.0
1.5
1.0
0.5
0.0
−0.5
−1
f1 (ppm)

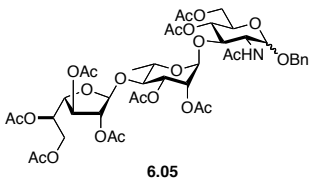

6.05

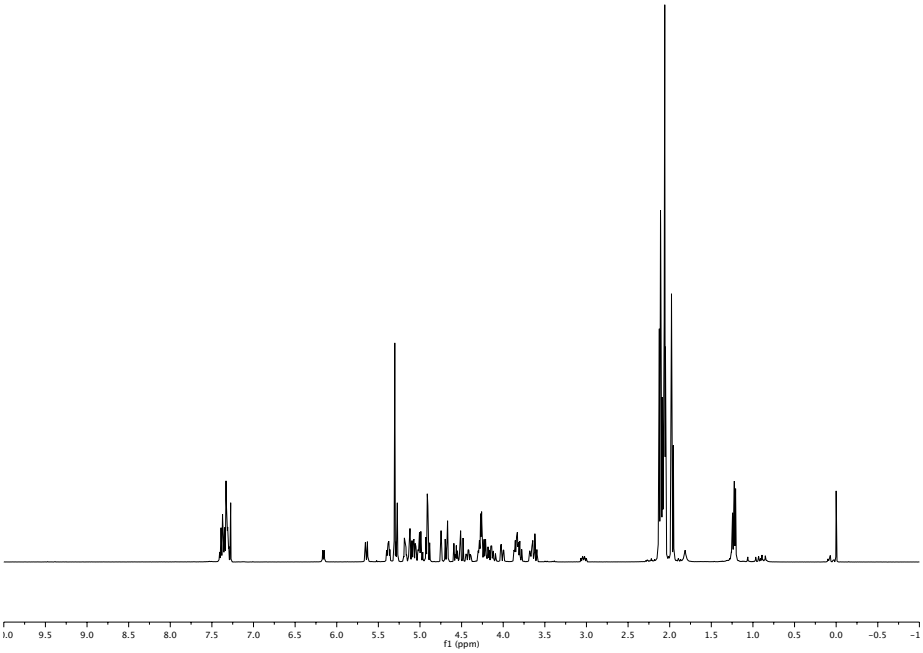

DEPT-45

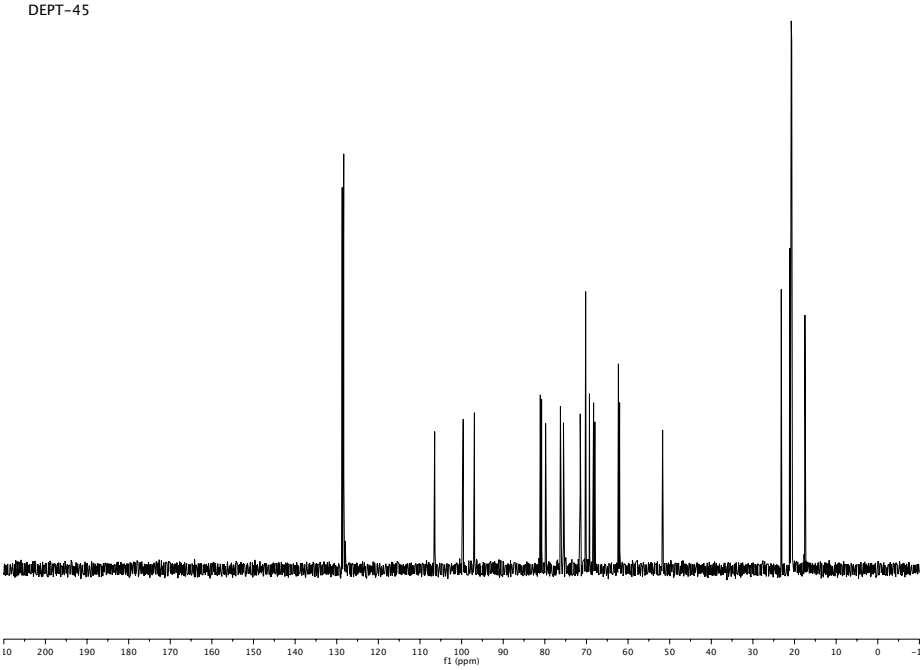

^{1}H-^{1}H COSY

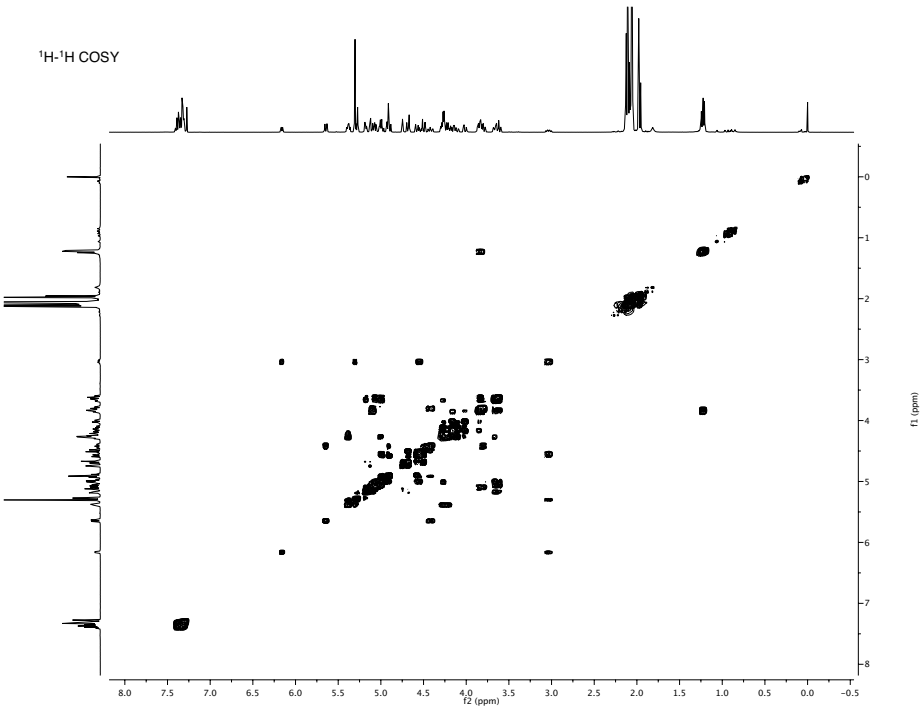

^{13}C–^{1}H HSQC

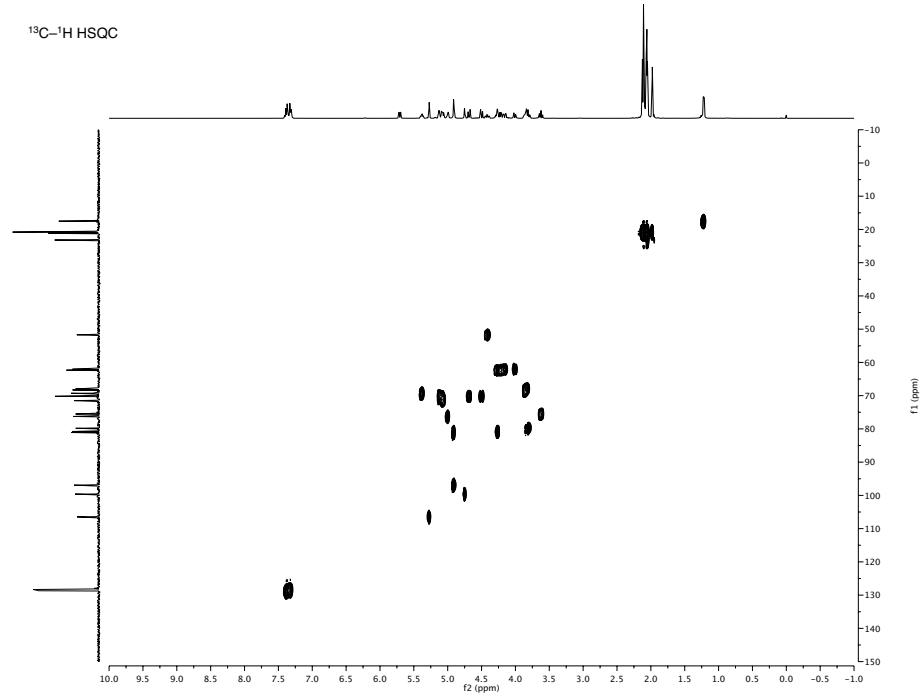

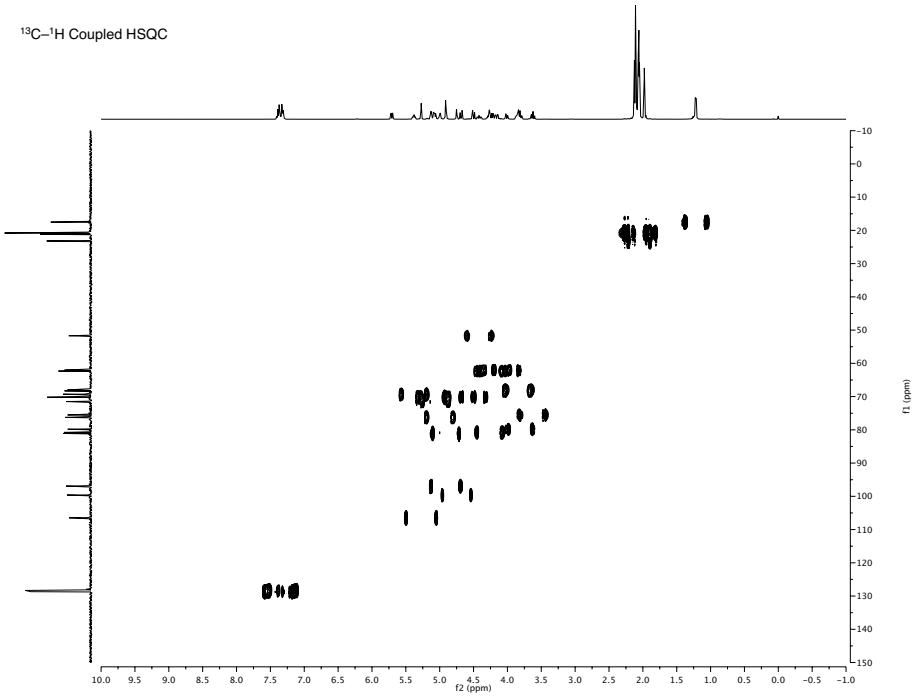
^{13}C–^{1}H Coupled HSQC
f2 (ppm)
f1 (ppm)

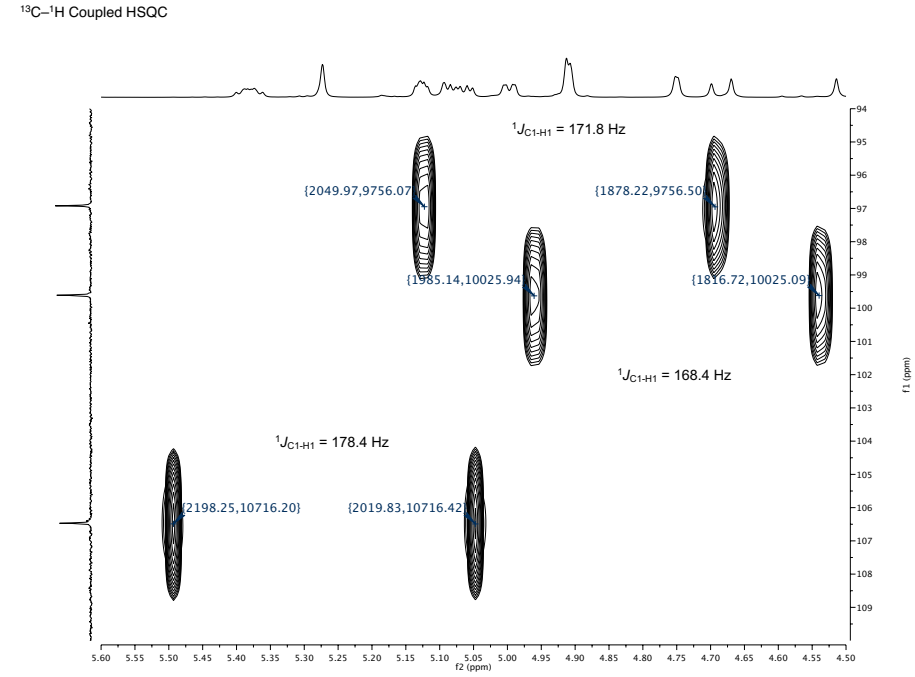
^{13}C–^{1}H Coupled HSQC
$^{1}J_{C1-H1}$ = 171.8 Hz
{2049.97,9756.07}
{1985.14,10025.94}
{1878.22,9756.50}
{1816.72,10025.09}
$^{1}J_{C1-H1}$ = 168.4 Hz
$^{1}J_{C1-H1}$ = 178.4 Hz
{2198.25,10716.20}
{2019.83,10716.42}
f2 (ppm)
f1 (ppm)

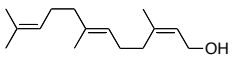
OH

6.08

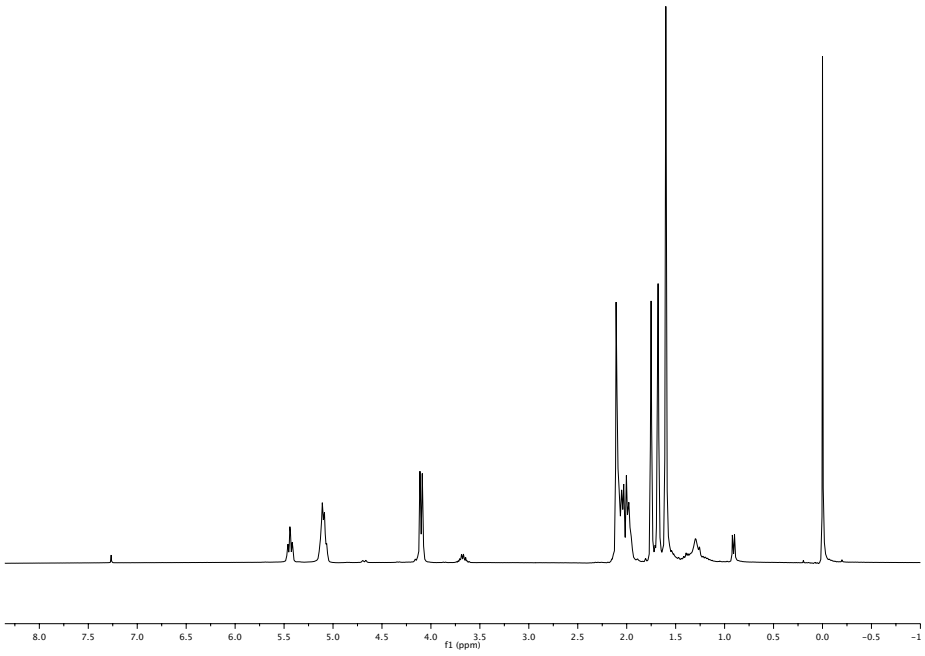
8.0
7.5
7.0
6.5
6.0
5.5
5.0
4.5
4.0
3.5
3.0
2.5
2.0
1.5
1.0
0.5
0.0
−0.5
−1
f1 (ppm)

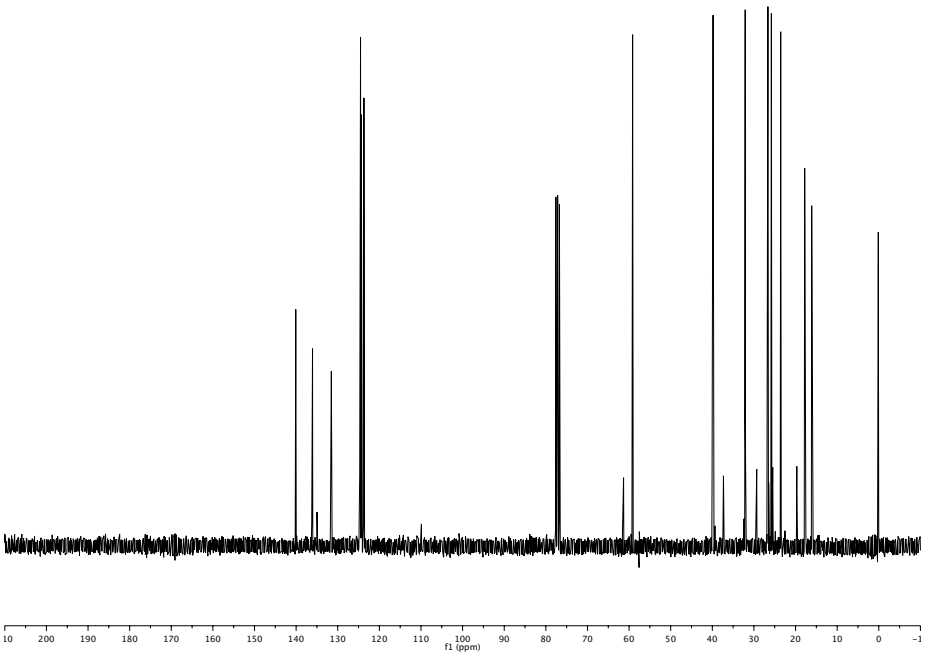
10
200
190
180
170
160
150
140
130
120
110
100
90
80
70
60
50
40
30
20
10
0
−1
f1 (ppm)

^{13}C–^{1}H HSQC

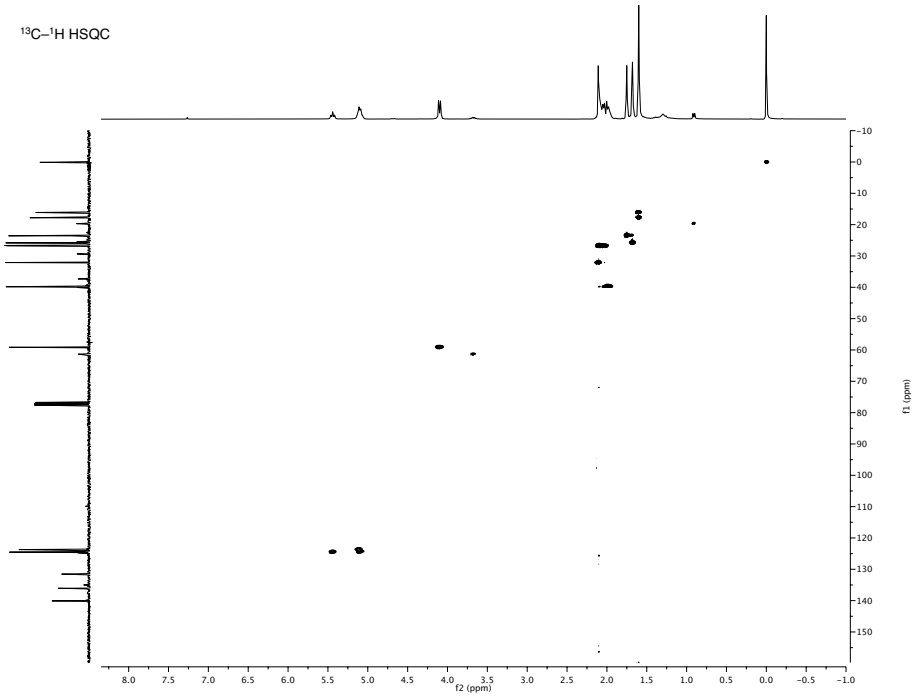

^{13}C–^{1}H HMBC

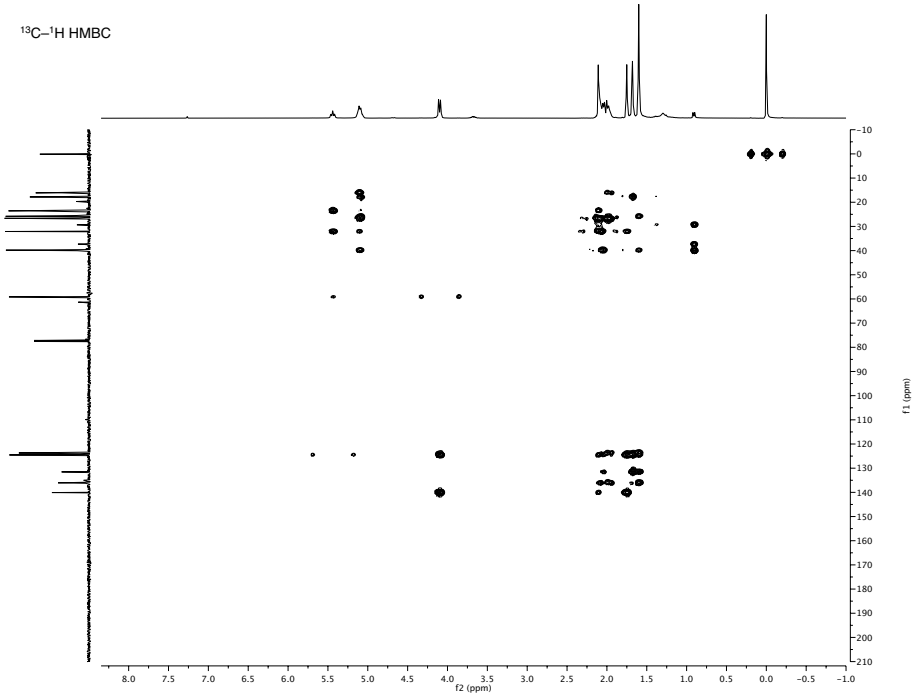

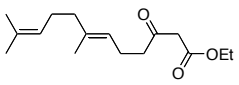
O
OEt
O

6.09

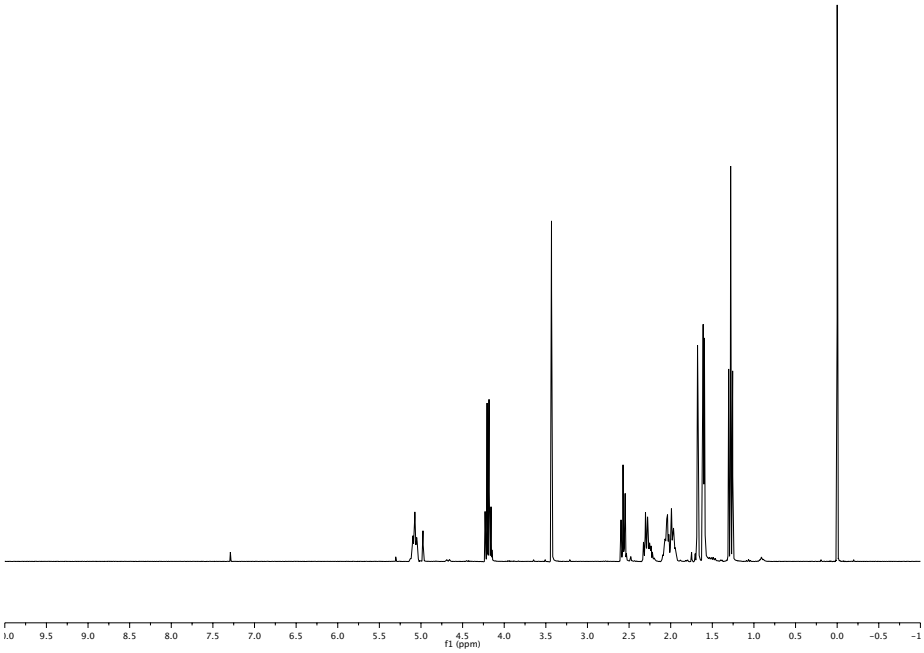
9.5
9.0
8.5
8.0
7.5
7.0
6.5
6.0
5.5
5.0
4.5
4.0
3.5
3.0
2.5
2.0
1.5
1.0
0.5
0.0
−0.5
f1 (ppm)

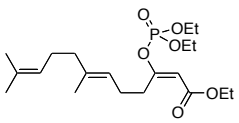

6.10

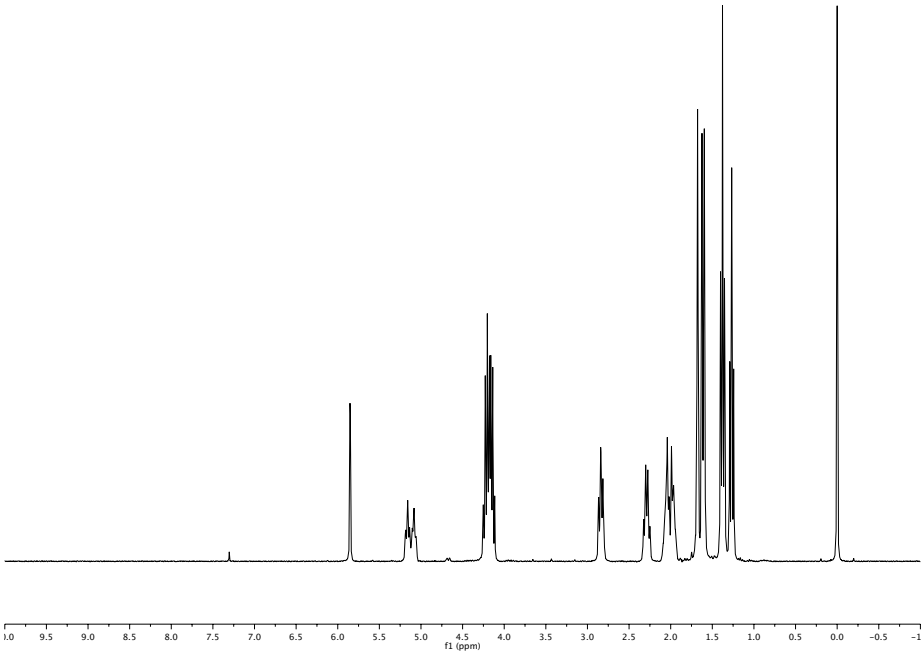

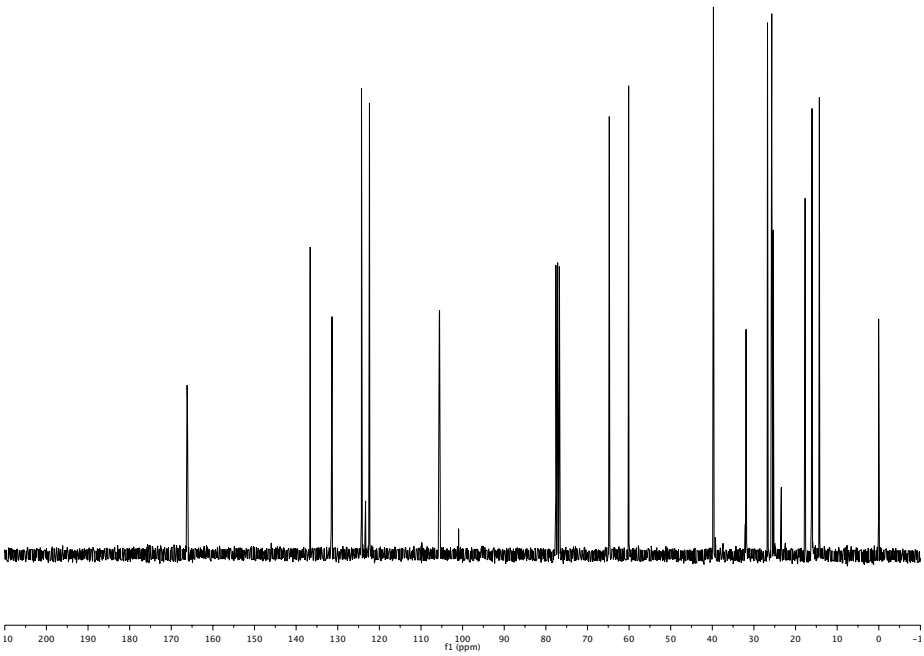

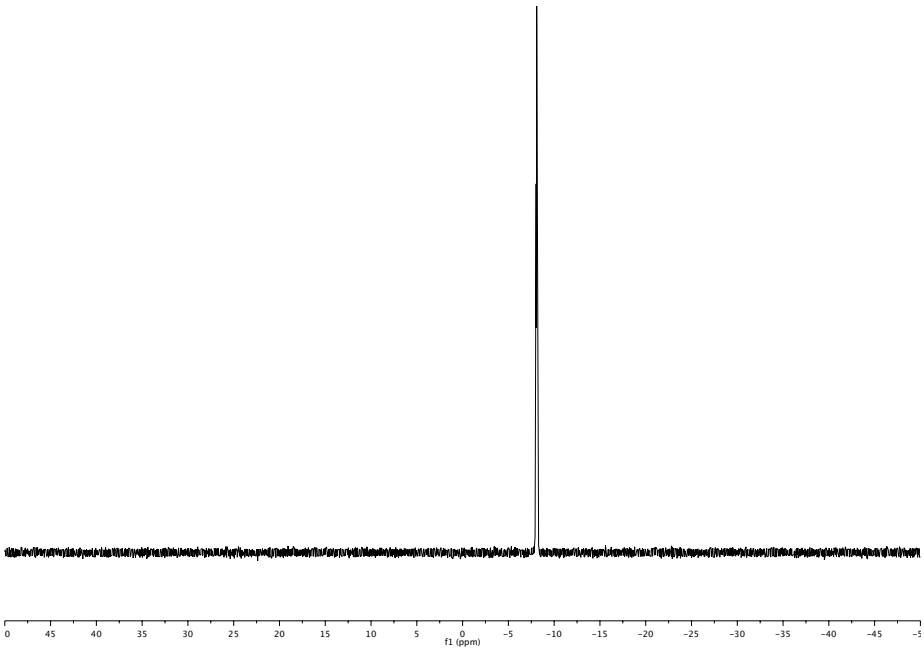
0
45
40
35
30
25
20
15
10
5
0
−5
−10
−15
−20
−25
−30
−35
−40
−45
f1 (ppm)

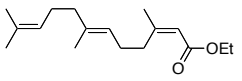

6.11

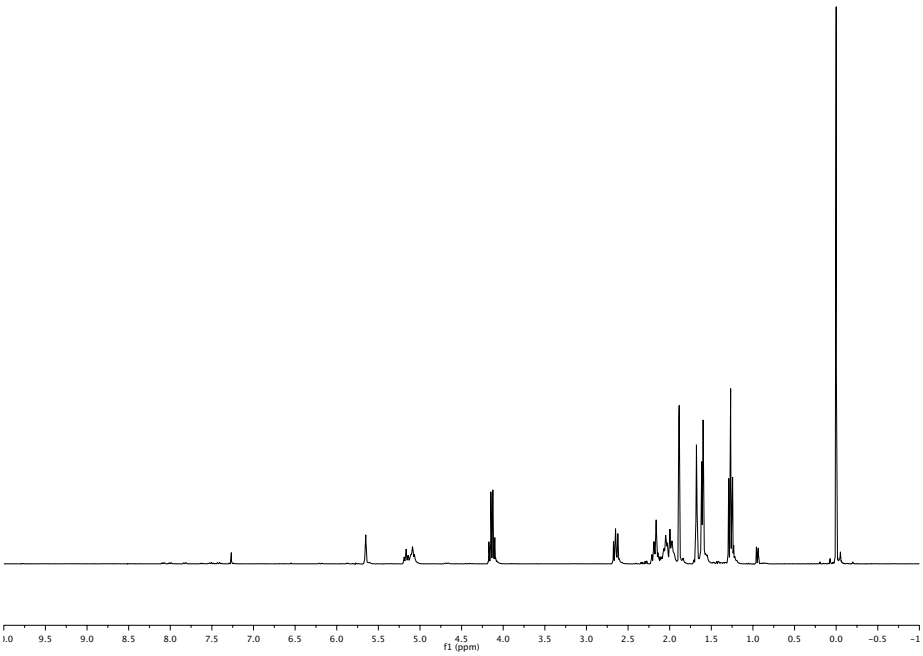

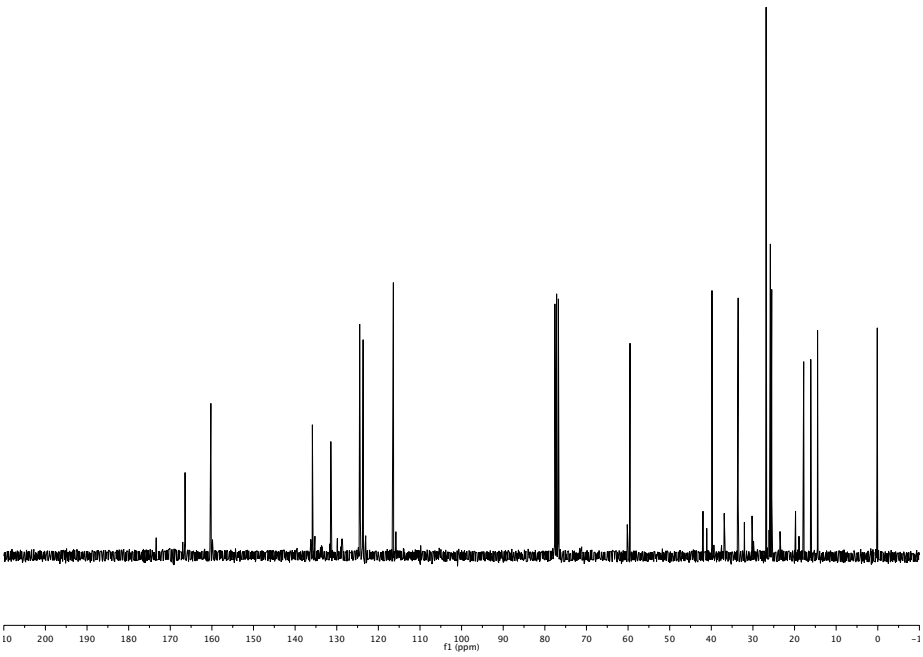

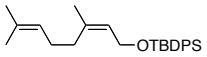

6.13

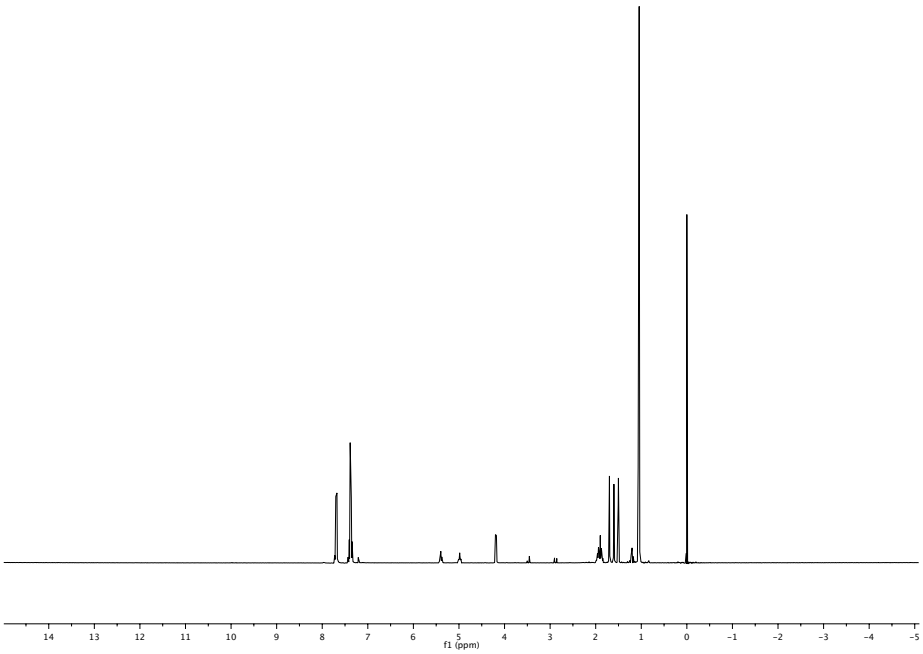

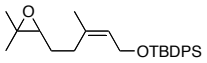
O
OTBDPS

6.14

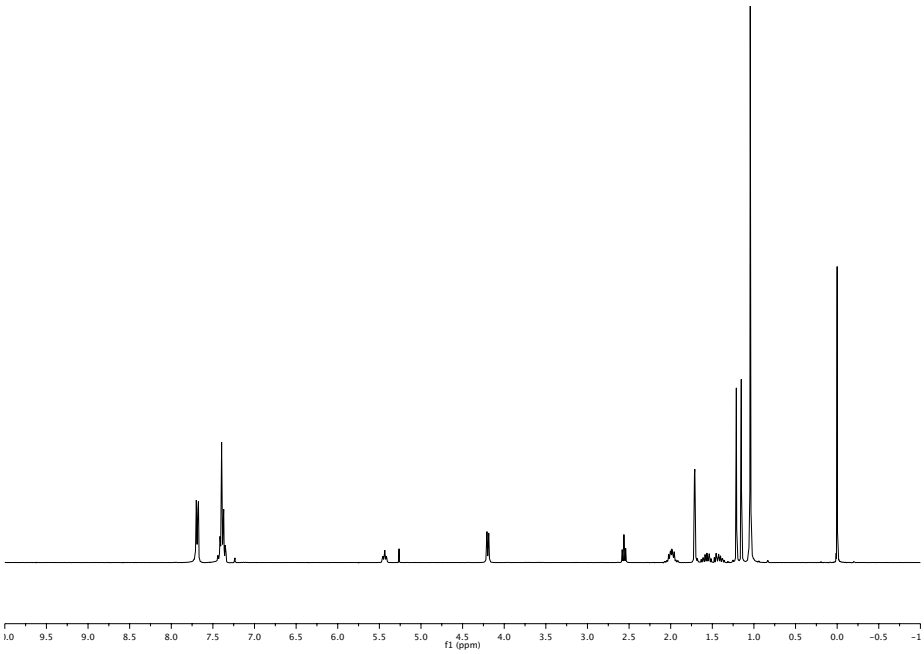
9.5
9.0
8.5
8.0
7.5
7.0
6.5
6.0
5.5
5.0
4.5
4.0
3.5
3.0
2.5
2.0
1.5
1.0
0.5
0.0
−0.5
f1 (ppm)

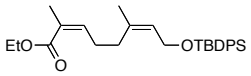
EtO
O
OTBDPS

6.16

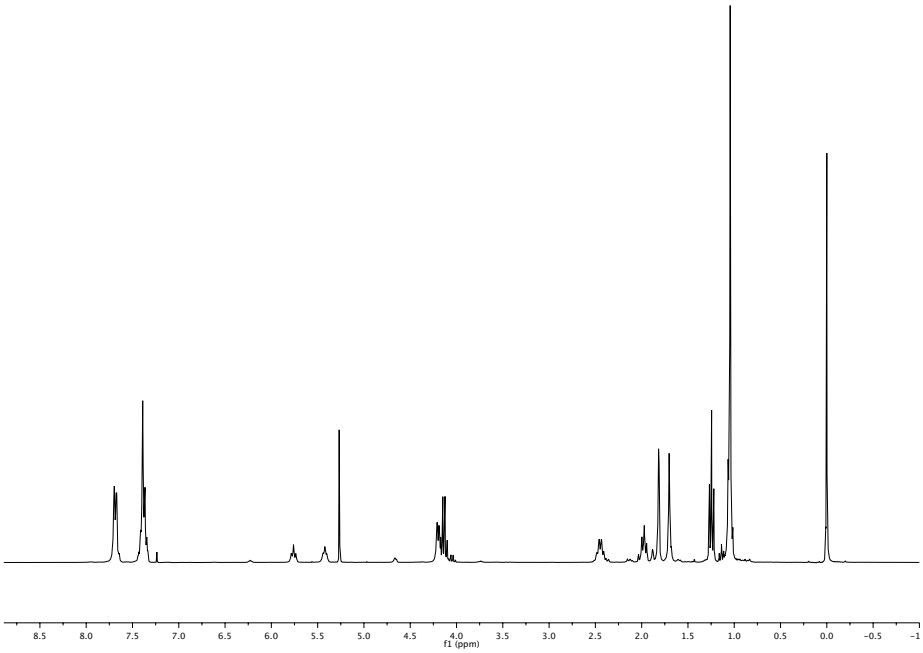
8.5
8.0
7.5
7.0
6.5
6.0
5.5
5.0
4.5
4.0
3.5
3.0
2.5
2.0
1.5
1.0
0.5
0.0
−0.5
−1
f1 (ppm)

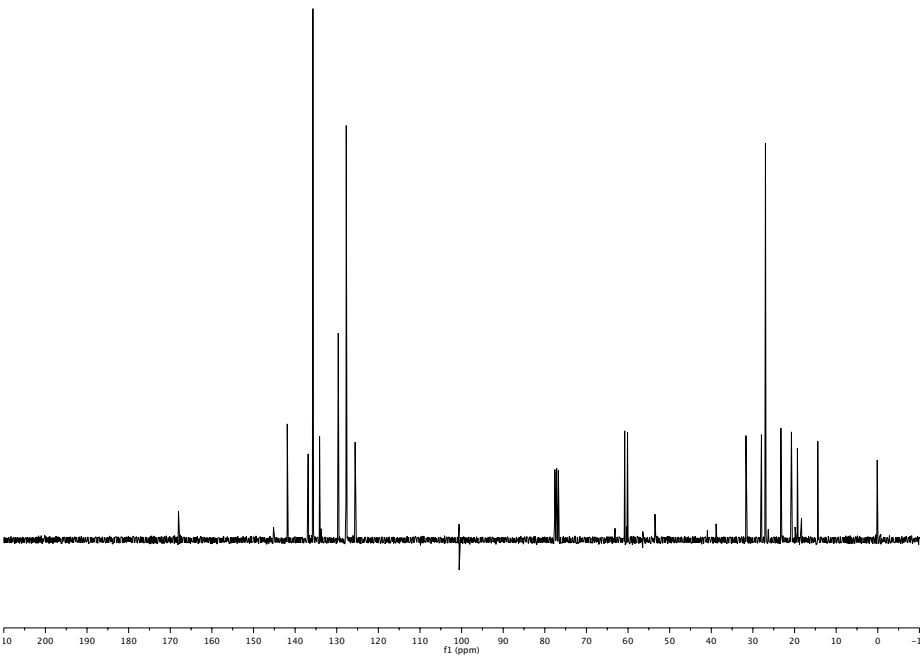
200
190
180
170
160
150
140
130
120
110
100
90
80
70
60
50
40
30
20
10
0
−1
f1 (ppm)

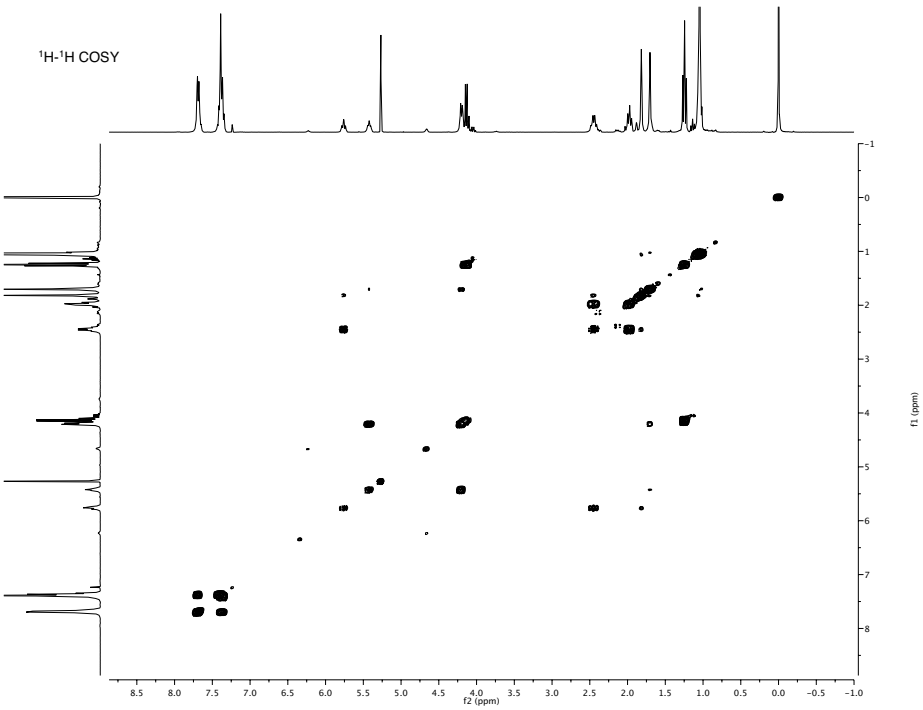
^{1}H-^{1}H COSY
f2 (ppm)
f1 (ppm)

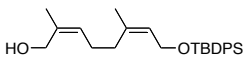

6.17

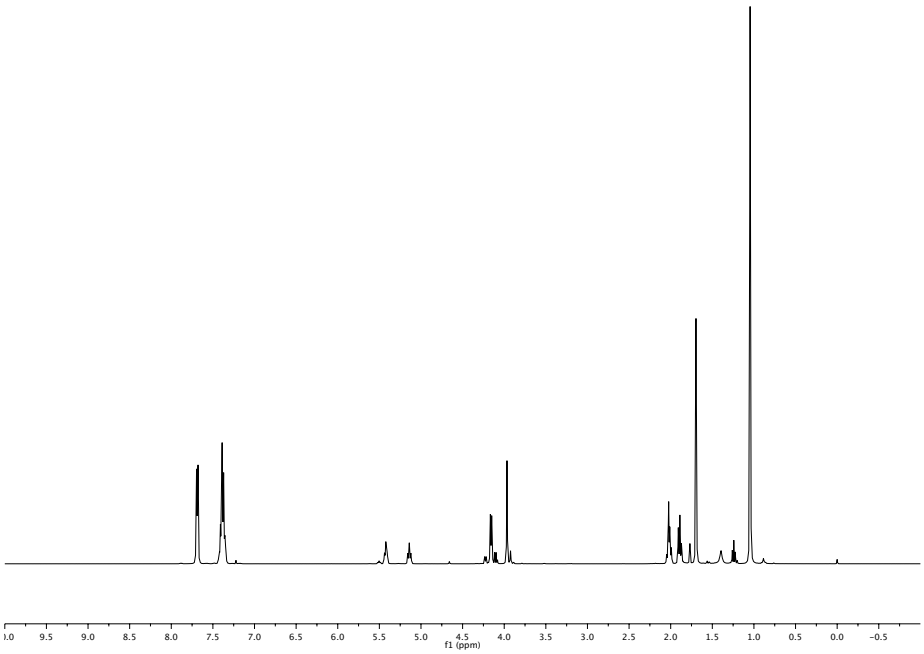

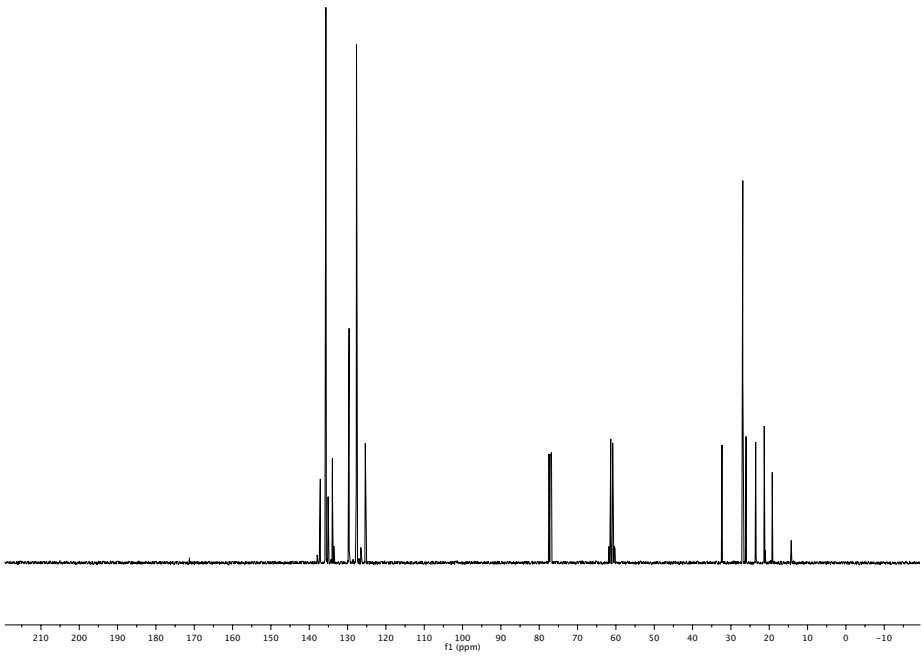

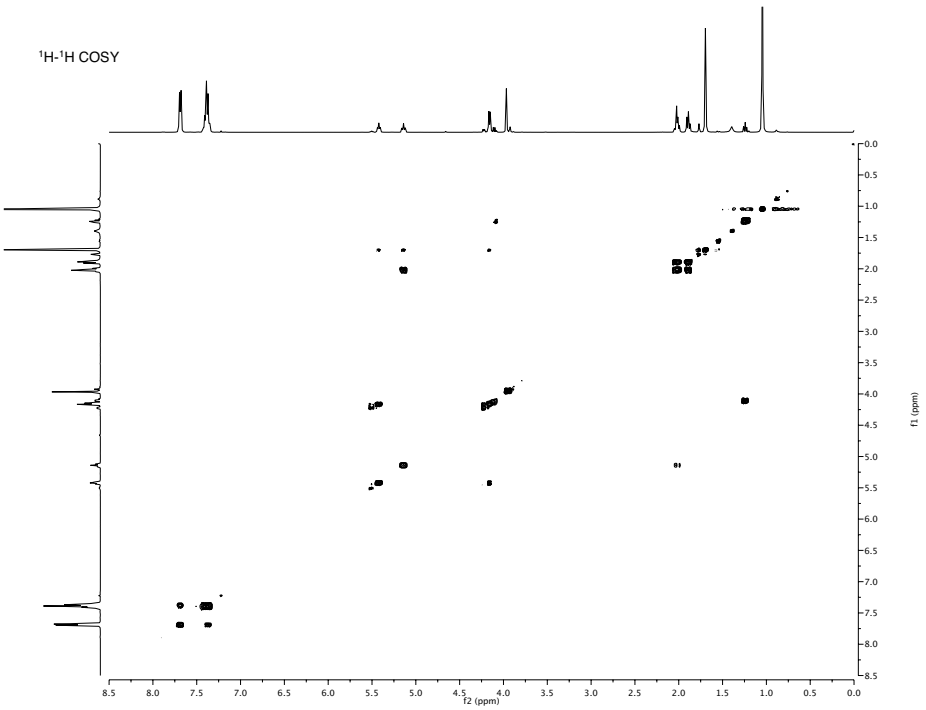
^{1}H-^{1}H COSY
f2 (ppm)
f1 (ppm)

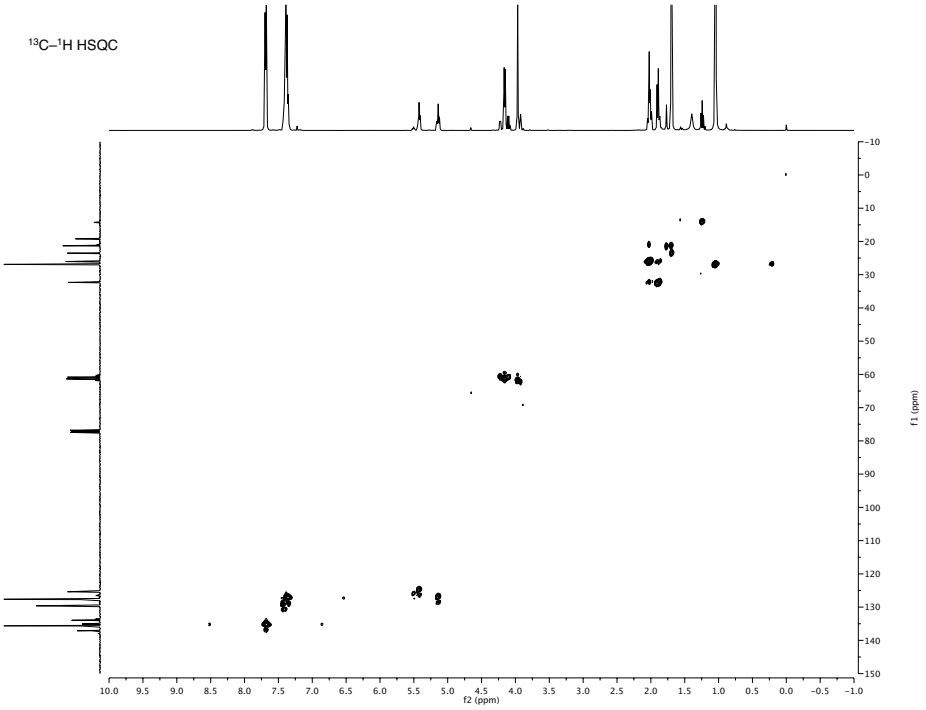
^{13}C–^{1}H HSQC
f2 (ppm)
f1 (ppm)

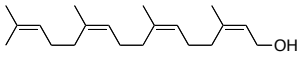

6.18

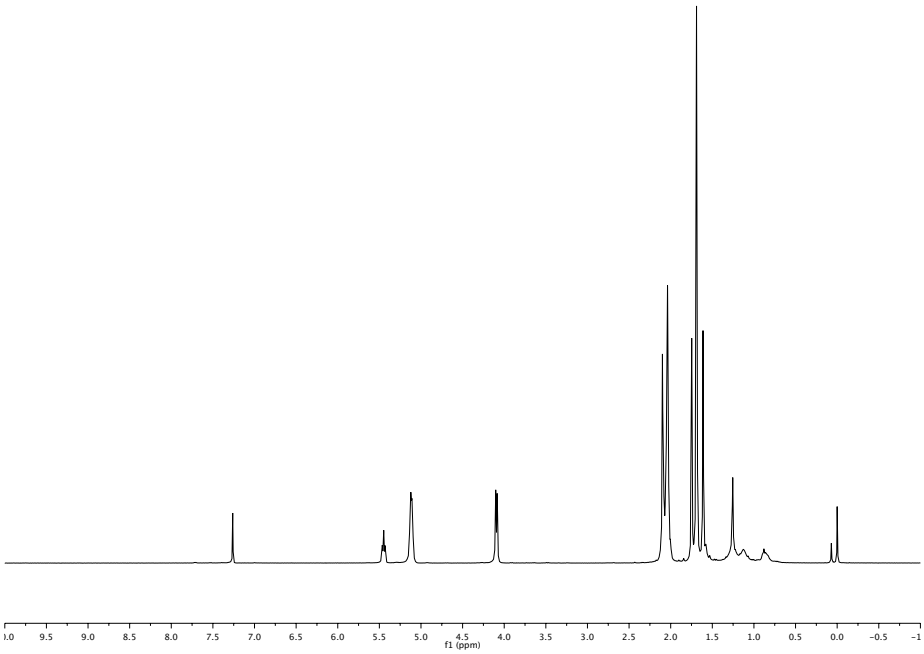

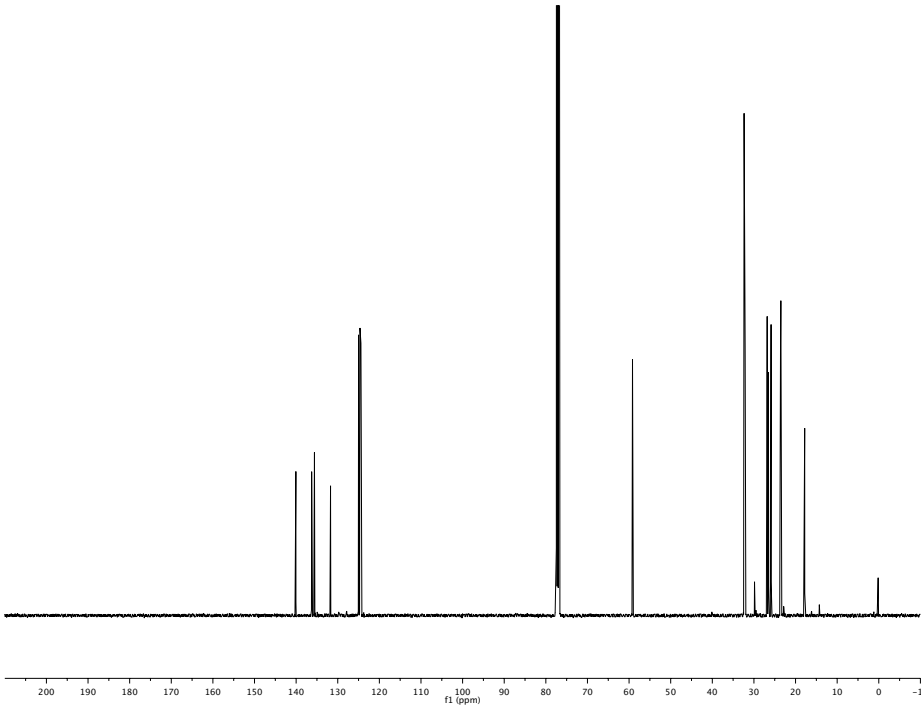

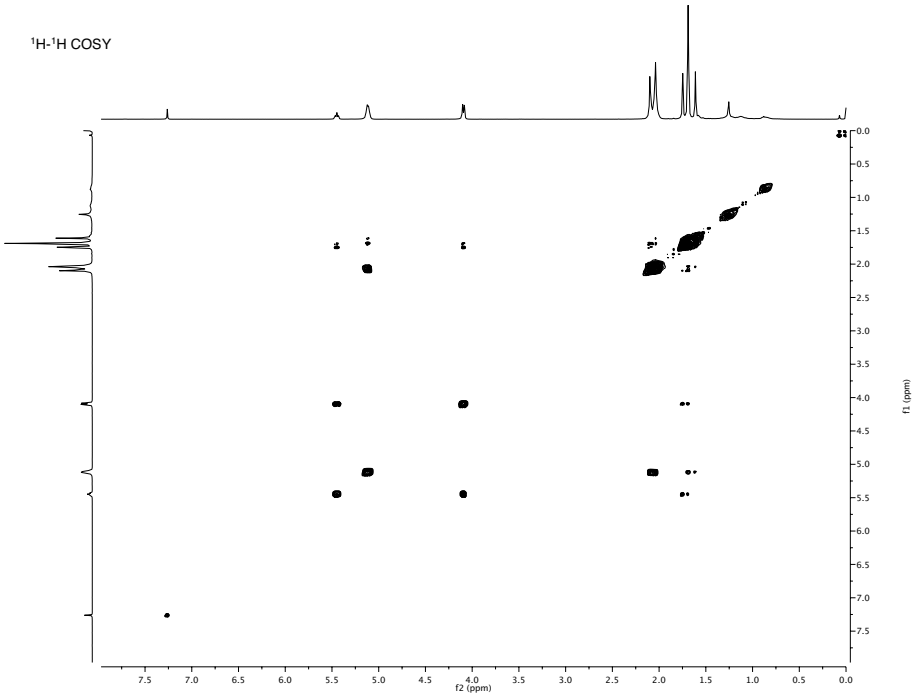
^{1}H-^{1}H COSY
f2 (ppm)
f1 (ppm)

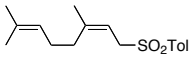

6.19

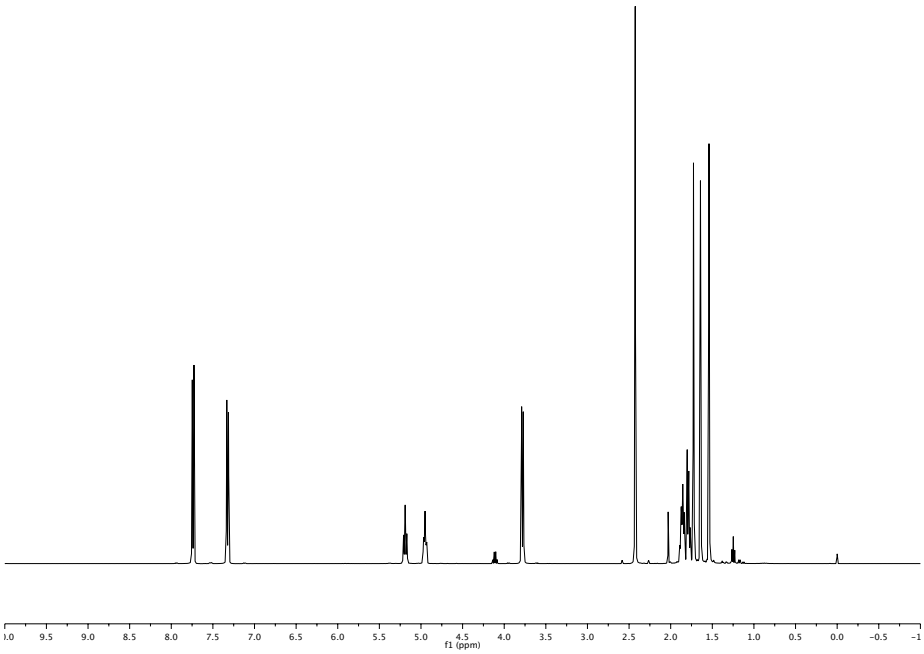

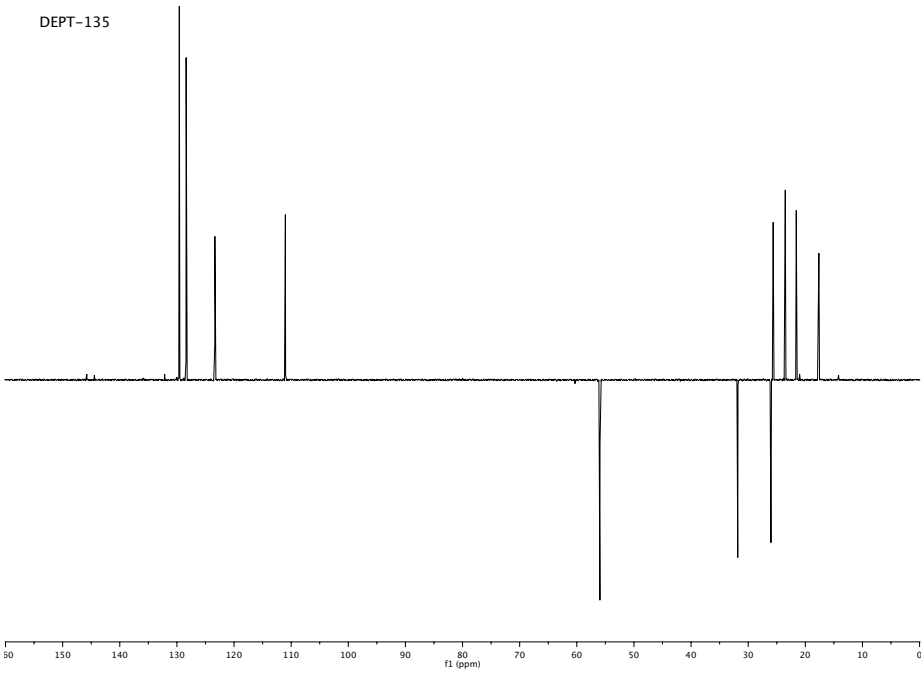

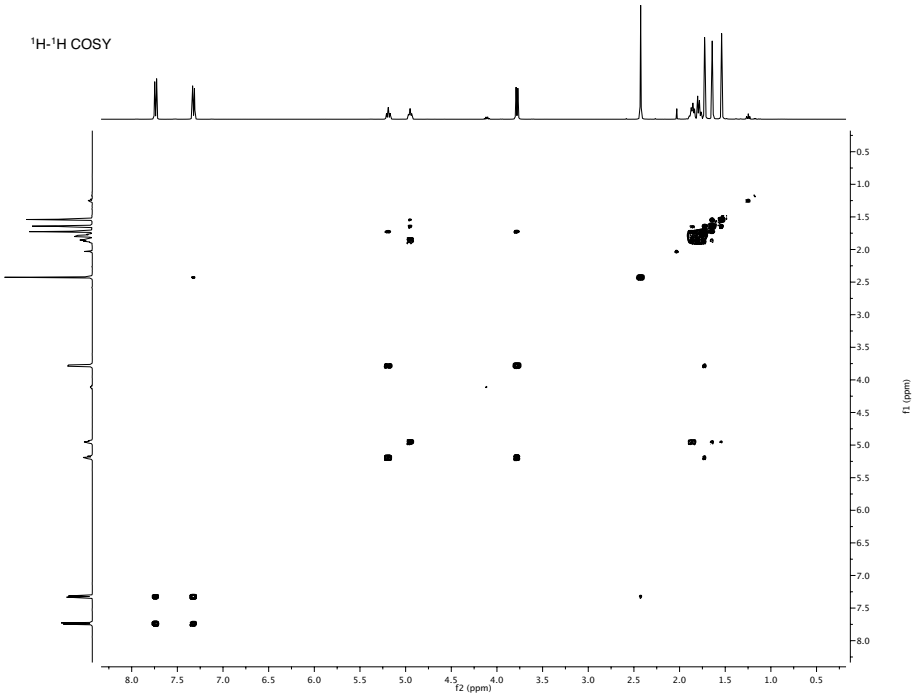
^{1}H-^{1}H COSY
f2 (ppm)
f1 (ppm)

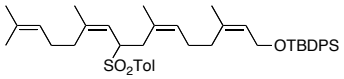

6.20

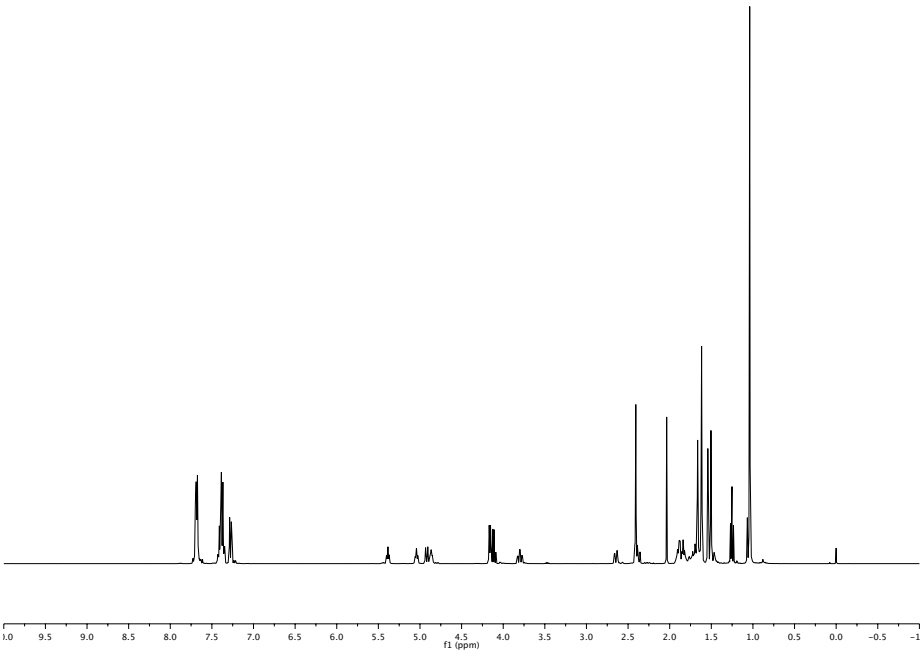

DEPT-135

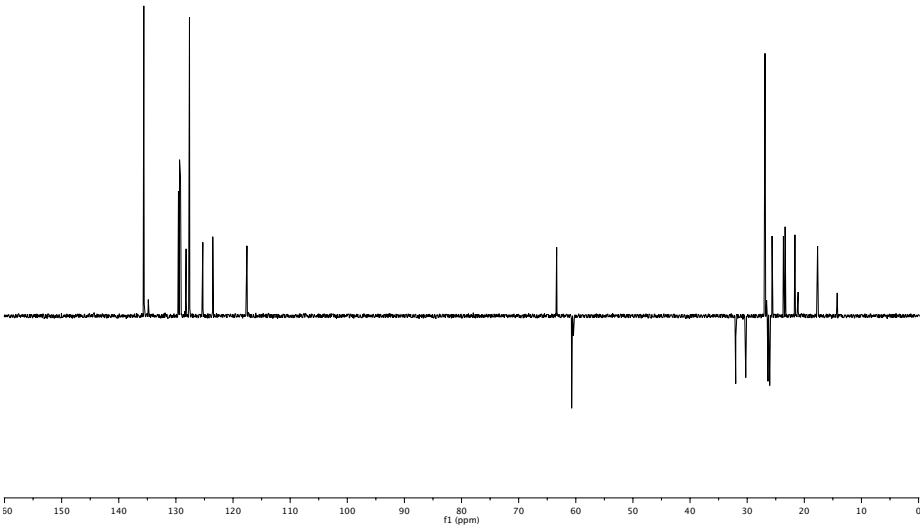

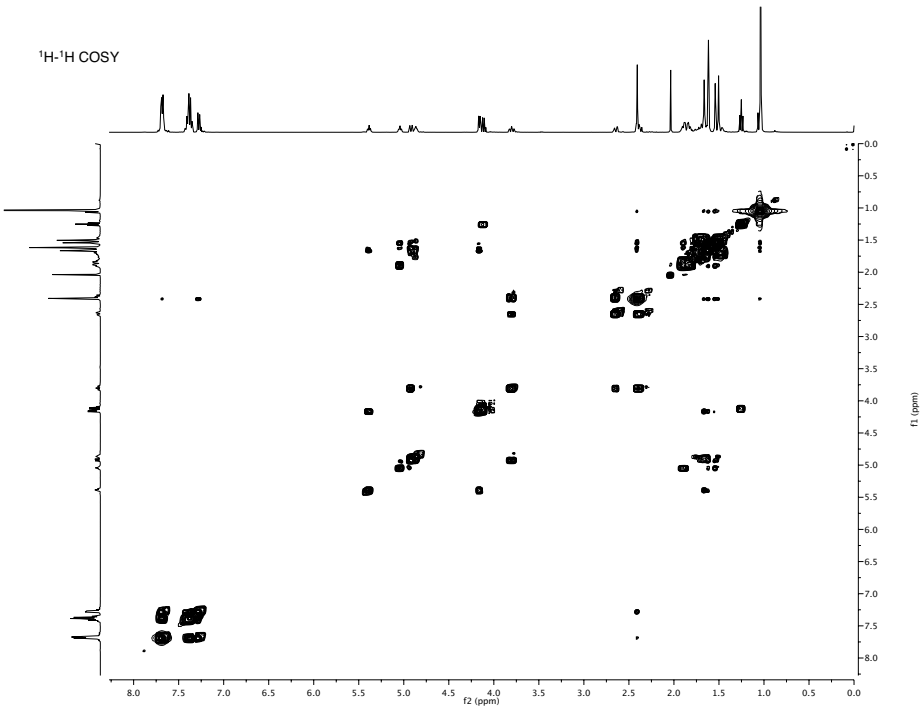
¹H-¹H COSY
f2 (ppm)
f1 (ppm)

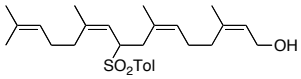

6.21

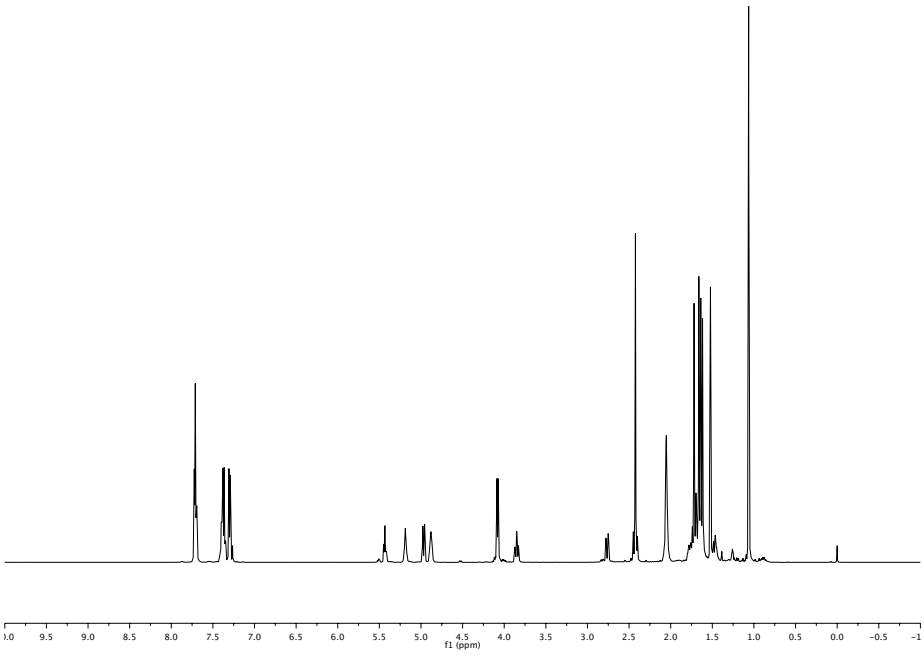

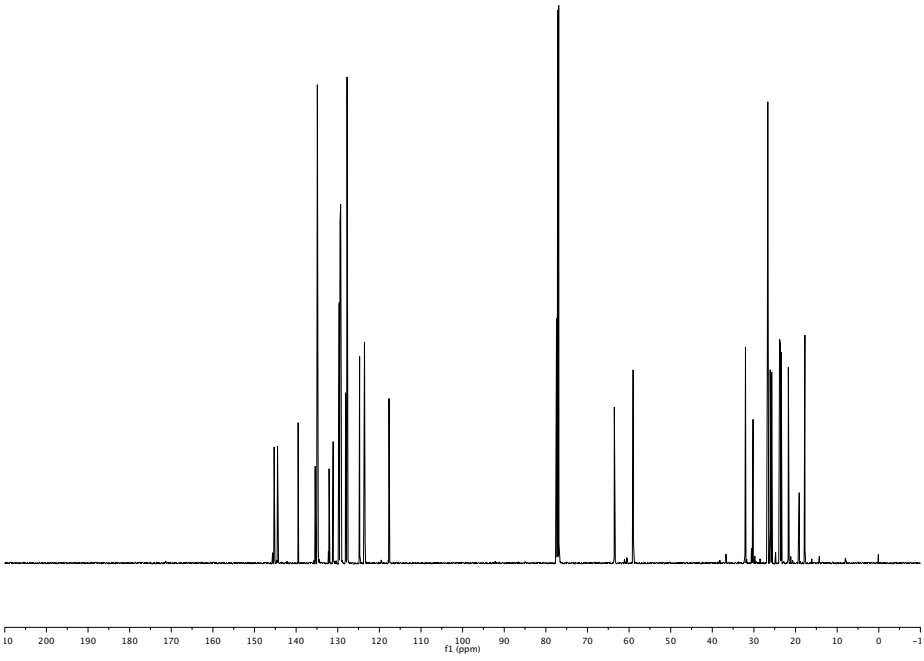

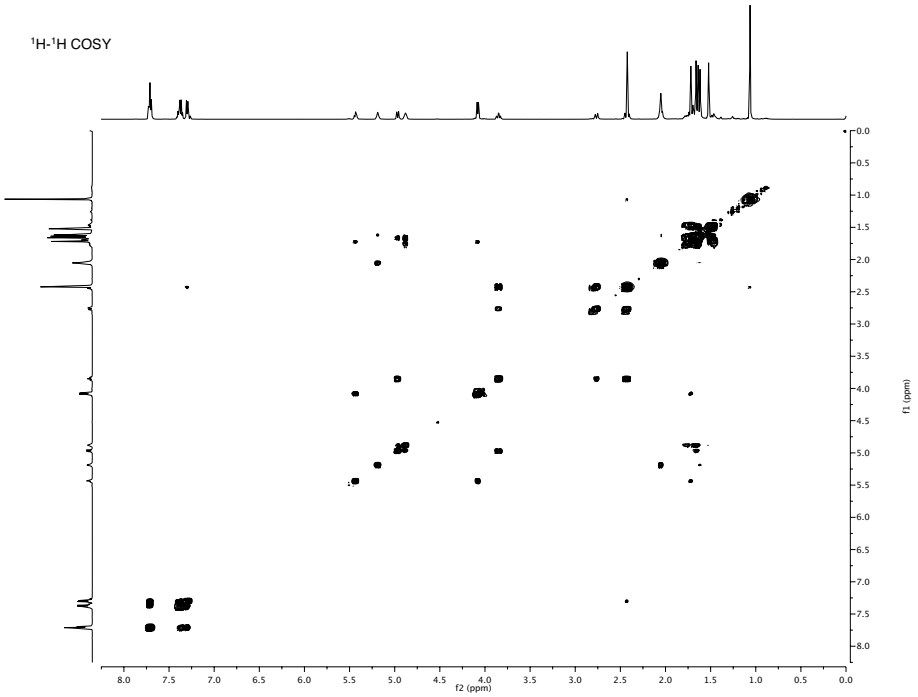
^{1}H-^{1}H COSY
f2 (ppm)
f1 (ppm)

Compiled References

1. Varki, A. Biological roles of oligosaccharides: all of the theories are correct. *Glycobiology* **1993**, *3*, 97-130.

2. Hart, G. W.; Housley, M. P.; Slawson, C. Cycling of O-linked [beta]-N-acetylglucosamine on nucleocytoplasmic proteins. *Nature* **2007**, *446*, 1017-22.

3. Spiro, R. G. Protein glycosylation: nature, distribution, enzymatic formation, and disease implications of glycopeptide bonds. *Glycobiology* **2002**, *12*, 43R-56R.

4. Bertozzi, C. R.; Kiessling; L., L. Chemical Glycobiology. *Science* **2001**, *291*, 2357-64.

5. Kiessling, L. L.; Splain, R. A. Chemical Approaches to Glycobiology. *Annu. Rev. Biochem.* **2010**, *79*, 619-53.

6. Blossom, D. B.; Kallen, A. J.; Patel, P. R.; Elward, A.; Robinson, L.; Gao, G.; Langer, R.; Perkins, K. M.; Jaeger, J. L.; Kurkjian, K. M.; Jones, M.; Schillie, S. F.; Shehab, N.; Ketterer, D.; Venkataraman, G.; Kishimoto, T. K.; Shriver, Z.; McMahon, A. W.; Austen, K. F.; Kozlowski, S.; Srinivasan, A.; Turabelidze, G.; Gould, C. V.; Arduino, M. J.; Sasisekharan, R. Outbreak of Adverse Reactions Associated with Contaminated Heparin. *New Engl. J. Med.* **2008**, *359*, 2674-84.

7. Seeberger, P. H.; Werz, D. B. Synthesis and medical applications of oligosaccharides. *Nature* **2007**, *446*, 1046-51.

8. Francis, C. W. Prophylaxis for Thromboembolism in Hospitalized Medical Patients. *New Engl. J. Med.* **2007**, *356*, 1438-44.

9. Asano, N. Glycosidase inhibitors: update and perspectives on practical use. *Glycobiology* **2003**, *13*, 93R-104R.

10. Moellering, R. C., Jr. In Vitro Antibacterial Activity of the Aminoglycoside Antibiotics. *Rev. Infect. Dis.* **1983**, *5*, S212-S32.

11. Wang, P.; Dong, S.; Shieh, J.-H.; Peguero, E.; Hendrickson, R.; Moore, M. A. S.; Danishefsky, S. J. Erythropoietin Derived by Chemical Synthesis. *Science* **2013**, *342*, 1357-60.

12. Coutinho, P. M.; Deleury, E.; Davies, G. J.; Henrissat, B. An Evolving Hierarchical Family Classification for Glycosyltransferases. *J. Mol. Biol.* **2003**, *328*, 307-17.

13. Lairson, L. L.; Henrissat, B.; Davies, G. J.; Withers, S. G. Glycosyltransferases: Structures, Functions, and Mechanisms. *Annu. Rev. Biochem.* **2008**, *77*, 521-55.

14. Tkacz, J. S.; Lampen, J. O. Tunicamycin inhibition of polyisoprenyl N-acetylglucosaminyl pyrophosphate formation in calf-liver microsomes. *Biochem. Biophys. Res. Commun.* **1975**, *65*, 248-57.

15. Ostash, B.; Walker, S. Moenomycin family antibiotics: chemical synthesis, biosynthesis, and biological activity. *Nat. Prod. Rep.* **2010**, *27*, 1594-617.

16. Liu, F.; Vijayakrishnan, B.; Faridmoayer, A.; Taylor, T. A.; Parsons, T. B.; Bernardes, G. J. L.; Kowarik, M.; Davis, B. G. Rationally Designed Short Polyisoprenol-Linked PglB Substrates for Engineered Polypeptide and Protein N-Glycosylation. *J. Am. Chem. Soc.* **2013**, *136*, 566-69.

17. Bugg, T. D. H. In *Comprehensive Natural Products Chemistry*; Barton, S. D., Nakanishi, K., Meth-Cohn, O., Eds.; Pergamon: Oxford, 1999, p 241-94.

18. Matsuhashi, M. Biosynthesis in the bacterial cell wall. *Tanpakushitsu Kakusan Koso* **1966**, *11*, 875-86.

19. Vollmer, W.; Höltje, J.-V. The Architecture of the Murein (Peptidoglycan) in Gram-Negative Bacteria: Vertical Scaffold or Horizontal Layer(s)? *J. Bacteriol.* **2004**, *186*, 5978-87.

20. Ikeda, M.; Wachi, M.; Jung, H. K.; Ishino, F.; Matsuhashi, M. The Escherichia coli mraY gene encoding UDP-N-acetylmuramoyl-pentapeptide: undecaprenyl-phosphate phospho-N-acetylmuramoyl-pentapeptide transferase. *J. Bacteriol.* **1991**, *173*, 1021-26.

21. Mengin-Lecreulx, D.; Texier, L.; Rousseau, M.; van Heijenoort, J. The murG gene of Escherichia coli codes for the UDP-N-acetylglucosamine: N-acetylmuramyl-(pentapeptide) pyrophosphoryl-undecaprenol N-acetylglucosamine transferase involved in the membrane steps of peptidoglycan synthesis. *J. Bacteriol.* **1991**, *173*, 4625-36.

22. Weppner, W. A.; Neuhaus, F. C. Fluorescent substrate for nascent peptidoglycan synthesis. Uridine diphosphate-N-acetylmuramyl-(Nepsilon-5-dimethylaminonaphthalene-1-sulfonyl)pentapeptide. *J. Biol. Chem.* **1977**, *252*, 2296-303.

23. Brandish, P. E.; Burnham, M. K.; Lonsdale, J. T.; Southgate, R.; Inukai, M.; Bugg, T. D. H. Slow Binding Inhibition of Phospho-N-acetylmuramyl-pentapeptide-translocase (Escherichia coli) by Mureidomycin A. *J. Biol. Chem.* **1996**, *271*, 7609-14.

24. Auger, G.; Crouvoisier, M.; Caroff, M.; van Heijenoort, J.; Blanot, D. Synthesis of an analogue of the lipoglycopeptide membrane intermediate I of peptidoglycan biosynthesis. *Lett. Pept. Sci.* **1997**, *4*, 371-76.

25. Auger, G.; van Heijenoort, J.; Mengin-Lecreulx, D.; Blanot, D. A MurG assay which utilises a synthetic analogue of lipid I. *FEMS Microbiol. Lett.* **2003**, *219*, 115-19.

26. Men, H.; Park, P.; Ge, M.; Walker, S. Substrate Synthesis and Activity Assay for MurG. *J. Am. Chem. Soc.* **1998**, *120*, 2484-85.

27. Ha, S.; Chang, E.; Lo, M.-C.; Men, H.; Park, P.; Ge, M.; Walker, S. The Kinetic Characterization of Escherichia coli MurG Using Synthetic Substrate Analogues. *J. Am. Chem. Soc.* **1999**, *121*, 8415-26.

28. Chen, L.; Men, H.; Ha, S.; Ye, X.-Y.; Brunner, L.; Hu, Y.; Walker, S. Intrinsic Lipid Preferences and Kinetic Mechanism of *Escherichia coli* MurG. *Biochemistry* **2002**, *41*, 6824-33.

29. Liu, H.; Ritter, T. K.; Sadamoto, R.; Sears, P. S.; Wu, M.; Wong, C.-H. Acceptor Specificity and Inhibition of the Bacterial Cell-Wall Glycosyltransferase MurG. *ChemBioChem* **2003**, *4*, 603-09.

30. Breukink, E.; van Heusden, H. E.; Vollmerhaus, P. J.; Swiezewska, E.; Brunner, L.; Walker, S.; Heck, A. J. R.; de Kruijff, B. Lipid II Is an Intrinsic Component of the Pore Induced by Nisin in Bacterial Membranes. *J. Biol. Chem.* **2003**, *278*, 19898-903.

31. Goffin, C.; Ghuysen, J.-M. Multimodular Penicillin-Binding Proteins: An Enigmatic Family of Orthologs and Paralogs. *Microbiol. Mol. Biol. Rev.* **1998**, *62*, 1079-93.

32. Barna, J. C. J.; Williams, D. H. The Structure and Mode of Action of Glycopeptide Antibiotics of the Vancomycin Group. *Annu. Rev. Microbiol.* **1984**, *38*, 339-57.

33. Chen, L.; Walker, D.; Sun, B.; Hu, Y.; Walker, S.; Kahne, D. Vancomycin analogues active against vanA-resistant strains inhibit bacterial transglycosylase without binding substrate. *Proc. Natl. Acad. Sci. USA* **2003**, *100*, 5658-63.

34. Ye, X.-Y.; Lo, M.-C.; Brunner, L.; Walker, D.; Kahne, D.; Walker, S. Better Substrates for Bacterial Transglycosylases. *J. Am. Chem. Soc.* **2001**, *123*, 3155-56.

35. Leimkuhler, C.; Chen, L.; Barrett, D.; Panzone, G.; Sun, B.; Falcone, B.; Oberthür, M.; Donadio, S.; Walker, S.; Kahne, D. Differential Inhibition of Staphylococcus aureus PBP2 by Glycopeptide Antibiotics. *J. Am. Chem. Soc.* **2005**, *127*, 3250-51.

36. Gampe, C. M.; Tsukamoto, H.; Wang, T.-S. A.; Walker, S.; Kahne, D. Modular synthesis of diphospholipid oligosaccharide fragments of the bacterial cell wall and their use to study the mechanism of moenomycin and other antibiotics. *Tetrahedron* **2011**, *67*, 9771-78.

37. Zhang, Y.; Fechter, E. J.; Wang, T.-S. A.; Barrett, D.; Walker, S.; Kahne, D. E. Synthesis of Heptaprenyl−Lipid IV to Analyze Peptidoglycan Glycosyltransferases. *J. Am. Chem. Soc.* **2007**, *129*, 3080-81.

38. Shih, H.-W.; Chen, K.-T.; Cheng, T.-J. R.; Wong, C.-H.; Cheng, W.-C. A New Synthetic Approach toward Bacterial Transglycosylase Substrates, Lipid II and Lipid IV. *Org. Lett.* **2011**, *13*, 4600-03.

39. Perlstein, D. L.; Zhang, Y.; Wang, T.-S.; Kahne, D. E.; Walker, S. The Direction of Glycan Chain Elongation by Peptidoglycan Glycosyltransferases. *J. Am. Chem. Soc.* **2007**, *129*, 12674-75.

40. Lebar, M. D.; Lupoli, T. J.; Tsukamoto, H.; May, J. M.; Walker, S.; Kahne, D. Forming Cross-Linked Peptidoglycan from Synthetic Gram-Negative Lipid II. *J. Am. Chem. Soc.* **2013**, *135*, 4632-35.

41. Schwartz, B.; Markwalder, J. A.; Seitz, S. P.; Wang, Y.; Stein, R. L. A Kinetic Characterization of the Glycosyltransferase Activity of Eschericia coli PBP1b and Development of a Continuous Fluorescence Assay. *Biochemistry* **2002**, *41*, 12552-61.

42. Huang, C.-Y.; Shih, H.-W.; Lin, L.-Y.; Tien, Y.-W.; Cheng, T.-J. R.; Cheng, W.-C.; Wong, C.-H.; Ma, C. Crystal structure of Staphylococcus aureus transglycosylase in complex with a lipid II analog and elucidation of peptidoglycan synthesis mechanism. *Proc. Natl. Acad. Sci. USA* **2012**, *109*, 6496-501.

43. Shih, H.-W.; Chang, Y.-F.; Li, W.-J.; Meng, F.-C.; Huang, C.-Y.; Ma, C.; Cheng, T.-J. R.; Wong, C.-H.; Cheng, W.-C. Effect of the Peptide Moiety of Lipid II on Bacterial Transglycosylase. *Angew. Chem. Int. Ed.* **2012**, *51*, 10123-26.

44. Neuhaus, F. C.; Baddiley, J. A Continuum of Anionic Charge: Structures and Functions of d-Alanyl-Teichoic Acids in Gram-Positive Bacteria. *Microbiol. Mol. Biol. Rev.* **2003**, *67*, 686-723.

45. Baddiley, J. Structure, biosynthesis, and function of teichoic acids. *Acc. Chem. Res.* **1970**, *3*, 98-105.

46. Doyle, R. J.; McDannel, M. L.; Streips, U. N.; Birdsell, D. C.; Young, F. E. Polyelectrolyte Nature of Bacterial Teichoic Acids. *J. Bacteriol.* **1974**, *118*, 606-15.

47. Yokoyama, K.; Miyashita, T.; Araki, Y.; Ito, E. Structure and functions of linkage unit intermediates in the biosynthesis of ribitol teichoic acids in Staphylococcus aureus H and Bacillus subtilis W23. *Eur. J. Biochem.* **1986**, *161*, 479-89.

48. Mauël, C.; Young, M.; Margot, P.; Karamata, D. The essential nature of teichoic acids in Bacillus subtilis as revealed by insertional mutagenesis. *Molec. Gen. Genet.* **1989**, *215*, 388-94.

49. Bhavsar, A. P.; Erdman, L. K.; Schertzer, J. W.; Brown, E. D. Teichoic Acid Is an Essential Polymer in Bacillus subtilis That Is Functionally Distinct from Teichuronic Acid. *J. Bacteriol.* **2004**, *186*, 7865-73.

50. Weidenmaier, C.; Kokai-Kun, J. F.; Kristian, S. A.; Chanturiya, T.; Kalbacher, H.; Gross, M.; Nicholson, G.; Neumeister, B.; Mond, J. J.; Peschel, A. Role of teichoic acids in Staphylococcus aureus nasal colonization, a major risk factor in nosocomial infections. *Nat. Med.* **2004**, *10*, 243-45.

51. Weidenmaier, C.; Peschel, A.; Xiong, Y.-Q.; Kristian, S. A.; Dietz, K.; Yeaman, M. R.; Bayer, A. S. Lack of Wall Teichoic Acids in Staphylococcus aureus Leads to Reduced Interactions with Endothelial Cells and to Attenuated Virulence in a Rabbit Model of Endocarditis. *J. Infect. Dis.* **2005**, *191*, 1771-77.

52. Marquis, R. E.; Mayzel, K.; Carstensen, E. L. Cation exchange in cell walls of gram-positive bacteria. *Can. J. Microbiol.* **1976**, *22*, 975-82.

53. Doyle, R. J.; Matthews, T. H.; Streips, U. N. Chemical basis for selectivity of metal ions by the Bacillus subtilis cell wall. *J. Bacteriol.* **1980**, *143*, 471-80.

54. Swoboda, J. G.; Campbell, J.; Meredith, T. C.; Walker, S. Wall Teichoic Acid Function, Biosynthesis, and Inhibition. *ChemBioChem* **2010**, *11*, 35-45.

55. Ginsberg, C.; Zhang, Y.-H.; Yuan, Y.; Walker, S. In Vitro Reconstitution of Two Essential Steps in Wall Teichoic Acid Biosynthesis. *ACS Chem. Biol.* **2006**, *1*, 25-28.

56. Zhang, Y.-H.; Ginsberg, C.; Yuan, Y.; Walker, S. Acceptor Substrate Selectivity and Kinetic Mechanism of Bacillus subtilis TagA†. *Biochemistry* **2006**, *45*, 10895-904.

57. Bhavsar, A. P.; Truant, R.; Brown, E. D. The TagB Protein in Bacillus subtilis 168 Is an Intracellular Peripheral Membrane Protein That Can Incorporate Glycerol Phosphate onto a Membrane-bound Acceptor in Vitro. *J. Biol. Chem.* **2005**, *280*, 36691-700.

58. Toshima, K.; Tatsuta, K. Recent progress in O-glycosylation methods and its application to natural products synthesis. *Chem. Rev.* **1993**, *93*, 1503-31.

59. Young, F. E.; Smith, C.; Reilly, B. E. Chromosomal Location of Genes Regulating Resistance to Bacteriophage in Bacillus subtilis. *J. Bacteriol.* **1969**, *98*, 1087-97.

60. Allison, S. E.; D'Elia, M. A.; Arar, S.; Monteiro, M. A.; Brown, E. D. Studies of the Genetics, Function, and Kinetic Mechanism of TagE, the Wall Teichoic Acid Glycosyltransferase in Bacillus subtilis 168. *J. Biol. Chem.* **2011**, *286*, 23708-16.

61. Bera, A.; Biswas, R.; Herbert, S.; Kulauzovic, E.; Weidenmaier, C.; Peschel, A.; Götz, F. Influence of Wall Teichoic Acid on Lysozyme Resistance in Staphylococcus aureus. *J. Bacteriol.* **2007**, *189*, 280-83.

62. Gross, M.; Cramton, S. E.; Götz, F.; Peschel, A. Key Role of Teichoic Acid Net Charge inStaphylococcus aureus Colonization of Artificial Surfaces. *Infect. Immun.* **2001**, *69*, 3423-26.

63. Qian, Z.; Yin, Y.; Zang, Y.; Lu, L.; Li, Y.; Jiang, Y. Genomic characterization of ribitol teichoic acid synthesis in *Staphylococcus aureus*: genes, genomic organization and gene duplication. *BMC Genomics* **2006**, *7*, 74.

64. Brown, S.; Zhang, Y.-H.; Walker, S. A Revised Pathway Proposed for Staphylococcus aureus Wall Teichoic Acid Biosynthesis Based on In Vitro Reconstitution of the Intracellular Steps. *Chem. Biol.* **2008**, *15*, 12-21.

65. Nothaft, H.; Szymanski, C. M. Protein glycosylation in bacteria: sweeter than ever. *Nat. Rev. Microbiol.* **2010**, *8*, 765-78.

66. Eichler, J. Extreme sweetness: protein glycosylation in archaea. *Nat. Rev. Microbiol.* **2013**, *11*, 151-56.

67. Szymanski, C. M.; Yao, R.; Ewing, C. P.; Trust, T. J.; Guerry, P. Evidence for a system of general protein glycosylation in Campylobacter jejuni. *Mol. Microbiol.* **1999**, *32*, 1022-30.

68. Szymanski, C. M.; Wren, B. W. Protein glycosylation in bacterial mucosal pathogens. *Nat. Rev. Microbiol.* **2005**, *3*, 225-37.

69. Young, N. M.; Brisson, J.-R.; Kelly, J.; Watson, D. C.; Tessier, L.; Lanthier, P. H.; Jarrell, H. C.; Cadotte, N.; St. Michael, F.; Aberg, E.; Szymanski, C. M. Structure of the N-Linked Glycan Present on Multiple Glycoproteins in the Gram-negative Bacterium, Campylobacter jejuni. *J. Biol. Chem.* **2002**, *277*, 42530-39.

70. Chen, M. M.; Weerapana, E.; Ciepichal, E.; Stupak, J.; Reid, C. W.; Swiezewska, E.; Imperiali, B. Polyisoprenol specificity in the Campylobacter jejuni N-linked glycosylation pathway. *Biochemistry* **2007**, *46*, 14342-48.

71. Lujan, D. K.; Stanziale, J. A.; Mostafavi, A. Z.; Sharma, S.; Troutman, J. M. Chemoenzymatic synthesis of an isoprenoid phosphate tool for the analysis of complex bacterial oligosaccharide biosynthesis. *Carbohydr. Res.* **2012**, *359*, 44-53.

72. Mostafavi, A. Z.; Troutman, J. M. Biosynthetic Assembly of the Bacteroides fragilis Capsular Polysaccharide A Precursor Bactoprenyl Diphosphate-Linked Acetamido-4-amino-6-deoxygalactopyranose. *Biochemistry* **2013**, *52*, 1939-49.

73. Aas, F. E.; Vik, Å.; Vedde, J.; Koomey, M.; Egge-Jacobsen, W. Neisseria gonorrhoeae O-linked pilin glycosylation: functional analyses define both the biosynthetic pathway and glycan structure. *Mol. Microbiol.* **2007**, *65*, 607-24.

74. Hartley, M. D.; Morrison, M. J.; Aas, F. E.; Børud, B.; Koomey, M.; Imperiali, B. Biochemical Characterization of the O-linked Glycosylation Pathway in Nesseria gonorrhoeae Responsible for Biosynthesis of Protein Glycans Containing N,N'-Diacetylbacillosamine. *Biochemistry* **2011**, *50*, 4936-48.

75. Voisin, S.; Houliston, R. S.; Kelly, J.; Brisson, J.-R.; Watson, D.; Bardy, S. L.; Jarrell, K. F.; Logan, S. M. Identification and Characterization of the Unique N-Linked Glycan Common to the Flagellins and S-layer Glycoprotein of Methanococcus voltae. *J. Biol. Chem.* **2005**, *280*, 16586-93.

76. Shams-Eldin, H.; Chaban, B.; Niehus, S.; Schwarz, R. T.; Jarrell, K. F. Identification of the Archaeal alg7 Gene Homolog (Encoding N-Acetylglucosamine-1-Phosphate Transferase) of the N-Linked Glycosylation System by Cross-Domain Complementation in Saccharomyces cerevisiae. *J. Bacteriol.* **2008**, *190*, 2217-20.

77. Chaban, B.; Logan, S. M.; Kelly, J. F.; Jarrell, K. F. AglC and AglK Are Involved in Biosynthesis and Attachment of Diacetylated Glucuronic Acid to the N-Glycan in Methanococcus voltae. *J. Bacteriol.* **2009**, *191*, 187-95.

78. Larkin, A.; Chang, M. M.; Whitworth, G. E.; Imperiali, B. Biochemical evidence for an alternate pathway in N-linked glycoprotein biosynthesis. *Nat. Chem. Biol.* **2013**, *9*, 367-73.

79. Shenoi, S.; Friedland, G. Extensively Drug-Resistant Tuberculosis: A New Face to an Old Pathogen. *Annu. Rev. Med.* **2009**, *60*, 307-20.

80. Nguyen, L.; Pieters, J. Mycobacterial Subversion of Chemotherapeutic Reagents and Host Defense Tactics: Challenges in Tuberculosis Drug Development. *Annu. Rev. Pharmacol. Toxicol.* **2009**, *49*, 427-53.

81. Aagaard, C.; Hoang, T.; Dietrich, J.; Cardona, P.-J.; Izzo, A.; Dolganov, G.; Schoolnik, G. K.; Cassidy, J. P.; Billeskov, R.; Andersen, P. A multistage tuberculosis vaccine that confers efficient protection before and after exposure. *Nat. Med.* **2011**, *17*, 189-94.

82. Azuma, I.; Thomas, D. W.; Adam, A.; Ghuysen, J. M.; Bonaly, R.; Petit, J. F.; Lederer, E. Occurrence of N-glycolylmuramic acid in bacterial cell walls: A preliminary survey. *Biochim. Biophys. Acta* **1970**, *208*, 444-51.

83. Mahapatra, S.; Scherman, H.; Brennan, P. J.; Crick, D. C. N Glycolylation of the Nucleotide Precursors of Peptidoglycan Biosynthesis of Mycobacterium spp. Is Altered by Drug Treatment. *J. Bacteriol.* **2005**, *187*, 2341-47.

84. Raymond, J. B.; Mahapatra, S.; Crick, D. C.; Pavelka, M. S. Identification of the namH Gene, Encoding the Hydroxylase Responsible for the N-Glycolylation of the Mycobacterial Peptidoglycan. *J. Biol. Chem.* **2005**, *280*, 326-33.

85. Bhakta, S.; Basu, J. Overexpression, purification and biochemical characterization of a class A high-molecular-mass penicillin-binding protein (PBP), PBP1* and its soluble derivative from Mycobacterium tuberculosis. *Biochem. J* **2002**, *361*, 635-39.

86. Goffin, C.; Ghuysen, J.-M. Biochemistry and Comparative Genomics of SxxK Superfamily Acyltransferases Offer a Clue to the Mycobacterial Paradox: Presence of Penicillin-Susceptible Target Proteins versus Lack of Efficiency of Penicillin as Therapeutic Agent. *Microbiol. Mol. Biol. Rev.* **2002**, *66*, 702-38.

87. Patru, M.-M.; Pavelka, M. S. A Role for the Class A Penicillin-Binding Protein PonA2 in the Survival of Mycobacterium smegmatis under Conditions of Nonreplication. *J. Bacteriol.* **2010**, *192*, 3043-54.

88. Meng, F.-C.; Chen, K.-T.; Huang, L.-Y.; Shih, H.-W.; Chang, H.-H.; Nien, F.-Y.; Liang, P.-H.; Cheng, T.-J. R.; Wong, C.-H.; Cheng, W.-C. Total Synthesis of Polyprenyl N-Glycolyl Lipid II as a Mycobacterial Transglycosylase Substrate. *Org. Lett.* **2011**, *13*, 5306-09.

89. Chen, K.-T.; Kuan, Y.-C.; Fu, W.-C.; Liang, P.-H.; Cheng, T.-J. R.; Wong, C.-H.; Cheng, W.-C. Rapid Preparation of Mycobacterium N-Glycolyl Lipid I and Lipid II Derivatives: A Biocatalytic Approach. *Chem. Eur. J.* **2013**, *19*, 834-38.

90. Liu, C.-Y.; Guo, C.-W.; Chang, Y.-F.; Wang, J.-T.; Shih, H.-W.; Hsu, Y.-F.; Chen, C.-W.; Chen, S.-K.; Wang, Y.-C.; Cheng, T.-J. R.; Ma, C.; Wong, C.-H.; Fang, J.-M.; Cheng, W.-C. Synthesis and Evaluation of a New Fluorescent Transglycosylase Substrate: Lipid II-Based Molecule Possessing a Dansyl-C20 Polyprenyl Moiety. *Org. Lett.* **2010**, *12*, 1608-11.

91. Huang, S.-H.; Wu, W.-S.; Huang, L.-Y.; Huang, W.-F.; Fu, W.-C.; Chen, P.-T.; Fang, J.-M.; Cheng, W.-C.; Cheng, T.-J. R.; Wong, C.-H. New Continuous Fluorometric Assay for Bacterial Transglycosylase Using Förster Resonance Energy Transfer. *J. Am. Chem. Soc.* **2013**, *135*, 17078-89.

92. Bhamidi, S.; Scherman, M. S.; Rithner, C. D.; Prenni, J. E.; Chatterjee, D.; Khoo, K.-H.; McNeil, M. R. The Identification and Location of Succinyl Residues and the Characterization of the Interior Arabinan Region Allow for a Model of the Complete Primary Structure of Mycobacterium tuberculosis Mycolyl Arabinogalactan. *J. Biol. Chem.* **2008**, *283*, 12992-3000.

93. Daffe, M.; Brennan, P. J.; McNeil, M. Predominant structural features of the cell wall arabinogalactan of Mycobacterium tuberculosis as revealed through characterization of oligoglycosyl alditol fragments by gas chromatography/mass spectrometry and by 1H and 13C NMR analyses. *J. Biol. Chem.* **1990**, *265*, 6734-43.

94. Richards, M. R.; Lowary, T. L. Chemistry and Biology of Galactofuranose-Containing Polysaccharides. *ChemBioChem* **2009**, *10*, 1920-38.

95. Tefsen, B.; Ram, A. F.; van Die, I.; Routier, F. H. Galactofuranose in eukaryotes: aspects of biosynthesis and functional impact. *Glycobiology* **2012**, *22*, 456-69.

96. Turco, S. J.; Descoteaux, A. The Lipophosphoglycan of Leishmania Parasites. *Annu. Rev. Microbiol.* **1992**, *46*, 65-92.

97. Brener, Z. Biology of Trypanosoma Cruzi. *Annu. Rev. Microbiol.* **1973**, *27*, 347-82.

98. de Lederkremer, R. M.; Agusti, R. In *Advances in Carbohydrate Chemistry and Biochemistry*; Derek, H., Ed.; Academic Press: 2009; Vol. 62, p 311-66.

99. Pan, F.; Jackson, M.; Ma, Y.; McNeil, M. Cell Wall Core Galactofuran Synthesis Is Essential for Growth of Mycobacteria. *J. Bacteriol.* **2001**, *183*, 3991-98.

100. Mikušová, K.; Mikuš, M.; Besra, G. S.; Hancock, I.; Brennan, P. J. Biosynthesis of the linkage region of the mycobacterial cell wall. *J. Biol. Chem.* **1996**, *271*, 7820-28.

101. Mills, J. A.; Motichka, K.; Jucker, M.; Wu, H. P.; Uhlik, B. C.; Stern, R. J.; Scherman, M. S.; Vissa, V. D.; Pan, F.; Kundu, M.; Ma, Y. F.; McNeil, M. Inactivation of the mycobacterial rhamnosyltransferase, which is needed for the formation of the arabinogalactan-peptidoglycan linker, leads to irreversible loss of viability. *J. Biol. Chem.* **2004**, *279*, 43540-46.

102. Sassetti, C. M.; Boyd, D. H.; Rubin, E. J. Genes required for mycobacterial growth defined by high density mutagenesis. *Mol. Microbiol.* **2003**, *48*, 77-84.

103. McNeil, M.; Daffe, M.; Brennan, P. J. Evidence for the nature of the link between the arabinogalactan and peptidoglycan of mycobacterial cell walls. *J. Biol. Chem.* **1990**, *265*, 18200-06.

104. Tsvetkov, Y. E.; Nikolaev, A. V. The first chemical synthesis of UDP-[small alpha]-D-galactofuranose. *J. Chem. Soc., Perkin Trans. 1* **2000**, 889-91.

105. Zhang, Q.; Liu, H.-w. Studies of UDP-Galactopyranose Mutase from Escherichia coli: An Unusual Role of Reduced FAD in Its Catalysis. *J. Am. Chem. Soc.* **2000**, *122*, 9065-70.

106. Marlow, A. L.; Kiessling, L. L. Improved Chemical Synthesis of UDP-Galactofuranose. *Org. Lett.* **2001**, *3*, 2517-19.

107. Mikušová, K. n.; Yagi, T.; Stern, R.; McNeil, M. R.; Besra, G. S.; Crick, D. C.; Brennan, P. J. Biosynthesis of the Galactan Component of the Mycobacterial Cell Wall. *J. Biol. Chem.* **2000**, *275*, 33890-97.

108. Mikušová, K.; Beláňová, M.; Korduláková, J.; Honda, K.; McNeil, M. R.; Mahapatra, S.; Crick, D. C.; Brennan, P. J. Identification of a novel galactosyl transferase involved in biosynthesis of the mycobacterial cell wall. *J. Bacteriol.* **2006**, *188*, 6592-98.

109. Alderwick, L. J.; Dover, L. G.; Veerapen, N.; Gurcha, S. S.; Kremer, L.; Roper, D. L.; Pathak, A. K.; Reynolds, R. C.; Besra, G. S. Expression, purification and characterisation of soluble GlfT and the identification of a novel galactofuranosyltransferase Rv3782 involved in priming GlfT-mediated galactan polymerisation in Mycobacterium tuberculosis. *Protein Expression Purif.* **2008**, *58*, 332-41.

110. Beláňová, M.; Dianišková, P.; Brennan, P. J.; Completo, G. C.; Rose, N. L.; Lowary, T. L.; Mikušová, K. Galactosyl transferases in mycobacterial cell wall synthesis. *J. Bacteriol.* **2008**, *190*, 1141-45.

111. Peltier, P.; Beláňová, M.; Dianišková, P.; Zhou, R.; Zheng, R. B.; Pearcey, J. A.; Joe, M.; Brennan, P. J.; Nugier-Chauvin, C.; Ferrières, V.; Lowary, T. L.; Daniellou, R.; Mikušová, K. Synthetic UDP-Furanoses as Potent Inhibitors of Mycobacterial Galactan Biogenesis. *Chem. Biol.* **2010**, *17*, 1356-66.

112. Martinez Farias, M. A.; Kincaid, V. A.; Annamalai, V. R.; Kiessling, L. L. Isoprenoid Phosphonophosphates as Glycosyltransferase Acceptor Substrates. *J. Am. Chem. Soc.*, DOI: 10.1021/ja500622v.

113. Kremer, L.; Dover, L. G.; Morehouse, C.; Hitchin, P.; Everett, M.; Morris, H. R.; Dell, A.; Brennan, P. J.; McNeil, M. R.; Flaherty, C.; Duncan, K.; Besra, G. S. Galactan Biosynthesis in

Mycobacterium tuberculosis : Identification of a Bifunctional UDP-Galactofuranosyltransferase. *J. Biol. Chem.* **2001**, *276*, 26430-40.

114. Pathak, A. K.; Pathak, V.; Seitz, L.; Maddry, J. A.; Gurcha, S. S.; Besra, G. S.; Suling, W. J.; Reynolds, R. C. Studies on (β ,1→5) and (β ,1→6) linked octyl Galf disaccharides as substrates for mycobacterial galactosyltransferase activity. *Bioorg. Med. Chem.* **2001**, *9*, 3129-43.

115. Rose, N. L.; Completo, G. C.; Lin, S.-J.; McNeil, M.; Palcic, M. M.; Lowary, T. L. Expression, purification, and characterization of a galactofuranosyltransferase involved in Mycobacterium tuberculosis arabinogalactan biosynthesis. *J. Am. Chem. Soc.* **2006**, *128*, 6721-29.

116. May, J. F.; Splain, R. A.; Brotschi, C.; Kiessling, L. L. A tethering mechanism for length control in a processive carbohydrate polymerization. *Proc. Natl. Acad. Sci. USA* **2009**, *106*, 11851-56.

117. Levengood, M. R.; Splain, R. A.; Kiessling, L. L. Monitoring processivity and length control of a carbohydrate polymerase. *J. Am. Chem. Soc.* **2011**, *133*, 12758-66.

118. Splain, R. A.; Kiessling, L. L. Synthesis of galactofuranose-based acceptor substrates for the study of the carbohydrate polymerase GlfT2. *Bioorg. Med. Chem.* **2010**, *18*, 3753-59.

119. May, J. F.; Levengood, M. R.; Splain, R. A.; Brown, C. D.; Kiessling, L. L. A Processive Carbohydrate Polymerase That Mediates Bifunctional Catalysis Using a Single Active Site. *Biochemistry* **2012**, *51*, 1148-59.

120. Wheatley, R. W.; Zheng, R. B.; Richards, M. R.; Lowary, T. L.; Ng, K. K. S. Tetrameric Structure of the GlfT2 Galactofuranosyltransferase Reveals a Scaffold for the Assembly of Mycobacterial Arabinogalactan. *J. Biol. Chem.* **2012**, *287*, 28132-43.

121. Szczepina, M. G.; Zheng, R. B.; Completo, G. C.; Lowary, T. L.; Pinto, B. M. STD-NMR studies of two acceptor substrates of GlfT2, a galactofuranosyltransferase from Mycobacterium tuberculosis: Epitope mapping studies. *Bioorg. Med. Chem.* **2010**, *18*, 5123-28.

122. Poulin, M. B.; Zhou, R.; Lowary, T. L. Synthetic UDP-galactofuranose analogs reveal critical enzyme-substrate interactions in GlfT2-catalyzed mycobacterial galactan assembly. *Org. Biomol. Chem.* **2012**, *10*, 4074-87.

123. Snitynsky, R. B.; Lowary, T. L. Synthesis of Nitrogen-Containing Furanose Sugar Nucleotides for Use as Enzymatic Probes. *Org. Lett.* **2013**, *16*, 212-15.

124. Brown, C. D.; Rusek, M. S.; Kiessling, L. L. Fluorosugar Chain Termination Agents as Probes of the Sequence Specificity of a Carbohydrate Polymerase. *J. Am. Chem. Soc.* **2012**, *134*, 6552-55.

125. Wen, X.; Crick, D. C.; Brennan, P. J.; Hultin, P. G. Analogues of the mycobacterial arabinogalactan linkage disaccharide as cell wall biosynthesis inhibitors. *Bioorg. Med. Chem.* **2003**, *11*, 3579-87.

126. Li, J.; Lowary, T. L. Sulfonium ions as inhibitors of the mycobacterial galactofuranosyltransferase GlfT2. *MedChemComm* **2014**, ASAP, doi:10.1039/C4MD00067F.

127. Carlson, E. E.; May, J. F.; Kiessling, L. L. Chemical Probes of UDP-Galactopyranose Mutase. *Chem. Biol.* **2006**, *13*, 825-37.

128. Dykhuizen, E. C.; May, J. F.; Tongpenyai, A.; Kiessling, L. L. Inhibitors of UDP-Galactopyranose Mutase Thwart Mycobacterial Growth. *J. Am. Chem. Soc.* **2008**, *130*, 6706-07.

129. Borrelli, S.; Zandberg, W. F.; Mohan, S.; Ko, M.; Martinez-Gutierrez, F.; Partha, S. K.; Sanders, D. A. R.; Av-Gay, Y.; Pinto, B. M. Antimycobacterial activity of UDP-galactopyranose mutase inhibitors. *Int. J. Antimicrob. Agents* **2010**, *36*, 364-68.

130. Alderwick, L. J.; Radmacher, E.; Seidel, M.; Gande, R.; Hitchen, P. G.; Morris, H. R.; Dell, A.; Sahm, H.; Eggeling, L.; Besra, G. S. Deletion of Cg-emb in Corynebacterianeae Leads to a Novel Truncated Cell Wall Arabinogalactan, whereas Inactivation of Cg-ubiA Results in an Arabinan-deficient Mutant with a Cell Wall Galactan Core. *J. Biol. Chem.* **2005**, *280*, 32362-71.

131. Wolucka, B. A.; McNeil, M. R.; de Hoffmann, E.; Chojnacki, T.; Brennan, P. J. Recognition of the lipid intermediate for arabinogalactan/arabinomannan biosynthesis and its relation to the mode of action of ethambutol on mycobacteria. *J. Biol. Chem.* **1994**, *269*, 23328-35.

132. Alderwick, L. J.; Seidel, M.; Sahm, H.; Besra, G. S.; Eggeling, L. Identification of a Novel Arabinofuranosyltransferase (AftA) Involved in Cell Wall Arabinan Biosynthesis in Mycobacterium tuberculosis. *J. Biol. Chem.* **2006**, *281*, 15653-61.

133. Birch, H. L.; Alderwick, L. J.; Bhatt, A.; Rittmann, D.; Krumbach, K.; Singh, A.; Bai, Y.; Lowary, T. L.; Eggeling, L.; Besra, G. S. Biosynthesis of mycobacterial arabinogalactan: identification of a novel $\alpha(1\rightarrow3)$ arabinofuranosyltransferase. *Mol. Microbiol.* **2008**, *69*, 1191-206.

134. Škovierová, H.; Larrouy-Maumus, G.; Zhang, J.; Kaur, D.; Barilone, N.; Korduláková, J.; Gilleron, M.; Guadagnini, S.; Belanová, M.; Prevost, M.-C.; Gicquel, B.; Puzo, G.; Chatterjee, D.;

Brennan, P. J.; Nigou, J.; Jackson, M. AftD, a novel essential arabinofuranosyltransferase from mycobacteria. *Glycobiology* **2009**, *19*, 1235-47.

135. McNeil, M. R.; Robuck, K. G.; Harter, M.; Brennan, P. J. Enzymatic evidence for the presence of a critical terminal hexa-arabinoside in the cell walls of Mycobacterium tuberculosis. *Glycobiology* **1994**, *4*, 165-74.

136. Escuyer, V. E.; Lety, M.-A.; Torrelles, J. B.; Khoo, K.-H.; Tang, J.-B.; Rithner, C. D.; Frehel, C.; McNeil, M. R.; Brennan, P. J.; Chatterjee, D. The Role of the embA and embB Gene Products in the Biosynthesis of the Terminal Hexaarabinofuranosyl Motif of Mycobacterium smegmatisArabinogalactan. *J. Biol. Chem.* **2001**, *276*, 48854-62.

137. Seidel, M.; Alderwick, L. J.; Birch, H. L.; Sahm, H.; Eggeling, L.; Besra, G. S. Identification of a Novel Arabinofuranosyltransferase AftB Involved in a Terminal Step of Cell Wall Arabinan Biosynthesis in Corynebacterianeae, such as Corynebacterium glutamicum and Mycobacterium tuberculosis. *J. Biol. Chem.* **2007**, *282*, 14729-40.

138. McNeil, M.; Daffe, M.; Brennan, P. J. Location of the mycolyl ester substituents in the cell walls of mycobacteria. *J. Biol. Chem.* **1991**, *266*, 13217-23.

139. Quémard, A.; Lacave, C.; Lanéelle, G. Isoniazid inhibition of mycolic acid synthesis by cell extracts of sensitive and resistant strains of Mycobacterium aurum. *Antimicrob. Agents Chemother.* **1991**, *35*, 1035-39.

140. Banerjee, A.; Dubnau, E.; Quemard, A.; Balasubramanian, V.; Um, K.; Wilson, T.; Collins, D.; de Lisle, G.; Jacobs, W. inhA, a gene encoding a target for isoniazid and ethionamide in Mycobacterium tuberculosis. *Science* **1994**, *263*, 227-30.

141. Baulard, A. R.; Betts, J. C.; Engohang-Ndong, J.; Quan, S.; McAdam, R. A.; Brennan, P. J.; Locht, C.; Besra, G. S. Activation of the Pro-drug Ethionamide Is Regulated in Mycobacteria. *J. Biol. Chem.* **2000**, *275*, 28326-31.

142. DeBarber, A. E.; Mdluli, K.; Bosman, M.; Bekker, L.-G.; Barry, C. E. Ethionamide activation and sensitivity in multidrug-resistant Mycobacterium tuberculosis. *Proc. Natl. Acad. Sci. USA* **2000**, *97*, 9677-82.

143. Larsen, M. H.; Vilchèze, C.; Kremer, L.; Besra, G. S.; Parsons, L.; Salfinger, M.; Heifets, L.; Hazbon, M. H.; Alland, D.; Sacchettini, J. C.; Jacobs, W. R. Overexpression of inhA, but not kasA, confers resistance to isoniazid and ethionamide in Mycobacterium smegmatis, M. bovis BCG and M. tuberculosis. *Mol. Microbiol.* **2002**, *46*, 453-66.

144. Takayama, K.; Kilburn, J. O. Inhibition of synthesis of arabinogalactan by ethambutol in Mycobacterium smegmatis. *Antimicrob. Agents Chemother.* **1989**, *33*, 1493-99.

145. Lee, R. E.; Mikušová, K.; Brennan, P. J.; Besra, G. S. Synthesis of the mycobacterial arabinose donor β -D-arabinofuranosyl-1-monophosphoryldecaprenol, development of a basic arabinosyl-transferase assay, and identification of ethambutol as an arabinosyl transferase inhibitor. *J. Am. Chem. Soc.* **1995**, *117*, 11829-32.

146. Makarov, V.; Manina, G.; Mikusova, K.; Möllmann, U.; Ryabova, O.; Saint-Joanis, B.; Dhar, N.; Pasca, M. R.; Buroni, S.; Lucarelli, A. P.; Milano, A.; De Rossi, E.; Belanova, M.; Bobovska, A.; Dianiskova, P.; Kordulakova, J.; Sala, C.; Fullam, E.; Schneider, P.; McKinney, J. D.; Brodin, P.; Christophe, T.; Waddell, S.; Butcher, P.; Albrethsen, J.; Rosenkrands, I.; Brosch, R.; Nandi, V.; Bharath, S.; Gaonkar, S.; Shandil, R. K.; Balasubramanian, V.; Balganesh, T.; Tyagi, S.; Grosset, J.; Riccardi, G.; Cole, S. T. Benzothiazinones Kill Mycobacterium tuberculosis by Blocking Arabinan Synthesis. *Science* **2009**, *324*, 801-04.

147. Lee, R. E.; Brennan, P. J.; Besra, G. S. Mycobacterial arabinan biosynthesis: the use of synthetic arabinoside acceptors in the development of an arabinosyl transfer assay. *Glycobiology* **1997**, *7*, 1121-28.

148. Ayers, J. D.; Lowary, T. L.; Morehouse, C. B.; Besra, G. S. Synthetic arabinofuranosyl oligosaccharides as Mycobacterial arabinosyltransferase substrates. *Bioorg. Med. Chem. Lett.* **1998**, *8*, 437-42.

149. Pathak, A. K.; Pathak, V.; Suling, W. J.; Gurcha, S. S.; Morehouse, C. B.; Besra, G. S.; Maddry, J. A.; Reynolds, R. C. Studies on n-Octyl-5-(α -d-arabinofuranosyl)- β -d-galactofuranosides for Mycobacterial Glycosyltransferase Activity. *Bioorg. Med. Chem.* **2002**, *10*, 923-28.

150. Khasnobis, S.; Zhang, J.; Angala, S. K.; Amin, A. G.; McNeil, M. R.; Crick, D. C.; Chatterjee, D. Characterization of a Specific Arabinosyltransferase Activity Involved in Mycobacterial Arabinan Biosynthesis. *Chem. Biol.* **2006**, *13*, 787-95.

151. Zhang, J.; Khoo, K.-H.; Wu, S.-W.; Chatterjee, D. Characterization of a Distinct Arabinofuranosyltransferase in Mycobacterium smegmatis. *J. Am. Chem. Soc.* **2007**, *129*, 9650-62.

152. Klement, M. L. R.; Öjemyr, L.; Tagscherer, K. E.; Widmalm, G.; Wieslander, Å. A processive lipid glycosyltransferase in the small human pathogen Mycoplasma pneumoniae: involvement in host immune response. *Mol. Microbiol.* **2007**, *65*, 1444-57.

153. Montoya-Peleaz, P. J.; Riley, J. G.; Szarek, W. A.; Valvano, M. A.; Schutzbach, J. S.; Brockhausen, I. Identification of a UDP-Gal: GlcNAc-R galactosyltransferase activity in Escherichia coli VW187. *Bioorg. Med. Chem. Lett.* **2005**, *15*, 1205-11.

154. Brockhausen, I.; Benn, M.; Bhat, S.; Marone, S.; Riley, J.; Montoya-Peleaz, P.; Vlahakis, J.; Paulsen, H.; Schutzbach, J.; Szarek, W. UDP-Gal: GlcNAc-R β 1,4-galactosyltransferase—a target enzyme for drug design. Acceptor specificity and inhibition of the enzyme. *Glycoconjugate J.* **2006**, *23*, 525-41.

155. Yi, W.; Yao, Q.; Zhang, Y.; Motari, E.; Lin, S.; Wang, P. G. The wbnH gene of Escherichia coli O86:H2 encodes an α -1,3-N-acetylgalactosaminyl transferase involved in the O-repeating unit biosynthesis. *Biochem. Biophys. Res. Commun.* **2006**, *344*, 631-39.

156. Brockhausen, I.; Larsson, E. A.; Hindsgaul, O. A very simple synthesis of GlcNAc- α -pyrophosphoryl-decanol: A substrate for the assay of a bacterial galactosyltransferase. *Bioorg. Med. Chem. Lett.* **2008**, *18*, 804-07.

157. Riley, J. G.; Xu, C.; Brockhausen, I. Synthesis of acceptor substrate analogs for the study of glycosyltransferases involved in the second step of the biosynthesis of O-antigen repeating units. *Carbohydr. Res.* **2010**, *345*, 586-97.

158. Al-Dabbagh, B.; Mengin-Lecreulx, D.; Bouhss, A. Purification and Characterization of the Bacterial UDP-GlcNAc:Undecaprenyl-Phosphate GlcNAc-1-Phosphate Transferase WecA. *J. Bacteriol.* **2008**, *190*, 7141-46.

159. Rush, J. S.; Rick, P. D.; Waechter, C. J. Polyisoprenyl phosphate specificity of UDP-GIcNAc:undecaprenyl phosphate N-acetylglucosaminyl 1-P transferase from E.coli. *Glycobiology* **1997**, *7*, 315-22.

160. Minami, A.; Uchida, R.; Eguchi, T.; Kakinuma, K. Enzymatic Approach to Unnatural Glycosides with Diverse Aglycon Scaffolds Using Glycosyltransferase VinC. *J. Am. Chem. Soc.* **2005**, *127*, 6148-49.

161. Kao, C.-L.; Borisova, S. A.; Kim, H. J.; Liu, H.-w. Linear Aglycones Are the Substrates for Glycosyltransferase DesVII in Methymycin Biosynthesis: Analysis and Implications. *J. Am. Chem. Soc.* **2006**, *128*, 5606-07.

162. Borisova, S. A.; Zhang, C.; Takahashi, H.; Zhang, H.; Wong, A. W.; Thorson, J. S.; Liu, H.-w. Substrate Specificity of the Macrolide-Glycosylating Enzyme Pair DesVII/DesVIII: Opportunities, Limitations, and Mechanistic Hypotheses. *Angew. Chem. Int. Ed.* **2006**, *45*, 2748-53.

163. Borisova, S. A.; Kim, H. J.; Pu, X.; Liu, H.-w. Glycosylation of Acyclic and Cyclic Aglycone Substrates by Macrolide Glycosyltransferase DesVII/DesVIII: Analysis and Implications. *ChemBioChem* **2008**, *9*, 1554-58.

164. Zhang, C.; Moretti, R.; Jiang, J.; Thorson, J. S. The in vitro Characterization of Polyene Glycosyltransferases AmphDI and NysDI. *ChemBioChem* **2008**, *9*, 2506-14.

165. Tang, L.; McDaniel, R. Construction of desosamine containing polyketide libraries using a glycosyltransferase with broad substrate specificity. *Chem. Biol.* **2001**, *8*, 547-55.

166. Freel Meyers, C. L.; Oberthür, M.; Anderson, J. W.; Kahne, D.; Walsh, C. T. Initial Characterization of Novobiocic Acid Noviosyl Transferase Activity of NovM in Biosynthesis of the Antibiotic Novobiocin†. *Biochemistry* **2003**, *42*, 4179-89.

167. Lu, W.; Leimkuhler, C.; Oberthür, M.; Kahne, D.; Walsh, C. T. AknK Is an l-2-Deoxyfucosyltransferase in the Biosynthesis of the Anthracycline Aclacinomycin A†. *Biochemistry* **2004**, *43*, 4548-58.

168. Zhang, C.; Griffith, B. R.; Fu, Q.; Albermann, C.; Fu, X.; Lee, I.-K.; Li, L.; Thorson, J. S. Exploiting the Reversibility of Natural Product Glycosyltransferase-Catalyzed Reactions. *Science* **2006**, *313*, 1291-94.

169. Thibodeaux, C. J.; Melancon, C. E.; Liu, H.-w. Unusual sugar biosynthesis and natural product glycodiversification. *Nature* **2007**, *446*, 1008-16.

170. World Health Organization Global tuberculosis control: WHO report 2013. **2013**, *WHO/HTM/TB/2013.11*.

171. Wells, W. F.; Ratcliffe, H. L.; Crumb, C. On the mechanics of droplet nuclei infection: II. Quantitative experimental air-borne tuberculosis in rabbits. *Am. J. Epidemiol.* **1948**, *47*, 11-28.

172. Bates, J. H.; Potts, W. E.; Lewis, M. Epidemiology of Primary Tuberculosis in an Industrial School. *New Engl. J. Med.* **1965**, *272*, 714-17.

173. Riley, R. L. Aerial dissemination of pulmonary tuberculosis. *Am. Rev. Tuberc.* **1957**, *76*, 931-41.

174. Comas, I.; Coscolla, M.; Luo, T.; Borrell, S.; Holt, K. E.; Kato-Maeda, M.; Parkhill, J.; Malla, B.; Berg, S.; Thwaites, G.; Yeboah-Manu, D.; Bothamley, G.; Mei, J.; Wei, L.; Bentley, S.; Harris, S. R.; Niemann, S.; Diel, R.; Aseffa, A.; Gao, Q.; Young, D.; Gagneux, S. Out-of-Africa migration and Neolithic coexpansion of Mycobacterium tuberculosis with modern humans. *Nat. Genet.* **2013**, *45*, 1176-82.

175. Philips, J. A.; Ernst, J. D. Tuberculosis Pathogenesis and Immunity. *Annual Review of Pathology: Mechanisms of Disease* **2012**, *7*, 353-84.

176. Zumla, A.; Nahid, P.; Cole, S. T. Advances in the development of new tuberculosis drugs and treatment regimens. *Nature Reviews Drug Discovery* **2013**, *12*, 388-404.

177. Koul, A.; Arnoult, E.; Lounis, N.; Guillemont, J.; Andries, K. The challenge of new drug discovery for tuberculosis. *Nature* **2011**, *469*, 483-90.

178. Ramakrishnan, L. Revisiting the role of the granuloma in tuberculosis. *Nature Reviews Immunology* **2012**, *12*, 352-66.

179. Bansal-Mutalik, R.; Nikaido, H. Mycobacterial outer membrane is a lipid bilayer and the inner membrane is unusually rich in diacyl phosphatidylinositol dimannosides. *Proc. Natl. Acad. Sci. USA* **2014**, *1211*, 4958-63.

180. Meroueh, S. O.; Bencze, K. Z.; Hesek, D.; Lee, M.; Fisher, J. F.; Stemmler, T. L.; Mobashery, S. Three-dimensional structure of the bacterial cell wall peptidoglycan. *Proc. Natl. Acad. Sci. USA* **2006**, *103*, 4404-09.

181. Besra, G. S.; Khoo, K.-H.; McNeil, M.; Dell, A.; Morris, H. R.; Brennan, P. J. A New Interpretation of the Structure of the Mycolyl–Arabinogalactan Complex of *Mycobacterium tuberculosis* As Revealed through Characterization of Oligoglycosylalditol Fragments by Fast-Atom Bombardment Mass Spectrometry and 1H Nuclear Magnetic Resonance Spectroscopy. *Biochemistry* **1995**, *34*, 4257-66.

182. Soltero-Higgin, M.; Carlson, E. E.; Gruber, T. D.; Kiessling, L. L. A unique catalytic mechanism for UDP-galactopyranose mutase. *Nature Structure & Molecular Biology* **2004**, *11*, 539-43.

183. Chad, J. M.; Sarathy, K. P.; Gruber, T. D.; Addala, E.; Kiessling, L. L.; Sanders, D. A. R. Site-Directed Mutagenesis of UDP-Galactopyranose Mutase Reveals a Critical Role for the Active-Site, Conserved Arginine Residues†. *Biochemistry* **2007**, *46*, 6723-32.

184. Gruber, T. D.; Borrok, M. J.; Westler, W. M.; Forest, K. T.; Kiessling, L. L. Ligand Binding and Substrate Discrimination by UDP-Galactopyranose Mutase. *J. Mol. Biol.* **2009**, *391*, 327-40.

185. Gruber, T. D.; Westler, W. M.; Kiessling, L. L.; Forest, K. T. X-ray Crystallography Reveals a Reduced Substrate Complex of UDP-Galactopyranose Mutase Poised for Covalent Catalysis by Flavin. *Biochemistry* **2009**, *48*, 9171-73.

186. Soltero-Higgin, M.; Carlson, E. E.; Phillips, J. H.; Kiessling, L. L. Identification of Inhibitors for UDP-Galactopyranose Mutase. *J. Am. Chem. Soc.* **2004**, *126*, 10532-33.

187. Dykhuizen, E. C.; Kiessling, L. L. Potent Ligands for Prokaryotic UDP-Galactopyranose Mutase That Exploit an Enzyme Subsite. *Org. Lett.* **2008**, *11*, 193-96.

188. Timmons, S. C.; Jakeman, D. L. Stereospecific synthesis of sugar-1-phosphates and their conversion to sugar nucleotides. *Carbohydr. Res.* **2008**, *343*, 865-74.

189. Westerduin, P.; de Haan, P. E.; Dees, M. J.; van Boom, J. H. Synthesis of methyl 3-[3-(2-O- α -L-rhamnopyranosyl- α -L-rhamnopyranosyloxy)decanoyloxy]decanoate, a rhamnolipid from Pseudomonas aeruginosa. *Carbohydr. Res.* **1988**, *180*, 195-205.

190. Warren, C. D.; Konami, Y.; Jeanloz, R. W. The synthesis of P1-(2-acetamido-2-deoxy- α -D-glucopyranosyl) P2-ficaprenyl pyrophosphate. *Carbohydr. Res.* **1973**, *30*, 257-79.

191. Lee, Y. J.; Ishiwata, A.; Ito, Y. Synthesis of undecaprenyl pyrophosphate-linked glycans as donor substrates for bacterial protein N-glycosylation. *Tetrahedron* **2009**, *65*, 6310-19.

192. Weerapana, E.; Glover, K. J.; Chen, M. M.; Imperiali, B. Investigating Bacterial N-Linked Glycosylation: Synthesis and Glycosyl Acceptor Activity of the Undecaprenyl Pyrophosphate-Linked Bacillosamine. *J. Am. Chem. Soc.* **2005**, *127*, 13766-67.

193. Woodward, R.; Yi, W.; Zhao, G.; Eguchi, H.; Sridhar, P. R.; Guo, H.; Song, J. K.; Motari, E.; Cai, L.; Kelleher, P.; Liu, X.; Han, W.; Zhang, W.; Ding, Y.; Wang, P. G. In vitro bacterial polysaccharide biosynthesis: defining the functions of Wzy and Wzz. *Nat. Chem. Biol.* **2010**, *6*, 418-23.

194. Engel, R. Phosphonates as analogs of natural phosphates. *Chem. Rev.* **1977**, *77*, 349-67.

195. Yengoyan, L.; Rammler, D. H. Nucleoside Phosphonic Acids. I. The Synthesis of 5'-Deoxyuridine 5'-Phosphonic Acids and Derivatives*. *Biochemistry* **1966**, *5*, 3629-38.

196. Rammler, D. H.; Yengoyan, L.; Paul, A. V.; Bax, P. C. Nucleoside Phosphonic Acids. II. The Synthesis of 5'-Deoxythymidine 5'-Phosphonic Acid and Its Pyrophosphate Derivatives*. *Biochemistry* **1967**, *6*, 1828-37.

197. Bax, P. C.; Morris, F.; Rammler, D. H. Nucleoside phosphonic acids III. A nucleoside phosphonic acid analog of UDP-glucose. *Biochim. Biophys. Acta* **1970**, *201*, 416-24.

198. Corey, E. J.; Volante, R. P. Application of Unreactive Analogs of Terpenoid Pyrophosphates to Studies of Multistep Biosynthesis. Demostration that "Presqualene Pyrophosphate" Is an Essential Intermediate on the Path to Squalene. *J. Am. Chem. Soc.* **1976**, *98*, 1291-93.

199. DeGraw, A. J.; Zhao, Z.; Strickland, C. L.; Taban, A. H.; Hsieh, J.; Jefferies, M.; Xie, W.; Shintani, D. K.; McMahan, C. M.; Cornish, K.; Distefano, M. D. A Photoactive Isoprenoid Diphosphate Analogue Containing a Stable Phosphonate Linkage: Synthesis and Biochemical Studies with Prenyltransferases. *J. Org. Chem.* **2007**, *72*, 4587-95.

200. Caravano, A.; Mengin-Lecreulx, D.; Brondello, J.-M.; Vincent, S. P.; Sinaÿ, P. Synthesis and Inhibition Properties of Conformational Probes for the Mutase-Catalyzed UDP-Galactopyranose/Furanose Interconversion. *Chem. Eur. J.* **2003**, *9*, 5888-98.

201. Partha, S. K.; Sadeghi-Khomami, A.; Slowski, K.; Kotake, T.; Thomas, N. R.; Jakeman, D. L.; Sanders, D. A. R. Chemoenzymatic Synthesis, Inhibition Studies, and X-ray Crystallographic Analysis of the Phosphono Analog of UDP-Gal*p* as an Inhibitor and Mechanistic Probe for UDP-Galactopyranose Mutase. *J. Mol. Biol.* **2010**, *403*, 578-90.

202. Kraft, M. B.; Martinez Farias, M. A.; Kiessling, L. L. Synthesis of Lipid-Linked Arabinofuranose Donors for Glycosyltransferases. *J. Org. Chem.* **2013**, *78*, 2128-33.

203. Codee, J. D. C.; Litjens, R. E. J. N.; van den Bos, L. J.; Overkleeft, H. S.; van der Marel, G. A. Thioglycosides in sequential glycosylation strategies. *Chem. Soc. Rev.* **2005**, *34*, 769-82.

204. Mootoo, D. R.; Konradsson, P.; Udodong, U. E.; Fraser-Reid, B. "Armed" and "Disarmed" n-pentenyl glycosides in saccharide couplings leading to oligosaccharides. *J. Am. Chem. Soc.* **1988**, *110*, 5583-84.

205. Tanikawa, T.; Fridman, M.; Zhu, W.; Faulk, B.; Joseph, I. C.; Kahne, D.; Wagner, B. K.; Clemons, P. A. Using Biological Performance Similarity To Inform Disaccharide Library Design. *J. Am. Chem. Soc.* **2009**, *131*, 5075-83.

206. Pedersen, C. M.; Nordstrøm, L. U.; Bols, M. "Super Armed" Glycosyl Donors: Conformational Arming of Thioglycosides by Silylation. *J. Am. Chem. Soc.* **2007**, *129*, 9222-35.

207. Yeager, A. R.; Finney, N. S. Synthesis of fluorescently labeled UDP-GlcNAc analogues and their evaluation as chitin synthase substrates. *J. Org. Chem.* **2005**, *70*, 1269-75.

208. Gold, H.; van Delft, P.; Meeuwenoord, N.; Codée, J. D. C.; Filippov, D. V.; Eggink, G.; Overkleeft, H. S.; van der Marel, G. A. Synthesis of Sugar Nucleotides by Application of Phosphoramidites. *J. Org. Chem.* **2008**, *73*, 9458-60.

209. Sim, M. M.; Kondo, H.; Wong, C.-H. Synthesis and use of glycosyl phosphites: an effective route to glycosyl phosphates, sugar nucleotides, and glycosides. *J. Am. Chem. Soc.* **1993**, *115*, 2260-67.

210. Caruthers, M. H.; Barone, A. D.; Beaucage, S. L.; Dodds, D. R.; Fisher, E. F.; McBride, L. J.; Matteucci, M.; Stabinsky, Z.; Tang, J. Y. In *Methods in Enzymology*; Wu, R., Grossman, L., Eds.; Academic Press: 1987; Vol. 154, p 287-313.

211. Daly, R.; McCabe, T.; Scanlan, E. M. Development of Fully and Partially Protected Fucosyl Donors for Oligosaccharide Synthesis. *J. Org. Chem.* **2012**, *78*, 1080-90.

212. Brown, R. C. D.; Bataille, C. J.; Hughes, R. M.; Kenney, A.; Luker, T. J. Permanganate oxidation of 1,5,9-trienes: stereoselective synthesis of tetrahydrofuran-containing fragments. *J. Org. Chem.* **2002**, *67*, 8079-85.

213. Casey, C. P.; Marten, D. F. A New General Synthesis of Isoprenoid Chains Employing the Reaction of Dialkylcuprates with β-Acetoxy α,β-unsaturated Esters. *Synth. Commun.* **1973**, *3*, 321-24.

214. Casey, C. P.; Marten, D. F.; Boggs, R. A. Reaction of lithium dialkylcuprates with β-Acetoxy α,β-unsaturated carbonyl compounds—a new synthesis of substituted α,β-unsaturated carbonyl compounds. *Tetrahedron Lett.* **1973**, *14*, 2071-74.

215. Casey, C. P.; Marten, D. F. Stereoselective syntheses of both Z- and E-β-acyloxy-α,β-unsaturated esters and their stereospecific conversion to β-alky-α,β-unsaturated esters. *Tetrahedron Lett.* **1974**, *15*, 925-28.

216. Sum, F.-W.; Weiler, L. Stereoselective synthesis of β-substituted α,β-unsaturated esters by dialkylcuprate coupling to the enol phosphate of β-keto esters. *Can. J. Chem.* **1979**, *57*, 1431-41.

217. Alderdice, M.; Spino, C.; Weiler, L. Synthesis of the three isomeric components of San Jose scale pheromone. *Tetrahedron Lett.* **1984**, *25*, 1643-46.

218. Snyder, S. A.; Treitler, D. S.; Brucks, A. P. Simple Reagents for Direct Halonium-Induced Polyene Cyclizations. *J. Am. Chem. Soc.* **2010**, *132*, 14303-14.

219. Wittmann, V.; Wong, C.-H. 1*H*-Tetrazole as Catalyst in Phosphomorpholidate Coupling Reactions: Efficient Synthesis of GDP-Fucose, GDP-Mannose, and UDP-Galactose. *J. Org. Chem.* **1997**, *62*, 2144-47.

220. Aguilera, B.; Fernández-Mayoralas, A.; Jaramillo, C. Use of cyclic sulfamidates derived from D-allosamine in nucleophilic displacements: Scope and limitations. *Tetrahedron* **1997**, *53*, 5863-76.

221. Perrin, D. D.; Armarego, W. L. F. *Purification of Laboratory Chemicals*; 3rd ed.; Pergamon Press: Oxford, 1988.

222. Rossi, E. D.; Aínsa, J. A.; Riccardi, G. Role of mycobacterial efflux transporters in drug resistance: an unresolved question. *FEMS Microbiology Reviews* **2006**, *30*, 36-52.

223. Viveiros, M.; Leandro, C.; Amaral, L. Mycobacterial efflux pumps and chemotherapeutic implications. *Int. J. Antimicrob. Agents* **2003**, *22*, 274-78.

224. Pasca, M. R.; Guglierame, P.; De Rossi, E.; Zara, F.; Riccardi, G. mmpL7 Gene of Mycobacterium tuberculosis Is Responsible for Isoniazid Efflux in Mycobacterium smegmatis. *Antimicrob. Agents Chemother.* **2005**, *49*, 4775-77.

225. Zegzouti, H.; Zdanovskaia, M.; Hsiao, K.; Goueli, S. A. ADP-Glo: A Bioluminescent and Homogeneous ADP Monitoring Assay for Kinases. *Assay Drug Dev. Technol.* **2009**, *7*, 560-72.

226. Completo, G. C.; Lowary, T. L. Synthesis of Galactofuranose-Containing Acceptor Substrates for Mycobacterial Galactofuranosyltransferases. *J. Org. Chem.* **2008**, *73*, 4513-25.

227. Karas, M.; Glückmann, M.; Schäfer, J. Ionization in matrix-assisted laser desorption/ionization: singly charged molecular ions are the lucky survivors. *J. Mass Spectrom.* **2000**, *35*, 1-12.

228. Zhou, P.; Altman, E.; Perry, M. B.; Li, J. Study of Matrix Additives for Sensitive Analysis of Lipid A by Matrix-Assisted Laser Desorption Ionization Mass Spectrometry. *Appl. Environ. Microbiol.* **2010**, *76*, 3437-43.

229. Faridmoayer, A.; Fentabil, M. A.; Mills, D. C.; Klassen, J. S.; Feldman, M. F. Functional Characterization of Bacterial Oligosaccharyltransferases Involved in O-Linked Protein Glycosylation. *J. Bacteriol.* **2007**, *189*, 8088-98.

230. Sievers, F.; Wilm, A.; Dineen, D.; Gibson, T. J.; Karplus, K.; Li, W.; Lopez, R.; McWilliam, H.; Remmert, M.; Söding, J.; Thompson, J. D.; Higgins, D. G. Fast, scalable generation of high-quality protein multiple sequence alignments using Clustal Omega. *Mol. Syst. Biol.* **2011**, *7*.

231. Peitsch, M. C. Protein Modeling by E-mail. *Nat. Biotechnol.* **1995**, *13*, 658-60.

232. Arnold, K.; Bordoli, L.; Kopp, J.; Schwede, T. The SWISS-MODEL workspace: a web-based environment for protein structure homology modelling. *Bioinformatics* **2006**, *22*, 195-201.

233. Kiefer, F.; Arnold, K.; Künzli, M.; Bordoli, L.; Schwede, T. The SWISS-MODEL Repository and associated resources. *Nucleic Acids Res.* **2009**, *37*, D387-D92.

234. Arosio, D.; Vrasidas, I.; Valentini, P.; Liskamp, R. M. J.; Pieters, R. J.; Bernardi, A. Synthesis and cholera toxin binding properties of multivalent GM1 mimics. *Org. Biomol. Chem.* **2004**, *2*, 2113-24.

235. DeNinno, M. P.; Danishefsky, S. J.; Schulte, G. Stereoselective reactions of alkenylpyranosides: the effect of double bond geometry on conformation. *J. Am. Chem. Soc.* **1988**, *110*, 3925-29.

236. Richardson, T. I.; Rychnovsky, S. D. Total Synthesis of Filipin III. *J. Am. Chem. Soc.* **1997**, *119*, 12360-61.

237. McDonald, F. E.; Wu, M. Stereoselective Synthesis of L-Oliose Trisaccharide via Iterative Alkynol Cycloisomerization and Acid-Catalyzed Glycosylation. *Org. Lett.* **2002**, *4*, 3979-81.

238. Corey, E. J.; Jones, G. B. Reductive cleavage of tert-butyldimethylsilyl ethers by diisobutylaluminum hydride. *J. Org. Chem.* **1992**, *57*, 1028-29.

239. Gaunt, M. J.; Yu, J.; Spencer, J. B. Rational Design of Benzyl-Type Protecting Groups Allows Sequential Deprotection of Hydroxyl Groups by Catalytic Hydrogenolysis. *J. Org. Chem.* **1998**, *63*, 4172-73.

240. Xia, J.; Abbas, S. A.; Locke, R. D.; Piskorz, C. F.; Alderfer, J. L.; Matta, K. L. Use of 1,2-dichloro 4,5-dicyanoquinone (DDQ) for cleavage of the 2-naphthylmethyl (NAP) group. *Tetrahedron Lett.* **2000**, *41*, 169-73.

241. Xia, J.; Alderfer, J. L.; Piskorz, C. F.; Matta, K. L. Total Synthesis of Sialylated and Sulfated Oligosaccharide Chains from Respiratory Mucins. *Chem. Eur. J.* **2000**, *6*, 3442-51.

242. Leonori, D.; Seeberger, P. H. *De Novo* Synthesis of the Bacterial 2-Amino-2,6-Dideoxy Sugar Building Blocks D-Fucosamine, D-Bacillosamine, and D-Xylo-6-deoxy-4-ketohexosamine. *Org. Lett.* **2012**, *14*, 4954-57.

243. Zakharova, A. N.; Madsen, R.; Clausen, M. H. Synthesis of a Backbone Hexasaccharide Fragment of the Pectic Polysaccharide Rhamnogalacturonan I. *Org. Lett.* **2013**, *15*, 1826-29.

244. Splain, R. A. Synthesis of Galactofuranose-based Acceptor Substrates for the Study of Galactan Biosynthesis. Ph.D. Dissertation, University of Wisconsin-Madison, Madison, WI, 2011.

245. Demchenko, A. V.; Pornsuriyasak, P.; De Meo, C.; Malysheva, N. N. Potent, Versatile, and Stable: Thiazolyl Thioglycosides as Glycosyl Donors. *Angew. Chem. Int. Ed.* **2004**, *43*, 3069-72.

246. Pornsuriyasak, P.; Demchenko, A. V. S-Thiazolinyl (STaz) Glycosides as Versatile Building Blocks for Convergent Selective, Chemoselective, and Orthogonal Oligosaccharide Synthesis. *Chem. Eur. J.* **2006**, *12*, 6630-46.

247. Pozsgay, V. A simple method for avoiding alkylthio group migration during the synthesis of thioglycoside 2,3-orthoesters. An improved synthesis of partially acylated 1-thio- α -L-rhamnopyranosides. *Carbohydr. Res.* **1992**, *235*, 295-302.

248. Chittenden, G. J. F. Synthesis of β -D-galactofuranose 1-phosphate. *Carbohydr. Res.* **1972**, *25*, 35-41.

249. Kiessling, L. L.; Grim, J. C. Glycopolymer probes of signal transduction. *Chem. Soc. Rev.* **2013**, *42*, 4476-91.

250. Zähringer, U.; Rietschel, E. T. 2-Deoxy-1,3,4,5,6-penta-O-methyl-2-(N-methylacetamido)-D-glucitol and Derivatives Undergo C-methylation at the N-methylacetamido Group on Repeated Hakomori Methylation. *Carbohydr. Res.* **1986**, *152*, 81-87.

251. Caroff, M.; Szabó, L. Loss of O-methyl Groups from Methylated 2-amino-2-deoxy-D-glucitol and -D-galactitol Derivatives Under Acidic Conditions Used During the Analysis of Glycoproteins. *Biochem. Biophys. Res. Commun.* **1979**, *89*, 410-13.

252. Funakoshi, I.; Yamashina, I. Quantitative Determination of Partially Methylated Alditol Acetate of Amino Sugar by Gas Chromatography-Mass Spectrometry. *Anal. Biochem.* **1980**, *107*, 265-70.

253. Caroff, M.; Szabó, L. O-demethylation of Per-O-methyl Derivatives of 2-amino-2-deoxyhexitols During Acid Hydrolysis and Acetolysis. *Carbohydr. Res.* **1980**, *84*, 43-52.

254. Levery, S. B.; Hakomori, S.-I. Microscale Methylation Analysis of Glycolipids Using Capillary Gas Chromatography-Chemical Ionization Mass Fragmentography with Selected Ion Monitoring. *Methods Enzymol.* **1987**, *138*, 13-25.

255. Sanger, F.; Nicklen, S.; Coulson, A. R. DNA sequencing with chain-terminating inhibitors. *Proc. Natl. Acad. Sci. USA* **1977**, *74*, 5463-67.

256. Bogachev, V. S. Synthesis of Deoxynucleoside 5'-Triphosphates Using Trifluoroacetic Anhydride as an Activating Reagent. □*uss. J. Bioorg. Chem.* **1996**, *22*, 599-604.

257. Barton, D. H. R.; McCombie, S. W. A new method for the deoxygenation of secondary alcohols. *J. Chem. Soc., Perkin Trans. 1* **1975**, 1574-85.

258. Pozsgay, V.; Neszmélyi, A. Synthesis and carbon-13 n.m.r.-spectral study of methyl 2,6- and 3,6-dideoxy- α -L-arabino- and methyl 4,6-dideoxy- α -L-lyxo-hexopyranoside. *Carbohydr. Res.* **1980**, *85*, 143-50.

259. Brimacombe, J. S.; Minshall, J.; Tucker, L. C. N. Nucleophilic displacement reactions in carbohydrates. Part XXII. Formation of 1,4-anhydropyranoses from 1-O-acetyl-6-deoxy-2,3-O-isopropylidene-4-O-methylsulphonyl-[small alpha]-L-manno- and -talo-pyranose with sodium azide. *J. Chem. Soc., Perkin Trans. 1* **1973**, 2691-94.

260. Ballestri, M.; Chatgilialoglu, C.; Clark, K. B.; Griller, D.; Giese, B.; Kopping, B. Tris(trimethylsilyl)silane as a radical-based reducing agent in synthesis. *J. Org. Chem.* **1991**, *56*, 678-83.

261. Liu, B.; Knirel, Y. A.; Feng, L.; Perepelov, A. V.; Senchenkova, S. y. N.; Wang, Q.; Reeves, P. R.; Wang, L. Structure and genetics of Shigella O antigens. *FEMS Microbiology Reviews* **2008**, *32*, 627-53.

262. Liu, B.; Knirel, Y. A.; Feng, L.; Perepelov, A. V.; Senchenkova, S. y. N.; Reeves, P. R.; Wang, L. Structural diversity in Salmonella O antigens and its genetic basis. *FEMS Microbiology Reviews* **2014**, *38*, 56-89.

263. McNulty, C.; Thompson, J.; Barrett, B.; Lord, L.; Andersen, C.; Roberts, I. S. The cell surface expression of group 2 capsular polysaccharides in Escherichia coli: the role of KpsD, RhsA and a multi-protein complex at the pole of the cell. *Mol. Microbiol.* **2006**, *59*, 907-22.

264. Steenbergen, S. M.; Vimr, E. R. Biosynthesis of the Escherichia coli K1 group 2 polysialic acid capsule occurs within a protected cytoplasmic compartment. *Mol. Microbiol.* **2008**, *68*, 1252-67.

265. Clarke, B. R.; Greenfield, L. K.; Bouwman, C.; Whitfield, C. Coordination of Polymerization, Chain Termination, and Export in Assembly of the Escherichia coli Lipopolysaccharide O9a Antigen in an ATP-binding Cassette Transporter-dependent Pathway. *J. Biol. Chem.* **2009**, *284*, 30662-72.

266. Marolda, C. L.; Tatar, L. D.; Alaimo, C.; Aebi, M.; Valvano, M. A. Interplay of the Wzx Translocase and the Corresponding Polymerase and Chain Length Regulator Proteins in the Translocation and Periplasmic Assembly of Lipopolysaccharide O Antigen. *J. Bacteriol.* **2006**, *188*, 5124-35.

267. Larrouy-Maumus, G.; Škovierová, H.; Dhouib, R.; Angala, S. K.; Zuberogoitia, S.; Pham, H.; Villela, A. D.; Mikušová, K.; Noguera, A.; Gilleron, M.; Valentínová, L.; Korduláková, J.; Brennan, P. J.; Puzo, G.; Nigou, J.; Jackson, M. A Small Multidrug Resistance-like Transporter Involved in the Arabinosylation of Arabinogalactan and Lipoarabinomannan in Mycobacteria. *J. Biol. Chem.* **2012**, *287*, 39933-41.

268. Borisova, S. A.; Zhao, L.; Melançon, C. E.; Kao, C.-L.; Liu, H.-w. Characterization of the Glycosyltransferase Activity of DesVII: Analysis of and Implications for the Biosynthesis of Macrolide Antibiotics. *J. Am. Chem. Soc.* **2004**, *126*, 6534-35.

269. Yuan, Y.; Chung, H. S.; Leimkuhler, C.; Walsh, C. T.; Kahne, D.; Walker, S. In Vitro Reconstitution of EryCIII Activity for the Preparation of Unnatural Macrolides. *J. Am. Chem. Soc.* **2005**, *127*, 14128-29.

270. Lu, W.; Leimkuhler, C.; Gatto Jr, G. J.; Kruger, R. G.; Oberthür, M.; Kahne, D.; T. Walsh, C. AknT Is an Activating Protein for the Glycosyltransferase AknS in L-Aminodeoxysugar Transfer to the Aglycone of Aclacinomycin A. *Chem. Biol.* **2005**, *12*, 527-34.

271. Rose, N. L.; Zheng, R. B.; Pearcey, J.; Zhou, R.; Completo, G. C.; Lowary, T. L. Development of a coupled spectrophotometric assay for GlfT2, a bifunctional mycobacterial galactofuranosyltransferase. *Carbohydr. Res.* **2008**, *343*, 2130-39.

272. Lee, R.; Monsey, D.; Weston, A.; Duncan, K.; Rithner, C.; McNeil, M. Enzymatic Synthesis of UDP-Galactofuranose and an Assay for UDP-Galactopyranose Mutase Based on High-Performance Liquid Chromatography. *Anal. Biochem.* **1996**, *242*, 1-7.

273. Buckstein, M. H.; He, J.; Rubin, H. Characterization of Nucleotide Pools as a Function of Physiological State in Escherichia coli. *J. Bacteriol.* **2008**, *190*, 718-26.

274. Battesti, A.; Bouveret, E. The bacterial two-hybrid system based on adenylate cyclase reconstitution in Escherichia coli. *Methods* **2012**, *58*, 325-34.

275. Miller, J. H. *A short course in bacterial genetics : a laboratory manual and handbook for Escherichia coli and related bacteria*; Cold Spring Harbor Laboratory Press: Plainview, N.Y. :, 1992.

276. O'Hare, H.; Juillerat, A.; Dianišková, P.; Johnsson, K. A split-protein sensor for studying protein–protein interaction in mycobacteria. *J. Microbiol. Methods* **2008**, *73*, 79-84.

277. Ciepichal, E.; Jemiola-Rzeminska, M.; Hertel, J.; Swiezewska, E.; Strzalka, K. Configuration of polyisoprenoids affects the permeability and thermotropic properties of phospholipid/polyisoprenoid model membranes. *Chem. Phys. Lipids* **2011**, *164*, 300-06.

278. Löw, P.; Peterson, E.; Mizuno, M.; Takigawa, T.; Chojnacki, T.; Dallner, G. Reaction of optically active S- and R-forms of dolichyl phosphates with activated sugars. *Biochem. Biophys. Res. Commun.* **1985**, *130*, 460-66.

279. Palamarczyk, G.; Lehle, L.; Mankowski, T.; Chojnacki, T.; Tanner, W. Specificity of Solubilized Yeast Glycosyl Transferases for Polyprenyl Derivatives. *Eur. J. Biochem.* **1980**, *105*, 517-23.

280. Rush, J. S.; van Leyen, K.; Ouerfelli, O.; Wolucka, B.; Waechter, C. J. Transbilayer movement of Glc-P-dolichol and its function as a glucosyl donor: protein-mediated transport of a water-soluble analog into sealed ER vesicles from pig brain. *Glycobiology* **1998**, *8*, 1195-205.

281. McLachlan, K. R.; Krag, S. S. Three enzymes involved in oligosaccharide-lipid assembly in Chinese hamster ovary cells differ in lipid substrate preference. *J. Lipid Res.* **1994**, *35*, 1861-68.

282. Dsouzaschorey, C.; McLachlan, K. R.; Krag, S. S.; Elbein, A. D. Mammalian Glycosyltransferases Prefer Glycosyl Phosphoryl Dolichols Rather Than Glycosyl Phosphoryl Polyprenols as Substrates for Oligosaccharyl Synthesis. *Arch. Biochem. Biophys.* **1994**, *308*, 497-503.

283. Sato, K.; Miyamoto, O.; Inoue, S.; Furusawa, F.; Matsuhashi, Y. Stereoselective synthesis of a cisoid C10 isoprenoid building block and some all-cis polyprenols. *Chem. Lett.* **1983**, *12*, 725-28.

284. Davisson, V. J.; Neal, T. R.; Poulter, C. D. Farnesyl-diphosphate synthase. Catalysis of an intramolecular prenyl transfer with bisubstrate analogs. *J. Am. Chem. Soc.* **1993**, *115*, 1235-45.

285. Muto, S.-e.; Nishimura, Y.; Mori, K. Synthesis of Germacrene-B and Its Extension to the Synthesis of (±)-9-Methylgermacrene-B, the Racemate of the Male-Produced Sex Pheromone of the Sandfly Lutzomyia longipalpis from Lapinha, Brazil. *Eur. J. Org. Chem.* **1999**, *1999*, 2159-65.

286. Still, W. C.; Gennari, C. Direct synthesis of Z-unsaturated esters. A useful modification of the horner-emmons olefination. *Tetrahedron Lett.* **1983**, *24*, 4405-08.

287. Malerich, J. P.; Trauner, D. Biomimetic Synthesis of (±)-Pinnatal and (±)-Sterekunthal A. *J. Am. Chem. Soc.* **2003**, *125*, 9554-55.

288. Jaenicke, L.; Siegmund, H.-U. Synthesis and characterization of dolichols and polyprenols of designed geometry and chain length. *Chem. Phys. Lipids* **1989**, *51*, 159-70.

289. Mohri, M.; Kinoshita, H.; Inomata, K.; Kotake, H.; Takagaki, H.; Yamazaki, K. Palladium-Catalyzed Regio- and Stereoselective Reduction of Allylic Compounds with LiHBEt3. Application to the Synthesis of Co-enzyme Q10. *Chem. Lett.* **1986**, *15*, 1177-80.

290. Jenn, T.; Heissler, D. Synthesis of tricyclopolyprenols via a radical addition and a stereoselective elimination. Part II: (Z)-tricyclopentaprenol, (E,E)- and (Z,Z)-tricyclohexaprenol, (Z,Z,Z)-tricycloheptaprenol. *Tetrahedron* **1998**, *54*, 107-18.

291. Terao, S.; Kato, K.; Shiraishi, M.; Morimoto, H. Synthesis of ubiquinones. Elongation of the heptaprenyl side-chain in ubiquinone-7. *J. Chem. Soc., Perkin Trans. 1* **1978**, 1101-10.